Making a medieval stained glass window:
An archaeometric study of technology and production

Laura Ware Adlington

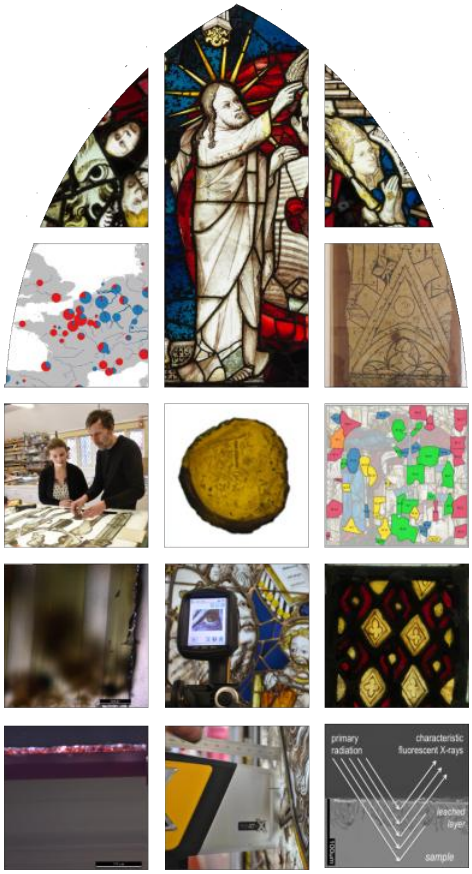

Thesis submitted in fulfilment of the requirements for the degree of
Doctor of Philosophy

UCL Institute of Archaeology

2019

UCL Institute of Archaeology
31-34 Gordon Square
London WC1H 0PY

Declaration of authorship

I, Laura Ware Adlington, confirm that the work presented in this thesis is my own. Where information has been derived from other sources, I confirm that this has been indicated in the thesis.

Signed:

9 September 2018

Decorative figures from the Great East Window in the front matter and final page: Page 2, detail from panel 8c. Page 32, detail from panel 5a. Page 364, detail from panel 2d. © The York Glaziers Trust: reproduced with the kind permission of the Chapter of York

Dedicated

To Edward
my steadfast source
of inspiration and support

and to the glass-painters of York
from John Thornton & his craftsmen
to the conservators of
York Glaziers Trust

Abstract

Medieval stained glass windows are relatively untapped sources of information about medieval technology and production, because the architectural context prohibits sampling glass for chemical analysis. This research focuses on the comprehensive study of York Minster's Great East Window (1405-1408) through chemical analysis, investigating glass-making technology and provenance, glass-painting craft organisation, and development of a methodology using the in situ technique, handheld/portable x-ray fluorescence (pXRF). This research also drew on historical documentation, art historical information, and analysis by EPMA-WDS, LA-ICP-MS, and TIMS.

Poor surface conditions make characterisation of most elements difficult. Through comparing pXRF with other techniques, five quantifiable elements were identified (Cu, Zn, Rb, Sr and Zr). These were used successfully to distinguish glass recipes and batches/sheets of glass, and potentially they may be used to provenance glass (see below). An attachment was designed to mitigate the interference of lead cames, which hold the glass pieces together, enabling high-precision in situ analysis.

Elemental analysis revealed two groups, one consistent with glass produced in Staffordshire and the other with glass produced in the Rhenish region. A longer-term relationship between York Minster and the Staffordshire glass-making industry was discussed. Results suggest medieval glass-makers were capable of greater control over colour generation and glass composition than previously recognised. Synthesis of legacy data proved a useful provenance tool, prompting reinterpretation of previous observations that English windows underwent a compositional change at the end of the fourteenth century. Instead of changes in glass-making technology, it appears glass-making production shifted towards the Rhine.

This study is the first to apply the concept of the "batch" to study craft organisation in medieval glass-painting workshops. Batches were identified chemically, and their distribution across the window studied. This yielded insights into the window's production, including identification of cellular-style production. Glass painted by John Thornton, the master glass-painter, is identified/suggested.

Impact statement

This research seeks to further the study of the enormous industry surrounding the production of medieval stained glass windows, focusing on three areas of study. The first and second contributions are in the study of the medieval crafts of glass-making and glass-painting (i.e., the craft of making stained glass windows). Medieval stained glass windows offer a rare, almost unique opportunity in archaeology to study the long-term output of a workshop; often the products of workshops have been dispersed through commerce and all that remains at the site are waste debris.

This thesis offers new insights into medieval glass-making, indicating that the craft was more sophisticated and glass-makers had greater control over their recipe than previously thought. A synthesis of legacy data shows that there exist regional trends in glass composition based on the characterisation of a few, commonly analysed major elements, which will be a powerful tool for studies of medieval glass to offer a regional provenance of production.

This study is the first application of the materials-based batch concept, recently used in archaeological studies of glass and metal production, to study the organisation of production of medieval windows. Previous studies have been based solely on a visual/stylistic approach, which has inherent limitations. This study brings together both disciplines as independent lines of evidence to gain insights into medieval craft organisation.

The third academic contribution is the development of a methodology for the study of medieval windows by handheld (portable) x-ray fluorescence spectrometry (pXRF), an inexpensive instrument that can be used in situ. This introduces many possibilities in the study of medieval windows, as chemical analysis is often inhibited by their architectural context.

This research has the potential to garner public interest, particularly regarding the organisation of production in the workshop that created the Great East Window of York Minster, the primary case study. For example, the images in this thesis can be easily translated into visual aids in an exhibition at York Minster.

A future output from this project will include a manual for pXRF analysis of archaeological materials that will be accessible to conservators and students with little or no scientific background. There is great potential for pXRF in conservation studios without access to a scientist or a laboratory, as it can be used for research and guide conservation decisions, but there is also potential to misunderstand or misuse the technique and the data.

The results of this thesis will be of special interest to stained glass conservators, particularly those working on the GEW. I have observed the close connection that stained glass artists and conservators feel to glass-painters of the past. The technology has hardly changed through the centuries, so this intimate connection is understandable. It is an often repeated wish of the York conservators to identify the hand of John Thornton, and I am pleased to put forth a strong candidate for his painted work. They have identified several artists in the window, and this result may allow them to identify more examples of his painting.

Table of contents

List of figures

List of tables

Acknowledgements

I have been very fortunate to be surrounded by a wonderful community of people who have supported me and this research. First and foremost, my supervisor Ian Freestone has had a tremendous impact on this research. He invited me to begin working on this project for my MSc research in 2013 and has coached me through all of the hurdles since then. His expertise, guidance and input have been invaluable and truly immeasurable.

Thank you also to my secondary and tertiary supervisors, Marcos Martinón-Torres and Sarah Brown. Although I have sought out your help less than I probably should have, that fault lies entirely with me. Whenever I did reach out, you were ready to advise; and furthermore your publications and research have had an enormous influence on this work.

Together with Sarah Brown, Nick Teed and the team at York Glaziers Trust have been actively supportive in granting me access to the panels, sharing their beautiful high-res images, and providing me detailed art historical reports they compiled. Each time I visited the studio, there was an incredible atmosphere of passion for their work, interest in my research, and a general feeling as though I had been welcomed into a tightknit community. I hope this project will contribute to the remarkable work that you have been undertaking at the York Glaziers Trust. Special thanks to Sarah, Nick, Laura Tempest, Jodie Hodgson, Monika Adamczak, and Merlyn Griffiths.

Leonie Seliger of the Canterbury Cathedral Studios has been very supportive of this research. She generously provided access to panels for analysis and to records pertaining to their history and conservation, and, in our few days working together, shared the wonderful colours of Canterbury Cathedral's windows and history. Although ultimately I decided to exclude this case study from the thesis, this was not because it was an uninteresting or in any way unworthy case study, but merely to preserve an overall narrative to the thesis that was becoming unwieldy in scope. I view the Canterbury case study as a crucial part of this research and I look forward to publishing the results.

Although not formally funded by the Leverhulme Trust, this research has benefitted enormously from collaboration with a Leverhulme Trust Project grant to Ian Freestone and Tim Ayers on the "Composition, Corrosion and Origins of Medieval Window Glass", both in access to the expert knowledge of the team and to samples and comparative data. The thermal ionisation mass spectrometry analyses were carried out in formal partnership with and funded by this Leverhulme Trust grant.

This research also benefitted from access to several laboratories and experts without which it would not have been possible to conduct on such a scale. At the Wolfson Archaeological Science Laboratories of the UCL Institute of Archaeology, Tom Gregory has been both a cheerful source of advice and guidance, as well as a fellow "classmate", as together we embarked on learning to operate the temperamental beast that is the EPMA. Thanks are also owed to Kevin Reeves, who conducted the EPMA-WDS analyses on a subset of the samples for my MSc research in 2013. Thanks to Harriet White also for the technical support, teaching and advice in sample preparation and microscopy.

The thermal ionisation mass spectrometry analyses were carried out at the Royal Holloway Department of Earth Sciences under the guidance of Matthew Thirlwall and with the help of his student, Steph Walker, who generously and patiently gave me their time to teach me the laborious process of sample preparation and analysis by TIMS.

The LA-ICP-MS analyses were carried out at the Cranfield Forensic Institute with Andrew Shortland and Fiona Brock. I not only received excellent training and support for this research, but was given an inordinate amount of Fiona's time and dedication in obtaining the analyses, for which I am very grateful.

A series of glass standards were mixed at UCL Institute of Archaeology with many chemicals provided by the UCL Department of Chemistry. In particular, Martyn Towner was very helpful in locating and granting access to the chemicals required. The glasses were melted by Mark Taylor of the Roman Glassmakers, who also gave appreciated advice. Bernard Gratuze gave valued feedback and advice on the compositions of the glass, and together with David Dungworth, generously agreed to analyse the standards to give a preliminary assessment of the final composition and homogeneity. Thank you also to Laure Dussubieux of The Field Museum, who has agreed to include the standards as part of an interlaboratory round robin for LA-ICP-MS analysis of glass and ceramics which will be invaluable in characterising their compositions as standards.

This research has benefitted enormously from financial support from several sources. The PhD was funded by a combination of the UCL Graduate Research Scholarship and the UCL Overseas Research Scholarship without which the project would not have gone ahead. These scholarships not only provided income but also have a generous and flexible budget for research costs that enabled me to travel to York, Canterbury, Royal Holloway and Cranfield for analyses and to participate in several conferences and

workshops in Europe and the Americas. These activities were also supported by monetary awards from the Institute of Archaeology. Other institutions also supported this research: the Association of the History of Glass (AHG grant), the Worshipful Company of Arts Scholars (the Arts Scholar Research Award), the Canterbury Historical and Archaeological Society (CHAS grant), the Society for Archaeological Sciences (MRS award), Durham University (the Rosemary Cramp Fund), and the Journal of Archaeological Sciences (UKAS presentation prize). I am very grateful for your support of my research, and for your support of research more generally.

Numerous other individuals have provided support and advice to me in various ways, and I am grateful for your attention and inspiration. Many have also given me the treasured gift of friendship, with a lot of silliness as well as personal support through the gruelling yet rewarding journey that is the PhD; please forgive me for not expressing the full, emotional extent of my gratitude here! Thank you to my fellow members of the Early Glass Technology Research Network (especially Ana Franjić, Andrew Meek, Matt Phelps, Daniela Rosenow, Umberto Veronesi, and of course Ian Freestone); Scott Chaussée; Lisa Daniel, Kathy Eremin; Timothy, Josephine, Thomas and Gaëlle Marks, Ole Nordland; Caitlin O'Grady; Hannah Page; Monica Petrescu; M. Teresa Plaza; Nadine Schibille; and Carlotta Gardner, my "work wife".

Finally, so much of who I am and what I have been able to pursue and accomplish is due to the love and support of my family. My parents-in-law, Jonathan and Carolyn Adlington; my sisters-in-law and their partners, Emily, Stu, Tamsin and Toby; my brother and his family, Donald, Ann and Richie Ware; my wonderful parents, Richard and Deborah Ware; and finally, Edward, upon whom I depend so much. Thank you so much, for everything.

CHAPTER 1

Introduction

1.1 Stained glass: Windows to medieval technology and production

Stained glass windows were increasingly important to medieval culture, in particular with the development of the Gothic style (*c.* 1130), the aim of which was to allow larger windows and bring in more light to create an earthly imitation of heaven within its walls (Bony, 1983; Nussbaum, 2000; Scott, 2003; von Simpson, 1962; Wilson, 1990). Besides fulfilling the practical purpose of admitting light into the interior space, stained glass windows are weighted with further meaning when connected to the association of light with the God of Christianity (Duby, 1981; Marks, 1993). The windows served an iconographic function, as they often illustrated religious scenes with sacred messages for the benefit of, and to inspire reflection in, the clergy and congregation. Beyond this, stained glass windows were a sign of conspicuous spending and wealth, and played a part in elevating the status and social power of the cathedral and its clergy; there formed an informal competition between bishops – whose cathedral could have the longest nave, or the highest vault – or the most magnificent stained glass (Scott, 2003). Frequently, windows were donated to the church and to God by patrons in order to curry favour for themselves in this life or the next (Marks, 1993). As an art form, medieval stained glass is one of the "least appreciated" (Marks, 1993, xxiv), perhaps due in part to the difficulty in observing it closely as well as the visual disruption of dirt, deterioration and centuries of conservation interventions. Today, medieval stained glass windows continue to serve their practical, iconographic and artistic functions, and

are furthermore regarded as valued objects of cultural heritage − the pride of local communities and an attraction for visiting tourists.

Beyond all this, medieval stained glass windows are a relatively untapped source of information about medieval craft production, a topic of indisputable importance, in particular in regards to the industry supporting the building of cathedrals. The medieval period is characterised by several periods during which art, craft and technology thrived. A rise in agricultural production enabled part of the population to focus on various trades and crafts, leading to greater specialisation; the institution of the guild developed as a mechanism for tradesmen and craftsmen to protect their interests in the transforming economy. A capital-based economy formed, through growing numbers of markets, increased commerce, the emergence of a merchant class, greater use of money, and increased wealth. The development of the medieval institutions of kingship and feudalism, and their role in and relationship to the Church, led to increased conspicuous and strategic spending. These highlight the medieval era as a significant period in the economic history of the Western world, and the industry of cathedral building is intimately related to the technological, political and social changes occurring at the time (Burnett, 2013; Epstein, 2009; Haskins, 1927; Ovitt, 2013; Scott, 2003; White, 1978, 1972).

Stained glass windows exist at the interesting intersection of art and craft, but have traditionally been studied with an art historical approach. A materials science approach has the potential to shed further light on the life history of a stained glass window, which represents a complex *chaîne opératoire*: from glass-making technology, to the acquisition of the glass, to the practices of the workshop that painted and constructed the window, as well as its life post-production of function and admiration, re-use and re-purposing, and deterioration and conservation. Monumental windows which are well dated and relatively undisturbed by historic conservation are a particularly interesting and rare opportunity to study a large volume of glass produced by one or more glasshouses, and to examine the output of a glass-painting workshop for an extended period of time. Studied through the lens of technological choice and within the historical framework of the medieval period, these topics will relate to technological expertise, trade and exchange patterns, workshop organisation, and guild influence on craft operations.

1.1.1 The Great East Window of York Minster

The Great East Window (GEW) of York Minster, created by John Thornton of Coventry and his workshop between 1405 and 1408, is the largest expanse of medieval stained

glass in England and is generally considered to be a masterpiece of artistry and iconography (Brown, 2018, 2014b; French, 2003; Marks, 1993). This magnificent window has recently been the focus of an important, comprehensive restoration project, "York Minster Revealed", an opportunity which has sparked careful study of the window by various means, including the present materials science approach. Through a comprehensive, multi-analytical study of the GEW, this investigation aims to explore aspects of medieval technology and production in the crafts of glass-making and glass-painting.

1.1.2 Glass-making technology and acquisition

This research engages with the closely related topics of glass acquisition and glass-making technology. This will entail a detailed review of the available information on medieval glass-making technology, drawing on both medieval treatises as well as previous work investigating medieval glass through chemical analysis. The glass in the GEW is thought to originate from both English and European glasshouses (Freestone *et al.*, 2010) and it is an aim of this study to provenance the glass to a region or glasshouse. Possible sources for the GEW glass will be suggested, referring to historical documentation where available. The GEW glass will be compared with glass from an English kiln site, and furthermore a synthesis of legacy data will allow the examination of regional patterns in glass composition for comparison to the GEW glass.

Different recipes will be identified using major and trace element compositions. The factors that affect the generation of colour in glass will also be reviewed. Colour is closely related to the composition of the glass as well as furnace conditions, and so one task will be to untangle the different glass recipes to determine which, if any, were made with the same raw materials and therefore presumably from the same place. The identification of the alteration of a base recipe will also inform about the technological skills of the glass-makers who supplied the window.

The results will also be interpreted outside the narrow scope of York in 1405, which will be possible by identifying and examining non-original medieval glass pieces in the window (removed from other windows and inserted during historical conservation interventions), which will inform about York glass acquisition at different times. In this way, York Minster's longer term relationship to their suppliers can be examined. By comparing the results to previously published work, this thesis will also comment on the acquisition of window glass in England at the end of the 14th and beginning of the 15th century.

1.1.3 The organisation of stained glass window production

This research also delves into the organisation of production in the glass-painting[1] workshop that produced the GEW through the new application of archaeology-based approaches related to technological choice and the concept of the batch to a topic that has traditionally been addressed through art historical and stylistic approaches. A review of current knowledge, including information based on medieval treatises, guild ordinances and other historical documentation; the evidence of the Girona glazing table; previous research based on art historical methods; and a review of the concepts of *chaîne opèratoire,* technological choice and the concept of the batch will provide the framework within which to interpret the results. The study of the GEW will be centred on the identification of different sheets of glass, and the interpretation of their distribution against different models of production. This will allow investigation of the organisation of skilled labour in the production of each panel, as well as tracking changes in production during the three year project. The intimate relationship between medieval craft and apprenticeship will also allow some discussion of learning in a medieval craft workshop and provide insights into a system that is known to have been highly stratified by skill.

1.2 Challenges in the study of medieval stained glass by materials science methods

The study of medieval stained glass by materials science methods has been inhibited by their architectural context; their position embedded in the walls of our ecclesiastical monuments makes the removal of samples impossible unless the window is dismantled, an expensive and intensive undertaking. Therefore, the removal of samples is generally only feasible when a conservation programme demands the dismantling of the window as well as the removal of the lead strips, called cames, that hold the glass pieces together.

Unsurprisingly, the use of in situ techniques such as handheld portable X-ray fluorescence spectrometry (pXRF) has become very popular in the archaeology and cultural heritage sectors. Handheld pXRF can be used directly on the surface of an

[1] In the medieval period, the term glazier was used to mean a range of craftsmen working with glass, from glass-makers, to those who installed plain glass quarries, to those who made the works of art known as stained glass windows (Brown and O'Connor, 1991; Lillich, 1985). The term "glass-painter" is first used in the late fifteenth century (Brown and O'Connor 1991, p 23) and will be used in this thesis as its meaning is unambiguous: it refers to the craftsmen who created stained glass windows, although this required more skills than just painting the glass.

object; the technique is completely non-invasive and non-destructive, thus there is no removal of sample material nor any sample preparation. The popularity of the technique in archaeology and cultural heritage studies can be explained by numerous factors, including that often a curator's or conservator's desire to preserve an object's physical integrity outweighs the desire to sample invasively, or, as is often the case for stained glass, removing a sample is simply impossible.

There are major reservations amongst archaeological scientists about the use of pXRF (e.g., Shackley, 2010). There are some limitations inherent in the technique; for example, handheld pXRF cannot be used to measure light elements (for example, sodium), due to the lack of a vacuum and the absorption of the characteristic x-rays in air. The most problematic limitation, however, lies not in the technology, but in the sample material itself: for best results, the test area must be flat, level, homogeneous, and its surface clean and free of corrosion or, for example, painted details or another surface treatment. This is not always or even often the case for archaeological materials.

In many ways, window glass is an ideal candidate for pXRF analysis; it is flat and level, and glass is homogeneous. Recent work on historic windows in England, mostly post-medieval, is an example of a highly successful application of this technique (Dungworth, 2012a). Unfortunately, the characterisation of medieval glass by pXRF is problematic, due to the presence of corrosion and painted detail, which in effect creates a layer of altered composition that dramatically affects the analyses by pXRF, and due to the presence of lead cames (the strips of lead which hold the glass pieces together), which prevent the placement of the spectrometer directly on the surface of the glass.

1.2.1 Trace element methodology

A key focus of this project is to develop a robust methodology for the in situ analysis of medieval stained glass windows, both to benefit the study of the GEW and to enable future work. This work builds upon previous work which focused on the in situ analysis of post-medieval window glass made in England (Dungworth, 2012a). This English Heritage (now Historic England) study identified three heavy trace elements (rubidium, strontium and zirconium) that were both analysed well by pXRF despite corrosion and other surface conditions, and that served to identify several glass types for the purpose of broadly dating the glass, focusing primarily on post-medieval glazing.

This investigation seeks to explore the resolution of these elements beyond the identification of glass types to test if they can be used to differentiate different recipes,

regional provenance, and even batches of glass. This component of the thesis will first survey the technical and practical considerations of handheld pXRF, the deterioration processes that affect medieval glass and its surface composition, and to identify other sources of surface heterogeneity (such as painted details). Tests will be carried out to test the performance of pXRF on medieval stained glass with the purpose of identifying which elements are affected by surface conditions, and results of the analysis of the GEW glass by pXRF will be compared to other more robust analytical techniques in order to identify their usefulness in addressing questions related to technology and production.

1.2.2 Interference of lead cames

The other major obstacle to the analysis of medieval stained glass by pXRF is the protrusion of lead cames that hold the glass pieces together. These cames can protrude several millimetres and the glass pieces themselves are often smaller than the face of the spectrometer; these two factors combine to prevent the placement of the spectrometer against the surface of the glass, resulting in a distance that can reach four to five millimetres. This study will attempt to mitigate this problem through an evaluation of what elements are affected by the increased distance between sample and spectrometer, and how, and furthermore to test whether this effect is predictable and can be corrected through empirical calibration if the distance is held constant. The ultimate aim is to produce an inexpensive, adaptive and portable solution for this problem while retaining a high degree of precision in the results.

1.3 Overview

The next chapter (Chapter 2) will introduce the Great East Window (GEW) of York Minster, the window that forms the focus of, and provides the materials for, this research. The chapter will identify the documentation available related to its construction, a brief background to York in 1400, and provide details related to its recent conservation and previous research.

The rest of the thesis is structured along three strains: glass-making technology, the organisation of glass-painting, and methodological development.

Chapter 3, ‘Glass-making in the medieval period’, provides a review of the available information related to medieval glass-making, including documentary sources, archaeological evidence, and previous work based on materials analysis. This chapter also reports a synthesis of a large amount of legacy data on medieval glass in Europe

with the purpose of defining regional characteristics in composition as a tool for provenance determination of medieval glass.

Chapter 4, 'Medieval glass-painting', will continue in a similar way on the topic of making stained glass windows, with a review of medieval treatises, other historical documentation including guild ordinances and financial records, and finally will outline how this research intends to try a new approach to the topic of organisation of artistic production of stained glass windows through the application of archaeology-based concepts and frameworks.

Chapter 5, 'Problems and possibilities in using handheld pXRF to study medieval stained glass windows', will begin with an overview of handheld pXRF technology and cover key parameters of which the typical user should be aware when planning an analytical programme. It will then build on the previous two chapters by identifying the key obstacles to analysis of medieval stained glass: poor surface conditions and the protrusion of lead cames.

Details of sampling, analytical methods, and statistical data treatment are given in Chapter 6, 'Methods'. A multi-analytical approach has been designed based on handheld pXRF as well as electron microprobe for the characterisation of major elements, laser ablation inductively coupled plasma mass spectrometry for the characterisation of trace elements, and thermal ionisation mass spectrometry for the measurement of isotopic ratios.

The results sections will begin with methodological development in Chapter 7, 'Performance of handheld pXRF in the analysis of medieval stained glass'. Through a series of tests, elements that are well measured by pXRF despite surface conditions will be identified as quantifiable elements in this study; all other elements reported are considered informational or qualitative. The identification of certain heavy trace elements as well analysed by pXRF is examined through a discussion of the varying depth of pXRF analysis. The relationship between these trace elements and glass-making technology as well as provenance will also be discussed. This chapter will also report the effect that distance between spectrometer and sample has on the analysis of different elements and investigate whether the results can be corrected through empirical calibrations if the distance is held constant. The development of an attachment for the spectrometer which will allow the analysis of in situ window glass despite lead cames will be introduced, and its successful use in the study of another case study, not reported in this document, will be briefly described.

In Chapter 8, 'Chemical characterisation of the GEW glass', the results of the analyses on the GEW glass will be reported. Different glass types will be identified, and then the chapter will focus on reporting the medieval glass in the window, with the original and non-original glass reported separately.

In Chapter 9, 'Original white glass batches and their distribution in the window', the results of the batch identification will be reported and images showing their distribution in each panel will be assessed.

Chapter 10, 'Recipes and procurement of the GEW glass', will discuss provenance and trade relationships specifically for York Minster in 1400 and for England in the 14th-15th centuries, and will examine glass-making technology, in particular in the generation of different colours, through the results of the coloured glasses in the GEW.

Chapter 11, 'Glass-painting and the organisation of production in John Thornton's workshop', examines the distribution of batches both in each panel and across the window to support previous hypotheses regarding the direction of work; to suggest which panels may have been created using the same glazing table; and finally, to compare with models of production based on well-known manufacturing techniques from the automobile manufacturing industry (Fordism and Toyotism). The identification of some of the painted work of John Thornton himself is also suggested.

Finally, the concluding chapter, Chapter 12, gives a summary of the key findings of this project and points towards areas for future research.

CHAPTER 2

The Great East Window of York Minster

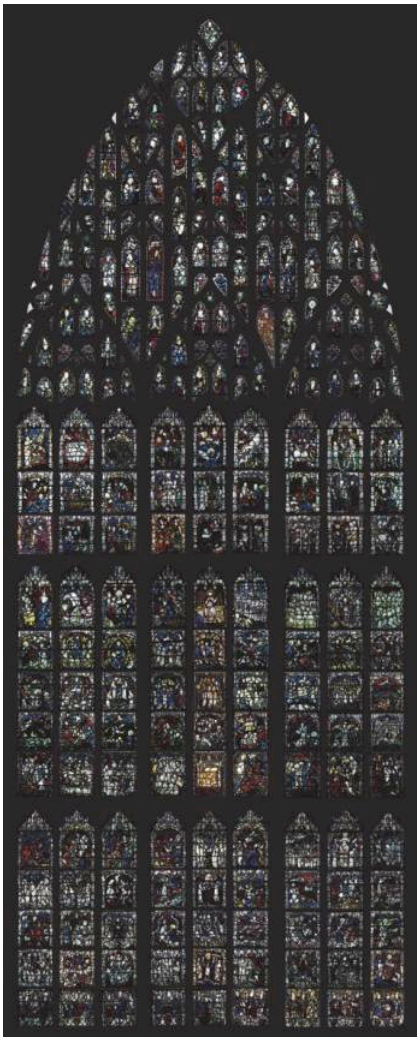

The Great East Window (GEW, Figure 2.1) of York Minster is of great importance in terms of art, history and cultural heritage. It is regarded as one of "the most impressive achievements of medieval glass-painting anywhere" (Marks, 1993, 181), "amongst the greatest work of medieval glaziers" (Brown, 2014a, 9) and is "a work of great imaginative power" that "contains some of the finest fifteenth-century stained glass in Europe" (French, 2003, 10 and 1). French went on to say, "The tremendous sweep of its iconography, the splendour of its design and layout, and the brilliance of its painting and colour, are all acknowledged wherever the glass is discussed" (French, 2003, 1).

Copies of the contract agreeing the terms of its production name the artist, John Thornton of Coventry, and the years of its production, 1405-1408 (Brown, 2014a; French, 2003). Thornton was an influential glass-painter painting in the International

Figure 2.1 The Great East Window of York Minster (compilation of individually photographed panels, circa 2011). A larger image is provided in Appendix A. © *The York Glaziers Trust with the kind permission of Mr Steve Farley.*

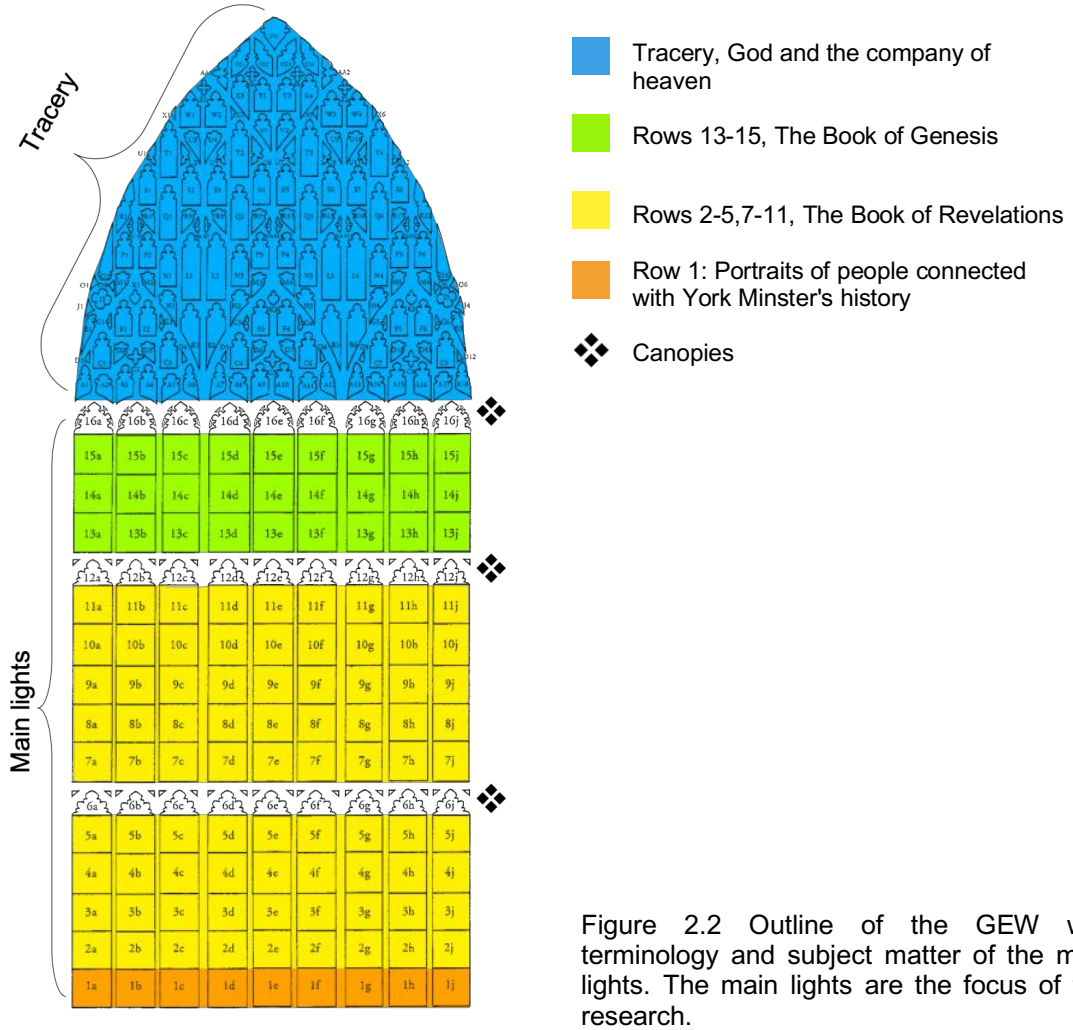

Figure 2.2 Outline of the GEW with terminology and subject matter of the main lights. The main lights are the focus of this research.

Gothic style, and this window is considered to be his masterpiece (Marks, 1993). It is the largest expanse of medieval stained glass surviving in Britain today, spanning 1680 ft^2, and is one of the largest windows created in the medieval period (Brown, 2014a; Osborne, 1997, 50).

The GEW, located at the East End of York Minster, depicts the Beginning and End of All Things, symbolised by the apex piece of the tracery[2] and window that shows God Almighty with the inscription "*Ego sum alpha et Ω*", a dictum which is repeated again at the bottom of the window (French, 2003, 7). God is accompanied in the tracery by the company of heaven, including figures from the Old Testament and martyred saints (Brown, 2014a; French, 2003). The main lights[3] tell the window's narrative with scenes

[2] *Tracery* refers to the pattern of stonework in the upper part of the window, but is also used to refer to the glass that resides there (see Figure 2.2).
[3] The majority of the window is populated by rectangular (almost square) panels that are called the *main lights*. Three rows of main lights are crowned with *canopies* (rows 6, 12 and 16 in Figure 2.1 and Figure 2.2.

Figure 2.3 Portrait of Bishop Walter Skirlaw. Skirlaw donated the funds to construct the GEW and is portrayed in the central position of the bottom row of the window, kneeling before an altar with an inscription that presents the window as an offering to God. Panel 1e of the GEW. © *The York Glaziers Trust with the kind permission of The Chapter of York.*

from the first and final books of the Bible, Genesis and Revelations (Figure 2.2). The top three rows (27 panels, in rows 13-15) illustrate scenes from Genesis beginning with Creation illustrated across the top-most row (row 15), followed by other stories such as Cain murdering Abel, Noah's ark, a Moses sequence (13a-13f), and David and Goliath (French, 2003). The following 9 rows (81 panels, in rows 2-5 and 7-11) depict scenes from Revelations, or the Apocalypse, which although to the current imagination evokes destruction and tragedy, was ultimately a message of hope and God's triumph over all evil (Gooder, 2014). The Apocalypse was a popular topic in medieval art, though primarily depicted in media other than stained glass; illuminated manuscripts depicting this topic were particularly popular in the 13th and 14th centuries and parallels have been drawn between the GEW and contemporary illuminated manuscripts (Brown, 2018, 2014a; Marks, 1993). The bottom row of the window (row 1) displays important figures connected with York Minster's history, including the donor of the window, Bishop Walter Skirlaw (panel 1e, Figure 2.3), who is positioned at the centre, depicted kneeling before an altar with an inscription offering "this magnificent work" to God (French, 2003, 1).

The outstanding qualities of the window have attracted the attention of scholars and antiquarians, who have written descriptions or provided sketches of parts or all of the GEW in records dating back to the late 1600s, including James Torre (1691), Thomas Gent (1762, 1730), Nathaniel Westlake (1886), John Knowles (1936), and Eric Milner-White (1950); for a complete bibliography see French (2003). This attention continues to the present day, and detailed analysis of the symbolism and iconography, with which

this window is rich, can be found in other works (Brown, 2014a; French, 2003; Gooder, 2014; Norton, 2005; Rickers, 1994).

2.1 York in 1400

York was a major city in the medieval period, the unofficial 'capital of the north' (Nightingale, 2010), whose prosperity was due in part to its access to the River Ouse and the nearby port at Hull (Brookes and Huynh, 2018). Towards the end of the 14th century, York was at a zenith of trade and economy, and Hull was the second largest eastern port in England (Kermode, 1998, 1987). The English company of overseas merchants, the Merchant Adventurers, had a branch in York, whose major export was cloth (Sellers, 1918; Sutton, 2009); much of the trade through Hull was with German merchants of the Hanseatic League (Kermode, 1987; Nightingale, 2010; Postan, 1987).

York was also a cosmopolitan centre home to a range of "skills, commerce and cultures, unrivalled outside London... importing ideas alongside almonds and liquorice" (Kermode, 2000, 678), although overall England was the "technological debtor" to mainland Europe throughout the medieval period (Epstein, 2008, 171), importing a wide range of technologies. York was an influential centre of glass-painting distinct from the London School, which interacted with craftsmen and stylistic influences from abroad (Knowles, 1936). From 1300 until the early 1500s, there are more glaziers recorded by name in association with York than with any other glazing centre in England (Marks, 1993); in contrast, there is "surprisingly little evidence" regarding London as a glass-painting hub until the 16th century (Marks, 1991, 275). York was of particular importance during the period in question, stylistically called the International Gothic (1350-1450), as the city contains "most of the finest surviving works in this style", including the famous GEW (Marks, 1993, 180). The glass-painters of York were arguably the most important and influential school in northern England and were likely granted a majority of the most important commissions in the region (Knowles, 1936; Marks, 1993).

Plague in the 14th century also had a profound impact on technology. After the Black Death of 1349 and local outbreaks of the plague throughout the 1300s, in particular in 1390/1391 (Knowles, 1922), the enormous death toll resulted in better, fuller employment for the surviving craftsmen, and led to greater specialisation via the apprenticeship and craft guild system (Britnell, 2000). In York, the shortage of craftsmen meant that some major works were delayed, and the city was forced to reach farther afield for skilled craftsmen, where before it normally drew from a more local region (Knowles, 1922). Knowles (Knowles, 1936, 1922) suggested that a local

dearth in glass-painters forced the Dean and Chapter to look as far as the Midlands for a master glass-painter to create the GEW; York's register of freemen actually show an increase in the numbers of glass-painters in the decades following the Black Death, which has been explained by the suggestion that the regulations for apprenticeship may have been relaxed in order to replete the numbers of craftsmen (Brown, 2018). This would have more or less the same result, in that there appears to have been a shortage in local talent.

2.2 Construction of the window

While the site where York Minster is situated today has been a place of public use since the Roman period when a basilica occupied the site (Ottaway, 2004), the present cathedral was built between 1220 and 1500 (Brown, 2003). The building of the nave began in the late 1200s; its completion and the construction of the East End were delayed by the Black Death in the mid 1300s and other local outbreaks of the plague (Brown, 2003; Knowles, 1922). Construction of the East End, including the quire and the Lady Chapel, began in 1361, and was completed by or around 1373 (French, 2003). The only remaining aspect of the Lady Chapel and East End was the huge window, left empty for over 30 years (French, 2003).

The funding for the outstanding project was provided by the Bishop of Durham, Walter Skirlaw, who was in the 1390s a favourite for the next Archbishop of York (French, 2003). His portrait in the window (Figure 2.3) is identified by his coat of arms. Evidence from medieval wills and other sources indicate that donors were often very involved in the determination of the subject matters of their gifts, sometimes providing images to be included, though this was not always the case (Marks, 1993). The complexity of the subject matter of the GEW suggests the contribution of someone educated in Christian theology (French, 2003). Therefore, Skirlaw should not be regarded as merely the source of funds but also potentially as an integral figure in the crafting of the complex subject matter and iconography of the GEW. Sadly, Skirlaw did not live to see the completion of the window, as he passed away in March 1406, within three months of the commencement of the glazing project (French, 2003, 6).

Copies of the contract for the commission survive, providing important information and interesting insights about the GEW's construction. The original document, now lost, was copied in the late seventeenth century by James Torre in English and in Latin, and by Matthew Hutton in Latin only (French, 2003; all three versions are provided in Appendix A). The following is a transcription of Torre's English version:

> On 10 Augst Ad 1405 6H4
>
> An Indenture was made between the Dean & Chapter on the one pt And John Thornton of Covintry glazier on the other Whereby The sd John covenanted to make a Great Window at the E: end of the Quire, according to the best of his skill & Cunning And undertook to glaze the same wth Glass, Lead, Sodder & other necessaries requisite, & to find all sufficient workmen to be disposed at the Costs of the sd Dean & Chapter. And to finish the same wthin 3 years from the date hereof And obliging himself wth his own hands to portraiture the sd Window wth Historicall Images & other painted work, in the best Mannor & form that he possibly could And likewise paynt the same where need required according to the Ordination of the Dean & Chapter. For all wch the Dean and Chapter should pay him 4s Sterling a week during the term aforesd that he wrought in his Art. And besides that 100s sterling every of those 3 years And if he performed his work well & truly, & perfect it according to the tenor of these Covenants, then he should receive more of the Dean & Chapter for his care therein, the sum of 10ll in Silver.
>
> Torre, York Minster Library LI/7, 7
> (Brown, 2014a; French, 2003)

The contract, dated 1405[4], is between the Dean & Chapter of York and John Thornton of Coventry. Thornton was given a deadline of three years, with a bonus to be paid if met; as the date of completion (1408) is depicted in glass in the tracery near the top of the window (Figure 2.4), it appears the deadline was met. The contract details the payment to be made (£46, plus the £10 bonus); furthermore Thornton was to supply the craftsmen and consumables (glass, lead, solder, and so forth) at the cost of the Dean & Chapter of York Minster. However, it was also noted in the fabric rolls (financial records) of York that were was already in 1399 a substantial supply of both white (i.e., colourless or unintentionally tinted) and coloured glass in stores set aside "pro magnis fenestris novi chori", for the great windows of the new choir (Raine, 1859, 18).

The contract also required that Thornton himself was to design the window (i.e., draw the cartoons, which are to-scale sketches or plans of individual panels), and to furthermore paint some of the glass as dictated by the Dean and Chapter of York. The GEW was constructed within the framework of the medieval guild system (to be discussed in further detail in Chapter 4), a highly stratified system in which different

[4] The three copies of the contract that survive today each record a different month of signing. Torre's Latin copy lists 10 October 1405; his English copy 10 August 1405; and Matthew Hutton's Latin copy lists 10 December 1405. The latter date of December is currently regarded as the most likely to be correct (French, 2003, 1989).

demands were made on craftsmen with different skill levels. The intensive study of a stained glass window provides a rare opportunity in archaeology and history, as the output of a crafts workshop for an extended period of time (three years in this case) can be studied in detail.

2.3 York Minster Revealed

The recent restoration project called "York Minster Revealed" (formally spanning 2011-2016, https://yorkminster.org/york-minster-revealed.html) was aimed at the East End of York Minster, sparked by an urgent need to conserve the stonework that would necessitate the temporary removal of the stained glass. After review, it was also decided to pursue extensive conservation of the Great East Window itself. The window was dismantled, and the glass pieces of the main lights were removed from their lead cames. The conservation programme is described in detail in the recent books on the window by Sarah Brown (2018, 2014a), Director of the conservation studio entrusted with this important work, York Glaziers Trust (YGT). The following summary of the treatment of the main lights (rows 1-5, 7-11 and 13-15; Figure 2.2) is based on her description (Brown, 2018, 69–87, and Brown, 2014a, 45–57).

After the panels were removed from the window, they were fully documented with photography under reflected and transmitted light, and a rubbing of the lead lines made, before the individual glass pieces were removed from the lead cames. The glass was then carefully cleaned, first using dry, soft brushes, and then by swabbing the

Figure 2.4 Panels Z1 and Z2 from near the top of the window, showing the date of completion, 1408. *Adapted from figure on page 106, Brown (2018).*

glass with deionised water and ethanol mixed 1:1. A careful study was made of each panel, in order to distinguish original glass and form an idea of the original composition. Extensive art historical and iconographical research was undertaken to facilitate this process (the art historical reports compiled for the panels studied in this research were made available to this research). Infills were identified and removed if visually obtrusive, while others were retained. New infills were painted based on extensive research, and clearly marked with a signature and the year as well as with faint diagonal lines painted on the exterior surface (Figure 2.5). Any broken glass that could be rebonded with epoxy resin was, reducing the number of leads in the panel. Finally, the panel was releaded, with thinner (and fewer) lead cames, more similar to how they think the medieval leading appeared, and waterproofed with cement under the cames (Brown, 2018, 69–87, and Brown, 2014a, 45–57).

The conservation programme was embedded in comprehensive research and has been a tremendous opportunity for study, including this PhD project and a larger research project with which this thesis dovetailed.

Figure 2.5 A replacement head made as part of the York Minster Revealed project, the most recent conservation of the GEW. Faint diagonal lines are painted across the glass to identify it clearly to future conservaters, and a signature is also scratched into the paint (indicated by an arrow: JP [conservator's initials] YGT 2014). Detail from panel 1h of the GEW. © *The York Glaziers Trust with the kind permission of The Chapter of York*.

2.3.1 Composition, Corrosion and Origins of Medieval Window Glass: The Cardiff-York project

This work dovetails with a larger project funded by the Leverhulme Trust under the leadership of Professor Ian Freestone (then affiliated with the School of History and Archaeology, Cardiff University) and Professor Tim Ayers (History of Art, University of York). This important project was focused on the chemical analysis of medieval window glass from the mid-twelfth to the early sixteenth centuries, predominantly from England but also with samples from mainland Europe; samples from English archaeological sites where glass-making production was carried out were also analysed. The key aims were to chemically characterise the glass, to investigate the relationship between composition and deterioration, and to determine sources of English medieval window glass.

2.3.1.1 Samples from the project

A large number of samples from the GEW (*n*=136), from six panels in the window were analysed as part of the Cardiff-York project. The entire dataset has been made available to this research, although it was used sparingly for the purposes of this thesis to avoid too much overlap between the projects and because most of the data from the project have not yet been published. For the purposes of this PhD, the focus was confined to comparative data from English glass-making sites. The data and how it will be used in this research will be described in more detail in the methods chapter (Chapter 6).

Two of the publications stemming from this project have particular relevance for the GEW and this research. In one, the results of chemical analysis from one of the GEW panels studied are reported (Freestone *et al.*, 2010), while another explored the technology and production of red window glass, including several samples from the GEW (Kunicki-Goldfinger *et al.*, 2014). Both papers will be described in the technological context of medieval glass-making in the next chapter (Chapter 3).

2.4 Summary: A window of opportunity

The GEW, painted and erected between the years of 1405-1408, is a widely celebrated work of art that has sparked the interest of scholars and antiquarians since at least the 17th century. The considerable attention it has received continues to the present day, as it has recently been the focus of an extensive, state-of-the-art conservation project called York Minster Revealed. The conservation programme included the removal of the glass pieces from their lead cames, and with the support of the YGT conservators

and the permission of the Dean and Chapter of York, this became a rare opportunity to conduct a programme of extensive chemical analysis, as will be described. The GEW, with its illustrious history and more recent conservation, presents an excellent opportunity to study topics related to the medieval crafts of both glass-making and glass-painting, as well as to address known issues with the in situ analysis of window glass.

CHAPTER 3

Glass-making in the medieval period

The twelfth century in Europe was a period of 'renaissance' (Haskins, 1927), which was not only academic with the revival of Roman and Greek culture (poetry, philosophy, science and law) and the beginnings of the first universities, but also in the beginning of Gothic art and architecture, and in technology and craft (Burnett, 2013). Several key technological inventions had a great impact on medieval culture and society (White, 1978, 1972), and more generally, a rise in agricultural production enabled part of the population to focus on various trades and crafts, which gave rise to increasing specialisation (Burnett, 2013; Ovitt, 2013).

The first Gothic great church is widely acknowledged as Saint-Denis near Paris, which was renovated under the direction of Abbot Suger beginning in the 1120s (Grant, 1998, 240ff). The Gothic church owed its advent to several key architectural developments, in particular the ogival arch (imported from India, see White, 1978), the ribbed vault and the flying buttress (Duby, 1981), all of which transferred the weight of the building and enabled larger openings for windows (Ovitt, 2013; Prak, 2011). Beginning with the construction works on St-Denis and throughout the later medieval period, a tremendous rise in the construction of ecclesiastical buildings saw the erection of hundreds of cathedrals, thousands of abbey churches, and tens of thousands of parish churches (Scott, 2003, 11). The building of churches and cathedrals underpinned an immense industry, such that it was calculated that in France between 1050 and 1350, more stone was quarried than during the entire history of ancient Egypt (Gimpel, 1984). This rise in ecclesiastical architectural also brought about an increase in the demand for glass to fill the windows; the glass industry during this time was enormous (Wedepohl, 2003, estimated about 40,000 tonnes of glass was produced in central

Europe between 1250 and 1500), and a large proportion of the glass produced during this period was designated for windows (Smedley and Jackson, 2002a; see also Stern and Gerber, 2004).

The making of "forest glass"[5], so-called because it was made using the ashes of wood and/or terrestrial plants such as ferns or bracken, marks a change in glass-making technology that occurred in northern Europe by the end of the first millennium. This technological change saw not only a shift in raw materials from soda-rich natron or ashes of halophytic plants to potash-rich ashes of wood or fern, but also other changes such as in production location, furnace design and types of products (Jackson and Smedley, 2008a; Thorpe, 1949; Willmott, 2005).

3.1 Medieval treatises on glass-making

Few historical treatises survive to give details about glass-making in the medieval period, the earliest and most comprehensive of which was penned by Theophilus Presbyter, a Benedictine monk writing in the early 12th century in northwest Germany (Dodwell, 1986; Hawthorne and Smith, 1979; White, 1964); Dodwell (1986) dates his work to between *c.* 1110 - 1140. *De Diversis Artibus,* or "On Diverse Arts", is an invaluable source of information on painting, metalworking, and glass-making in the medieval period and is today still the most widely cited primary source on the latter subject (Hawthorne and Smith, 1979).[6] His treatise is exceptional as the first European account to provide an intimate level of detail, such that it suggests that he was a craftsman himself - or that he at least 'dabbled' (Hawthorne and Smith, 1979). He details not only the most primary steps of each craft, but also the making of the tools and equipment (such as furnaces) and the preparation of raw materials (Figure 3.1).

The recipe for glass-making as described by Theophilus has been compared to, and proved compatible with, medieval glass compositions (Freestone, 1992), and although it is recognised that precise recipes will have varied regionally and through time, the basic recipe he reports is generally accepted as an accurate description of medieval glass-making. His recipe is to use the ashes of dried out beech logs, and to mix two

[5] This type of glass has been given various names, including "wood ash glass", "potash glass", "potash lime glass" and "calco-potassic glass", but "forest glass" is preferred in this work as it includes the use of terrestrial plants as well as trees for ashes, reflects the connection of the industry with forested areas, and adds no restrictions on the chemical composition.

[6] There are two seminal translations into English that are used today, the first a "very nearly definitive text" (White, 1964, 225) by C. R. Dodwell (first published in 1961) and the other by classicist John G. Hawthorne and metallurgist Cyril Stanley Smith (first published in 1963), whose book has focused more on technology. It is therefore this latter version that was used more heavily in this research.

THEOPHILUS ON DIVERS ARTS

1 How to prepare the beechwood ashes, and how to build the furnace;

2 How to build the annealing furnace;

3 How to build the furnace for spreading out the glass; and also the tools needed for the craft;

4 How to mix the beechwood ashes and sand, and heat the mixture ("fritting");

5 How to make the glass-making crucibles, and melt the fritted mixture;

6 How to form sheets of glass (using the cylinder method);

7 How to make yellow glass;

8 How to make flesh-coloured and purples glasses;

9 How to spread out the glass sheets and anneal them;

12 How to melt opaque glass used in Roman mosaics for repurposing;

17 How to draw out the plan for a window panel;

18 How to cut the glass for the window, and grozing the edges of the glass pieces;

19 How to prepare and apply pigment onto the glass;

20 Different techniques for applying the pigment to achieve different effects;

21 Further techniques for painting the glass;

22 How to make the kiln for firing the painted glass;

23 How to fire the glass;

Figure 3.1 Selected chapters from the second book of *De Diversis Artibus* by Theophilus (trans. Hawthorne and Smith, 1979).

parts of the ash with one part sand; experimental work and calculations have suggested that these parts were measured by weight rather than volume (Smedley and Jackson, 2002a; see also Stern and Gerber, 2004). This mix is then fritted, or heated until hot but not melting. The fritted mix is then melted in a ceramic working pot overnight. Theophilus describes making sheets of glass by what is called the "muff" or cylinder method, in which the glass-blower blows a long bubble, opening the ends and cutting it down the centre to make a rectangular sheet of glass. An alternate method of making a glass sheet is the crown method, in which the glass-blower rolled the blowpipe until the gather of glass flattened out into a circular disc. Both techniques were known in Europe during the medieval period (Caen, 2009; Charleston, 1991; Godfrey, 1975; Kenyon, 1967; Marks, 1993; see also Wood, 1982). After shaping, the sheet was annealed in a separate furnace. These basic steps are illustrated in an early 15th century manuscript, Sir John Mandeville's *Travels* (Figure 3.2), which show men digging up sand and carrying the raw materials from the forest (a), workers tending to the fuel and melting of the glass in the main furnace (b), a glass-blower (c), and the annealing furnace with finished vessels (d).

Another early text describing glass-making, dating to the late 12th - early 13th century (Marks, 1993), is the text *De coloribus et artibus Romanorum* by Eraclius, who was probably writing in Italy (Merrifield, 1967).[7] His recipe varies somewhat from that of Theophilus, in that he prescribes the use of both ferns and young beech trees, both ashed separately, combined in a ratio of two parts fern ash to one part beech ash, and baked. Despite doubts that fern or bracken ashes were a sustainable raw material for large-scale glass-making (Stern and Gerber, 2004), these concerns were challenged by Verità (2005), citing several papers reporting chemical compositions that could have been achieved through the addition of fern ash; an earlier paper by Smedley and Jackson (2002b) offered an extensive defence of the use of fern/bracken in glassmaking, citing a range of documentary sources aside from technological treatises, including Chaucer and purchase records, and archaeological evidence. Subsequently, experiments by Smedley and Jackson (2006) focused on the sustainability of using ferns as a source for ash in glass-making, concluding it was sustainable although they acknowledged that the collection of fern and bracken was more labour- and time-intensive, and suggested that fern ash was added for specific properties it could bring to the glass.

Theophilus also describes the process of making variously coloured glass. His account as it survives to us today makes no mention of the addition of colourants, beyond a brief description of the Frankish practice of repurposing opaque mosaic pieces and cullet to melt with a base glass for making coloured sheets for windows, in particular blue (*Theophilus* 2:12). Evidence of this practice of reusing tesserae has been detected in the archaeological record in the early

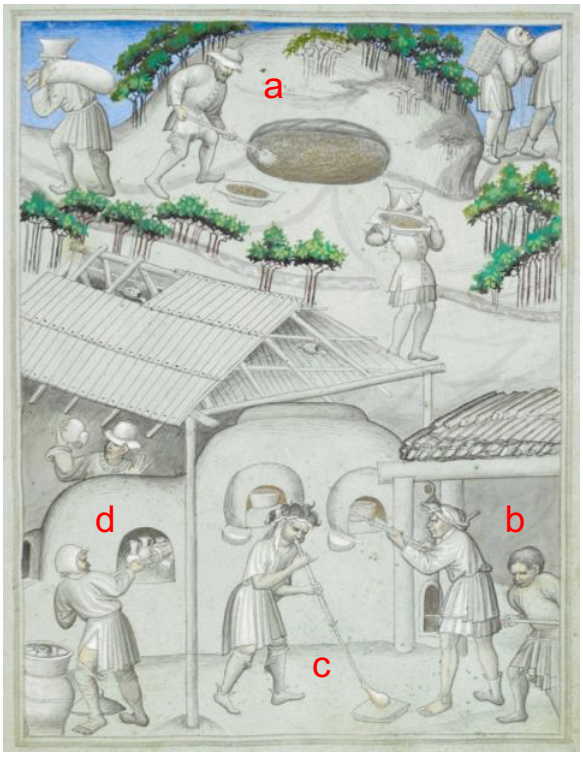

Figure 3.2 'Glassmaking at the Pit of Memnon' from Sir John Mandeville's *Travels* (c. 1410). Different stages of glassmaking and glassblowing have been marked and described in text. *British Library Add. 24189 f.16*

[7] This treatise was translated into English with commentary by Mary Philadelphia Merrifield in 1849, which remains the only English translation (see Merrifield, 1967; Introduction by editor S. M. Alexander).

medieval period (Schibille and Freestone, 2013) and blue window glass pieces in twelfth centuries windows at York Minster and St Denis have also been suggested as the product of such recycling (Cox and Gillies, 1986; Kunicki-Goldfinger *et al.*, 2014a). Many copies of the treatise also list the name of additional chapters which are no longer extant, which evidently described the making of pigments from copper, lead and salt, and how to make green, blue and red glass (Hawthorne and Smith, 1979, 58, fn. 1). Instead, the surviving chapters recount a method that depends on optimising the conditions of each batch during the melt (*Theophilus* 2:7-8; Hawthorne and Smith, 1979). If upon melting, the glass begins to turn either yellow or purple-ish, Theophilus advises on how to proceed in order to enhance the colour. Modern experiments recreating medieval glass production have confirmed that the same glass recipe can yield a range of different colours with different redox conditions in the furnace (Royce-Roll, 1994).

The account by Eraclius does include details on producing colours through the addition of extra raw materials. Copper filings burnt to a powder produce green if the ashes are well baked, red if they are not, and yellow with the addition of extra ashes. Other colours are made without added colourants, like Theophilus describes: purple, *membranaceum* and *membranum*[8] (Eraclius 3:7; Merrifield, 1967). Merrifield made no attempt to translate the last two terms, but some further information may form an idea of their colour: *membranaceum* has since become part of the binomial name for the plant huckleberry, which has berries with a dark, reddish or blueish purple colour; while the word *membranum* is translated as 'skin' (or “parchment”, Aune, 2003) and may therefore refer to flesh tones in this context (Eraclius writes that the purple glass will turn pale after extended firing, and after further time will become *membranum*).

3.2 The chemical composition of medieval forest glass

Most man-made glasses, and virtually all glass pre-dating the twentieth century, are composed predominantly of silica. Flux is necessary to lower the melting temperature of pure silica (1713°C) to attainable temperatures and to extend the cooling time (or working range), the time (and range of temperatures) the glass may be shaped (Drees *et al.*, 1989; Moretti and Hreglich, 2013). For centuries, the flux used was the mineral natron, sourced from the Wadi Natrun in Egypt; in the 8th-9th centuries, this source

[8] Merrifield (1967, 213, ft. 8) includes the word *membrun* in her text, but notes that one manuscript uses the variant *membranum* (the oldest manuscript, formerly at Cambridge, but now in the British Museum).

was exhausted and replaced in the Near East and Mediterranean with the use of soda-rich plant ash as a flux (Phelps *et al.*, 2016; Shortland *et al.*, 2006). In Western Europe (north of the Alps), a glass-making tradition using the ashes of wood and terrestrial plants such as ferns developed beginning in the eighth century (Pactat *et al.*, 2017; Rehren and Freestone, 2015; Velde, 2013; Wedepohl, 1998). Medieval forest glass is generally characterised by its high concentrations of potash and lime, and relatively low silica; other markers include relatively high concentrations of phosphate and magnesia.

3.2.1 Factors affecting the chemical composition of medieval glass

The chemical composition of wood or plant ash, and therefore the composition of the glass made from these ashes, is highly variable dependent on numerous factors. The underlying geology where the tree or plant grows is arguably the most significant factor determining the chemical composition of the plant ash and resultant glass, as this determines which elements the plant takes up from the substratum (Drobner and Tyler, 1998; Meiwes and Beese, 1988; Sanderson and Hunter, 1981; Stern and Gerber, 2004; Turner, 1956a). Sanderson and Hunter (1981) collected branches of oak and beech trees from six locations in the Weald (Surrey), and found a high degree of variability even within that one region. For example, the beech ash compositions ranged from 7.8% − 16.3% K2O, 14.0% − 26.3% CaO, and 0.17% − 4.0% MnO. Stern and Gerber (2004) compared the ash compositions of trees growing on specific substrata, e.g. calcareous versus silicate (clayish), and found, for example, that the lime contents of the calcareous beech ash was approximately twice that of the silicate beech ash (68% CaO compared to 33%).

Other factors also impact the composition of the wood ash, including the plant species (such as different types of tree, or the use of fern or bracken), time of harvest (seasonally as well as year to year), and the part of the tree/plant used (for example, trunk versus bark) (Jackson *et al.*, 2005; Jackson and Smedley, 2008b; Turner, 1956a; Wedepohl, 1998; Wedepohl and Simon, 2010). In a study by Jackson, Booth and Smedley (2005), the ashes of beech, oak and bracken collected from the same region in Sheffield/Derbyshire showed significant differences in their major and trace element concentrations (for example, beech ashes contained 31.1% CaO and 18.8% K_2O; bracken 10.5% CaO and 42.5% K_2O; and oak 65.4% CaO and 14.5% K_2O). Another part of that study compared the composition of bracken ash from plants collected from the same place, one year apart, and found that some elements were present in very different concentrations: for example, soda (0.26% Na2O versus 2.66%) and iron

(0.35% Fe2O3 versus 4.21%). The ash of bracken collected regularly throughout the growing season also showed significant changes in composition (Jackson and Smedley, 2008b).

The sand raw material furthermore adds several minor and trace elements to the glass batch, and varies by geological origin. Several studies have focused on the Mediterranean coastal sands used in the ancient Egyptian and Roman traditions, reporting high concentrations of aluminium and calcium, as well as iron and other impurities (for trace element compositions, see Brems *et al.*, 2012; Silvestri *et al.*, 2006; Turner, 1956a). Fewer studies have reported the compositions of northern European sands used in many forest glass recipes; these sands can have high concentrations of alumina but typically have very low calcium contents, along with various other impurities including iron and titanium (Boswell, 1917; Hartmann, 1994; Jackson and Smedley, 2004; Stern and Gerber, 2004). Reverse calculations on medieval high-lead glass, made with lead oxide and sand, suggest that highly pure sands were used for this type of glass, though early medieval finds in York showed very high alumina that could originate in the sand, or alternatively from the crucible (Mecking, 2013).

3.2.2 Transition to high lime, low alkali (HLLA) glass

Studies tracking changes through time in Germany (Wedepohl and Simon, 2010), Bohemia/Czechia (Smrček, 1999), France (Barrera and Velde, 1989), and Belgium (Schalm *et al.*, 2007) have noted that over time, silica concentrations increase slightly, potash concentrations drop, and lime contents increase (or increase relative to potash). The beginning of the fifteenth century appears to be a particularly transitional period for medieval glass-making technology; two of these studies (Schalm *et al.*, 2007; Wedepohl and Simon, 2010) use the year 1400 to divide their glass types, while Barrera and Velde (1989) use the year 1450. Therefore, the GEW (1405-8) was constructed at a time of development in glass-making technology in Europe.

This transition towards a glass with higher lime and low potash (called "high lime low alkali" or HLLA glass[9]) is a technological development interpreted in various ways. Wedepohl (2003) put forth the theory that, due to increasing pressure on timber

[9] HLLA is sometimes a problematic term, as some publications use the phrase to describe high-lime glasses with potash levels similar to potash glasses with lower lime (see Schalm *et al.*, 2007; Sedláčková *et al.*, 2014). In this research, the term HLLA will only be used to refer to glass with a high proportion of lime and low alkali - specifically, a $CaO/[CaO+K_2O]$ ratio above about 0.75, and about 10% or less alkali (Na_2O+K_2O); these cut-offs were identified as a natural separation in data for this period (see section 3.5). The term "mixed alkali" will be used to describe glass with approximately equal concentrations of Na_2O and K_2O, but this designation does not exclude the glass from also being HLLA.

resources, glassmakers began to use a higher proportion of twigs and smaller branches to trunk, and that the higher proportion of bark imparted a higher amount of calcium to the glass. Although his data strongly supports this theory (Figure 40 in Wedepohl, 2003), other studies report that ash from beech twigs and smaller branches have less calcium than larger branches and the trunk (Table 3 in Jackson *et al.*, 2005; Table IX in Turner, 1956a), and in another study, the analysis of pine bark had significantly less calcium than the rest of the tree (Table 1 in Stern and Gerber, 2004).

Stern and Gerber (2004) argue that washing the ashes, and using some combination of the potash extract with the leached ash, could have been used to achieve target melt compositions; however this has been criticised as being contradictory to the available evidence both literary and compositional (Verità, 2005). The purification of plant ash by washing it and extracting the alkali salt for glass-making is usually associated with the development of the Venetian *cristallo* glass in the mid-15th century (Verità, 1985), though an argument has been made for an earlier, less sophisticated version of this technique being used in western Europe for enamelling in the 14th and 15th centuries (Wypyski and Richter, 1997). The first reference to the production of potash for glassmaking does not occur until the 16th century (Agricola: Hoover and Hoover, 1950; Biringuccio: Smith and Gnudi, 1943). However, it has also been argued that in eastern Europe, where glass was produced with particularly high K_2O:CaO ratio, that wood ash and potash were used together as early as the 14th century (Cílová and Woitsch, 2012), suggesting the technology to extract potash existed already.

Another possibility is the addition of limestone to the batch (Hartmann, 1994). However, limestone is strontium-poor (Katz *et al.*, 1972; Kinsman, 1969) and the high concentration of strontium in most forest glass, and the increasing concentrations usually seen in higher lime glasses, suggests this may not be the case until the post-medieval period, when fewer impurities associated with wood ash (such as magnesium and phosphorus) are observed in the glass (Cílová and Woitsch, 2012; Dungworth, 2012a; Kunicki-Goldfinger *et al.*, 2008). The first literary reference to the deliberate addition of lime was not until the late 17th century (Johann Kunckel, 1689, in Turner, 1956b), though this does not exclude the possibility of earlier use as the addition of cobalt is not referenced until 1540 (Biringuccio: Smith and Gnudi, 1943).

The development of HLLA is often associated with increasing sodium concentrations, usually associated with higher chlorine and negatively correlated with potassium; this is interpreted as the addition of salt (NaCl) to the batch to adjust the viscosity of the low-potash recipe (Gerth *et al.*, 1998; Kunicki-Goldfinger *et al.*, 2009; Schalm *et al.*, 2007; Wedepohl and Simon, 2010). The solubility of chlorine in a glass melt is affected by

numerous factors including furnace temperature and length of time in the molten state (Obranovic *et al.*, 2005; Rehren, 2000); however, the higher calcium would have resulted in a higher melting temperature (Hunault *et al.*, 2017b), which should result in less chlorine in the final glass.

Changing recipes also impacted furnace technology and the skill requirements for glassmakers. The melting temperature of forest glass is in the region of 1250 - 1350°C (Morey *et al.*, 1930; Stern and Gerber, 2004). A recent study (Hunault *et al.*, 2017b) into the thermodynamic properties of various medieval glass compositions found that the transition from soda ash glass, to high potash forest glass, to HLLA glass, meant higher furnace temperatures, decreased working range (the range of temperatures that the glass can be worked), and increased viscosity.

In English glassmaking, the transition to HLLA does not appear to have taken place until the late 16th century, when glassmakers immigrated from the Continent and set up in the Weald in 1567 (Dungworth, 2012a; Thorpe, 1949).

3.3 Colour technology

There were three main techniques used for achieving a desired colour in window glass: first, as described by Theophilus, relying on control over the furnace redox conditions and length of melting; second, as described by Eraclius, by including additional raw materials (colourants) into the batch; and third by forming composite glasses, the most prevalent of which was red flashed glass.

3.3.1 Control over the furnace and redox conditions

Theophilus and Eraclius both describe making different colours from the same base glass. The standard wood ash and sand recipe results in a glass with significant incidental concentrations of both iron and manganese, which in various concentrations and more importantly, oxidation states, impart a wide range of colours to glass (Geilmann and Brückbauer, 1954; Weyl, 1951).

The colour that iron imparts to a glass depends on ratio of $FeO:Fe_2O_3$ and furthermore the role that these play in a glass; $Fe^{3}+$ ions can act either as a network former (corresponding to the silica tetrahedra) or in glass with higher alkali, as a network modifier (by bonding with the alkali ions). The furnace atmosphere, temperature, length of melting, and base glass composition all affect the oxidation of iron ions and the $Fe^{2+}:Fe^{3+}$ ratio, which produces colours including browns, greens, yellows, and blues.

The deliberate and separate addition of manganese oxide, which later became known as "glass-maker's soap" as it served to decolourise the glass, was practiced in northern Europe during the Roman period (Sayre, 1963). However, the naturally high contents of manganese found in wood ashes (about 1-11% MnO in beech ashes, Turner 1956a; see also Cílová and Woitsch, 2012; Jackson *et al.*, 2005; Jackson and Smedley, 2008b; Royce-Roll, 1994; Stern and Gerber, 2004) made the separate addition of manganese unlikely in most medieval forest glass recipes, until recipes such as that recorded by Biringuccio (16th century), which used manganese added to purified ash from soda-rich saltwort ashes or fern ashes (Smith and Gnudi, 1943; see also discussion in footnote, Hawthorne and Smith, 1979, 56; Turner, 1956b). Under oxidising conditions, the manganic ion (Mn^{3+}) imparts purplish colours to the glass; to produce purple, the glass should be high in alkalis and melted at a low temperature (Weyl, 1951). Sulphur also oxidises iron, but in doing so this also changes the ratio of sulphites and sulphides, producing amber yellow (Beerkens, 2003). When reduced to the manganous ion Mn^{2+}, it serves to oxidise the iron present in the glass resulting in a colourless glass (Weyl, 1951).

Experiments with glass-making have shown that the typical compositions of medieval forest glass can achieve a range of colours through varying redox conditions of the melting, with purples and violets formed with oxidising conditions and yellow-ish greens and browns produced by reducing conditions (Sellner *et al.*, 1979). While it was posited that furnace design might have played a large role in this, in particular the inclusion/exclusion of a chimney (Sellner *et al.*, 1979), a further experiment showed that the standard medieval furnace (i.e., chimney-less) could be controlled well enough to produce the range of redox conditions required to produce these colours (Royce-Roll, 1994). From this it was concluded that the full range of colours observed in medieval stained glass windows could be achieved through manipulation of furnace conditions, excluding cobalt blue and copper red (Newton, 1980, 1978; Royce-Roll, 1994).

3.3.2 Addition of colourants to the melt

Blue glass in the medieval period was frequently made using cobalt to colour the glass. Cobalt has been used in glass-making since its beginnings in the Late Bronze Age, though in the early medieval period, the knowledge or access to ores was either lost briefly, or it was less expedient, as blue Roman mosaic tesserae were often used to colour glass instead (Cox and Gillies, 1986; Kunicki-Goldfinger *et al.*, 2014a; Schibille and Freestone, 2013). Other cobalt pigments were used by the end of the twelfth

century, and after this, the recycling of Roman mosaic tesserae became less common (Gratuze *et al.*, 1995).

A very small amount of cobalt can give a vibrant blue colour; although different oxidation states of cobalt will exist in a glass, CoO_4 has such a strong absorption that it easily overpowers other cobalt ions (and other colourant ions) and therefore the colour is not affected by furnace redox conditions. However, a deeper blue can be achieved with higher furnace temperature and rapid cooling (rather than slow annealing; Weyl, 1951). Different ore groups in use during the medieval period, most of which probably originated in Germany, have been identified on the basis of associations with several other trace elements (Gratuze, 2013; Gratuze *et al.*, 1996, 1995, 1992).

Glass coloured using copper can be blue, green or red depending on redox conditions as well as the composition of the base glass. Under oxidising conditions, the Cu^{2+} ion is formed and produces shades of blue, green and brown (with lead and zinc oxides in the melt resulting in a blue colour and alumina resulting in green), while under reducing conditions, Cu^{+} and metallic Cu nanoparticles form, the latter of which results in ruby red (Weyl, 1951). However, for the copper ruby to be used as window glass, glass-makers employed an extra technique (see next section), since this glass transmits light poorly and appears nearly opaque at the typical thickness of window glass.

3.3.3 Flashed glass and other composite glasses

Another method of achieving colour in window glass was to "flash" the glass: flashed glass was created by gathering a blob of molten glass on the blowpipe, dipping this into another colour glass, and blowing them together so that two (or more) layers are created (Whall, 1905). Blue, green and light pink flashed glass (on white or tinted base glasses), as well as blue-and-purple glass, have been reported in medieval windows (e.g. Brill, 1999; Marchesi *et al.*, 2006; Schalm *et al.*, 2007); however, by far the most extensive use of the technique in the medieval period was in the production of ruby red glass. Red glass produced before the medieval period was opaque (see Freestone *et al.*, 2003). The flashing technique enabled the fabrication of translucent red colour through the combination of a very thin red glass layer overlaid a thicker white glass base.

The current understanding is that the precipitation of metallic copper nanoparticles results in the red colour of the glass, the colour resulting from light scattering (Mie scattering) and depending on the size and shape of the nanoparticles (Bamford, 1977; Durán *et al.*, 1984; Farges *et al.*, 2006; Kunicki-Goldfinger *et al.*, 2014b). Up to four types of red flashed glass have been identified (Newton and Davison, 1989; Spitzer-

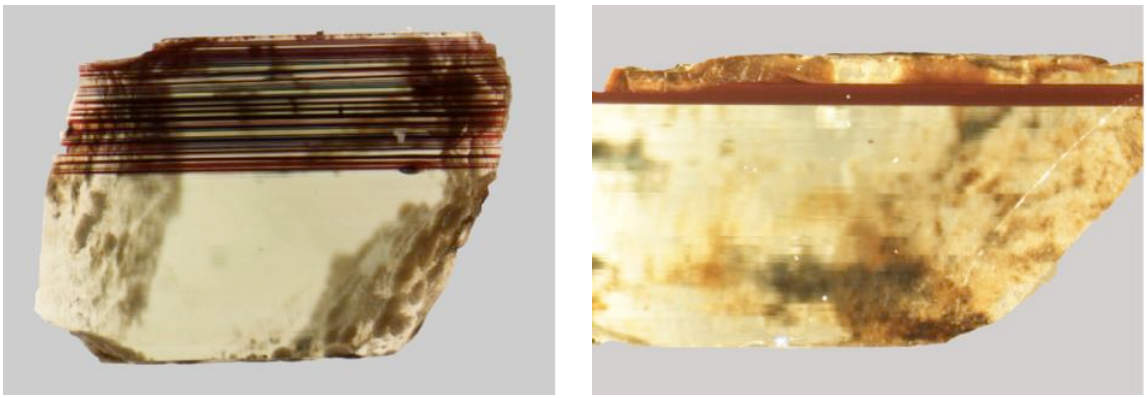

Figure 3.3 Images of red flashed glass in cross-section: on the left, Type A, and on the right, Type B3. Type B2 glasses do not have the thin layer of white on top of the red layer. *Figures 2 and 4 from Kunicki-Goldfinger et al. (2014b).*

Aronson, 1975) but this paper will conform to the typology set out by Kunicki-Goldfinger *et al.* (2014b): Type A, in which the red layer is striated, or composed of numerous thin stripes of alternating red and white glass; and Type B, in which the red layer is more homogeneous and easily distinguished from the white layer(s) (Figure 3.3). These mostly correspond to the feiulleté and plaqué types (Spitzer-Aronson, 1975). Type A glass was made up until the 14th century, while Type B began to be produced from at least the 14th century until the modern day. Type B glass is further subdivided into B-2 (a red flash on a white glass base) and B-3 (in which there is an additional thin white layer of glass overtop the red, see Figure 3.3); the Type A technology was also possible regional, as no Type A red glass has yet been observed in Germany (Kunicki-Goldfinger *et al.*, 2014b).

Both types of red glass were produced by the basic technique described above, but Type A was flashed with a mixture of high and low copper glasses, and Type B with a high copper glass. After forming the glass, it was heat treated, which in Type A resulted in the diffusion of copper between the mixed glasses to form metallic copper at their boundaries, and in Type B simply caused the reduction of Cu^{+} ions to metallic copper through the donation of an electron by other ions such as Fe^{2+} (Kunicki-Goldfinger *et al.*, 2014b).

Visually, many red glasses appear as homogeneous in their colour as any other coloured glass of the period, though a special effect could be achieved with Type A through uneven mixing resulting in a streaky red (Figure 3.4).

No medieval description of the technique survives, as Theophilus' chapter on making red glass is not extant, and Eraclius describes how to make red-coloured glass but makes no mention of flashing (Hawthorne and Smith, 1979; Merrifield, 1967). The

Figure 3.4 Detail of a medieval stained glass panel with different textures achieved using Type A technology. A streaky appearance like this was achieved through the uneven mixing of the copper-rich red striations. Detail from panel 7,8c (Ezekias) from window SXXVIII at Canterbury Cathedral © *Dean and Chapter of Canterbury*

technique had been forgotten by the end of the seventeenth century and became a topic of fascination in the centuries following (Knowles, 1927).

Other types of composite glasses exist and bear mentioning, including striped glass such as those described in a recent paper by Hunault *et al.* (2017a) that are white glasses with stripes of blue, purple and red.

3.4 Possible sources for the GEW glass

Unlike the preceding period, when it is suggested that glass-making was separated into primary and secondary production centres (Freestone *et al.*, 2002), glass was melted and shaped into its final form at the same site in the medieval period (Marks, 1993; Welch, 1997; Willmott, 2005)[10]. Glasshouses were often located in forested areas for direct access to the large quantity of wood needed as fuel and raw materials in making glass (Maitte, 2014; Marks, 1993). The exception is those short-term glasshouses built in association with a large construction project, such as the one at Salisbury Cathedral in the 15th century (Willmott, 2005).

The two primary areas for glass production in England during the medieval period (from the 13th century onwards) were foremost in the Weald and secondarily in Staffordshire (Kenyon, 1967; Thorpe, 1949; Welch, 1997; Willmott, 2005). Although glass produced in the two areas are largely similar in composition, with high magnesia, phosphate and soda contents, subtle differences in manganese concentrations have been noted; the two regions can be distinguished with greater certainty by their isotopic signatures (Meek *et al.*, 2012). Unfortunately, most of the glass found at English kiln sites date to

[10] M. Lillich (1985) argued that in France until the late 13th century, the same craftsmen carried out glass-making and glass-painting. In England, the crafts appear to have been distinct from an early date, as evidenced by the purchase of glass for glazing Westminster Abbey in the 1250s (Marks, 1993), perhaps due to the lack of glass-making expertise in England during the medieval period.

the early 16th century and later; for example, at Little Birches Wolseley, almost no glass was excavated associated with the 14th century furnace (Welch, 1997).

It has been suggested previously that York Minster sourced some of their glass from the Staffordshire glass-making region during the early fifteenth century (Welch, 2003). In the fabric rolls of York Minster, there is a purchase record in the year 1418 (ten years after the completion of the GEW) for white glass from John Glasman of Ruglay (Rugeley) in Staffordshire (Raine, 1859, 37). Unfortunately there are no records specifically pertaining to the sources for the GEW glass, beyond the record in the fabric rolls of 1399 that a supply of white and coloured glass had been set aside for the windows of the choir (Raine, 1859, 18).

Although the Weald has been considered to be the largest glass-making industry in England during the medieval period, archaeological evidence at kiln sites near the River Trent in Staffordshire show intensive activity spanning the late 14th through mid-16th century; this coincides with a dearth of documentary evidence for Weald production, which may indicate an increased reliance on Staffordshire glass during this period (Kenyon, 1967; Linford and Welch, 2002; Welch and Linford, 2005; Willmott, 2005).

English glass was less expensive than glass imported from mainland Europe; it was also not as highly regarded in quality, as illustrated by a mid-15th century contract that directed that no English glass was to be used in the window, only imported glass (Marks, 1993). If English glass-makers supplied any glass to the GEW, they only potentially supplied white window glass. There are no archaeological finds at medieval kiln sites in England to support the production of coloured glass, and furthermore, a 1449 patent to John Utynam, for making coloured glass and for teaching others the practice, suggests that the craft had not yet been mastered in England (Marks, 1993, 30). Therefore, it is generally considered that all the coloured glass in English medieval windows was imported from Europe (Freestone *et al.*, 2010).

The limited documentary evidence available suggests that the two principal areas from which the English sourced their coloured glass were from forested areas surrounding the Rhine and its tributaries, which enabled the transportation of the glass to the coast and from there shipped; and Normandy and those areas surrounding the Seine and its tributaries (Knowles, 1936; Marks, 1993). Norman glass was more expensive, and regarded as higher quality, as the Antwerp guild regulating stained glass window production decreed in 1470 that only high quality Norman glass was to be used by its members (Caen, 2009; Caen *et al.*, 2006). The purchase of both Norman and Rhenish

glass are documented in York during this period, though Rhenish glass might have been more easily available due to the strong trade relations between York/Hull and the German Hanseatic League (Kermode, 1987; Marks, 1993; Nightingale, 2010; Postan, 1987).

3.5 Regional trends in glass composition: Synthesis of previous analytical work on medieval European glass

The regional geology, the availability of different plant species, and differing recipes result in a wide range of compositions found in medieval glass, which opens the possibility that glass can be traced to its region of manufacture based on its major, minor and trace elements. Many publications that have mentioned generalisations of regional composition, however, tend to focus on areas defined by modern-day national borders, and not, for example, regions related to geology or river systems that may cross these borders (the former which affects the composition and the latter being the primary mode of transport), making regional characterisation difficult. For example, Wedepohl (2003) noted that French and English glass are higher in MgO and P_2O_5. Other data (e.g., Wedepohl and Simon, 2010) show that some German glasses have high concentrations of P_2O_5, while a study of French glass compositions (Barrera and Velde, 1989) found high magnesia glass in only some areas of France.

Therefore, to better understand the regional geology, compositional data on glass from the 12th through 15th centuries were examined for regional trends. Only forest glass (including HLLA) was considered; high lead and soda glasses were excluded. Major and minor elemental composition for over 1300 glass samples were analysed using QGIS to study regional distribution, with data taken from 36 sources (Table 3.1). The glass reported in this synthesis include window glass, vessel fragments, and glass production waste, from archaeological sites (production and otherwise) and church windows. The data come from modern day Austria, Belgium, Croatia, Czech Republic, England, France, Germany, Hungary, Italy, Netherlands, Poland, Portugal, Slovakia, Spain, and Switzerland, although the focus will be on the northern European regions. English window glass data were excluded, since the colours are known to be imported from continental Europe; the only English glass included are from archaeological kiln sites.

Table 3.1 Data sources providing city/state, date range and number of analyses. The sources of the data are numbered and correspond to the list on the next page. (continued next page)

City/Site	Century	n	References	City/Site	Century	n	References
Ebriach, Austria (CE)	14	3	27	Marseille/Rougiers, France	12-14	12	4,9
Kremsmunster, Austria (CE)	15	1	21	Montpellier, France	13	2	4
Spitz, Austria (CE)	14	1	27	Saint-Jean-des-Vignes, France	13-16	47	2
St Martin im Muhlkreis, Aust. (CE)	14	5	21	Cologne, Germany (R)	14	31	14, 34
Strassengel, Austria (CE)	14	12	21, 24	Frankfurt/vicinity, Germany (R)	12-15	8	4, 21, 30, 34
Vienna/vicinity, Austria (CE)	12-15	22	4, 21, 22, 24, 27	Freiburg, Germany (R)	13-14	12	4
Raversijde, Belgium (R)	15-16	223	25	Lautenbach, Germany (R)	15	1	4
(Various), Belgium (R)	12-17	135	26	Nuremburg, Germany (R)	14-15	3	4, 32
Dunave, Croatia (CE)	14-15	1	31	Ulm, Germany (R)	14-15	11	3, 4, 21
Bohušov, Czechia (CE)	13-14	1	28	Altenberg/Naumberg, Ger.(CE)	13-15	17	4,14
Brno-stred, Czechia (CE)	13-14	2	28	Augsburg/Munich, Ger. (CE)	14	8	4,14, 21
Chrudim, Czechia (CE)	14-16	1	28	Braunschweig, Germany (CE)	12-13	1	28
Moldava and Most, Czechia (CE)	14-16	12	7, 8	Budapest, Hungary (CE)	14-18	1	13
Olomouc, Czechia (CE)	15	1	7	Erfurt, Germany (CE)	14	7	4
Opava, Czechia (CE)	14-16	2	28	Halberstadt, Germany (CE)	15	2	4
Plasy, Czechia (CE)	14	2	8, 28	Höxter/vicinity, Germany (CE)	11-16	42	4, 8, 29, 34
Prague, Czechia (CE)	13-15	6	8	Jerichow, Germany (CE)	12-16	6	20
Staffordshire, England (W)	13-14	4	35	Leck, Germany (CE)	13	1	21
Weald, England (W)	13-14	19	18	Meissen, Germany (CE)	14	1	30
Amiens, France (W)	13	11	4, 21, 32	Regensburg, Germany (CE)	13-14	4	4
Angers, France (W)	14	5	1	Wienhausen, Germany (CE)	13-15	4	21
Bourges, France (W)	13-15	6	4,15	Florence, Italy	14 -16	5	4
Brittany/Brennilis, France (W)	15	4	4,15	Orvieto, Italy	13-14	1	28
Évron (Mayenne), France (W)	14	1	4	Pavia, Italy	15	33	17
Le Mans, France (W)	13-15	1	21	St. Leonhard in Passeier, Italy	14	1	21
Orleans & Chartres, France (W)	12-16	51	1, 4, 24, 33	Heemskerk, Netherlands (R)	15-16	1	14
Paris/vicinity, France (W)	12-16	213	1, 4, 5,14,15, 21, 32	Zutphen, Netherlands (R)	14 -16	23	14
Poitiers, France (W)	11-12	2	1	Elblag, Poland (CE)	Late medieval	11	12
Provins, France (W)	15	4	15	Grodziec, Poland (CE)	15	13	36
Rouen/vicinity, France (W)	13-16	78	1, 4,15,16, 21, 30, 32	Turuń, Poland (CE)	Medieval	1	12
Tours, France (W)	13-14	3	32, 30	Batalha, Portugal	15-16	9	4
Argonne and Metz, France (R)	14-15	62	1	Bratislava, Slovakia (CE)	13-16	4	28
Châlons-en-Champagne, Fra. (R)	12-15	10	1, 32	Avila, Spain	15	1	19
Reims, France (R)	12	1	4	Barcelona, Spain	14	23	10,11, 23
Troyes/Aube, France (R)	13-16	8	4, 21	Burgos, Spain	13	1	14
Avignon, France	14	10	3, 4	León, Spain	12-15	7	6
Chambaran, France	15	2	1	Palencia, Spain	15	1	19
Digne, France	12-13	5	30	Tarragona, Spain	14	17	10, 23
Léon, France	13-15	23	4	Bern, Switzerland (R)	15	3	4

Table 3.1 (continued from previous page) Some of the data given in the table exceed the range of 12th-15th centuries; these data were assigned a broad date range in the original source but were consistent with typical medieval compositions and therefore included. References, below, correspond to the numbered sources on the previous page.

1 Barrera & Velde 1989
2 Brill & Pongracz 2004
3 Brill 1970
4 Brill 1999
5 Calligaro 2008
6 Carmona *et al.* 2006
7 Cílová & Woitsch 2012
8 Cílová *et al.* 2015
9 Foy 1985
10 Garcia-Vallès *et al.* 2003
11 Gimeno *et al.* 2008
12 Kunicki-Goldfinger *et al.* 2008
13 Kunicki-Goldfinger *et al.* 2013
14 Kunicki-Goldfinger *et al.* 2014
15 Lagabrielle & Velde 2005
16 Lombardo *et al.* 2010
17 Marchesi *et al.* 2006
18 Meek *et al.* 2012
19 Molina *et al.* 2013
20 Muller & Bochynek 1989
21 Newton 1976
22 Newton 1977
23 Piñar *et al.* 2013
24 Pollard 1979
25 Schalm *et al.* 2004
26 Schalm *et al.* 2007
27 Schreiner 1984
28 Sedláčková *et al.* 2014
29 Stephan & Wedepohl 1997
30 Sterpenich & Libourel 2001
31 Topić *et al.* 2016
32 Vassas 1971
33 Velde & Barrera 1986
34 Wedepohl & Simon 2010
35 Welch 1997
36 Wilk *et al.* 2017

Since the data used in this synthesis were from both archaeological production sites and church windows, it was anticipated that there would be considerable overlap in compositions due to trade. Despite this, regions are well distinguished. Maps showing the distribution of compositional characteristics as well as scatterplots show three regions of interest to this study (Figure 3.5 – Figure 3.7): England and north-western France, areas surrounding the Rhine and its tributaries, and central/eastern Europe which includes Germany east of the Rhenish region. Glass from England/NW France are differentiated by higher MgO and Na_2O, and lower CaO, while glass from the eastern region tend to have lower P_2O_5 and Na_2O, and high K_2O. Rhenish glass generally has low MgO and Na_2O and high CaO and P_2O_5; the exception is HLLA glass from this region, which has higher Na_2O.

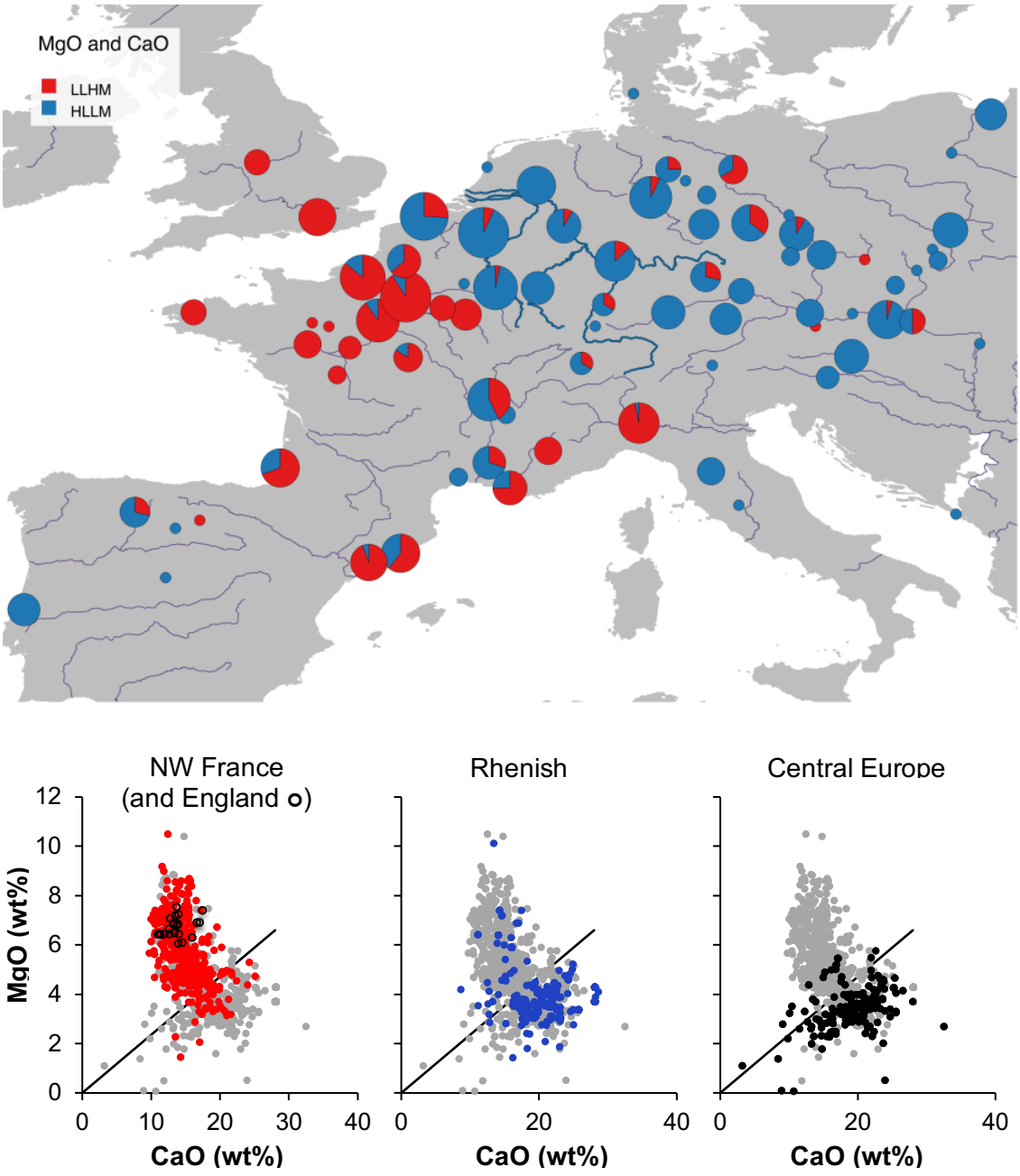

Figure 3.5 Map showing the regional distribution of LLHM and HLLM glasses using a threshold of MgO/CaO=0.24., with scatterplots showing magnesia and lime contents of glass from the three regions The high magnesia type is characteristic of glass found in western and central parts of northern France and England (the latter marked with an open circle, **O**, in the scatterplot).

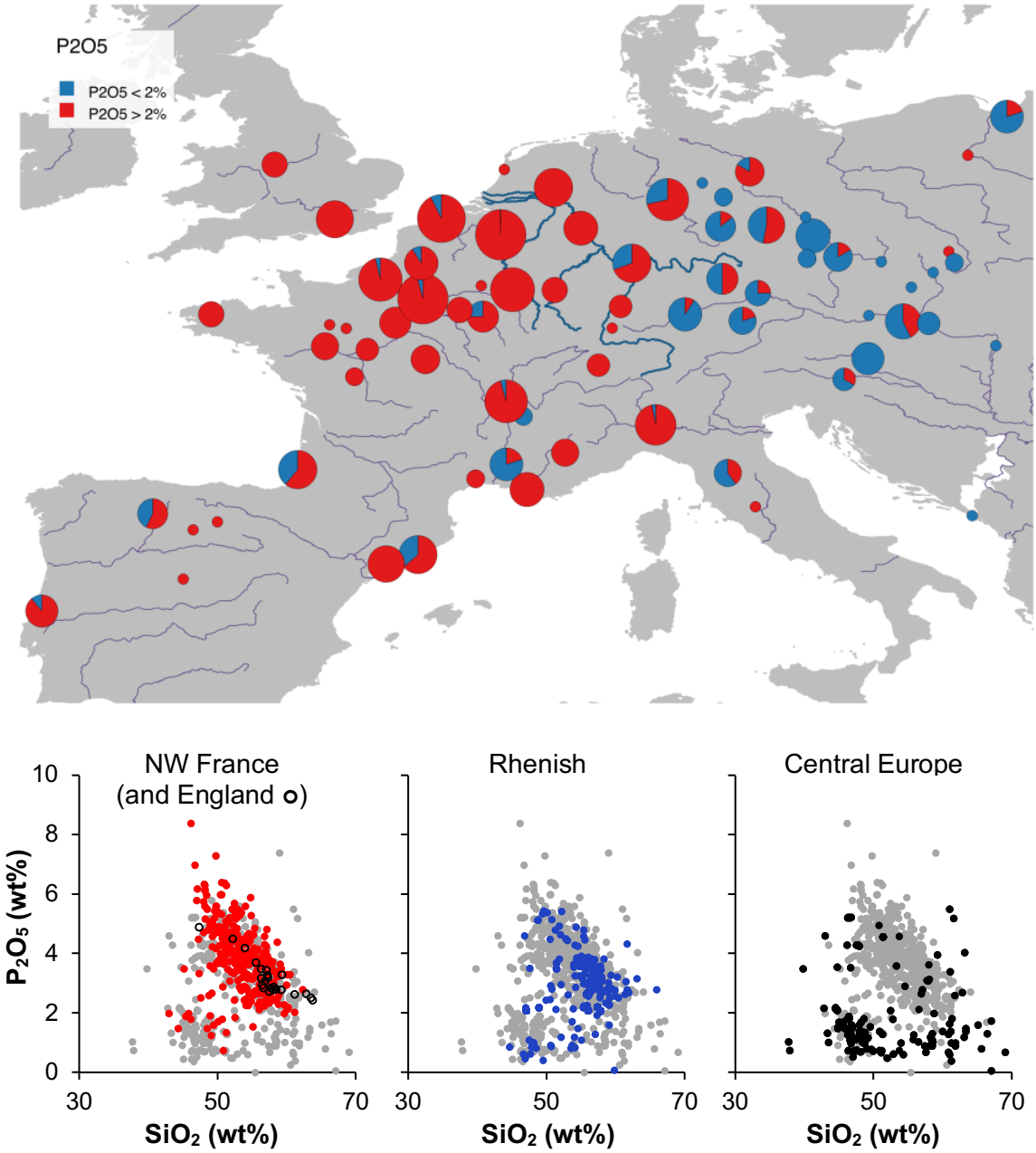

Figure 3.6 Regional distribution of glass with high and low phosphate (threshold at 2% P_2O_5), and scatterplots showing phosphate and silica contents of the three regions The low phosphate type is characteristic of glass found in central Europe, excluding areas near the Rhine and its tributaries.

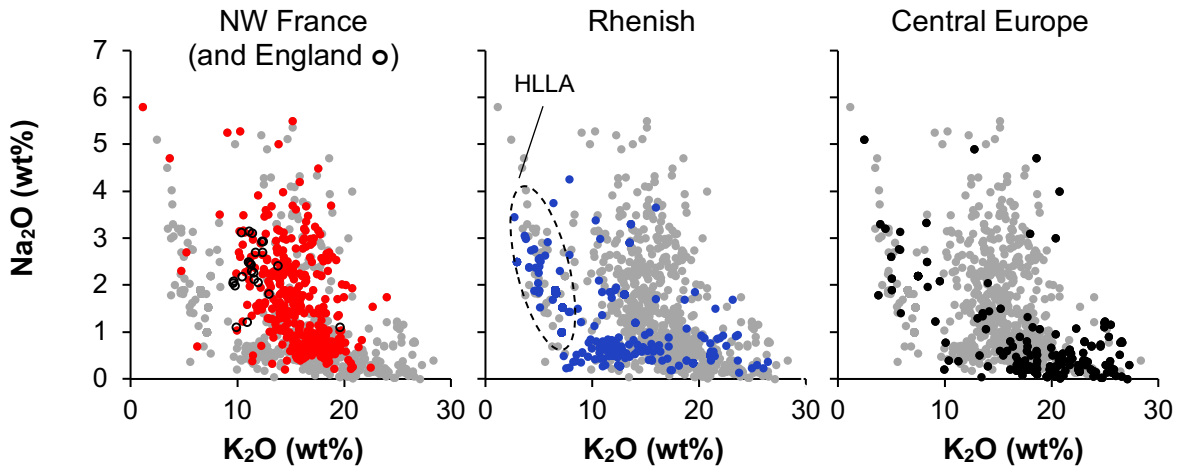

Figure 3.7 Scatterplots showing the soda and potash contents of glass in the three regions.

3.6 The GEW and glass-making technology

The GEW was constructed in the midst of changing glass-making technology on the continent as glass recipes moved towards a HLLA composition, a transition that is still not fully understood. Chemical characterisation of the glass in the GEW has the potential to further our understanding of this technological change, as well as other technological topics related to medieval glass-making such as colour generation. Further, synthesis of previous analytical work for regional characterisation of European glass from this period may allow identification of (regional) sources for the coloured window glass.

The probable/possible English source of the white glass in the window also presents an opportunity to illuminate our knowledge of English glass-making technology, for which most of the surviving evidence dates to a later period. The glass will be compared to Staffordshire glass, as well as available data on both Staffordshire and Wealden glass (Meek *et al.*, 2012; Welch, 1997), in chemical composition and in isotopic composition in order to suggest a regional provenance and to examine the English glass-making technology at the end of the 14th century.

CHAPTER 4

Medieval glass-painting

The later medieval period in Europe was a time of increasing populations and urbanisation, plague and famine, warfare and social upheaval – but also a time in which art, craft and technology thrived (Haskins, 1927; White, 1972). The guild system grew around the flourishing craft technology and production as an institution to protect and support its members, practitioners of that craft. Although the medieval guild system is contentious – did it foster technological creativity and progress? or stifle it? – it is recognised as a significant development in the economic history of the Western world, and the medieval economy, of which it was an aspect, as the predecessor to the modern economies of the West (Epstein, 2009).

The surge in the construction of ecclesiastical buildings that brought such an enormous demand for window glass (as discussed in the previous chapter) and the greater capacity for specialisation in craft technology during this period also saw increased specialisation in the making of stained glass windows. In an earlier period, glaziers were craftsmen who both made the glass as well as created windows (Lillich, 1985), but by this period, glass-painters practiced a separate craft requiring highly specialised skills, often organised within a guild organisation. At the intersection of art and craft, medieval glass-painting presents an interesting opportunity to marry the fields of art history with an archaeology-based technological approach. A monumental window such as the GEW provides a rare and significant opportunity to gain a detailed insight into the organisation of production within the workshop that created it.

4.1 Medieval treatises on glass-painting

The technical steps and tools used in the art of making stained glass windows were described in detail by Theophilus in his second book of *De Diversis Artibus* (2:17-2:28, trans. Hawthorne and Smith, 1979; see also Figure 3.1). However, it should be emphasised that Theophilus, although intimately acquainted with the details of the technology he describes, seems to have been unconcerned with issues of production on a larger scale such as time- and resource-efficient practices, the organisation of production, or the management of a workshop responsible for large-scale projects.

First, Theophilus describes the preparation of a glazing table with chalk, upon which an exact, life-sized image of the panel (the cartoon) was drawn upon it, including indications of glass colour and the outlines where strips of lead (cames) would hold the glass pieces together. Pieces of glass of various colours were cut according to the drawing using a hot iron cutting tool. The hot end of the iron was drawn along the glass surface, causing a crack that would follow the tool's path and allowing a clean break. The use of a diamond for cutting glass is referenced as early as the latter part of the 14th century, in the treatise by Antonio da Pisa (Bugslag, 1998). After cutting, a tool called a grozing iron was used to chip away at the glass until the exact shape was achieved, with rounded edges.

Theophilus then described the preparation of the pigment, a mixture of ground copper (or iron - Marks, 1993) oxide and specific types of ground glass with a binder of wine or urine. The paint was then applied with a brush. He describes how to create different shades, and the technique of scratching away dried pigment with the brush handle to create inscriptions, shadows, or backgrounds like the *rinceau* found in the GEW (Figure 4.1).

The pigment is then fired onto the glass; Theophilus describes how to build the appropriate kiln and where to lay the different colours so that they don't discolour in the kiln. The glass is heated to a degree hot enough to allow the pigment to melt and fuse

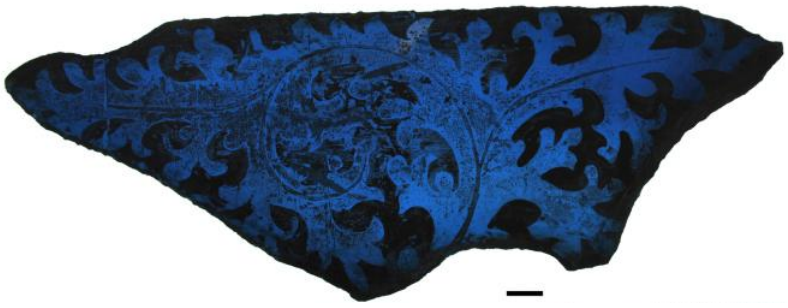

Figure 4.1 An example of *rinceau*, a design used frequently in the GEW, painted on blue or red glass for the background of many panels. Scale bar is 1 cm. *(GEW 15g-B7)*

with the softened glass surface, but not enough that the glass re-melts and loses its shape.

The glass pieces are fitted together with lead strips, called cames, which are cast using a prepared iron mould; the shape of the cast cames in cross-section is like a capital "H". The mould is heated, closed and encased in a wooden holder, and molten lead poured inside.

According to Theophilus, the assembly of a panel began in one corner. The flexible lead cames are bent around a piece of glass, which is held tightly in place using nails struck into the table all around the glass piece. When the next piece is ready to be added, a nail is removed and the piece fitted into place in the lead came, and held into place with further nails. After the panel is fitted together in this way, the lead cames are soldered together at the joins using a tin solder and a hot iron on both sides of the panel.

After Theophilus' time, there emerged an additional technology called yellow silver staining, which was described in the treatise by Antonio da Pisa in the late 14th century (Moretti and Hreglich, 2013) and is first observed in windows around the same time (Heaton, 1947). Silver stain is a cementation technology in which a silver compound dispersed in a carrier medium such as clay or ochre is applied and fired onto the surface of the glass at a temperature below the softening point. The colour achieved by this process can vary widely, from gold to brownish orange (Figure 4.2), and depends on

Figure 4.2 Detail from the GEW, showing different shades of yellow/orange silver stain. Detail of panel 10e of the GEW. © *The York Glaziers Trust with the kind permission of The Chapter of York*

numerous factors, including the duration and temperature of the firing, and the composition of the raw materials used for the silver stain (Jembrih-Simbürger *et al.*, 2002; Molina *et al.*, 2013; Zhang *et al.*, 2007); this process will be described in greater detail in the next chapter (Chapter 5).

The above sequence would often result in multiple firings - one to apply the major details and lines, another to add shading, and possibly an additional to add the yellow stain.

Aside from the use of modern tools such as light boxes, electric soldering irons, and diamond glass cutting tools, much of the above remains the same to the present day, with the exception that from about the 16th century, cement or putty was pushed underneath the lead cames (after the panel was soldered together) in order to securely fix the glass in place and make the panel wind- and waterproof (Caen *et al.*, 2006; Cortés Pizano, 2000).

4.2 Cartoons and glazing tables

The drawing out of the cartoon was of utmost importance; so much so that in Italy, the designer of a window was usually a prominent artist who was distinct from the craftsmen who painted the glass (Burnam, 1988). However in northern parts of Europe, glass-painters were artists in their own right, although there are known exceptions in which a separate artist supplied a window's design (Ramsay, 1987). Still, evidence including the contract for the GEW, which dictated that Thornton was to draw the cartoons himself, suggests that the most skilled artists in the workshop would be entrusted with the task. According to Theophilus' description, the cartoon drawn on the glazing table was highly detailed; this practice would then reduce the craftsmen who painted the glass to copyists. However, the discovery of a glazier's table in Girona, dating to the 14th century, paints a different picture (Brown, 2014a): the markings are minimal, little more than cut lines (Figure 4.3), leaving more up to the creativity of the glass-painter. Glazing tables were washed and reused, as evidenced by examination of the Girona table as well as documentary records showing the purchase of beer for the purpose (Brown, 2014a; Santolaria Tura, 2014).

The glazing table was gradually replaced by paper, which was being used in Italy by the latter part of the 14th century, but is not recorded in England until 1443, when it was used together with tables at Westminster (Brown, 2014b, 25; Marks, 1993, 34). Paper cartoons are not recorded in York until 1503, and it is currently suggested that the GEW was produced using glazing tables (Brown, 2014b, 26). The use of paper was an enormously important transition, as it could be reserved and used again for other windows, and

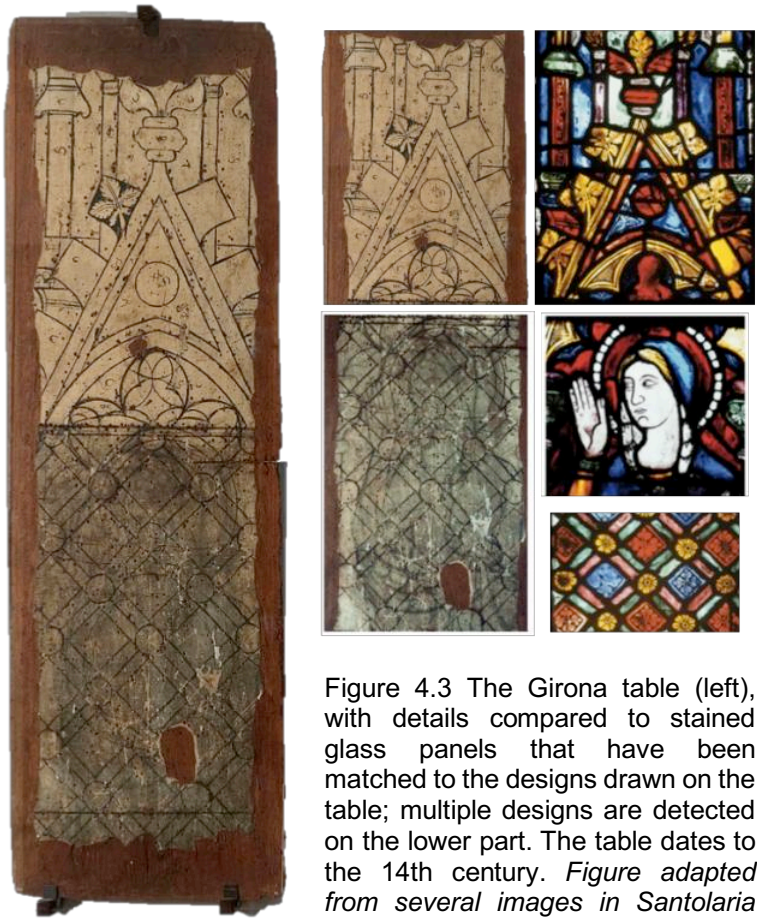

Figure 4.3 The Girona table (left), with details compared to stained glass panels that have been matched to the designs drawn on the table; multiple designs are detected on the lower part. The table dates to the 14th century. *Figure adapted from several images in Santolaria Tura (2014).*

passed down through generations. Conversely, the use of glazing tables would bring with it particular demands on the practical operation of a busy workshop (Brown, 2014b).

4.3 Medieval craft guilds and glass-painting

The art and craft of glass-painting in major centres such as York was carried out within the framework of the medieval guild; ordinances of the York Glaziers guild survive from circa 1380 and from 1463-4 (Brown and O'Connor, 1991; Knowles, 1936; Marks, 1993). The role and purpose of craft guilds in medieval society have been portrayed in a very negative light since the eighteenth century as an institution in opposition to economic and technological progress (e.g., Adam Smith's Wealth of Nations, 1776; for a history of the scholarship, see Richardson, 2001). In more recent years, economic historians sought to re-evaluate this position and examine the guild system within its economic, political, and technological contexts, arguing that craft guilds were instrumental in creating an environment that supported technological innovation (Epstein and Prak, 2008), ensured high quality craftsmanship (Caen *et al.*, 2006), encouraged the development and flourishing of the arts (Prak, 2008), protected and ensured the transfer of technical knowledge through apprenticeship (Croix *et al.*, 2015; Epstein, 1998), and

otherwise was highly beneficial to its members (Richardson, 2001), while another argues that medieval guilds in England had very little impact on the economy (Swanson, 1988).

The high demand for specialised and skilled labour after the devastation of the Black Death (1347-1351, Gottfried, 2010) resulted in higher wages for skilled workers, due not only to the labour shortage but also lobbying by guilds and journeymen associations (Lis and Soly, 1994); more and more people invested in apprenticeship and guild membership (Britnell, 2000). Although guild membership was not compulsory for a craftsmen in any trade, the numerous benefits provided compelling incentives to join (Richardson, 2001). Among these were the sharing of risks and costs, the negotiation of contracts both for the acquisition of raw materials and for sale of the final product, and the provision of a brand name and reputation.

A study of guild ordinances related to the glass-painting craft in the 16th-18th century Netherlands found that a primary concern implied by the regulations were for quality control and quality assurance (Caen *et al.*, 2006). These regulations included restrictions on glass sources (i.e., only allowing the use of high quality glass), a demand that the glass should be fitted snugly into the cames so that they do not rattle, and instructions on what technology was acceptable in the making of lead cames. The guild could further ensure quality control in other ways; in the ordinances of the York glass-painting guild of c. 1380, it was dictated that stained glass commissions above a certain value had to be inspected before being exported out of the city (Knowles, 1936). Regulations such as these protected the craft and the customer, and elevated the brand name to the benefit of all the guild's members.

The regulation of apprenticeship was a core function and purpose of the craft guild (Epstein, 1998), which could offer incentives to both the master and apprentice while also ensuring that neither took advantage of the other. A model for technological progress in pre-industrial economies showed that the regulation of the master-apprentice relationship by the guild supported technological progress by providing a larger network of craftsmen, and therefore a larger body of technical knowledge upon which to build and innovate (Croix *et al.*, 2015). The long term of an apprenticeship (in England, the Statute of Apprentices of 1563 dictated that apprenticeships should last seven years; Knoop and Jones, 1932) helped to offset the costs of training to the master craftsmen through the low cost labour of the apprentice towards the end of that period, and there were fees associated with leaving an apprenticeship early (Epstein, 1998). The apprentice was also protected from the opportunism of the master, via regulations ensuring proper training, and through ordinances such as those of the York Glaziers guild in 1463-4, which forbade master glass-painters from taking a second apprentice until the first had

completed at least four years of training (Epstein, 1998; Knowles, 1936; Marks, 1993; Sellers, 1912). This would prevent master craftsmen running workshops on the backs of cheap, low-skilled labour, and in turn helped to protect the integrity of the craft.

After the successful completion of an apprenticeship, the craftsman would enter a period during which he would move, sometimes to foreign countries, to work with and learn from others masters, before he would be considered a fully trained craftsman (Bednarski and Courtemanche, 2009; Harvey, 1972; Knowles, 1936). Alternatively, he might continue working in the workshop where he was apprenticed (Thomas, 1995). As a fully skilled craftsman, called a journeyman, he would work for a daily rate, an employee for a master's workshop, and many craftsmen continued in this status for the rest of their career (Lis and Soly, 1994). Journeymen sometimes had their own associations and considered themselves the equals of master craftsmen; this was particularly true of crafts where a flexible supply of labour was required (Lis and Soly, 1994). Their mobility is thought to have been a major contributor to the circulation of technical knowledge (Reith, 2008).

Eventually, a craftsman might apply to become a master of the craft, which would allow him to set up shop for himself. This status usually had to be approved by the guild on examination of a submitted piece of work, which was set by the guild, such as a small panel with a specific design that would test various skills and techniques (Brown and O'Connor, 1991; Caen *et al.*, 2006). The earliest references to the master's test[11] date to the late 15th century (Caen *et al.*, 2006), but there is no explicit evidence of this practice in England (Harvey, 1972).

Medieval glass-painting workshops are thought to have been quite small, consisting of a master glass-painter with a couple apprentices, journeymen, and/or servants; a letter of patent from Durham towards the end of the 15th century restricts a glass-painter's workshop to three to four men (Brown and O'Connor, 1991; Marks, 1993). The ordinances of the York glass-painting guild in 1363-4 indicate that there were eight firms or workshops in York at the time (Knowles, 1936). Although there are records of glass-painters resident in York at the time the GEW was created, it is thought that they were unsuited for designing the largest expanse of medieval stained glass in the country,

[11] The work of art submitted for promotion to master status was also called a *masterpiece*. However, modern usage of the word means *magnus opus* or the best, most significant work an artist creates in his career. The reference to the GEW being Thornton's masterpiece (e.g., Marks, 1993, 180) is in the modern meaning of the word.

forcing the Dean and Chapter to look as far as the Midlands for their master glass-painter (Brown, 2018, 2014b; French, 2003; Knowles, 1936, 1922; Marks, 1993).

The small size of the typical glass-painting workshop may not have applied to the production of the GEW. A financial record pertaining to another glazing campaign in Westminster (dated 1351) refers to the employment of 33 craftsmen (Marks, 1993, 44). Collaboration between two workshops for the fulfilment of large projects is documented during this period (Brown and O'Connor, 1991; Marks, 1993), and is practical in light of the inconstant, fluctuating demand for this work. The contract for the GEW does not record the number of workmen but states that Thornton was in charge of gathering them, probably in addition to his existing workshop in Coventry (Brown and O'Connor, 1991; French, 2003); the project may have attracted itinerant journeymen from other parts of the country.

There is limited documentary evidence for the organisation of labour within the workshop. The financial records previously mentioned, in which 33 craftsmen were employed for a large glazing project for St. Stephen's Chapel at Westminster in 1351, lists the craftsmen by the task they were employed to do, with their pay adjusted accordingly (Marks, 1993, 44). Six master glaziers designed the panels and drew the cartoons on the glazing tables, eleven glaziers painted the glass, fourteen glaziers and two assistants cut and fit the glass. However, this project was exceptional for its size, and this degree of specialisation is unlikely in most other circumstances due to the small size of most workshops (Marks, 1993).

4.4 Workshop practice

In the absence of textual evidence, the study of glass-painting workshops has by necessity been confined largely to stylistic analysis of windows. This pursuit has traditionally focused on the identification of an atelier or school through observed stylistic and iconographical similarities, often in windows of different cities suggesting that ateliers were extremely mobile (Caviness, 1990; Grodecki, 1948; Raguin, 1976). The latter interpretation can be faulted in that it minimises the role of itinerant journeymen in the dissemination of technique and style, and neglects to acknowledge the availability of stained glass to public view, enabling craftsmen to visit churches and cathedrals in other cities to study, and probably sketch, the stained glass (Caviness, 1990; Reith, 2008). At the same time, glass-painters were at the mercy of fluctuating demand, like other artists and craftsmen associated with building works, and in the early medieval period before the craft was organised in and advanced by the guild system, some degree of mobility was probably necessary (Knoop and Jones, 1932; Prak, 2008; Thomas, 1995).

Successful studies which have penetrated into the organisation of production within the workshop have set out to determine whether, for example, a single craftsmen designed an entire glazing programme including drawing the cartoons, and other painters carried out the work; or if multiple craftsmen worked semi-autonomously although with a common vision and using a common repertoire of forms and style; or if glass-painters (working in different styles) would be brought in from elsewhere to meet an unusual level of demand (Caviness, 1981; Frodl-Kraft, 1985). One model for the organisation of a glass-painting workshop is that work was divided according to the skills of individual craftsmen; for example, that the most skilled craftsmen would work on figures while the lesser skilled craftsmen might work on border motifs and architectural canopies. However, as put by Eva Frodl-Kraft, "this type of technical division of labor cannot be proven from extant intact windows [through stylistic analysis], for the production of ornament relied on traditional formulas and its execution did not require – in fact precluded – individual artistic expression" (Frodl-Kraft, 1985, 108).

To impose the identity of master or apprentice on different hands identified in a glazing programme inevitably introduces some assumptions, as described by art historian Michael Cothren:

> ...we initially assume that there was a hierarchy of skilled labor - masters and apprentices and assistants of various sorts - in early medieval shops. Then we assign to the masters those portions of a glazing, window or panel that we judge to be highest in quality or narrative significance, such as the prominent parts of figural compositions. Areas we consider marginal or substandard in execution, such as minor figures or ornamental borders and backgrounds, we consign to the work of assistants of apprentices.
>
> (Cothren, 1999, 118)

Cothren was speaking of assumptions made about early medieval craft, for which there is less documentary evidence regarding workshop organisation, and suggests that we may be projecting backwards from the late medieval or Renaissance workshops for which there is more evidence. Other differences related to this craft have been detected for the early medieval period; for example, as noted earlier (footnote 10, page 57), it has also been suggested that early glaziers were responsible for both making glass and painting it (Lillich, 1985). In essence, however, Cothren's caution is entirely relevant. Although in the later medieval period, there is more contemporary documentation that workshops were organised around a hierarchy of skill, visual cues such as relative skill required to paint different parts of a panel are sometimes used to attribute parts of panels to apprentices and to support the division of tasks based on technical skill, thus

reinforcing our existing concepts of apprenticeship in the medieval craft workshop (see also Brown and O'Connor, 1991, 15). For example, an often ignored possible model of workshop organisation is that craftsmen focused on any of the many and varied skills required to make a stained glass window, from making and joining the lead cames, to sizing the glazing tables and panels to the window cavity, to cutting the glass, to the preparation of the pigment, to firing the glass in a kiln (Caviness, 1990).

4.5 A multidisciplinary approach

From a modern perspective, the production of stained glass windows could be viewed as existing in the crossing between art and craft. This distinction may not have been recognised in the medieval period; it is argued that the distinction was not fully made until the late 18th century when the creation of the Royal Academy differentiated between the "fine" arts and other crafts (Williams, 1976, in Ingold, 2001). Cennini's account of making stained glass windows, however, suggests this distinction was made earlier:

> It is true that this occupation [of glass-painting] is not much practiced by our profession [painters/artists], and is practiced more by those who make a business of it. And ordinarily those masters who do the work possess more skill than draftsmanship, and they are almost forced to turn, for help on the drawing, to someone who possesses finished draftsmanship, that is, to one of all-round, good ability.
>
> (Thompson, 1960, 111)

The distinction between skill (the glass-painter) and draughtsmanship (the artist/designer) correlate to the distinction between technology and art discussed by Ingold (2001). The separate and disparate roles of the glass-painter and designer that was prevalent in Italy (for example, see Thompson, 2014) has been connected to the earlier and predominant use of paper in that area, as mentioned previously (Santolaria Tura, 2014). The use of paper transformed the role of the master glass-painter, as paper allowed a cartoon to be drawn by another artist, rolled up and transported to a glazing workshop, where it could be translated to glass by a craftsman with technical skill; furthermore, it could be stored and reused for future windows. There are documented examples of glass-painters bequeathing their cartoons to their apprentices upon their death (Brown and O'Connor, 1991; Marks, 1993).

The marriage of artistry with technical skill in stained glass window production means that, although stained glass windows have traditionally been studied with more art historical approaches based on the visual and stylistic analysis of the painted work, it is also appropriate to use a technological approach derived from anthropology and

archaeology, with reference to the frameworks of *chaîne opèratoire* and technological choice. The *chaîne opèratoire* approach is the reconstruction of the technical steps involved in the transformation of raw materials in to a final product (Leroi-Gourhan, 1964; Sellet, 1993). In more recent years, this approach has been transformed and enriched by the concept of technological choice, in which both the technical steps and the technological choices involved in material production are studied within their cultural, political, economic, environmental and ideological contexts (Jones, 2004; Sillar and Tite, 2000). Technological choices are made related to the selection of raw materials, the use of different tools, the use of one technique over another, as well as the sequence of steps (Sillar and Tite, 2000). This approach not only allows researchers to connect technological studies to social or cultural meaning, but also provides a framework within which to interpret the results: in the present research, for example, it will allow the historical framework regarding medieval guilds to inform the interpretation of the compositional results.

This is also a useful and popular approach underpinning pedagogical studies in archaeology (e.g., Tehrani and Riede, 2008), particularly if we employ the concept of the individual craftsman as a tool (Mauss, 1979, in Crown, 2014). Apprenticeship is closely tied to craft production in the medieval system, as it not only ensures the continuation of the craft through transmission of knowledge to the next generation, but it is also a valuable yet inexpensive source of skilled labour. The costs of training an apprentice were offset by the long term of the apprenticeship, which ensured the master was repaid through low-cost skilled labour and which was an incentive for the master to take apprentices. The value of an apprentice's labour is evidenced by the ordinance of the York glass-painters guild that restricted how many apprentices one craftsman could have. Therefore, the medieval master running a successful crafts workshop must have balanced the demands of the project, the learning needs of the apprentices, and the management of varied skill levels in the workshop.

Learning is of key importance to the study of technology and past societies. Learning is socially and culturally embedded, and intrinsically tied to identity (Budden, 2008; Crown, 2014; Wenger, 1998). In the medieval guild system, apprenticeship took place during adolescence, with the child learning to be an adult and full participant in his society under the tutelage of his master, who was given the rights and privileges of a father (Bednarski and Courtemanche, 2009; Reyerson, 1992). Technologically speaking, different styles of learning or apprenticeship have a direct impact on how well technology is passed on, and what degree of conservatism or innovation are fostered in the next generation of craftsmen (Wallaert-Pêtre, 2001). Pedagogical studies are often based on ethnography

(e.g., Gamble, 2001; see also Tehrani and Riede, 2008). Evidence of learning in archaeology is often identified by the presence of irregular forms or designs, which are attributed to learners (Minar and Crown, 2001). Greater skill is characterised by greater regularity, as a result of repetition and practice leading to brain's automatic processing of specific motor tasks, as well as the use of specialised tools that increase efficiency and regularity (Bleed, 2008; Schneider and Fisk, 1983, in Minar and Crown, 2001). Although the reasoning is embedded in evidence, this approach can still result in circular arguments (like Cothren's description of stylistic analysis of art, above), as the work of learners is identified through their irregularity, and then the irregularity is studied as the work of learners. A more robust approach is that employed by Kamp (2001; 1999), who measured fingerprints on objects to argue that children (learners) had made certain pots, thereby using an independent line of evidence to identify the work of learners and then interpreting their work within the framework of pedagogy and childhood.

In this research, a chemical analysis approach will be used as an independent line of evidence to identify the work of different craftsmen, by relying on the identification of batches of glass. The batch is all of the artefacts made from a single working pot of molten glass; the origin of glass as a fluid melt results in the contents of each working pot having a relatively homogeneous composition, especially if stirred while molten (Freestone *et al.*, 2009; Price *et al.*, 2005). The limited control over raw materials and recipes in traditional methods of glass-making mean that, in theory, individual batches of glass can be identified by their chemical composition. Topping up the mixture with more raw materials or cullet, or melting a new pot of glass although following the same basic recipe, will result in a distinct chemical composition that can be measured (Figure 4.4). The size of a batch depends on several factors, including the size of the working pot, whether or not the glassmakers topped up the pot frequently, the amount of waste, and also the degree to which the pot's contents were actually homogenised (e.g., Freestone *et al.*, 2015b). To suggest that different glass objects are from the same batch, all elements analysed must be identical within experimental error (Freestone *et al.*, 2009), although high standardisation of working practices and raw materials have the potential to obscure the identification of a batch through this method.

Recent studies on both ancient glass (Freestone *et al.*, 2015a, 2015b, 2009; Price *et al.*, 2005) and metalwork (which also originates as a fluid melt; Martinón-Torres *et al.*, 2012; Martinón-Torres and Uribe-Villegas, 2015) have demonstrated the value of the concept of the batch in addressing questions related to the organisation of production. Examples include the reconstruction of the sequence of firing events, or the "life" of a furnace, at a glass-making workshop (Freestone *et al.*, 2015a) and the identification of a cellular

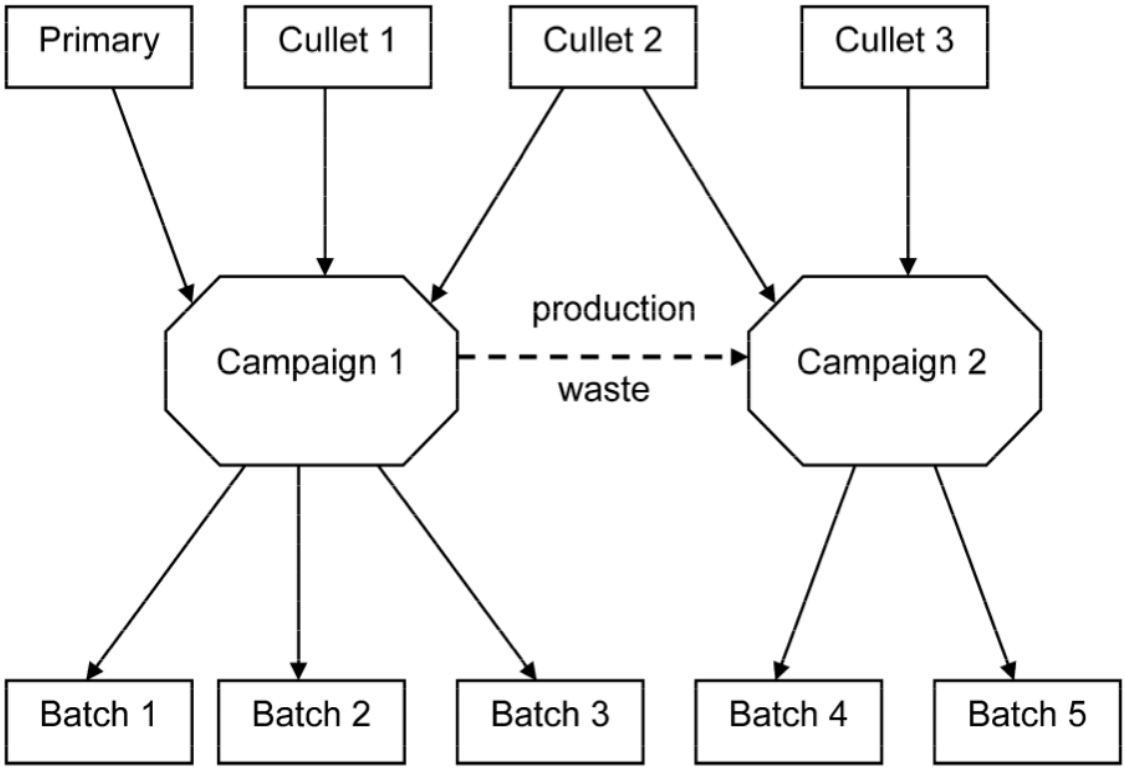

Figure 4.4 Illustration showing batches of glass are made, based on the primary/secondary workshop set up typical of the natron glass-making tradition; here, a secondary workshop melts chunks of glass from a primary workshop together with cullet (Figure 3 from Freestone, Price and Cartwright, 2009).

model of production in the making of the weapons for the Terracotta Army (Martinón-Torres *et al.*, 2012).

As in the latter aforementioned study, this research will involve the definition of models for the spatial distribution of batches under different possible production modes for the division and assignation of tasks, that are based loosely on concepts borrowed from automobile manufacturing. For example, if different workers were assigned to the tasks of cutting glass and painting (similar to an assembly line approach), a different distribution of glass sheets in a panel is expected than if different craftsmen were responsible for different parts of the panel, both cutting and painting the glass. The spatial distribution of batches, therefore, will enable the identification of the work of separate individuals within a single panel, and their status as an apprentice or master will be interpreted with respect to visual evidence and within the context of medieval guilds and craft workshop practice.

CHAPTER 5

Problems and possibilities in using handheld pXRF to study medieval stained glass windows

Chemical analysis of a medieval stained glass window such as the GEW can be used to study and understand key aspects related to the technology involved in producing such a window, in particular the crafts of glass-making and glass-painting. A well-dated window with minimal historical interventions presents an uncommon opportunity in the study of past technologies because it represents the output of glass-making and glass-painting workshops over an extended period of time; unlike the more common situation faced by archaeologists, in which the products of workshops are widely dispersed to consumers, often becoming disconnected from a precise production context. The same trait that preserves this context of a window, however, also prohibits its sampling for analysis; the removal of a window from the walls of our cathedrals and churches is an expensive and infrequent undertaking, and even when this occurs, the glass pieces are not always removed from their lead cames. If in situ techniques can be applied, it would be very valuable to this field of study.

Handheld pXRF is a popular technique in archaeology. The primary benefits are its capability for *in situ* analysis, the high speed of analysis, and the relatively low cost of the machine. Restrictions on invasive sampling are commonplace, as curators and conservators seek to protect an object's physical integrity; pXRF can be used directly on the surface of the object and requires no sampling. It can be transported to the object, bypassing regulations on exporting objects and samples, and can be used in the field on excavation. The speed of analysis allows the examination of hundreds of samples in a relatively short period of time. As a result of these advantages, the technique is used around the world on a range of archaeological materials (e.g.,

Dungworth, 2012a; Gabler, 2017; Janssens *et al.*, 2016; Koleini *et al.*, 2017; Martinón-Torres *et al.*, 2012; O'Grady and Hurst, 2011; Roxburgh *et al.*, 2018; Tykot, 2016). For stained glass, pXRF has enormous potential as it can allow analysis despite the window's architectural context, and furthermore allows analysis of a large area across the window, meaning a more comprehensive study of a window's life history may be conducted.

However, there are many limitations inherent in the technique, and pXRF should only be used with a thorough understanding of the technology and the material to be analysed (Frahm and Doonan, 2013; Scott *et al.*, 2012). Therefore, this chapter will provide an overview of the basic principles behind XRF analysis, address practical considerations in the instrumentation and analytical settings, review relevant archaeological applications for this technique in particular the English Heritage Historic Window Glass project (Dungworth, 2012b, 2012a), and identify the key obstacles anticipated in the analysis of medieval stained glass windows.

5.1 An introduction to handheld pXRF

5.1.2 The basic principles behind XRF analysis

Table 5.1 Characteristic x-ray emission lines, and the orbital transition they represent

Emission line	Orbital transition
$K_{\alpha1}$	$L_3 \rightarrow K$
$K_{\alpha2}$	$L_2 \rightarrow K$
$K_{\beta1}$	$M_3 \rightarrow K$
$K_{\beta2}$	$M_2 \rightarrow K$
$L_{\alpha1}$	$M_3 \rightarrow L$
$L_{\alpha2}$	$M_2 \rightarrow L$
$L_{\beta1}$	$N_3 \rightarrow L$
$L_{\beta2}$	$N_2 \rightarrow L$

X-rays are electromagnetic radiation with short wavelength and high energy, produced by electron transitions from states of higher to lower energy between the inner-most orbitals or shells within heavier atoms. Instruments using x-ray fluorescence (XRF) for compositional analysis do so by irradiating the sample material with an x-ray beam (the primary radiation), creating vacancies in the inner electron orbitals of the atoms within the sample material. Once a vacancy is created, an electron from an outer orbital moves to fill that position, an event which generates secondary radiation characteristic of the element. The fluoresced x-ray is characteristic of the particular transition (from one orbital to another) within an atom of a specific element; moreover, when the higher energy electron vacates a space in order to fill the inner electron space, this leaves another vacancy that must be filled, creating another transition and characteristic x-ray. Therefore, there may be numerous characteristic x-rays specific to any one element (Table 5.1). The detection of these characteristic x-rays allow the instrument to identify which elements are

present and, through quantification calculations, in what concentrations (Jenkins, 1999; Pollard *et al.*, 2007).

5.1.3 Handheld (portable) XRF: Practical considerations

Recent years have seen the development of portable, handheld spectrometers capable of XRF analysis. The term "portable XRF" or "pXRF" can refer to a range of systems, from large machines on wheels that can be moved into galleries, to portable benchtop systems, to lightweight handheld devices; while some have adopted various acronyms to more specifically denote the handheld variety (including "hXRF", "HHXRF", "HHpXRF" or "HH-XRF"), "pXRF" remains the most widespread and recognised term to indicate handheld XRF spectrometers. Therefore the terms "pXRF" or "handheld pXRF" (albeit somewhat redundant) will be used here.

Handheld pXRF spectrometers are designed to be used directly on the surface of the sample material and to produce rapid results. The consequence of the design, however, is that (1) due to the lack of a vacuum during analysis, light elements such as sodium cannot be measured, and (2) due to the lack of sample preparation, the material itself can present problems for analysis; for example, the sample may not be flat, homogeneous or free from surface corrosion, and/or the x-rays may pass unpredictable distances through the sample, meaning that the quantification corrections may not be valid.

There is a range of instrumentation available, with a variety of settings that can be selected to optimise analysis of different materials. The full range will not be detailed here, as the information can be found in any XRF textbook or handbook (Jenkins, 1999; Potts *et al.*, 2001). The following details regarding the sample, instrumental settings, and quantification of the data are ones that the typical analyst should be aware of before planning an analytical programme.

5.1.3.1 The sample material

Sample composition (matrix). The sample matrix can have a major effect on the resulting measurements, and should determine the analyst's selection of analytical settings and the type of quantification used. The elements of interest should be identified, as well as the sensitivity required to address the research question(s), as pXRF performance will vary from element to element (Hall *et al.*, 2014). Furthermore, the sample should be horizontally and vertically homogeneous if the results are to be representative, otherwise the results may be characteristic of some combination of stratified layers or influenced by corrosion or paint layers. The presence of corrosion

can prevent the use of pXRF for the characterisation of the bulk composition, but the technique can still be used in some cases to provide useful information (Nørgaard, 2017).

Sample thickness. Samples that are not of an adequate thickness ("infinite thickness") may require corrections (Sitko, 2009). The "infinite thickness" of a sample is the minimum thickness required for the sample material to absorb all of the primary radiation and to emit the characteristic x-rays of the elements within the sample; it therefore must be at least as thick as the maximum critical depth of the elements analysed. The critical depth is the depth from which 99% of the fluorescent x-rays are emitted, and depends upon the energy of the primary radiation, the geometry of the instrument, the density and composition of the sample material, and on the energy of the element's characteristic fluorescent radiation (Potts *et al.*, 1997b). The practical outcome of this is that elements with higher atomic number (hence higher energy characteristic x-rays) are measured from a greater depth in the sample. Typically, samples less than 1mm thick are likely to be problematic for fully quantitative pXRF analysis, and for samples with a matrix similar to stained glass, 1.5mm thickness is desirable (e.g., Dungworth and Girbal, 2011; this will be discussed in greater detail).

Sample geometry. The material should be flat and level in order to yield quantitative results. However, these conditions are frequently not met in archaeology and cultural heritage, and for surfaces that are not flat and level, corrections should be applied to account for surface geometry and irregularity. Compton or Rayleigh normalisation has been found to be an adequate correction for minor surface irregularity (Potts *et al.*, 1997a), though a recent study found that normalisation to the Rayleigh peak may be better suited for the correction of more extreme effects due to curvature like that found in pottery (Wilke *et al.*, 2016).

5.1.3.2 Instrumental settings

Anode/target. The anode is part of the x-ray generator, which produces the primary radiation by bombarding the anode with a beam of electrons, thereby producing x-rays with a continuous spectrum of energies called bremsstrahlung radiation. Characteristic x-rays of the anode material will also be emitted and have the potential to interfere with the measurement of elements of interest. For example, if an Ag anode is used, Ag cannot be analysed in the sample (Cesareo, 2010). Therefore, popular anodes, such as Rh, have characteristic x-rays that do not interfere with the most common elements of interest.

Primary radiation: accelerating voltage, current and filters. These are settings that the analyst can typically change to optimise analysis of specific elements (unlike other specifications like the anode and detector type which are generally fixed). The **accelerating voltage** describes the energy of the primary radiation (specifically, the maximum energy of the continuous spectrum emitted, called bremsstrahlung radiation). A lower accelerating voltage of 15kV is better for measuring lighter elements, while a much higher accelerating voltage of 40kV is necessary for measuring heavier elements. To analyse a particular element using XRF, a general rule of thumb is to use an accelerating voltage of approximately twice the energy of the target characteristic x-ray (Amuda *et al.*, 2014). The **current** reflects the number of electrons that bombard the anode and controls the resultant intensity of the primary radiation and of the characteristic spectra generated from the sample. A higher intensity is usually recommended for the analysis of light elements and for trace elements, and a lower intensity for mid-Z elements, to avoid oversaturating the detector. **Primary beam filters** may be used between the primary radiation source and sample, in order to reduce background "noise" resulting from the x-ray tube target. It blocks out segments of the continuous spectrum of energies produced by the x-ray generator, can reduce or eliminate characteristic lines originating from the tube and/or anode, reduce the intensity to avoid saturation of the detector, and reduce the signal-to-noise ratio.

Acquisition time. A longer acquisition time, *i.e.* the time allotted to each analysis, will increase the signal-to-noise ratio, hence lower the limits of detection (e.g., Dungworth and Girbal, 2011), and it is up to the analyst to weigh the 'need for speed' against the limits of detection (LOD). An inter-laboratory study of laboratory-based XRF showed that acquisition time did not affect the laboratory's data quality for the elements of interest (copper alloys; Heginbotham *et al.*, 2011).

Spot size. The spot size, or the area of analysis, is dependent on the size of the beam of primary radiation and the angle of incidence. Unless the sample material is completely homogeneous, a smaller spot size may mean a less representative area; however, a smaller spot size might be desired if there is only a small area of clean surface available or if the object itself is very small. Some instruments have a collimator, which restricts the spot size but can also limit the detection of lighter elements due to overall reduced intensity.

5.1.3.3 Quantification

Spectra. The spectra produced during analysis will include peaks that are not due to characteristic fluorescence, and a user should be able to identify them. These include

- Rayleigh scatter (x-rays that are deflected by the sample and are measured by the detector without loss in energy; these appear as characteristic x-rays of the anode material);
- Compton scatter (similar to Rayleigh, except that some energy is absorbed by the sample material, and appears as a broad bump or peak just preceding the Rayleigh peak; this relates to the density and composition of the sample material);
- escape peaks (when the silicon material of the detector fluoresces when bombarded by the characteristic x-rays of the sample, reducing the energy of the x-rays by the value of the energy of the silicon Kα x-ray);
- sum peaks (when two characteristic x-rays arrive at the detector at the same moment, and are recorded as a single x-ray with an energy equal to the sum of the two x-rays)
- and for crystalline materials, Bragg scattering (which is due to diffraction).

A good overview of these spectral effects is given in Shugar and Mass (2012). The bremsstrahlung radiation, or the continuous spectrum emitted by the spectrometer, also appears in the spectrum, underlying the peaks as background noise.

Calibration: fundamental parameters and Compton normalisation. Many commercially available spectrometers come with built-in software that applies calibrations to the measured counts per second, in order to produce absolute compositions for a range of elements. The two main methods of quantification are fundamental parameters (Heginbotham and Solé, 2017; Sherman, 1955; also see Solé *et al.*, 2007) and Compton normalisation (Giauque *et al.*, 1993; Wilke *et al.*, 2016), and either can be combined with empirical calibration (see below). The fundamental parameters method is based on measurement of pure elements, x-ray physics (including absorption data and other known behaviour of x-rays under the analytical conditions), and the specific instrumental settings (Shugar and Mass, 2012). This method returns normalised data (*i.e.,* the concentrations sum 100%), and this can be problematic for materials that include elements that are too light for analysis in air (such as Na in glass). The fundamental parameters method has been shown to be the superior method of calibration for metal samples (Heginbotham *et al.*, 2011). The Compton normalisation method, also called Compton ratioing, involves normalisation against the Compton scatter, which can help to reduce matrix effects, for example in silicate-rich minerals (Wilke *et al.*, 2016), and while not as effective in the quantification of light elements, is optimal for mid-Z or high-Z trace elements (Conrey *et al.*, 2014).

Empirical calibration. It is generally recommended that analysts apply empirical calibrations to the data generated by the spectrometer, as the built-in or factory calibrations are not always adequate, especially for complex samples such as glass (Brand and Brand, 2014; Goodale *et al.*, 2012). Regression lines based on the analysis

of multiple matrix-matched standards of known composition yield a slope or calibration factor that can be applied to the data to correct it to the known standards. The standards should cover the full range of concentrations expected in the sample(s). The flaw in this approach, however, is that often there are not sufficient or suitable standards available in archaeology; standards of the right matrix may not be available, standards may not be well characterised, or available standards may not contain the right concentrations of the elements of interest. One way to bypass this problem is to create a series of standards specifically tailored to the research (Wilke *et al.*, 2016), but this can be resource- and time-intensive. Another approach is to calibrate the pXRF data to the analysis of a subset of the samples analysed by a complementary technique, such as lab-XRF or LA-ICP-MS (e.g., Frahm, 2014).

Secondary standards. As for any analytical programme, secondary standards should be used throughout the analysis in order to provide information about the machine's performance in terms of accuracy and precision. It is best practice to analyse widely available standards and to report the results (Shackley, 2010). It is also best to avoid self-standardisation; i.e., the same standards used to develop empirical calibrations should not be used as secondary standards to monitor accuracy and precision.

5.1.3.4 Performance, problems and potential

Despite the problems that the lack of a vacuum or sample preparation can present, studies comparing handheld spectrometers and laboratory-based XRF systems have shown that the handheld systems generally compare favourably, in particular in terms of precision (Craig *et al.*, 2007; Goodale *et al.*, 2012; see also Williams-Thorpe *et al.*, 1999). The accuracy of the absolute concentrations generated by a spectrometer's built-in calibrations, on the other hand, can be more problematic (Brand and Brand, 2014), in part because it is difficult to take into account all of the matrix effects present in the wide variety of archaeological materials with just a few calibration programmes. An inter-laboratory comparison of lab-XRF (Heginbotham *et al.*, 2011) showed that by far the most important factor affecting a laboratory's data quality (*i.e.,* accuracy) was the method of quantification, rather than any instrumentation or setting (such as detector type or acquisition time). This appears to be mostly true for handheld pXRF as different brands with different instrumentation perform comparatively (see also Brand and Brand, 2014; cf. conference poster by Hunt *et al.*, 2014). Researchers at the Corning Museum of Glass did find they could use calibrations developed using their lab-based handheld pXRF on data collected by their field pXRF (both instruments were the same make and model, using the same settings; Kaiser and Shugar, 2012).

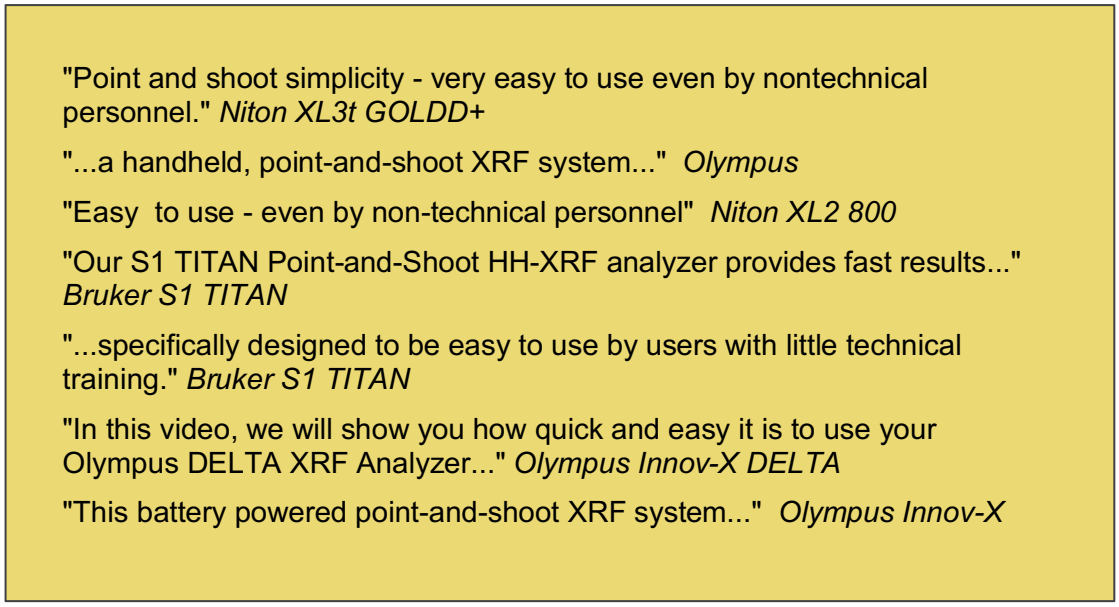

Figure 5.1 Handheld pXRF spectrometers are marketed in such a way as to encourage non-scientists to use the machines without an understanding of how it works or what the data really mean.

Retrieved from (in order): www.thermofisher.com/order/catalog/product/XL3TGOLDDPLUS, www.olympus-ims.com/en/applications/portable-xrf-technology-archaeometry-authentication-conservation-art-objects/, www.nitonuk.co.uk/xl2/, www.bruker.com/products/x-ray-diffraction-and-elemental-analysis/handheld-xrf/applications/food-agriculture.html, www.bruker.com/products/x-ray-diffraction-and-elemental-analysis/handheld-xrf.html, www.youtube.com/watch?v=W9HCYYK93RE, https://www.olympus-ims.com/en/applications/xrf-technology-analysis-arsenic-lead-soil/

However, inter-laboratory comparison continues to be a concern, mostly due to less-than-rigorous and non-standard applications of the technique.

Handheld pXRF spectrometers are widely marketed as "simple" and "easy to use" alternatives to laboratory equipment (Figure 5.1). The ease of use of these spectrometers means that non-scientists can easily operate the machine and generate a table of data about their material, but the user may have little to no understanding of the spectrometer, how the technology works, or of their material, meaning that there is a risk that the data is meaningless (Scott *et al.*, 2012). Those who have raised concerns have stressed the need for rigorous scientific protocol, in particular the use of secondary standards and recognition of quantitative versus qualitative data (Shackley, 2010). These concerns have resulted in a general scepticism towards the technique and studies that rely upon it, due to a "perceived lack of analytic rigour or understanding" (Grave *et al.*, 2012, 1674). While many studies respond by focusing on developing a methodology for specific materials (Dungworth, 2012a; Grave *et al.*, 2012; Wilke *et al.*, 2016), Frahm (2013a) responded with a paper testing the use of deliberately suboptimal conditions (including relying solely on the built-in calibration

programmes, and using materials that were too small and irregular in shape) for obsidian sourcing. Among other things, Frahm argued that the distinction between accuracy and precision is often ignored, and that accuracy often seems to be held as the marker of the data's reliability and validity when in many studies, precision might be the more important of the two. This is an important argument, as accuracy can be corrected but precision cannot; and furthermore, as Frahm argues, some studies need only internal consistencies and do not rely on comparison with other data. The paper by Frahm prompted a spirited debate with a response by Speakman and Shackley (2013, 1435), in which they decried Frahm's supposed support for dismissing reliability and validity in science and encouragement of the general population to "play scientist", to which Frahm (2013b, 1444) replied by characterising their objections as an "artificial crisis triggered by specialists' concerns about a hitherto restricted technique becoming available to a wider community".

This spirited exchange underlines the contentious position held by pXRF in archaeology, yet both parties are right: the analyst must understand the technique, the material, and how to conduct scientific analysis; however, data that is appropriate for one study may not be for another and it is important to recognise this. An analyst would not use energy dispersive scanning electron microscopy (SEM-EDS) to characterise trace elements, just as one should not use pXRF to characterise light elements. Similarly, a study which requires high precision may not also require high accuracy.

5.2 Handheld pXRF in archaeology and cultural heritage

Applications of pXRF for archaeology and cultural heritage are hugely varied. The technique is now commonly used for obsidian provenance studies and more widely to study exchange relationships, transportation of trade goods, and the migration of both people and material culture (Craig *et al.*, 2007; Ferguson, 2012; Frahm, 2013a; Frahm *et al.*, 2014; Milić, 2014; Tykot, 2017). This is an apt application because the material is homogeneous, and this research is focused on the analysis of a few discriminative trace elements, many of which are high *Z* elements. A recent paper by Wilke, Rauch and Rauch (Wilke *et al.*, 2016) also relied on the analysis of a few discriminative heavy trace elements for the provenance determination of late medieval pottery, with success despite the limitations presented by the material. Another interesting and relevant application was in the study of the bronze weapons of the terracotta army (*Imperial Logistics*), which relied on the internal precision of the pXRF analyses to identify metal batches and the large numbers of samples made possible by the technique, in order to

conduct a thorough study of the organisation of production in the metallurgical workshops that armed the warriors (Martinón-Torres *et al.*, 2012). The most important and most relevant research to this thesis, however, is the English Heritage Historic Window Glass project.

5.2.2 The English Heritage Historic Window Glass project

The English Heritage (now Historic England) Historic Window Glass project was a two-phase project under David Dungworth that began as an initiative to preserve, and advocate the importance of, the window glass in historic buildings, which is often regarded as of little value in comparison to other aspects of historic architectural contexts. The project involved the characterisation of the chemical composition of historic window glass and the association of these compositions to a chronology of glass-making technology. Phase 1 involved the characterisation of over 500 samples of glass from architectural as well as archaeological contexts, including materials from production sites in England, using laboratory techniques SEM-EDS and XRF (Dungworth, 2011a). Phase 2 focused on the in situ analysis of window glass by handheld pXRF (Dungworth, 2012b, 2012a). The project not only yielded a compositional chronology that tracked changes in English glass-making technology through the centuries since the medieval period, but for individual case studies, the data was used to provide a history of construction, repairs and renovation for the historical buildings in question, and to date and characterise original glass for the purposes of conservation and preservation.

In addition to the journal articles previously cited, case studies from the project are detailed in English Heritage Research Department reports (Dungworth, 2014, 2011b; Dungworth *et al.*, 2011; Dungworth and Girbal, 2011; Dungworth and Harrison, 2011; Girbal and Dungworth, 2011), which allowed the authors to provide more detail than is normally permitted in a journal's typical word count allotment. Dungworth and his colleagues took advantage of this to explore more fully the use of pXRF for window glass.

Some parameters explored in these reports were

- the count time, which was found to impact the limits of detection, but in the end quite short count times (25s per analysis) were found to be adequate for purposes of data quality with the equipment and settings used in the study, as well as enabling rapid analysis of hundreds of pieces of glass per day (Dungworth and Girbal, 2011);
- the thickness of the glass, which through tests using microscope slides determined that analyses of glass less than 2mm were affected, and that the

effect was most extreme for glass less than 1mm thick (under their analytical settings; Dungworth and Girbal, 2011); and

- the effect of corrosion, which was explored both by performing line scans using SEM-EDS on cross-sections of glass, across both corroded and uncorroded layers (Dungworth *et al.*, 2011) and through the analysis of glass pieces by pXRF before and after the removal of corrosion (Dungworth and Girbal, 2011), both of which showed the most dramatic differences were found in lighter elements.

The spectrometer was flushed with helium to enable and improve the detection of lighter elements (Mg and heavier), though the equipment could be problematic (Girbal and Dungworth, 2011). Even when there were no reported issues with the helium flush, the benefits can be minimal: sodium is still too light to measure, and silicon measurements were poor as well; SEM-EDS and pXRF analysis of the same glass pieces showed that silicon measurements were not relative, as the sample with the highest silicon concentrations was recorded by pXRF as having the lowest (cf. SiO2 concentrations in Tables 1 and 2, in Dungworth *et al.*, 2011).

Despite this, pXRF was more than adequate for distinguishing types of post-medieval glass and identifying a date of manufacture and/or insertion, using the compositional timeline established in Phase 1 of the project (Dungworth, 2011b; Dungworth and Girbal, 2011). The difficulty in measuring lighter elements was compounded, however, when medieval forest glass was thrown into the mix: the effect of the corrosion present was often so severe that types of glass could not be identified based on the analysis of the major elements. Instead, it was discovered that trace elements rubidium, strontium, and zirconium were less affected by corrosion, and could be used to distinguish the different glass types through the ages (Dungworth, 2012a; Dungworth *et al.*, 2011; Girbal and Dungworth, 2011). The present research is partially based on developing this approach further.

Phase 2 of the Historic Window Glass project exploited the speed of pXRF, covering large datasets quickly to provide a comprehensive history of the building's construction and renovation, and the non-invasive, in situ applications possible with the technique, which allowed analysis of glass that was not already broken or removed from its context as well as glass from a wider variety of historic buildings (such as prestigious houses) that would not have permitted invasive sampling of more expensive glass. The project would not have been possible without Phase 1 and the use of SEM-EDS to establish the compositional chronology, but with that database in place, it is now relatively easy to identify types of window glass using handheld pXRF. Furthermore, the methodology was adapted when confronted with one of the pitfalls of pXRF, the

problems surrounding the analysis of lighter elements (which, unfortunately, constitute the major elements of most glass), and turned its focus towards the analysis of heavy trace elements, Rb, Sr and Zr, to distinguish broad glass types.

Another study of relevance used a macro-XRF scanning spectrometer to scan a late 15th century stained glass panel in Belgium, and similarly encountered problems attributed to surface corrosion and found that trace elements Rb and Sr distinguished high potash forest glass from HLLA glass types (Van der Snickt *et al.*, 2016).

5.3 Surface conditions of medieval stained glass

Analysis by pXRF depends on the assumption that the surface has an identical composition to the bulk. This assumption is not necessarily valid for medieval stained glass, as it may have paint and silver stain on the surface, and even more problematic, it is very prone to deterioration. Rb, Sr, and Zr can be used to distinguish medieval forest glass from other types of glass (Dungworth, 2012a; Dungworth *et al.*, 2011; Girbal and Dungworth, 2011); this work will seek to methodically identify which elements are affected by surface conditions and which are well measured by pXRF, and explore the use of Rb, Sr, Zr and other elements as markers of glass-making technology, production sources, and tools for the identification of glass batches for the study of the organisation of production.

5.3.2 Composition and corrosion of medieval stained glass

The deterioration of glass is a complex phenomenon that is dependent on both intrinsic properties of the glass (its chemical composition) and external factors (the environment and its exposure to certain conditions; Newton, 1982).

The chemical composition of medieval glass makes it one of the least durable glasses of pre-modern times. The recipes described in Chapter 3 resulted in a glass that is relatively low in silicon and high in potassium and calcium. The addition of alkaline and alkaline earth ions disrupts the silica network (Figure 5.2) through the creation of non-bridging oxygens (NBOs) and formation of weaker ionic bonds between NBOs and M^{+} and M^{2+} ions in place of the stronger Si-O covalent bonds within the silica tetrahedra (Pollard and Heron, 1996). The higher the ratio NBO/T (non-bridging oxygens per tetrahedron, Mysen, 1988), the higher the rate of corrosion (Sterpenich and Libourel, 2001). For example, a threshold at about 60 mol% SiO_2 has been observed for medieval glass; with glass containing less silica showing various signs of weathering and glass containing more appearing unweathered (Cox *et al.*, 1979).

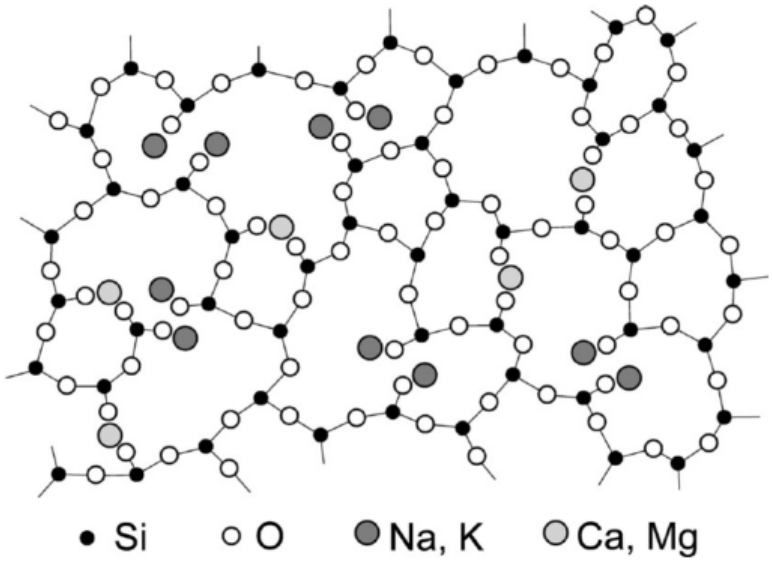

Figure 5.2 Structure of a typical man-made silicate glass (Figure 1, in Melcher *et al.*, 2010). The presence of network modifiers (e.g., K^+, Ca^{2+}) result in the creation of nonbridging oxygens (NBOs). If the silica content of a glass is too low (below about 60 mol% SiO2, Cox et al., 1979), the glass is particularly prone to deterioration.

Furthermore, the bond between K^+ and NBO is weaker than that between Na^+ and NBO, due to the larger volume of K^+ and resultant lower field strength, and therefore K^+ is leached out of the glass more easily than Na^+. The low silica concentrations and the disruption of the silica network by high alkali concentrations, and secondarily the presence of K^+ rather than Na^+, results in a glass that is particularly prone to deterioration (Cox *et al.*, 1979; De Bardi *et al.*, 2013; Fernández-Navarro and Villegas, 2013).

Several environmental factors drive the deterioration of medieval stained glass windows, the most compelling of which is rainwater (Gentaz *et al.*, 2011), which reacts with the glass in such a way that results in leaching; the formation of corrosion crusts, cracks and pits; and the dissolution of the silica network. Leaching (see Figure 5.3) is the process by which modifying ions are drawn out from the surface layer of the glass and replaced by the diffusion of hydrogen-containing species, including H^+, H_3O^+, and H_2O, from the rainwater (Carmona, 2013; Fernández-Navarro and Villegas, 2013; Melcher *et al.*, 2010). This exchange forms a hydrated "gel" layer that is depleted in modifying ions, in particular the weakly bonded K^+, which is preferentially leached from the surface of the glass in comparison to all other elements (Melcher and Schreiner, 2006; Sterpenich and Libourel, 2001). The depth of leaching on in situ window glass has been measured in the range of 40-220μm (Lombardo *et al.*, 2010; Sterpenich and Libourel, 2001). Analytical work comparing the compositions of the bulk glass and the

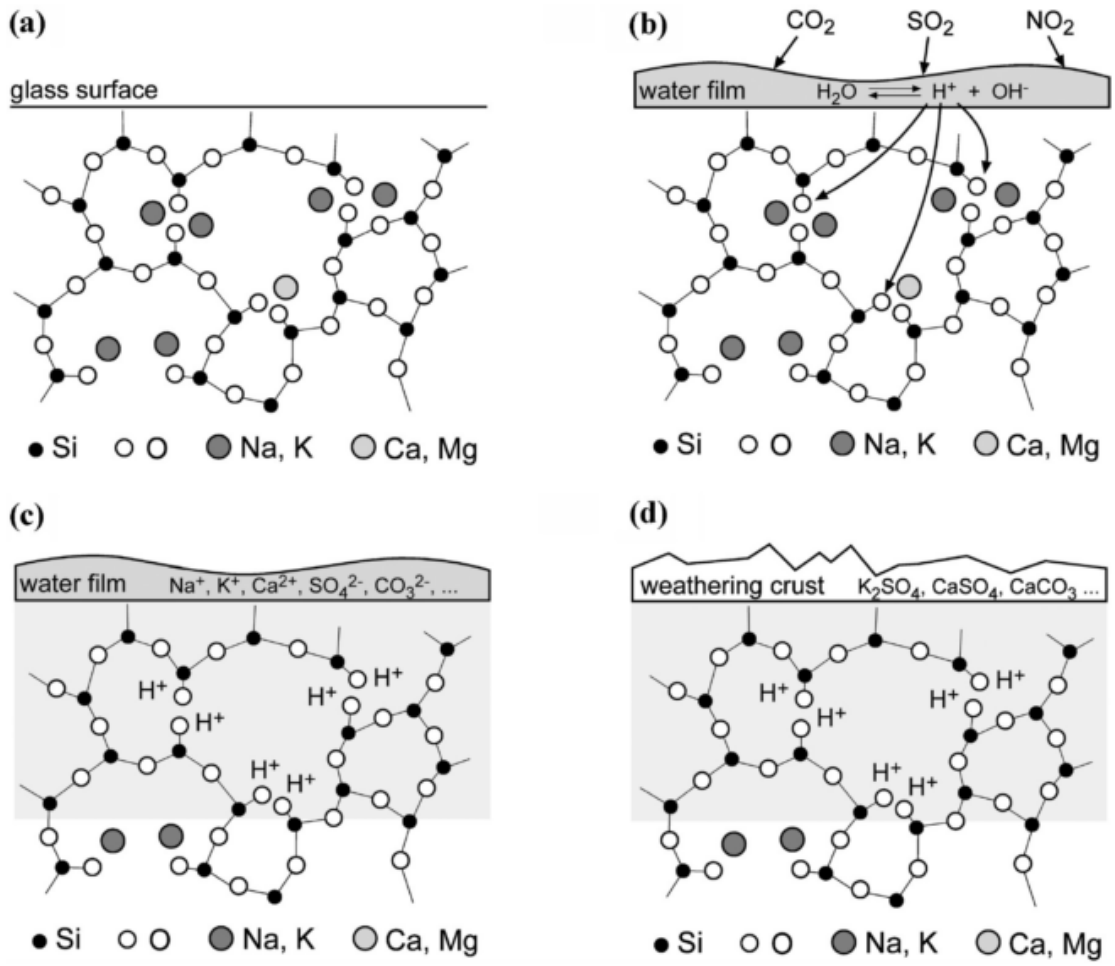

Figure 5.3 An illustration of some deterioration processes affecting medieval stained glass exposed to the environment (Figure 5, in Melcher *et al.*, 2010). (a) The first image shows clean, unweathered glass. (b) A watery film forms on the surface on the glass, and an ion exchange begins between the hydrogens in the watery film and the alkaline ions in the glass; meanwhile the water also incorporates gases from the ambient atmosphere. (c) A hydrated layer forms in the glass. (d) Weathering crusts form through the combination of the leached alkaline ions from the glass with atmospheric compounds. This illustration does not depict the formation of cracks (etc.) nor the dissolution of the silicate network that may result from these processes.

leached layer generally find that the leached layer is severely depleted in K, is also depleted in Na, Ca and Mg, and that Si and many other elements are enriched as a result (Carmona *et al.*, 2005; Lombardo *et al.*, 2010; Melcher and Schreiner, 2006; Schreiner *et al.*, 1999). One study also examined the behaviour of trace elements in archaeological stained glass (i.e., buried; the leached layers on the in situ glass samples in that study were too small for analysis), and found that Rb (also Cs, Ba and Sb) is depleted and Sr and Zr (and most transition metals and REEs) were enriched in the leached layer in comparison to the unweathered bulk glass (Sterpenich and Libourel, 2001). The leaching process also leads to the formation of cracks, lamination and scaling (Gentaz *et al.*, 2016; Schalm and Anaf, 2016). Brown manganese-rich areas on the surface glass amongst the leached areas may also form (Ferrand *et al.*,

2015). SEM images of deterioration of medieval glass, in cross-section as well as on the surface, are included in Figure 5.4, as well as a photograph of stained glass depicting several of these deterioration effects.

Through this ion exchange, hydroxyl ions (OH^-) remain in the watery film on the surface of the glass, increasing its pH; at a pH larger than ~9, OH^- react with the silica in the glass, breaking the siloxane bonds to form silanol groups (Si-OH) and leading to the dissolution of the silica network (Fernández-Navarro and Villegas, 2013; Melcher *et al.*, 2010; Newton and Davison, 1989). Random packing of the silanol nanoparticles with variable packing density may result in lamellae structure (Schalm and Anaf, 2016).

The rainwater on the glass surface also contains compounds absorbed from atmospheric gases, which then react with the modifying ions that are leached from the glass. When the water evaporates, hard crusts form on the glass, composed of sulphates, carbonates, chlorides and nitrates of the modifiers (K, Na, Ca, Mg...) as well as organic compounds (Melcher and Schreiner, 2006; Newton, 1982; Sterpenich and Libourel, 1997; Woisetschläger *et al.*, 2000). The most common corrosion crusts identified on medieval stained glass windows are gypsum ($CaSO_4 \cdot 2H_2O$) and syngenite ($K_2SO_4 \cdot CaSO4 \cdot 2H_2O$), though a wide range of crystalline phases have been identified (Carmona *et al.*, 2005; Lombardo *et al.*, 2013; Melcher and Schreiner, 2006). Calcium oxalate (CaC_2O_4) discovered on stained glass in the Mediterranean especially are evidence of the presence of fungi, lichen and bacteria, which use calcite as a nutrient and secrete calcium oxalate; similarities have been noted in the species found on medieval stained glass and on stone monuments (Aulinas *et al.*, 2009; Carmona, 2013; Piñar *et al.*, 2013; Rodrigues *et al.*, 2014; Vilarigues *et al.*, 2013, 2011). Finally, another effect of the deterioration of medieval stained glass is the loss of paintwork (grisaille, see next section). This is due in part to the deterioration of the underlying glass, but also due to significant differences in the thermal expansion properties of the paint and the glass (Becherini *et al.*, 2008).

The severe susceptibility of medieval window glass to deterioration is perhaps best illustrated by the studies that have manufactured fresh glass with medieval compositions and exposed them to the ambient environment in several European cities for as little as six months, and already leaching and the presence of corrosion products could be detected (Melcher and Schreiner, 2006, 2005; Woisetschläger *et al.*, 2000).

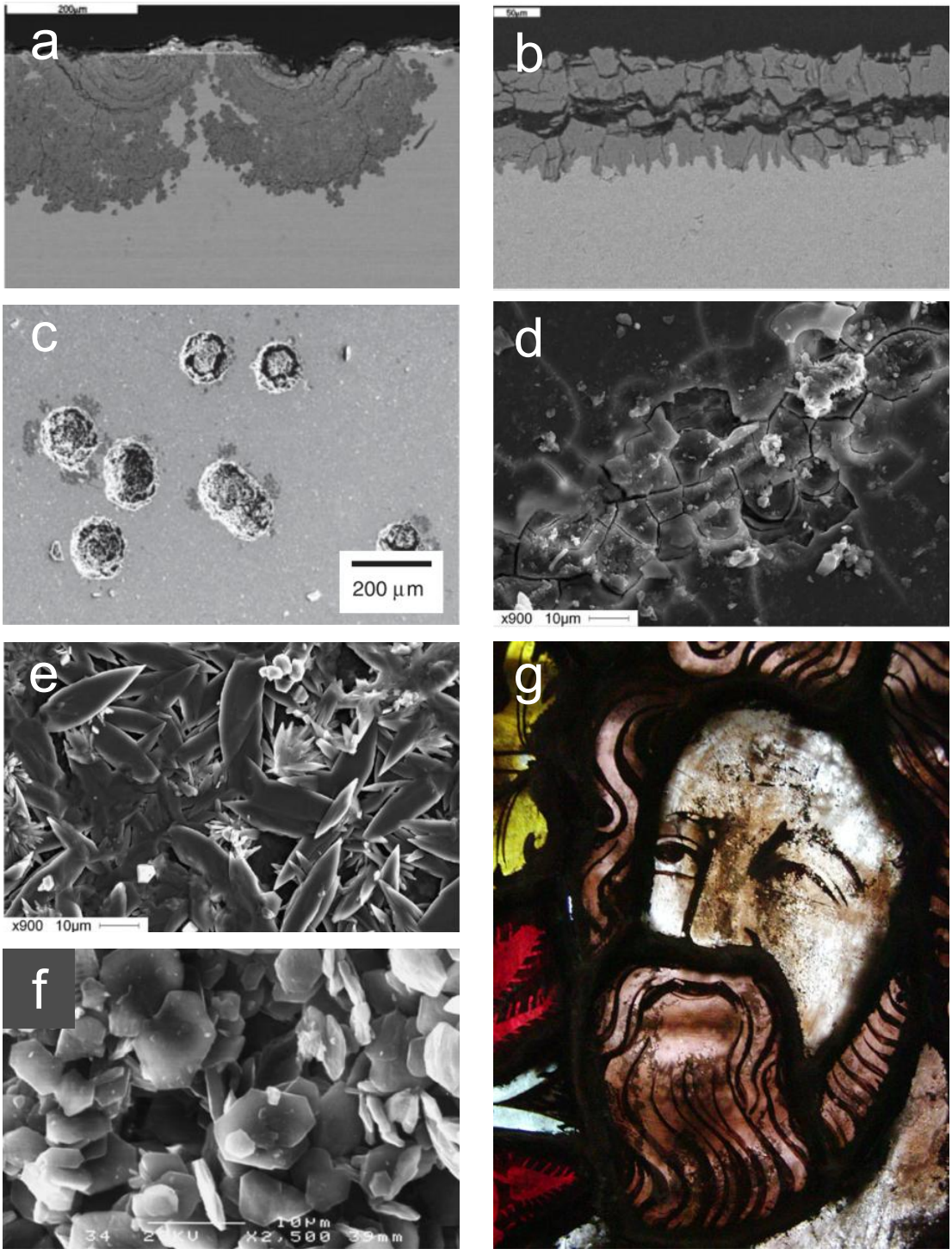

Figure 5.4 SEM images and one photograph showing the effects of deterioration on medieval stained glass: At top, a view in cross-section of the leached layer is associated with the formation of a pit/crater (a) and cracks resulting in scaling (b) (reproduced from Figure 1, in Lombardo *et al.*, 2010). These phenomena are also pictured on the surface of the glass, pits or craters in (c) (Figure 8, in Carmona, 2013) and cracking and scaling of the glass surface in (d) (Figure 4, in Melcher and Schreiner, 2006). Also pictured on glass surface are the formation of crystals of corrosion productions: syngenite (e) (Figure 4, in Melcher and Schreiner, 2006) and gypsum (f) (Figure 14, in Woisetschläger *et al.*, 2000). Pitting, paint loss and manganese-browning are all visible in (g), a photograph detail of a medieval stained glass panel (Figure 2, in Rauch, 2004).

5.3.3 Decorative details: grisaille and silver stain

5.3.3.1 Grisaille

The surface conditions of stained glass are also affected by the presence of painted detail, usually found on the interior surface but also found on the exterior. A grey-, black- or brown-monochrome pigment called grisaille[12] was used to add both line drawing as well as shading to the glass to depict the subject matter (Figure 5.5); shading on the exterior could be added to create a sense of depth. Grisaille preparation varies, but generally includes mixing ground glass (often a lead silicate) with powdered metal oxides (usually iron or copper) as the pigment, and the use of wine or urine as a binder (Carmona *et al.*, 2009; Pradell *et al.*, 2016; Verità, 1996; Vilarigues and da Silva, 2004). As described in the medieval account by Theophilus, one recipe included equal parts ground green glass, ground Byzantine blue glass, and powdered copper, mixed together with wine or urine as a binder (*De diversus artibus*, 2:19, trans. Hawthorne and Smith, 1979). The pigment is painted onto the surface and then fired onto the glass, at temperatures in the range of 500-750°C (Carmona *et al.*, 2009; Verità, 1996; Vilarigues and da Silva, 2004). Grisaille compositions have often been found to be high in lead and iron in particular (Carmona *et al.*, 2006; Machado *et al.*, 2017; Pradell *et al.*, 2016; Van Wersch *et al.*, 2016). In one study, some metals (Pb, Zn) have been found to diffuse into the surrounding glass, affecting both the durability of the glass and paint adhesion, but also the composition (Vilarigues and da Silva, 2004). This may be problematic for surface analysis, as it suggests that even if an area of the glass can be selected that appears free of grisaille, there may be some migration of certain elements affecting the analysis.

5.3.3.2 Silver stain

Despite the implications of the term "stained glass", most colours present in stained glass windows were provided by pieces of glass that were coloured throughout the glass via the addition of colourants to the melt (so-called “pot metal” colours) rather than through the application of a surface stain. The prominent exception is silver stain, a cementation technology adopted for use on window glass in the early 14th century

[12] The term ‘grisaille’ is also sometimes used to refer to stained glass windows typical of the late 14th/early 15th century, which was dominated by grisaille-painted white glass, or to refer to the white glass itself (see Simmons and Mysak, 2010). In this research, grisaille will be used to refer to the pigment only.

Figure 5.5 Detail of a medieval stained glass panel, showing different shades of yellow/orange silver stain, as well as details painted on using grisaille pigment. Detail of panel 10h of the GEW. © *The York Glaziers Trust with the kind permission of The Chapter of York*.

(Molina *et al.*, 2013). Silver stain was mostly used on white glass to give a yellow colour (ranging from gold to brownish/orange, see again Figure 5.5 and 4.2), and could be used on all or part of the piece of glass (for details such as halos, for example).

The technology is based upon the application of a silver compound dispersed in a carrier medium such as clay or ochre, and fired onto the surface of the glass at a temperature below the softening point. The chemical reactions are described by Weyl (1951): the silver ions (Ag^+) undergo an exchange reaction with the alkali ions of the glass (K^+ or Na^+), allowing the silver ions to diffuse up to about 0.5mm into the glass. The silver ions are then reduced to neutral silver atoms through the donation of electrons by other ions, such as Fe^{2+}. The low solubility of silver results in the crystallization of the metallic silver, resulting in the observed colour.

The colour achieved by this process can range widely, and depends on numerous factors, including: the duration and temperature of the firing (Zhang *et al.*, 2007); the composition of the silver compound (such as $AgNO_3$, Ag_2SO_4, AgCl, Ag_3PO_4 or Ag_2O; Jembrih-Simbürger *et al.*, 2002); and the addition of copper oxide, which was also sometimes used (Delgado *et al.*, 2011). It is worth noting that the experimental studies by Zhang *et al.* (2007) and by Jembrih-Simbürger *et al.* (2002) were both carried out on

soda-lime-silicate glasses, and so the applications of their work may not translate fully to potash-lime-silicate glasses. Delgado *et al.* (2011) carried out experimental work on both potash- and soda-containing glasses, and found that soda glass was more easily stained (the potash glass could only be stained with a mixture of 2:1 Ag:Cu). Studies from the early 1900s suggested that overall, the major element composition of the base glass does not have a significant effect on the staining and final colour, though Weyl also adds, "soda glasses seem to take the stain better than potash glasses" (Weyl, 1951, 418; and references therein). The minor elements present (iron, arsenic and antimony, for example) affect the ease with which the glass may be stained due to their role in the reduction of the silver ions (Weyl, 1951).

5.4 The interference of lead cames

The use of handheld pXRF for the analysis of medieval stained glass windows has the potential to address problems of accessibility to the glass for sampling, which is often inhibited by the position of the windows in the walls of cathedrals and other monuments. However, analysis of in situ medieval stained glass is further complicated by the relatively small size of the individual glass pieces, therefore increasing the likelihood that the spectrometer cannot be placed flush against the glass surface due to the protrusion of the lead cames.

The interference of lead cames on the analysis of windows is of particular relevance to medieval stained glass, though it is not limited to this period. As already stated, colour in medieval stained glass windows was achieved through the use of differently coloured glass pieces rather than the use of enamels on the surface of a glass pane. The glass pieces are therefore cut into shapes that are often too narrow or otherwise incompatible to accommodate the dimensions of the pXRF spectrometer's face. The lead cames can therefore prevent the placement of the spectrometer flush against the surface of the glass material for analysis for all but the largest pieces of glass (Figure 5.6).

The problem of distance between sample and detector is not a new one, and has usually been addressed in the context of materials that do not have flat surfaces, creating distance between the detector and (parts of) the sample and resulting in reduced intensity. Potts *et al.* (1997a) established a simple correction for the lost intensity caused by irregular surfaces, based on normalising the intensity of characteristic peaks to the intensity of Rayleigh scatter peaks. A more recent study on curved pottery fragments (Wilke *et al.*, 2016) confirmed the superiority of using Rayleigh scatter over Compton scatter to normalise and correct distance errors.

However, both studies advise only using this correction for distances up to 1mm for mid-Z elements and up to 3mm for heavy elements.

The lost intensity is attributed both to absorption of the x-rays (both incident and characteristic) in air, and to the changed angle of detection affecting the relative intensity of the scatter peaks (Potts *et al.*, 1997a). The relevant conclusions of this study for the application of this correction were:

- Normalisation to Rayleigh scatter is a sufficient correction for distances up to 1mm for mid-Z elements (such as Fe) and up to 3mm for heavy elements (Sr, Ba);
- The correction cannot be applied to light elements successfully, as it does not account for absorption in air, which more drastically affects lower energy characteristic x-rays;
- Different excitation sources, with different scatter peaks, perform differently in terms of this correction (^{55}Fe was preferred over ^{109}Cd and ^{241}Am in that study);
- The increased angle of detection resulted in an increase in the relative intensity of the scatter (particularly for the ^{55}Fe Rayleigh scatter), limiting the application of the correction for larger distances.

However, there are key differences between the study conducted by Potts *et al.* (1997a) and the present study. The matrix in this work is non-crystalline (and therefore

Figure 5.6 Lead cames can protrude multiple millimeters, and together with the use of small pieces of glass, prohibit the placement of the pXRF spectrometer directly on the surface of the glass for analysis. The glass in this image has been recently conserved and re-leaded, and the modern lead cames in these panels protrude by about 2-4mm.

will have different matrix effects); the spectrometer in this study uses a different excitation source (Rh anode) than those tested by Potts and will have a different geometry (i.e., angles of incidence and detection). Furthermore, distances larger than 3mm can be expected, and therefore a different solution may be required. Finally, a proprietary algorithm, known to include Compton normalisation along with other corrections, is used by the Innov-X/Olympus programme to transform the counts into concentrations, and it will be necessary to examine how this affects the results.

5.5 Developing a methodology for the study of medieval stained glass windows by handheld pXRF

Although this research has benefitted from the invaluable opportunity to sample glass from across the GEW, more generally the study of medieval windows has been impeded by the difficulty in access. Therefore, a key aim of this research and a hopeful contribution to the field of study is to develop a methodology based on pXRF analysis, which can be used on in situ windows. The two primary problems identified for the analysis of medieval stained glass windows by handheld pXRF are suboptimal surface conditions and the protrusion of lead cames creating distance between the sample and spectrometer.

To address the obstacle of poor surface conditions, this work derives itself from the English Heritage Historic Window Glass Project, which showed that heavy trace elements could be used to distinguish glass types of different periods. This work will compare pXRF analyses to analyses by more established laboratory-based techniques that produce high quality results, so that elements that are well measured might be identified (or confirmed).

To understand and mitigate the problem of lead cames, a series of tests were carried out to illustrate the effect that lead cames might have on the analysis of different elements, and possible solutions explored.

CHAPTER 6

Methods

This research is a multi-analytical study with two core aims: the investigation of the technology and production of the GEW of York Minster, and the development of a methodology using handheld pXRF for the study of medieval stained glass windows.

PXRF allowed a large number of samples to be analysed, a subset of which was chosen for cross-sectional analysis by various methods. Sampling and the analytical methods used are described in this chapter. Experiments conducted to test the performance of pXRF as well as statistical data processing will also be described.

6.1 Materials and sampling

The window glass pieces of the main lights of the GEW are the focus of this thesis. Sampling terminology (Table 6.1) has been adapted from the Analytical Methods Committee of the Royal Society for Chemistry (AMC, 2005) and the sections on cluster sampling by Levy and Lemeshow (2008). Panels from the GEW were selected for study in order to provide information on the life history of the window, constituting the first-stage sampling; however they will simply be referred to as "panels" in this thesis. Numerous pieces of glass from each panel were selected for analysis - the second-stage sampling, and what will be referred to as the *sample*. All samples were analysed on the surface by pXRF (the area of analysis will be called *test area*). A subset of the samples, called the *control group*, was also chosen for removal of a small amount of glass (which, after preparation for analysis, can be termed *sub-samples* or *cross-sections*), which were analysed by various laboratory-based methods.

Table 6.1 Guide to the terminology used in this thesis as regards sampling.

Statistical terminology	**Terminology used in this thesis**	**Description**
Primary sample (first-stage sampling)	Panel	Panels refer to a portion of the window that contains its own finite subject matter, that fits into the overall subject matter of the window (or series). Panels are surrounded by a metal frame and can be removed as a unit, and internally are composed of the individual glass pieces connected with lead cames.
Secondary sample (second-stage sampling)	Sample	piece of glass analysed
Sub-sample, Test sample	Sub-sample *or* Cross-section	portion of glass removed from sample for analysis on the cross-section by laboratory means or for dissolution for TIMS analysis
	Control group	the samples from which sub-samples were removed
Test portion, Test sample	Test area	area on the surface of the sample analysed by pXRF

Samples were all named according to a similar formula, adapted from a longer version used by the Freestone Leverhulme project (Freestone *et al.*, 2010; Kunicki-Goldfinger *et al.*, 2014) including window information (generally excluded in this thesis unless distinction is required), panel code, and a sample code including colour information and a number:

(WINDOW CODE)-(PANEL CODE)-(SAMPLECOLOURANDNUMBER)

For example, GEW-3b-B4 is the name for a blue glass piece from panel 3b of the Great East Window of York Minster. B is used for blue, W for white (i.e., colourless or unintentionally tinted glass), R for red, G for green, Y for yellow, and M for manganese-coloured glasses, which covers a range of purple, pink, murrey, and flesh tones. This sample name refers to the piece of glass analysed by pXRF and is also applied to any cross-sectioned sub-samples removed from it.

For archaeological glass, samples were named by their site name and sample number:

(SITE CODE)-(SAMPLENUMBER)

For example, LBW-1.1 is sample 1.1 from Little Birches, Wolseley.

6.1.1 Great East Window, York Minster

A total of twelve panels from the GEW were studied for this thesis. Only panels from the main lights were studied due to availability and access. The panels are located from across the window (Figure 6.1): three from the bottom row (panels 1e, 1h and 1j), four from the middle parts of the window (3b[13], 10c, 10e, and 10h) and five from the topmost row (15a, 15b, 15f, 15g, 15h). High resolution images of the panels (courtesy the York Glaziers Trust, or YGT) along with sample maps, brief descriptions and other pertinent information are provided in Appendix A. Art historical reports for each panel, which were written by the YGT as part of the conservation programme (reports in reference list under author "YGT"), were also made available. The selection of panels was largely determined by the schedule of conservation works. As the window was conserved row by row, groups of panels from the same row were studied during each analytical visit as these were available for analysis, having been removed from their lead cames and cleaned.

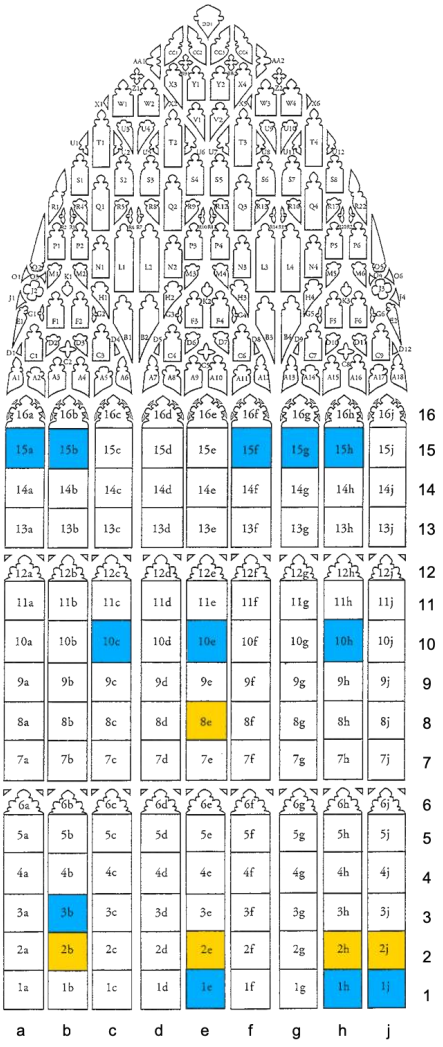

Figure 6.1 Plan of the GEW with panels analysed shaded blue; six panels analysed previously in the Cardiff-York project (see below) are shaded yellow. Panels are named according to their position in the window: a row number and column letter (noted on the plan).

A total of 906 samples were analysed by pXRF, with cross-sections removed from 253 of these to form the control group. The final sampling decisions for the control group were made by the YGT conservators following discussion with the author. The main focus of this sampling was on original glass, although some non-original glass

[13] Panel 3b was studied as part of an MSc dissertation by the author (Ware, 2013). The results of that dissertation led to this PhD. The results and interpretation of the panel have been revisited and revised since the MSc dissertation.

was deliberately included. Samples representing all colours in a given panel were cross-sectioned, and a more-or-less even distribution across the panel was attempted.

The majority of the panels were studied after they had been removed from their lead cames and cleaned (see Chapter 2). The exception is the row 10 panels, which were studied after their conservation had been completed, and the panels had been releaded and framed. Since the beginning of the conservation programme, the conservators at YGT were in the habit of sampling every third panel in the window, in anticipation of future study such as the Cardiff-York project (described below). For example, 39 panels were sampled between rows 1 and 11, for a total of at least 395 samples that have not been analysed in this study or by the Cardiff-York project. Therefore, the row 10 panels were subsampled before the commencement of this PhD, and the panels were selected based on the number of, and the diversity of colours present in, the cross-sectioned subsamples.

The selection of samples for pXRF analysis were decided with some advice from the YGT conservators. Significant coverage of the panels was attempted, covering all colours, with a focus on original glass pieces. Thorough coverage of the original white glass was a particular focus, for spatial analysis of white glass batches across the panels. For most panels, approximately 50% of the surface area of the panel was analysed, excluding the panels of row 1 (the bottom row), which covered about 25% due to the low survival of original glass.

6.1.2 The Cardiff-York project: Data and samples

A Leverhulme Trust Project grant to Professor Ian Freestone (then based at the School of History and Archaeology, Cardiff University) and Professor Tim Ayers (Department of History of Art, University of York) funded the study of medieval window glass including the chemical analysis of some 900 samples. With the kind permission of Freestone and Ayers, the Cardiff-York project provided both data and samples to this project for comparative purposes. Samples from six other panels in the GEW (panels 2b, 2e, 2h, 2j, 83 and 11e, see Figure 6.1 and Appendix A) were characterised by scanning electron microscopy with energy dispersive spectrometers (SEM-EDS n=136) and by laser ablation inductively coupled plasma mass spectrometry (LA-ICP-MS, n=52). The results from one panel have been published (Freestone *et al.*, 2010), as well as the data for the red glass in the window (n=21) in a paper on red glass production and technology (Kunicki-Goldfinger *et al.*, 2014). Data from kiln sites in the Weald and in Staffordshire was also made available (n=30), and the following samples were provided by the project for a joint investigation of the provenance determination of

the white glass in the GEW and another York Minster window by Thornton. Data from the project will also be used in Chapter 7 to characterise trace element concentrations of glass in different regions in Europe; preliminary empirical calibrations were applied to these data to correct discrepancies noted with the GEW glass analysed in this study.

6.1.2.2 Little Birches Wolseley, Staffordshire

Archaeological glasses from Little Birches, Wolseley (LBW), in Staffordshire, were studied for comparison to the GEW white glasses and for possible provenance identification. The excavation (1991-1992) uncovered four furnaces (and four tips), three of which belong to the South Site and were dated by archaeomagnetic dating to the mid-16th century (1533-1557 at 68% CL, Welch, 1997, 16). The fourth furnace, in the North Site, was poorly preserved in comparison due to the later creation of a pond as well as quarrying, and could not be dated by archaeomagnetic dating; the associated pottery, however, gave a date of 13th or 14th century (Welch, 1997, 15–16). Very few glass fragments were found in the North Site.

Six glass samples were analysed in this research, all of which are reported with context and major element composition by C. Mortimer in Appendix I of Welch's publication on the archaeological site (Welch, 1997). Three of these samples (LBW-22, LBW-23, and LBW-24) are from the earlier North Site. The other three samples (LBW-1.1, LBW-36, and LBW-45) are from the South Site.

6.1.2.2 St William Window, York Minster

The St William Window (SWW), in the north-east transept of York Minster and dated to c. 1414, is another window attributed to John Thornton (French, 1987). Four samples (SWW-20b-W52, SWW-21b-M44, SWW-24e-B26, and SWW-25c-W37) were also submitted for comparison to the LBW glass by isotopic characterisation in collaboration with the Cardiff-York project.

6.2 Analytical methods

6.2.1 Handheld pXRF analyses

Most of the pXRF analyses were carried out directly on the surface of the glass using a test stand, after the glass had been removed from their lead cames are part of the conservation interventions; the row 10 panels, as previously mentioned, were analysed after conservation had been completed (i.e., they had been reinstalled within lead cames), and were analysed using a tripod or handheld using a vertical lightbox (Figure 6.2).

Figure 6.2 Analyses by handheld pXRF were carried out using a test stand (left) whenever possible; if the glass pieces were not removed from their lead cames, the analyses were carried out using a tripod (right) or handheld.

The pXRF analyses were carried out using Innov-X/Olympus Delta Premium spectrometers (DP4000 and DP6000CC, see Table 6.2), which have a Rh anode, a silicon drift detector, and a spot size of 10mm. The built-in programme called the "Soils" mode was chosen for analysis, as this mode is optimised for oxygen-rich matrices, using Compton normalisation rather than fundamental parameters for quantification. The Soils mode uses three so-called "beams", or settings with different combinations of primary radiation voltage, current and filters. Beam 1 operates with a 40kV accelerating voltage, 89μA tube current, and a 1.5mm copper filter (optimised for heavier elements with higher energy characteristic x-rays); Beam 2 uses a 40kV accelerating voltage, 52μA tube current, and a 2.0mm aluminium filter (targeting mid-Z elements); and Beam 3 runs with a 15kV accelerating voltage, 68μA tube current, and a 0.1mm aluminium filter (for the analysis of lighter elements with lower energy characteristic x-rays). For the test stand analyses, the three beams were run sequentially for 20s each for a total of 60s; for the tripod/handheld analyses, they were operated for 10s, 5s and 5s respectively, for a total of 20s, in order to reduce strain during handheld analyses. Tests carried out on glass standards (data not reported) showed that accuracy and precision were unaffected unless concentrations were close to LOD, in keeping with similar previous tests on copper alloys (Heginbotham *et al.*, 2011). The analytical parameters, and variations within them, are summarised in Table 6.2.

The pXRF data is transformed into concentrations by the Innov-X/Olympus algorithm, proprietary information which includes Compton normalisation as well as other

Table 6.2 Summary of different analytical parameters used in the pXRF analyses of medieval glass in this research.

Handheld pXRF	**GEW Panel 3b**	**GEW Row 1**	**GEW Row 15**	**GEW Row 10**
Spectrometer brand:	Innov-X/Olympus Delta Premium XRF Analyzers			
Model:	DP4000	DP6000CC		
Machine specs:	Rh anode/target; Silicon Drift Detector; 10mm spot size			
Apparatus:	Test stand			Handheld or tripod (in situ conditions)
Mode	Soils			
"Beam" 1	40kV accelerating voltage; 80μA tube current; 1.5mm copper primary beam filter			
"Beam" 2	40kV accelerating voltage; 52μA tube current; 2.0mm aluminium primary beam filter			
"Beam" 3	15kV accelerating voltage; 68μA tube current; 0.1mm copper primary beam filter			
Acquisition time: (Beam 1/2/3)	20s/20s/20s			10s/5s/5s
Date of analysis:	May 2013	October 2014	February 2016	June 2015

necessary corrections. A set of empirical calibrations based on the analysis of matrix-matched standards (Appendix B) and on the analysis of a subset of the control group that was also analysed by LA-ICP-MS (see later section) were applied on top of that quantification. A separate calibration based on the same standards was developed for each variation of the pXRF method (Table 6.2).

The panels of row 10 are a special case; the calibration of this data by the above method is problematic because the panels were analysed under in situ conditions. For many samples, the lead cames surrounding them interfered with analysis by preventing the placement of the spectrometer directly on the glass. Although this was somewhat anticipated, as it was expected that it would not be possible to analyse the smallest glass pieces, ultimately most of the glass pieces were smaller than the spectrometer face. As the analytical programme was scheduled to accommodate the conservation programme timeline, it was not possible to delay the analysis in order to seek a solution. Encountering this problem led to a series of tests to examine the effect distance between spectrometer and sample has on analysis and to develop a practical way to alleviate the problem (experimental procedure described in a later section).

Table 6.3 Analysis of Corning D by handheld pXRF (in ppm) with accuracy and precision reported; for the Row 10 analyses (*), a comparison is made between test stand analyses of 3b samples ("TS", used as the accepted values) and handheld analyses ("HH") of the same samples under in situ conditions (described more fully in text). Accepted values are compiled from several sources as reported in Adlington (2017).

		Mn	**Fe**	**Co**	**Ni**	**Sn**	**Cu**	**Zn**	**Rb**	**Sr**	**Zr**
	Accepted	**4260**	**3637**	**181**	**393**	**788**	**3036**	**803**	**46**	**482**	**93**
Panel 3b	Mean	4258	3557	172	386	779	3030	801	45	500	90
n=15	Accuracy	0.0	-2.2	-5.0	-1.8	-1.1	-0.2	-0.3	-1.8	3.6	-2.9
	RSD	1.3	1.6	11.5	4.2	2.9	1.1	2.3	5.4	2.1	2.7
Row 1	Mean	4251	3663	176	401	783	2822	839	47	493	92
n=22	Accuracy	-0.2	0.7	-3.0	2.0	-0.6	-7.0	4.5	2.8	2.3	-0.3
	RSD	1.2	1.8	6.0	4.0	1.7	1.5	1.7	3.3	1.6	3.6
Row 15	Mean	4260	3526	168	382	779	2850	800	45	472	88
n=45	Accuracy	0.0	-3.1	-7.0	-2.9	-1.1	-6.1	-0.4	-0.7	-2.0	-5.1
	RSD	0.9	1.4	6.0	2.6	2.4	1.0	1.4	3.2	2.1	3.5
Row 10*	3b-W1, Accepted (TS)	10505	3723		*(Corn D)*	139	123	440	208	568	49
	Mean (HH)	10770	3925		373	141	132	462	216	570	53
	Accuracy	2.5	5.4		-5.0	1.5	6.7	5.1	3.6	0.3	6.7
	3b-B1, Accepted (TS)	8640	7390	758		195	1119	1323	307	835	110
	Mean (HH)	8926	7089	787		202	1114	1241	302	812	110
	Accuracy	3.3	-4.1	3.8		3.5	-0.4	-6.2	-1.9	-2.7	-0.9

For the purposes of calibrating the pXRF data of row 10, a subset of glass from panel 3b was reanalysed under the same in situ conditions. The panel had previously been analysed using a test stand, and the data calibrated using matrix-matched standards and LA-ICP-MS analysis, as described above. These final compositions for panel 3b were compared to the in situ 3b analyses to develop empirical calibrations for the row 10 data.

Corning D was used as a secondary standard throughout the analytical campaigns, and the results, accuracy and precision are reported in Table 6.3. Since the Corning D standard was analysed under different circumstances than the row 10 panels due to the circumstances described above, the reanalysis of 3b samples are reported to show accuracy for that campaign.

Overall the accuracy is very good; Co and Cu are the least accurate with relative accuracy of up to -7.0%. Rb and Sr are both very well characterised. RSDs are generally good, excluding analysis of Co, with an RSD of up to 11.5%. Most elements have an RSD of about 3% or better; the exceptions are Ni, Rb, Zr and Sb (up to 5.4% RSD). Ni is present in very low concentrations in the medieval GEW glass, except for Ni in a small number of blue glasses. Rb is present in Corning D in concentrations well below the medieval GEW glass (with Rb contents of about 200ppm and above), and so the precision is likely to be significantly better in the analysis of the samples. Zr is also

present in concentrations below 100ppm; this is approximately the concentration found in the medieval GEW glass.

The thickness of a subset (276 glass pieces) of the GEW samples was measured, with an average of 2.3mm thickness and with only three glass pieces falling below 1.5mm. Therefore, no corrections were applied for thickness, as the critical depth above which 99% of the x-rays of Zr (the element of interest with the highest energy characteristic x-ray) were emitted is calculated to be 1.2-1.5mm based on the analytical parameters used. Furthermore, it was not possible to measure the thickness of in situ glass.

As discussed in Chapter 5 and explored in future chapters, many of the elements analysed are likely to have been affected by surface conditions and cannot be used fully quantitatively. The measurement of some elements is more informative about the analysis and the condition of the glass surface (for example, sulphur). In Chapter 7, five elements (Cu, Zn, Rb, Sr, and Zr) are identified as being well measured by pXRF for the study of medieval stained glass, and only these elements will be reported as quantitative numbers. All other elements are reported as informational numbers only.

6.2.2 Electron microprobe analyses

Electron microprobe (electron probe micro-analyser, EPMA) is a type of electron microscope that is closely related to the scanning electron microscope (SEM), but is optimised for X-ray microanalysis over imaging. It provides elemental composition of a material for major and minor elements present. Electron microscopy operates under similar principles to XRF, but instead of a primary beam of x-rays, it uses a beam of electrons to irradiate the sample material to produce the characteristic x-rays. The EPMA at UCL Wolfson Archaeological Laboratories operates with wavelength dispersive spectrometers (WDS), which disperses the characteristic x-rays by their wavelength rather than their energy. WDS typically has better limits of detection than EDS (Pollard *et al.*, 2007); the detection limits of the UCL instrument is approximately 0.03%. The characteristic x-rays are dispersed by a crystal, which has a crystalline structure with atomic spacings similar to the short wavelength of x-rays; usually multiple crystals are used to accommodate the full range of x-ray wavelengths to be measured (Pollard *et al.*, 2007). The angle at which the x-rays are dispersed is dependent on the wavelength, and the detector is positioned at different locations in order to measure x-rays of different wavelength (i.e., different elements); it records the x-rays as pulses to measure the intensity at each measured wavelength. The WDS for the EPMA at UCL Wolfson Archaeological Laboratories uses moving sequential detectors, which move their positions relative to the crystal to record x-rays of different

wavelengths, one element at a time. Analyses are carried out in a vacuum, in order to reduce x-rays attenuating and scattering in air. Samples are prepared by polishing until flat, and if the material being analysed is electrically insulating, samples are covered with a thin layer of carbon to prevent electrical charging.

Subsamples were removed from the 253 samples of the GEW control group and the four SWW samples, mounted in epoxy resin with the cross-section exposed, and polished to 1µm using diamond paste. The resin blocks were vacuum-coated with carbon and analysed using a JEOL JXA-8100 electron probe microanalyser with three

Table 6.4 Analysis of Corning A, B and D by EPMA with accuracy and precision (RSD) calculated.

	Na_2O	MgO	Al_2O_3	SiO_2	P_2O_5	SO_3	Cl	K_2O	CaO	TiO_2
Given (A)	14.30	2.66	1.00	66.56	0.13	0.14	0.09	2.87	5.03	0.79
Mean (*n*=78)	14.20	2.63	0.94	66.94	0.11	0.14	0.09	2.80	5.04	0.74
Accuracy	-0.73	-1.04	-6.41	0.57	-14.93	-2.15	1.17	-2.29	0.13	-6.27
RSD	3.57	1.93	1.79	0.63	15.15	11.65	7.16	2.24	2.01	12.59
Given (B)	17.00	1.03	4.36	61.55	0.82	0.49	0.16	1.00	8.56	0.089
Mean (*n*=98)	16.95	1.02	4.26	61.93	0.86	0.49	0.17	1.02	8.61	0.09
Accuracy	-0.29	-1.26	-2.29	0.61	5.11	-0.28	3.88	1.54	0.54	3.41
RSD	2.82	3.08	0.97	0.72	6.53	9.71	6.66	2.36	2.23	25.18
Given (D)	1.20	3.94	5.30	55.24	3.93	0.23	0.16	11.3	14.8	0.38
Mean (*n*=103)	1.30	3.89	5.24	55.31	4.16	0.21	0.16	11.05	14.86	0.37
Accuracy	8.17	-1.20	-1.10	0.12	5.90	-10.60	2.40	-2.18	0.41	-2.70
RSD	4.29	1.60	0.78	0.55	2.78	11.37	5.48	1.84	1.89	8.57

	MnO	Fe_2O_3	CoO	CuO	ZnO	SnO_2	Sb_2O_5	BaO	PbO	Total
Given (A)	1.00	1.09	0.17	1.17	0.044	0.19	1.75	0.46	0.0725	**99.47**
Mean (*n*=78)	1.01	1.03	0.17	1.18	0.05	0.19	1.65	0.39	0.07	99.35
Accuracy	0.96	-5.39	-1.75	1.28	14.52	1.22	-5.68	-16.25	-5.78	
RSD	2.41	3.27	8.03	4.64	54.23	7.35	2.47	12.09	22.18	
Given (B)	0.25	0.34	0.046	2.66	0.19	0.0241	0.46	0.077	0.61	**99.72**
Mean (*n*=98)	0.24	0.33	0.04	2.65	0.19		0.41	0.07	0.45	99.76
Accuracy	-4.33	-3.65	-14.38	-0.36	-2.47		-11.12	-11.90	-25.98	
RSD	4.10	5.00	29.09	3.08	15.01		8.89	24.68	6.86	
Given (D)	0.55	0.52	0.023	0.38	0.10	0.10	0.97	0.291	0.241	**99.66**
Mean (*n*=103)	0.54	0.47		0.36	0.10	0.08	0.88	0.25	0.22	99.45
Accuracy	-2.02	-9.65		-4.59	-4.85	-15.54	-9.46	-13.03	-8.17	
RSD	3.08	4.09		7.56	24.54	14.65	4.66	11.44	10.39	

attached wavelength dispersive spectrometers. The machine was operated with an accelerating voltage of 15kV, a beam current of 50nA, a count time of 50s (30s peak, 10s per background), a working distance of 11mm and on area dimensions determined by 800x magnification giving an analysed area of approximately 150 by 110µm. Standard practice was to analyse each subsample five times unless the subsample itself was too small. The elements analysed were Na, Mg, Al, Si, P, S, Cl, K, Ca, Ti, Mn, Fe, Co, Cu, Zn, Sn, Ba and Pb; crystals and peak lines used are reported in Appendix B. The data are reported as oxide weight percent, with totals in the range of 98.3-100.7% (mean 99.5%). Corning A, B and D were used as secondary standards to monitor the machine performance and data quality (Table 6.4). Generally accuracy is good; exceptions include PbO in Corning B and Fe_2O_3 in Corning D. Better accuracy for Na_2O in Corning D (1.2% Na_2O; analysed at 1.3%) would be desired. The measurements with the poorest precision are those present in trace amounts (<0.1%), close to the detection limits. Analysis of ZnO has particularly poor precision (from 15% RSD in Corning B at 0.19% ZnO, to 54% RSD in Corning A at 0.044% ZnO).

The subsamples from panel 3b were analysed by Dr. Kevin Reeves. The rest were analysed by myself with help and advice from Dr. Tom Gregory.

6.2.3 OM and SEM imaging

Clean resin blocks (*i.e.,* without a carbon coating) were examined using a Leica DM 4500 P LED polarising light microscope (optical microscope, OM) equipped with a camera. Carbon-coated resin blocks were examined using a Hitachi S-3400 scanning electron microscope in back-scattered mode. This allowed the investigation of any microstructure of the glass, such as the presence of flashed layers, bubbles or striations. It also allowed the examination of surface conditions such as the presence of grisaille paint or different types of corrosion.

6.2.4 Laser ablation ICP-MS analyses

Laser ablation inductively coupled plasma mass spectrometer (LA-ICP-MS) is similar to its sister technique, (solution-) ICP-MS, but does not require the same lengthy sample preparation in which the sample is digested in acid. Instead, the solid sample is placed inside an ablation cell (or chamber) and a laser is used to remove small particles of sample, producing an aerosol that is then transported to the ICP-MS via a carrier gas. The high temperature (over 6000K, Fricker and Günther, 2016, 1) ICP converts the aerosol to ionised atoms, which pass through the quadrupole mass filter and are separated by their mass to charge ratio to be collected by the detector. The technique

has been used for the analysis of archaeological glasses and other vitreous materials for more than 20 years (Gratuze, 2016; Gratuze *et al.*, 1993) and is an especially powerful tool for the characterisation of trace elements. A small subset of the control group was analysed using this method to help calibrate the pXRF data (see earlier section). Therefore, the subsamples were primarily selected to cover a wide range of trace element concentrations based on the pXRF analyses, although a subsample from each original colour group was also a priority.

19 subsamples from the control group of the GEW were analysed by LA-ICP-MS. The polished resin blocks were re-polished to remove the carbon coating. The LA-ICP-MS analyses were carried out at the Rutherford Laboratory at the Cranfield Forensic Institute by Dr. Fiona Brock (with the kind permission and advice of Professor Andrew Shortland), using a New Wave 213 laser attached to a Thermo Series II ICP-MS. The resin blocks were placed in the ablation cell and the location of analyses controlled using a camera and the computer. The New Wave laser was operated at a wavelength of 213 nm in the spot-scan mode (<1500 µm path, 10 µm/s), with a spot diameter of 30µm, an energy of 0.42 mJ and density (fluence) of >15 J/cm, and a pulse with duration of 2 ns and frequency of 10 Hz.

The RF power of the Thermo Series II ICP-MS was set at 1350-1450 W. Helium was used as the carrier gas (with a flow rate of 500-550 L/min), while argon was used as the coolant, auxiliary and nebuliser gas (coolant gas flow rate 15 L/min, auxiliary gas flow rate 0.9 L/min, and nebuliser gas flow rate 0.8-1.2 L/min), with extraction of -720 to -750 V. The data acquisition was performed in the peak hopping mode, with 18-20 sweeps, a dwell time of 20 ms, measuring 51 elements, with three ablations per sample, with a total acquisition time of about 60s per sample. Each run began with three gas blank analyses, in which gas was collected without ablation, followed by three ablations each on NIST612, NIST610 and Corning A; three to four samples were each ablated three times, each sample separated by three gas blanks to ensure no residual ablated material remained in the chamber. This cycle of standards and samples was repeated up to four times, always ending on the analysis of standards followed by three gas blanks. The unknowns were calibrated against the NIST standards using the consensus values (Jochum *et al.*, 2011); the NIST standards were also used to correct instrumental drift. The concentrations were calculated using a mathematical approach (Gratuze, 1999) rather than using an internal standard following the procedure of van Elteren *et al.* (2009). Further details about the procedures for LA-ICP-MS analysis used in the Rutherford Laboratory can be found in a paper by Giannini *et al.* (2017). The repeated analyses of Corning A were calibrated

Table 6.5 Summary of the analysis of Corning A by LA-ICP-MS (*n*=10). Concentrations are reported as parts per million.

	Given	Mean	Acc.	RSD
Li	46	46	-0.2	6.7
B	621	585	-5.9	5.0
Na	106083	104457	-1.5	4.3
Mg	16041	15832	-1.3	2.0
Al	5292	4620	-12.7	4.5
Si	311144	311481	0.1	1.0
P	370	617	67.0	11.7
K	23825	25504	7.0	12.1
Ca	35949	35654	-0.8	4.1
Ti	4736	4789	1.1	4.8
V	34	37	8.9	2.6
Cr	23	21	-8.8	3.9
Mn	7745	7780	0.5	1.9
Fe	7624	6807	-10.7	7.0
Co	1337	1376	2.9	2.2
Ni	157	181	15.3	2.3
Cu	9347	10165	8.8	2.7
Zn	353	456	29.0	11.7
Rb	91	86	-5.5	4.4
Sr	846	899	6.3	3.1
Zr	37	38	2.3	7.3
Ag	19	17	-7.0	6.5
Sn	1497	1560	4.3	6.8
Sb	13174	15842	20.3	4.0
Ba	4120	4348	5.5	5.9
Pb	628	693	10.3	11.7
Bi	9	9	-3.7	7.8

and corrected in the same way, and used as a secondary standard (Table 6.5). Many elements are well analysed. Exceptions are P, which is difficult to analyse by this technique, and Zn.

6.2.5 Isotope ratio analyses

Thermal ionization mass spectrometry (TIMS) is a technique for measuring isotope ratios in a sample. Sample preparation is a rather laborious process in which the sample material is digested in acid and the fractions containing the element(s) of interest are filtered out. This is placed on a thin metal ribbon which is heated under vacuum until ionisation is achieved. The resultant ions are focused into a beam, which then passed through a magnetic field so that is disperses by mass. This data is used in this research to suggest a provenance for a subset of the GEW, by comparing the Sr and Nd isotope ratios to that of the LBW samples. The samples from SWW were also

analysed as this portion of the project was conducted jointly with, and funded by, the Cardiff-York project (Leverhulme Trust).

Sample preparation and analysis by TIMS was carried out at the Department of Earth Sciences at Royal Holloway, under the supervision of Professor Matthew Thirlwall. Subsamples of glass weighing approximately 125mg were washed with HCl to remove unwanted contaminants and then digested in nitric and hydrofluoric acid and evaporated, digested in nitric acid and then evaporated again, and finally digested in nitric acid again and the solutions placed in a centrifuge. The centrifuged subsamples were then filtered through cation-exchange columns which preferentially absorbed strontium, which was then released using water, and dried. The subsample was dissolved in phosphoric acid and precipitated onto degassed tantalum filaments. These were analysed for strontium isotopes using a multi-collector VG354 thermal ionisation mass spectrometer (TIMS). Accuracy was measured using SRM 987, which yielded $^{87}Sr/^{86}Sr = 0.710228 \pm 0.000003$.

The subsample remaining after the extraction of the Sr was digested in nitric acid and placed in the centrifuge. The centrifuged subsample was passed through two cation exchange columns to isolate the neodymium. The subsamples were loaded onto degassed rhenium filaments and analysed for neodymium isotopes using the same spectrometer. Accuracy was measured by using a laboratory Nd standard (also see Table VI, Part 1 in Thirlwall, 1991; see Vance and Thirlwall, 2002), which yielded $^{143}Nd/^{144}Nd = 0.511406 \pm 0.000007$.

One run failed for unknown reasons, possibly due to low subsample mass. The affected subsamples were therefore rerun on a multicollector (MC)-ICP-MS in static mode, using the Royal Holloway GV Instruments IsoProbe. This technique results in less accurate and less reproducible results (Thirlwall and Anczkiewicz, 2004), but accuracy measured on the Nd standard yielded $^{143}Nd/^{144}Nd = 0.5111310 \pm 0.000008$, which was adequate for the purposes of the present investigation.

6.2.6 Development of glass calibration standards

Three glass standards (AD1, AD2 and AD3) were produced during the course of this research that approximate the composition of medieval glasses with both major and trace elements. Full data sheets are in Appendix C. The raw materials were mixed together at the UCL Institute of Archaeology Wolfson Archaeological Laboratories. The raw materials were sourced from both the UCL Institute of Archaeology and UCL Department of Chemistry, and were of varying purity. The materials were weighed out

beginning with the smallest concentrations, and thoroughly stirred between each addition.

The glasses were melted by Mark Taylor of the Roman Glassmakers, using a ceramic crucible with a lid. The crucibles were made with 60% powdered (120 grit) molochite (calcined kaolin), 30% powdered kaolin, 10% powdered ball clay and a very small amount of deflocculent (c. 1 level teaspoon each of sodium carbonate and sodium silicate dissolved in a yoghurt-potful of boiling water). The slip is made with 10kg of mixed powder to 4.0-4.5 litres of cold water. The crucibles and lids are slipcast using small plaster moulds. They were allowed to dry, then fired to 1400°C.

The glasses were melted in a propane gas furnace. The batches were melted at 1350°C for 4.5 hours, with a c. 15s stir using a stainless steel rod every 30 minutes; the rod was cleaned between stirs to remove the remains of glass from the previous stir. The melts were then annealed at 600°C.

The three standards were characterised by both EPMA and LA-ICP-MS and are currently the subject of an international LA-ICP-MS round robin organised by Dr. Laure Dussubieux, which will allow better characterisation. The target compositions, the proportions of raw materials, and the preliminary recommended compositions for all elements are reported in the data sheets given in Appendix C.

6.3 Tests for methodological development

6.3.1 Elements affected by surface conditions

A series of 23 glass reference standards were analysed by handheld pXRF in order to evaluate the performance of the instrument under ideal circumstances (clean, uncorroded, unpainted flat glass with infinite thickness). A list of these standards can be found in Appendix B (as they are the same standards used to create the empirical calibrations), and includes Corning A, B and D, the Newton/Pilkington medieval glasses, and three glass standards made during the course of this research (see previous section, 6.2.6).

The pXRF data was also evaluated by comparing the data to the data produced by EPMA and LA-ICP-MS on the same GEW glass of the control group. This allows a direct comparison of a range of elements and identification of possible problems due to surface conditions of the medieval window glass.

6.3.2 The interference of lead cames on in situ analysis

A series of tests were designed to evaluate the effect that distance between sample and spectrometer has on analysis of medieval stained glass by handheld pXRF. A group of 30 pieces of glass from panel 3b of the GEW was analysed by handheld pXRF both using a test stand (directly on the surface) and again under in situ conditions, when the pieces had been restored into their lead came framework. Both datasets were calibrated to the same range of matrix-matched standards as described above in order to correct any differences between them due to the unavoidable change in spectrometer model (DP-4000 and DP-6000CC, both by Innov-X/Olympus).

Three glass standards, Corning A, B and D, and three medieval pieces from York Minster stores (YGT A, B and C) were analysed repeatedly at discrete and increasing distances using microscope slides (thickness 1mm) to hold the standards over the spectrometer using a test stand. Analyses were conducted at working distances from 0-8mm from the face of the spectrometer. Raw counts (i.e., the net counts at the specific energy peak, rather than a sum volume from underneath the peak) are examined as well as the final data after being transformed by the Innov-X/Olympus algorithm.

The standards used for empirical calibrations (Appendix B) were analysed with a working distance equal to 0mm (i.e., flush against the spectrometer face) and 5mm (a distance chosen to accommodate most lead cames). The R^2 values for all elements are examined as a measure of how well the analysed data are in linear agreement with the known concentrations of the standards (NB: not a measure of accuracy, but if and how well the data can be corrected). This will be used to determine the possibility of correcting the data collected if a constant working distance is maintained between the spectrometer and sample.

6.4 Identification of glass batches

The identification of the batch of glass is an important tool in this research that will enable the study of the organisation of production within John Thornton's workshop. Like other windows of the International Gothic style (Marks, 1993), the GEW is characterised by the predominant use of white glass over other colours, and therefore this study focuses on the identification of original white glass batches in a panel as this has the most spread across a panel. Glass of different colours cannot be compared as they were by definition created in separate pots and are therefore different batches.

Groups of glass can be suggested as a batch if their composition is "identical", i.e., their concentrations fall within the experimental error of the analytical equipment, for all elements measured (Freestone *et al.*, 2009). However, this method of identification is not always practical for large datasets with a similar origin that therefore have overlapping compositions. In the present research, for example, multiple batches were found to have shared possible members, i.e., a glass piece might be identical to the members of two groups which are not identical to each other. Another study utilising the concept of the batch suggested batches by examining metal arrowheads that were deposited in bundles with the soldiers of the Terracotta Army, and found that each bundle formed a compositional cluster (although in many cases overlapping each other). This approach, too, does not translate perfectly to the present situation.

Two approaches were tested, both based upon hierarchical cluster analysis. The first approach examined the data panel by panel, separately (panel-by-panel approach), and the second examined all of the original white glass in the window (cross-window approach).

In the panel-by-panel approach, batches in the control group were identified based on major element compositions as analysed by EPMA-WDS. The criterion of identical composition was applied using a standard deviation. As every subsample analysed by EPMA was analysed multiple times, the standard deviation of the multiple analyses could be calculated for every element on every white glass subsample. The maximum of these for each element from the original white glass group was set as the boundary; as each subsample is generally less than 2mm in either direction, this number should encompass both machine error and a small amount of heterogeneity in the glass. Two glass pieces were designated identical in composition if they are within two standard deviations for all elements analysed.

To address the problem of overlapping compositions, the EPMA data of the control group was also analysed using hierarchical cluster analysis with R software. Elements which were below detection limits for some samples were excluded. The data were standardized to range of 0-1 and analysed using squared Euclidian distances with average linkage. The cophenetic distance at which to delineate the clusters (i.e., the height at which to cut the “tree” in the resulting dendrogram) was guided by the identicalness of groups as determined above. In many cases, the combination of these approaches allowed the distinction of different batches; in some cases, some batches could not be separated and were instead included as one group (clearly marked) in order to avoid the imposition of meaningless groups on the data.

Hierarchical cluster analysis was also carried out on the pXRF data of the five quantifiable elements (Cu, Zn, Rb, Sr, and Zr, see Chapter 7) and the cophenetic distance at which to delineate batches were guided by the control group batches.

The trace element data from across the window were also examined together by hierarchical cluster analysis on the five quantifiable elements by pXRF (cross-window approach), and compared to the batches identified in the panel-by-panel approach. The results of both methods will be reported, and the degree to which they agree.

6.5 Summary of the research methods

The majority of the materials analysed in this study come from the GEW, with some comparative samples from an archaeological kiln site at Little Birches, Wolseley in Staffordshire, provided by the Cardiff-York project. Selection of panels was partly directed by availability and the schedule of the conservation works being carried out by YGT. Analysis of the glass was carried out using pXRF, EPMA-WDS, LA-ICP-MS, TIMS, and OM and SEM for imaging. This multi-analytical approach is designed to address the three topics of this research: medieval glass-making technology, the organisation of production in the glass-painting workshop of John Thornton, and the further development of a pXRF methodology for medieval stained glass windows.

For the development of a methodology using pXRF, the analysis of the control group by EPMA-WDS and LA-ICP-MS will allow the evaluation of the performance of pXRF on medieval stained glass with variable surface conditions compared to pXRF performance on glass standards. A series of tests was also designed to show the effect that increased distance between the spectrometer and sample has on the final result. The methodology will also be evaluated in light of its performance in the study of technology and production.

A study into the glass-making technology evidenced in the GEW will be based mostly on the analysis of major elements by EPMA-WDS, and the determination regional provenance will be attempted based on synthesis of previously published data (Chapter 3). The trace element data analysed by pXRF will be used to show the same groups for a larger dataset, and preliminary observations about possible trace element signatures based on regional recipes will be made. The white glass of the GEW will be compared to English sources; in particular, the GEW glass will be compared to Staffordshire glass by means of TIMS analysis of isotope ratios.

The identification of batches in the original white glass will be a useful tool for the study of the organisation of production in John Thornton's workshop. The use of different

batches within a panel will be compared to different models of production based on well-known methods used in automobile manufacturing, and these results will be interpreted within the historical framework of medieval guilds and apprenticeship.

CHAPTER 7

Performance of handheld pXRF in the analysis of medieval stained glass

This chapter reports results pertaining to the evaluation of the performance of pXRF in the analysis of medieval stained glass windows, in light of the obstacles discussed in Chapter 5 (surface conditions and the interference of lead cames). The first part is focused on assessing the analysis of different elements, through (1) comparison of pXRF analyses of matrix-matched standards against the consensus values in order to assess how well the pXRF performs under ideal conditions, and (2) comparison of pXRF analyses of a subset of the GEW glass against the results obtained using EPMA-WDS or LA-ICP-MS on the cross-section in order to assess how well the pXRF performs on medieval glass with suboptimal surface conditions. Through these results, elements that are well-measured despite surface conditions are identified. This is followed by an overview of the depth of analysis by pXRF, which serves to explain the superior analysis of certain heavy trace elements despite poor surface conditions. The raw material origins of the quantifiable elements identified in this study is also addressed.

The latter part of the chapter is focused on determining the effect that distance between spectrometer and sample (such as that caused by lead cames) has on the analytical results, through (1) comparison of pXRF analysis of one disassembled GEW panel (3b) versus analysis of the same panel when encased in lead cames (i.e., in situ conditions) and (2) a controlled laboratory experiment in which matrix-matched standards and medieval glass pieces were analysed at increasing discrete distances from 0mm (on the surface) up to 8mm. This is followed by an overview of the factors affecting the intensity measured by pXRF when the spectrometer is not placed directly against the sample

surface. These tests were conducted with the aim of developing an attachment for the spectrometer that maintains a constant distance between spectrometer and sample, and which bypasses the interference of lead cames. The production of the attachment, nicknamed the WindoLyzer 5, is described, and health and safety concerns addressed.

7.1 Trace element methodology[14]

7.1.1 pXRF performance on standards and medieval glass

Analysis of matrix-matched standards by handheld pXRF (Figure 7.1, left column) show that the accuracy of the proprietary algorithm for the "Soils" mode is variable between different elements (represented in Figure 7.1 by the slope value of y=mx; the closer m is to 1, the more accurate the analyses). For example, analyses of Ca, Cu and Sr were relatively well measured in terms of accuracy, while S is very poorly characterised. However, for most elements, there is good linear agreement between the measured intensity and the given concentrations (represented in Figure 7.1 by the coefficient of determination, R^2).[15]

The control group of the GEW window glass were analysed by EPMA-WDS (*n*=253), and a smaller group by LA-ICP-MS (*n*=19), allowing comparison with pXRF results (after applying empirical calibrations based on the analysis of the matrix-matched standards) for the identification of interferences due to surface conditions. The GEW glass showed variable surface conditions; most pieces have grisaille, several with yellow silver stain covering part of or all of the surface, and the deterioration of the glass varied from very minimal (nearly perfect or with very minor micro-pitting) to highly corroded (including large areas of pitting and loss of the glassy surface). Comparison of pXRF with EPMA-WDS or LA-ICP-MS for several elements are also reported in Figure 7.1 (right column), with the line y=x also plotted to illustrate over- and under-reported values. In comparison with the standards analysis, the analysis of many elements by pXRF on the surface have poor linear agreement with EPMA-WDS or LA-ICP-MS on the cross-section, suggesting that analysis of those elements is affected by surface conditions. Table 7.1 summarises the findings (reported using the R^2 value of the analyses on standards and on medieval glass) with possible sources of interference (corrosion processes, grisaille, etc.) noted.

[14] Part of the results of this section have been published (Adlington and Freestone, 2017).
[15] The coefficient of determination R^2 describes how well the linear regression explains the data, and in this case is a measurement of how well the pXRF results correlate to the “actual” concentrations (i.e., consensual values of the standards, or the EPMA/ICP results of the medieval glass). The closer R^2 is to 1, the better the correlation. Regardless of accuracy, a good correlation means the data can be corrected through empirical calibration with greater confidence.

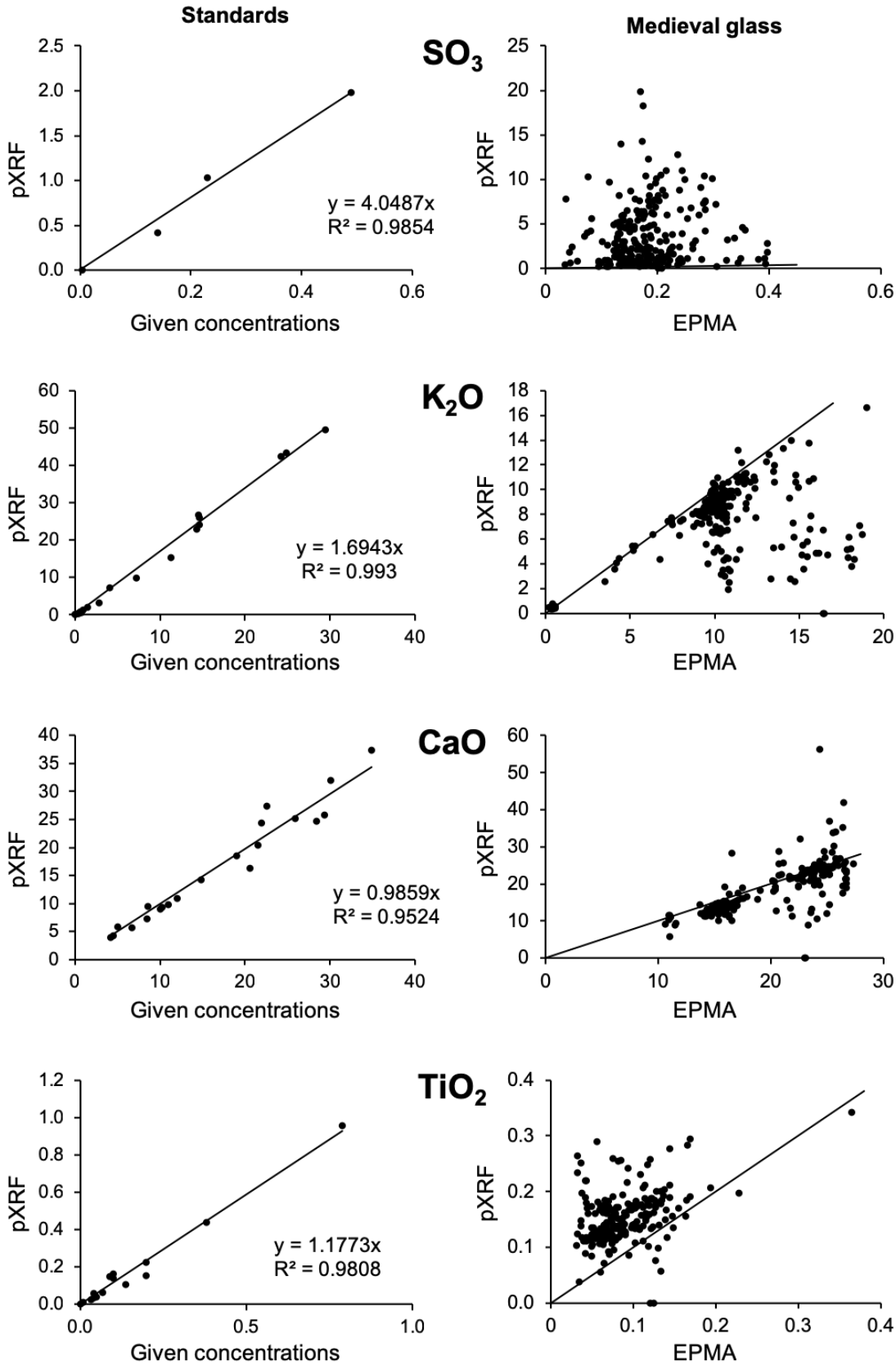

Figure 7.1 Evaluation of pXRF performance analysing medieval glass for several elements. On the left, pXRF analysis of standards are plotted against their known compositions, with a best-fit line forced through 0. For most elements there is an excellent correlation. On the right, surface analysis by pXRF is compared to EPMA or LA-ICP-MS analysis of the cross-section, with the line y=x plotted so that over- or underreported values can be easily identified. Surface

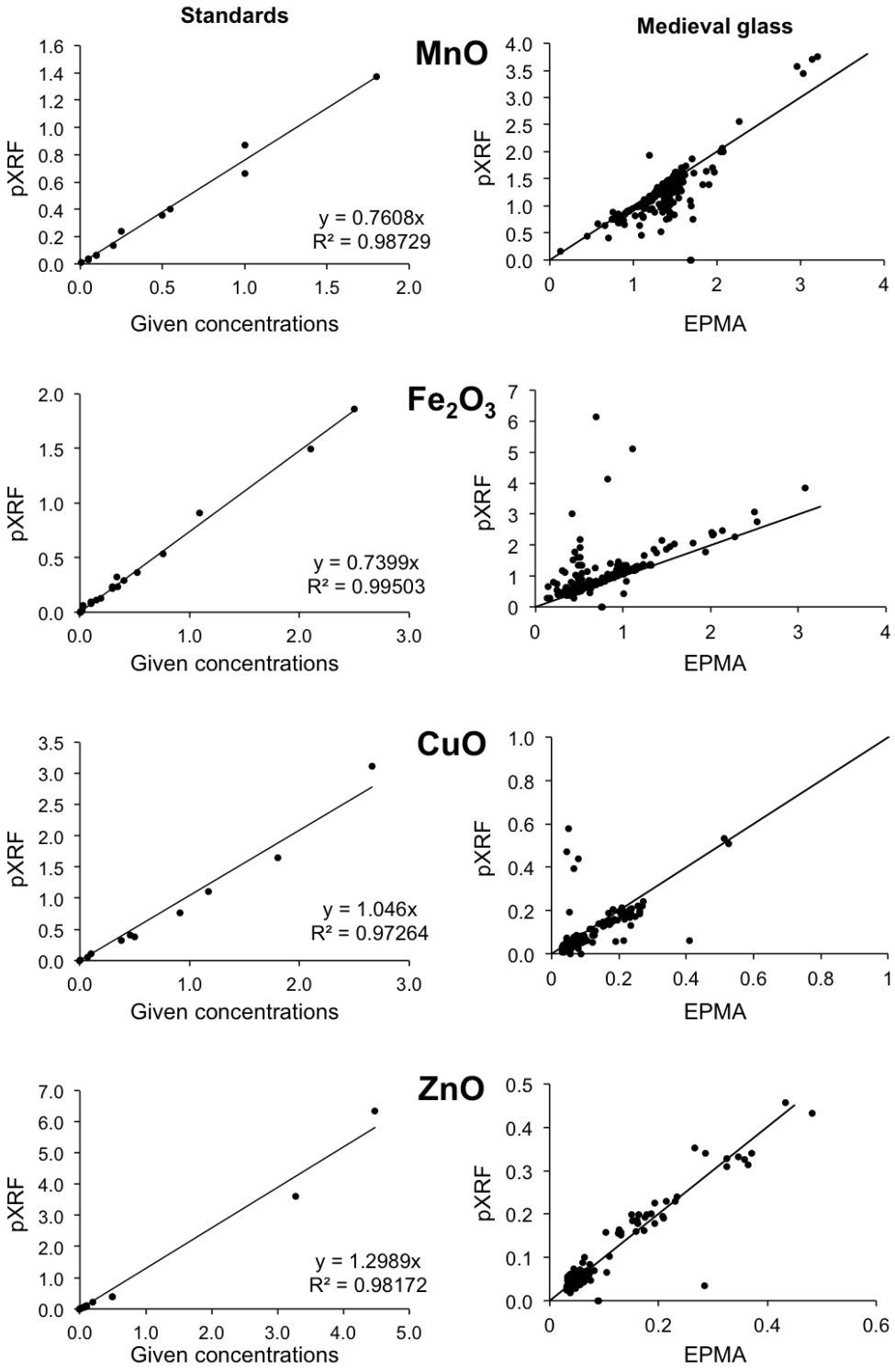

(Figure 7.1 continued) conditions affected the analysis of most elements; rubidium, strontium and zirconium are well analysed. All elements are reported as oxide weight percentage, except for rubidium, strontium and zirconium (marked with an asterisk), which are reported as element parts per million.

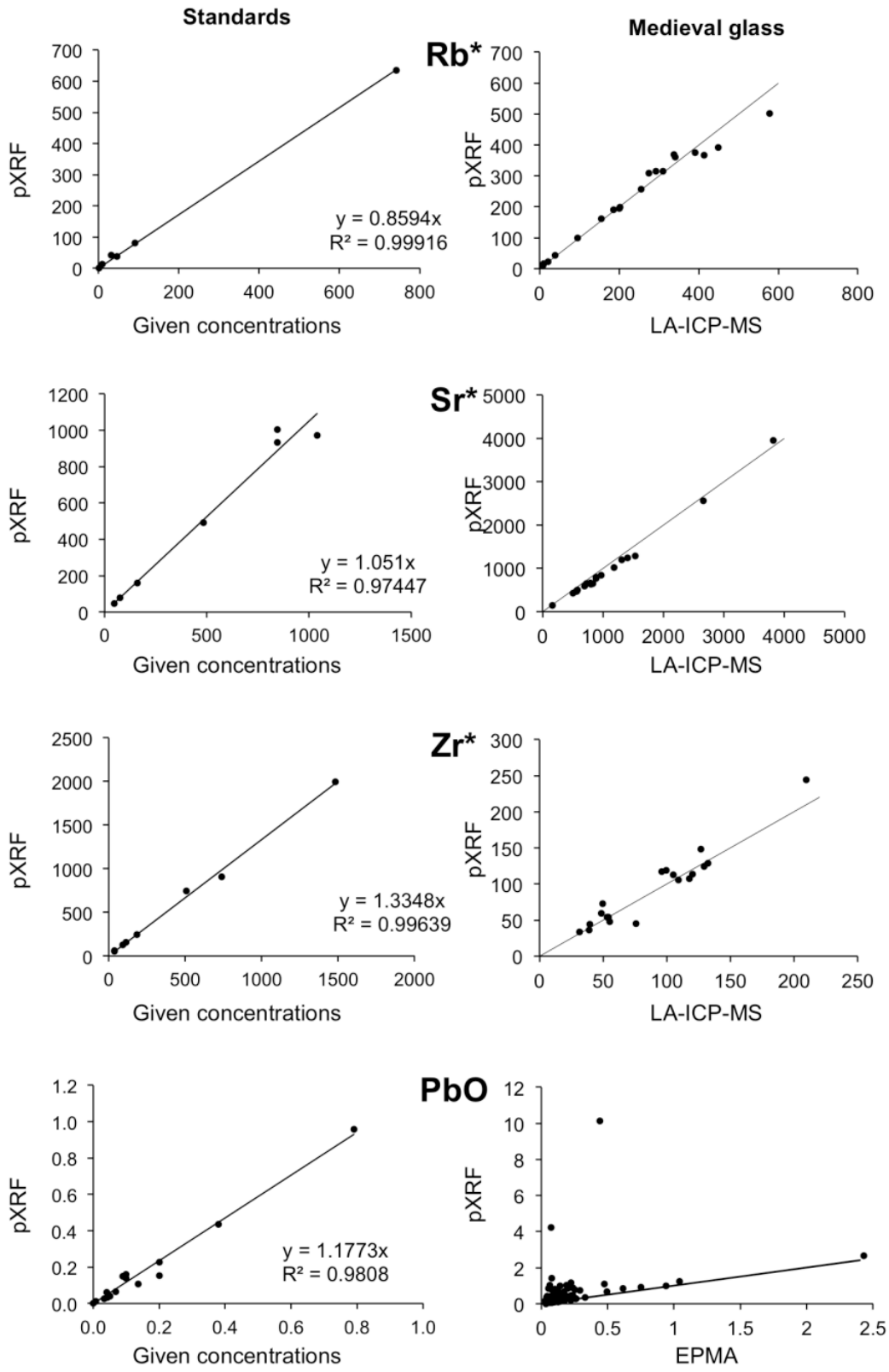

(Figure 7.1 continued)

Table 7.1 A summary of pXRF performance on standards and on medieval stained glass. The pXRF data was compared to known composition of standard glass, with R^2 (st) reported; also, it was compared to EPMA or LA-ICP-MS analysis of the same medieval glass pieces, with R^2 (med) reported. R^2 is not a measure of accuracy, but shows the linear agreement between the two values, indicating whether the analysis can be corrected through empirical calibration. Elements marked by an asterisk were analysed by LA-ICP-MS rather than EPMA. The up and down arrows indicate whether the element concentration is generally over- or underreported in the pXRF data. Possible sources of influences due to surface conditions are given in the final column.

Element	R^2 (st)	R^2 (med)	Possible source(s) of interference
P	0.970	0.167 ↑↓	Variably affected by leached layer, sometimes depleted and others enriched (e.g., Sterpenich and Libourel, 2001)
S	0.985	-0.049 ↑	Corrosion products in the form of sulphates; Enrichment in the leached layer**.** Also may be present in grisaille (cf. Carmona, Villegas and Navarro, 2006).
Cl	0.842	-0.720 ↑	Corrosion products in the form of chlorides
K	0.993	-0.251 ↓	Leaching of potassium ions from the surface layer
Ca	0.953	0.530 ↑↓	Ca-containing corrosion products such as gypsum; Leaching from the surface
Ti	0.975	-0.795 ↑	Enriched in the leached layer**;** Present in grisaille.
Mn	0.987	0.688 ↓	Leaching from the surface layer*
Fe	0.995	0.402 ↑	A major element in grisaille; Enriched in the leached layer
Co	0.950	0.450 ↑↓	Enriched in the leached layer**;** Present in grisaille
Ni*	0.949	0.943	Well analysed, but close to or below detection limits for most of the GEW glasses
Cu	0.973	0.953	Well analysed except for several red-flashed glasses, which are coloured with copper and are heterogeneous
Zn	0.982	0.891	Well analysed - good linear agreement on both glass standards and medieval glass of GEW
Rb*	0.999	0.969	
Sr*	0.974	0.983	
Zr*	0.996	0.922	
Pb	0.997	0.089 ↑	A major component in grisaille; Pb also migrates to surrounding glass

The comparative scatterplots for some elements show linear agreement for some of the glass pieces, with other samples showing either enrichment (e.g., Fe_2O_3 and PbO) or depletion (e.g., K_2O and MnO) in the surface.

The results of the analyses on the medieval glass pieces agree with expectations based on the available literature. Sulphur and chlorine are both severely elevated in the pXRF

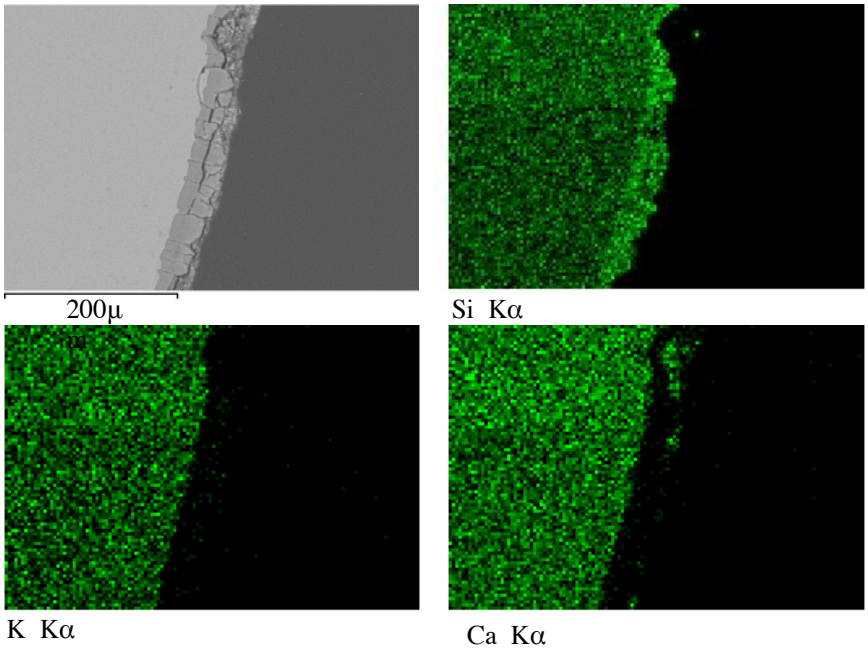

Figure 7.2 SEM-EDS mapping of a GEW sample cross-section (15g-G1) showing the distribution of Si, K and Ca in the bulk glass compared to weathered glass. Si is enriched, while both K and Ca are depleted. Ca is also present in a corrosion deposit on the surface

analyses, due to the accumulation of corrosion products in the form of sulphates and chlorides. Potassium is underreported, due to the preferential leaching of K^+ ions from the surface of the glass. Analysis of calcium was not as poor; for many samples, the calcium concentrations are underreported, but for others, the results are elevated, due to the incorporation of the leached Ca^{2+} ions into corrosion crusts (such as gypsum or calcite, see Figure 7.2). For this set of glass (as the precise corrosion process will vary with composition and environment), it is possible that the greater solubility of potassium resulted in it being washed away by rain rather than incorporated into the weathering crusts on the surface of the glass. Many of the transition metals were better analysed. Some of these (Ti, Fe, Co) are generally enriched in the leached layer, and can also be found in grisaille; Fe in particular is a major component of typical grisaille recipes. In previous studies, the behaviour of manganese has been variable: sometimes it is found to have been leached, and other to have been enriched in the surface layer (in particular, see Lombardo *et al.*, 2010; also see studies cited in Chapter 5). In the glass of the GEW, it appears that manganese has been leached from the surface. Lead is typically over-reported, due to its significant presence in grisaille and its migration through the surrounding glass (Figure 7.3).

Despite the presence of copper and zinc in grisaille, sometimes in significant concentrations (Machado *et al.*, 2017; Vilarigues and da Silva, 2004), both were well analysed in the medieval glass and appear unaffected by surface conditions. All of the

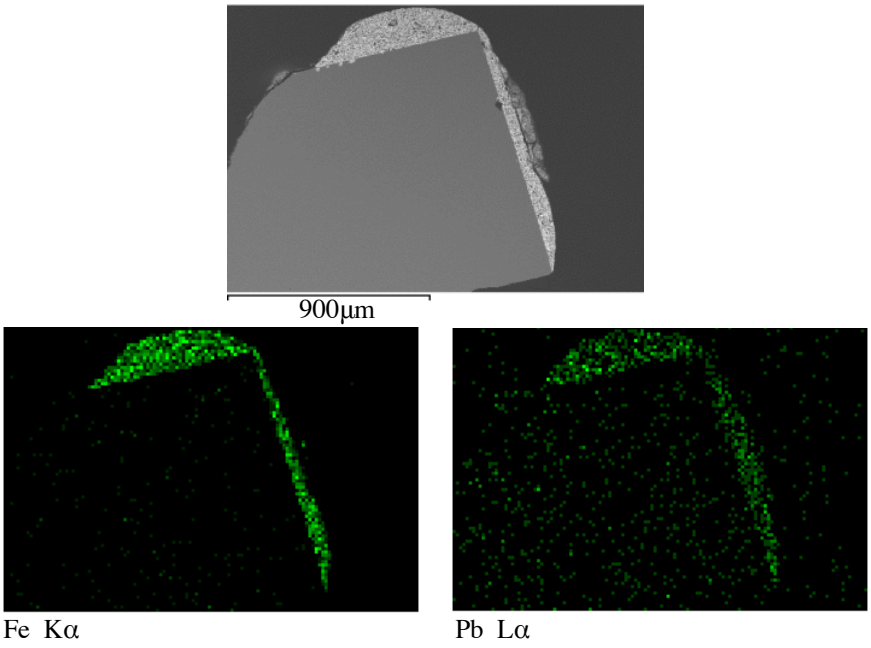

Figure 7.3 SEM-EDS mapping of a GEW sample cross-section (15g-W3) showing the distribution of of Fe and Pb in the bulk glass compared to the grisaille painted on the surface. All three are major components in the grisaille layers.

samples whose copper concentrations were significantly over- or under-reported are red glass pieces, which are coloured by copper and are heterogeneous by definition (as flashed glass). While the R^2 for Ni is favourable, the element is present in concentrations below the detection limits for about two thirds of the GEW control group and therefore will have limited use except for the identification of Ni-rich blue glass pieces.

In keeping with previous observations by Dungworth (2012b), rubidium, strontium and zirconium are also well analysed in the GEW glass, and these elements do not appear to have been greatly affected by surface conditions despite previous work indicating that rubidium is leached from and strontium and zirconium enriched in the altered surface layer (Sterpenich and Libourel, 2001).

Therefore, Cu, Zn, Rb, Sr and Zr are considered the quantifiable elements in this research, while all other reported are considered semi-quantitative or informational only.

7.1.2 Deterioration and the depth of analysis

The effect of a layer of altered composition on surface analyses by pXRF can be explained through a consideration of the depth of analysis: how far the primary radiation penetrates into the sample material, and from what depth the characteristic X-rays able to escape. More simply, these explain what the data is characterising - the first 20µm on the surface, or the first 2000µm? The depth of analysis is dependent on the specific configuration of the spectrometer (the energy of the primary radiation, and the angles of

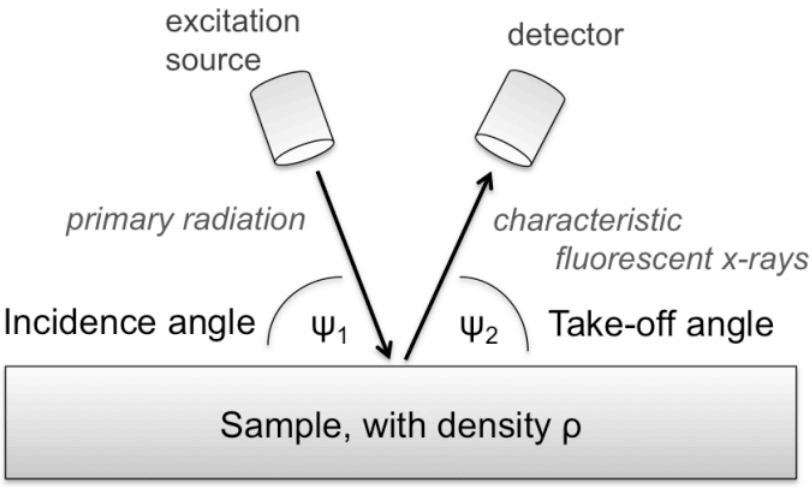

Figure 7.4 An illustration of the parameters of XRF analysis, including the identification of the angles, ψ_1 and ψ_2, which are variables in Equation 2. This equation describes both the primary radiation penetrating the sample at angle ψ_1 and the characteristic fluorescent X-ray travelling out of the sample to the detector at angle ψ_2.

take-off and incidence), on the density of the sample material, and on the energy of the element's characteristic fluorescent radiation (Potts *et al.*, 1997b). Equation 7.1, adapted from Potts, Williams-Thorpe and Webb (1997b) and Kaiser and Shugar (2012), may be used to calculate the depth, x, from which a percentage of fluorescent X-rays, $\frac{I_x}{I_0}$, are emitted from a sample. To calculate the critical depth, x_c, from which 99% of the fluorescent X-rays are emitted, $\frac{I_x}{I_0}$ is set to 0.99.

$$x = -\frac{\ln\left(1-\frac{I_x}{I_0}\right)}{[\rho \cdot \mu_{net}]} \quad \text{(Equation 7.1)}$$

ρ is the density of the sample and μ_{net} is the bulk mass attenuation coefficient, defined by Equation 7.2 (Potts *et al.*, 1997b). It is the sum of two terms, the first describing the attenuation of the primary radiation penetrating the sample at an angle of ψ_1 (the incidence angle, between the excitation source and the sample); and the second describing the attenuation of the fluorescent X-rays travelling out of the sample to the detector at an angle of ψ_2 (the take-off angle, between the detector and sample; Figure 7.4).

$$\mu_{net} = \frac{\mu_{source}}{\sin\psi_1} + \frac{\mu_{K\alpha}}{\sin\psi_2} \quad \text{(Equation 7.2)}$$

The mean average of the original glass was used to estimate the composition and density of the sample material matrix. The mass attenuation coefficients were obtained using the NIST website[16].

As the depth of analysis is dependent upon the energy of the characteristic X-rays of each element, different elements are read from different depths within the sample; heavier elements with higher energy characteristic X-rays are read from deeper within the glass. The depth function is logarithmic (Figure 7.5), meaning a greater percentage of the emitted X-rays will originate from the shallower layers. Even in the present case, in which much of the weathered layer has been removed in conservation, there is a leached layer of altered composition (Figure 7.6), which has an observable effect on the lighter elements as seen by the comparison between EPMA and pXRF (refer again to Figure 7.1). However, pXRF analyses of prepared standard reference materials under

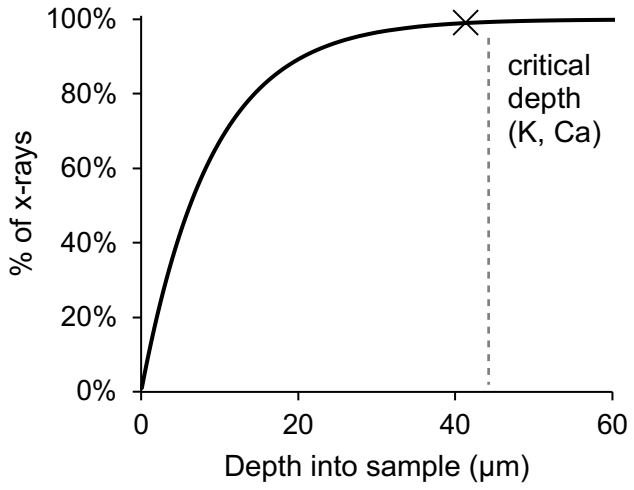

Figure 7.5 Graph of the logarithmic function that describes the percentage of the characteristic X-rays, $I_x \ / \ I_0$, that originate from within a depth, x, in a sample. The critical depth, from which 99% of X-rays originate, is marked with a cross. This graph illustrates the depth of analysis of potassium and calcium. The average composition of the original glass from the original GEW glass was used to approximate the sample density, and the parameters of the pXRF analysis were used in the calculation.

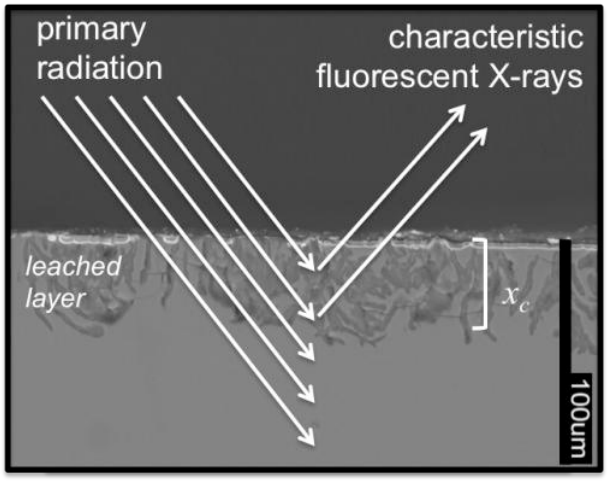

Figure 7.6 Illustration of the critical depth of analysis, x_c, of potassium and calcium, imposed on a back-scattered electron image of a glass from the GEW (3b-R3), which shows the extent of the leached layer and the resultant effect on surface analysis.

[16] http://physics.nist.gov/PhysRefData/Xcom/html/xcom1.html

the same operating conditions show a good linear correlation with the given values, indicating that the errors in the analysis of the medieval glass are an artefact of the corroded glass surface and not, for example, due to the conduct of the analyses in air.

By selecting heavy elements with higher energy characteristic X-rays, which are generated in deeper areas of the glass, there is observable improvement in the data. In particular, the elements Cu, Zn, Rb, Sr and Zr were well measured by pXRF. Although it has been shown that these trace elements are also altered by corrosion (Sterpenich and Libourel, 2001), due to the greater depth of analysis associated with these heavy elements (Table 7.2, Figure 7.7), they are still measured with great enough precision to identify batches (see Chapter 9). It is possible that for more heavily deteriorated glasses the trace element proxy methodology may not be adequate, particularly in the analysis of the transition metals Cu and Zn. It is also important to note that the internal- and

Table 7.2 The depths, in micron, at which different percentages of the characteristic x-rays are read for a selection of elements. Calculations are based on the analytical parameters of the current study and a sample of the average composition of the GEW glass.

I_x / I_0	P	K	Ca	Cu	Zn	Rb	Sr	Zr	Pb
99%	12	41	41	218	265	872	999	1325	741
90%	6.1	21	21	109	132	436	500	662	371
75%	3.7	12	12	66	80	262	301	399	223
50%	1.8	6.2	6.2	33	40	131	150	199	112
25%	0.8	2.6	2.6	14	17	54	62	83	46

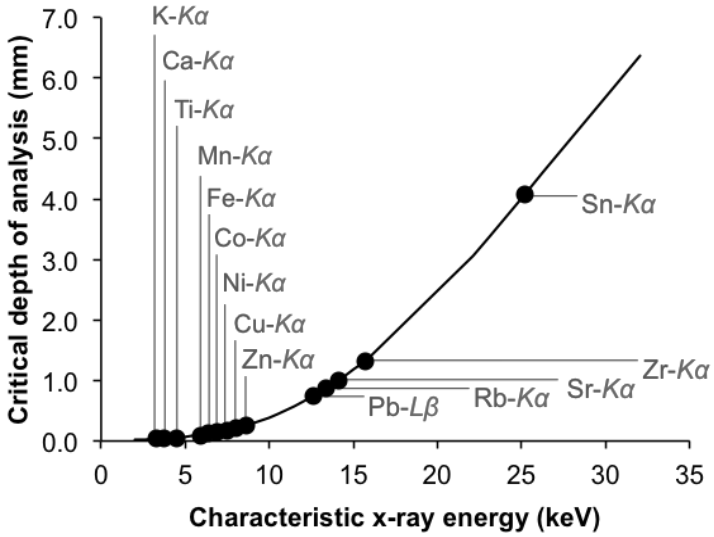

Figure 7.7 Graph showing the critical depths of analysis for selected elements under the analytical parameters of the current research, showing the relationship between the energy of the characteristic x-ray and the critical depth of analysis (the depth from which 99% of x-rays are measured).

external-facing surfaces of the glass will have experienced different environmental exposure and will therefore display different levels and/or types of deterioration, and the analyst should examine the glass and select the surface to be analysed carefully to optimise the results.

The presence of grisaille, as well as yellow stain, similarly has a great effect on certain elements, in particular iron and lead, which make up a large part of the grisaille pigment. Despite the depth of analysis of these elements (note that lead is read from the L_β line, as a very high accelerating voltage is required to excite the K_α x-rays), the logarithmic depth function means that the influence of the grisaille layer is great enough to distort the results for these elements.

The calculation of the depth of analysis of the elements of interest is also important in the evaluation of the sample's thickness and suitability for quantitative pXRF analysis. In the present study, the glass of Great East Window was generally 2mm, which exceeds the critical depth of analysis of the heavy trace elements. Depending on the spectrometer parameters and the composition of the glass being analysed, corrections may need to be made if the critical depth exceeds the sample thickness (Kaiser and Shugar, 2012; Sitko, 2009).

A further implication is the need for tailored calibration in order to improve accuracy and inter-laboratory comparability. Varying surface conditions between medieval glass of different composition, date and environmental exposure may necessitate the development of empirical calibrations based at least in part on the analysis of a control group on the cross-section with a technique such as LA-ICP-MS. Doing so helps to correct not only machine-related error but errors due to surface conditions.

7.1.3 Trace elements in medieval forest glass

Trace elements are included in a glass recipe unconsciously, as they are present in such small quantities that they have negligible impact on the properties of the raw materials and the final glass. However, the trace element composition of a glass can impart important information regarding its production and provenance (e.g., Brems and Degryse, 2014; Gratuze, 2013; Janssens *et al.*, 2013; Kunicki-Goldfinger *et al.*, 2008).

The wood ash used in medieval forest glass contributes to the trace element contents of the glass. Strontium concentrations enter glass primarily through the lime-bearing raw materials, as strontium and calcium are a geochemically coherent pair; due to similar chemical properties including their ionic charge and ionic radius (Sr^{2+}: 118 pm; Ca^{2+}: 100 pm), they frequently occur together in nature in particular minerals (the Goldschmidt

Rules, revised by Ringwood, 1955; also cf. Brems *et al.*, 2013a; Salminen *et al.*, 2005; Shannon, 1976). Similarly, rubidium (Rb^+, ionic radius 152 pm) and potassium (K^+ 138 pm) are geochemically coherent (the Goldschmidt Rules, revised by Ringwood, 1955; also cf. Brems *et al.*, 2013a; Salminen *et al.*, 2005; Shannon, 1976). The composition of wood ash and glass made from wood ash are highly variable, and dependent on numerous factors, as detailed in Chapter 3. While trace elements are not often included in compositional studies comparing different ashes and/or their resultant glasses, it is reasonable to assume that the same factors affect their concentration in the glass. Analysis of beech, oak and bracken ashes in England (Sheffield/Derbyshire) showed that bracken ashes had higher rubidium (250 ppm) and lower strontium (130 ppm) concentrations than both tree species (80-110 ppm Rb; 530-620 ppm Sr); all three ashes contained low zirconium (30-40ppm: Jackson *et al.*, 2005). Glass made using kelp (seaweed) contains strontium in very high concentrations (over 2000 ppm, Dungworth, 2009). Analyses on medieval glass from Germany relates the major elements to parts of the beech tree: potassium with the trunk, calcium with the bark, and magnesium with chlorophyll (Wedepohl, 1998); observations of correlations between trace elements and those majors led the authors to conclude that rubidium is concentrated in the trunk with potassium and strontium in the bark with calcium (Wedepohl and Simon, 2010). As these correlations are based upon glass compositions and not on plant or ash compositions, the particular factors affecting the glass composition is inconclusive; given the geochemical coherence between strontium/calcium, and rubidium/potassium, the observed correlations are not unexpected.

Zirconium concentrations are mostly related to the sand raw material, and is present in sand as zircons, $ZrSiO_4$ (Henderson, 2013). The relative and absolute concentrations of zirconium can help identify changes in the silica source, and distinguish production centres (Aerts *et al.*, 2003; Freestone *et al.*, 2002; Janssens *et al.*, 2013; Velde, 2013). The strontium contents of sand have been widely studied, usually under the study of Roman glass (Brems *et al.*, 2013a; Degryse *et al.*, 2006; Freestone *et al.*, 2003, 2000, Silvestri *et al.*, 2008a, 2008b). The strontium contents varies in different minerals; for example, aragonite (the polymorph of calcium carbonate, $CaCO_3$, found in seashells) contains higher concentrations of strontium than calcite (the polymorph of calcium carbonate found in limestone; Brems *et al.*, 2013a; Katz *et al.*, 1972; Kinsman, 1969; Silvestri *et al.*, 2008b). Therefore, the strontium concentration of a natron glass can indicate the lime source - aragonite-bearing marine sand, limestone-bearing river sands, and/or the addition of an extra lime source such as crushed seashells (Freestone *et al.*, 2003; Silvestri *et al.*, 2008b; Wedepohl and Baumann, 2000). The mixture of these and

other minerals present in the sand contribute to the strontium concentrations of different sand sources and the glasses made from them (Degryse *et al.*, 2006; Freestone *et al.*, 2005). Roman natron glasses made with marine sands generally contain about 400ppm strontium, while glasses made with inland sands contain about 150ppm strontium (Brems *et al.*, 2013a; Silvestri *et al.*, 2008a).

Concentrations of copper and zinc in medieval forest glass can be affected by both the basic raw materials (sand or wood ash) as well as by colouring agents. Copper is found in wood and fern ashes (c. 125-180 ppm, Jackson *et al.*, 2005). Analyses of marine beach sand report very low concentrations of copper (Brems and Degryse, 2014; Silvestri *et al.*, 2006), but fewer studies have been undertaken on the trace element composition of inland river sands. Similarly, zinc is found in significant concentrations in wood and fern ashes (Jackson *et al.*, 2005 reports c. 2100 ppm in beech ashes and c. 730 ppm in bracken ashes), and is variably present in marine sands (Brems and Degryse, 2014; Silvestri *et al.*, 2006). However, both elements are commonly associated with colouring medieval glass. Copper was widely used in the medieval period to colour red glass (Kunicki-Goldfinger *et al.*, 2014). The original blue glass of the GEW was coloured using a cobalt ore containing zinc that was in use in the medieval period and may have come from Germany (Gratuze *et al.*, 1995; see next chapter); the blue also has high concentrations of copper, which can also be used to colour glass blue. Therefore, the characterisation of these elements will be less useful for study base glass recipes and provenance.

In Chapter 3, regional patterns in medieval glass composition were characterised based on major element concentrations. These patterns are presumed to be the result of various factors, including bioavailability of elements in the underlying substratum, regional availability of plant species, and technological traditions and/or choices by the craftsmen. Trace element compositions are less widely measured and published, and so unpublished LA-ICP-MS data from the Cardiff-York project are used to compare medieval compositions from St.-Denis, the Weald and Staffordshire in the NW French/English region; Zutphen, Heemskerk, Cologne, and Oppenheim in the Rhenish region; and Altenberg, Stendal, Esslingen and Erfurt in the Central European region.

In this limited dataset, there are observable differences between the three regions in terms of their trace element contents (Figure 7.8). The glass found in central Europe have rubidium contents above about 300ppm. The English/French and Rhenish glass generally have less than 300ppm Rb, and the latter are further distinguished by their higher Sr contents (above about 1300 ppm). Several glass pieces from windows in the Rhenish region were more similar to central European glass in both major elements (i.e.,

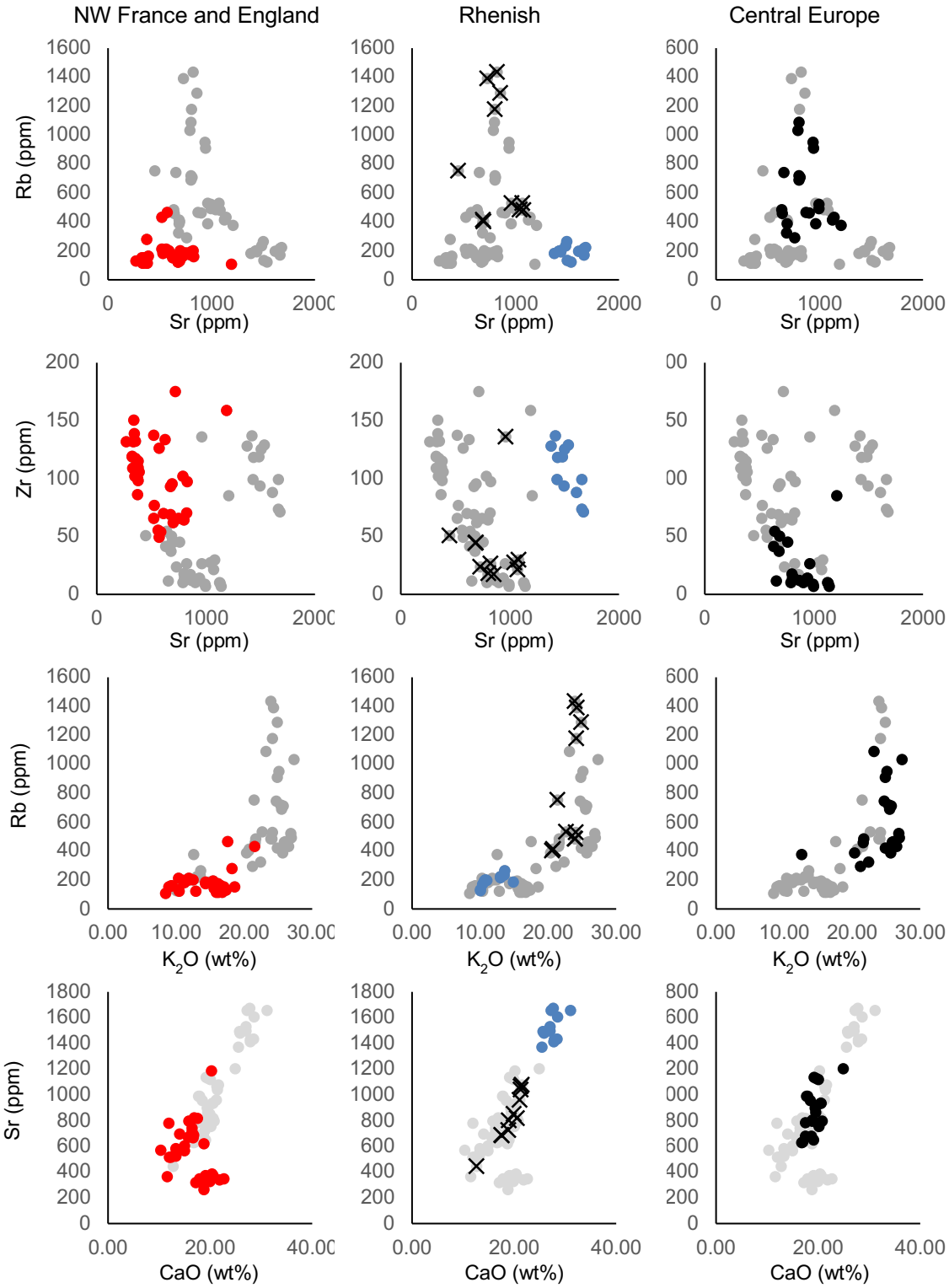

Figure 7.8 Scatterplots showing the trace element composition for three regions in northern Europe: (left) England and St.-Denis in NW France; (middle) areas surrounding the Rhine and its tributaries; and (right) areas of Germany east of the Rhine. Several of the samples from this dataset that originate from the Rhenish region had major element compositions more similar to central European glasses, and so these are marked with an "×" on the Rhenish graph.

HLLM with low phosphate) and trace elements (high Rb), and have been marked with an "x" to distinguish them in Figure 7.8. The glass from the central European region are also characterised by low Zr (less than about 50ppm). HLLA glass found in the different regions, on the other hand, are difficult to distinguish from each other but can be identified by their low Rb contents (not pictured). The correlations between major and trace elements are also of interest (Figure 7.8); in particular, the Rb:K_2O ratio, which is much higher for the Central European glasses.

7.2 Bypassing the interference of lead cames

7.2.1 Comparison of in situ and test stand analyses by pXRF

The control group of panel 3b (*n*=30) was analysed twice by pXRF, first using a test stand after the panel had been dismantled for conservation, and again after the conservation of the panel had been completed and the glass pieces had been releaded, ready for its return to the window (Figure 7.10). The latter analyses were carried out under in situ conditions, using the spectrometer handheld or with a tripod. Ultimately, two in the selected group could not be analysed under the in situ conditions because they were too small and too close to the edge of the panel (where the frame encasing the panel becomes a larger obstacle). Empirical calibrations based on the analysis of matrix-matched standards were applied to both sets of data.

For the elements of interest, the in situ analyses reported concentrations 10-20% lower than the analyses taken directly on the surface, although Cu and Zn were both reported as about 10% higher. More importantly, the relative concentrations are not always comparable. The zirconium concentrations of the blue glasses have a wider spread (Figure 7.10), and two pieces (one red and one green) have been severely affected, to the point that they no longer appear to be part of the same compositional groups.

Regarding the identification of batches in the white glass group (see Chapter 9), most of the pieces were still closely clustered with their previously identified batches; one batch was actually closer in composition when reanalysed after releading. For one batch, however, one piece could not be analysed due to its size and proximity to the edge, and the other, which was also small, was relatively underreported causing it to overlap with another batch (Figure 7.9).

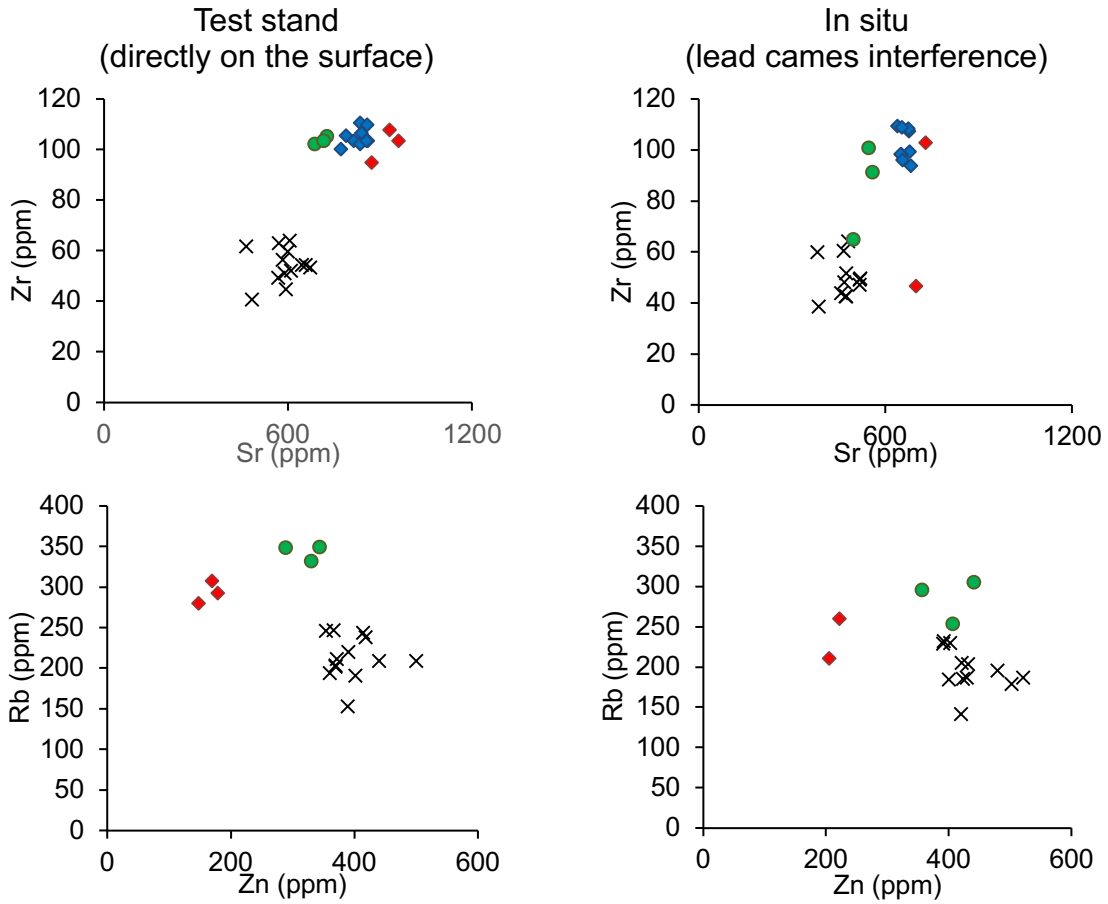

Figure 7.10 Comparison of the same glass pieces, analysed using a test stand directly on the surface of the glass (left) and after conservation when the glass had been re-leaded (on the right), shows an overall decrease in reported concentrations, with different levels of severity for different pieces of glass. The variability in the amount of lost intensity is a loss in precision that affects the identification of different glass groups.

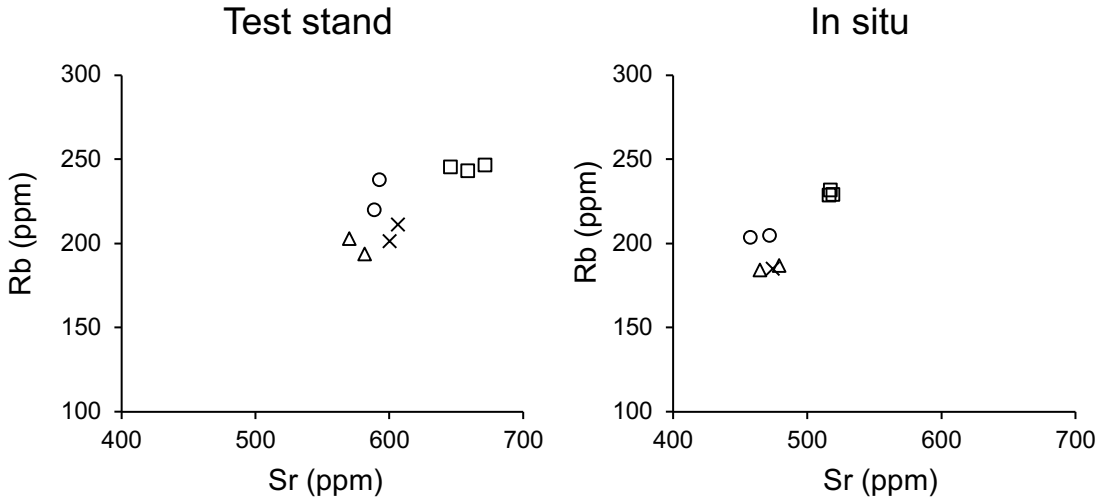

Figure 7.9 The identification of batches (each batch represented by differently shaped data points) was also affected by the poor precision resulting from the variable interference of lead cames.

7.2.2 Analysis of glass at increasing distances

Repeated analysis of standards at increasing distances showed a great effect on the measured counts, with loss of about 45-55% of the measured intensity by 8mm from the detector for all elements measured (Figure 7.11, top). Examination of the same data after converted into concentrations shows that the effect of distance is lessened but not fully corrected by the Innov-X/Olympus algorithm, with concentrations underreported by about 20% at 8mm (Figure 7.11, bottom).

Three glass pieces of uncertain date (possibly medieval) from YGT glass stores were also analysed at increasing distances. For many elements, the trend was similar as those observed for the tests on standards. However, for Fe, Cu and Pb, the results did not progressively decrease with more distance between detector and sample (Figure 7.12). The increased distance makes aiming for areas clear of corrosion, grisaille and silver stain more difficult, as the area of analysis will shift as the spectrometer moves farther from the sample material.

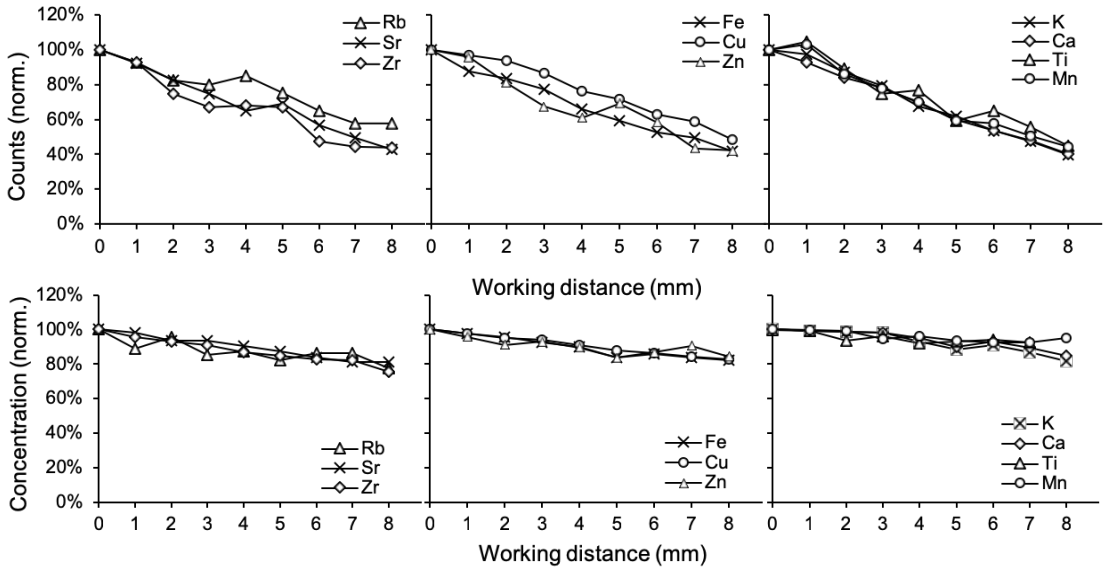

Figure 7.11 Analysis of Corning A and D (selected based on which glass had higher concentration for each element) at increasing distances, reported in counts (top) and as concentrations (bottom), both normalised to their value at working distance equal to 0mm.

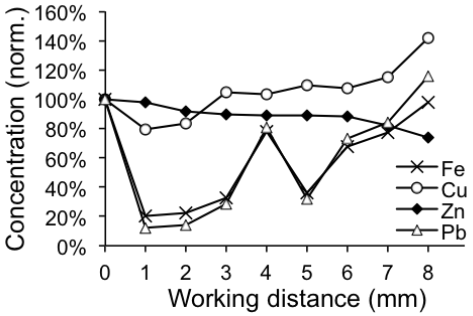

Figure 7.12 Analysis of glass A from YGT stores at increasing distances, normalised to its concentration reported at 0mm. Zn is included in order to show behaviour typical of most other elements. Fe, Cu and Pb concentrations are influenced by the presence of grisaille and silver stain and the difficulty in aiming the spectrometer for clean areas of the glass.

7.2.3 Comparison of empirical calibrations

25 glass standards were analysed directly on the surface, and again with a working distance of 5mm in order to compare the resultant calibration curves and their suitability for data correction, again using R^2 as a tool. Since the R^2 values for the calibration curves are comparable at 0mm and 5mm (Table 7.3), this shows that the data behaves in a consistent and predictable way when the distance between the spectrometer is increased, and can be corrected using calibration curves without an observable loss of precision.

Table 7.3 The R^2 values for the calibration curves (forced through 0), based on the analysis of up to 25 glass standards, both on the surface and with a working distance of 5mm. The R^2 values for all elements are comparable under both conditions.

Element	R^2 (0mm)	R^2 (5mm)
K	0.988	0.989
Ca	0.988	0.988
Ti	0.992	0.989
Mn	0.995	0.993
Fe	0.999	0.998
Co	0.954	0.976
Ni	0.983	0.993
Cu	0.994	0.995
Zn	0.996	0.996
Rb	0.999	0.999
Sr	0.989	0.991
Zr	0.982	0.981
Pb	0.962	0.967

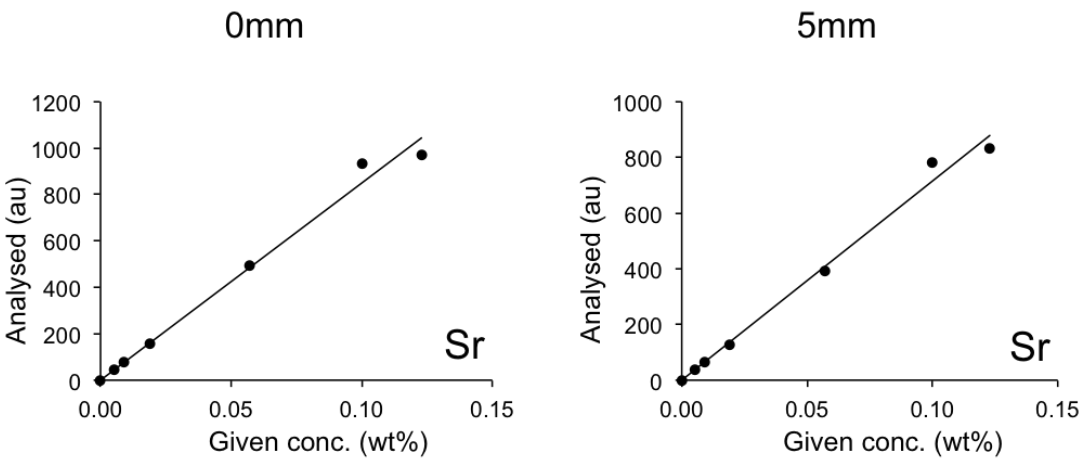

Figure 7.13 Calibration curves based on the analysis of matrix-matched standards at working distance equal to 0mm (i.e., on the surface of the glass) and at working distance equal to 5mm (on the right). The calibration curves are comparable, and as can be noted in Table 7.2, the R^2 values are also comparable.

Therefore, for most of the elements of interest, Rb, Sr, Zr and Zn, the loss in measured intensity can be corrected through the development of calibrations based on the analysis of matrix-matched standards (Figure 7.13). In light of the results depicted in Figure 7.12, it will be difficult to confidently correct Cu for medieval glass.

7.2.4 Factors affecting the measured intensity with increased working distance

The expectation for this study was that the major factor affecting the analyses would be the absorption of the characteristic x-rays in air, which affects lighter elements exponentially more drastically. However, this trend is not consistent with the observed data, in which the percent loss in intensity shows no correlation to characteristic x-ray energy and instead is mostly consistent for all elements (Figure 7.14). This observation applies to both the measured counts, and to the data after transformation into concentrations by the Innov-X/Olympus algorithm (which includes Compton normalisation); in both graphs in Figure 7.14, the data have been normalised to their values at 0mm.

Another factor affecting the final measured intensity is the angular dependence of the intensity of the fluorescent x-rays (de Boer, 1989). This is due in part to the custom in which we measure the distance between detector and sample perpendicularly, not the actual distance travelled by the x-rays, which is based upon the angle of detection (Figure 7.15). In de Boer's models, he also accounts for the width of the primary radiation and the detected beam, and the surface area projected by these beams onto the sample

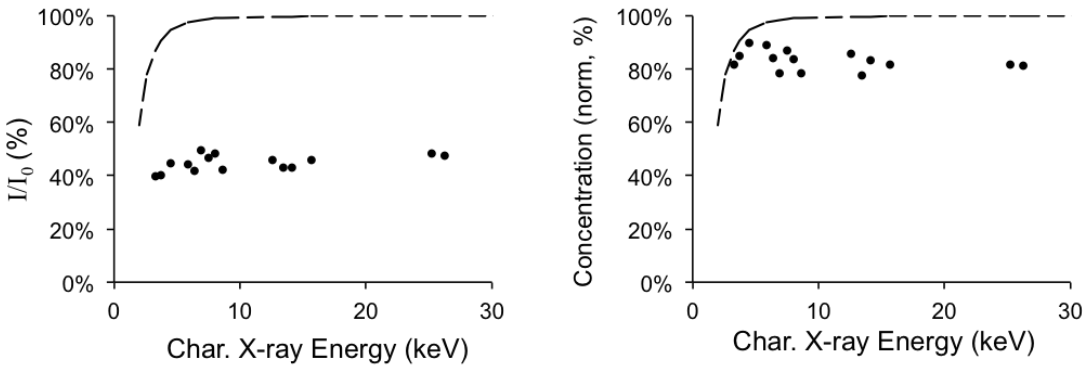

Figure 7.14 Analysis of Corning D at a working distance of 8mm, compared to the theoretical absorption in air. On the left, the data points represent the percentage of net counts of various elements, normalised to the intensity at 0mm. On the right, the same data after transformation by the Innov-X algorithms including Compton normalisation, also normalised to the concentration at 0mm. Both graphs show a line of the equation $\frac{I}{I_0} = e^{-\rho\mu d}$, the theoretical intensity of x-rays of different energies after travelling through d cm of air (equal to 0.8•sin(ψ_2) with 0.8 cm being the perpendicular distance and ψ_2 the angle of detection), normalised to the intensity at 0mm (I_0). ρ is the density of the material the x-rays travel through, in this case air, and μ is the mass attenuation coefficient of the x-rays of different energies passing through air. Neither set of data shows the logarithmic shape predicted by the theoretical absorption in air.

that are also dependent on the sine of the angle of incidence and of detection. The most common arrangement is depicted in Figure 7.16, in which the detected surface area is smaller than both the sample and the irradiated area. With ψ_1 held constant, the resultant intensity varies by $1/\sin \psi_2$. This model also takes into account that as the angle of detection gets very small, the detected surface area increases.

Under the conditions of the present study, as the spectrometer is moved away from the glass surface, the incident angle does not change, but the angle of detection gets larger. De Boer's models show that if the angle of detection increases while the angle of incidence is held constant, elements measured via higher energy characteristic x-rays are more affected (Figure 7.17). With the increased angle of detection affecting the intensity of higher energy x-rays more heavily and the absorption of x-rays in air affecting lighter elements, it is possible that these two effects resulted in the observed reduction in intensity that was more or less consistent across the measured elements.

It should be noted that de Boer's models and experiments assume the repositioning of the excitation source and detector. In the present case, a spectrometer with stationary parts is moved farther from the sample, which will have other unique effects on the analysis. The increased distance will result in defocusing the incident beam and shifting the irradiated area, making it difficult to accurately aim the spectrometer at clean areas

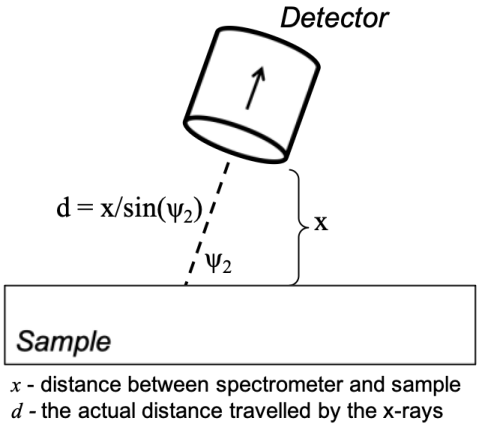

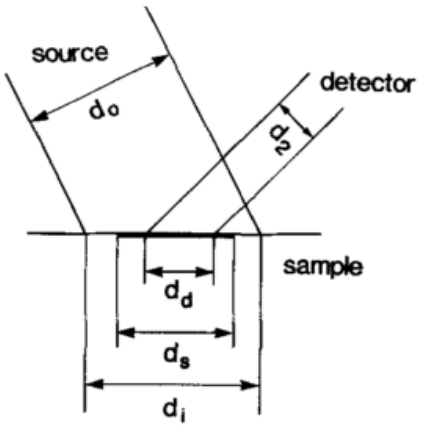

Figure 7.15 (left): An illustration depicting the actual distance travelled by x-rays from sample to detector, in relation to the perpendicular distance customarily used to describe the distance between spectrometer and sample. This illustration assumes the angle of detection is unchanging with increased distance (which is untrue).

Figure 7.16 (right): Figure 2 from de Boer (1989), showing the dependence of the detected surface area on the angle of detection between the detector and sample. $d_d = \frac{d_2}{\sin(\psi_2)}$, where d_d is the surface area on the sample that is both irradiated and detected, and d_2 is the width of the detected beam.

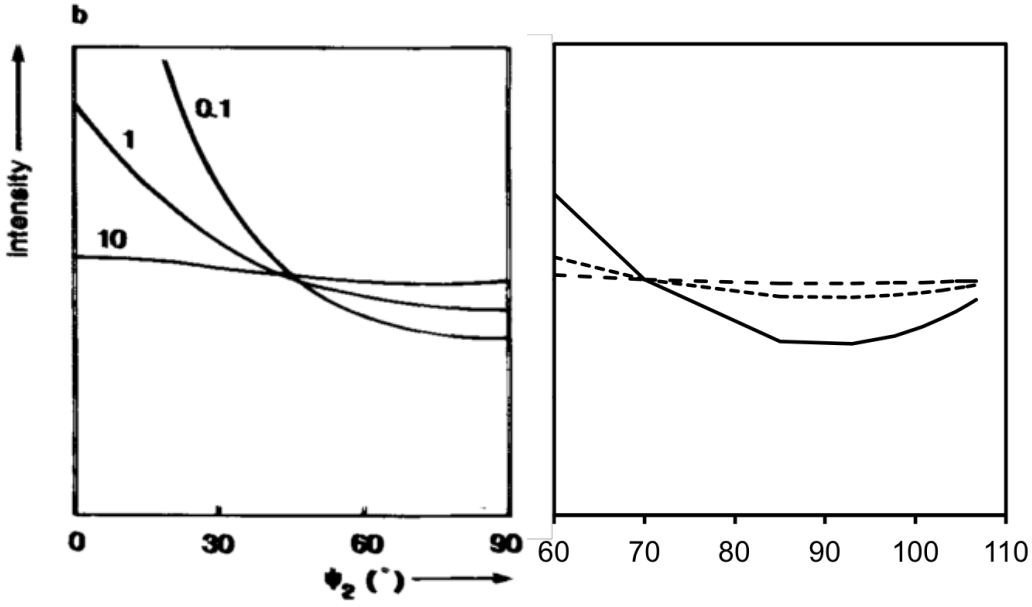

Figure 7.17 On the left, Figure 4 from de Boer (1989) Showing the effect that the angle of detection has on the intensity of different characteristic x-rays up to 90°; On the right, a graph, showing a continuation of the previous graph for larger angles, with the intensity normalised to 70°, which is closer to the angle of detection of the present study's machine when at a working distance of 0mm. On the left, lower energy x-rays are labelled "10" and harder radiation "0.1"; on the right, lower energy x-rays are depicted with a long-dashed line and higher energy with a solid line. The decrease in measured intensity attributed to the change in the angle of detection is greater for higher energy characteristic x-rays.

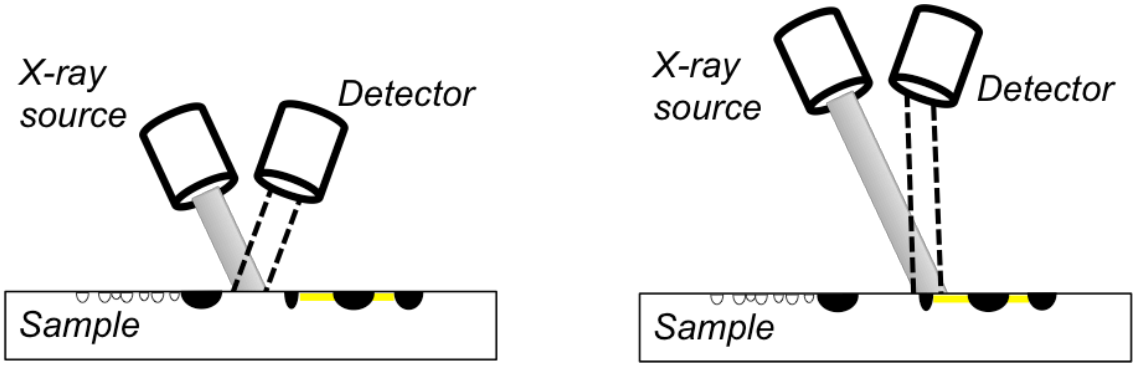

Figure 7.18 An illustration depicting the analysis of medieval glass with corrosion (depicted as pitting here), grisaille (the solid black) and yellow stain. As the spectrometer is moved away from the glass, the irradiated area shifts, making it difficult to aim the spectrometer for areas free of corrosion and decorative details. The increased angle of detection is also visible in this illustration.

of the sample. This explains why increasing the working distance in the analysis of medieval glass pieces resulted in an increase in Fe, Cu and Pb despite aiming at the same spot; the irradiated area evidently shifted to include decorative elements grisaille paint and yellow stain (Figure 7.18). Similarly, this also means that the detected area grows smaller, thus reducing measured counts, and furthermore there will be a point where the irradiated area has been moved out of the range of the detector, as the detector will still be positioned to receive x-rays from the intended irradiated area.

The transformation of the data into concentrations has lessened the effects of increasing the distance between spectrometer and sample (see again Figure 7.14), but has not fully corrected it, in part due to the relative increase in the intensity of scatter x-rays experienced with an increased scatter angle, as well as scatter in air (Potts *et al.*, 1997a). Since this algorithm also corrects for numerous other interferences (such as overlapping peaks and escape peaks, and so on), it was decided to continue with the transformed data and apply calibrations on top of the programmed algorithm (see next section).

7.2.5 Development of an attachment for in situ window analysis, the WindoLyzer 5

The most important finding in these results is that if the distance is held constant, the data remains consistent and precise, and can be corrected using empirical calibrations (see again Figure 7.13 and Table 7.3). It is expected that analysing at an increased working distance will increase the limits of detection, in particular for lighter elements, but this should not affect the analysis of the key elements of interest, Rb, Sr, Zr and Zn. The analysis of Cu may be made more difficult in light of the difficulty of aiming the spectrometer at areas free of decorative elements including yellow stain.

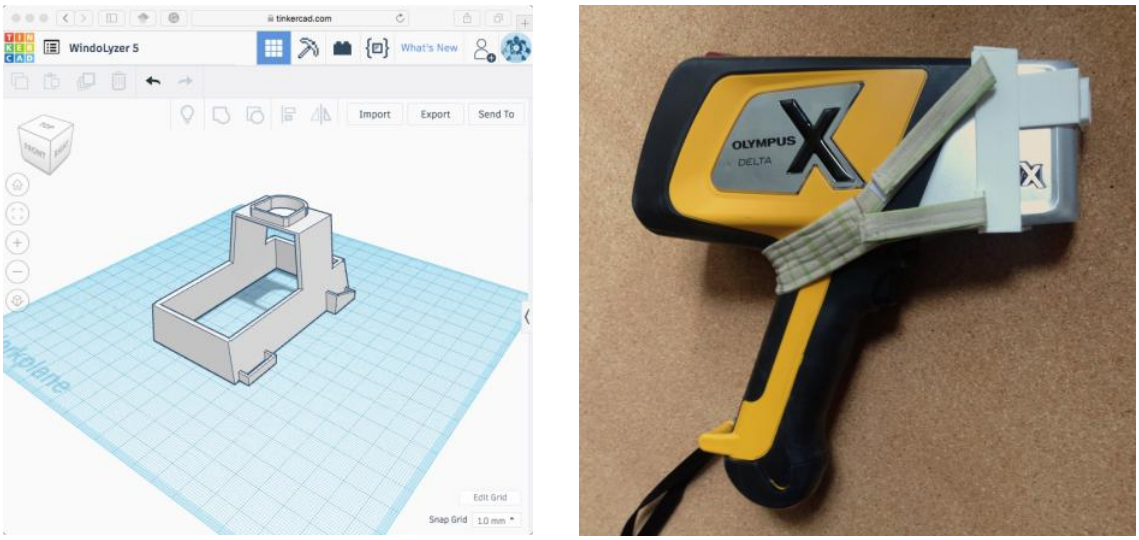

Figure 7.19 A window analyser attachment nicknamed the WindoLyzer 5 was designed using tinkercad.com (left) and 3D printed at the UCL Institute of Making out of polylactic acid. The attachment is secured to the spectrometer using velcro on a fabric strap (right).

Therefore, an attachment for the Innov-X/Olympus DP6000CC was designed and 3D-printed with the purpose of bypassing lead cames and maintaining a constant distance from the glass surfaces. The window analyser attachment, nicknamed the WindoLyzer 5, was designed using a freely available, simple to use, browser-based programme called Tinkercad (tinkercad.com, Figure 7.19).[17] Since most lead cames only protrude 3-4mm, a working distance of 5mm was chosen, with accommodation up to 4mm for lead came protrusion; however this distance could be easily adjusted on Tinkercad and reprinted. The design was imported to the Cura software for selection of printing parameters (100% fill density, print speed 80 mm/s, layer height 0.1mm, shell thickness 1.2mm and bottom/top thickness 0.8mm) and creation of the gcode file for input into the printer. The WindoLyzer 5 was printed in polylactic acid (PLA) using the Ultimaker2 3D printer with a 0.4mm nozzle at the UCL Institute of Making with a printing time of 3-4 hours. The supports on the printed WindoLyzer 5 were then removed with a scalpel and where need, it was sanded with 2500 grit sand paper to smooth any jagged edges that might damage the glass surface. A fabric strap with Velcro was made using a Janome DC3050 sewing machine in order to securely fix the attachment to the spectrometer for analysis.

The development of the WindoLyzer 5 was not completed in time for the in situ analyses of the GEW (as the difficulties in those analyses actually prompted this area of

[17] The "5" refers to the working distance, 5mm, that was chosen in this instance. However, the working distance can be adjusted and the attachment reprinted based on the geometry of a different window.

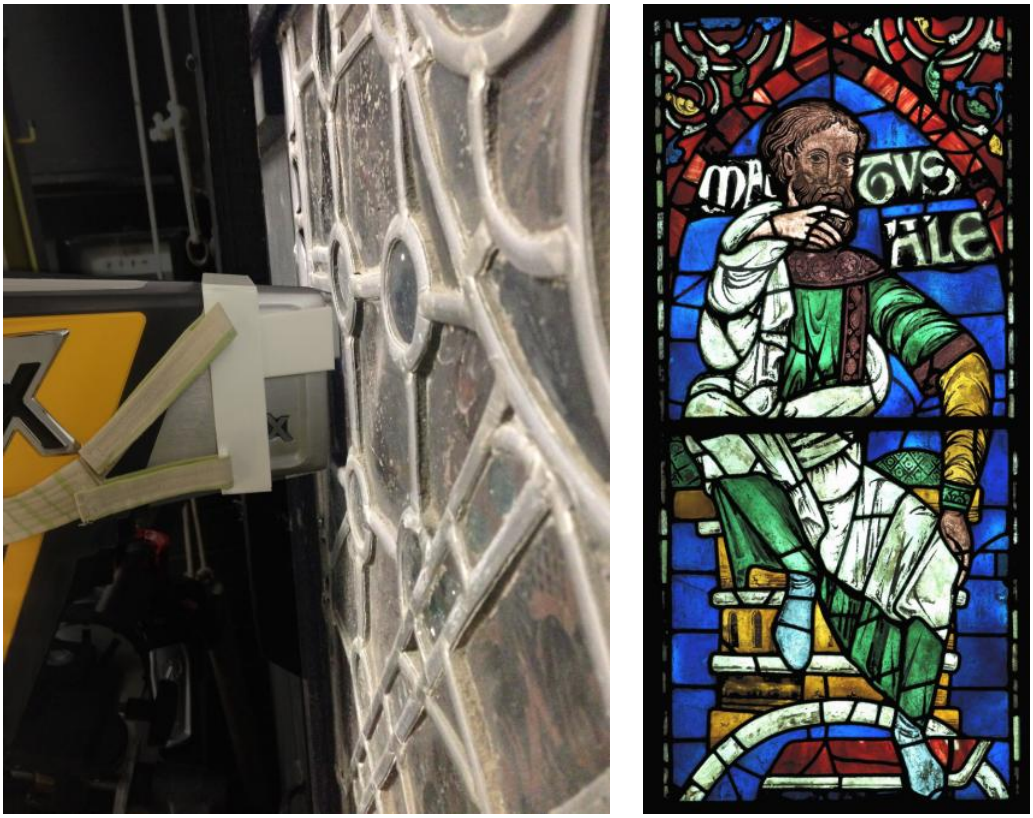

Figure 7.20 The WindoLyzer 5 (left) was used in a case study focused on the Ancestors of Christ series at Canterbury Cathedral as part of this research but ultimately not reported in this thesis. However, the preliminary results are very encouraging and highlight the potential of this attachment. *Image, right: panels 2,3e (Methuselah) from window SXXVIII at Canterbury Cathedral, originally from the Ancestors of Christ series © Dean and Chapter of Canterbury*

methodological development), but a prototype was used to analyse a case study as part of this research (Figure 7.20), although the case study will not be reported in the thesis. The glass was not removed from its lead cames and so sampling was impossible and obstruction due to the lead cames was anticipated. The Ancestors of Christ panels from Canterbury Cathedral date to an earlier period (12th century) and pXRF analyses could be used to identify a change in glass recipe/source between the earlier part and later part of the glazing programme (*c.* 1180 vs. 1220). Furthermore, the research strongly supported an earlier hypothesis by M. Caviness (1987) that some of the figures from the later part of the glazing programme were re-used from windows pre-dating the 1174 fire at Canterbury Cathedral (publication forthcoming).

7.2.6 Health & Safety

The WindoLyzer 5 was 3D printed in a material composed of very light elements (polylactic acid, $C_3H_4O_2$), and so will not interfere with analysis but also will not stop scattered x-rays. It was anticipated that the use of the WindoLyzer might increase radiation risks to the user, necessitating health and safety tests.

Tests were carried out using a Geiger counter to measure the radiation at various points relative to the spectrometer's nose to determine whether analysing a stained glass panel using this attachment increases the radiation dose to the analyst. As the scatter of x-rays from a pXRF is highly dependent on the material being analysed (Rouillon *et al.*, 2015), a small, modern stained glass panel (within its lead cames) was used as the analysed material during these tests. The spectrometer was placed against a glass piece in the panel, and run using the settings used in this research: the Soils mode, with 20s per beam setting. The analyst is unlikely to stand directly in front of the spectrometer while it is running, but instead may stand adjacent/parallel to the direction of analysis (for example, using the spectrometer on a tabletop, faced downwards towards the sample) or behind it (holding the spectrometer facing away from him/her, Figure 7.21). Therefore, the areas that were measured were 20cm and 40cm to the right of the spectrometer and 50cm behind the spectrometer (measuring from the nose), which is the approximate distance of the analyst's torso if using the spectrometer handheld. Measurements were recorded every 10s, throughout the 60s analysis. The tests were repeated using the WindoLyzer 5, and again using the WindoLyzer 5 with a lead shield surrounding the spectrometer's nose.

The results of the health and safety tests are reported in Figure 7.22. The use of a device such as the WindoLyzer significantly increases the amount of radiation detected adjacent

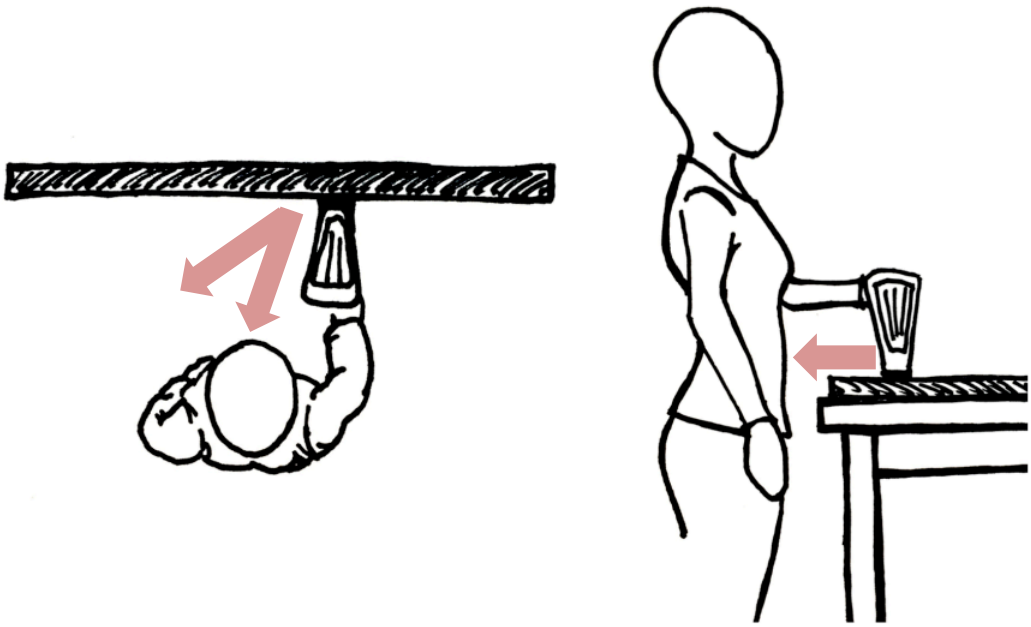

Figure 7.21 Sketches showing the two areas of radiation risk to an analyst using pXRF to study a stained glass panel: when using a vertical lightbox or stand, the analyst is behind the spectrometer, while for tabletop analyses, the analyst is adjacent to the spectrometer's nose. Sketches are illustrative only and not to scale.

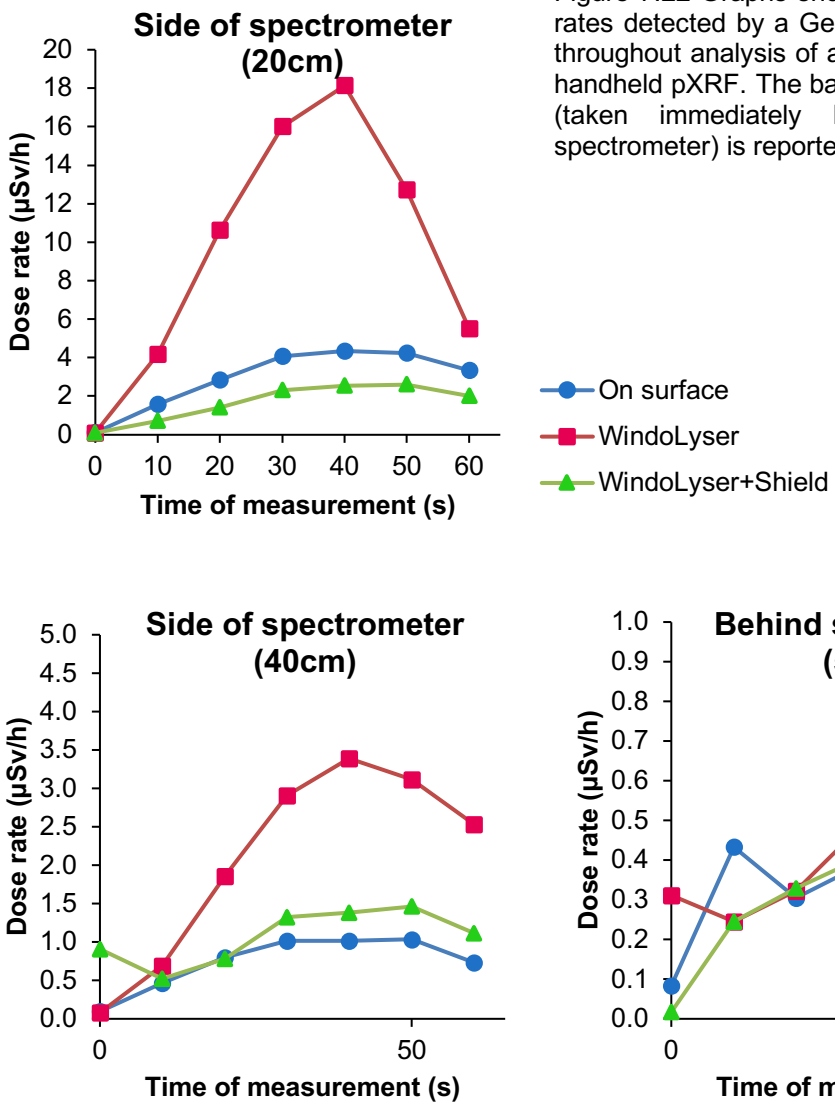

Figure 7.22 Graphs showing the radiation dose rates detected by a Geiger counter at intervals throughout analysis of a stained glass panel by handheld pXRF. The background measurement (taken immediately before operating the spectrometer) is reported as *t*=0s.

to the spectrometer at both 20cm and 40cm; this effect was mitigated through the use of a lead shield, which is already standard practice at UCL Institute of Archaeology for analyses taking place on a tabletop or similar set up. The radiation detected behind the spectrometer remained the same or with a negligible increase. The dosage was found to be within acceptable ranges.

The Ionising Radiations Regulations of 2017 (IRR 2017, which came into force on 1 January 2018) dictate the dose limitations for both employees who work with radiation (above and below 18 years of age) and the general public, as well as special cases such as pregnant women. These dose limits are reported in Table 7.4: the annual whole body dose limit for a radiation worker is set at 20 mSv, and for the public, 1 mSv. UCL policy regarding radiation is to investigate a whole body dose above 0.2mSv and advises that radiation exposure should not approach the IRR 2017 limits; doses should be kept "as low as reasonably possible" (UCL, n.d.).

To compare the amount of radiation detected in these tests to the dose limits in IRR 2017, a few calculations must be made. First the radiation rates reported by the Geiger counter (in μSv per hour) must be transformed to an absorbed dose by dictating the numbers of hours the exposure occurred. The absorbed dose must then be converted to a whole body dose equivalent. The whole body dose equivalent is a function of the absorbed dose, the type of radiation, and the type of body tissue where the radiation occurred, and can be calculated according to the equation and constants reported by Rouillon *et al.* (2015, 820):

$$E = W_T \times H_T \times W_R \quad \text{(Equation 7.3)}$$

where E is the effective whole body dose, W_T is the tissue weighting factor (0.01 for skin), H_T is the absorbed dose to the tissue, and W_R is the radiation weighting factor (dependent on the type of radiation: 1 for x-rays).

Table 7.4 Annual dose limits according to IRR 2017 Sch 3. "Employee" refers to employees over the age of 18; employees and trainees below the age of 18 have different limits.

	Employees	Others/Public
Effective dose (whole body dose)	20mSv	1mSv
Lens of the eye	20mSv	15mSv
Skin (averaged over any area of 1cm^2)	500mSv	50mSv
Extremities	500mSv	50mSv

Table 7.5 Annual whole body dose equivalents for different use parameters of pXRF analysis on stained glass panels, for different hours of usage per year. 21 hours is the estimated hours of use during an analytical trip to Canterbury which took place over 3 days; 260 hours was an annual usage estimate used by Rouillon *et al.* (2015; 1 hour per week day); and 1820 hours is an extreme case of 7 hours per week day.

	No WindoLyzer		**WindoLyzer**		**WindoLyzer with Lead Shield**	
	20cm side	*50cm behind*	*20cm side*	*50cm behind*	*20cm side*	*50cm behind*
μSv/h (max. measured)	4.4	0.43	18.1	0.5	2.6	0.5
Whole body dose equivalent (μSv)						
21 hours (Canterbury analytical trip)	9.1	0.9	38.1	1.1	5.5	1.1
260 hours (1 hour/day annually)	113.2	11.3	471.4	14.2	67.7	13.1
1820 hours (7 hours/day annually)	792.2	78.8	3299.7	99.2	473.7	91.5
Annual dose limit for public (μSv)	1000					
UCL limit for investigation (μSv)	200					

The effective whole body dose for analysing a stained glass panel directly on the surface and with the use of the WindoLyzer are calculated for different scenarios and reported in Table 7.5: first, for 21 hours, which was the estimated time of use of the pXRF over three days for the case study undertaken at Canterbury Cathedral using the WindoLyzer; second, for 260 hours, equivalent to one hour of use per working day, an estimation of an analyst's annual use used by Rouillon *et al.* (2015); and finally, a more extreme case, 1820 hours, or 7 hours per working day. All calculations were based upon the maximum dose rate recorded during the above tests.

Most of the calculated whole body doses do not exceed UCL's limit for investigation (0.2mSv); only when using the WindoLyzer without a shield and standing 20cm from the side of the spectrometer for 7 hours/day annually does the dose (3.3mSv) exceed the IRR 2017 limit on public exposure (1mSv), but still does not approach the limits for employees (20mSv). Standing behind the spectrometer is the safer option, as even at the most intensive usage the annual dose remains below 0.1mSv. 260 hours per year (1 hour per day, or the equivalent of more than ten trips to Canterbury) would result in an effective whole body dose of 0.014mSv, well below all limits.

There is negligible difference in the radiation exposure to the handheld user standing behind the spectrometer when using the WindoLyzer. The increased exposure at the sides of the spectrometer, however, is of greater concern. With or without the WindoLyzer, it is advisable to use a lead shield for tabletop analyses, when the analyst has the greatest risk of being exposed to radiation at the side of the spectrometer. This protective measure is even more important when using a device such as the WindoLyzer. Whenever possible, when analysing a stained glass panel, it is always safer to secure the panel on an upright stand for analysis as it is always safer to stand behind the spectrometer. Use of a tripod (Figure 7.23) not only alleviates the strain on the analyst's arms and the risk of pressure on the glass, but allows the analyst to step back several paces during analysis, which greatly reduces exposure.

7.3 Summary

The key obstacles anticipated or encountered in the use of handheld pXRF for the study of medieval stained glass were first, the effect that surface conditions including both deterioration and the presence of grisaille and yellow silver stained, and second, the obstruction presented by the small surface area of many medieval stained glass pieces and the protrusion of their surrounding lead cames. In these results, there is a greater focus on precision than accuracy, under the premise that accuracy can be corrected with

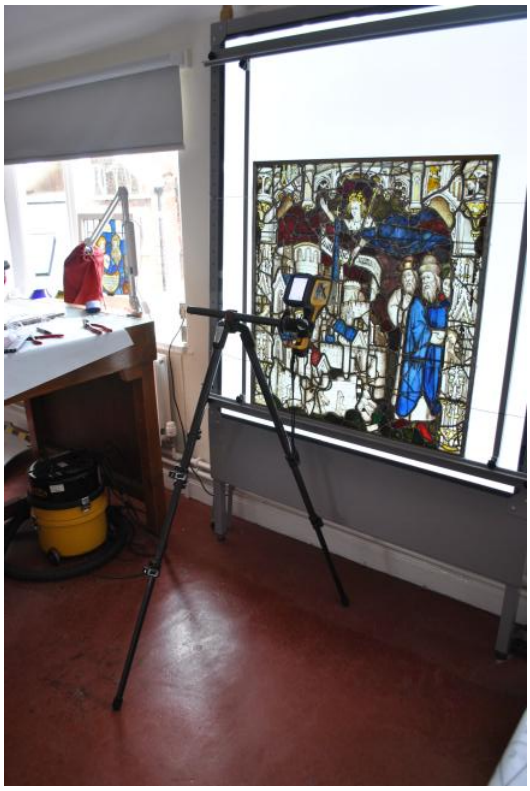

Figure 7.23 Use of a tripod with handheld pXRF allows the analyst to initiate the analysis and then step back several paces, reducing exposure to radiation.

empirical calibrations if there is a good linear agreement between the raw pXRF data and the "true" composition of the sample or standard.

Tests were carried out to determine which elements were well analysed by pXRF on medieval window glass, and which were affected by surface conditions. The pXRF spectrometer performed well in the analysis of standards, with good linear agreement between the analyses and the known compositions of the standards. However, many elements are poorly characterised in medieval glass, as demonstrated by a comparison of pXRF with analyses by EPMA-WDS or LA-ICP-MS on the cross-section of subsamples. This is attributed to poor surface conditions. Some elements are well analysed; in this study, Cu, Zn, Rb, Sr and Zr were identified as well analysed in the medieval glass by pXRF, which is consistent with previous studies of window glass (Dungworth, 2012a). This is despite previous work indicating that the composition of these elements is also altered by deterioration processes affecting medieval glass (Sterpenich and Libourel, 2001). The superior measurement of these elements is attributed to their greater depth of analysis, which is dependent on several factors including the energy of the characteristic x-ray; higher-Z elements have higher energy characteristic x-rays and are read from deeper within the sample. Therefore, the potential of this methodology relies in large part on the condition of the glass; for more corroded glass, even the measurement of these heavy trace elements may be affected. However, these five elements were identified as quantifiable elements in this study and will be the

focal point for the pXRF analyses. Other elements may be used semi-quantitatively; for example, both Co and Ni can be used to characterised the colourants used in blue glass.

The interference of lead cames also presented a significant problem. Previous work has shown that small distances between spectrometer and sample (up to 1mm for mid-Z elements, and up to 3mm for high-Z elements) can be corrected by Rayleigh or Compton normalisation (Potts *et al.*, 1997a; Wilke *et al.*, 2016); however larger distances can be expected in the analysis of in situ medieval windows. Laboratory tests showed that increased distance between the spectrometer and the glass sample yielded an observable decrease in measured intensity, which was only partially corrected by the Innov-X/Olympus algorithm based on Compton normalisation. The decrease in measured intensity does not fit the expected model if increased absorption in air were the dominant factor affecting analyses, and instead this was explained by the disruptions to and changes in the angles of detection at increased working distances. In practice (in the analysis of a panel encased in lead cames), the variable working distance between each analysis disrupted the precision of the analyses and obscured compositional groups. Increased distance on medieval glass were unpredictable for elements associated with grisaille and silver stain. However, if the distance is held constant, the linear agreement between the analysed values and standard values remained good and it appears empirical calibrations would be effective under these analytical parameters. Therefore, an attachment for the spectrometer was developed, which was designed to be adjustable and inexpensive. The attachment, nicknamed the “WindoLyzer 5”, maintains a constant distance between the spectrometer and sample so that the data may be corrected through empirical calibrations.

CHAPTER 8

Chemical characterisation of the GEW glass

This chapter reports the results of the chemical analyses of the GEW glass by EPMA-WDS, pXRF, LA-ICP-MS and TIMS (full results reported in Appendix D); the next chapter will report the identification and distribution of white glass batches in each panel. The EPMA-WDS data was used to analyse the control group to characterise the major element compositions of the different glass types, and for comparison to legacy data for medieval glass (see Chapter 3) and the post-medieval compositions defined by Dungworth (2012a, 2012b). The pXRF analyses focused on elements Cu, Zn, Rb, Sr and Zr (see previous chapter) and were used to identify glass types for a larger number of glass pieces through comparison with the control group. Although the primary purpose of the LA-ICP-MS analyses was to develop empirical calibrations for the pXRF data, REEs will also be examined. TIMS analyses were used to compare isotope ratios of the GEW glass to samples from Little Birches, Staffordshire, and previously published data from both Staffordshire and the Weald.

8.1 Characterising major glass types

Four main glass types were detected in the control group (Table 8.1, Figure 8.1). The majority have compositions characteristic of medieval forest glass, with major components silica, lime and potash, with high magnesia, phosphate and manganese. A smaller group have HLLA compositions characteristic of the later medieval period, with higher lime and lower potash than the forest potash glass, but with similar silica, magnesia, phosphate and manganese concentrations. Two control group glasses have mixed alkali concentrations (with similar concentrations of soda and potash); the high strontium of this group identifies it as kelp ash glass, made with the ashes of seaweed,

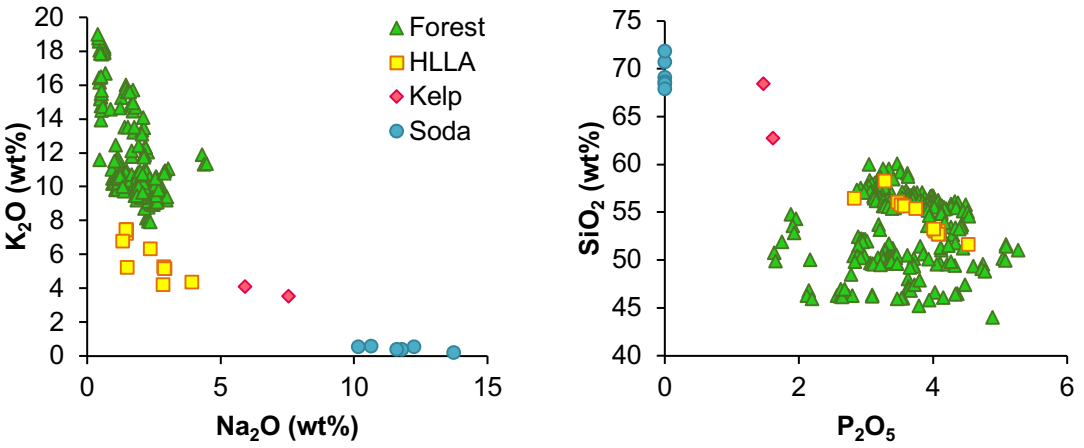

Figure 8.1 Scatterplots showing the major element compositions of the glass types found in the GEW. Results are measured by EPMA and reported in oxide weight percent.

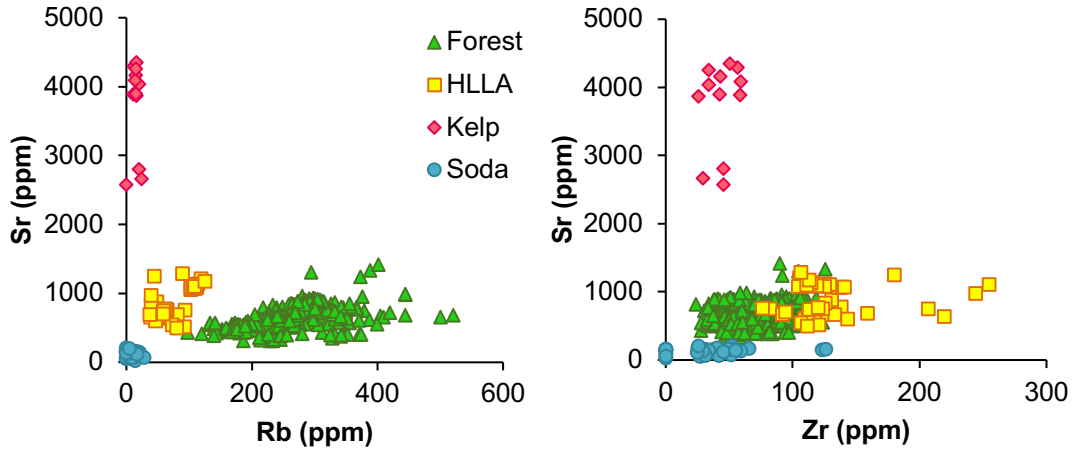

Figure 8.2 Scatterplots showing the trace element compositions of the glass types found in the GEW. Results are measured by pXRF and reported in parts per million.

which was produced in England *c.* 1700-1835 (Dungworth, 2012a, 2009). One of these (10h-M2) was a composite glass, with the thicker base glass (colourless) having a mixed alkali composition, and a thinner flash of purple glass on the surface, which is a lead glass (52% SiO_2, 36% PbO, with 6.7% K_2O; full results in Appendix D). Finally, several soda glasses were identified, with no phosphate detected, suggesting the use of synthetic soda rather than sodic plant ash. The very low concentrations of magnesia suggest these glasses date to between 1835-1930; the potash contents make the latter part of the period, 1870-1930, the more likely origin (see Dungworth, 2012a).

Trace element concentrations also distinguish these groups (in keeping with Dungworth, 2012b), and allowed glass type identification for the larger sample set analysed by handheld pXRF. Rubidium and strontium are the strongest identifiers (Figure 8.2) Glass made using synthetic soda has low concentrations of trace

Table 8.1 The four types of glass observed in the GEW, as characterised by EPMA (reported in oxide weight percent) and pXRF (trace elements Rb, Sr, and Zr, reported in element parts per million). Cu and Zn are excluded as these elements are associated with colourants.

	Forest		HLLA		Kelp/Mixed Alkali		Soda	
Na_2O	1.77	*0.72*	2.21	*0.86*	6.71	*1.15*	11.62	*1.16*
MgO	5.83	*1.46*	3.87	*0.57*	4.96	*0.43*	0.14	*0.21*
Al_2O_3	1.54	*0.41*	2.63	*0.55*	1.70	*0.65*	1.89	*0.97*
SiO_2	53.16	*3.93*	54.50	*2.01*	65.58	*4.02*	69.55	*1.41*
P_2O_5	3.56	*0.66*	3.77	*0.46*	1.54	*0.10*	<	
SO_3	0.18	*0.05*	0.18	*0.17*	0.12	*0.01*	0.34	*0.06*
Cl	0.25	*0.15*	0.42	*0.14*	0.56	*0.22*	0.10	*0.03*
K_2O	11.32	*2.38*	6.01	*1.24*	3.82	*0.40*	0.43	*0.14*
CaO	19.26	*4.41*	23.08	*1.27*	12.17	*2.21*	11.07	*0.22*
TiO_2	0.08	*0.03*	0.13	*0.09*	0.13	*0.00*	0.12	*0.07*
MnO	1.35	*0.22*	1.56	*0.51*	0.07	*0.09*	2.53	*1.01*
Fe_2O_3	0.69	*0.44*	0.67	*0.12*	0.67	*0.37*	1.00	*0.48*
BaO	0.24	*0.09*	0.29	*0.08*	<		<	
PbO	0.14	*0.13*	<		1.22	*1.72*	<	
Rb	248	*50*	79	*28*	15	*6*	9	*14*
Sr	623	*141*	897	*226*	3705	*677*	165	*313*
Zr	67	*22*	131	*38*	44	*12*	31	*33*
EPMA n=	*234*		*12*		*2*		*7*	
pXRF n=	*808*		*41*		*12*		*42*	

elements, in particular rubidium, while kelp ash glass has very high concentrations of strontium. The forest glass has high rubidium (more than about 100ppm) and moderate strontium (more than 300ppm), while the HLLA glass generally has lower rubidium and higher strontium contents than the forest glass. The distinction between the forest and HLLA glass types is not very well defined in terms of trace elements, and some pieces appear borderline between the two classifications. Zirconium contents are less discriminating; HLLA glass tends to have higher zirconium, and kelp ash and synthetic soda glasses tend to have lower zirconium (Figure 8.2). Due to their association with colourants, copper and zinc are not useful markers of glass types, and were excluded from the table.

A small group of pieces analysed only by pXRF (*n*=13) were measured as having very high lead, sulphur and chlorine, and some also are also measured with extraordinarily high iron (up to 17% Fe_2O_3). This is attributed to the surface conditions of the glass; elevated iron and lead may come from the painted detail (grisaille), while sulphur and chlorine are probably due to the presence of corrosion products (see Chapter 5). On the basis of their trace element compositions, two of this group are consistent with HLLA compositions, and the rest with synthetic soda glass.

8.1.1 Identification of original and non-original glass

Due to the date of the window, the post-medieval glass types (the kelp ash glass and the synthetic soda glass) are considered not original to the window. Various medieval forest glass compositions, both potash and HLLA, were detected in this window, all characterised by silica, potash and lime as major components, and significant concentrations of phosphorus, magnesium and manganese oxides, which is consistent with the use of the ashes of wood and terrestrial plants in the glass recipes. However, not all of the medieval glasses are original to the window, due to the practice of using miscellaneous medieval stained glass pieces to patch up windows during historical repair campaigns (e.g., Milner-White, 1950).

The non-original medieval glasses were identified on the basis of their painted detail and chemical composition. Visual identification was often made with the help of YGT conservators (both through the provision of conservation records and verbal observations and discussion); this includes both stylistic evaluation as well as physical characteristics such as very different weathering (indicating it has been exposed to a different environment and/or is of different composition) or deliberate abrasion (which indicates that details have been removed when inserted into the window as an infill). Chemical composition was evaluated by colour group; e.g., if a blue glass piece is dissimilar in composition to all the other blue glass pieces, it is unlikely to be original. The original and non-original medieval glass are reported separately, as are a small group of glasses with HLLA composition, as visual identification suggests they are original; however if original, this would be a very early occurrence of HLLA glass.

8.2 Glass original to the window

The colours original to the window include white, blue, red, green, yellow and manganese colours (various shades of purple, pink and murrey). The white, blue and red are the most prevalent, due in part to the original colour scheme (the white is used copiously for architectural details, the frames, and figures, while blue and red were used as the backgrounds for all panels as well as other details including demons, drapery, rooftops, etc.) and in part to the condition of the glass (the green, yellow and Mn-glass are generally in much poorer conditions than the other colours, and are more likely to have been replaced in earlier conservation interventions). The original glass in the GEW fall into two major groups based on their lime and magnesia concentrations (Figure 8.3, Table 8.2): a low lime, high magnesia group (LLHM) that comprises all of and only the white glass, and a high lime, low magnesia group (HLLM) that comprises

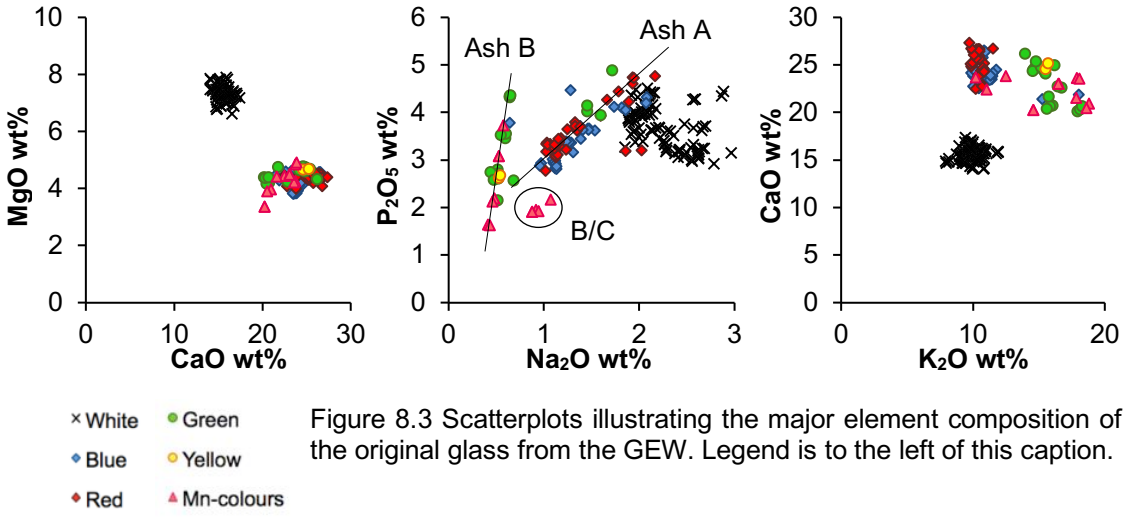

Figure 8.3 Scatterplots illustrating the major element composition of the original glass from the GEW. Legend is to the left of this caption.

all of and only the coloured glass. These groups are consistent with the data published by Freestone *et al.* (2010) and the rest of the unpublished GEW data from the Cardiff-York project.

The HLLM colours can be further subdivided based on their soda and phosphate contents (Figure 8.3); the two oxides are strongly correlated, suggesting the use of two distinct ashes, ash A and ash B. The A group colours include blue, red and some green (green A, Figure 8.3), and the B group includes the rest of the green, yellow, and manganese colours. The group A glasses mostly have about 11% K_2O, except the green A group which has higher potash (about 16% K_2O); the group B glasses tend to have higher potash (about 16% K_2O), excluding some of the Mn colours (Mn B/C), which have lower potash, 11-14% K_2O (Figure 8.3). These exceptions, green A and Mn B/C, are interpreted as having extra raw materials added to the batch to alter the base glass composition; the following sections will go into more detail.

The white glass is distinguished from the coloured glasses by their lower Rb, Sr and Zr concentrations (Figure 8.4, Figure 8.5). The blue/red group tends to have higher Sr and lower Rb than the green/yellow group, while the Mn-colours are highly variable in trace element composition. Most of the colours have a similar Sr:CaO ratio, excluding some of the high Sr Mn-colours (most of them "murrey" coloured); most of the colours and the white glasses have similar Rb:K_2O ratios, excluding the green, yellow, and Mn-coloured glasses (Figure 8.6). In comparison with the white glasses, the colours were made with a sand richer in Zr (Figure 8.6). The blue glass has higher Cu and Zn; some of the red glasses were measured with higher Cu although they were analysed by pXRF on the white/unflashed side (Figure 8.7).

Table 8.2 Mean composition and standard deviation of the original glass groups in the GEW, grouped by colour. The oxides are the results by EPMA-WDS and are reported in weight percent. The elements Cu, Zn, Rb, Sr, and Zr are the results by pXRF and are reported in parts per million.

	White		Blue		Red		Green A		Green B		Yellow		Mn-B		Mn-B/C	
Na_2O	2.26	*0.28*	1.32	*0.31*	1.33	*0.34*	1.55	*0.13*	0.56	*0.08*	0.88	*0.61*	0.48	*0.06*	0.94	*0.08*
MgO	7.32	*0.24*	4.23	*0.26*	4.43	*0.14*	4.35	*0.28*	4.54	*0.19*	4.52	*0.29*	4.25	*0.24*	4.19	*0.77*
Al_2O_3	1.36	*0.11*	1.77	*0.18*	1.66	*0.07*	1.65	*0.02*	1.24	*0.29*	1.27	*0.33*	0.86	*0.31*	1.34	*0.24*
SiO^2	56.65	*1.27*	50.04	*1.77*	49.97	*0.84*	45.64	*1.14*	46.30	*0.21*	46.60	*0.67*	47.58	*1.97*	52.88	*1.66*
P_2O_5	3.68	*0.45*	3.41	*0.49*	3.62	*0.55*	4.25	*0.43*	3.17	*0.75*	3.08	*0.74*	2.50	*0.81*	1.97	*0.11*
SO_3	0.17	*0.04*	0.19	*0.05*	0.18	*0.03*	0.27	*0.03*	0.22	*0.04*	0.25	*0.01*	0.25	*0.06*	0.27	*0.06*
Cl	0.33	*0.07*	0.05	*0.02*	0.06	*0.02*	0.04	*0.01*	0.03	*0.04*	<		<		0.06	*0.07*
K_2O	9.91	*0.78*	11.02	*1.59*	10.39	*0.37*	15.78	*0.18*	15.85	*1.43*	15.58	*0.09*	17.72	*0.92*	12.55	*2.00*
CaO	15.62	*0.72*	24.08	*1.17*	25.53	*1.15*	20.88	*0.57*	23.58	*1.96*	23.39	*2.59*	22.32	*1.31*	22.09	*1.78*
TiO_2	0.07	*0.02*	0.10	*0.02*	0.08	*0.02*	0.13	*0.03*	0.07	*0.03*	0.08	*0.06*	0.10	*0.02*	0.05	*0.04*
MnO	1.45	*0.07*	1.26	*0.09*	1.31	*0.13*	1.47	*0.03*	1.44	*0.19*	1.50	*0.01*	1.69	*0.23*	1.70	*0.14*
Fe_2O_3	0.47	*0.05*	1.01	*0.16*	0.52	*0.08*	2.51	*0.47*	1.73	*0.35*	1.22	*1.62*	0.37	*0.27*	0.29	*0.14*
CoO	<		0.11	*0.03*	<		<		<		<		<		<	
CuO	<		0.20	*0.05*	0.07	*0.03*	0.06	*0.01*	0.08	*0.02*	<		0.04	*0.02*	0.04	*0.02*
ZnO	0.05	*0.01*	0.22	*0.10*	<		0.04	*0.01*	0.05	*0.01*	<		0.04	*0.03*	0.04	*0.03*
BaO	0.18	*0.02*	0.29	*0.04*	0.27	*0.02*	0.37	*0.02*	0.42	*0.07*	0.43	*0.05*	0.43	*0.06*	0.43	*0.06*
PbO	0.07	*0.04*	0.18	*0.05*	0.26	*0.24*	<		<		<		<		<	
Cu	137	*55*	1334	*292*	783	*910*	380	*160*			277	*92*	348	*296*	113	*22*
Zn	423	*37*	1775	*653*	236	*38*	389	*73*			320	*25*	388	*81*	265	*37*
Rb	226	*20*	293	*20*	286	*15*	320	*31*			341	*14*	362	*97*	401	*51*
Sr	560	*41*	810	*61*	839	*66*	681	*70*			769	*55*	730	*64*	1134	*187*
Zr	53	*7*	97	*9*	94	*8*	97	*14*			101	*5*	75	*20*	102	*25*
EPMA n=	101		33		32		4		14		3		5		5	
pXRF n=	457		76		90		37				7		10		9	

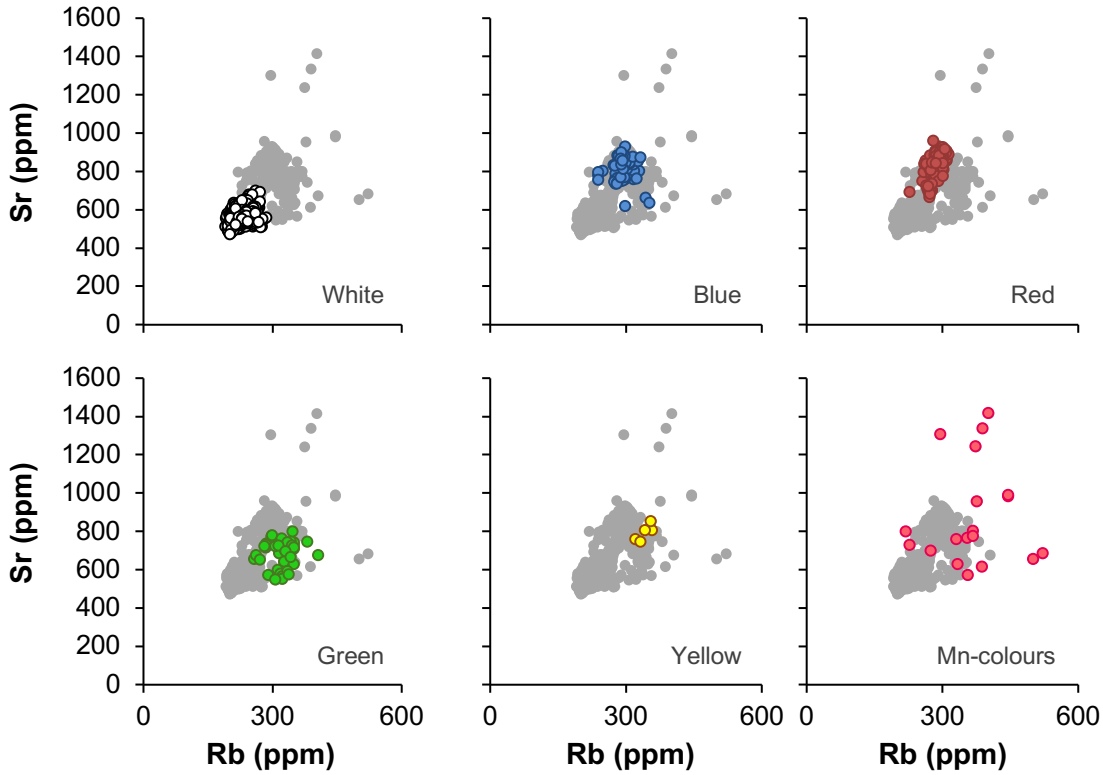

Figure 8.4 Scatterplots illustrating the strontium and rubidium contents of the original glass from the GEW, by colour.

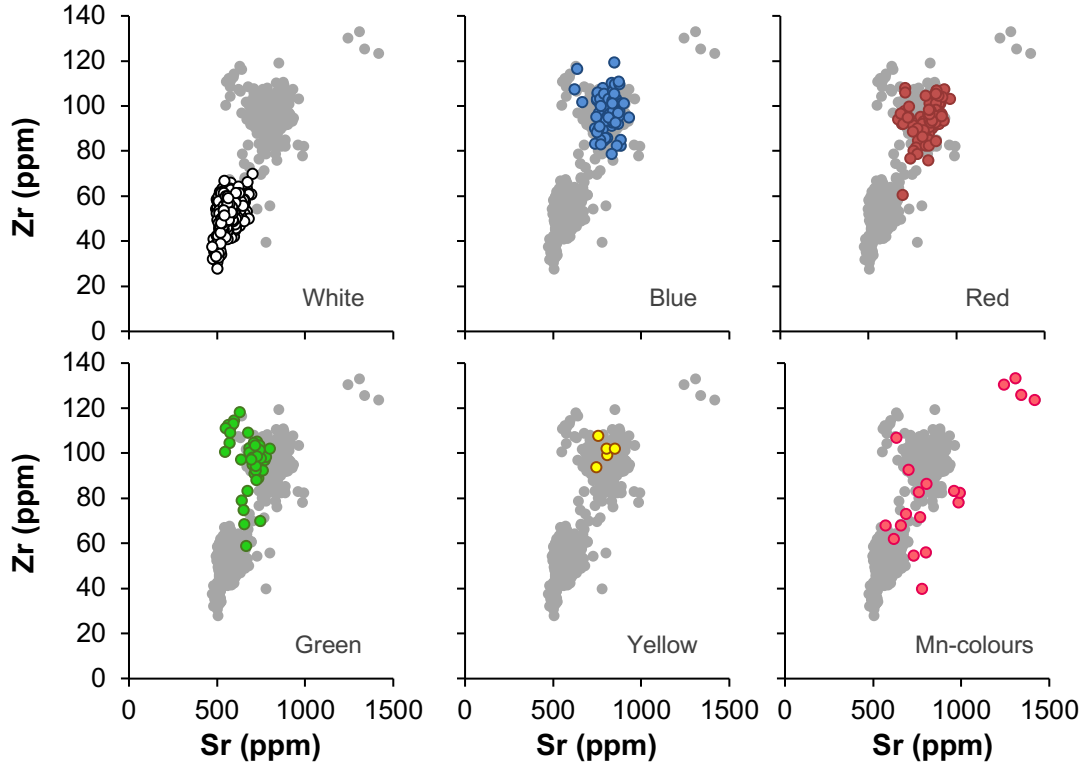

Figure 8.5 Scatterplots illustrating the zirconium and strontium contents of the original glass from the GEW, by colour.

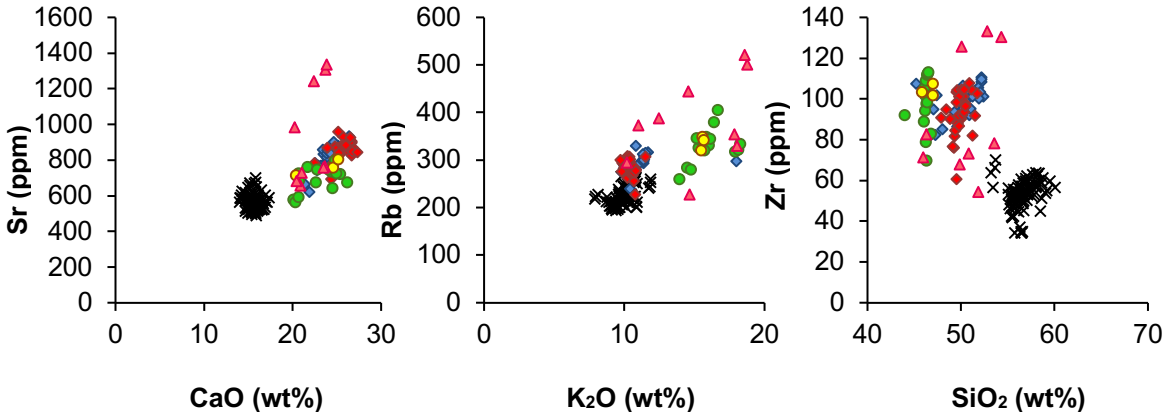

Figure 8.6 Trace element contents (pXRF) compared with major element concentrations (EPMA-WDS).

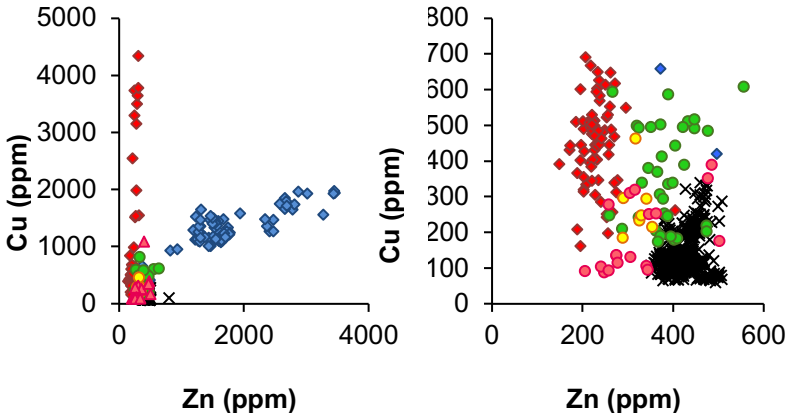

Figure 8.7 Scatterplots illustrating the Cu and Zn compositions of the original glass from the GEW. Legend as in Figure 8.4.

Thirteen of the samples analysed by LA-ICP-MS were identified as original or possibly original to the window; as stated previously, these were primarily selected to calibrate the pXRF data, so for example a higher proportion of Mn-coloured glasses were included in the sample set than are present in the window due to their high Sr or Rb concentrations. This group comprises four original white glass pieces, four Mn-coloured glasses, and one each of red, blue, light blue, green and yellow. The rare earth element (REE) contents of the analysed glasses are reported in Figure 8.8, normalised to the composition of the continental crust (Wedepohl, 1995). The white glass pieces are distinct from the rest, with higher light REEs and lower heavy REEs. Despite the differences in their major element compositions, the colours are mostly consistent with each other, with a positive anomaly at Eu and higher heavy REEs.

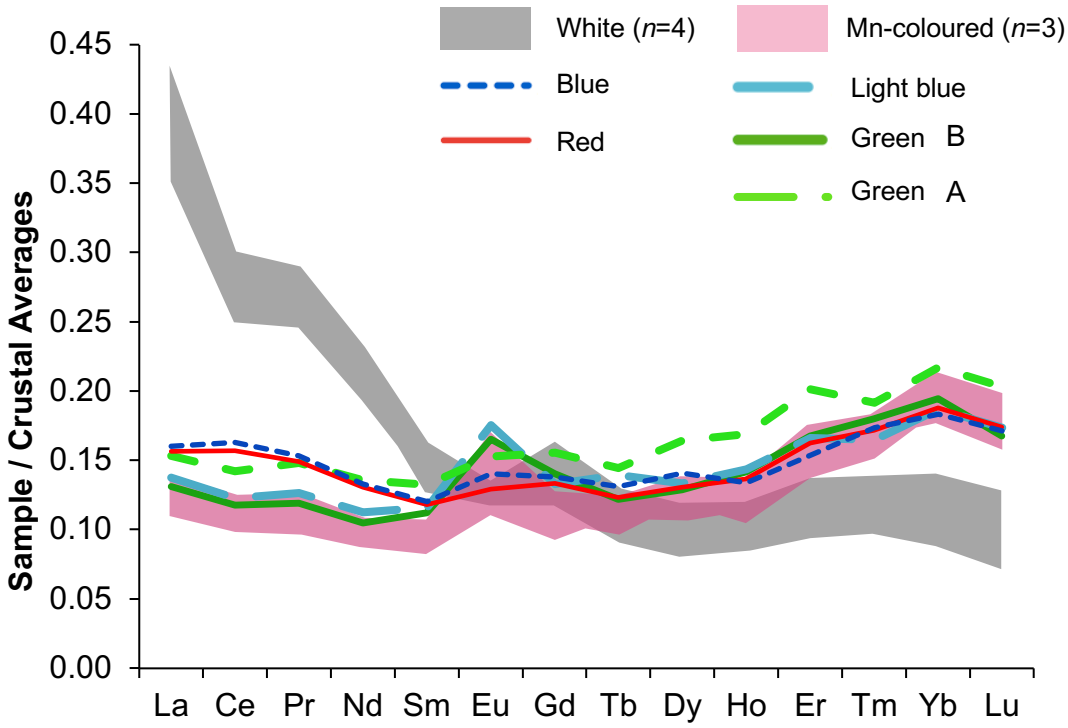

Figure 8.8 REE contents of original GEW glass, normalised to the composition of the continental crust (Wedepohl 1995). The shaded areas show the full range of the four white glass samples and the four Mn-coloured samples (maximum to minimum).

8.2.1 The original white glass

The white glass pieces (Figure 8.10) are generally in superior condition, with only light micro-pitting on the surface and in some cases, minor paint loss. Many white glass pieces have yellow silver stain on the surface, and this technique is used copiously throughout the window. In composition, the white glass pieces have high magnesia, lower lime, and higher soda (about 2.3% Na_2O), and are consistent with previous analyses of glasses produced in England during the medieval period (see next section). Overall the chemical composition of the original white glass is fairly consistent across the window. However, two subgroups can be distinguished based on P_2O_5, K_2O, and Na_2O concentrations; a similar trend was noted in the SEM-EDS data from the Cardiff-York project. The lower P_2O_5 group is concentrated in the lower part of the window (Figure 8.9).

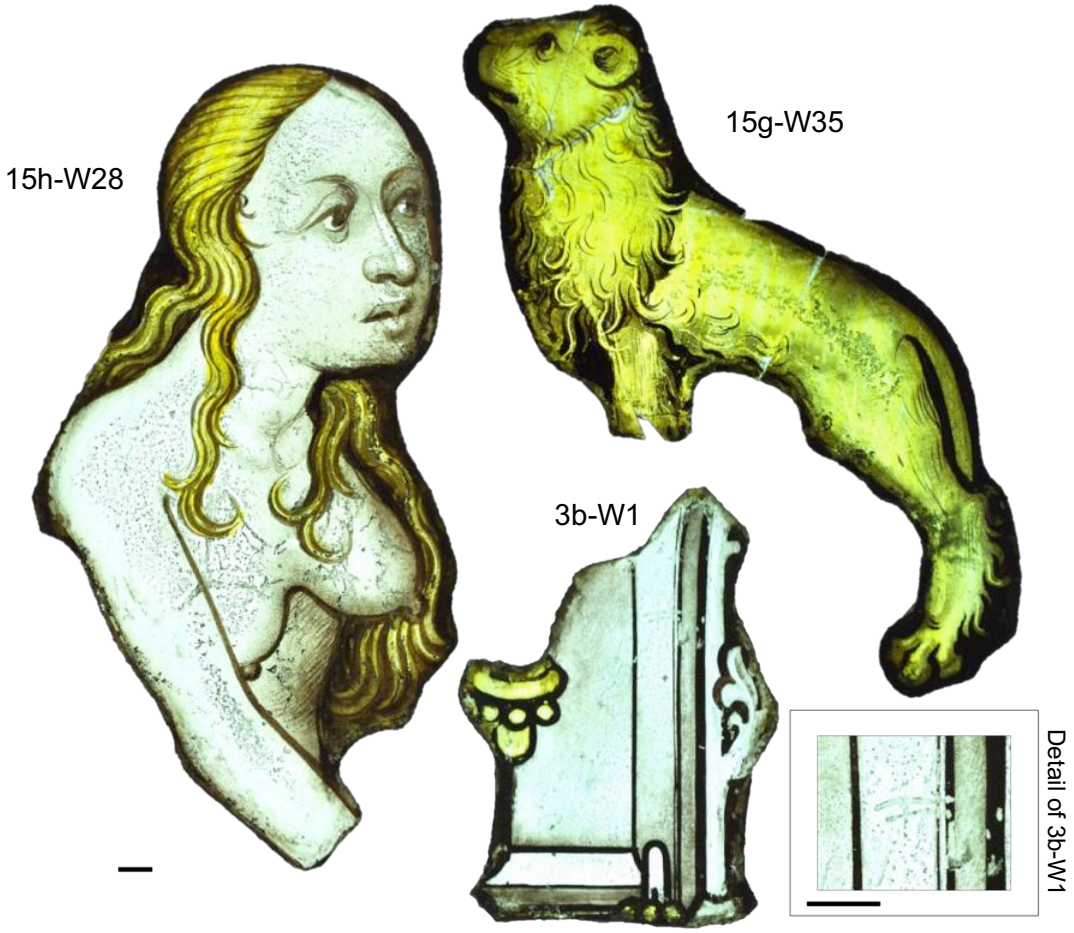

Figure 8.10 White glass pieces from the GEW. A golden colour was applied by silver staining, either to achieve two colours in a single piece of glass (such as Eve's hair in 15h-W28, or in 3b-W1, part of the architectural frame) or to colour the entire piece (15g-W35, the lion). A detail of the architectural piece (3b-W1), shows an original glazier's mark from Thornton's workshop (N. Teed, *pers. comm.*). Scale bars (lower left, and inside the box showing the detail) show 1cm.

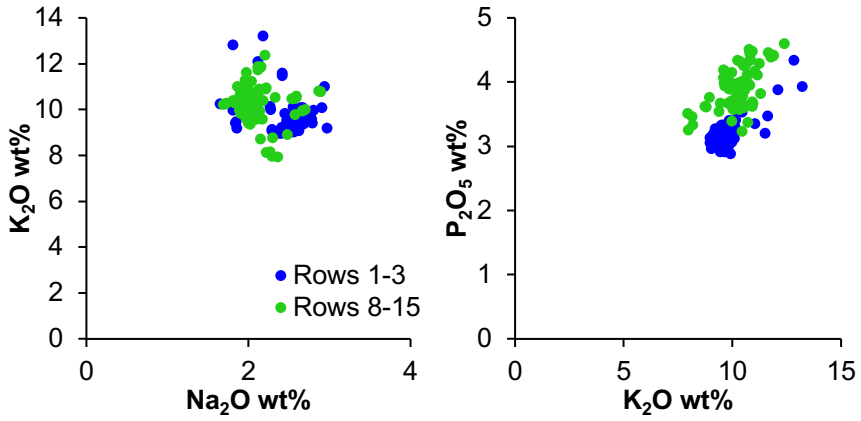

Figure 8.9 Scatterplots showing the distribution of two consignments of glass; the colours relate to the panels analysed in the lower (rows 1-3) and upper (rows 8-15) parts of the main lights of the GEW. Note: these plots include data from the Cardiff-York project.

8.2.1.1 Comparison with Staffordshire glass

The original white glass from the GEW are compared to previously published data for glasses from kiln sites in both Staffordshire and the Weald (Table 8.3); the available data include samples from two sites at Little Birches, Wolseley (LBW) in Staffordshire, the first dated to the 13th or early 14th centuries and the second to the early 16th century, a 16th century kiln site at Bagot's Park in Staffordshire, and from the Weald, a 14th century kiln site at Blunden's Wood, and 16th century kiln sites at Idehurst (North and South) and Knightons (Dungworth and Clark, 2004; Meek *et al.*, 2012; Mortimer, appendix in Welch, 1997). It has been previously observed that Staffordshire glasses tend to contain higher concentrations of manganese than Wealden glasses (Meek *et al.*, 2012); it is also generally lower in iron for both the earlier and later periods (Figure 8.11). On the basis of manganese and iron contents, the GEW white glasses are more similar to glasses from Staffordshire than those from the Weald (Figure 8.11).

The glasses from LBW show differences in composition between those from the 13th/14th century context (North Site) and those from the early 16th century context (South Site): the earlier glasses have lower soda and magnesia, and higher lime. The

Table 8.3 Chemical composition of glass samples from Staffordshire and the Weald, compared to GEW white glass compositions. The Little Birches (LBW) and Bagot's Park (BP) data are from Mortimer (appendix in Welch, 1997) and Meek *et al.* (2012); the Blunden's Wood (BW) and Knightons (KT) data are from Meek *et al.* (2012), and the Idehurst (IH, North and South sites) data are from Dungworth and Clark (2004).

	Staffordshire			The Weald			
Site	**LBW**	**LBW**	**BP**	**BW**	**IH**	**KT**	**GEW**
Century	**13th-14th**	**early 16th**	**16th**	**14th**	**16th**	**16th**	**1405-8**
Na_2O	1.30	2.42	2.76	2.53	2.60	2.42	2.26
MgO	6.88	7.53	7.39	6.72	6.82	6.70	7.32
Al_2O_3	1.95	1.31	1.80	0.89	1.63	1.96	1.36
SiO_2	52.83	57.22	60.19	58.41	54.93	56.02	56.65
P_2O_5	4.15	3.31	3.24	2.97	3.63	3.80	3.68
SO_3	0.69	0.35	0.29	0.14	0.30	0.30	0.17
Cl	0.10	0.16	0.23	0.50	0.54	0.34	0.33
K_2O	13.33	12.34	10.00	11.26	10.07	10.79	9.91
CaO	16.73	13.13	11.61	13.09	17.88	13.66	15.62
TiO_2	0.20	0.15	0.15	0.09	0.23	0.21	0.07
MnO	1.48	1.49	1.55	1.08	1.04	0.94	1.45
Fe_2O_3	0.68	0.54	0.63	0.72	0.63	0.80	0.47
***n*=**	4	51	23	20	24	10	101

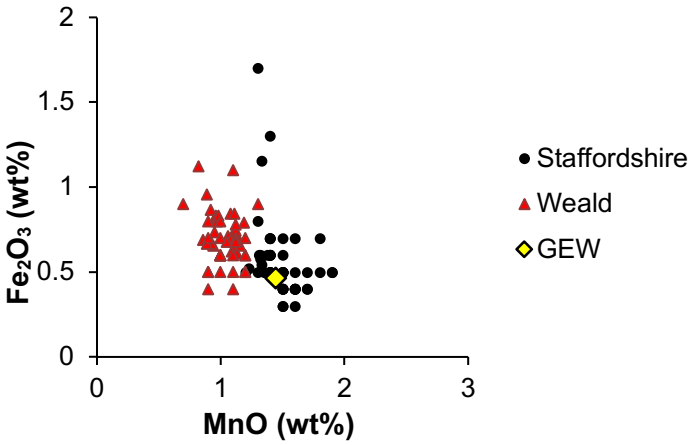

Figure 8.11 Manganese and iron contents of glass from kiln sites in Staffordshire and the Weald, compared to the mean composition of the GEW white glass. Data from Staffordshire and the Weald are from Mortimer (Appendix in Welch, 1997), Dungworth and Clark (2004), and Meek *et al.* (2012).

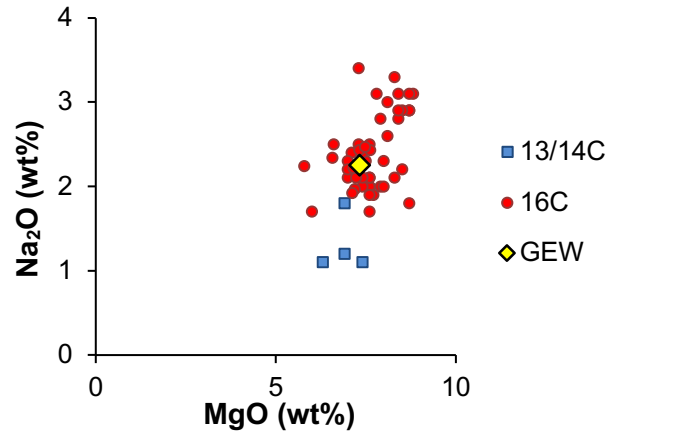

Figure 8.12 Soda and magnesia contents of Staffordshire glass from the earlier (13th-14th century) and later (16th century) contexts, compared to the mean composition of the original white glass of the GEW.

GEW white glasses have soda and magnesia contents more similar to the 16th century LBW glasses (Figure 8.12).

Some of these previously published samples from LBW were made available through the Cardiff-York project for analysis of isotopic ratios by TIMS. The results of the $^{143}Nd/^{144}Nd$ and $^{87}Sr/^{86}Sr$ analyses of three samples from the 13th/14th century context of LBW, three samples from an early 16th century context of LBW, six samples from the GEW (three white and three coloured glass pieces), and five samples from the St. William Window (SWW, also attributed to Thornton and dating to *c.* 1415) of York Minster (two white and three coloured glass pieces) are reported in Appendix D and Figure 8.13 (excluding the SWW glass). Figure 8.13 also shows data from Meek *et al.* (2012), who reported the isotopic ratios of four sites from Staffordshire (both 16th century, including LBW) and the Weald (a 14th century and a 16th century site; major element compositions from these four sites are included in Table 8.3).

The isotopic ratios of the present analyses of 16th century samples from LBW are consistent with those published by Meek et al., but the 13th/14th century samples have a lower $^{143}Nd/^{144}Nd$ ratio and a wider range of $^{87}Sr/^{86}Sr$ ratios. The GEW original white

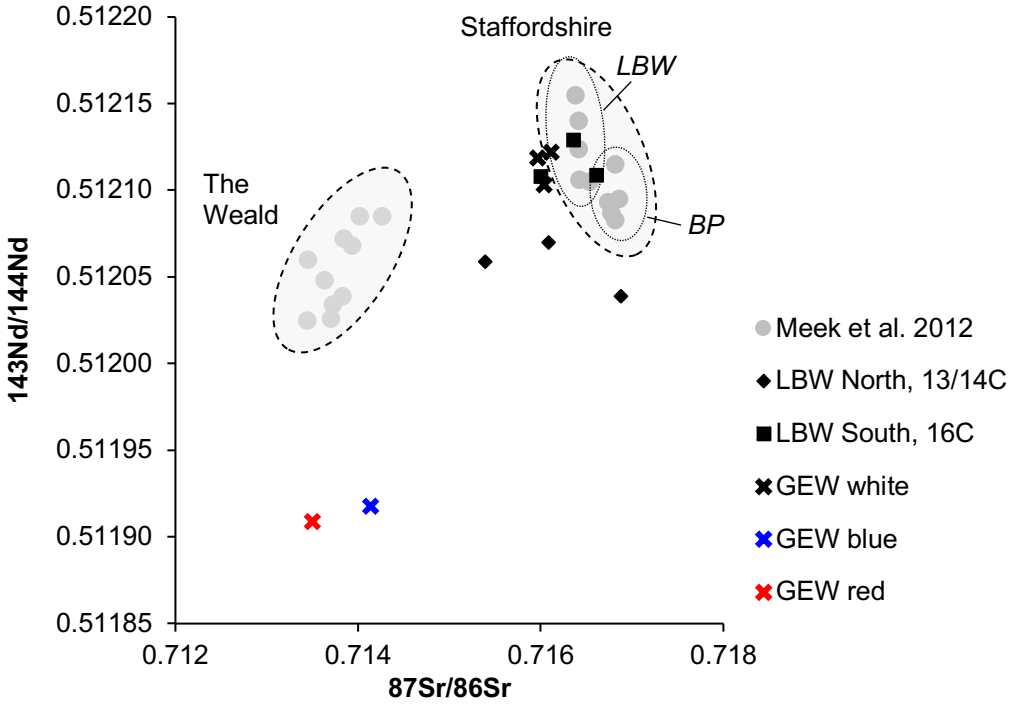

Figure 8.13 Graph showing the isotope ratios of glass from the two LBW kiln sites and the GEW (white, blue and red). The data is superimposed on ellipses showing the range of previous data from 16th century kiln sites in Staffordshire (from LBW and Bagot's Park, BP) and 14th and 16th century sites in the Weald (Meek *et al.*, 2012).

glass samples are consistent in their isotopic ratios with the early 16th century LBW data. The SWW white glass (not shown in Figure 8.13) are also consistent with the GEW white glass and the early 16th century LBW samples (see Appendix D).

The major element composition and isotope ratios of the GEW original white glass are overall consistent with glass produced in Staffordshire, with more similarities to the glass found in the early 16th century context at Little Birches than in the late 13th/early 14th century. However, it is uncertain whether the samples associated with the earlier site were produced there, due to the poor preservation of the North Site and the low incidence of associated glass. It is possible that some or all of the excavated glass are cullet collected for recycling.

8.2.2 The original blue and red glass

The original blue and red glass pieces (Figure 8.14) show variable deterioration, with the blue glass generally in good or moderate condition (with minor pitting), and the red glass ranging from poor to good condition. Some of the red glass pieces had deteriorated to the point of loss of the flash layer, while others only showed minor pitting on the surface. After white glass, red and blue are the most common colours in

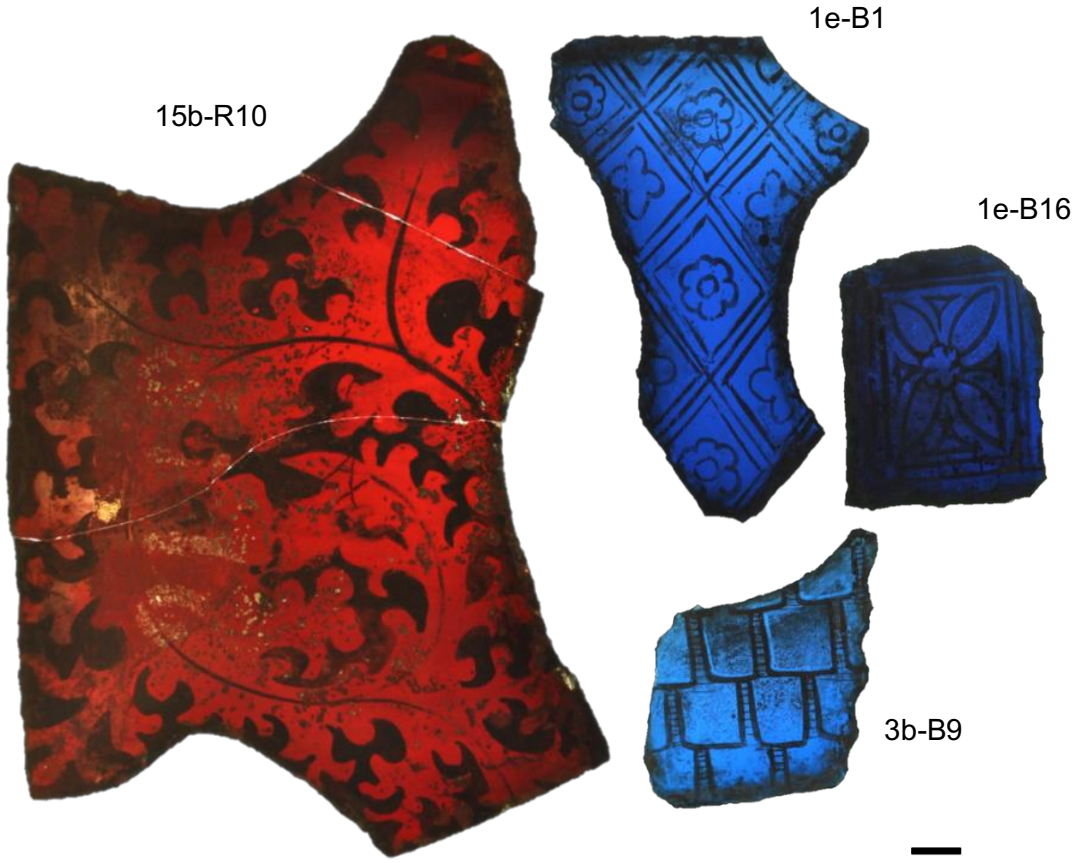

Figure 8.14 Blue and red glass pieces from the GEW. The red glass is painted with a *rinceau* design used throughout the window. One of the blue glasses pictured include a HLLA blue (1e-B1), which will be discussed in a later section. Scale bar is 1cm.

the window, used for the background of the panels with a painted seaweed foliage pattern (*rinceau*), as well as for other details such as clothing or rooftops.

The original blue and red glass pieces are part of ash group A, and are made with a very similar base glass recipe, with about 50% SiO_2, 25% CaO, 10% K_2O, 4.3% MgO, 3.5% P_2O_5, and 1.3% Na_2O (refer again to Figure 8.3). They also contain higher concentrations of the trace elements Rb, Sr, and Zr than the white glass (about 290; 825; and 95 ppm respectively, Figure 8.4; see also Figure 8.15). The blue glass is coloured with cobalt and is rich in zinc, with at least two groups defined by Zn contents (most with less than 2000ppm Zn, and a smaller group with more, Figure 8.7). The latter group are found concentrated in panels 1e and 15a, and one or two in 3b, 15g and 15h. The red glass are coloured by flashing (Type B, Kunicki-Goldfinger *et al.*, 2014; see later section). Isotope ratios of a blue (1h-B2) and a red glass piece (1h-R5) are very similar (see Figure 8.13), indicating a common origin.

Three light blue glass pieces (10c-B6, 15f-B1 and 15f-B2) were analysed, which if original are a rarity in the window. This glass has higher potash (15% K_2O) and lower

lime and silica (21% CaO, 47% SiO_2) than the rest of the blue potash glass pieces, and trace element contents more similar to the green glasses (e.g., lower Sr, see Figure 8.4).

8.2.1.2 Blue colour: Comparison with Gratuze cobalt ores

As mentioned previously (Chapter 3), Gratuze and colleagues (Gratuze, 2013; Gratuze *et al.*, 1996, 1995, 1992; Soulier *et al.*, 1996) have identified several cobalt ores that were used for colouring blue glass during the medieval period in Europe. The compositional data for the blue glass allow comparison with these previously characterised ore groups.

Most of the original blue glass pieces were coloured with a Zn-rich cobalt ore. This glass was probably coloured using the Co-Zn-Pb-In ore, which originated in Freiberg, Germany, where mining was carried out from 1168 AD, and which was in use for colouring blue glass from the end of the 12th century through the 14th or 15th centuries (Gratuze, 2013; Gratuze et al., 1995, 125; B. Gratuze, *pers. comm.* 22 June 2018).

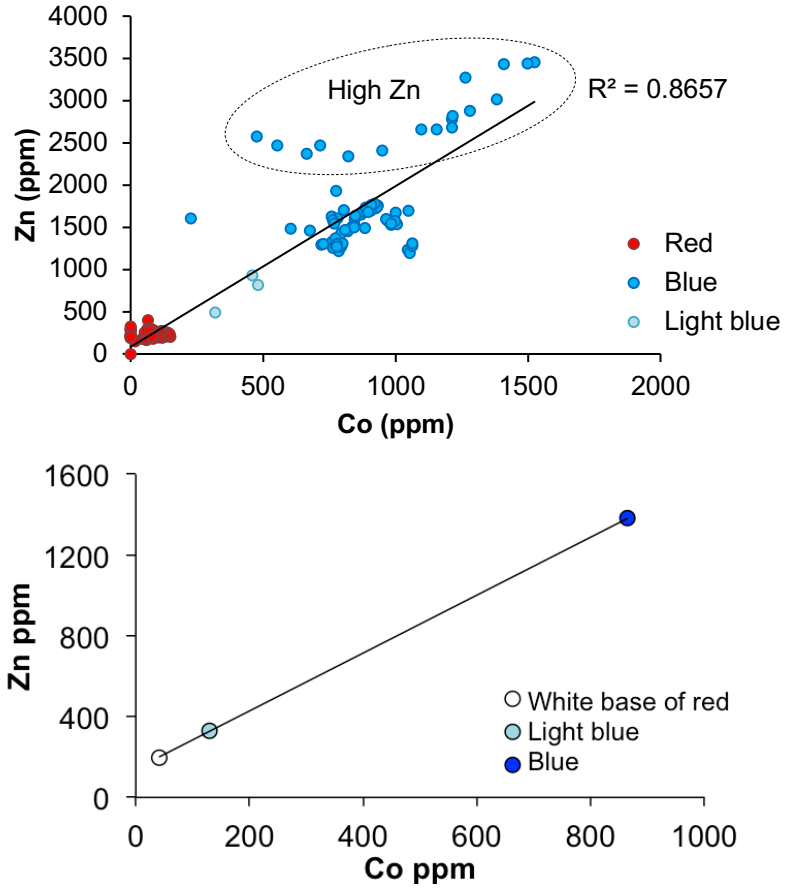

Figure 8.15 Biplots showing a linear relationship and mixing line between the red, light blue and blue (above, pXRF; below, LA-ICP-MS). Since the reds and blues share such a similar composition, the red is assumed to have the same composition as the blue base glass before the cobalt was added.

The higher Zn group of blue glasses is also marked. These glasses are mostly confined to panels 1e and 15a (with one or two samples found in panels 3b, 15g and 15h).

Although indium was not analysed by LA-ICP-MS in this study, the Cardiff-York project data show high In for the Zn-rich blue glasses.

The light blue pieces are also coloured with a Zn-rich cobalt ore, and it appears that the same ore was used. As the red and (dark) blue glasses have the same base glass composition and the same origin (see again Figure 8.13), the white glass base of the red glasses can be used as a proxy for the blue glass composition before the addition of the cobalt colourant. Figure 8.15 shows the cobalt and zinc concentrations of the blue, light blue and red glasses (pXRF and LA-ICP-MS data); the linear relationship suggests that the same ore was used for both light and dark blue, and that similar zinc levels were present in both base glass compositions. As the light blue glasses are consistent with the other colours from the GEW in REE patterns (see again Figure 8.8), it is probable that they were from the same region.

8.2.1.3 Red glass: Comparison with Kunicki-Goldfinger *et al.* (2014)

Various types of red flashed glass have been categorised (Kunicki-Goldfinger *et al.*, 2014; Newton and Davison, 1989; Spitzer-Aronson, 1975) as described in Chapter 3. The most recent paper by Kunicki-Goldfinger *et al.* (2014) noted that Type A (striated) was dominant up until the late 14th century and was mostly made with LLHM glass, while Type B (simple flashing) was produced from at least the 14th century and was generally made with HLLM glass. All of the original red glass from the GEW were Type B with a single layer of red glass overlaid a thicker white glass base, often with another thin layer of white glass atop the red (Figure 8.16). The typology, the base glass composition (high lime, low magnesia) and the date of the GEW red glass are all consistent with the trends reported in that paper (which included GEW samples from

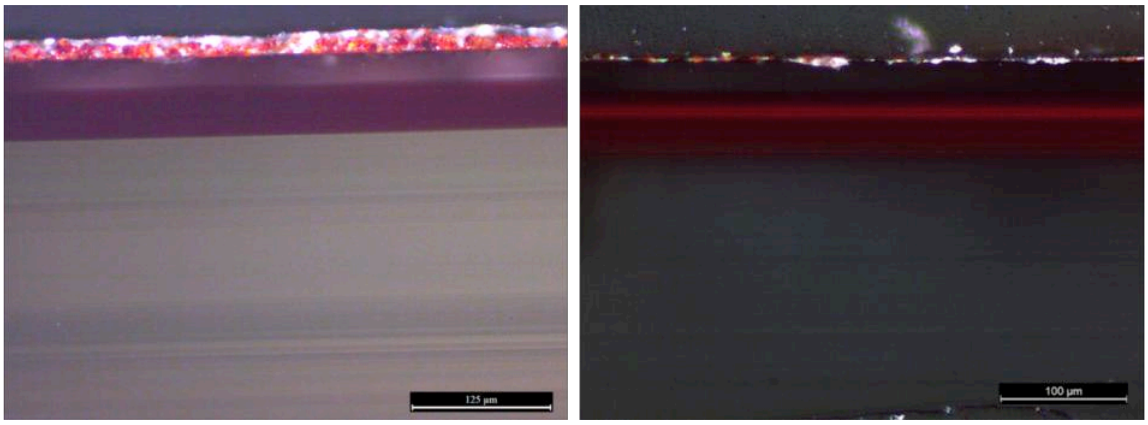

Figure 8.16 Micrographs of the cross-section of two red glass pieces from the GEW, showing a Type B3 structure (Kunicki-Goldfinger *et al.*, 2014). The image on the left is also a good image of the grisaille paint in cross-section, red due to the presence of iron in the form of hematite.

the Cardiff-York project).

8.2.3 The original green and yellow glass

The original green and yellow glass pieces (Figure 8.17) generally are in poorer condition, with pitting, loss of paint, and in some cases loss of the glossy surface. Fewer pieces of this colour are present in the window, perhaps due in part to replacement of the glass because of its more advanced deterioration.

The original green and yellow glasses are characterised by high potash (about 15.7% K_2O) and also contain about 46% SiO_2, 23% CaO, and 4.5% MgO. In trace element composition, the green/yellow glasses contained higher Rb, Sr and Zr than the white glass, and compared to the blue/red glasses contained higher Rb, lower Sr and similar amounts of Zr.

The major element compositions of the green and yellow glass pieces are less consistent as a group than the blue and red glass groups, with higher standard deviations for most elements analysed (refer to Table 8.2). For example, phosphate

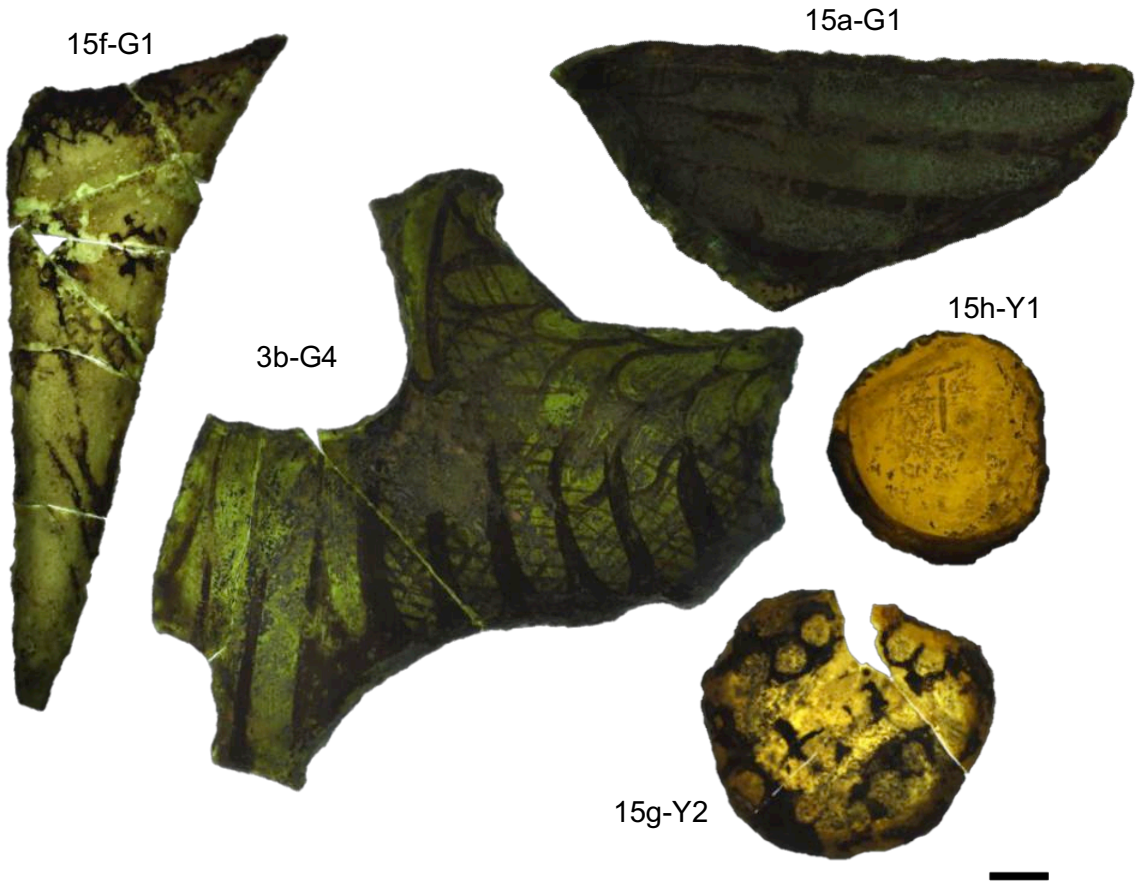

Figure 8.17 Green and yellow glass pieces from the GEW. 3b-G4 was originally one piece with the glass piece pictured in cross-section in Figure 8.19, with composite morphology. 15h-Y1 is a HLLA yellow, bearing an original glazier's mark (N. Teed *pers. comm.;* refer also to Figure 8.10); this will be discussed in a later section. Scale bar is centimeters.

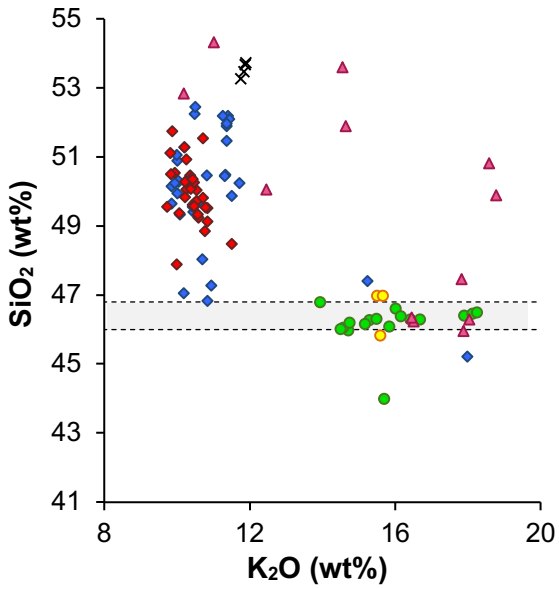

Figure 8.18 Scatterplot showing the narrow range of values for silica present in the green and yellow glasses, in comparison to other groups.

ranged from 2.2 - 4.8% P_2O_5, sodium concentrations from about 0.6% to 1.6% (Figure 8.3), and manganese from 0.7% - 1.7% MnO. The exception to this wide variability is silica (Figure 8.18), which was measured as between 46.0-46.8% for nearly all of the green samples (excluding two out of 18: 3b-G3, 45.8% SiO_2; 15f-G1, 44.0% SiO_2); the two original yellow glasses in the control group have 47.0% SiO_2.

The green glasses may be subdivided into two groups by their soda and phosphate contents and were possibly made using different ashes (see again Figure 8.3; Table 8.4). One subsample from each ash group (A and B) was analysed by LA-ICP-MS, and both glasses appear to be from the same region as the other coloured glasses on the basis of their REE patterns (Figure 8.8). The green A glasses with higher soda (1.5-1.7% Na_2O), found in panels 2j (n=2, Cardiff-York project), 3b (*n*=3) and 15f (*n*=1) are in some ways very similar to the blue/red group in their base composition; these have a Na_2O:P_2O_5 ratio consistent with the blue/reds rather than the lower soda green glasses (Figure 8.3). The primary differences between the base glass compositions of the blue/red group and green A group are the higher potash and iron of the green A glasses (Table 8.4). Removing about 5% K_2O and 1.5% Fe_2O_3 from this group of green glasses results in a base glass composition that is very similar to the blue/red glasses, with about 50% SiO_2 and 23% CaO.

The green glasses (A and B) are characterised by high concentrations of Fe_2O_3 (1.2-2.5%). One of the green A glasses comprises 2-3 layers of low-iron colourless glass on a high-iron (3.1% Fe_2O_3) olive-coloured base (Figure 8.19). The thickness and uniformity of the low iron layers make mixing an unlikely explanation for this morphology, but no parallels to this glass, with several flashing treatments, are known

Table 8.4 Major element composition of green and yellow groups, and the blue/red group for comparison.

	Green B - low Na		Yellow		Green A- high Na		Blue/Red	
Na2O	0.56	*0.08*	0.88	*0.61*	1.55	*0.13*	1.32	*0.32*
MgO	4.54	*0.19*	4.52	*0.29*	4.35	*0.28*	4.33	*0.23*
Al2O3	1.24	*0.29*	1.27	*0.33*	1.65	*0.02*	1.71	*0.14*
SiO2	46.30	*0.21*	46.60	*0.67*	45.64	*1.14*	50.00	*1.38*
P2O5	3.17	*0.75*	3.08	*0.74*	4.25	*0.43*	3.51	*0.53*
SO3	0.22	*0.04*	0.25	*0.01*	0.27	*0.03*	0.18	*0.04*
Cl	0.03	*0.04*	<		0.04	*0.01*	0.05	*0.02*
K2O	15.85	*1.43*	15.58	*0.09*	15.78	*0.18*	10.71	*1.20*
CaO	23.58	*1.96*	23.39	*2.59*	20.88	*0.57*	24.79	*1.36*
TiO2	0.07	*0.03*	0.08	*0.06*	0.13	*0.03*	0.09	*0.02*
MnO	1.44	*0.19*	1.50	*0.01*	1.47	*0.03*	1.28	*0.11*
Fe2O3	1.73	*0.35*	1.22	*1.62*	2.51	*0.47*	0.77	*0.28*
CoO	<		<		<		0.07	*0.05*
CuO	0.06	*0.03*	<		0.06	*0.01*	0.14	*0.07*
ZnO	0.03	*0.02*	<		0.04	*0.02*	0.12	*0.12*
BaO	0.42	*0.07*	0.43	*0.05*	0.37	*0.02*	0.28	*0.03*
PbO	<		<		0.06	*0.02*	0.22	*0.17*

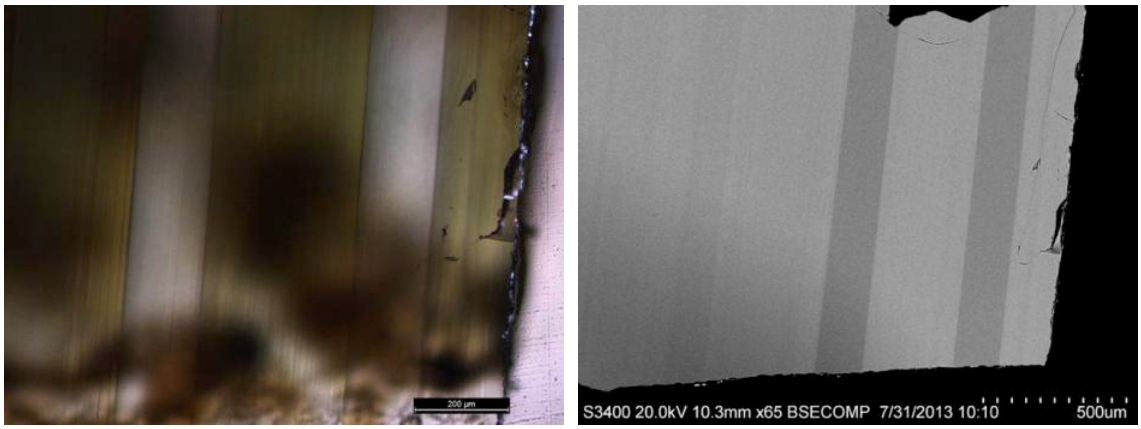

Figure 8.19 Optical micrograph and backscattered electron image of a green/yellow glass (3b-G3) with 2-3 layers of colourless glass with low iron. Two low iron layers are visible in the optical micrograph; in the BSE image, a more faint, third line is also visible. The presence of so many layers is unusual unless they are striae produced by mixing two glasses which failed to fully homogenise in the working pot; however, the layers are thick and consistent in width and therefore that interpretation is unlikely.

to the author. The two yellow glasses have lower iron contents (0.26-0.30% Fe_2O_3) with compositions otherwise similar to the green B glass.

The colouring effect of iron in glass is dependent on the iron concentrations and the ratio of the Fe^{2+} and Fe^{3+} ions; strongly reduced Fe^{2+} yields a fairly strong blue and strongly oxidised Fe^{3+} yields a weak yellow-brown, so that green is produced with

intermediate Fe^{3+}/Fe^{2+} ratios (Bamford, 1977; Weyl, 1951). The higher K_2O (and lower SiO_2) would have increased the basicity of the glass and also lowered the temperature at which the glass needed to be melted, both of which favour the formation of Fe^{3+} relative to Fe^{2+} and hence the development of a green colour (Cable and Smedley, 1987; Morey *et al.*, 1930; Stern and Gerber, 2004; Weyl, 1951). As the yellow glasses are likely to have a higher Fe^{3+}/Fe^{2+} ratio than the green glasses, but are compositionally similar in other respects, they are likely to have been produced at lower temperatures, or in a less smoky furnace, than the green glasses.

While the REE patterns suggest a common regional origin for the green glasses, the above model calculation suggests that the high soda group of green glasses were made using a similar recipe to the blues and reds, except that additional potash (and iron) was added to the iron-coloured glasses. The green B glasses and the yellows, on the other hand, although made using an ash with a different $Na_2O:P_2O_5$ ratio, also appear to be from the same region as the blues/reds and other original colours in terms of their REE.

8.2.4 The original manganese-coloured glass

Like the green and yellow glasses, the original manganese-coloured glasses (Figure 8.20) are generally in poorer condition and are less well represented in the window than the white, blue and red glass. This group includes a range of different pink and purplish hues (including a glass colour known as "murrey", which ranges from purplish to brownish pink to reddish brown), and similarly have a range of compositions (Figure 8.3). Due to the frequent lack of definitive painting (as in Figure 8.20), it was difficult to determine the originality of the glass based on visual examination, so all glasses in this group with forest glass compositions are provisionally considered "original".

The Mn-colours and contain about 1.3-1.9% MnO and 0.3-0.5% BaO. The higher contents of barium compared to the ash group A glasses could indicate the separate addition of "glass-maker's soap" in the form of psilomelane, which typically has a significant Ba-rich composition (Hunault *et al.*, 2017). However, the concentrations of both Mn and Ba in the Mn-colours are within range of typical wood ash compositions, and are similar to the concentrations of the ash group B glasses (1.1-1.7% MnO, and 0.3-0.5% BaO). It is considered unlikely that additional MnO was added and instead these characteristics are related to the use of ash B. As with the green and yellow glasses, the colours are produced by the redox conditions of the glass. Pink and purple colours are produced by the Mn^{3+} ion, and as with the green glasses, higher alkali would have increased the basicity of the glass and lowered the melting temperature,

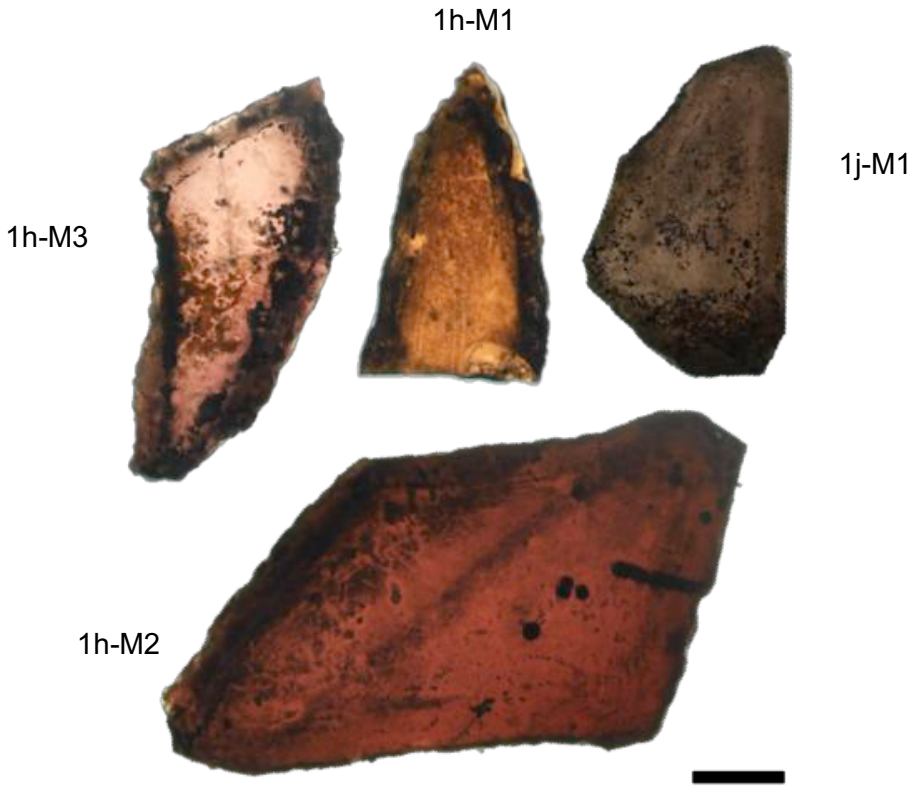

Figure 8.20 Various shades of purples, pinks, and murreys found in the GEW. These were grouped together due to the role of manganese in colouring the glass, and also due to the difficulty in assigning colours to the variety of shades. Scale bar is 1cm.

both which aid in the oxidation of the glass melt; furthermore, the base glass composition, including the proportions of potash and sodium as well as phosphate and divalent oxides, can affect the final hue (Weyl, 1951).

The Mn-colours are not a compositionally coherent group. Two groups are identifiable in the control group based on soda and potash concentrations, but this becomes three when strontium concentrations (pXRF) are also considered. One group has lower Na_2O and Sr and higher K_2O than the other, and a single sample in the control group has higher Na_2O and lower K_2O, but also lower Sr (Figure 8.21). This latter sample, 15g-M2, is thought to be a possible infill. The higher K_2O group is consistent with the ash B glasses, while the lower K_2O group (labelled "B/C" in Figure 8.3) was either made with a different ash, or with an additional raw material added to the batch.

It is difficult to distinguish the two lower strontium groups (i.e., the original glass versus the infills) solely on the basis of pXRF analysis of trace elements; however, this is an example in which the elements that were poorly measured by pXRF might be still useful in the characterisation of glass. As shown in Chapter 7, calcium is poorly determined by pXRF on the GEW glass due to poor surface conditions. Despite this, the calcium and strontium results help to differentiate the three groups observed in the

control group data (Figure 8.21). All of the Mn-colours have similar lime concentrations as analysed by EPMA in cross-section (about 20-23% CaO), but the concentrations measured by pXRF range from 9% to 34%. Therefore the different groups distinguished by their calcium contents in pXRF are related to differing surface conditions. Both glass composition and exposure to different environments are contributing factors to differences in corrosion. The higher potash and lower silica of the group B Mn-colours would have led to accelerated deterioration, probably resulting in the leaching of the Ca^{2+} ions out of the glass, forming a Ca-rich crust which was later removed during cleaning of the window glass; this would explain the lower levels of calcium measured by pXRF. The lower potash and higher silica of the group B/C Mn-colours would have undergone less severe deterioration under the same environmental conditions and so the measurement of calcium by pXRF was less affected. The infill group shows a different trend due to both its differing chemistry and also possible due to its movement from a different window, with different environmental exposure. Therefore, although the calcium measurements cannot be used to characterise the glass compositions, they can be used to draw out other information about the glass.

The mean compositions of the three subgroups are reported in Table 8.5, with the lower Na group labelled “B” as they are consistent in their base glass composition with the ash group B glasses (green and yellow) while the higher Sr group is labelled “B/C” as it appears they were made with an additional ingredient.

The B and B/C Mn-colours show a strong correlation between their Sr and Na contents. The higher strontium B/C glasses (with two clusters at 950-1000ppm and at 1250-1400ppm, see Table 8.5), have higher soda (0.9-1.0% Na_2O) and lower potash (10.2-14.6% K_2O). The B/C group have similar REE patterns to the other colours, in

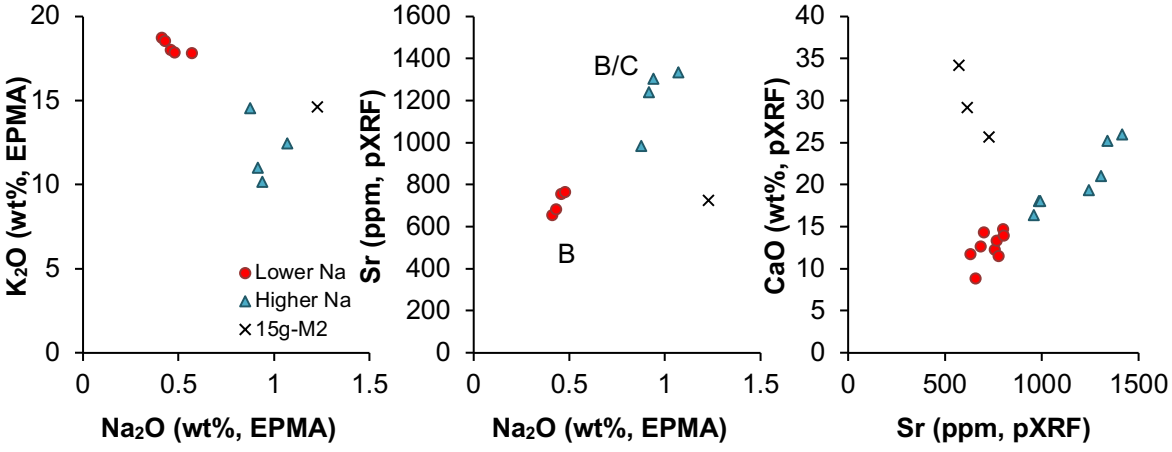

Figure 8.21 Biplots showing the composition of three groups of Mn-glass. K_2O and Na_2O were measured by EPMA-WDS (control group only), while Sr and CaO contents were analysed by pXRF.

Table 8.5 Mean compositions of different subgroups of Mn-coloured glasses. Symbols correspond to scatterplots in Figure 8.21.

	B ●		B/C(1) ▲		B/C(2)		Not orig. ×	
Na2O	0.47	*0.06*	0.88		0.98	*0.08*	1.23	
MgO	4.15	*0.21*	3.37		4.73	*0.25*	4.21	
Al2O3	0.70	*0.16*	1.08		1.51	*0.02*	1.50	
SiO2	48.09	*2.17*	53.59		52.41	*2.16*	51.90	
P2O5	2.26	*0.86*	1.91		2.01	*0.13*	1.75	
SO3	0.27	*0.06*	0.24		0.28	*0.08*	0.30	
Cl	<		0.13		<		0.08	
K2O	18.22	*0.43*	14.55		11.22	*1.15*	14.64	
CaO	22.03	*1.48*	20.23		23.33	*0.77*	21.07	
TiO2	0.06	*0.04*	0.03		0.07	*0.05*	<	
MnO	1.69	*0.28*	1.72		1.69	*0.19*	1.69	
Fe2O3	0.22	*0.06*	0.14		0.40	*0.05*	0.31	
CuO	0.03	*0.01*	<		<		<	
ZnO	0.04	*0.01*	<		<		0.05	
BaO	0.41	*0.05*	0.51		0.49	*0.04*	0.35	
PbO	<		<		<		<	
Cu	348	*296*	122	*24*	95	*7*	215	*88*
Zn	388	*81*	296	*40*	237	*23*	293	*47*
Rb	362	*97*	422	*40*	364	*48*	323	*84*
Sr	730	*64*	977	*18*	1325	*72*	638	*81*
Zr	75	*20*	81	*3*	128	*4*	61	*7*
EPMA (*n*)	*5*		*1*		*3*		*1*	
pXRF (*n*)	*10*		*3*		*4*		*3*	

particular the group B green subsample (refer again to Figure 8.8), suggesting a similar source. One subsample from the B/C group (1h-M1) was analysed by TIMS, although due to an analytical issue, the $^{143}Nd/^{144}Nd$ ratio determination was not successful. However, the $^{87}Sr/^{86}Sr$ ratio of this glass was higher than the blue/red pieces (0.716196, compared to about 0.713818 for the blue and red pieces), which could indicate a different provenance but is probably due to the use of a different raw material rich in strontium. In light of the elemental and isotopic results, it appears that the Mn-colours were made with a similar base glass recipe, with an additional raw material added to the B/C Mn-colours, which, along with the higher proportion of silica sand, has resulted in overall lower potash contents.

The positive correlation of sodium, aluminium and strontium concentrations between the B and B/C groups could suggest the addition of kelp ash to the batch (compare to kelp ash glass compositions reported by Dungworth, 2009, which have elevated

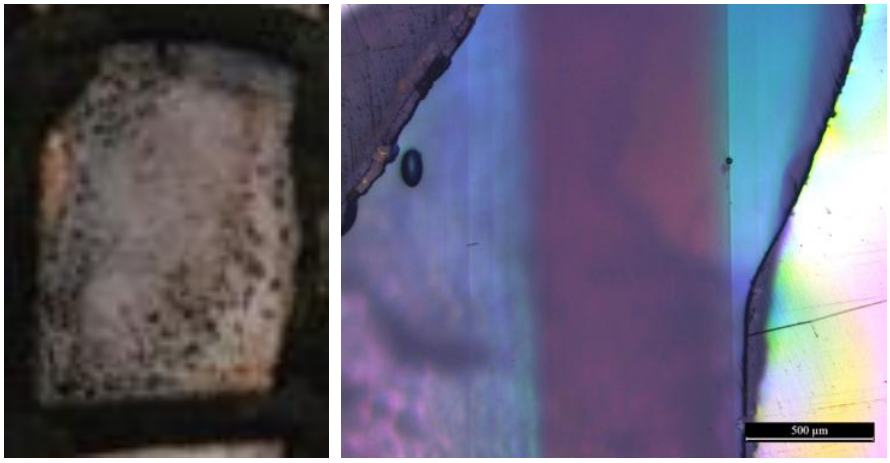

Figure 8.22 In situ photograph (left, 10h-M13), and micrograph of the cross-section (right, 10h-M5) of a glass coloured using flashing, with a blue-purple-blue morphology.

sodium, aluminium and strontium), possibly in order to adjust the alkalinity of the melt or to adjust the final hue by altering the proportion of soda and potash. However, in that case it would be expected that the $^{87}Sr/^{86}Sr$ would be lowered, not raised, by the marine signature of the strontium isotopes (*c.* 0.7092 $^{87}Sr/^{86}Sr$) in the kelp ash (Dungworth, 2009; Dungworth *et al.*, 2009; Freestone *et al.*, 2003; Wedepohl and Baumann, 2000).

Two subsamples in the ash B group are composite glasses coloured using a flashing technique, with three layers, blue-purple-blue, that result in a pale violet or pink colour (Figure 8.22). These are members of the lower strontium group, and are compositionally similar to the other glasses in the ash B group in both major and trace element concentrations. The similarities in the compositions of the different layers suggest that the same base glass was used before colouring. The blue layers contain about 0.06% CoO and have higher concentrations of copper and zinc, as well as aluminium, titanium, and iron, than the purple layer. Three other glass pieces from the same panel appear to be similar in hue, are consistent in trace element concentrations and are presumably also composite glasses; however, several other Mn-coloured glasses in panel 10h are consistent in their trace elements and are visually distinct in colour.

8.2.5 Original HLLA glass?

A small group of glasses which appear original have HLLA composition, with 7% K_2O and 23% CaO (Figure 8.23, Table 8.6). The soda (1.5% Na_2O) and chlorine (0.3% Cl) contents may indicate the addition of rock salt to the melt, as has been suggested by others (Kunicki-Goldfinger *et al.*, 2008; Schalm *et al.*, 2007; Wedepohl, 2003; Wedepohl and Simon, 2010). The soda to phosphate ratios are consistent with those

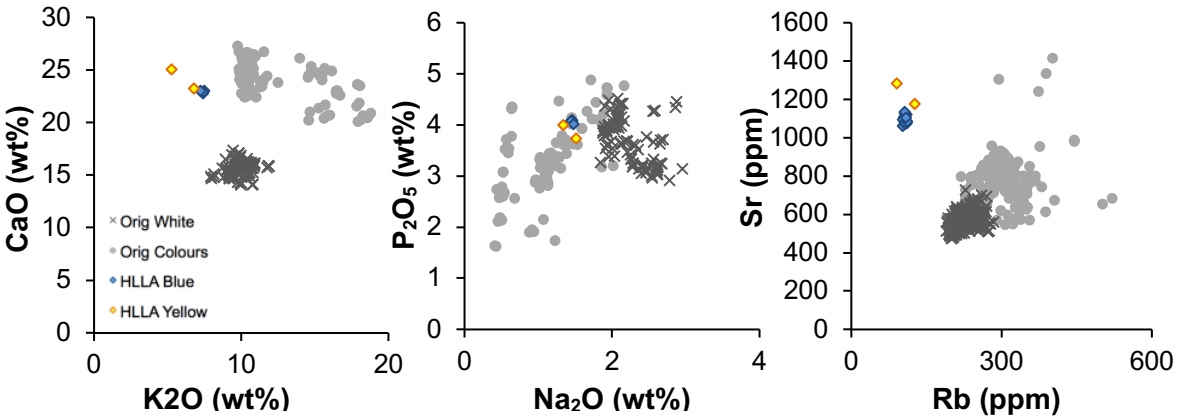

Figure 8.23 Major and trace element concentrations of the HLLA glass (the blue and yellow data points) compared to the other original glass of the GEW.

found in the original blue and red glasses (Figure 8.23), although this could be coincidence. The lower Rb and higher Sr are consistent with HLLA trace compositions previously reported (e.g., Dungworth, 2012b).

The blue HLLA glasses (*n*=13; see Figure 8.14, which shows a HLLA blue alongside the original blues in the GEW) are all situated in panel 1e in the bottom row. Although these differ in composition from the rest of the blue analysed in the window, based on the painted detail on many of the glass pieces, they appear to be original to the window. The elevated nickel of these glasses (0.05% NiO) suggests they were coloured with a Ni-rich cobalt ore. Gratuze identified two Ni-rich ores, a Co-As-Ni ore, in use from the beginning of the sixteenth century, and a Co-Ni ore, which was less commonly represented in his dataset but date to the end of the thirteenth century through the beginning of the sixteenth (Gratuze *et al.*, 1995; Soulier *et al.*, 1996)[18].

One sample of this Ni-rich group of cobalt blue glasses was analysed by LA-ICP-MS (1e-B4) and contains arsenic contents above the rest of the analysed samples (48ppm compared to 2-12 ppm), but this concentration is more consistent with the Co-Ni ore group rather than the Co-As-Ni (the Co-Ni group contained less than about 75ppm As, while the Co-As-Ni group contained in the range of 200-500ppm As; see Figure 8 in Gratuze *et al.*, 1995). This ore is of an uncertain geographical origin, although it was suggested that it is possibly the same ore as the Co-As-Ni group originating from Schneeberg, Germany; if so, the ore may have been roasted, burning away (most of) the arsenic, and the transition from Co-Ni to Co-As-Ni was a technological change in

[18] A more recent paper dates a Co-Ni-Mo-Fe group to "around 1500" (Gratuze, 2013, 323); however upon further enquiry from the author, Gratuze confirmed the range of the end of the thirteenth century through the beginning of the sixteenth (B. Gratuze, *pers. comm.* 22 June 2018).

Figure 8.24 Heraldic shield from panel 1j with lead cames that may be original. 1j-Y1 is a similar hue and painted in the same design as the other yellow glasses in the shield, although the grisaille is more faded than some of the pieces.

Table 8.6 Mean compositions of the blue and yellow HLLA glasses.

	Blue HLLA		Yellow HLLA	
Na2O	1.47	*0.01*	1.42	*0.12*
MgO	3.54	*0.02*	3.63	*0.01*
Al2O3	2.81	*0.02*	2.76	*0.50*
SiO2	52.89	*0.19*	54.31	*1.51*
P2O5	4.07	*0.03*	3.87	*0.19*
SO3	0.05	*0.01*	0.06	*0.03*
Cl	0.29	*0.01*	0.37	*0.01*
K2O	7.40	*0.10*	6.01	*1.08*
CaO	22.94	*0.10*	24.20	*1.31*
TiO2	0.06	*0.01*	0.08	*0.04*
MnO	2.06	*0.01*	1.85	*0.03*
Fe2O3	0.71	*0.02*	0.46	*0.03*
CoO	0.15	*0.02*	<	
NiO	0.05	*0.00*	<	
CuO	0.16	*0.01*	<	
ZnO	0.03	*0.00*	<	
BaO	0.30	*0.01*	0.30	*0.01*
PbO	<		<	
Cu	1078	*19*	60	*7*
Zn	237	*7*	292	*3*
Rb	106	*3*	108	*25*
Sr	1091	*27*	1231	*77*
Zr	111	*4*	103	*39*
EPMA	*4*		*2*	
pXRF	*13*		*2*	

ore processing, taking place around the beginning of the 16th century (Gratuze *et al.*, 1995, 125–126).

The other two HLLA glasses which are possibly original are yellow. One of these bears an original glazier's mark identified throughout the window (N. Teed, *pers. comm.*; see Figure 8.17, which shows 15h-Y1 alongside the original yellows and greens in the GEW; see also Figure 8.10 for another glazier's mark). The other is part of what is thought to be an original heraldic shield, containing the only lead cames in the window that are possibly original (N. Teed, *pers. comm.*; Figure 8.24). Iron concentrations are not particularly high (0.46% Fe_2O_3) and they also contain low sulphur in comparison to the yellow glasses original to the window made of potash-lime glass (HLLA: 0.06% SO_3; potash-lime: 0.25% SO_3), but these lower concentrations are within the range of

possible compositions for glass coloured by the amber chromophore Fe^{3+}-S^{2-} if other criteria are met (such as the addition of reducing agents to the melt, and the furnace temperature; Beerkens, 2005, 2003, 1999).

In light of the visual evidence including the painting style and glazier's mark, it would appear these glasses are original. If so, they are an early example of the HLLA recipe, although not inconsistent with previous findings; the appearance of HLLA is dated to 1400 in Germany (Wedepohl and Simon, 2010) and Belgium (Schalm *et al.*, 2007), and 1450 in France (Barrera and Velde, 1989).

8.3 Non-original medieval forest glass

Most of the non-original medieval glasses were identified using both visual observation of their painted detail and analysis of their chemical composition. Some pieces do not have distinctive painted detail, due to corrosion or deliberate abrasion (the latter is observed on some infills, as painted detail was removed in order to insert it into its new position); these pieces were identified by chemical composition alone. A small group of glass pieces, mostly white glasses, were identified as non-original on the basis of painted detail alone, as their chemical compositions did not distinguish them from the original glasses (these are marked in Appendix D; also see later section).

The chemical compositions of the non-original medieval glasses fall into both the potash lime and HLLA types. Although low rubidium contents are usually associated with HLLA glass, in the GEW examples of glass with low Rb and potash contents exceeding HLLA levels were identified (for example, 10c-B2, with 93 ppm Rb and

Table 8.7 Ratio of Rb:Sr and trace element contents (in parts per million) for the potash-lime glass, HLLA and kelp ash glass in this study.

		Potash-lime	HLLA	Kelp Ash
Rb/Sr	*Min*	0.180	0.031	0.003
	Mean	0.408	0.085	0.005
	Max	0.925	0.133	0.009
Rb	*Min*	93	38	*bd*
	Mean	248	78	17
	Max	520	126	24
Sr	*Min*	313	548	2578
	Mean	623	943	3743
	Max	1416	2091	4354
Zr	*Min*	*bd*	76	26
	Mean	67	132	44
	Max	133	255	59

11.6% K_2O, Appendix D). Rb alone is therefore considered an unreliable indicator of HLLA, and glasses for which only pXRF data had been collected were assigned to HLLA or potash-lime on the basis of the Rb:Sr ratio (Table 8.7). For potash-lime forest glass, this value range from 0.18 to 0.93, and for HLLA glass, 0.03 to 0.13. Kelp ash glass (although not medieval, it is another type of glass characterised by low Rb and high Sr) had a Rb:Sr ratio below 0.01.

8.3.1 Non-original white forest glass (potash-lime)

Several white glass pieces (7 in the control group, 21 in total) were identified as non-original on the basis of their painted detail, and were otherwise identical or very similar to the original white glass in composition (Figure 8.25). Several examples are given in Figure 8.26, which shows stylistic differences in the painting, differences in scale, or significant differences in deterioration (indicating different environmental exposure). These glasses probably represent glass from other windows that were glazed using white glass from the same source in Staffordshire, and which were later used to patch the GEW during conservation as was formerly customary (e.g., Milner-White, 1950).

Another group of non-original white forest glass (8 in control group) are compositionally distinct from the original glass, with higher Al_2O_3, Fe_2O_3, and K_2O and lower MgO and MnO (Figure 8.25); these also have high Zr contents. These glasses are still LLHM glasses, with compositional parallels in both England and NW France. The low concentration of MnO (0.7-0.9%) and higher Al_2O_3 (2-3%) may suggest a possible Wealden origin, with similar concentrations reported for glass from the site at Knightons in particular (Meek *et al.*, 2012). A further 20 glass pieces, analysed by pXRF only,

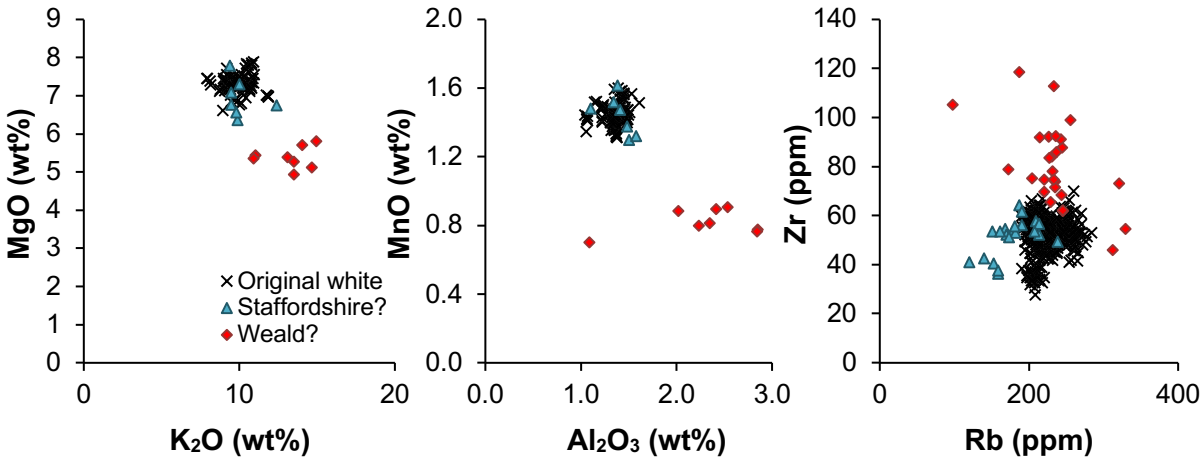

Figure 8.25 Scatterplots showing the composition of non-original white glass compared to the original white glass. Some glass are very similar in major element composition (examples pictured in Figure 8.26) while others have key differences, including lower MnO which may indicate a Wealden origin (Meek *et al.*, 2012). Some of the glass that were similar in major element composition have lower Rb; whereas glass with lower MnO has high Zr.

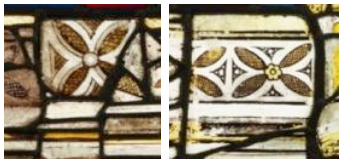

The piece on the left (1e-W43) is painted in a different style and scale (compare to original piece, right).

Both pieces (3b-W2 & W13, top centre of each image) are visually identified as infills, but their chemical compositions are very similar to the original glass.

The hand on the lower right (1j-W28) is painted in a different style and is heavily corroded, but pXRF analysis showed no difference in composition.

Although this head (10c-W7) is painted in the Thornton style, the scale is wrong for the panel. It was in place by 1884, when Camidge illustrated the window (YGT, 2015a).

These pieces (10c-W25 & W9), which belonged together originally, are painted in a style distinct from the Thornton style observed in the GEW.

This piece (10c-W10) was moved to its present location during the Milner-White (EMW) conservation campaign, who noted that it "had patched the Old Testament scene above of the dying Jacob blessing his sons, but certainly belonged to an Apocalypse panel" (YGT, 2015a). However, the style is dissimilar to Thornton's and the positioning and scale of the head do not fit this panel.

The animal's head on the right (15f-W47) is not painted in the same style (compare to the original sheep's head from the same panel, right).

Figure 8.26 Examples of white glass that were identified as not original to the window by visual evidence, but were indistinguishable or very similar to the original glass in chemical composition.

were consistent with this group and so have been tentatively identified as from the Weald (Figure 8.25).

8.3.2 Non-original coloured forest glass (potash-lime)

Most of the coloured medieval forest glass with potash-lime compositions that were identified as not original to the window were so identified by visual examination and chemical analysis, or in cases with little or no painted detail, by chemical analysis alone. Most of these were red and green glasses that have a low lime, high magnesia

composition (LLHM; Figure 8.27). All of these LLHM glasses also contained more chlorine than the original coloured glasses, similar to the concentrations measured in the original LLHM white glasses (Figure 8.27). The medieval infills were also distinguished by their lower concentrations of strontium and/or zirconium (Figure 8.27).

The green glasses in this group were coloured with about 3% CuO and also had higher ZnO (about 0.3%), unlike the original greens (which are of HLLM composition and coloured with iron). Most of the control group red glasses were Type A (with multiple

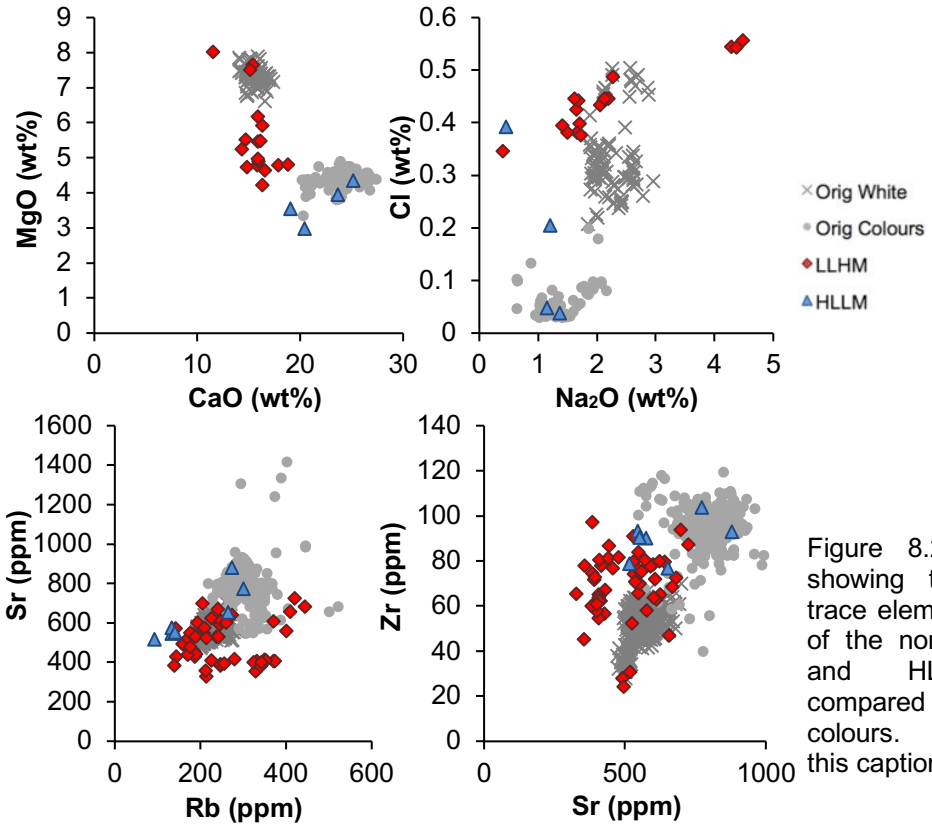

Figure 8.27 Scatterplots showing the major and trace element composition of the non-original LLHM and HLLM glasses compared to the original colours. Legend above this caption.

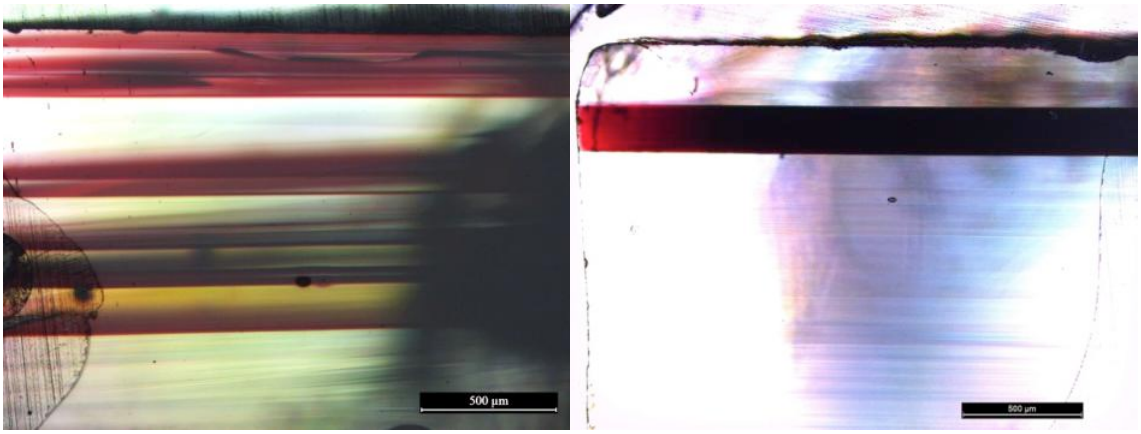

Figure 8.28 Two non-original red glass pieces with low lime composition. Most of the red glasses in this group have Type A structure, like the glass piece on the left (10e-R2). One non-original red has Type B structure (on the right, 3b-R5).

Figure 8.29 An example of a non-original blue glass (top, 10c-B3) that is identical in composition to the original blues, but painted in a different style. At the bottom is a picture of *rinceau* painted in the typical style of the GEW, This pattern was used throughout the window for the backgrounds of panels.

striated layers, Figure 8.28), which is in keeping with previous observations on association between red flash morphology and base glass composition (Kunicki-Goldfinger *et al.*, 2014); only one non-original red glass was Type B-3 (Figure 8.28**).** Three of the reds were distinguished by their higher magnesia and soda contents (about 7.7% and 4.4% respectively).

Seven blue glasses were identified as non-original potash-lime glasses, all of which have HLLM composition. Two of these were identical to the original blue glasses in major and trace element composition, but visual examination distinguished them (Figure 8.27**,** Figure 8.29). Another, analysed only by pXRF, had similar concentrations of rubidium and strontium but lower zirconium contents (Figure 8.27).

The remaining four HLLM blues, all found in panel 10c, could be identified using pXRF by their lower rubidium concentrations, although the Rb:Sr ratios were within potash-lime forest glass ranges (Figure 8.27; see again Table 8.7). Three glasses in this lower rubidium group were coloured using a Ni-rich cobalt, and are characterised by 11.5% K_2O, 19.0% CaO, 3.6% MgO, and 1.9% P_2O_5. The fourth was coloured with a Zn-rich cobalt and is characterised by about 11.6% K_2O, 20% CaO, 3.0% MgO, and 4.0% P_2O_5.

8.3.3 Non-original HLLA glass

There were several pieces of glass of various colours which were identified as high lime low alkali, and not original to the window (Figure 8.30). Those sampled for EPMA analysis contained about 56% SiO_2, 5% K_2O, 22.8% CaO, 4.2% MgO, 3.5% P_2O_5, and 3.0% Na_2O with high Cl (0.5%); they also contain low concentrations of Rb (less than about 100ppm), and all contained high Zr (100-250ppm). Sr concentrations were

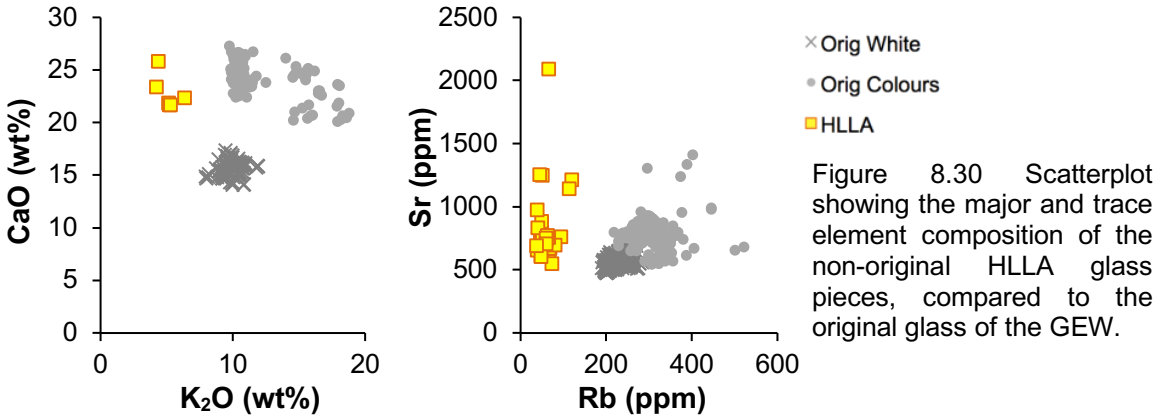

Figure 8.30 Scatterplot showing the major and trace element composition of the non-original HLLA glass pieces, compared to the original glass of the GEW.

Table 8.8 Composition of the Ni-rich HLLA blues, measured by pXRF, comparing the group that may be original to the panel and the glasses that are not original (reporting mean and standard deviation, parts per million).

	Original?		Not Original	
Co	1268	*24*	1235	*498*
Ni	451	*19*	707	*269*
Cu	1053	*30*	802	*295*
Zn	247	*12*	323	*172*
Rb	107	*3*	62	*17*
Sr	1096	*23*	709	*79*
Zr	112	*5*	155	*57*

variable, ranging from 430- 1220ppm. Ten of these are white, and resemble Welch's "Composition X" discovered at Little Birches, Staffordshire, in the early 16th century context (Welch, 1997). Two of this group are red glasses; one of these was examined in cross-section and is flashed using Type B technology.

Eleven pieces of blue glass were identified as HLLA and coloured with a Ni-rich cobalt ore; these were distinct from the blue HLLA group that was designated as possibly original in their Co, Ni, Cu, Zn, Rb, Sr and Zr concentrations (Table 8.8). Unlike the original group, which had very consistent compositions across the group, these non-original glasses have a wide range of concentrations for the elements analysed. Unfortunately, none of them were sampled for cross-sectional analysis.

Two yellow glass pieces were also identified as HLLA and not original; these are distinct from the two original yellow HLLA pieces both visually and with their significantly lower strontium concentrations (500-700ppm, compared to 1200ppm).

8.4 Summary of the compositional results

The results of the chemical analyses of the GEW glass show a range of medieval compositions present in the window. Amongst the original glass group are LLHM white glass and HLLM colours. These are also distinguished by their trace elements; the LLHM white glass have lower rubidium, strontium and zirconium than the HLLM colours.

The LLHM composition of the white glass is similar to glasses found in NW France and England. Comparison with glass produced in both the Weald and in Staffordshire showed that the GEW white glasses have manganese contents more similar to Staffordshire glass. Analysis of isotope ratios by TIMS showed consistency between the GEW white glass and glass produced at Little Birches, Wolseley in Staffordshire.

The HLLM colours include blue, red, green, yellow and Mn-colours, which are purplish or pinkish. All of these have phosphate contents above about 2% and are similar to compositions found in the Rhenish region. Compositionally, these glasses can be grouped by their P:Na ratio, which appears to be related to use of different ashes (see Figure 8.3).

The ash group A consists mostly of blues and red, as well as a small number of green glasses. The blues and reds, with about 11% K_2O, are highly consistent in their base glass composition excluding the elements related to colourants. The blues are coloured with a Zn-rich cobalt, while the reds are coloured with Type B flash technology. These glasses have higher strontium than the greens and yellows. The group A greens have very similar base glass compositions if the excess Fe_2O_3 and K_2O are removed.

The ash group B consists of green, yellow and Mn-coloured glass. These glasses are higher in K_2O. The higher potash of the greens and yellows would have facilitated the colouring of these glasses by iron, and may indicate the deliberate adjustment of the recipe in medieval glass colouring technology, either by the addition of potash to ash A as above or in the selection of a different, higher potash ash (ash B).

The Mn-colours (ash group B) have a range of K_2O compositions; examination of positive and negative correlations between different elements suggests that the Mn-colours have similar base glass recipe, with some of the glasses having an additional raw material added to the batch, which was high in Na_2O and Sr, and had similar concentrations of CaO. The purpose of this may have been to adjust the proportions of K_2O and Na_2O, which is known to affect the hue of colours produced by manganese in

glass, and as with the greens and yellows, higher alkali would have assisted in the colouring of the glasses.

A small group of blue and yellow glasses appear to be original, and have HLLA composition. The blues in this group are coloured with a Ni-rich cobalt. If original, these glasses are an early occurrence of HLLA (usually dated from about 1400 in Germany).

Several medieval compositions which were not original to the window were also identified, including some which were identical or very similar in composition to the original glass but which could be clearly identified by visual examination. It is suggested that these glasses originated in another window of a similar date, using glass from the same source, that at some point was removed and used to patch the GEW. Other non-medieval compositions, including kelp ash glasses and synthetic soda glasses, were also found in the window and are evidence of historical restorations.

CHAPTER 9

Original white glass batches and their distribution in the window

The identification of glass batches is an important approach to this research that will enable the study of the organisation of production in John Thornton's workshop through the spatial analysis of the batches (roughly equated to sheets of glass in the panels). This chapter focuses on the identification of batches in the original white glass. The GEW is an example of the International Gothic style, which is characterised by an increasing use of white glass to portray most of the scene (Marks, 1993). Therefore, the higher incidence and more widespread distribution of the white glass will allow the best coverage for examining how the panels were put together and the organisation of production in the workshop of John Thornton.

9.1 Identification of batches using compositional data

There is no established methodology for the identification of batches for a dataset such as this one. The criteria that all members of a batch must be identical (i.e., within the experimental error of the analytical equipment) for all elements analysed (Freestone *et al.*, 2009) is difficult to apply in this case; in a large group of glass from the same place and period such as the white glass of the GEW, considerable overlap is expected to obscure the identification of chemically identical batches. Another study dealing with a large dataset of overlapping compositions examined archaeologically defined groups (i.e., bundles of arrows) to determine if they clustered together compositionally (Martinón-Torres *et al.*, 2012); this approach, too, is difficult to apply to the present situation. Therefore, as described in Chapter 6 (Methods), different approaches based

on hierarchical cluster analysis were explored in order to ensure that the groupings are robust.

9.1.1 Panel-by-panel identification

In the panel-by-panel approach, chemically identical batches were identified in the control group first, using the criterion that all members of a batch must be identical in composition within experimental error. However, for several panels, the narrow range of chemical compositions present in a panel resulted in overlapping ranges of batches, such that several batch groups had shared members. In order to separate these groups, the data were analysed by hierarchical clustering, and the identicalness criterion used to determine the cluster boundaries (dendrogram 'cutree' or cophenetic distance).

The control group batches were then used to identify batch groups in the larger sample set analysed by pXRF. The five quantifiable elements using this method (Cu, Zn, Rb, Sr, and Zr) were analysed by hierarchical clustering, and the control group batches were used to determine the cluster boundaries. These were checked and confirmed through the examination of scatterplots with error bars equal to $\pm 1\sigma$.

Identification of batches through this approach was carried out with variable success. For many panels (in particular panels 3b, 10c, 10e, 10h, 15a and 15h), identification was straightforward. Cluster analysis was not necessary to identify control group batches (although still carried out for confirmation purposes). The control group batches for these panels translated well to the pXRF batches, with each control group batch confined to a distinct cluster and could also be easily identified by examining scatterplots of the pXRF data. In other panels, cluster analysis was necessary, but corresponded well to pXRF clusters (panels 15b and 15g).

For the row 1 panels, the variation in both major and trace element composition was very low, resulting in overlapping batches that were distinguished through cluster analysis, but which did not correspond as well to pXRF clusters; for example in panels 1e and 1j, two control group batches were combined in the pXRF clusters. Panel 1h white glass were almost all in one batch/cluster. Panel 15g was also characterised by overlapping batches and very poor correlation between the control group batches and pXRF clusters.

The full results for the panel-by-panel approach are reported in Appendix E.

9.1.2 The cross-window approach

In the cross-window approach, the trace element compositions of the original white glass pieces from across the window were also examined together and analysed using

hierarchical clustering and principal component analysis. While the panel-by-panel approach was viewed as the more robust approach, the advantage of the cross-window approach is that it would allow not only examination of batches within each panel, but examination of the use of batches across a row and across the window. A secondary benefit is that human error is less likely to enter the calculations compared to the panel-by-panel approach, in which cluster boundary decisions were made for every panel and therefore introduced the possibility that the boundaries would vary in sensitivity across the window.

The results of the cross-window cluster analysis were compared to the panel-by-panel approach, and six clusters were identified that corresponded well to the batches identified in each panel (Figure 9.1, Figure 9.2, Figure 9.3). Only 39 out of 350 samples (11%) were grouped in different batches using the two approaches, and only one sample (15g-W1) was separated from its control group batch.

The primary difference between the two approaches is that in some panels, batches that were distinct in the panel-by-panel approach were joined in the cross-window approach. This effect was constrained to panels that had a narrow range of compositions in the original white glass pieces, making the identification of a chemically-identical batch difficult. The foremost example is the row 1 panels, which in the panel-by-panel approach were difficult to divide into batches. In the original white glass of the first row, 102 of the 106 samples were part of cluster 1 in the cross-window approach.

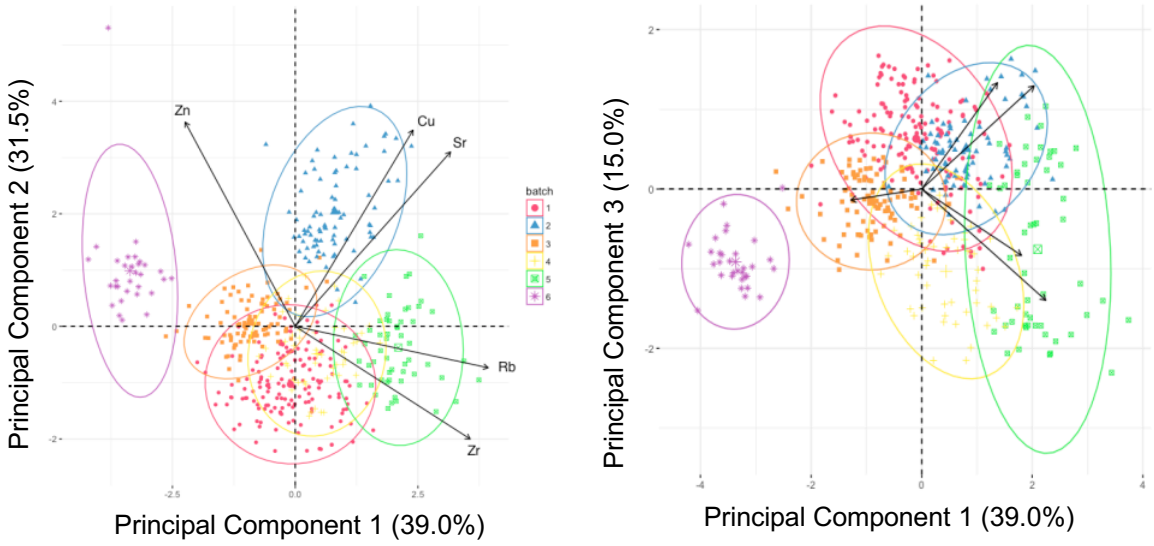

Figure 9.1 Principal components 1, 2 and 3 for the six batches identified in the original white glass of the GEW based on trace element concentrations measured by handheld pXRF.

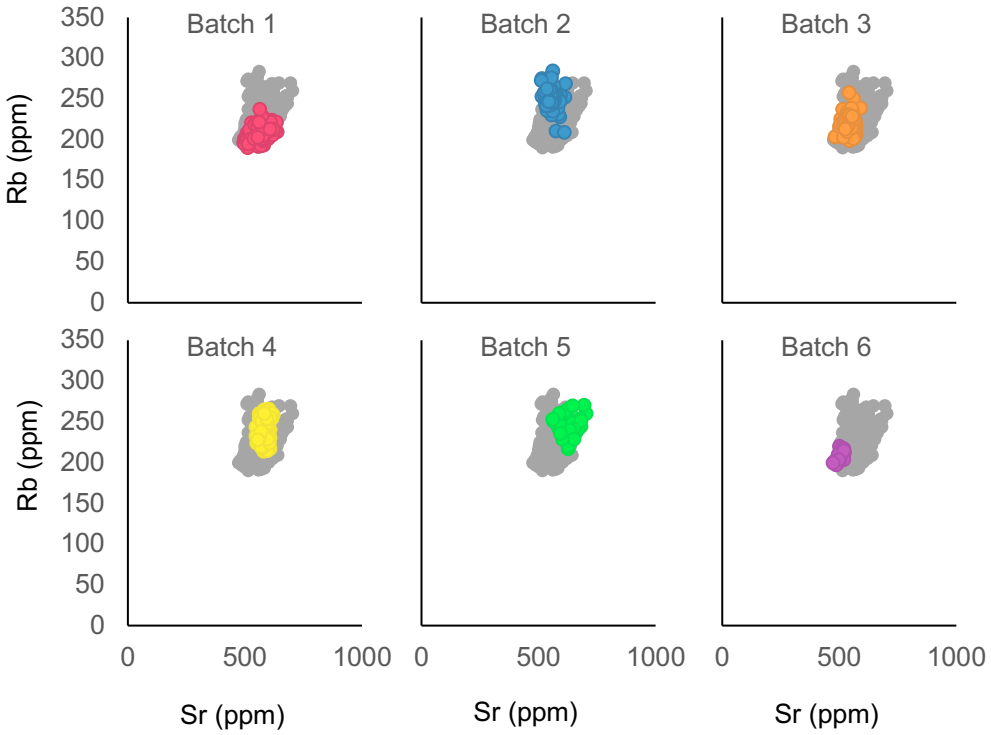

Figure 9.2 Strontium and rubidium contents of the six clusters/batches identified in the original white glass of the GEW.

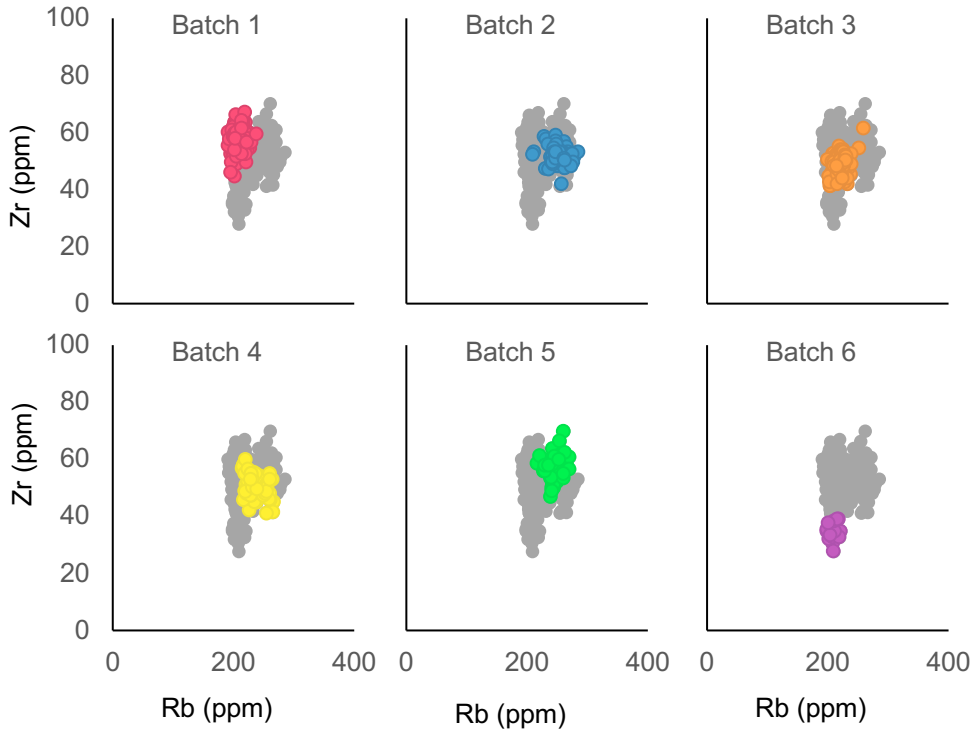

Figure 9.3 Rubidium and zirconium contents of the six clusters/batches identified in the original white glass of the GEW.

9.1.3 Significance of clusters

Although the cross-window clusters are based upon the trace element data only, they correspond moderately well to major elements (Figure 9.4, Figure 9.5). Within each panel, the control group batches correspond very well to the batches. The cross-window clusters do, however, contain batches from different panels that are in some cases chemically distinct in their major element compositions (i.e., not all of the control group glass in each cluster are identical within experimental error), and, as previously stated, the key differences between the results of the two approaches was that some batches defined by the panel-by-panel approach were combined in the cross-window approach.

The identification of the glass batch as a production event using chemical analysis is complicated by the uncertainty that the molten glass within a working pot was completely homogenised. If heterogeneous, there may arise two realisations of the batch: (1) the chemical batch, or the group of glass which was produced from the same pot of molten glass and is identical in chemical composition, and (2) the production batch, which is all of the glass originating from the same pot of molten glass (Figure 9.6). If the contents of a working pot are homogeneous, then the chemical batch and the production batch are the same, but if not, a production batch may contain multiple chemical batches. In the GEW white glass, it appears that the batches defined by the panel-by-panel approach

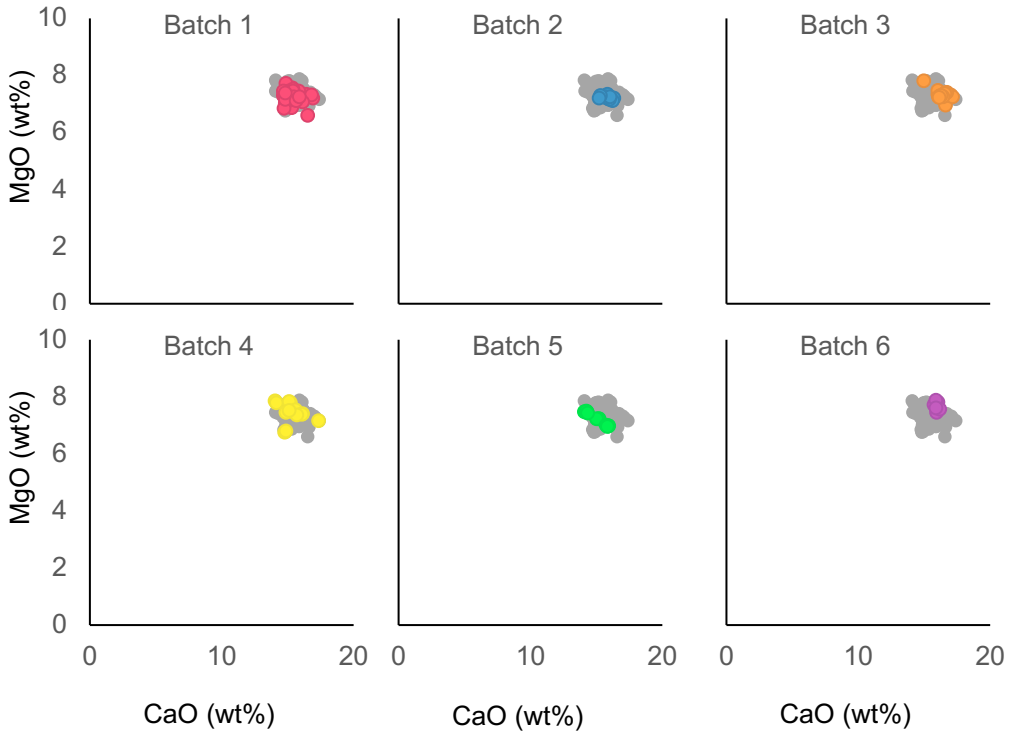

Figure 9.4 Magnesia and lime contents of the six clusters/batches identified in the original white glass of the GEW. The data in these plots are major elements measured by EPMA, with batches identified using trace element concentrations measured by pXRF.

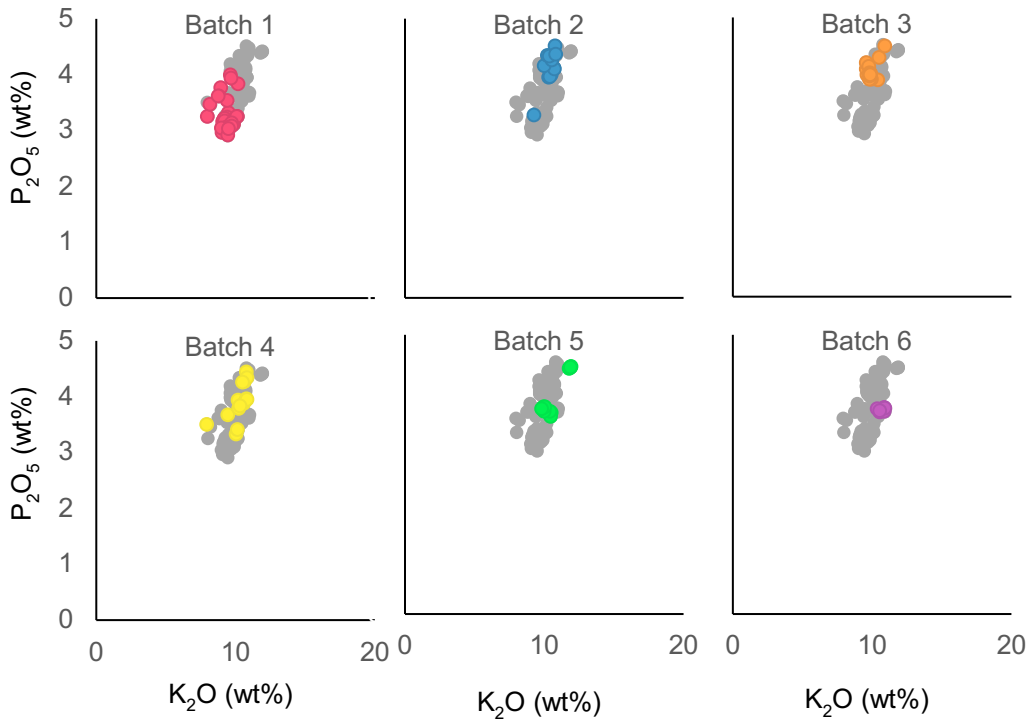

Figure 9.5 Phosphate and potash contents of the six clusters/batches identified in original white glass of the GEW. The data in these plots are major elements measured by EPMA, with batches identified using trace element concentrations measured by pXRF.

are chemical batches, while the batches defined by the cross-window approach are related to production batches, thus explaining the incorporation of multiple chemical batches in some clusters. Some error due to overlapping compositions is also expected using either the cross-window or panel-by-panel approach, and cannot be avoided.

In light of the agreement between the two approaches at the panel level, the delineation between chemical and production batches, and the advantages presented by the ability to observe trends across rows and across the window, the cross-window clusters are used as the final groupings.

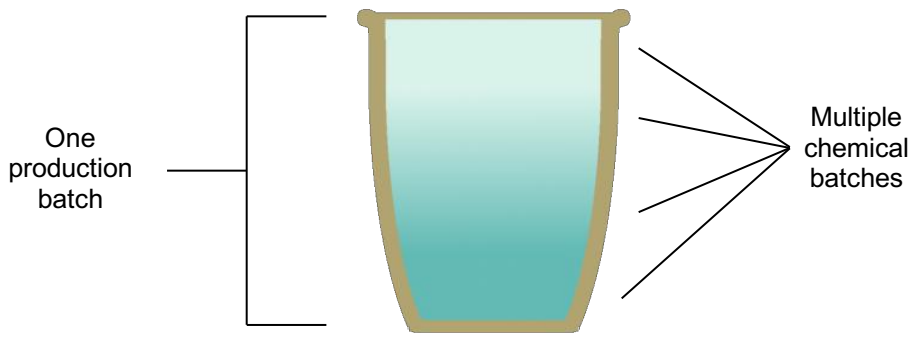

Figure 9.6 An illustration showing the relationship between the "production batch" and the "chemical batch" when a working pot is not completely homogenised.

9.2 Distribution of batches across the panels

In the following sections, each panel will be presented separately with a report on the degree to which the two approaches for the identification of batches in the GEW original white glass (cross-window and panel-by-panel) agree. The different (cross-window) batches are then colour-coded and superimposed on an image of each panel to show their distribution. The batches are colour-coded consistently in all graphs and panel images in this chapter. The distribution of the batches in each panel was evaluated for spatial tendencies; the three outcomes were distribution according to aspect (i.e., parts of the panel according to subject matter, such as frame, interior scene or figures); distribution according to coordinate area (i.e., parts of the panel dictated by geometry irrespective of subject matter, such as upper left quadrant, lower quarter, and so forth); or finally some mixture of both.

9.2.1 Row 1 panels (1e, 1h, 1j)

As mentioned previously, the original white glass of row 1 panels (Figure 9.7) have low variation in composition across the row in both major and trace elements. Chemical batches were identified in the control group; however this required the use of hierarchical clustering to separate the batches with overlapping compositions. Three batches were identified in panel 1e, one in panel 1h, and four in panel 1j. It was furthermore impossible to fully distinguish these batches using trace element data in the panel-by-panel approach.

Nearly all of the original row 1 white glass (102 out of 106) were found to belong to batch 1. The exceptions were 1e-W36, 1h-W26 (batch 2), 1h-W23 and 1j-W18 (batch 3). The former two were ungrouped in the panel-by-panel clusters, and may have been moved

Figure 9.7 Panels 1e, 1h and 1j (left to right). All three panels are from the bottom row, and almost entirely compsed of batch 1 glass. Therefore, no batch distribution images have been produced for these panels. © *The York Glaziers Trust with the kind permission of The Chapter of York.*

from elsewhere in the window or from another window using the same glass source (see previous chapter). The other two may have been grouped with batch 3 in error.

9.2.2 Panel 3b

Panel 3b primarily contains glass from four batches (1, 2, 4 and 5) and a single piece in batch 3 (3b-W1). The cross-window clusters are an excellent match to the panel-by-panel clusters, with one sample (3b-W30) grouped differently. The clusters also correlate to three control group batches.

The distribution of these batches across the panel are strongly related to different aspects of the panel (Figure 9.8): one batch (1) consists of almost every analysed glass piece in the border, while two others (4 and 5) are confined to the left and right parts of the interior scene. Batch 2 consists of scattered pieces, including two border pieces, the head of one figure, the inscribed scroll and pieces from the city.

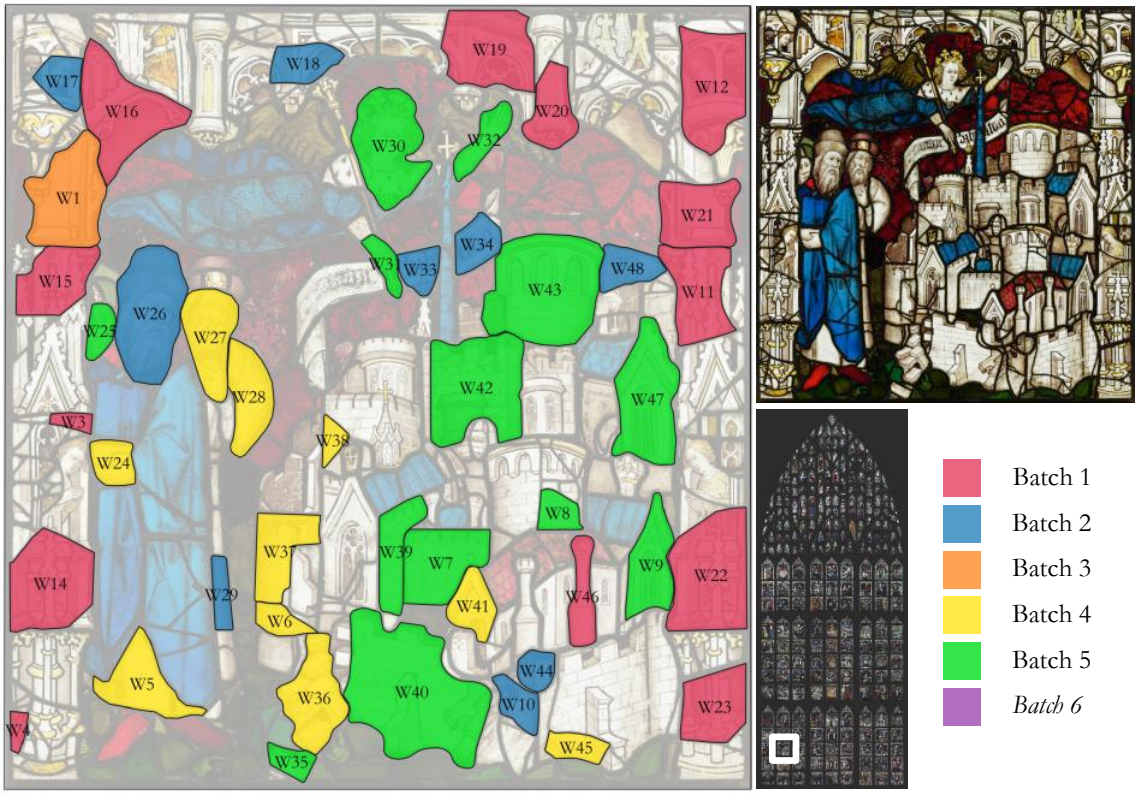

Figure 9.8 Distribution of the batches identified in panel 3b. *Panel image: © The York Glaziers Trust with the kind permission of The Chapter of York.*

9.2.3 Panel 10c

Panel 10c contains glass mostly from batch 2, as well as glass from batches 1, 3, 4, and a single piece analysed from 5. Again, the correlation between the cross-window and panel-by-panel approaches was very good; two samples in batch 1 were grouped in other batches by the panel-by-panel method (10c-W31 and 10c-W36). Of the thirteen white glass subsamples in the control group from panel 10c, only four were original to the window, all of which were identical within experimental error; these were all grouped in batch 2 (one, 10c-W3, was too small to analyse by pXRF but has been included in batch 2).

The distribution of the batches in the panel (Figure 9.9) are mostly segregated by aspect within the panel, with batch 2 concentrated in the interior scene and batches 3, 4 and 5 in the architectural frame; batch 1 was used to glaze miscellaneous parts of both.

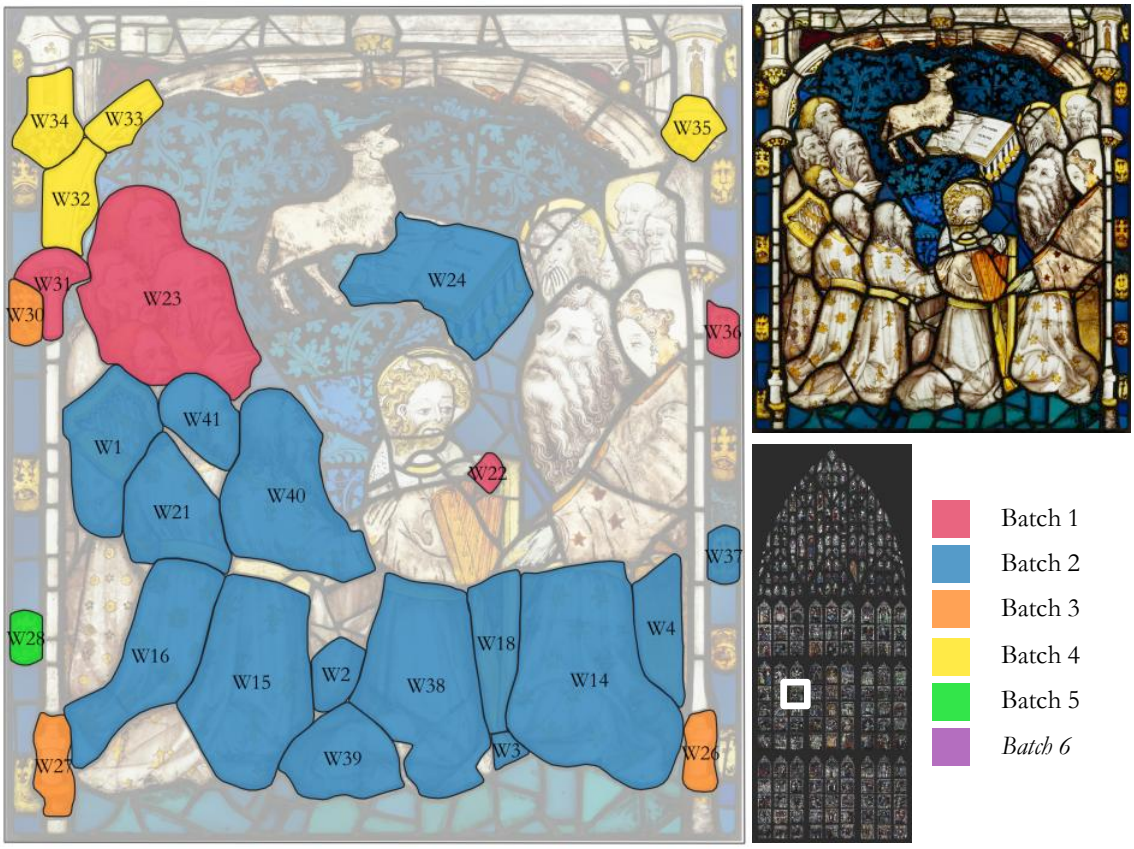

Figure 9.9 Distribution of the batches identified in panel 10c. *Panel image: © The York Glaziers Trust with the kind permission of The Chapter of York.*

9.2.4 Panel 10e

Panel 10e contains glass from batches 1-5. Agreement between the cross-window and panel-by-panel approach is more moderate, with five out of 33 samples showing different groupings. Two pairs of samples were found to be identical within experimental error in the control group; one of these four (10c-W6) could not be analysed using pXRF, as the sample was too small to put the spectrometer flush against the glass, but the other two were grouped into batch 5.

The distribution of the batches in the panel show a relationship according to aspect, architectural frame versus interior scene (Figure 9.10). The batches represented in fewer numbers (1, 2 and 4) appear to have been used to fill in areas across the panel. Batch 3 is concentrated on the interior scene, while batch 5 was used to glaze the frame. The exceptions are the two pieces at the base of the frame, which belong to batch 3; possibly this is due to filling in gaps in the same way that batches 1, 2 and 4 appear to have been used in this panel.

Figure 9.10 Distribution of the batches identified in panel 10e. *Panel image: © The York Glaziers Trust with the kind permission of The Chapter of York.*

9.2.5 Panel 10h

Panel 10h contains glass from batches 3 and 5, as well as a few pieces from batch 2 and one each from batch 1 and 4. Agreement between the cross-window and panel-by-panel approach is good; the three disagreements in this panel are the sample from batch 1 (10h-W26) and two from batch 2 (10h-W36 and 10h-W56). Three easily distinguished batches (i.e., no overlapping groups) were identified in the control group, two of which were included in batch 5 and the other in batch 3.

One piece, 10h-W13, which was grouped with 10h-W9 in a control group batch, was excluded by the cluster analysis due to the elevated measurements of zinc on this sample (about twice the concentration found in the other samples). As the sample is completely covered with silver stain, it was assumed that this affected the analysis. Its concentrations of the other trace elements were consistent with batch 3, and so it was included in that batch.

The distribution of the three batches in the panel (Figure 9.11) are distributed across the panel by coordinate area, with one focused at the top and the lower right part of the panel (batch 5), another present in a diagonal band near the top (batch 3), and the other batches used for miscellaneous pieces throughout the panel.

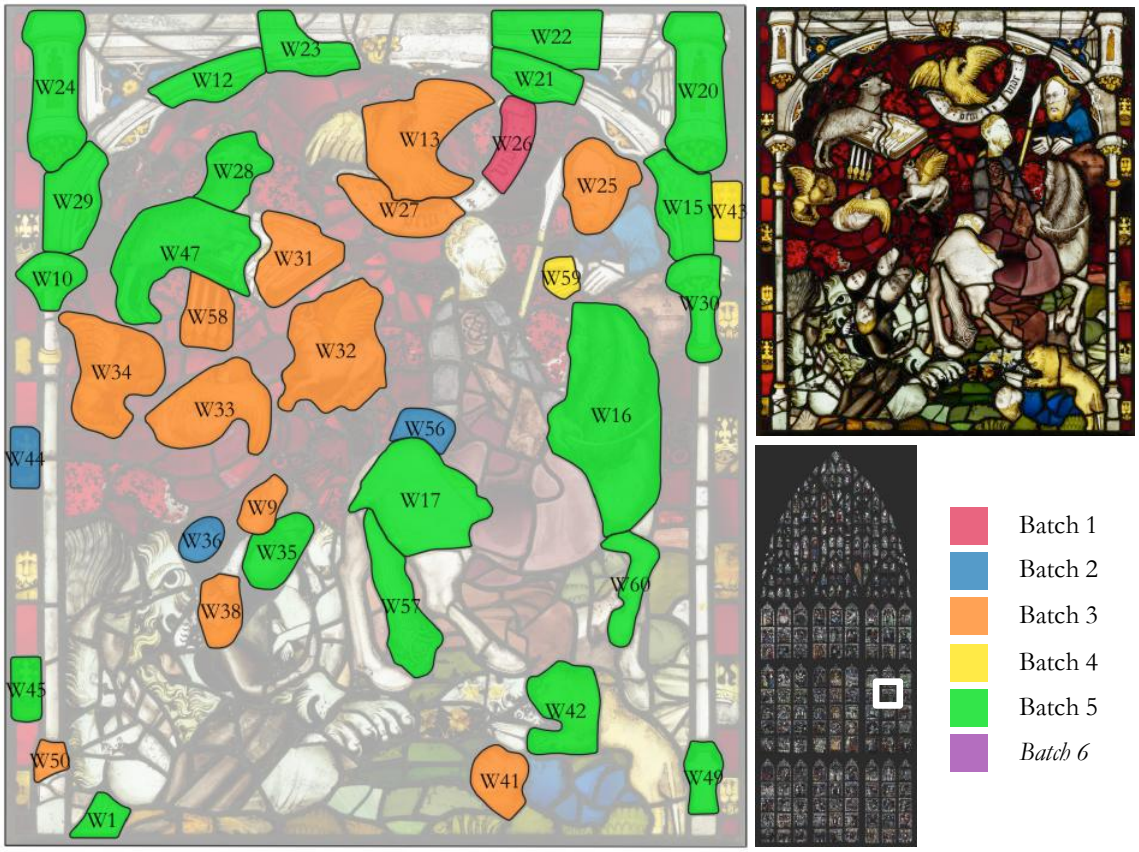

Figure 9.11 Distribution of the batches identified in panel 10h. *Panel image: © The York Glaziers Trust with the kind permission of The Chapter of York.*

9.2.6 Panel 15a

Panel 15a contains glass from batches 1, 3, 4, 5 and 6. Identification of batches by the panel-by-panel approach was difficult; while batch 6 is clearly distinguished in composition (refer again to Figure 9.3, showing the lower Zr contents of batch 6), the other batches were overlapping in their trace element composition and no further separation of the groups was attempted. Two batches were identified in the control group, both of which were grouped in batch 4.

The distribution of the batches across the panel is singular; batch 6 was used to glaze the figure of God, while the rest are more or less randomly used around the panel (Figure 9.12). Whether the latter result is due to the act of glazing or due to overlapping compositions confusing batch identification, the separate glazing of God is an important result.

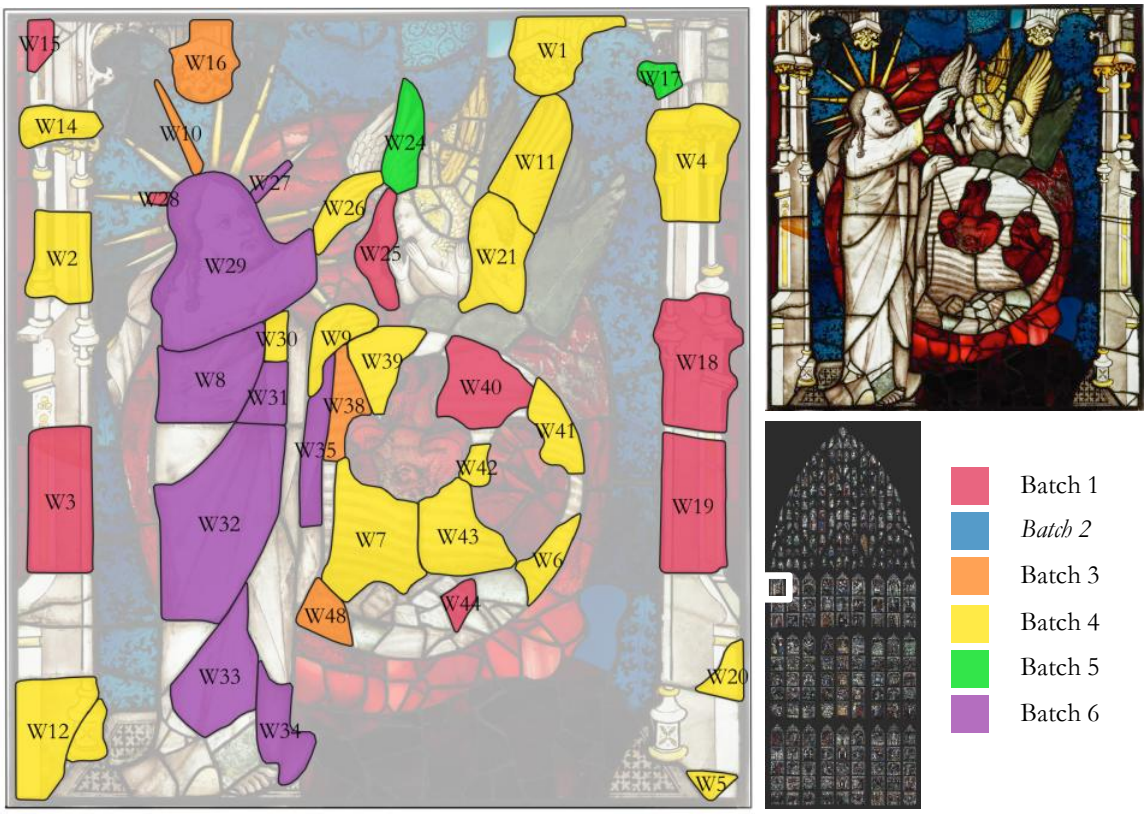

Figure 9.12 Distribution of the batches identified in panel 15a. *Panel image: © The York Glaziers Trust with the kind permission of The Chapter of York.*

9.2.7 Panel 15b

Panel 15b contains glass from all six batches. Identification of batches by the panel-by-panel approach was made difficult due to overlapping groups; as in panel 15a, batch 6 is easily distinguished but the other glass pieces were simply grouped together as a multi-batch group in the panel-by-panel approach. Two batches were identified in the control group, which correspond to batches 4 and 6.

The distribution of the pXRF groups in the panel show a relationship primarily to coordinate areas of the panel, with some relationship to subject matter as well (Figure 9.13); batch 6 was used to glaze the hand of God and the upper part of the earth (roughly a square area), and the floor along with a few pieces in the frame (i.e., the bottom part of the panel). Batch 4 was used for most of the frame; the other groups were used for the rest of the frame and the earth in the interior scene.

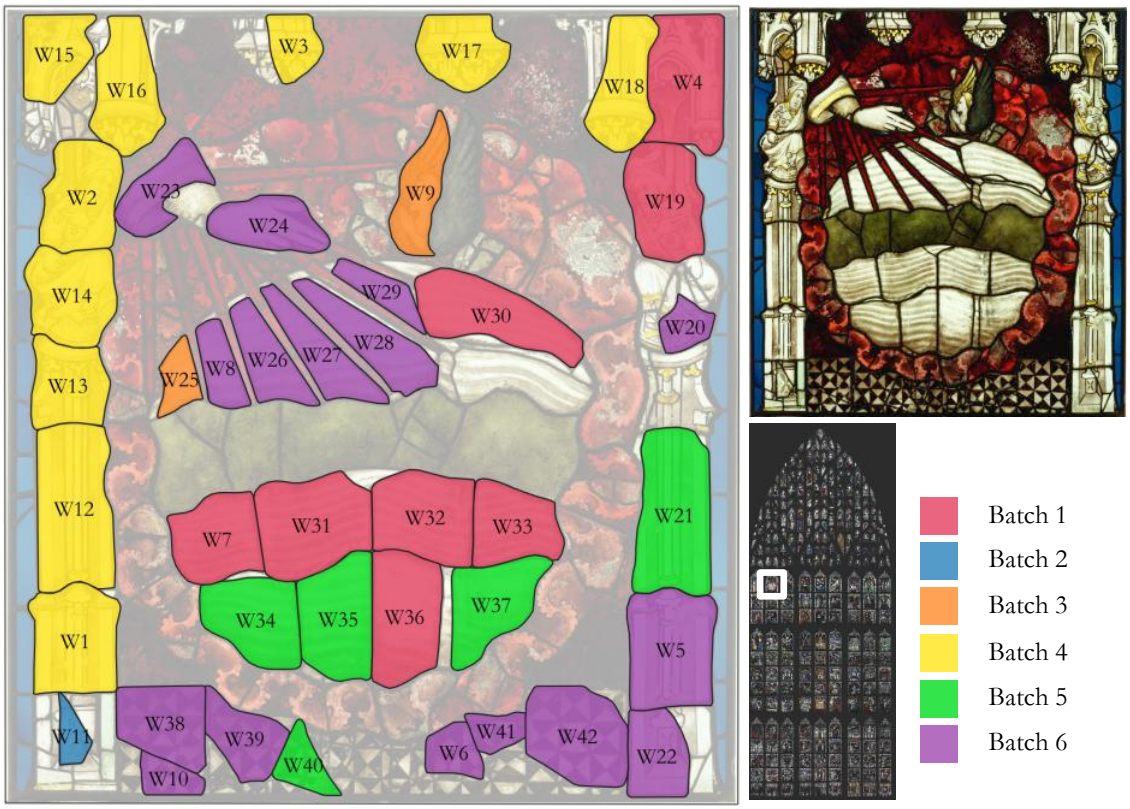

Figure 9.13 Distribution of the batches identified in panel 15b. *Panel image: © The York Glaziers Trust with the kind permission of The Chapter of York.*

9.2.8 Panel 15f

Panel 15f contains glass from batches 2 and 3, with a single piece analysed from batch 1. These batches correspond perfectly to the panel-by-panel approach, with no disagreements between them. No subsamples were taken from the panel for EPMA analysis; this panel was analysed by pXRF alone, providing a small trial of the use of this technique in isolation of other analytical methods. Therefore, in the panel-by-panel approach, the groups had to be determined without the guidance of control group batches.

The distribution of the batches are mostly confined to coordinate areas of the panel, unrelated to aspects such as frame or interior (Figure 9.14). In particular, one batch covers an area at the bottom left of the panel, while another covers the top/top-left area of the panel. The figures of Adam and the horse are both dissected by batches. The angel in the upper righthand corner was reconstructed during the Milner-White campaign (YGT, 2016), and although the one wing appears to be original glass, it was possibly moved from elsewhere in the window (or another window entirely, see chapter 8).

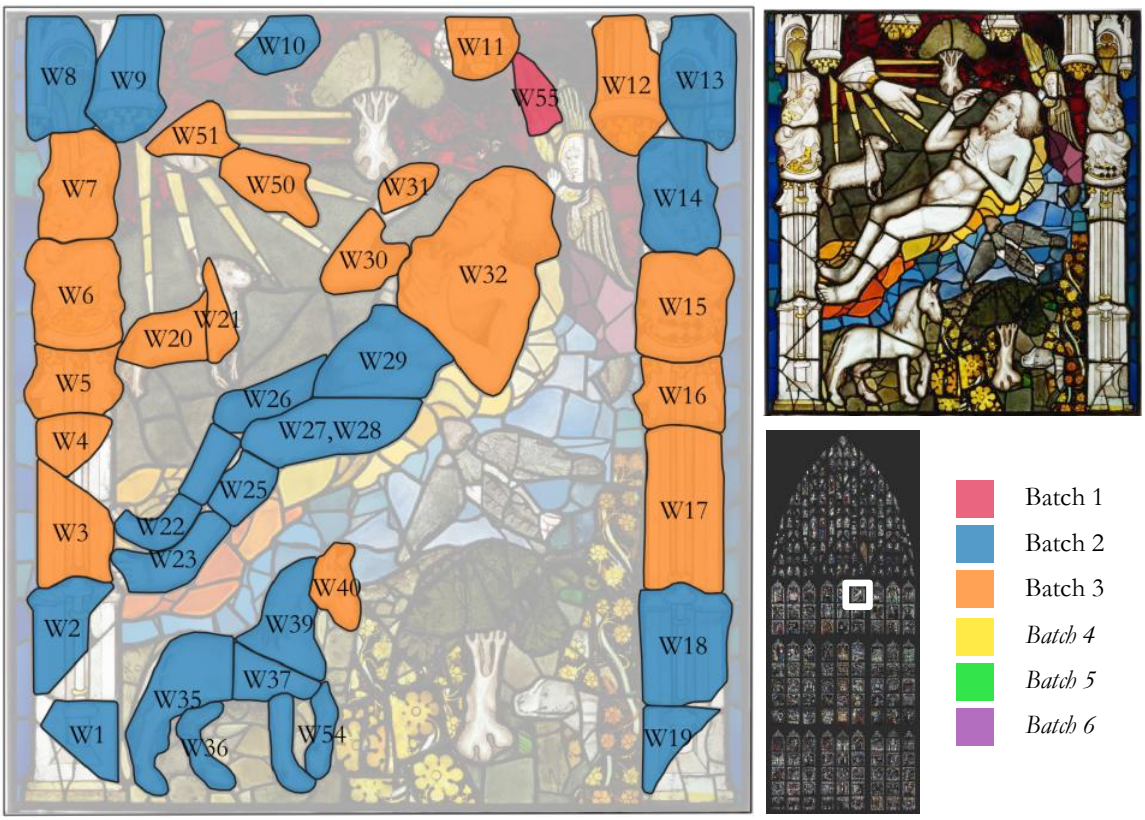

Figure 9.14 Distribution of the batches identified in panel 15f. *Panel image: © The York Glaziers Trust with the kind permission of The Chapter of York.*

9.2.9 Panel 15g

Panel 15g contains glass from batches 2 and 3, along with a few pieces from batches 1 and 5. Identification of batches under the panel-by-panel approach was problematic. Two of the three control group batches were separated between clusters or were ungrouped, and no grouping was attempted. However, in the cross-window approach, two of the three control group batches correspond to batch 3 and the third to 2, although one sample, 15g-W1 is separated from its control group batch.

The distribution of the batches is less well-defined spatially than other panels, which may be due to overlapping compositions confusing batch identification. There is a trend, however, that batch 2 tends to populate the frame (74% by sample numbers, 66% by surface area of the glass pieces) and batch 3 tends to glaze the interior scene (74% by sample numbers, 78% by surface area; Figure 9.15). Alternatively, the distribution may reflect the use of several fragmented batches of glass to glaze this panel. Either way, it is notable that this panel, like those in row 1, was glazed using sheets of glass that were of similar composition, such that no batches were distinguished in the panel-by-panel method.

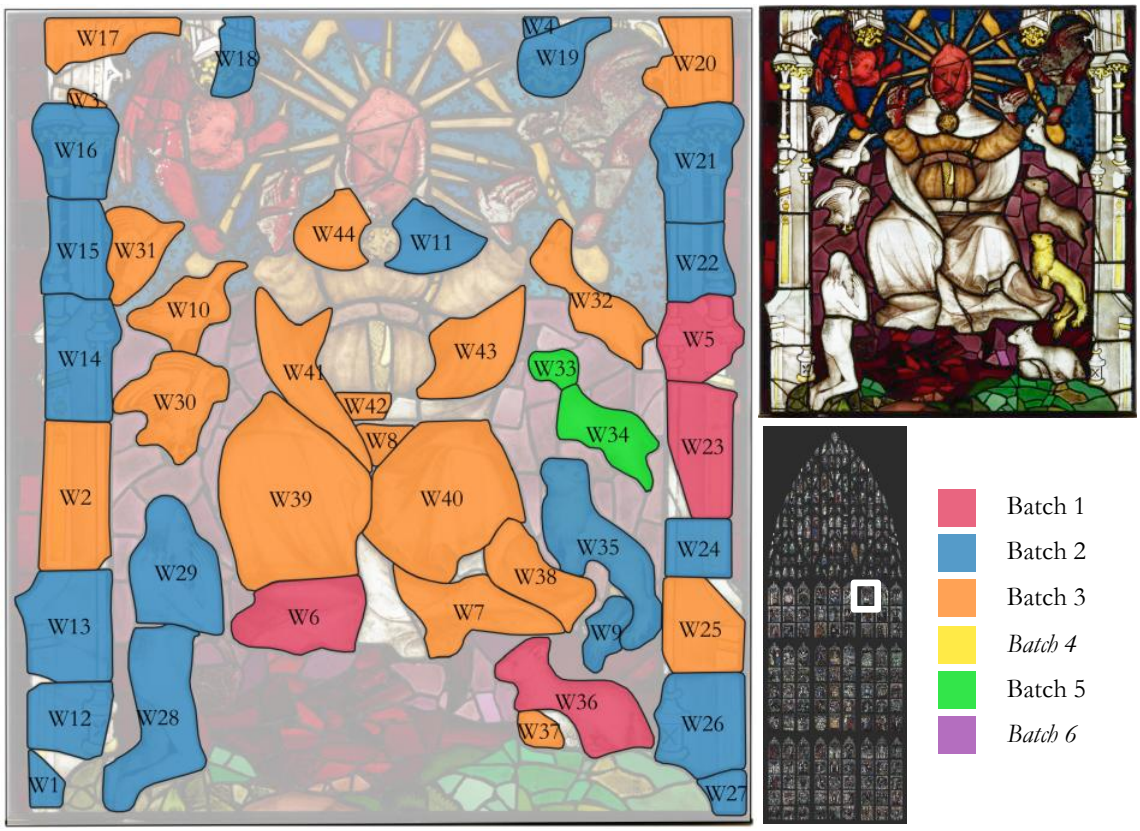

Figure 9.15 Distribution of the batches identified in panel 15g. *Panel image: © The York Glaziers Trust with the kind permission of The Chapter of York.*

9.2.10 Panel 15h

Panel 15h predominantly contains glass from batch 3, as well as pieces in batch 1, 2, 4 and 6. The cross-window approach corresponds well with the panel-by-panel approach, with three disagreements all of which were grouped with batch 3 in the panel-by-panel method and batch 1 in the cross-window (15h-W7, 15h-W28 and 15h-W31). Two batches were identified in the control group; a large one consisting of six subsamples (two of these, 15h-W7 and 15h-W3, have CaO contents differing by more than two standard deviations, but both were included in the group as there was no way to exclude one over the other) and a pair, 15h-W8 and 15h-W9. These correspond to batches 3 and 2, respectively, although 15h-W7 was grouped with batch 1 in the cross-window approach.

The distribution of these batches across the panel are mostly related to coordinate area, although some relationship to aspect is also evident (Figure 9.16). In particular, the hands and forearms of Adam and Eve, extended towards each other to exchange the fruit from the Tree of Knowledge, are the only two glass pieces analysed from batch 2. The two glass pieces with Adam's and Eve's faces and upper bodies are also distinct from their lower bodies and from the same batch (1), although this batch was also used to glaze parts of the frame and part of the Tree of Knowledge.

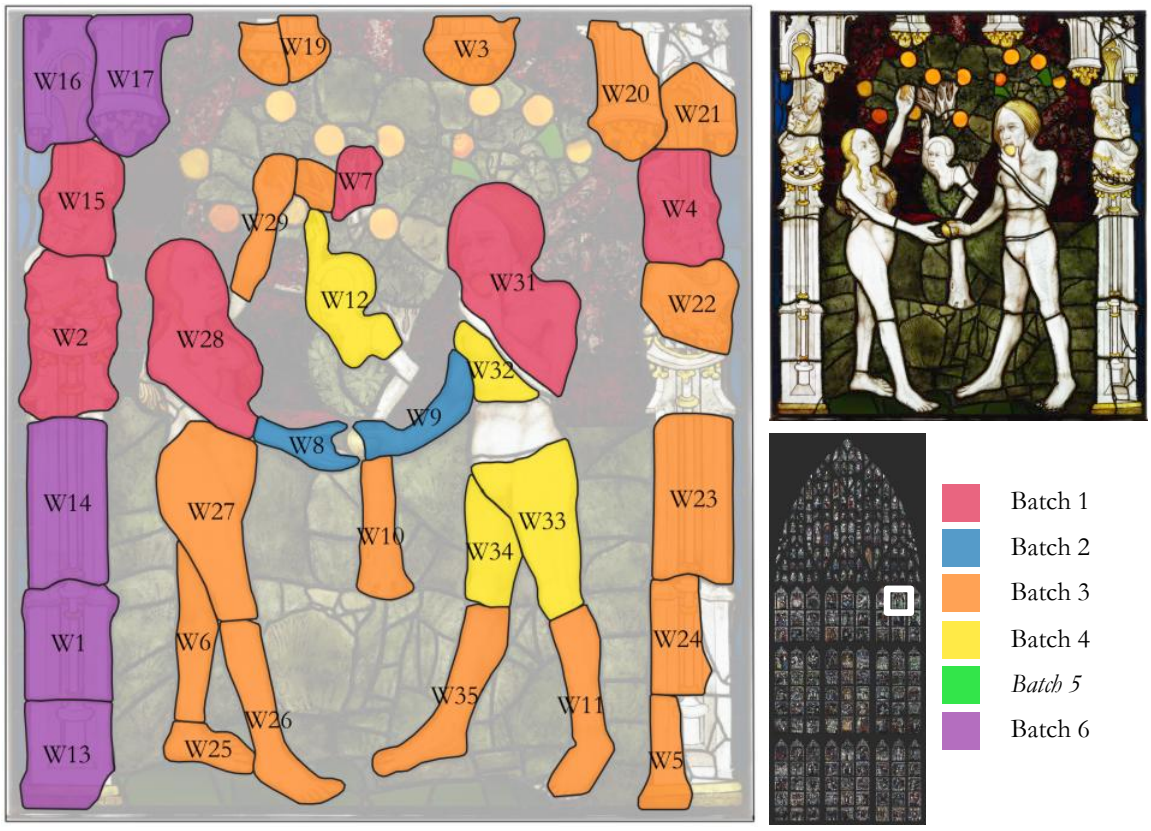

Figure 9.16 Distribution of the batches identified in panel 15h. *Panel image: © The York Glaziers Trust with the kind permission of The Chapter of York.*

9.3 Summary

Two approaches were tested in the identification of batches in the original white glass of the GEW. The first was a panel-by-panel approach, in which each panel was examined separately. The second approach was to examine all of the trace element data from the window together. In general, there was excellent agreement between the two approaches, and so the batches identified by the cross-window approach were ultimately used as this will allow examination of the use of different batches across a row and the window. A distinction was made between the "chemical batch" and the "production batch" for glass originating from molten glass in a working pot that was not fully homogenised. This situation could result in multiple groups of glass which are identical in chemical composition (the chemical batch) and yet the production event itself yields the production batch, which may contain multiple chemical batches with close compositions.

Table 9.1 shows a summary of the results reported in this chapter. The three panels in the bottom row were almost entirely composed of batch 1 glass. Distribution according to aspect (i.e., subject matter including architectural frame, the interior scene or more specifically, figures) was found in several of the panels in the upper part of the window. In others, the distribution was more closely related to coordinate area of the panel, or appeared somewhat random.

Table 9.1 Summary of white glass batch distribution for each panel studied.

	Distribution in Panel
1e	One batch
1h	One batch
1j	One batch
3b	Aspect
10c	Aspect
10e	Aspect
10h	Coordinate
15a	Aspect (Figure of God distinct)
15b	Mixture of coordinate and aspect
15f	Coordinate
15g	Aspect (trend)
15h	Mixture of coordinate and aspect

CHAPTER 10

Recipes and procurement of the GEW glass

The results of this thesis have allowed exploration of several topics related to glass-making; first in the identification of the English suppliers for the GEW and the ongoing relationship between York Minster and their suppliers of white window glass, second in the identification of the regional provenance for the coloured glasses and the examination of colouring technology at this time, and finally a preliminary examination of the transition to HLLA glass.

10.1 White glass

10.1.1 Provenance

The origins of the GEW white glass have been traced to the Staffordshire glass-making region, with major element contents and isotope ratios consistent with glass produced there (see section 8.2.1.1). Two areas in Staffordshire are thought to have been producing glass during the medieval period, in Wolseley and Abbot's Bromley. Bagot's Park, in Abbot's Bromley, comprises the largest concentration of furnaces so far found in the region, with eighteen furnaces. These have been studied with archaeomagnetic dating, showing production in the area from the 13th century to the 16th century (Crossley, 1967; Linford and Welch, 2004, 2002); however only 16th century furnaces have been fully excavated and no earlier glass samples were available for analysis. Analysis of samples from the 16th century context were published by Meek *et al.* (2012). In Wolseley on the Cannock Chase were two nearby sites at Cattail Pool and Little Birches (LBW), the latter which was excavated with samples taken from both 16th century furnaces and a late 13th/early 14th century furnace.

Chronologically, the GEW white glass falls between the comparative materials from Staffordshire. Isotopically, however, the glass from the 13th/14th century context had lower $^{143}Nd/^{144}Nd$ ratios than the 16th century Staffordshire glass and the GEW white glass (Figure 8.13). An explanation for this change can, at present, only be speculated. It is possible that a different local sand source was exploited (as the Nd ratios are still within one standard deviation of local sediments as reported by Meek *et al.*, 2012). In the same vein, it is possible that some of the change is due to a different ash; although the assumption is that Nd derives almost entirely from the sand raw material (e.g., Brems *et al.*, 2013b; Degryse *et al.*, 2014, 2010), data from an unpublished thesis showed surprisingly low Nd contents in English silica sources (0.4-6.8 ppm), and high Nd in one of the three analysed bracken ash samples (25 ppm, from the Weald; Meek, 2011, 124ff). The strontium ratios, however, which would derive from a combination of the sand and ash (probably weighted towards the latter), remains consistent for the two periods. Another possible explanation is that the few fragments of glass uncovered in the waste heaps of the 13th/14th century context were cullet, collected for remelting, rather than waste from on-site production.

The GEW white glass is consistent with the 16th century Staffordshire glass, and is furthermore more similar to the LBW samples than the Bagot's Park samples, which have a slightly higher $^{87}Sr/^{86}Sr$ ratio (Figure 8.13). Therefore, it seems likely that the GEW was sourced from LBW, although it would be preferable to compare with contemporary glass from Bagot's Park.

10.1.1.1 Consignments of white glass

The intensive analysis from across a single, well-dated window provides a rare opportunity to study the output of a glass-making workshop, in particular for the production of the white glass (the dominant colour in the window). For example, under the assumption that each batch within a panel derived from a sheet of glass (see Chapters 4 and 9), the identification of different batches/sheets within a panel allow an estimation of minimum glass sheet size. Based on batch distribution in panel 3b and panel 15f[19], each batch/sheet covered a surface area equal to approximately 2000-2500cm^2 (45 x 45cm to 55 x 55cm), therefore requiring a sheet larger than that to accommodate waste. This is within range of previous estimations of window glass sheet size of later date (late 15th to mid-16th century), which ranged from 1600 cm^2 (40 x 40cm) to about 3600cm^2 (60 x 60cm; Caen, 2009, 232).

[19] These panels were chosen because they had well-defined batch areas that could allow deduction of the batch identity of the unanalysed glass for the purposes of this calculation.

Table 10.1 Mean composition for major elements of the two consignments of white glass.

	Cons. 1	Cons. 2
Na_2O	2.58	2.08
MgO	7.20	7.21
Al_2O_3	1.38	1.26
SiO_2	57.71	56.33
P_2O_5	3.16	3.86
K_2O	9.48	10.40
CaO	15.16	15.77
MnO	1.48	1.45
Fe_2O_3	0.54	0.49

The compositions of the white glass are highly consistent across the window, although at least two groups based on soda, phosphate and potash concentrations were identified (Figure 8.10); while the compositional differences between these two groups were first observed using bivariate analysis, the ultimate designation of each piece of glass as belonging to each group was determined using cluster analysis in R (Ward's method with squared Euclidean distance on scaled data, *k*=2). The differences between the two consignments of glass are small, but are summarised in Table 10.1.[20] The concentration of one group (corresponding to batch 1, Chapter 9) towards the bottom of the window and the other (batches 2-6) towards the top supports the hypothesis that these two groups represent two consignments of glass, perhaps produced in two different furnace campaigns (Figure 10.1).[21] The glass produced during two different campaigns is more likely to show an abrupt or well defined change in composition, as is observed in the white glass. If glass-making was a seasonal occupation (Jackson and Smedley, 2008a), the campaigns might have been separated by several months or years and have the potential to show significant changes in composition, given the documented variability in ash composition of different plant species, harvested at different times of year, and so forth.

[20] The consignments of glass were identified using the major element concentrations of the glass analysed by EPMA in this study and the glass analysed by SEM as part of the Cardiff-York project. The batches of glass identified in Chapter 9 were determined based on trace element data measured by pXRF. Although the consignments and batches were determined separately, consignments 1 corresponds to batch 1, and consignment 2 corresponds to batches 2-6.

[21] A furnace campaign is the period during which it is operated at a high temperature, and ends when it is allowed to cool again; it begins with starting raw materials, which are topped up throughout the campaign, resulting in a sequence of slightly altered compositions, or batches of glass (Freestone *et al.*, 2009).

There is evidence suggesting that the window was painted beginning with the panels at the bottom and working upwards (this will be discussed in greater detail in the next chapter). Therefore, "consignment 1" is the name given to the consignment concentrated at the bottom of the window, while "consignment 2" is concentrated at the top, with some overlap in rows 2 and 3 (Figure 10.1). Possibly the first consignment was part of the glass in storage, set aside for the GEW, as recorded in the city's Fabric Rolls in 1399 (Raine, 1859, 18), and that the second consignment was ordered not long after the project's beginning, when Thornton had been hired and the design

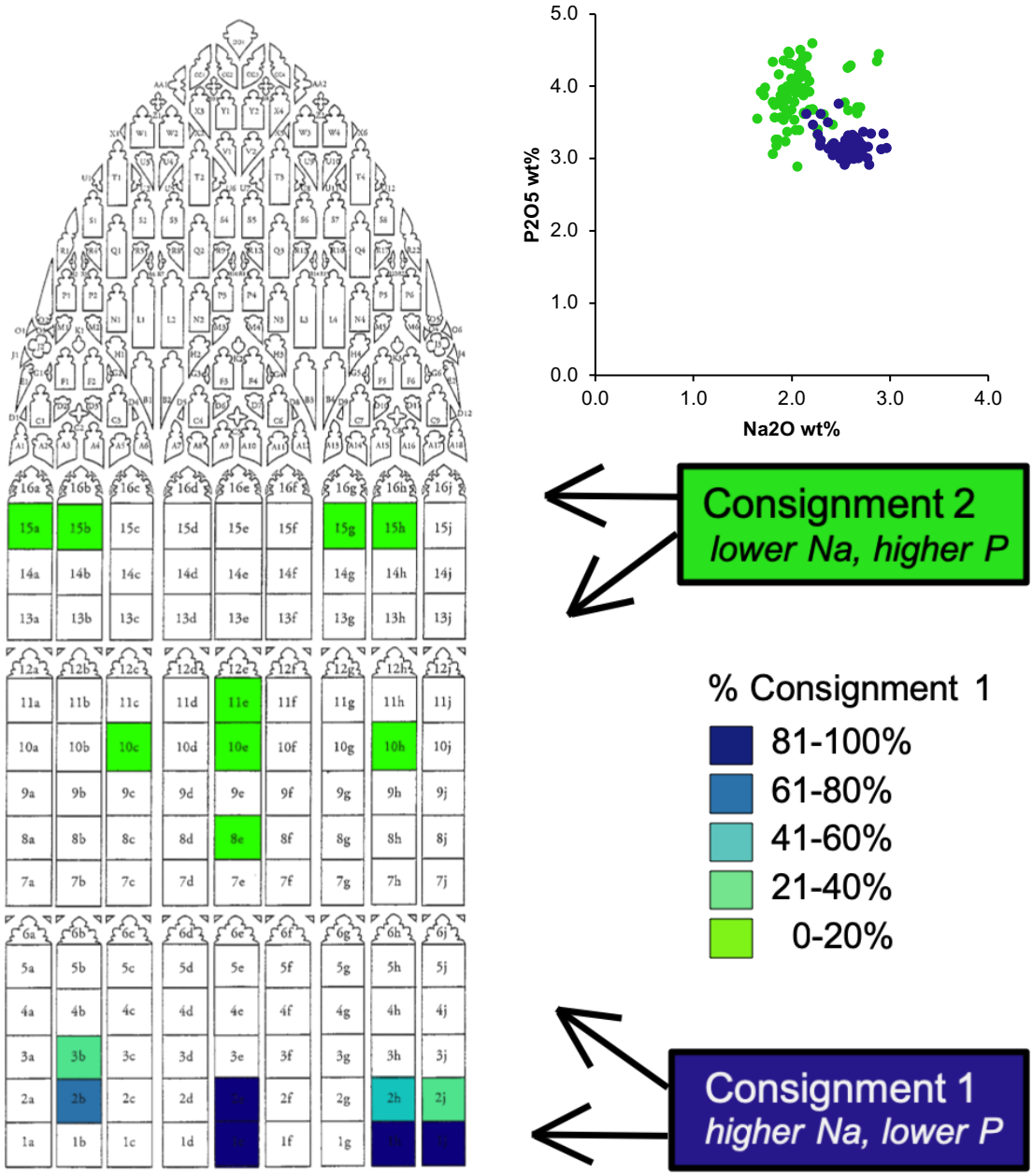

Figure 10.1 Distribution of Consignments 1 and 2 mapped onto an outline of the GEW.

finalised, allowing more accurate calculation of the amount of glass required. Consignment 2 is larger, and has a larger spread of compositions, which is consistent with a longer furnace campaign, with more top-ups of the raw materials and more small alterations to the batch compositions. A difference between glass in the first row and the upper rows can also be observed in the blue glass (to be discussed later in this chapter).

10.1.2 Customer-supplier relationship

Taken together with documentary evidence, the results of this research suggest that York Minster had a steady relationship with the Staffordshire glassmakers, as it appears that they supplied the white window glass for multiple projects during this period. The GEW, in 1405, was one. Another was the St. William Window (SWW) in *c*. 1414, which was studied within the Cardiff-York project; one white glass sample from this window was also submitted for TIMS analysis, and was found to be consistent with the GEW and LBW glasses in its isotopic ratios. As referenced previously (Chapter 3), the fabric rolls of York Minster record the purchase of white glass from John Glasman of Ruglay (Rugeley, in/near Wolseley) in the year 1418 (Raine, 1859, 37) and again in 1478/9 (Welch, 2003).

The presence of several white glass pieces which were identical in major and trace element composition to the original glass, yet which may confidently be identified as not original to the window in terms of their painting style, suggests the use of this glass source outside the Thornton era. The GEW is thought to be Thornton's debut in Yorkshire, after which he became a freeman of York (Knowles, 1936, 1920; Marks, 1993). The International Gothic style, in which Thornton painted, began to appear in York in the final decades of the 14th century, but Thornton is credited with being a key actor in its dissemination in the north and his style dominates early 15th century stained glass in York (Marks, 1993). Other glass pieces, for example the oversized head in panel 10h (10c-W7, see again Figure 8.26; see also Milner-White, 1950), are painted in the Thornton style but are disproportionate to the rest of the panel, and are either from another Thornton window or were for some reason moved within the GEW.

A further observation of note is that the products from this glasshouse or region appear to have been very stable over several years if not decades, such that glasses considered original and non-original on the basis of art historical considerations and physical condition were sometimes indistinguishable from each other by either EPMA or pXRF. This seems remarkable in view of the wide variability of compositions reported for medieval glasses generally, and the demonstrated variability inherent in

factors beyond the control of the craftsmen, such as seasonal or annual differences in ash composition (Jackson and Smedley, 2008a). The consistency in composition suggests that the glass-makers had greater control over their recipe than previously assumed, and implies that numerous factors were held constant, such as harvesting site and time of year (Jackson *et al.*, 2005; Jackson and Smedley, 2008a; Sanderson and Hunter, 1981).

10.2 Coloured glass

10.2.1 Regional provenance

The synthesis of available data for forest glass in Europe has shown three regional compositions (section 3.5). The two western groups correspond to well-known areas of glass-making in Normandy (NW France) and Lorraine as well as areas such as the Spessart Forest (Rhenish area), while in the east the area appears related to the traditional glass-making area centred on Bohemia.

The regional differences in glass composition reflect the ash components of the glass: K_2O, CaO, MgO and P_2O_5 and the trace element proxies, Rb and Sr. There are a number of potential influences on vegetal ash compositions, including geology, species and technological choice and the relative influences of these remain to be unravelled for each of the three regions. However, whatever the origins of the compositional differences observed, they are reasonably consistent over a single region and the logical explanation is that this reflects the characteristics imparted by the dominant manufacturing process and raw materials used in each region. Therefore these regional variations may be used to make sensible suggestions about the regions of origin of the glass analysed. The coloured glass original to the GEW, with HLLM composition and phosphate contents above about 2%, is consistent with Rhenish glass production.

Chapter 7 (section 7.1.3) reported preliminary results (from the Cardiff-York project) for trace elements showing similar differences between these three regions; although based on a very limited dataset at present, this is promising and the coloured glasses original to the GEW are generally consistent with the trend that Rhenish glass is higher in strontium than the other regions.

It is unexpected that the regional patterns are so well defined, as greater movement of different glass types through trade might have been expected, in particular when the limited documentary evidence suggests that glass-painting guilds controlled the glass source used by its members in order to ensure quality (Caen *et al.*, 2006). While some

spread of glass types between regions was observed (see Figures 3.5-3.7), the strong regional patterns in glass composition from both archaeological sites (from production sites and otherwise) and windows suggests that glass during this period did not spread as widely through trade as the documentation would suggest, and that frequently glass was sourced from the closest source. It is possible that the craft guilds protecting the interests of glass-makers were generally able to negotiate "exclusive access to local markets" as is documented in other craft guilds (Prak, 2008, 166) or perhaps the closer source was preferred due to ease of access and lower transportation costs. The documentation tends to date to the latter part of the 15th century, towards the end of the range of the data synthesised in this study, so perhaps this simply reflects more specific demands enabled by wider trade in the later period.

10.2.2 Glass-making technology

Interpretation of the coloured glass in the GEW is not straightforward, however there exist several links between the different colours and compositional groups that lead to the conclusion that all of the coloured glass originate from the same glasshouse or regionally associated glasshouses, i.e. a cooperative or group of glasshouses that used the same raw materials (and probably organised together as a guild or similar organisation). Based on the links between the glasses described below, the inferred reconstruction of the different recipes (summarised in Figure 10.2) is that the same or similar sand source was used for all of the coloured glass, and two different ashes were used for the base glass recipe.

The primary differences between the two ash groups ("A" and "B") are their potash and soda contents (and various colourants), aside from which there are no significant differences. However, the simplest explanation, that some potash and soda was added separately to some recipes, cannot be accepted due to the strong correlations noted between phosphate and soda (see again Figure 8.3) that indicates these elements were added together in ashes with different P:Na ratios. Often forest glass with Na_2O in excess of about 1.0-1.5% is attributed to the separate addition of sodium chloride (e.g., Velde, 2013), but this model does not account for the P:Na correlation observed in the GEW coloured glass. Furthermore, the chlorine levels of the coloured glass are generally below about 0.1% and are therefore unlikely to originate from NaCl (Gerth *et al.*, 1998). It therefore seems more probable that two ashes, one lower in potash and higher in soda (ash A) and the other higher in potash and lower in soda (ash B), were in use by the glasshouse(s).

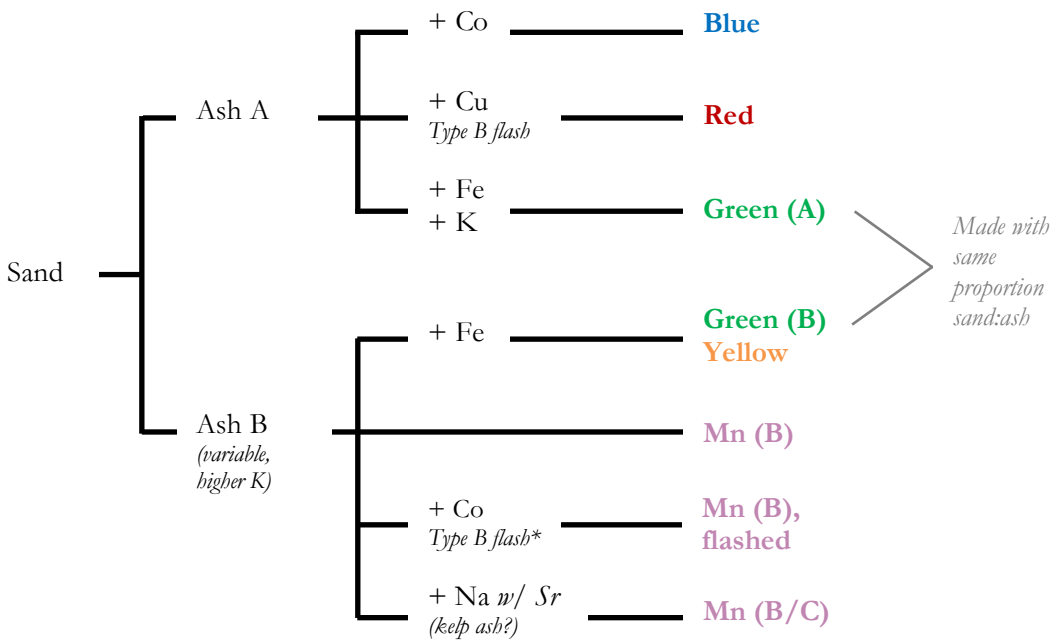

Figure 10.2 Flow chart illustrating the basic recipes used to make the colours of the GEW. *The Mn-colours which are flashed have a blue-purple-blue structure, with the purple layer in the centre of the sheet.

Ash "A" had lower potash and higher soda concentrations. The colours made using this ash were the blue, red, and some of the green glasses (green "A"; see Figure 8.3 and section 8.2.2). The blue and red glasses have the same base glass recipe when the colouring oxides (CoO, ZnO, CuO) are excluded. Model calculations by the author showed that the green A glasses have the same base glass recipe as the blues and red when its excess Fe_2O_3 and K_2O are removed, both of which contribute to the colouring of the glass.

Ash "B" was overall more variable in composition but is characterised by higher potash and lower soda contents. This ash was used to make the rest of the green (green "B"), yellow, and the Mn-colours. A group of Mn-colours (Mn B/C) appear to have had a high strontium source of sodium added to the batch (lowering the potash contents as a result), presumably to affect the final hue of the glass.

Links between these groups suggest a common origin. The coloured glasses in both groups have similar REE patterns (Figure 8.8), suggesting the use of the same sand or closely similar sand. All of the green glasses, both green A and green B, have a very narrow range of SiO_2 values, suggesting they were all made with the same proportion of sand to ash in a tightly controlled recipe. This narrow range of silica concentrations (the full range of 44-46.8%, with all but two of the 18 green subsamples analysed were within the range 46.0-46.8% SiO_2; the yellow glasses had similar concentrations) is too narrow to be coincidental in glasses from different sources. Instead it suggests that the

greens (both A and B) and yellow originate from the same source, where the ratio between sand and ash was kept constant in the glass recipe, but the composition of the ash was not tightly controlled, either because it was not possible or because it was unimportant. These glasses are coloured by high concentrations of iron, which is an impurity included incidentally in forest glass but in this case was probably also added; therefore control over the glass composition (as is seen in the Staffordshire white glass) might not have been necessary or even desired.

The addition of potash to the green A glasses and the addition of kelp ash or some other source of strontium-rich soda to the Mn-coloured B/C glasses are two examples of a similar practice of modifying the alkali content of the base glass in order to produce oxidised colours; the probable common origin of the colours also suggests the selection of higher potash ashes for the production of greens, yellows, and the various purples and pinks produced by manganese. This level of sophistication in the manipulation of colour has not previously been recognised in medieval glass and is beyond that normally attributed to medieval glass-makers.

To summarise the above, the coloured glasses were made with the same or similar sand source. The blue, red, and some of the green glasses ("green A") were made using an ash with lower potash and higher soda ("ash A"); blue was made from this base recipe using added cobalt, red using copper and a flashing technique, and green (A) was made through the addition of both iron and extra potash. The Mn-colours, yellow and the rest of the green glasses ("green B") were made using another ash that was more variable in composition but generally higher in potash and lower in soda ("ash B"); many of the Mn-colours were made without additional colourants, while a few were achieved through a flashing technique (with blue-purple-blue layers), and another group had a further raw material, high in soda and strontium (possibly kelp ash), added to the recipe. The green (B) and yellow glasses were achieved through the addition of iron as a colourant.

10.2.3 Importation of European glass to England

In light of the previous section, it appears that the majority of the coloured glasses in the GEW came from a single source, a glasshouse that was versatile and sophisticated using flashing techniques, the manipulation of furnace temperatures, and the adaption of the base melt to improve colour generation. Another study has noted that all of the colours from 13th/14th century windows in Siena and Barcelona appear to have been made at the same workshop with the same raw materials (Gimeno *et al.*, 2008). This result suggests that various colours from a single source were packaged and sold

together, whether this was due to monopolisation of certain markets by a major glass-making industry or due to purchaser preference in the selection of a trusted brand. The explanation might lie in the medieval guild system; the source might have been a regional glass-making craft guild comprising multiple glasshouses, which would have provided the brand name, overseen the purchasing of raw materials including sand or colouring materials, and overseen the sale of the final product (see Epstein, 1998; Richardson, 2001). As with the white glass, the presence of non-original blues and reds with composition identical to the original glass suggests a longstanding relationship with a particular supplier, whether due to preference or lack of alternatives.

Previous work from the Cardiff-York project has noted that a general change from LLHM to HLLM coloured glasses appears to occur in medieval windows towards the end of the 14th century; at about the same time, the technology of the red glass changes from striated Type A to simple Type B flashing, leading to the suggestion that these changes reflected two technological changes in European glass making (Kunicki-Goldfinger *et al.*, 2014). However, the original study was based on a dataset of red glass that was primarily from English windows, and therefore probably imported from Europe; the regional patterns noted in this research suggest the situation is more complex.

HLLM glass was produced well before the 14th century since the early medieval period (e.g., Wedepohl and Simon, 2010), and LLHM glass continued in Normandy and England in the form of white glass (Barrera and Velde, 1989; Caen, 2009). The “new” HLLM composition observed in English windows, therefore, may be explained as a change in the source of coloured glass in the late fourteenth century from Normandy to the Rhenish area.

Political upheavals associated with the Hundred Years War restricting the accessibility of Norman glass is one possible explanation for the change in the source of coloured glass (Neillands, 2001). There are a few instances where trade disruption due to wars has evidently affected the craft of glass-painting in York, identified both through documentation and through the evidence of the windows themselves (Knowles, 1936, 200ff). For example, Knowles (1936, 200–203) notes that windows c. 1470 contained very little red glass, which he attributes to the trade disruptions resulting from the Wars of Roses.

However, temporary trade disruption is not an entirely satisfactory explanation for the apparently nation-wide, long-term change (as observed by Kunicki-Goldfinger *et al.*, 2014) in coloured window glass procurement. It seems more plausible that the

combination of the devastation of the Black Death and the pressures exerted by the War (e.g., Gottfried, 2010) caused a major downturn in glass-making in Normandy, and perhaps a loss in skills (such as the Type A red glass technology, which required a high degree of skill; Kunicki-Goldfinger *et al.*, 2014) and/or access to colourant materials such as cobalt, which was obtained from Saxony (Gratuze, 2013; Gratuze *et al.*, 1995). The intensity of glass-making activity seems to have shifted to the Rhenish region for coloured glass production in particular.[22]

Returning to focus on York, the available historical evidence suggests that most of the glass traded through Hull was from the Rhenish region (and Flanders), transported by the Hanseatic League or the York Merchant Adventurers (Kermode, 1998; Knowles, 1936; Marks, 1993); however, most of the available documentary evidence reported in these studies date to the fifteenth century or later. Analysis of artistic styles recognises a heavy influence of a Normandy style on early York glass, up to and during the 14th century (Westlake 1886, in Knowles, 1936). However, a strong influence of Flemish and Rhenish style is observed on York painting of the 14th and 15th centuries (Knowles, 1936, 117ff), a timeline that loosely coincides with the change in (coloured) glass sources. It is possible that artistic influence and glass procurement went hand-in-hand, and that the elevation of the Rhenish glass-making industry in York/England resulted in a closer relationship between their glass-painters, encouraging the presence of foreign glaziers in York, as well as the travel abroad by English journeyman having just completed their apprenticeships (for the role played by travelling journeymen in the transmission of technical knowledge, see Epstein, 1998; Knowles, 1936, 9 and 117ff).

Most of the medieval coloured glass that are not original to the GEW are of the LLHM type, and therefore are probably from the Normandy region and pre-date the window (Kunicki-Goldfinger *et al.*, 2014). This conforms with a theory posited by Milner-White, who suggested that much of the non-original medieval glass in the window once belonged to the south clerestory windows in York Minster, which dated to c. 1385 and which disappeared between 1690 and 1730 (Milner-White, 1950, 182).

[22] This is the subject of a forthcoming paper co-authored with I. Freestone, J. Kunicki-Goldfinger, T. Ayers, H. Gilderdale Scott and A. Eavis.

10.3 HLLA glass

Although not outside the chronological range previously suggested for this glass type (e.g., Wedepohl and Simon, 2010), the presence of a small group of HLLA glasses that appear to be original to the GEW requires special consideration.

A comprehensive study of Belgian windows throughout the medieval period showed that although HLLA compositions dominated from the fifteenth century, higher potash glass continued to be made through the seventeenth century (Schalm *et al.*, 2007). Analysis of a late fifteenth century stained glass panel showed that most of the original glass was of the higher potash type, while some colours were of the HLLA type (Van der Snickt *et al.*, 2016). These examples suggest that the transition to HLLA recipes in northern Europe was not a technology that totally replaced the higher potash recipe, but was instead the development of a new, parallel recipe that came to dominate the industry. Furthermore, Schalm *et al.* (2007) noted several trends or developments that applied to both HLLA and higher potash glass, including an increase in relative silica and the addition of sodium chloride, which suggested that the same glass-makers used different recipes and/or raw materials. This view aligns with the interpretation of the present results, which appear to indicate that all of the coloured glass originated from a single yet versatile glasshouse or regionally associated group of glasshouses. The origins of the HLLA glass are probably also in the Rhenish region, in light of the apparently earlier emergence of HLLA in Germany than France (compare Wedepohl and Simon, 2010, and Barrera and Velde, 1989) and its P_2O_5 contents above 2% (Figure 3.6 and Figure 8.23). They are unlikely to originate from the same glasshouse as the other colours, however, given the use of a different cobalt ore for colouring the blue glass.

The concentration of the blue HLLA glass in a single panel is significant. The panel (1e) is positioned in the centre of the bottom row, and depicts the donor of the window, Bishop Walter Skirlaw, kneeling before an altar giving the window to God in offering. There are two types of blue glass in this panel, the HLLA blues and a small group of higher potash blues, the latter of which are generally consistent with the rest of the window but form a compositional cluster with higher Zn and Co (see again Figures 8.7 and 8.15). As mentioned previously and will be discussed more fully in the next chapter, evidence suggests that the window was constructed beginning at the bottom. The concentration of compositionally distinct blue glasses in this panel may be evidence of a “pilot” panel, the first panel produced as a showcase of what was to come to both Skirlaw and the Dean and Chapter of York. It is not clear why a change in

glass would occur after this panel; perhaps there was only a small amount of blue glass set aside for the window in 1399, or perhaps Thornton supplied some glass for the pilot panel. The high Zn potash blues reappear in panel 15a, towards the end of the project.

An alternate explanation for the presence of this glass in panel 1e is that the glass is not original, despite the visual evidence, and that it is the product of early repairs of exceptionally high quality. Such repairs have not been detected elsewhere in the window, but perhaps the position of this panel in the bottom row, making it more accessible to deliberate destruction and also highly visible, dictated that extra care and expense was demanded for its restoration. The glass might have come from the same region, but sometime later. The two yellow HLLA glasses are found in the first and fifteenth row, but as there are also only five higher potash yellows (two of which were subsampled) studied in this research, there is not much to compare with. The explanation of repair does not explain the presence of an original glazier's mark on one of these yellow pieces, unless perhaps the repair was undertaken by Thornton's workshop some years later when HLLA was more available; however, it is uncertain that the use of glazier's marks (which helped to identify glass belonging to different panels in the kiln) would be necessary on such a smaller scale.

10.4 Summary

The comprehensive study of a single, well-dated window has resulted in several key insights into medieval glass-making both in England and in Europe. The white glass in the GEW has been connected to a kiln site in Little Birches, Wolseley, in Staffordshire, and the chemical and documentary evidence suggests a long-standing relationship between York Minster and the Staffordshire glass-making industry. Two consignments of glass were detected in the window, with the one concentrated towards the bottom and the other towards the top. The first consignment was smaller, and may have been the glass set aside in stores for the GEW as recorded in 1399. The second was much larger, and may represent a second order once the window was designed and more accurate calculations of supplies could be made.

The coloured glass appear to be from a similar source in the Rhenish region, made by a single glasshouse or regional association of glasshouses organised by a guild and possibly brand name (see Chapter 4; also Richardson, 2001). Two different ashes were in use, with the higher potash ash used for oxidised colours. Two compositional groups had another raw material added; the green A glass was made with the lower-potash ash with extra potash added, and the Mn-coloured B/C glasses were made with the addition of a strontium-rich sodium source, possibly kelp ash. The control over the

alkalinity of the base glass in order to facilitate the creation of certain colours is a level of sophistication in colour generation that is not normally attributed to medieval glass-makers.

CHAPTER 11

Glass-painting and the organisation of production in John Thornton's workshop

This chapter will employ multiple lines of evidence to support an interpretation of how the workshop was organised (as described in Chapter 4), including the distribution of batches, the use of models of production adapted from the automobile manufacturing industry, art historical information (in particular a recent book on the GEW by Brown, 2018), pertinent medieval documents, and the historical context of medieval crafts and guilds.

11.1 The long-term progress of the glazing project

Knowles (1936, 220) argued that the GEW was glazed beginning at the bottom and moving upwards, despite the fact that the window is 'read' chronologically from top to bottom. Bishop Skirlaw, the donor depicted in the central panel of the bottom row (1e, Figure 2.3), passed away in March 1406, three months after the contract was signed and the work begun. In his portrait in panel 1e, however, there is no indication that he had passed away at the time of glazing, as would have been customary, thus suggesting that the first row was completed in the initial months of the project. Furthermore, the year of completion, 1408, is inscribed at the top of the window with John Thornton's initials, suggesting this was the last part of the window to be completed (Brown, 2018, 2014a; French, 2003; Knowles, 1936; Figure 2.4).

The distribution of glass in the window appears to support Knowles' argument, in particular the exclusive use of batch 1 at the bottom of the window (see again Figure

10.1). There are several possible explanations for this result, all of which suggest that the bottom row was the first row to be completed.

Evidence for the presence of two consignments of white glass, concentrated in the upper and lower parts of the window respectively, was presented in chapter 10 (Figure 10.1). The row 1 panels were glazed almost entirely of glass from consignment 1 (corresponding to "batch 1"), and while the batch continues to be used higher in the window, the analysed panels in rows 8, 10, 11 and 15 all contained less than 20% consignment 1 glass. The most logical explanation of this pattern is that batch 1 was the first consignment of glass (possibly representing the glass in storage for this window as was recorded in the city's Fabric Rolls of 1399; Raine, 1859, 18), and the only batch of glass available to use at the beginning of the glazing works before the full supply was procured. Therefore the lower row was glazed exclusively from batch 1, following which this glass became part of the general stock.

Another factor that may have contributed to this distribution is the likelihood that Thornton's workshop did not immediately operate at full capacity. It is generally accepted that the GEW represents Thornton's first commission in York, although he already had a workshop in Coventry that he continued to run concurrently (Brown, 2018, 2014a; French, 2003; Knowles, 1936). Therefore, while the contract allowed Thornton to select his own workforce (for the text of the contract, Chapter 2; Appendix A), he probably employed local craftsmen for the GEW so that he could leave his Coventry craftsmen to run his workshop there (Brown, 2018). The employment of Coventry glass-painters would also have countered potential local hostility to his operation, as in York in 1407 local masons attacked a London architect brought up to work on the Minster (Brown, 2018, 23). It may have taken some time, however, to find, test and perhaps train suitable local artists. The quality of the painting on the GEW is observed to be consistently of a very high standard (Brown, 2018, 2014a), so presumably Thornton was very discerning. When compounded with the view that Thornton was brought in due to a shortage of local talent (see Chapters 2 and 4), it seems even more likely that it would have taken some time to source his craftsmen. To begin with, therefore, Thornton's workshop may have consisted of a very small team, perhaps picked from his Coventry craftsmen, until he was able to gather a larger number of craftsmen. If this was the case, the pace of work at the beginning would be slower and more deliberate, with fewer glazing tables, possibly resulting in a narrower range of compositions observed in the early part of the window, as seen in row 1.

Finally, the use of closely related sheets of glass at the beginning of the project versus the use of a wider array of sheets as time progressed is consistent with the normal

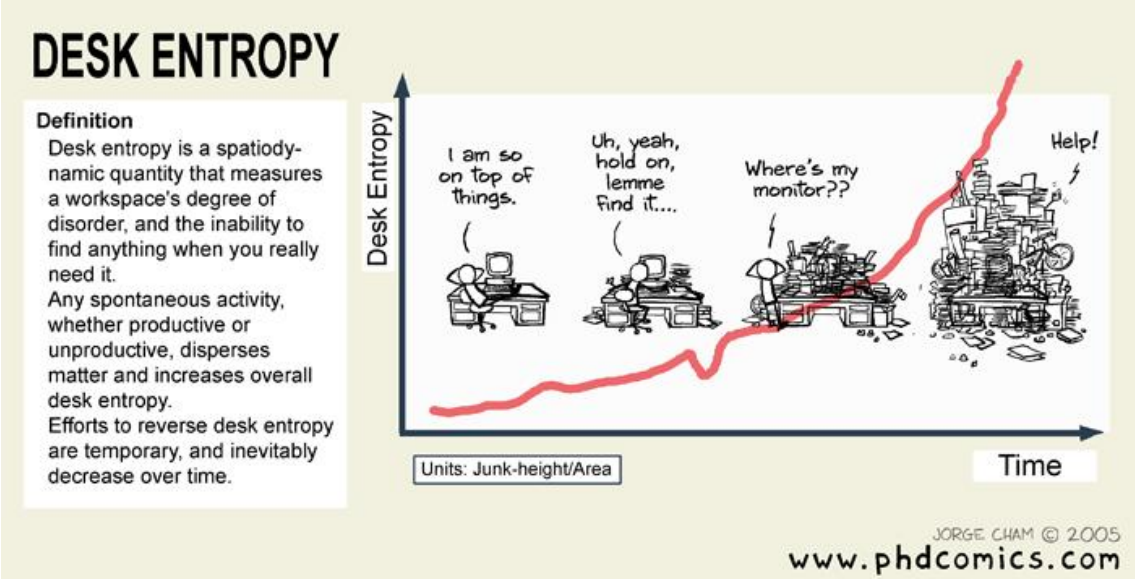

Figure 11.1 "Desk entropy" by Jorge Cham. This comic illustrates a more negative manifestation of the progression of a workspace from neat to 'broken in' (in this case, disorganised) through time. © *Jorge Cham*

progression of a project. While apparently not a formally studied or documented phenomenon, the concept of "desk (or workspace) entropy" is useful here; a new workspace at the start of a project tends to be neater and tidier than it ever will be again, while later on in a project the workspace is more likely to be 'broken in' for the more efficient and organised people, or in total disarray for the less organised (Figure 11.1). At the beginning of the project, Thornton was setting up shop for the first time in the workshop associated with the Minster, at which time it was likely to been well-stocked with consumables, which well-organised and carefully stored. Over time, the workspace would have been adapted to support the work. One way this might have manifested is in the progression from a single, central store of glass to several stacks kept where they were needed most frequently, along with some accumulation of off-cuts set aside. This model would result in a narrower range of compositions at the beginning of the project, and a wider range of compositions (i.e., multiple batches) higher in the window, possibly with a scattering of singular glass pieces as is observed in the data.

In section 10.3, it was also suggested that panel 1e may have served as a "pilot panel", the first panel to be completed as an example of the planned window to show to Bishop Skirlaw and the Dean and Chapter. This could explain the presence in the panel of blue glass with different composition from the blue in the rest of the window; some are HLLA glass that appear to be original, and the rest are similar to the blue glass found in the rest of the window, but with almost twice as much zinc and higher cobalt (Figure 8.15); this high-Zn, high-Co glass, along with consignment 1 of the white glass, might have been in stores at the beginning of the project and more glass ordered once accurate

estimates based on the final design could be made. This possibility would be amenable to testing by the analysis of the remaining panels in this row.

11.2 The glazing table as a workspace

The examination of the relative proportions of batches used in panels across a row show an interesting pattern, suggesting that pairs of panels have similar proportions of glass from the same batches. In row 10 (Figure 11.2), panels 10e and 10h are both composed predominantly of batches 3 and 5, while 10c is mostly composed of batch 2. In row 15 (Figure 11.3), there are similarities between panels 15a and 15b, and 15f and 15g. The presence of pairs in both rows suggests at least two panels were under production at any one time, and at least two glazing tables were in use in the workshop. There are two probable explanations for the pairing pattern: that the panels in a pair were completed at more or less the same time, by craftsmen using different glazing tables but by workmen accessing the same store of glass; or alternatively that the two panels were produced in close succession at the same glazing table, and each glazing table had its own store of glass.

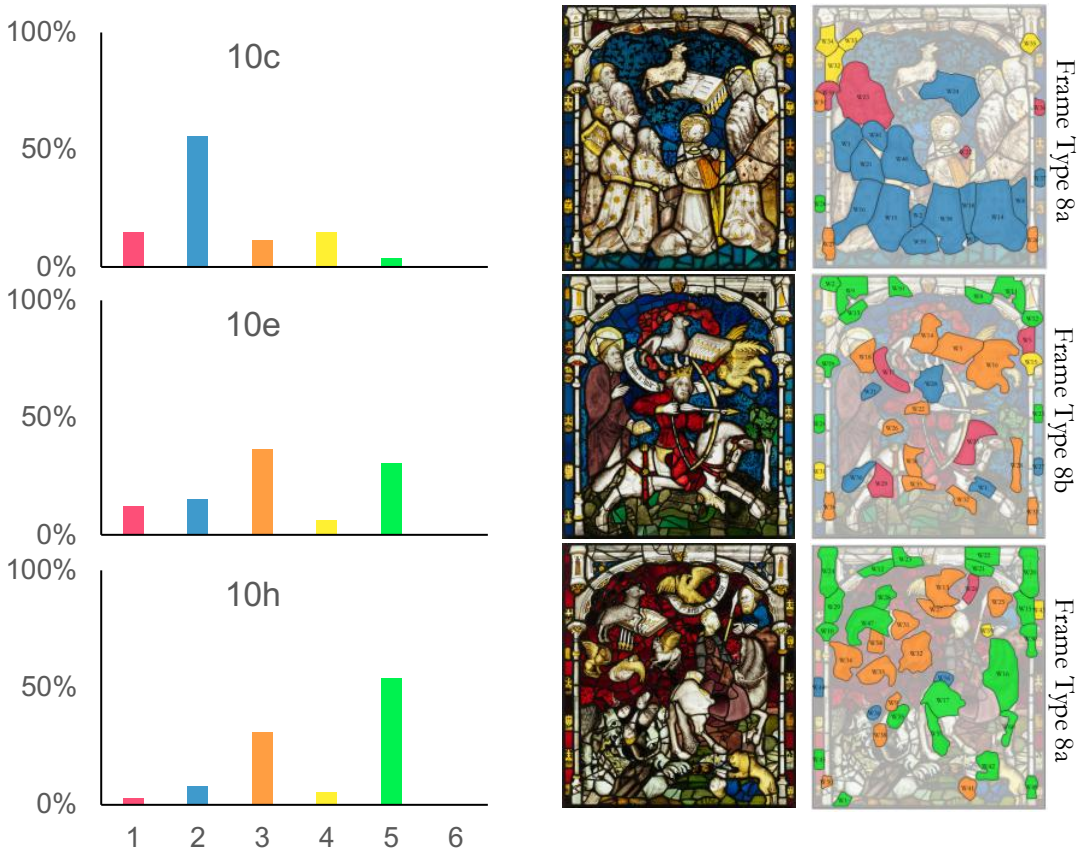

Figure 11.2 Column charts showing the relative distribution of batches used in row 10 panels, alongside images of the panels and the distribution of the batches in each panel as presented in Chapter 9. Small variations on the frame type (Type 8; French, 2003) are denoted by “a” and “b”. *Panel images: © The York Glaziers Trust with the kind permission of The Chapter of York.*

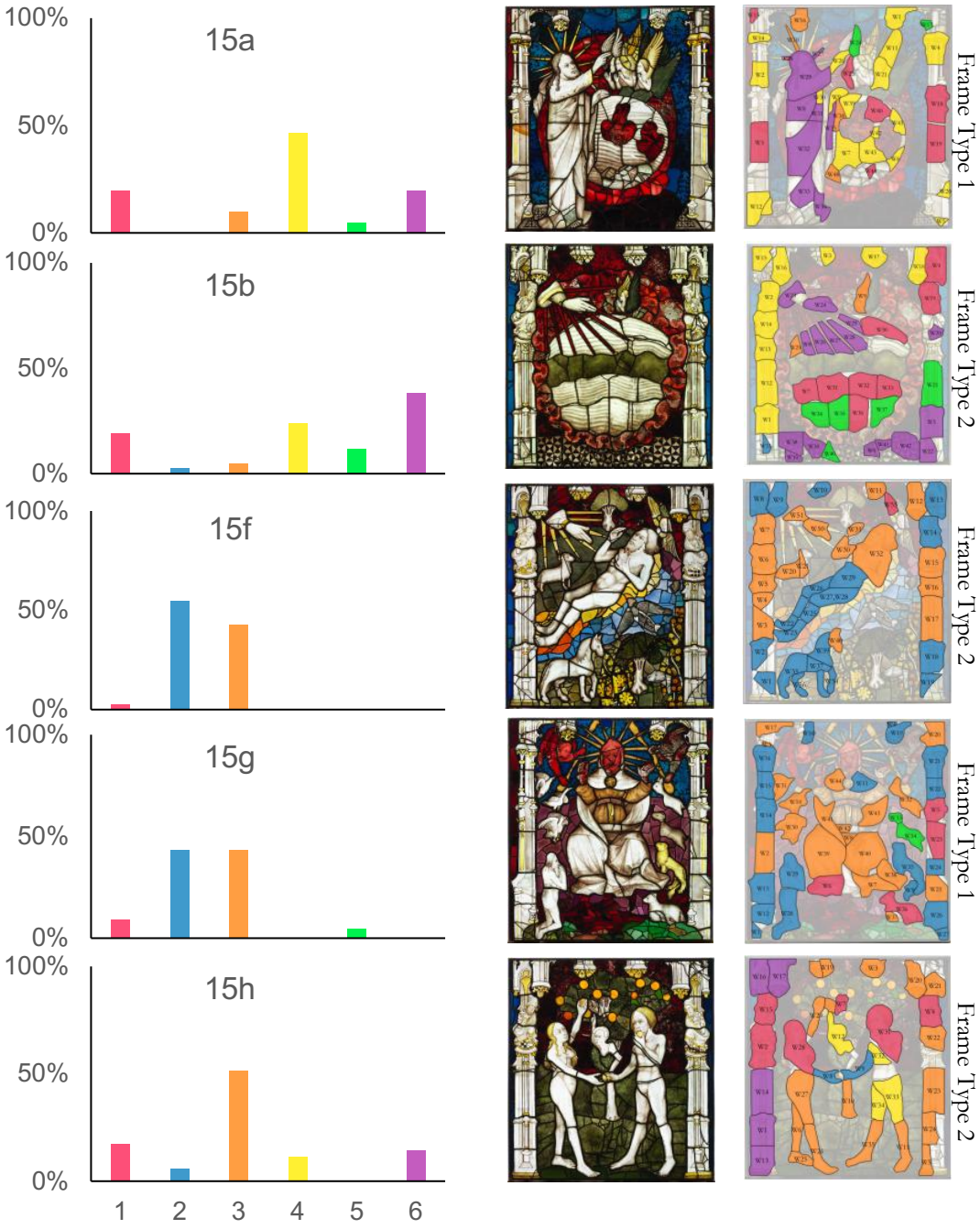

Figure 11.3 Column charts showing the relative distribution of batches used in row 15 panels, alongside images of the panels and the distribution of the batches in each panel as presented in Chapter 9. Frame types defined by French (2003) are also given. *Panel images: © The York Glaziers Trust with the kind permission of The Chapter of York.*

The stylistic analysis of the panels suggests the former explanation. Although there are numerous kinds of architectural frames in the GEW panels, there are usually one or two types that are repeated across a row. For example, in row 15, panel 15a and 15g have one type of frame (Type 1, French, 2003), while 15b, 15f and 15h have another (Type 2, French, 2003). In row 10, the difference is more nuanced; all are categorised as Type 8 by French (2003), but they show small differences, in particular in the turrets in the upper corners. Panels 10c and 10h have trefoil windows in the turrets, while panel 10e has a

circular window. Certain discrepancies in the assignment of a frame type to a panel (for example, one row 9 panel has a row 8 frame) have led to the conclusion that after a panel was completed, all of the cartoon except the frame could be wiped or cleaned from the surface of the glazing table, and the cartoon for the next panel drawn inside it (Brown, 2018, 2014). The implication is that panels 15a and 15g were prepared on one worktable, while 15b, 15f and 15h were prepared on another.

Therefore, under this model, it appears that the panels showing similar patterns in the use of different batches were completed at the same time, and that craftsmen working at multiple glazing tables were drawing on the same supply of glass rather than using separate stacks. In row 15, therefore, 15a and 15b were glazed at the same time, and 15f and 15g at the same time; 15a and 15g were glazed on the same table at different times while 15b and 15f were glazed on another (Figure 11.4). In row 10, 10e and 10h were glazed at the same or similar time, and 10h was glazed on the same table as 10c. The minute differences observed in row 10 may not have been deliberate variations on

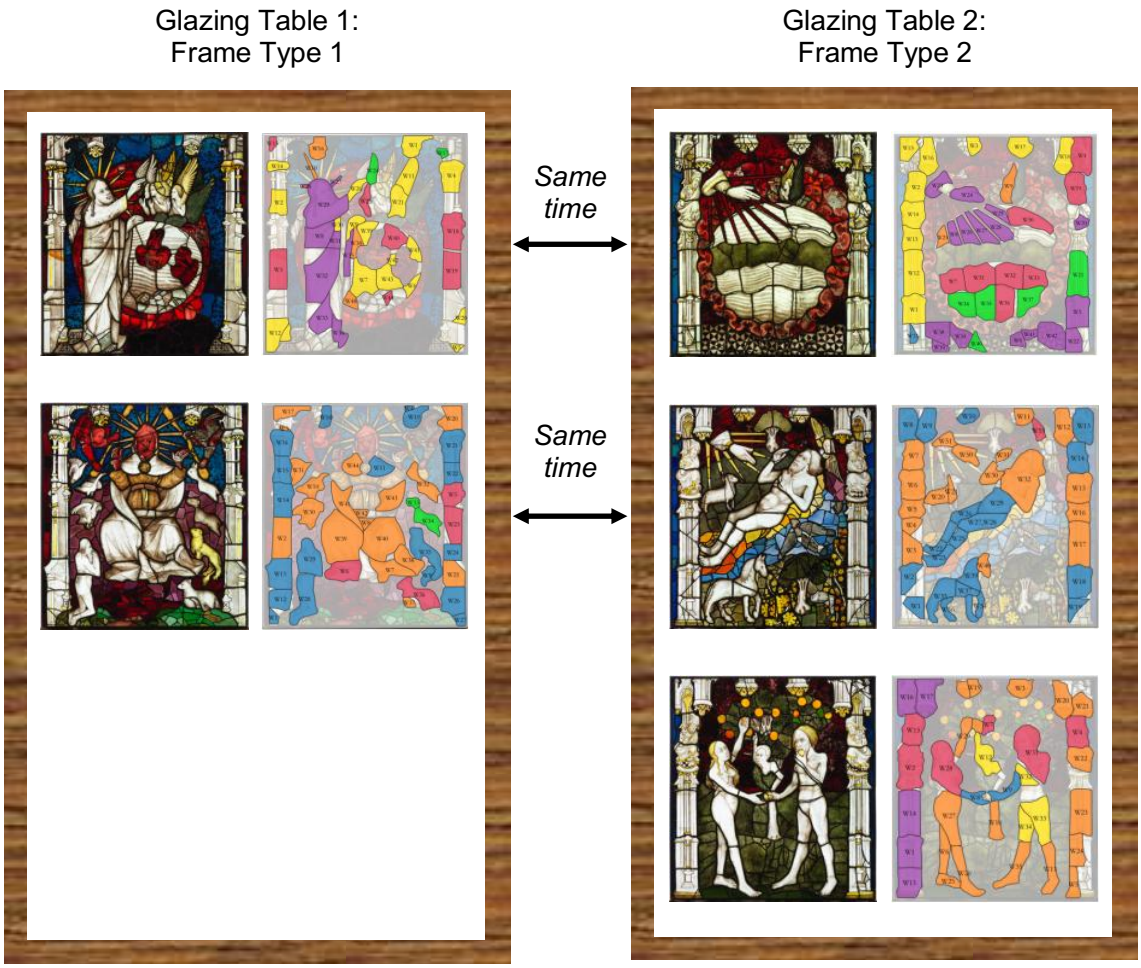

Figure 11.4 Diagram showing the proposed model for the production of the row 15 panels. Panels 15a and 15g, both with Type 1 frames, were completed at one glazing table, while panels 15b, 15f and 15h (Type 2 frames) were glazed at another. The panels with similar proportions of glass batches were likely glazed around the same time, at separate tables.

the frame, but could be due to different interpretations of the design by craftsmen at different glazing tables.

11.3 The division of labour in the production of panels

On the basis of painting style, the YGT conservators have identified three to four painters who worked on the faces in the GEW and at least two painters who worked on rinceau, with the possibility that others specialised in the details such as inscriptions, which were skilfully painted (Brown, 2018, 36). No attempt to untangle the hierarchy in skilled labour was made, however, in large part due to the consistently high quality of the painted work.

How the labour was divided in the production of individual panels is the subject of this section. The distribution of batches within panels are compared against two models of how artistic production might have been organised within the workshop, based on concepts borrowed from automobile manufacturing that have recently been successfully applied as frameworks for understanding the organisation of production in the past (Li *et al.*, 2015; Li, 2007; Martinón-Torres *et al.*, 2012). These are models of mass production, but can be reinterpreted and understood in terms of production on a smaller scale. The distribution of batches derives from the act of cutting the glass, but through this approach, some inference regarding the division of labour in the cutting and painting of the glass may be made. These models will first be applied to interpret the production of individual panels, by examining how labour was assigned or divided: by technical step (e.g., assigned to cutting glass, or painting glass; the assembly line model) or by segment of complete work (e.g., assigned to complete the frame in a panel, with responsibility for all steps; the cellular model). After this evaluation, it will be possible to examine the overall organisation of the workshop.

11.3.1 Taylorism-Fordism: the assembly line model

The first model is based upon the assembly line manufacturing approach (Taylorism-Fordism), in which there is a flow of technical steps to be undertaken until the product is finished (Dioguardi, 2010). In a medieval glass-painting workshop, the manifestation of this model would have been the division of labour by technical steps, in which each craftsman completed one step in the production of a panel before the next craftsman fulfilled his role: e.g., Thornton designed and drew the cartoon, apprentices or lower skilled craftsmen cut and grozed the glass, then master glass-painters painted the glass.

This model is explicitly evidenced in medieval glass-painting by financial records in 1351 for the glazing of St Stephen's Chapel in Westminster:

> Masters John de Chestre, John Athelard, John Lincoln, Hugh Licheffeld, Simon de Lenne, and John de Lenton, **6 master glaziers, designing and painting on white tables various designs for the glass windows of the chapel, for 6 days, at 12d each, 36s.** William Walton, John Waltham, John Carleton, John Lord, William Lichesfeld, John Alsted, Edward de Bury, Nicholas Dadyngton, Thomas Yong, Robert Norwic, and John Geddyng, **11 glaziers painting glass for the said windows, each at 7d, 28s 6d.** John Couentr', William Hamme, William Hereford, John Parson, William Nafreton, John Cosyn, Andrew Horkesle, W. Depyng, Geoffrey Starley, William Papelwic, John Brampton, Thomas Dunmowe, John atte Wode and William Bromle, **14 glaziers breaking and fitting glass upon the painted tables, for the same time, at 6d a day, 42s.** Thomas Dadyngton and Robert Yerdesle, **2 glaziers' mates (garcionibus vitriariis) working with the others at breaking glass, each of them at 4½d a day, 4s 6d.**
>
> (Salzman, 1927, 35; in Marks, 1993, 44; emphasis added)

The example of St Stephen's Chapel is thought to be exceptional for the level of specialisation (Frodl-Kraft, 1985; Marks, 1993), but a similar yet less intensive version of the model could be applied to the GEW. The advantages of this model would have been ensured high quality of the final painted work as it focuses the time of the most highly

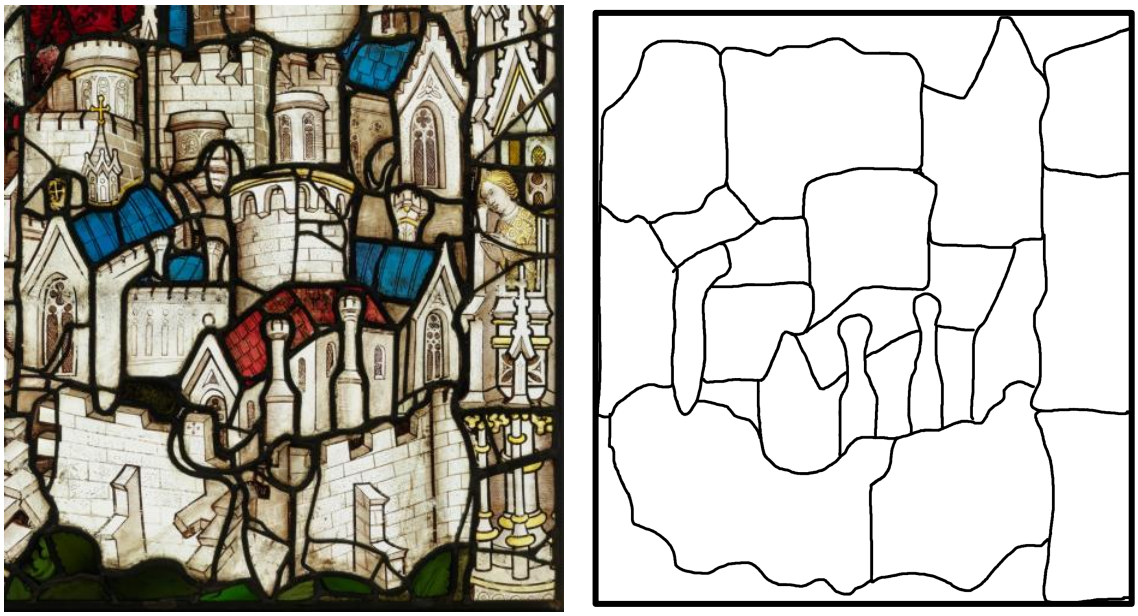

Figure 11.5 An illustration of how a sheet of white glass might be used in a panel by a craftsman assigned to cut all of the glass in the panel (detail from panel 3b). This has been simplified for illustrative purposes; it ignores the few coloured glass pieces in this part of the panel, and some shapes, such as thin, tapering towers, might be difficult to cut with a single cut (from personal experience). However, a stained glass artist and conservator who had the opportunity to work with glass with medieval composition described it as much "softer" than modern glass (pers. comm., M. Adamczak, Feb. 2016) and possibly it was easier to form shapes with that material. *Detail of panel 3b of the GEW: © The York Glaziers Trust with the kind permission of The Chapter of York.*

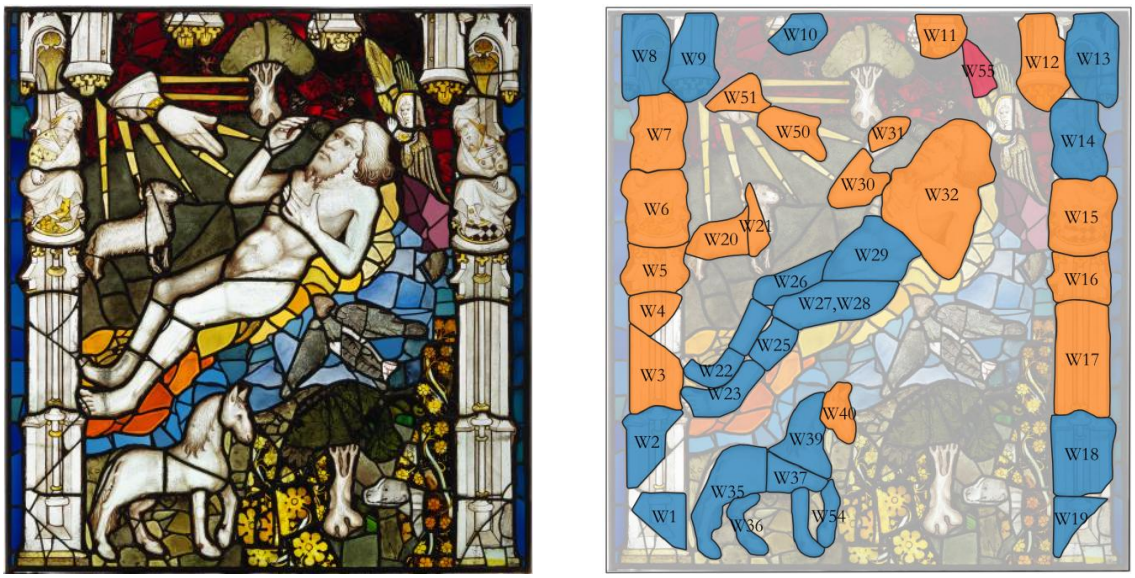

Figure 11.6 An example from the GEW of coordinate area batch distribution (panel 15f), a distribution which fits the model of the assembly line, in which a craftsman or craftsmen were tasked with all of the glass cutting for the panel. *Panel image: © The York Glaziers Trust with the kind permission of The Chapter of York.*

skilled on the most important technical step; it is in some ways an efficient use of skill and the resource that is the craftsman. Some practical difficulty might arise, however, as this model would have required a very detailed and explicit cartoon drawn on the glazing table, which is in line with Theophilus' account but at odds with the evidence from the only well preserved example of a medieval glazing table at Girona (see Chapter 4). In terms of the education of the apprentice, the repetition of manual motions develops motor skills by making the movements automatic rather than requiring conscious thought (Crown, 2014), although this would be confined to the tasks of cutting and grozing glass, not painting. Ultimately, this system might prioritise the skills of the higher skilled glass-painters, but allow little individual expression or autonomy, and would minimise the education of the apprentices.

The expected result of the assembly line model in the production of a panel is the presence of only or mostly one batch of glass in a panel if cut by a single craftsman, or batches of glass distributed by coordinate area within the panel if cut by a team (e.g., Figure 11.5, Figure 11.6). Cutting the glass in this way minimises the number of cuts that must be made on a sheet of glass as well as minimising waste, and is the sensible technological choice for the glass-cutter to make. This distribution would reflect the most logical and practical way of approaching the task if the acts of glass-cutting and glass-painting were stratified by skill.

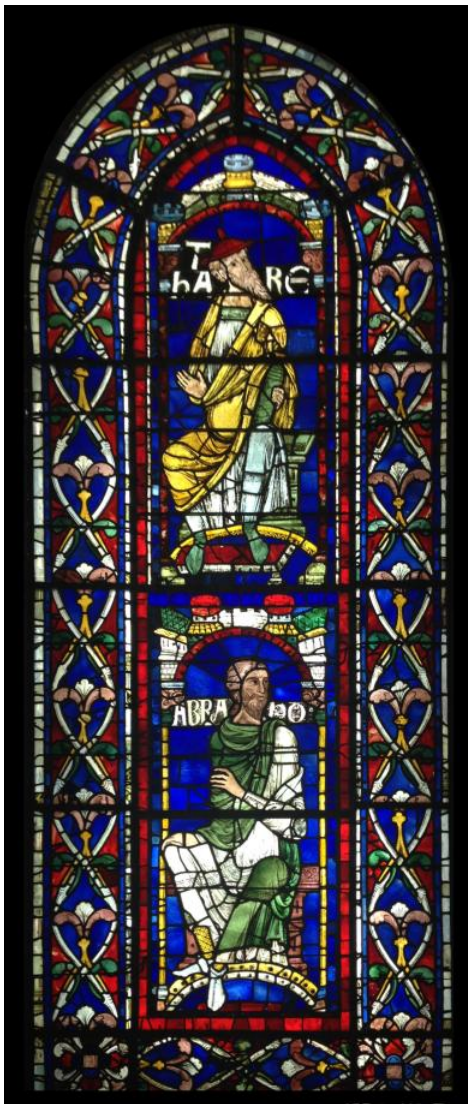

Figure 11.7 Figures from the Ancestors of Christ series that once adorned the upper clerestory windows of Canterbury Cathedral, and which are now in the Great South Window (panels 2c/3c and 7a/8a). In this photograph from a recent exhibition, the figures are displayed with their original borders, which remain in the clerestory with modern replicas of the figures.

11.3.2 Toyotism: the cellular model

The other model is similar to cellular manufacturing (Toyotism), in which smaller, independent teams are responsible for several or all technical steps involved in making a product (Dioguardi, 2010). In a stained glass workshop, this model would see different parts of a panel assigned to different craftsmen according to their skill, and the individual or team would be responsible for both the cutting and painting of the glass. This type of organisation is more or less assumed for windows with borders that are separate panels from the figurative scene, such as that shown in Figure 11.7, as the borders could be produced at a separate glazing table, even in a separate part of the workshop, and furthermore they require repetition and little artistic expression (Frodl-Kraft, 1985). The

borders or frames of the GEW panels, however, are part of the same panel and so must have been completed at the same glazing table.

There would have been several advantages to this pattern of work. It is more time-efficient, as no craftsman would be held up waiting for another to finish a previous step. Furthermore, it would have allowed Thornton to rely more heavily on the members of his workshop: a less detailed cartoon could have been drawn on the glazing table, allowing the craftsmen working on the panel to make their own decisions about where to place subsidiary cames and what details to include to embellish the scene. It would have prioritised the skill of the higher skilled craftsmen by allowing them to focus on the more expressive and more challenging aspects of a panel (such as figures and faces) and not on simple, routine designs such as rinceau or frames. As artists, they may have preferred to select and cut their own glass, particularly when using coloured glasses[23], as the hue can vary not only as a result of its recipe, but also in the sometimes highly variable thickness of the glass, producing lighter or darker colours. It would have allowed all of the craftsmen to engage with the panel creatively, and in terms of the education of the apprentice, this model would have allowed him to practice all of the skills of the trade through assignation to simpler, repetitive, and low risk parts of a panel such as the architectural frames or the rinceau used for backgrounds.

The materialisation of the cellular production model in the production of a panel would be the distribution of glass batches by aspect or subject matter rather than coordinate

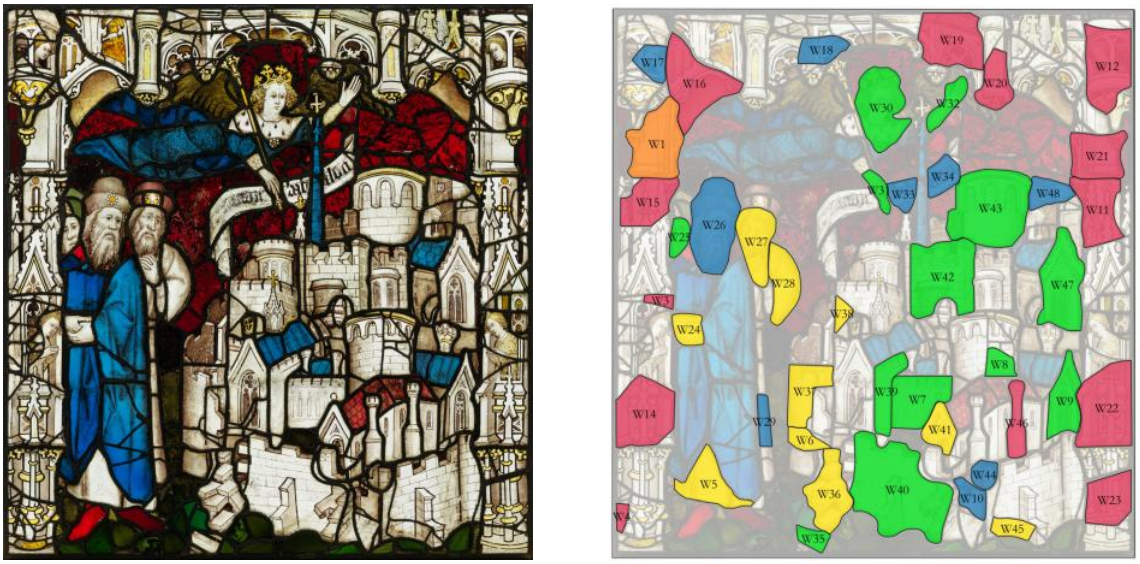

Figure 11.8 An example from the GEW of aspect batch distribution (panel 3b), a distribution which fits the cellular production model, in which a craftsmen were assigned to different parts of a panel and completed both the cutting and painting of the glass. *Panel image: © The York Glaziers Trust with the kind permission of The Chapter of York.*

[23] This idea was first suggested in conversation with Nadine Schibille (September 2015).

area (Figure 11.8). The craftsman, or perhaps pair or team of craftsmen, would cut the glass for the parts of the panel he has been assigned, and presumably paint them as well.

11.3.3 Panel production

By necessity, the application of these models simplifies a far more complex reality, neglecting other actions such as shading and yellow staining (both of which would be applied after the main painting was fired onto the glass, with a subsequent firing) and fitting the glass into cames; the organisation of these tasks is invisible to the present study. Furthermore, the distribution of batches will be obscured by other practicalities of a workshop, such as the likelihood that spare pieces of glass were stockpiled or otherwise scattered around the workshop, having been set aside by a craftsman who has either temporarily finished cutting glass, or who upon whittling down a sheet of glass was left with a size or shape that could not immediately be used. These spare pieces could be used at any time, perhaps by a colleague working on another part of the same panel, or later, in another panel entirely. Obfuscation also occurs through the documented and undocumented movement of pieces within the window and from other windows that were glazed with white glass from the same source, with compositions that may incidentally overlap glass original to a panel.

Despite the many possible sources of interference to the final distribution, batches were spatially well defined in most of the panels in the upper part of the window (see again Table 9.1). While the row 1 panels are all composed of a single batch and could be interpreted as the work of a single glass-cutter under the assembly line model of production, the exclusive use of batch 1 in this row was instead interpreted as symptomatic of the early days of the project, as discussed previously. In the upper part of the window, batches in several panels were clearly segregated by aspect, in particular between the frame and the interior; this suggests a model similar to cellular production, in which craftsmen were assigned to parts of a panel and were responsible for both cutting and painting the glass. In panel 15h, one batch of glass is dominant in the panel and possibly reflects the work of a single glass-cutter, while in other panels there is a coordinate distribution, or a mixture of coordinate and aspect distribution; this suggests an assembly line approach to assignation of tasks, as the glass for the panels appears to have been cut by a craftsman or team of craftsmen who were tasked with cutting the glass for the entire panel, which was then presumably painted by another glass-painter.

11.4 Workshop organisation

The previous section is focused on the division of labour in the production of a single panel without consideration of the overall workshop organisation, however these models can also be applied to understand the latter topic.

The expected result of an overall assembly line approach is that all or most panels would show coordinate distribution of batches or the use of mostly one batch. In this model, one or more glass-cutters (presumably lower-skilled apprentices) work together to cut the glass of one panel, and then move on to the next glazing table while the glass-painters then begin work on the prepared glass.

However, the evidence for both types of organisation in the production of panels (with panels showing both coordinate and aspect distribution of batches), as well as the evidence of the glazing tables discussed previously, suggest a cellular model of production. The change in labour division from one panel to the next implies a flexible and adaptive approach to the operation of the workshop, which is characteristic of cellular production. Although several panels showed evidence of an assembly line approach to the division of labour in the production of individual panels, all but one of these (panel 15h) showed a coordinate distribution of batches, which suggests the collaboration of multiple craftsmen in the cutting of the glass (i.e., a team, rather than a single glass-cutter). The identification of at least two glazing tables that were operating concurrently also lends itself to cellular production. The similar distribution of batches in panels prepared at different glazing tables suggests not only that the craftsmen working at the two tables were drawing from a common stock of glass, but that the glass was being cut at the same time, by different people – in other words, not by perpetual glass-cutters who cut the glass for one panel, and then another. Instead, it appears that small teams were assigned to panels and they themselves divided the work, probably under the management of a master glass-painter. Thornton would have retained overall responsibility and oversee all the work, drawing the cartoons and communicating which parts of a panel he might paint himself (see next section).

Brown's visual analysis is consistent with this; in part due to the consistent high standard of painting seen across the window (suggesting Thornton employed highly skilled glass-painters who could operate with autonomy), as well as in the identification of "close copying" in the frames of the panels (Brown, 2018, 39): in many of the panels, the two sides of the frame are such perfect mirror-images of each other that she concluded it could not have been accomplished by free-handed painting, but must have been closely copied from the same cartoon. This, combined with the repetitive use of a frame design

throughout a row, suggests the work of apprentices. Meanwhile, higher skilled master glass-painters might be entrusted to interpret from a vidimus or a less-detailed cartoon.

The changes in the assignation of labour between different panels, and the apparent concentration of an assembly line division of labour in the upper part of the window (row 15), raises the question of why different approaches were used. One explanation is that for more important panels, either theologically- or technically-speaking, Thornton drew more detailed cartoons for the glass-painters to copy; however this seems inconsistent with the overall flexible production model of the workshop. Alternatively, perhaps less technically-demanding panels were not so clearly or definitely assigned, and the craftsmen worked collaboratively on the panel without any need for assignation to specific parts of the panel.

There may be a technical explanation for their changing modus operandi. The coordinate distribution is predominant in row 15 (the top row of the main lights), while the aspect distribution is dominant in the panels in the middle of the window. The panels of row 15 are glazed with much larger pieces of glass in row 15, for purposes of perspective. The placement of lead cames, which is not only aesthetic but functionally important, must be carefully planned to avoid making "weak 'hinge points'" in the panel (Brown, 2018, 42). With fewer, larger pieces of glass and fewer subsidiary cames, the placement of the cames becomes more important and strategic, and perhaps necessitated the collaboration of the whole team (i.e., the supervision of the team's leader, the master glass-painter) to ensure that the panel was of high technical quality.

11.4.1 The work of John Thornton?

No study of the GEW is complete without attention to the identification of painted work by John Thornton himself. The phrase in the contract for the GEW in which Thornton is instructed to paint certain parts of the window "where need required according to the Ordination of the Dean & Chapter" has stimulated the imaginations of all those who have studied the window, most recently including Sarah Brown and the conservators of YGT (Brown, 2018, 34–42). Although the YGT conservators have identified three to four painters who worked on the faces in the GEW (mentioned previously), there was no correlation to the identity or relative importance of the figures; for example, the various depictions of God were painted by different hands, as were depictions of St. John.

The importance of the need to identify Thornton's work is evoked by an excerpt from Brown's book, which echoes words heard several times at the YGT studio:

> A question that continues to intrigue us is the meaning of the words 'paint the same where need required according to the Ordination of the Dean & Chapter'. In other words, can we identify the hand of John Thornton himself in the painting of the Great East Window? Sadly … We are forced to conclude that we will probably never know which parts of the Great East Window were actually painted by John Thornton's own hand. The status of the figure and the scene to be represented, its iconographic or technical challenges, and its proximity to the viewer may all have played a part in determining his contribution to the painting of the glass 'according to the ordination of the Dean and Chapter'. But through the agency of the cartoon and in his role as designer, mentor, manager and leader, John Thornton's influence must have pervaded the spirit of every panel and influenced every stage in the conduct of the work.
>
> (Brown, 2018, 34–41)

Under the present approach, however, a suggestion might finally be made. The distinction of the figure of God from the rest of the white glass in panel 15a is a singular result and suggests that a different (presumably higher-skilled) glass-painter than those working on the rest of the panel cut and painted this figure. As a figure, it is amongst the more technically-demanding aspects of the window, and as it is large and in the forefront, it is the dominant feature of the panel. The subject matter is of enormous iconographical importance; it is difficult to propose a more important figure in Genesis or Revelations than God creating the world. It is therefore considered that there is a strong possibility that this reflects the painted work of John Thornton himself (Figure 11.9).

11.5 Summary

The application of the concept of the batch to the study of a medieval stained glass window has yielded interesting insights into the workshop of John Thornton. The identification of consignments of glass and the concentration of the first at the bottom of the window, evaluated within a practical consideration of the operation of Thornton's workshop in its early days, has given support for the previous hypothesis that the glazing project was begun at the bottom of the window. The examination of how batches were used across a row allowed the identification of panels that were glazed using the same table.

Through a multidisciplinary approach based both on the identification and distribution of batches in the GEW panels and drawing heavily on the stylistic analysis published by Sarah Brown, a detailed analysis of the workshop operations under Thornton has been carried out. It was argued that Thornton ran his workshop in a flexible, adaptable manner

Figure 11.9 Detail of panel 15a, showing God creating the world. The figure of God in this panel was painted on a batch of glass distinct to the rest of the glass in the panel, and is a strong candidate for being the work of John Thornton himself. *Detail of panel 15a of the GEW: © The York Glaziers Trust with the kind permission of The Chapter of York.*

that gave a significant autonomy to his trusted master glass-painters, in something resembling a cellular model of production. The master craftsmen could adapt the way his team approached the glazing of each panel; in row 15, it appears that the glass was cut collaboratively, which may have been due to a need for greater supervision in the decision of where to place lead cames.

It has been a historical and contemporary debate, did guilds stifle or support technological innovation in the medieval period (Croix *et al.*, 2015; Epstein, 2009, 2008; Richardson, 2005; Smith, 1776)? This workshop, operating within the framework of medieval guilds, appears to have supported it. The modus operandi was flexible, efficient, relied on and encouraged individual creativity and responsibility, and highlighted the education of and acquirement of practical skills by the more junior craftsmen.

Finally, this section concluded with the suggestion given that it was cut from a different sheet of glass than the rest of the panel, the figure of God creating the world in panel

15a may have been painted by John Thornton himself, which is consistent with the high technical skill required and its great iconographic importance.

CHAPTER 12

Conclusions

Medieval stained glass windows were an important part of, and a valuable clue about, medieval culture, serving practical, aesthetic, religious, cultural and even political functions. Their heyday occurred against the backdrop of a boom in ecclesiastical construction, the development of the Gothic style, and advances made in technology and art. They present a rare opportunity to study medieval technology and craft organisation, as they hold within their cames the output of a workshop over an extended period of time. The craft of glass-painting in particular is known to have been carried out within the guild system, which is an important subject in medieval history both in the ongoing debate on whether guilds were regressive and progressive, and as a key stage in the economic development of Europe. A materials science approach has much to offer this field of study, and yet these treasures of cultural heritage are rarely studied by these techniques, due to practical obstacles related to their architectural context.

The GEW of York Minster, painted and constructed between 1405 and 1408 by John Thornton of Coventry and his workshop, has recently been the subject of an extensive, comprehensive, state-of-the-art conservation project, York Minster Revealed. This project has been an exceptional opportunity for research, including this project as well as extensive art historical research. Although this thesis has focused on only one window, the intensive analysis of the GEW has yielded results with wider significance, regarding medieval glass-making technology, the organisation of production in a glass-painting workshop, and in the development of a robust, sensitive methodology for the study of medieval stained glass windows by handheld pXRF.

12.1 Development of a methodology

The study of the technology and production of medieval stained glass windows has previously been inhibited by the inaccessibility of the glass for sampling, and therefore a key focus and contribution of this research was to develop a methodology based on handheld pXRF that can be used in situ.

12.1.1 The trace element methodology

The first part of this aim was to further develop a methodology centred on the analysis of heavy trace elements, building upon the work conducted by Dungworth (2012a, 2012b) and the English Heritage Historic Windows project. Comparison of pXRF results compared to the results of EPMA-WDS and LA-ICP-MS on the cross-section of medieval glass showed that although pXRF performed well on glass standards, the poor surface conditions of medieval glass interfered with the analysis of most elements. Five elements (Cu, Zn, Rb, Sr and Zr) were determined to be well-measured by pXRF on the GEW glass, in large part due to the higher energy characteristic x-rays of these elements that results in a greater depth of analysis. The latter three elements in particular were useful in differentiating not only medieval forest glass from other glass types (as has been demonstrated previously by Dungworth), but could be used to show different forest glass recipes, and even batches of glass.

The usefulness of this methodology for the study of medieval glass-making is at present limited. The successful use of this approach on the GEW glass is by no means a guarantee that it would work on more heavily corroded glass; this requires further exploration. Furthermore, a number of nuances regarding glass-making technology will be lost in a study that relies solely on pXRF analysis of trace elements, especially since trace elements are added incidentally, unlike major elements that affect the properties of the glass enough so that a craftsman could observe and attempt to manipulate the recipe. Ideally, a study would combine pXRF analysis with one or more techniques involving analysis on the cross-section, both for the development of tailored empirical calibrations and for invaluable major element information.

However, this is not always possible and despite the present limitations, the potential for handheld pXRF to be used in isolation of other techniques is still encouraging. Different recipes used within a window can be distinguished, and if a larger database of trace element compositions from across Europe is compiled, there is potential that these trace elements may point to a regional provenance, as is suggested by the preliminary evaluation of the Cardiff-York project data in Chapter 7. If so, pXRF might

be used to quickly and inexpensively provide a regional provenance of the glass production, a potentially powerful tool in medieval glass studies.

The use of trace element data in the identification of batches of glass made in the same glasshouse was carried out with a similar degree of success as identification of batches based on major element data. Although previous work has recommended that a batch be identified by ensuring all members are identical within experimental error for all elements analysed (Freestone *et al.*, 2009), this approach could not be directly applied to the GEW. The procurement of large consignments of glass from a glasshouse is likely to consist of numerous batches/sheets produced in sequence and which may have only slightly varying compositions. The large number of glass sheets of any given colour used in a window forecasts the likelihood of overlapping compositions, which can partially obscure the groups. Although in concept the batch (the "production batch") is all of the objects made from a single pot of homogenised molten glass (until it is topped up with further raw materials, creating a new batch), in practice the homogeneity of the pot may have been less than perfect and continual topping up of the pot might not have been necessary to result in multiple "chemical batches" (i.e., groups which are identical in chemical composition).

A combination of approaches involving hierarchical cluster analysis were tried and proved comparable to each other and to batches identified in the control group based on EPMA data. The distribution of these batches in the panels and in the window proved informative for the study of the organisation of production in John Thornton's workshop (summarised in section 12.3). This degree of success is encouraging because handheld pXRF is particularly suited to this type of study: the rapidity of the analyses and the lack of necessary sample preparation allows enormous numbers of data to be collected in a short amount of time so that a comprehensive view may be formed of the window's construction (for example, although this project progressed at a more deliberate pace, Dungworth and Girbal, 2011, report an average of 220 glass panes analysed per day). This widespread scale of study would not be practical by EPMA or other laboratory methods requiring more laborious sample preparation. The study of batch distribution in panels and in the window led to interesting new insights into medieval craft production.

12.1.2 The WindoLyzer 5

An attachment for the spectrometer, designed to facilitate in situ analysis, was also developed as part of this project. Test analyses of a panel that was not dismantled (i.e., the pieces encased in lead cames) showed that the variable interference of the

protruding lead cames affected both the measured intensity and the precision of the analyses. Laboratory tests showed that this effect was consistent at a given distance, although not fully explained by the increased absorption in air; the disruption to the geometry of the spectrometer (i.e., the angles of incidence and detection) appears to have greatly affected the measured intensity. However, if the distance between spectrometer and sample were held constant, the data could be corrected through empirical calibrations. The attachment (the "WindoLyzer 5") was inexpensively produced using a 3D printer, will be easy to adjust for different windows (with different lengths to account for different lead came sizes), and is safe to use if the proper precautions are made. The WindoLyzer was successfully used to study a case study on the Ancestors of Christ series from Canterbury Cathedral as part of this research (not reported in this thesis).

A limitation of this part of the project was the lack of foresight in the anticipation of problems due to lead cames. It would have been very useful to have developed the WindoLyzer before the analysis of the row 10 panels, and the precision of the analyses for those panels is likely to have suffered.

The development of a methodology for the study of in situ medieval stained glass windows by handheld pXRF has opened up the possibility of studying other windows that would have otherwise been inaccessible for sampling.

12.2 Glass-making and procurement of the glass

The chemical characterisation of the glass original to the GEW revealed two major compositional groups, with the white glass forming one group (LLHM) and the coloured glasses forming another (HLLM). The white glass was found to be consistent with glass produced at Little Birches, Wolseley, in Staffordshire, in its elemental and isotopic composition. The coloured glasses, although several different compositions were identified within the group, appear to have been made at the same glasshouse or conglomerate of glasshouses in the Rhenish region using the same raw materials in different proportions or recipes to produce the range of colours.

A long-term relationship between York Minster and the Staffordshire glass-making industry was established through purchase records, analysis of a few comparative samples from the St. Williams Window (dated to *c.* 1414), and the identification of several white glass pieces that were identified as not original to the window on the basis of its painted detail, and yet were indistinguishable in chemical composition from the original white glass in the GEW. Like many of the non-original medieval glass

pieces in the window, these were taken from other windows and used to patch the window during historical conservation interventions. The consistency of their compositions, in glass that may have been produced decades before or after the GEW glass, suggests that glass-makers had far greater control over the glass recipe than previously supposed, in particular when the high variability of plant ash composition is considered.

The synthesis of legacy data for medieval glass compositions in Europe (chapter 3) is a valuable contribution in itself as a useful tool for determining the regional provenance of medieval glass production based on just a few, commonly analysed major elements. In this work, it allowed the provenance determination of the coloured glasses to the Rhenish region, and also prompted a reinterpretation of a previously made observation that the coloured glass in English windows tend to be of LLHM composition before the end of the fourteenth century and of HLLM afterwards (Kunicki-Goldfinger *et al.*, 2014). A new consideration of this change in composition suggests that the change was related to a change in the source of glass rather than a sweeping change in technology; however, rather than a change in trading patterns, it appears that the intensity of glass-making activity, in particular for coloured glass, shifted from Normandy to the Rhenish region, perhaps prompted by numerous upheavals suffered in the former region during the fourteenth century.

Despite the variety in compositions found in the coloured glass group, several compositional links exist between the different groups that suggests that they are all variations of recipes based on the use of two different ashes. A higher potash ash was used for green, yellow and Mn-colours; some of the green glasses were made using the lower potash glass but with an additional source of potash. The higher potash would have facilitated the production of these highly oxidised colours. The apparently deliberate selection of different ashes and the alteration of the base glass composition in order to produce colour is a level of sophistication in glass-making technology that has not previously been attributed to medieval glass-makers.

This research suffered some limitations, in particular as the results are based on the study of only one window. However, this work represents the first study of its kind and scale, a comprehensive analytical study of a single, large and well-documented window, and while this has proved valuable, it will require further studies to collaborate the findings. Furthermore, a larger number of subsamples was planned for LA-ICP-MS analysis, and the study would have benefitted greatly from more varied selection in the samples. Ultimately these samples were chosen in order to provide the full range of trace element values for the development of empirical calibrations for the pXRF data,

which introduced its own limitations. For example, only high-Sr Mn-glasses (group B/C) were analysed, and no lower Sr Mn-glasses (group B).

The identification of regional trends in medieval glass composition also raises questions for future research. The factors affecting the strong regional patterns in chemical composition, for example, are presumably determined by some combination of the bioavailability of elements in the underlying substratum, the regional availability of different species, and/or regional technological traditions. One starting step towards untangling these factors might be in the fuller characterisation of ashes from different plant species and from different regions.

12.3 The organisation of production in Thornton's workshop

This is the first study to apply the concept of the batch to study the organisation of production in a medieval stained glass window workshop. Batches were identified based on hierarchical cluster analysis of their chemical composition, and their distribution within each panel and across the window were examined within the historical context of guild practice and an art historical context provided in large part by Brown (2018, 2014a).

The analysis provided insights into several details regarding the windows production, including supporting a previous hypothesis that the window was begun at the bottom and identifying panels that were produced at the same glazing table. The latter supported the suggestion that, upon finishing one panel, all of the cartoon except the overarching frame would be wiped away, and the cartoon for the next panel drawn inside it.

Comparison of the distribution of batches to common models of production (based on the automobile manufacturing industry) allowed investigation into the division of labour in the making of different panels as well as the overall model of production. This was accomplished together with art historical perspective as well as a consideration of technological practicalities under the model of technological choice. The results indicate that Thornton ran his workshop in a flexible, adaptable manner that gave greater autonomy to his trusted master glass-painters, in something resembling a cellular model of production.

Finally, an exciting result was the identification of a strong candidate for the painted work of John Thornton himself: the figure of God creating the world (panel 15a).

There were limitations in the identification of batches as there is no established methodology for a dataset such as this one, comprising a large body of work from a single glasshouse and from a short span of time, resulting in overlapping compositions. There were certainly errors in the groupings, however it may prove impossible to avoid error in this case. There is furthermore a limitation inherent in this application as it is anticipated that it will only be useful for the study of windows of this style, which are characterised by a high dependence on one colour (white glass) over others. In other medieval windows of other styles, there is a more or less equal distribution of the different colours. Therefore, the identification of batches will relate to the use of different colours of glass, not to the work patterns of the craftsmen.

In hindsight, it would have been useful to study panels from two adjacent rows (i.e., rows 14 and 15). With the current sample set, it appears there were two glazing tables in operation in the production of the GEW, however a larger number cannot be discounted at present. As glazing tables have been connected to frame types (chapter 11), and generally only one or two frame types were used in any row, evidence of more than two glazing tables used in a single row is unlikely.

This research was focused on only one window, and work on others will be necessary to form a more complete picture of medieval glass-painting workshops. Future work on the GEW or other windows might also include a closer collaboration with art historical experts, who might identify visually the work of different painters, for more direct comparison with the chemical results.

12.4 A window to the past

Medieval stained glass windows offer a rare, almost unique opportunity in our investigation of the past, containing within their cames the long-term output of a workshop. Often, the products of workshops are dispersed through commerce, a large percentage lost forever, and the remaining rarely linked to their origins and to each other. At workshop sites, what remains are waste debris and few finished products. Meanwhile, the GEW for example contains three years of artistic output from John Thornton's workshop, and about 1,680 ft^2 of sheet glass from a couple glasshouses. This research contributed to filling this gap in our knowledge, both through the study of technology and production evidenced in the GEW and through the facilitation of future studies using handheld pXRF to study medieval windows.

References

Adlington, L.W., 2017. The Corning Archaeological Reference Glasses: New Values for “Old” Compositions. *Pap. from Inst. Archaeol.* 27(1), 1–8.

Adlington, L.W., Freestone, I.C., 2017. Using handheld pXRF to study medieval stained glass: A methodology using trace elements. *MRS Adv.* 2(33–34), 1785–1800. doi:10.1557/adv.201

Aerts, A., Velde, B., Janssens, K., Dijkman, W., 2003. Change in silica sources in Roman and post-Roman glass. *Spectrochim. Acta - Part B At. Spectrosc.* 58, 659–667. doi:10.1016/S0584-8547(02)00287-2

AMC Analytical Methods Committee, 2005. Terminology – the key to understanding analytical science. Part 2: Sampling and sample preparation. *AMC Tech. Br.* 19, 1–2.

Amuda, A.K., Okoh, S., Ekwuribe, S., Bashir, M., 2014. Implication of X-Ray Path, Region of Interest, Tube Current and Voltage in Calibration of X-ray Fluorescence Instrument: A Case Study of X-Supreme 8000. *Int. J. Sci. Technol. Res.* 3(2), 113–117.

Aulinas, M., Garcia-Vallès, M., Gimeno, D., Fernandex-Turiel, J.L., Ruggieri, F., Pugès, M., 2009. Weathering patinas on the medieval (S. XIV) stained glass windows of the Pedralbes Monastery (Barcelona, Spain). *Environ. Sci. Pollut. Res.* 16, 443–452. doi:10.1007/s11356-008-0078-0

Aune, D.E., 2003. *The Westminster Dictionary of New Testament and Early Christian Literature and Rhetoric*. Westminster, Louisville, KY.

Bamford, C.R., 1977. *Colour generation and control in glass*. Elsevier, Amsterdam.

Barrera, J., Velde, B., 1989. A study of french medieval glass composition. *Archéologie Médiévale* XIX, 81–130.

Becherini, F., Bernardi, A., Daneo, A., Geotti, F., Nicola, C., Verità, M., 2008. Thermal Stress as a Possible Cause of Paintwork Loss in Medieval Stained Glass Windows. *Stud. Conserv.* 53(4), 238–251. doi:10.1179/sic.2008.53.4.238

Bednarski, S., Courtemanche, A., 2009. Learning to be a man: public schooling and apprenticeship in late medieval Manosque. *J. Mediev. Hist.* 35(2), 113–135. doi:10.1016/j.jmedhist.2009.01.003

Beerkens, R.G.C., 2005. Sulphate decomposition and sulphur chemistry in glass melting processes. *Glas. Technol.* 46(2), 39–46.

Beerkens, R.G.C., 2003. Amber chromophore formation in sulphur- and iron-containing soda-lime-silica glasses. *Glas. Sci. Technol.* 76(4), 166–175.

Beerkens, R.G.C., 1999. Redox and sulphur reactions in glass melting processes. *Ceram. - Silikáty* 43(3), 123–131.

Bleed, P., 2008. Skill matters. *J. Archaeol. Method Theory* 15(1), 154–166. doi:10.1007/s10816-007-9046-0

Bony, J., 1983. *French Gothic Architecture of the Twelfth and Thirteenth Centuries*. University of California Press, Berkeley.

Boswell, P.G.H., 1917. British glassmaking sands. *J. Soc. Glas. Technol.* 1, 3–61.

Brand, N.W., Brand, C.J., 2014. Performance comparison of portable XRF instruments. *Geochemistry Explor. Environ. Anal.* 14(2), 125–138.

Brems, D., Degryse, P., 2014. Trace element analysis in provenancing Roman glass-making. *Archaeometry* 56, 116–136. doi:10.1111/arcm.12063

Brems, D., Degryse, P., Hasendoncks, F., Gimeno, D., Silvestri, A., Vassilieva, E., Luypaers, S., Honings, J., 2012. Western Mediterranean sand deposits as a raw material for Roman glass production. *J. Archaeol. Sci.* 39(9), 2897–2907. doi:10.1016/j.jas.2012.03.009

Brems, D., Ganio, M., Latruwe, K., Balcaen, L., Carremans, M., Gimeno, D., Silvestri, a., Vanhaecke, F., Muchez, P., Degryse, P., 2013a. Isotopes on the Beach, Part 1: Strontium Isotope Ratios As a Provenance Indicator for Lime Raw Materials Used in Roman Glass-Making. *Archaeometry* 55(2), 214–234. doi:10.1111/j.1475-4754.2012.00702.x

Brems, D., Ganio, M., Latruwe, K., Balcaen, L., Carremans, M., Gimeno, D., Silvestri, a., Vanhaecke, F., Muchez, P., Degryse, P., 2013b. Isotopes on the Beach, Part 2: Neodymium Isotopic Analysis for the Provenancing of Roman Glass-Making. *Archaeometry* 55(3), 449–464. doi:10.1111/j.1475-4754.2012.00701.x

Brill, R.H., 1999. *Chemical analyses of early glasses*. Corning Museum of Glass, Corning, NY.

Brill, R.H., 1970. Scientific Studies of Stained Glass: A Progress Report. *J. Glass Stud.* 12(3), 185–192.

Brill, R.H., Pongracz, P., 2004. Stained glass from Saint-Jean-des-Vignes (Soissons) and comparisons with glass from other medieval sites. *J. Glass Stud.* 46, 115–144.

Britnell, R.H., 2000. The economy of British towns 1300–1540, in: Palliser, D.M. (Ed.), *The Cambridge Urban History of Britain, Volume 2: 600-1540*. Cambridge University Press, Cambridge, 313–333.

Brookes, S., Huynh, H.N., 2018. Transport networks and towns in Roman and early medieval England: An application of PageRank to archaeological questions. *J. Archaeol. Sci. Reports* 17, 477–490. doi:10.1016/j.jasrep.2017.11.033

Brown, S., 2018. *The Great East Window of York Minster: An English Masterpiece*. Third Millennium Publishing LTD, London.

Brown, S., 2014a. *Apocalypse: The Great East Window of York Minster*. Third Millennium Publishing LTD, London.

Brown, S., 2014b. The Girona Glazier's Table: An English Perspective, in: Santolaria Tura, A. (Ed.), *Vitralls Sobre Taules de Vitraller: La Taula de Girona*. Institut Catal de Recerca en Patrimoni Cultural, Girona.

Brown, S., 2003. *York Minster: An Architectural History c 1220-1500*. English Heritage, Swindon, UK.

Brown, S., O'Connor, D., 1991. *Medieval Craftsmen: Glass-painters*. British Museum Press, London.

Budden, S., 2008. Skill amongst the sherds: Understanding the role of skill in the early to late Middle Bronze Age in Hungary, in: *Breaking the Mould: Challenging the Past through Pottery*, Prehistoric Ceramic Research Group Occasional Paper. BAR 1861, Oxford, 1–17.

Bugslag, J., 1998. Valentin Bousch's Artistic Practice in the Stained Glass of Flavigny-sur-Moselle. *Metrop. Museum J.* 33, 169–182.

Burnam, R.G., 1988. Medieval stained glass practice in Florence, Italy: The case of Orsanmichele. *J. Glass Stud.* 30, 77–93.

Burnett, C., 2013. The twelfth-century renaissance, in: Lindberg, D.C., Shank, M.H. (Eds.), *The Cambridge History of Science Volume 2: Medieval Science*. Cambridge University Press, New York, NY, 365–384.

Cable, M., Smedley, J.W., 1987. Liquidus temperatures and melting characteristics of some early container glasses. *Glas. Technol.* 28(2), 94–98.

Caen, J., 2009. *The Production of Stained Glass in the County of Flanders and the Duchy of Braband From the XVth to the XVIIIth Centuries*. Turnhout, Brepols.

Caen, J., De Munck, B., De Laet, V., 2006. Technical Prescriptions and Regulations for Craftsmen in the Southern Netherlands during the Sixteenth, Seventeenth and Eighteenth Centuries. A Confrontation of Archival and Material-Technical Information regarding Glazing and Stained-Glass Windows, in: Lagabrielle, S. (Ed.), *Verre et Fenêtre Del'antiquité Au 18e Siècle: Actes Du Premier Colloque International de l'association Verre et Histoire (Paris-La Défense / Versailles, 13-14-15 Octobre 2005)*. Verre et Histoire, Paris.

Calligaro, T., 2008. PIXE in the study of archaeological and historical glass. *X-Ray Spectrom.* 37, 169–177. doi:10.1002/xrs

Carmona, N., 2013. Corrosion of Stained Glass Windows: Applied Study of Spanish Monuments of Different Periods, in: Janssens, K. (Ed.), *Modern Methods for Analysing Archaeological and Historical Glass*. John Wiley & Sons, Chichester, UK.

Carmona, N., Oujja, M., Rebollar, E., Römich, H., Castillejo, M., 2005. Analysis of corroded glasses by laser induced breakdown spectroscopy. *Spectrochim. Acta - Part B At. Spectrosc.* 60(7–8), 1155–1162. doi:10.1016/j.sab.2005.05.016

Carmona, N., Villegas, M.A., Ferna, J.M., 2006. Study of glasses with grisailles from historic stained glass windows of the cathedral of León (Spain). *Appl. Surf. Sci.* 252, 5936–5945. doi:10.1016/j.apsusc.2005.08.023

Carmona, N., Wittstadt, K., Römich, H., 2009. Consolidation of paint on stained glass windows: Comparative study and new approaches. *J. Cult. Herit.* 10(3), 403–409. doi:10.1016/j.culher.2008.12.004

Caviness, M.H., 1990. *Sumptuous arts at the Royal Abbeys in Reims and Braine: Ornatus elegantiae, varietate stupendes*. Princeton University Press, Princeton.

Caviness, M.H., 1987. Romanesque "belles verrières" in Canterbury, in: Stratford, N. (Ed.), *Romanesque and Gothic: Essays for George Zarnecki*. Boydell Press, Woodbridge, NH, 35–38.

Caviness, M.H., 1981. The Windows of Christ Church Cathedral Canterbury.

Cesareo, R., 2010. X-Ray Fluorescence Spectrometry. *Ullmann's Encycl. Ind. Chem.*

Charleston, R.J., 1991. Vessel Glass, in: Blair, J., Ramsay, N. (Eds.), *English Medieval Industries: Craftsmen, Techniques, Products*. Hambledon Press, London, 237–264.

Cílová, Z., Woitsch, J., 2012. Potash - A key raw material of glass batch for Bohemian glasses from 14th-17th centuries? *J. Archaeol. Sci.* 39(2), 371–380. doi:10.1016/j.jas.2011.09.023

Cílová, Z.Z., Kučerová, I., Knížová, M., Trojek, T., 2015. Corrosion damage and chemical composition of Czech stained glass from 13th to 15th century. *Glas. Technol. Eur. J. Glas. Sci. Technol. Part A* 56(5), 153–162. doi:10.13036/17533546.56.5.153

Conrey, R.M., Goodman-Elgar, M., Bettencourt, N., Seyfarth, A., Van Hoose, A., Wolff, J.A., 2014. Calibration of a portable X-ray fluorescence spectrometer in the analysis of archaeological samples using influence coefficients. *Geochemistry Explor. Environ. Anal.* 14(3), 291–301. doi:10.1144/geochem2013-198

Cortés Pizano, F., 2000. Medieval window lead cames from Pedralbes (Catalonia) and Alten- berg (Germany): a comparative study. *CVMA Newsl.* 47, 25–31.

Cothren, M.W., 1999. Production practices in medieval stained glass workshops: Some evidence in the Glencairn Museum. *J. Glass Stud.* 41, 117–134.

Cox, G.A., Gillies, K.J.S., 1986. The X-ray fluorescence analysis of medieval durable blue soda glass from York Minster. *Archaeometry* 28(1), 57–68.

Cox, G.A., Heavens, O.S., Newton, R.G., Pollard, A.M., 1979. A study of the weathering behaviour of medieval glass from York Minster. *J. Glass Stud.* 21, 54–75.

Craig, N., Speakman, R.J., Popelka-Filcoff, R.S., Glascock, M.D., Robertson, J.D., Shackley, M.S., Aldenderfer, M.S., 2007. Comparison of XRF and PXRF for analysis of archaeological obsidian from southern Perú. *J. Archaeol. Sci.* 34(12), 2012–2024. doi:10.1016/j.jas.2007.01.015

Croix, D. De, Doepke, M., Mokyr, J., 2015. Clans, Guilds, and Markets: Apprenticeship Institutions and Growth in the Pre-Industrial Economy (9828), 73.

Crossley, B.D.W., 1967. Glassmaking in Bagot's Park, Staffordshire, in the Sixteenth Century. *Post-Medieval Archaeol.* 1(1), 44–83. doi:10.1179/pma.1967.003

Crown, P.L., 2014. The Archaeology of Crafts Learning: Becoming a Potter in the Puebloan Southwest. *Annu. Rev. Anthropol.* 43(1), 71–88. doi:10.1146/annurev-anthro-102313-025910

De Bardi, M., Wiesinger, R., Schreiner, M.R., 2013. Leaching studies of potash-lime-silica glass with medieval composition by IRRAS. *J. Non. Cryst. Solids* 360(1), 57–63. doi:10.1016/j.jnoncrysol.2012.06.035

de Boer, D.K.G., 1989. Angular Dependence of X-Ray Fluorescence Intensities. *X-Ray Spectrom.* 18, 119–129.

Degryse, P., Freestone, I.C., Schneider, J., Jennings, S., 2010. Technology and provenance of Levantine plant ash glass using Sr-Nd isotope analysis, in: Drauschke, J., Keller, D. (Eds.), *Glass in Byzantium - Production, Usage, Analyses*. Verlag des Römisch-Germanischen Zentralmuseums, Mainz, 83–90. doi:10.1017/CBO9781107415324.004

Degryse, P., Schneider, J., Haack, U., Lauwers, V., Poblome, J., Waelkens, M., Muchez, P., 2006. Evidence for glass 'recycling' using Pb and Sr isotopic ratios and Sr-mixing lines: the case of early Byzantine Sagalassos. *J. Archaeol. Sci.* 33, 494–501. doi:10.1016/j.jas.2005.09.003

Degryse, P., Scott, R.B., Brems, D., 2014. The archaeometry of ancient glassmaking: reconstructing ancient technology and the trade of raw materials. *Perspective* 2.

Delgado, J., Vilarigues, M., Ruivo, A., Corregidor, V., Silva, R.C., Alves, L.C., 2011. Characterisation of medieval yellow silver stained glass from Convento de Cristo in Tomar, Portugal. *Nucl. Instruments Methods Phys. Res. B* 269(20), 2383–2388. doi:10.1016/j.nimb.2011.02.059

Dioguardi, G., 2010. *Network Enterprises: The evolution of organizational models from guilds to assembly lines to inovation clusters*. Springer, New York.

Dodwell, C.R., 1986. *The various arts: de diversis artibus by Theophilus, translated from the Latin with introduction and notes by C. R. Dodwell*. Clarendon Press, Oxford.

Drees, L.R., Wilding, L.P., Smeck, N.E., Senkayi, A.L., 1989. Silica in Soils: Quartz and Disordered Silica Polymorphs, in: Dixon, J.B., Weed, S.B. (Eds.), *Minerals in Soil Environments*. Soil Science Society of America, Madison, WI, 35–153.

Drobner, U., Tyler, G., 1998. Conditions controlling relative uptake of potassium and rubidium by plants from soils. *Plant Soil* 201(2), 285–293. doi:10.1023/A:1004319803952

Duby, G., 1981. *The Age of Cathedrals: Art and Society, 980-1420*. University of Chicago Press, Chicago.

Dungworth, D., 2014. *Oxburgh Hall, Oxborough, Norfolk: Portable XRF analysis of some window glass from the gatehouse*, Research Report Series. English Heritage.

Dungworth, D., 2012a. Historic windows: Investigation of composition groups with nondestructive pXRF. *Glas. Technol. Eur. J. Glas. Sci. Technol. Part A* 53(5), 192–197.

Dungworth, D., 2012b. Historic Window Glass: The Use of Chemical Analysis to Date Manufacture. *J. Archit. Conserv.* 18(1), 7–25. doi:10.1080/13556207.2012.10785101

Dungworth, D., 2011a. The value of historic window glass. *Hist. Environ.* 2(1), 21–48. doi:10.1179/175675011X12943261434567

Dungworth, D., 2011b. *Kenwood House, Uxbridge, London: An investigation of the Music Room window glass*, Research Report Series. English Heritage.

Dungworth, D., 2009. Innovations in the 17th-century glass industry: the introduction of kelp (seaweed) ash in Britain, in: Lagabrielle, S., Philippe, M. (Eds.), *Les Innovations Verrières et Leur Devenir (Paris)*. 119–123.

Dungworth, D., Clark, C., 2004. *SEM-EDS analysis of Wealden glass*, Centre for Archaeology Report, Centre for Archaeology Report. English Heritage, Portsmouth.

Dungworth, D., Cooke, J., Cookie, R., Jaques, R., Martlew, D., 2011. St Michael's and All Angels Church, Thornhill, Dewsbury, West Yorkshire: Scientific examination of stained window glass., Research Department Report Series. English Heritage, Portsmouth.

Dungworth, D., Degryse, P., Schneider, J., 2009. Kelp in historic glass: the application of strontium isotope analysis, in: *Isotopes in Vitreaous Materials*. 113–130.

Dungworth, D., Girbal, B., 2011. Walmer Castle, Deal, Kent: Analysis of the glass. Technology report, Research Department Report. English Heritage, Portsmouth.

Dungworth, D., Harrison, S., 2011. Belsay Castle, Belsay, Northumberland: Scientific analysis and historic interpretation of decorated window glass by Henry Gyles of York, Research Department Report Series. English Heritage.

Durán, A., Fernández Navarro, J.M., García Solé, J., Agulló-López, F., 1984. Study of the colouring process in copper ruby glasses by optical and EPR spectroscopy. *J. Mater. Sci.* 19(5), 1468–1475. doi:10.1007/BF00563041

Epstein, S.R., 2009. *An Economic and Social History of Later Medieval Europe, 1000 - 1500*. Cambridge University Press, Cambridge:

Epstein, S.R., 2008. Craft guilds in the pre-modern economy: a discussion. *Econ. Hist. Rev.* 61(1), 155–174. doi:10.1111/j.1468-0289.2007.00411.x

Epstein, S.R., 2008. Craft guilds, apprenticeship, and technological change in pre-industrial Europe. *Guilds, Innov. Eur. Econ. 1400-1800* 52–80. doi:10.1017/CBO9780511496738.003

Epstein, S.R., 1998. Craft Guilds, Apprenticeship, and Technological Change in Preindustrial Europe. *J. Econ. Hist.* 58(3), 684–713.

Epstein, S.R., Prak, M., 2008. *Guilds, Innovation, and the European Economy, 1400-1800*.

Farges, F., Etcheverry, M.-P., Scheidegger, A., Grolimund, D., 2006. Speciation and weathering of copper in "'copper red ruby"' medieval flashed glasses from the Tours cathedral (XIII century). *Appl. Geochemistry* 21, 1715–1731. doi:10.1016/j.apgeochem.2006.07.008

Ferguson, J.R., 2012. X-Ray fluorescence of obsidian: approaches to calibration and the analysis of small samples, in: Shugar, A.N., Mass, J.L. (Eds.), *Handheld XRF for Art and Archaeology*, Studies in Archaeological Sciences. Leuven University Press, Leuven, Belgium, 401–422.

Fernández-Navarro, J.-M., Villegas, M.-Á., 2013. What is Glass? An Introduction to the Physics and Chemistry of Silicate Glasses, in: Janssens, K. (Ed.), *Modern Methods for Analysing Archaeological and Historical Glass*. John Wiley & Sons, Chichester, UK, 1–22.

Ferrand, J., Loisel, C., Trcera, N., Hullebusch, E.D. Van, Bousta, F., Pallot-frossard, I., 2015. Browning Phenomenon of Medieval Stained Glass Windows. *Anal. Chem.* 87, 3662–3669. doi:10.1021/ac504193z

Foy, D., 1985. Essai de typologie des verres medievaux d'apres les fouilles provencales et languedociennes. *J. Glass Stud.* 27, 18–71.

Frahm, E., 2014. Characterizing obsidian sources with portable XRF: Accuracy, reproducibility, and field relationships in a case study from Armenia. *J. Archaeol. Sci.* 49(1), 105–125. doi:10.1016/j.jas.2014.05.003

Frahm, E., 2013a. Validity of "off-the-shelf" handheld portable XRF for sourcing Near Eastern obsidian chip debris. *J. Archaeol. Sci.* 40(2), 1080–1092. doi:10.1016/j.jas.2012.06.038

Frahm, E., 2013b. Is obsidian sourcing about geochemistry or archaeology? A reply to Speakman and Shackley. *J. Archaeol. Sci.* 40(2), 1444–1448. doi:10.1016/j.jas.2012.10.001

Frahm, E., Doonan, R., Kilikoglou, V., 2014. Handheld Portable X-Ray Fluorescence of Aegean Obsidians. *Archaeometry* 56(2), 228–260. doi:10.1111/arcm.12012

Frahm, E., Doonan, R.C.P., 2013. The technological versus methodological revolution of portable XRF in archaeology. *J. Archaeol. Sci.* 40(2), 1425–1434. doi:10.1016/j.jas.2012.10.013

Freestone, I.C., 1992. Theophilus and the composition of medieval glass, in: Vandiver, P.B. (Ed.), *Materials Issues in Art and Archaeology III: Symposium Held April 27-May 1, 1992, San Francisco, California, U.S.A.* Materials Research Society, 739–745.

Freestone, I.C., Gorin-Rosen, M.Y., Hughes, M.J., 2000. Primary Glass from Israel and the Production of Glass in Late Antiquity and the Early Islamic Period, in: *La Route Du Verre. Ateliers Primaires et Secondaires Du Second Millénaire Av. J.-C. Au Moyen Âge. Colloque Organisé En 1989 Par*

l'Association Française Pour l'Archéologie Du Verre (AFAV) Lyon : Maison de l'Orient et de La Méditerranée Jean Pouilloux. 65–83.

Freestone, I.C., Gutjahr, M., Kunicki-Goldfinger, J.J., McDonald, I., Pike, A., 2015a. Composition, technology and origin of the glass from the workshop at 35 Basinghall Street, in: Wardle, A. (Ed.), *Glass Working on the Margins of Roman London*. Museum of London Archaeology, London, 75–90.

Freestone, I.C., Jackson-Tal, R.E., Taxel, I., Tal, O., 2015b. Glass production at an Early Islamic workshop in Tel Aviv. *J. Archaeol. Sci.* 62, 45–54. doi:10.1016/j.jas.2015.07.003

Freestone, I.C., Kunicki-Goldfinger, J.J., Gilderdale-Scott, H., Ayers, T., 2010. Multidisciplinary Investigation of the Windows of John Thornton, Focusing on the Great East Window of York Minster, in: Shepherd, M.B., Pilosi, L., Strobl, S. (Eds.), *The Art of Collaboration: Stained-Glass Conservation in the Twenty-First Century*. The International Committee of the Corpus Vitrearum for the Conservation of Stained Glass, London, 151–158.

Freestone, I.C., Leslie, K.A., Thirlwall, M.F., Gorin-Rosen, Y., 2003. Strontium isotopes in the investigation of early glass production: Byzantine and Early Islamic glass from the Near East. *Archaeometry* 45, 19–32.

Freestone, I.C., Ponting, M., Hughes, M.J., 2002. The origins of Byzantine glass from Maroni Petrera, Cyprus. *Archaeometry* 44(s), 257–272.

Freestone, I.C., Price, J., Cartwright, C.R., 2009. The Batch: Its Recognition and Significance, in: Janssens, K., Degryse, P., Cosyns, P., Caen, L., Van't dack, L. (Eds.), *Annales Du 17e Congrès de l'Association Internationale Pour l'Histoire Du Verre, Anvers 2006.* AIHV, Corning, NY, 130–135.

Freestone, I.C., Stapleton, C.P., Rigby, V., 2003. The production of red glass and enamel in the Late Iron Age, Roman and Byzantine periods. *Through a Glas. Bright. Stud. Byzantine Mediev. Art Archaeol. Present. to David Buckt.* (November 2015), 142–154.

Freestone, I.C., Wolf, S., Thirlwall, M.F., 2005. The production of HIMT glass: elemental and isotopic evidence, in: *Annales Du 16e Congrès de l'Association Internationale Pour l'Histoire Du Verre, Nottingham UK 2003*. 153–157.

French, T., 2003. *York Minster: The Great East Window*, Corpus Vitrearum Medii Aevi: Great Britain, Summary Catalogue 2. Oxford University Press, Oxford.

French, T., 1989. John Thornton's Monogram in York Minster. *J. Stain. Glas.* XIX(1).

French, T., 1987. The Glazing of the St William Window in York Minster. *J. Br. Archaeol. Assoc.* 140(1), 175–181. doi:10.1179/jba.1987.140.1.175

Fricker, M.B., Günther, D., 2016. Instrumentation, Fundamentals, and Application of Laser Ablation-Inductively Coupled Plasma-Mass Spectrometry, in:

Recent Advances in Laser Ablation ICP-MS for Archaeology. 1–19. doi:10.1007/978-3-662-49894-1

Frodl-Kraft, E., 1985. Problems of Gothic Workshop Practices in Light of a Group of Mid-Fourteenth-Century Austrian Stained-Glass Panels, in: *Corpus VItrearum: Selected Papers from the XIth International Colloquium of the Corpus Vitrearum, New York, 1-6 June 1982*. The Metropolitan Museum of Art, New York, 107–123.

Gabler, C. V, 2017. Craft Production and Exchange in the Pre-Hispanic Andes: LA-ICP-MS and pXRF Analyses of Tiwanaku Ceramics. Georgia State University.

Gamble, J., 2001. Modelling the Invisible: The pedagogy of craft apprenticeship. *Stud. Contin. Educ.* 23(2), 185–200. doi:10.1080/01580370120101957

Garcia-Vallès, M., Gimeno-Torrente, D., Martínez-Manent, S., Fernández-Turiel, J.L., 2003. Medieval stained glass in a Mediterranean climate: Typology, weathering and glass decay, and associated biomineralization processes and products. *Am. Mineral.* 88, 1996–2006.

Geilmann, W., Brückbauer, T., 1954. Bieträge zur Kenntnis alter Gläser II. Der Mangangehalt alter Gläser. *Glas. Berichte* 27(456).

Gent, T., 1762. *The Most Delectable, Scriptural and Pious History of the Famous and Magnificent Great Eastern Window (According to Beautiful Portraiture) in St Peter's Cathedral, York*. York.

Gent, T., 1730. *The Antient and Modern History of the Famous City of York*. York.

Gentaz, L., Lombardo, T., Chabas, A., Loisel, C., Neff, D., Verney-Carron, A., 2016. Role of secondary phases in the scaling of stained glass windows exposed to rain. *Corros. Sci.* (April). doi:10.1016/j.corsci.2016.04.005

Gentaz, L., Lombardo, T., Loisel, C., Chabas, A., Vallotto, M., 2011. Early stage of weathering of medieval-like potash – lime model glass: evaluation of key factors. *Environ. Sci. Pollut. Res.* 18, 291–300. doi:10.1007/s11356-010-0370-7

Gerth, K., Wedepohl, K.H., Heide, K., 1998. Experimental melts to explore the technique of medieval wood ash glass production and the chlorine content of medieval glass types. *Chemie der Erde* 58, 219–232.

Giannini, R., Freestone, I.C., Shortland, A.J., 2017. European cobalt sources identified in the production of Chinese famille rose porcelain. *J. Archaeol. Sci.* 80, 27–36. doi:10.1016/j.jas.2017.01.011

Giauque, R.D., Asaro, F., Stross, F.H., Hester, T.R., 1993. High-precision non-destructive x-ray fluorescence method applicable to establishing the provenance of obsidian artifacts. *X-Ray Spectrom.* 22(1), 44–53. doi:10.1002/xrs.1300220111

Gimeno, D., Garcia-Valles, M., Fernandez-Turiel, J.L., Bazzocchi, F., Aulinas, M., Pugès, M., Tarozzi, C., Riccardi, M.P., Basso, El., Fortina, C., Mendera, M., Messiga, B., 2008. From Siena to Barcelona: Deciphering colour recipes of Na-rich Mediterranean stained glass windows at the XIII-XIV century transition. *J. Cult. Herit.* 9, 10–15. doi:10.1016/j.culher.2008.08.001

Gimpel, J., 1984. *The Cathedral Builders*. Evergreen Books, New York.

Girbal, B., Dungworth, D., 2011. Ightham Mote, Ightham, Kent: Portable XRF Analysis of the Window Glass, Archaeological Science, Research Department Report Series. English Heritage, Portsmouth.

Godfrey, E., 1975. *The Development of English Glassmaking 1560-1640*. University of North Carolina Press, Chapel Hilll, NC.

Goodale, N., Bailey, D.G., Jones, G.T., Prescott, C., Scholz, E., Stagliano, N., Lewis, C., 2012. PXRF: A study of inter-instrument performance. *J. Archaeol. Sci.* 39(4), 875–883. doi:10.1016/j.jas.2011.10.014

Gooder, P., 2014. The Apocalypse in the New Testament and the Church Today, in: Brown, S., Hartshorne, P. (Eds.), *Apocalypse: The Great East Window of York Minster*. Third Millennium Publishing LTD, 59–67.

Gottfried, R.S., 2010. *Black Death: Natural and Human Disaster in Medieval Europe*. The Free Press, New York.

Grant, L., 1998. *Abbot Suger of St-Denis: Church and State in early Twelfth-Century France*. Longman, New York, NY.

Gratuze, B., 2016. Analysis of Vitreous Archaeological Materials by LA-ICP-MS, in: Dussubieux, L., Golitko, M., Gratuze, B. (Eds.), *Recent Advances in Laser Ablation ICP-MS for Archaeology*, Natural Science in Archaeology. Springer, Berlin, 137–139.

Gratuze, B., 2013. Provenance Analysis of Glass Artefacts, in: Janssens, K. (Ed.), *Modern Methods for Analysing Archaeological and Historical Glass*. John Wiley & Sons, Chichester, UK.

Gratuze, B., 1999. Obsidian characterization by laser ablation ICP-MS and its application to prehistoric trade in the Mediterranean and the Near East: Sources and distribution of obsidian within the Aegean and Anatolia. *J. Archaeol. Sci.* 26(8), 869–881. doi:10.1006/jasc.1999.0459

Gratuze, B., Giovagnoli, A., Barrandon, J.N., Telouk, P., Imbert, J., 1993. Apport de la méthode ICP-MS couplée à l'ablation laser pour la caractérisation des archéomatériaux. *Rev. d'Archéométrie* 17, 89–104. doi:10.3406/arsci.1993.908

Gratuze, B., Soulier, I., Barrandon, J.-N., Foy, D., 1995. The origin of cobalt blue pigment in French glass from the thirteenth to the eighteenth centuries, in: Hook, D.R., Gaimster, D.R.M. (Eds.), *Trade and Discovery: Scientific Study*

of Artefacts from Post-Medieval Europe and Beyond, British Museum Occasional Paper. British Museum, London, 123–133.

Gratuze, B., Soulier, I., Barrandon, J.-N., Foy, D., 1992. De l'origine du cobalt dans les verres. *Rev. d'archéométrie* 16, 97–108. doi:10.3406/arsci.1992.895

Gratuze, B., Soulier, I., Blet, M., Vallauri, L., 1996. De l'origine du cobalt: du verre à la céramique. *Rev. d'archéométrie* (20), 77–94. doi:10.3406/arsci.1996.939

Grave, P., Attenbrow, V., Sutherland, L., Pogson, R., Forster, N., 2012. Non-destructive pXRF of mafic stone tools. *J. Archaeol. Sci.* 39(6), 1674–1686. doi:10.1016/j.jas.2011.11.011

Grodecki, L., 1948. A Stained Glass Atelier of the Thirteenth Century: A Study of Windows in the Cathedrals of Bourges, Chartres and Poitiers. *J. Warburg Courtauld Inst.* 11, 87–111.

Hall, G.E.M., Bonham-Carter, G.F., Buchar, A., 2014. Evaluation of portable X-ray fluorescence (pXRF) in exploration and mining: Phase 1, control reference materials. *Geochemistry Explor. Environ. Anal.* 14, 99–123. doi:10.1144/geochem2013-241

Harrison, F., 1927. *The Painted Glass of York: An Account of the Medieval Glass of the Minster and the Parish Churches*. Society for promoting Christian knowledge, London.

Hartmann, G., 1994. Late medieval glass manufacture in the Eichsfeld region (Thuringia, Germany). *Chemie der Erde* 54, 103–128.

Harvey, J., 1972. *The Medieval Architect*. Wayland Publishers, London.

Haskins, C.T., 1927. *The Renaissance of the Twelfth Century*. Harvard University Press, Cambridge, MA.

Hawthorne, J.G., Smith, C.S., 1979. Introduction, in: *On Divers Arts: The Foremost Medieval Treatise on Painting, Glassmaking and Metalwork.* xv–xxxv.

Heaton, N., 1947. The Origin and Use of Silver Stain. *J. Br. Soc. Master Glas.* 10(1), 9–16.

Heginbotham, A., Bezur, A., Bouchard, M., Davis, J.M., Eremin, K., Frantz, J.H., Glinsman, L., Hayek, L., Hook, D., Kantarelou, V., Karydas, G., Lee, L., Mass, J., Matsen, C., Mccarthy, B., 2011. An evaluation of inter-laboratory reproducibility for quantitative XRF of historic copper alloys, in: Mardikian, P., Chemello, C., Watters, C., Hull, P. (Eds.), *Metal 2010: International Conference on Metal Conservation*. Clemon University, Clemson, SC, 244–255.

Heginbotham, A., Solé, V.A., 2017. CHARMed PyMca Part I: A Protocol for Improved Inter-laboratory Reproducibility in the Quantitative ED-XRF Analysis of Copper Alloys. *Archaeometry*. doi:10.1111/arcm.12282

Henderson, J., 2013. *Ancient Glass: An Interdisciplinary Exploration*. Cambridge University Press, New York, NY.

Hoover, H.C., Hoover, L.H., 1950. *Georgius Agricola: De Re Metallica, Translated from the First Latin Edition of 1556*. Dover Publications, New York.

Hulme, E.W., 1894. English Glass-making in the Sixteenth and Seventeeth Centuries. *Antiq.* 30, 210–214.

Hunault, M.O.J.Y., Loisel, C., Bauchau, F., Lemasson, Q., Pacheco, C., Moignard, B., Boulanger, K., Hérold, M., Calas, G., Pallot-Frossard, I., 2017a. Non-destructive redox quantification reveals glassmaking of rare French Gothic stained glasses. *Anal. Chem.* 89, 6277–6284.

Hunault, M.O.J.Y., Vinel, V., Cormier, L., Calas, G., 2017b. Thermodynamic insight into the evolution of medieval glassworking properties. *J. Am. Ceram. Soc.* 2017(00), 1–5. doi:10.1111/jace.14819

Hunt, A., Thomas, D.H., Speakman, R., 2014. Characterization of Archaeological Copper Alloys by pXRF, in: *Poster Presented at the 80th Annual Meeting of the Society for American Archaeology*.

Ingold, T., 2001. Beyond art and archaeology: the anthropology of skill, in: Schiffer, M.B. (Ed.), *Anthropological Perspectives on Technology*. University of New Mexico Press, Albuquerque, 17–31.

IRR, 2017. *Ionising Radiations Regulations 2017 Sch 3, Reg 2(1) and 12*.

Jackson, C.M., Booth, C.A., Smedley, J.W., 2005. Glass by design? Raw materials, recipes and compositional data. *Archaeometry* 47(4), 781–795.

Jackson, C.M., Smedley, J.W., 2008a. Theophilus and the Use of Beech Ash as a Glassmaking Alkali, in: Martinón-Torres, M., Rehren, T. (Eds.), *Archaeology, History and Science: Integrating Approaches to Ancient Materials*. Left Coast Press, Walnut Creek, CA, 117–130.

Jackson, C.M., Smedley, J.W., 2008b. Medieval and post-medieval glass technology: Seasonal changes in the composition of bracken ashes from different habitats through a growing season. *Glas. Technol. Eur. J. Glas. Sci. Technol. Part A* 49(5), 240–245.

Jackson, C.M., Smedley, J.W., 2004. Medieval and post-medieval glass technology: Melting characteristics of some glasses melted from vegetable ash and sand mixtures. *Glas. Technol. Eur. J. Glas. Sci. Technol. Part A* 45(1), 36–42.

Janssens, K., Cagno, S., De Raedt, I., Degryse, P., 2013. Transfer of Glass Manufacturing Technology in the Sixteenth and Seventeenth Centuries from Southern to Northern Europe: Using Trace Element Patterns to Reveal the Spread from Venice via Antwerp to London, in: Janssens, K. (Ed.), *Modern Methods for Analysing Archaeological and Historical Glass*. John Wiley & Sons, Chichester, UK.

Janssens, K., Van der Snickt, G., Vanmeert, F., Legrand, S., Nuyts, G., Alfeld, M., Monico, L., Anaf, W., De Nolf, W., Vermeulen, M., Verbeeck, J., De Wael, K., 2016. Non-Invasive and Non-Destructive Examination of Artistic Pigments, Paints, and Paintings by Means of X-Ray Methods. *Top. Curr. Chem.* 374(6), 1–52. doi:10.1007/978-3-319-52804-5

Jembrih-Simbürger, D., Neelmeijer, C., Schalm, O., Fredrickx, P., Schreiner, M.R., De Vis, K., Mäder, M., Schryvers, D., Caen, J., 2002. The colour of silver stained glass-analytical investigations carried out with XRF, SEM/EDX, TEM, and IBA. *J. Anal. At. Spectrom.* 17, 321–328. doi:10.1039/b111024c

Jenkins, R., 1999. *X-Ray Fluorescence Spectrometry*, 2nd ed, Chemical Analysis: A Series of Monographs on Analytical Chemistry and its Applications. John Wiley & Sons, Inc., Honoken, NJ.

Jochum, K.P., Weis, U., Stoll, B., Kuzmin, D., Yang, Q., Raczek, I., Jacob, D.E., Stracke, A., Birbaum, K., Frick, D.A., Günther, D., Enzweiler, J., 2011. Determination of reference values for NIST SRM 610-617 glasses following ISO guidelines. *Geostand. Geoanalytical Res.* 35(4), 397–429. doi:10.1111/j.1751-908X.2011.00120.x

Jones, A., 2004. Archaeometry and materiality: Materials-based analysis in theory and practice. *Archaeometry* 46(3), 327–338.

Kaiser, B., Shugar, A.N., 2012. Glass analysis utilizing handheld X-ray fluorescence, in: Shugar, A.N., Mass, J.L. (Eds.), *Handheld XRF for Art and Archaeology*, Studies in Archaeological Sciences. Leuven University Press, Leuven, Belgium, 449–470.

Kamp, K.A., 2001. Where Have All the Children Gone?: The Archaeology of Childhood. *J. Archaeol. Method Theory* 8(1), 1–34. doi:10.1023/A

Kamp, K.A., Timmerman, N., Lind, G., Graybill, J., Natowsky, I., 1999. Discovering Childhood: Using Fingerprints to Find Children in the Archaeological Record. *Am. Antiq.* 64(2), 309–315. doi:10.2307/2694281

Katz, A., Sass, E., Starinsky, A., Holland, H.D., 1972. Strontium behavior in the aragonite-calcite transformation: An experimental study at 40-98??C. *Geochim. Cosmochim. Acta* 36(4), 481–496. doi:10.1016/0016-7037(72)90037-3

Kenyon, G.H., 1967. *The Glass Industry of the Weald*. Leicester University Press.

Kermode, J.I., 2000. Northern towns, in: Palliser, D.M. (Ed.), *The Cambridge Urban History of Britain, Volume 2: 600-1540*. Cambridge University Press, Cambridge, 657–679.

Kermode, J.I., 1998. *Medieval Merchants: York, Beverley and Hull in the Later Middle Ages*. Cambridge University Press, Cambridge.

Kermode, J.I., 1987. Merchants, Overseas Trade, and Urban Decline: York, Beverley, and Hull c. 1380--1500. *North. Hist.* 23(1), 51–73. doi:10.1179/007817287790176082

Kinsman, D.J.J., 1969. Interpretation of Sr+2 Concentrations in Carbonate Minerals and Rocks. *J. Sediment. Res.* 39(2), 486–508.

Knoop, D., Jones, G.P., 1932. Masons and Apprenticeships in Medieval England. *Econ. Hist. Rev.* 3(3), 346–366.

Knowles, J.A., 1936. *Essays in the History of the York School of Glass-Painting*. Macmillan, New York.

Knowles, J.A., 1927. The History of Copper Ruby Glass. *Trans. Newcom. Soc. Study Hist. Eng. Technol.* 6(November), 66–74. doi:10.1179/tns.1925.003

Knowles, J.A., 1922. The periodic plagues of the second half of the fourteenth century and their effects on the art of glass-painting. *Archaeol. J.* 79, 343–352.

Knowles, J.A., 1920. John Thornton of Coventry and the Great East Window in York Minster. *Notes & Queries* 140, 481–483.

Koleini, F., Colomban, P., Antonites, A., Pikirayi, I., 2017. Raman and XRF classification of Asian and European glass beads recovered at Mutamba, a southern African Middle Iron Age site. *J. Archaeol. Sci. Reports* 13(November 2016), 333–340. doi:10.1016/j.jasrep.2017.04.004

Kunicki-Goldfinger, J.J., Freestone, I.C., Gilderdale-Scott, H., Ayers, T., McDonald, I., 2014a. Problematyka badań witraży średniowiecznych. *Archeol. Pol.* 59(1–2), 47–78.

Kunicki-Goldfinger, J.J., Freestone, I.C., McDonald, I., Hobot, J.A., Gilderdale-Scott, H., Ayers, T., 2014b. Technology, production and chronology of red window glass in the medieval period - rediscovery of a lost technology. *J. Archaeol. Sci.* 41, 89–105. doi:10.1016/j.jas.2013.07.029

Kunicki-Goldfinger, J.J., Keirzek, J., Freestone, I.C., Małożewska-Bućko, B., Nawrolska, G., 2009. The composition of window glass from the cesspits in the old town in Elbląg, Poland, in: Ignatiadou, D., Antonaras, A. (Eds.), *Annales Du 18e Congrès de l'Association Internationale Pour l'Histoire Du Verre, Thessaloniki 2009*. ZITI Publishing, Thessaloniki, 395–400.

Kunicki-Goldfinger, J.J., Mester, E., Freestone, I.C., 2013. The chemical composition of glass from the Hungarian glasshouses and glass utilized in

Hungary from the 14th century to the 17th century, in: Michalik, J., Smułek, W., Godlewska-Para, E. (Eds.), *Annual Report 2012*. Institute of Nuclear Chemistry and Technology, Warszawa, 73–75.

Kunicki-Goldfinger, J.J., Pańczyk, E., Dierżanowski, P., Waliś, L., 2008. Trace element characterization of medieval and post-medieval glass objects by means of INAA and EPMA. *J. Radioanal. Nucl. Chem.* 278(2), 307–311. doi:10.1007/s10967-008-0507-z

Lagabrielle, S., Velde, B., 2005. Evolution of French stained glass compositions during the Middle Ages - Analyses and observations made on the Cluny Collection, in: *Annales Du 16e Congrès de l'Association Internationale Pour l'Histoire Du Verre, Nottingham UK 2003*. AIHV, 341–346.

Leroi-Gourhan, A.A., 1964. *Le Geste et la Parole I: Technique et Language*. Michel Albin, Paris.

Levy, P.S., Lemeshow, S., 2008. *Sampling of Populations: Methods and Applications*, 4th ed. John Wiley & Sons, Inc., Hoboken, NJ. doi:10.1002/9780470374597

Li, X.J., Bevan, A., Martinón-Torres, M., Rehren, T., Cao, W., Xia, Y., Zhao, K., 2015. Crossbows and imperial craft organisation: the bronze triggers of China's Terracotta Army. *Antiquity* 88(339), 126–140. doi:10.1017/S0003598X00050262

Li, Y.T., 2007. Co-craft and multicraft: Section-mold casting and the organization of craft production at the Shang capital of Anyang, in: Shimada, I. (Ed.), *Craft Production in Complex Societies: Multicraft and Producer Perspectives*. University of Utah Press, Salt Lake City, 184–223.

Lillich, M.P., 1985. Gothic Glaziers: Monks, Jews, Taxpayers, Bretons, Women. *J. Glas.* 27(1985), 72–92.

Linford, P., Welch, C., 2004. Archaeomagnetic analysis of glassmaking sites at Bagot's Park in Staffordshire, England. *Phys. Earth Planet. Inter.* 147(2–3 SPEC.ISS.), 209–221. doi:10.1016/j.pepi.2004.07.002

Linford, P., Welch, C.M., 2002. Bagot's Park, Abbots Bromley, Staffordshire, III: Archaeomagnetic Dating Report [Unpublished Report].

Lis, C., Soly, H., 1994. "An Irresistible Phalanx": Journeymen Associations in Western Europe, 1300–1800. *Int. Rev. Soc. Hist.* 39(S2), 11–52. doi:10.1017/S0020859000112921

Lombardo, T., Gentaz, L., Verney-Carron, A., Chabas, A., Loisel, C., Neff, D., Leroy, E., 2013. Characterisation of complex alteration layers in medieval glasses. *Corros. Sci.* 72, 10–19. doi:10.1016/j.corsci.2013.02.004

Lombardo, T., Loisel, C., Gentaz, L., Chabas, A., Verita, M., Loisel, C., Gentaz, L., Chabas, A., Verita, M., Lombardo, T., Loisel, C., Gentaz, L., Chabas, A., Verita, M., 2010. Long term assessment of atmospheric decay of stained

glass windows. *Corros. Eng. Sci. Technol.* 45(5), 420–424. doi:10.1179/147842210X12710800383800

Louw, H., 1991. Window-Glass Making in Britain c. 1660-c. 1860 and its Architectural Impact. *Constr. Histroy* 7, 48–68.

Machado, A., Wolf, S., Alves, L.C., Katona-serneels, I., Serneels, V., 2017. Swiss Stained-Glass Panels: An Analytical Study. *Microsc. Microanal.* doi:10.1017/S1431927617000629

Maitte, C., 2014. The Cities of Glass: Privileges and Innovations in Early Modern Europe, in: Davids, K., De Munck, B. (Eds.), *Innovation and Creativity in Late Medieval and Early Modern European Cities*. Ashgate Publishing, Farnham, 35–53. doi:10.1590/S1516-18462008000300012

Marchesi, B., Negri, E., Messiga, B., Riccardi, M.P., 2006. Medieval stained glass windows from Pavia Carthusian monastery (northern Italy). *Geomaterials Cult. Herit.* 257, 217–227. doi:10.1144/GSL.SP.2006.257.01.17

Marks, R., 1993. *Stained Glass in England during the Middle Ages*. Routledge, London.

Marks, R., 1991. Window Glass, in: Blair, J., Ramsay, N. (Eds.), *English Medieval Industries: Craftsmen, Techniques, Products*. Hambledon Press, London, 265–294.

Martinón-Torres, M., Li, X.J., Bevan, A., Xia, Y., Zhao, K., Rehren, T., 2012. Forty Thousand Arms for a Single Emperor: From Chemical Data to the Labor Organization Behind the Bronze Arrows of the Terracotta Army. *J. Archaeol. Method Theory* 21(3), 534–562. doi:10.1007/s10816-012-9158-z

Martinón-Torres, M., Uribe-Villegas, M.A., 2015. The prehistoric individual, connoisseurship and archaeological science: the Muisca goldwork of Colombia. *J. Archaeol. Sci.* 63. doi:10.1016/j.jas.2015.08.014

Mecking, O., 2013. Medieval Lead Glass in Central Europe. *Archaeometry* 55(4), 640–662. doi:10.1111/j.1475-4754.2012.00697.x

Meek, A., 2011. The chemical and isotopic analysis of English forest glass.

Meek, A., Henderson, J., Evans, J., 2012. Isotope analysis of English forest glass from the Weald and Staffordshire. *J. Anal. At. Spectrom.* 27(5), 786. doi:10.1039/c2ja10364h

Meiwes, K.J., Beese, F., 1988. Ergebnisse der Untersuchung des Stoffhaushaltes eines Buchenwaldökosystems auf Kalkgestein. *Berichte Forschungszentrum Waldökosysteme* B9, 1–142.

Melcher, M., Schreiner, M.R., 2006. Leaching studies on naturally weathered potash-lime-silica glasses. *J. Non. Cryst. Solids* 352(5), 368–379. doi:10.1016/j.jnoncrysol.2006.01.017

Melcher, M., Schreiner, M.R., 2005. Evaluation procedure for leaching studies on naturally weathered potash-lime-silica glasses with medieval composition by scanning electron microscopy. *J. Non. Cryst. Solids* 351(14–15), 1210–1225. doi:10.1016/j.jnoncrysol.2005.02.020

Melcher, M., Wiesinger, R., Schreiner, M.R., 2010. Degradation of glass artifacts: Application of modern surface analytical techniques. *Acc. Chem. Res.* 43(6), 916–926. doi:10.1021/ar9002009

Merrifield, M.P., 1967. *Medieval and Renaissance Treatises on the Arts of Painting: Original Texts with English Translations*. Dover Publications, New York.

Milić, M., 2014. PXRF characterisation of obsidian from central Anatolia, the Aegean and central Europe. *J. Archaeol. Sci.* 41, 285–296. doi:10.1016/j.jas.2013.08.002

Milner-White, E., 1950. The Restoration of the East Window of York Minster. *Antiq. J.* 30(3–4), 180–184. doi:10.1017/S0003581500087850

Minar, C.J., Crown, P.L., 2001. Learning and craft production: An introduction. *J. Anthropol. Res.* 57(4), 369–380. doi:10.2307/3631351

Molina, G., Murcia, S., Molera, J., Roldan, C., Crespo, D., Pradell, T., 2013. Color and dichroism of silver-stained glasses. *J. Nanoparticle Res.* 15(1932), 1–13. doi:10.1007/s11051-013-1932-7

Moretti, C., Hreglich, S., 2013. Raw Materials, Recipes and Procedures Used for Glass Making, in: Janssens, K. (Ed.), *Modern Methods for Analysing Archaeological and Historical Glass*. John Wiley & Sons, Chichester, UK, 23–47.

Morey, G.W., Kracek, F.C., Bowen, N.L., 1930. The ternary system K2O-CaO-SiO2. *J. Soc. Glas. Technol.* 14, 149–187.

Müller, W., Bochynek, G., 1989. Possibilities of approximate dating of medieval glasses using their chemical composition, in: Mazurin, O. V. (Ed.), *Proceedings of the XVth International Congress on Glass, Leningrad*. 47–52.

Mysen, B.O., 1988. Structure and properties of silicate melts, in: *Developments in Geochemistry, Vol. 4*. Elsevier Science, Amsterdam.

Neillands, R., 2001. *The Hundred Years War*. Psychology Press.

Newton, R.G., 1982. *The deterioration and conservation of painted glass: A critical bibliography*, Corpus Vitrearum Medii Aevi Great Britain Occasional Papers II. Oxford University Press, Oxford.

Newton, R.G., 1980. Recent views on ancient glasses. *Glas. Technol.* 21(4), 173–183.

Newton, R.G., 1978. Colouring Agents used by Medieval Glassmakers. *Glas. Technol.* 19(3), 59–60.

Newton, R.G., 1977. Simulated medieval glasses. *CV News Lett.* 25(April), 3–5.

Newton, R.G., 1976. Chemical Analyses of Medieval Window Glasses - Part 1. *Corpus Vitr. Newsl.* 21, 9–16.

Newton, R.G., Davison, S., 1989. *Conservation of glass*. Butterworth & Co., London.

Nightingale, P., 2010. The rise and decline of medieval York: A reassessment. *Past Present* 206(1), 3–42. doi:10.1093/pastj/gtp043

Nørgaard, H.W., 2017. Portable XRF on Prehistoric Bronze Artefacts: Limitations and Use for the Detection of Bronze Age Metal Workshops. *Open Archaeol.* 3(1), 101–122. doi:10.1515/opar-2017-0006

Norton, C., 2005. Sacred Space and Sacred History: The Glazing of the Eastern Arm of York Minster, in: Becksmann, R. (Ed.), *Glasmalerei in Kontext: Bildprogramme Und Raumfunktionen*. Germanisches Nationalmuseum, Nuremberg, 167–80.

Nussbaum, N., 2000. *German Gothic Church Architecture*. Yale University Press, New Haven.

O'Grady, C., Hurst, H., 2011. Lost Walls/Murals Rebuilts: Interdisciplinary Approaches to the Conservation of Preclassic Maya Wall Paintings from San Bartolo, Guatemala, in: Bridgland, J. (Ed.), *ICOM-CC 16th Triennial Preprints - Lisbon, Portugal*. ICOM, 1–10.

Obranovic, D., Barham, D., Hancock, R.G. V, 2005. On the Behaviour of Chlorine in Glass-melting, in: Burke, E., Kars, H. (Eds.), *Proceedings of the 33rd International Symposium on Archaeometry, 22-26 April 2002, Amsterdam*. Vrije Universiteit Amsterdam, Amsterdam, 229–231.

Osborne, J., 1997. *Stained Glass in England*, 2nd ed, History Handbooks. Sutton Publishing, Stroud, Gloucestershire.

Ottaway, P., 2004. *Roman York*. Tempus / The History Press, Stroud.

Ovitt, G., 2013. Technology and science, in: Lindberg, D.C., Shank, M.H. (Eds.), *The Cambridge History of Science Volume 2: Medieval Science*. Cambridge University Press, New York, NY, 630–644.

Pactat, I., Guérit, M., Simon, L., Gratuze, B., Raux, S., Aunay, C., 2017. Evolution of glass recipes during the early Middle Ages in France: Analytical evidence of multiple solutions adapted to local contexts, in: Wolf, S., de Pury-Gysel, A. (Eds.), *Annales Du 20e Congrès de l'Association Internationale Pour l'Histoire Du Verre, Fribourg/Romont 7-11 Septembre 2015*.

Phelps, M., Freestone, I.C., Gorin-Rosen, Y., Gratuze, B., 2016. Natron glass production and supply in the late antique and early medieval Near East: The effect of the Byzantine-Islamic transition. *J. Archaeol. Sci.* 75, 57–71. doi:10.1016/j.jas.2016.08.006

Piñar, G., Garcia-Valles, M., Gimeno-Torrente, D., Fernandez-Turiel, J.L., Ettenauer, J., Sterflinger, K., 2013. Microscopic, chemical, and molecular-biological investigation of the decayed medieval stained window glasses of two Catalonian churches. *Int. Biodeterior. Biodegradation* 84, 388–400. doi:10.1016/j.ibiod.2012.02.008

Pollard, A.M., 1979. X-Ray Fluorescence and Surface Studies of Glass, with Application to the Durability of Mediaeval Window Glass. University of York.

Pollard, A.M., Heron, C., 1996. The chemistry and corrosion of archaeological glass, in: Pollard, A.M., Heron, C. (Eds.), *Archaeological Chemistry*. Royal Society of Chemistry, Cambridge, 149–195.

Pollard, M., Batt, C., Stern, B., Young, S.M.M., 2007. *Analytical Chemistry in Archaeology*, Cambridge Manuals in Archaeology. Cambridge University Press, Cambridge.

Postan, M.M., 1987. The Trade of Medieval Europe: the North, in: Postan, M.M., Miller, E. (Eds.), *The Cambridge Economic History of Europe, Volume II: Trade and Industry in the Middle Ages*. Cambridge University Press, Cambridge, 168–305.

Potts, P.J., Ellis, A.T., Kregsamer, P., Marshall, J., Streli, C., Uk, S., 2001. Atomic Spectrometry Update. X-ray fluorescence spectrometry. *J. Anal. At. Spectrom.* 16, 1217–1237. doi:10.1039/b106821k

Potts, P.J., Webb, P.C., Williams-Thorpe, O., 1997a. Investigation of a Correction Procedure for Surface Irregularity Effects Based on Scatter Peak Intensities in the Field Analysis of Geological and Archaeological Rock Samples by Portable X-ray Fluorescence Spectrometry. *J. Anal. At. Spectrom.* 12(July), 769–776.

Potts, P.J., Williams-Thorpe, O., Webb, P.C., 1997b. The bulk analysis of silicate rocks by portable X-ray fluorescence: Effect of sample mineralogy in relation to the size of the excited volume. *Geostand. Newsl.* 21(1), 29–41. doi:10.1111/j.1751-908X.1997.tb00529.x

Pradell, T., Molina, G., Murcia, S., Ibáñez, R., Liu, C., Molera, J., Shortland, A.J., 2016. Materials, Techniques, and Conservation of Historic Stained Glass "Grisailles." *Int. J. Appl. Glas. Sci.* 7(1), 41–58. doi:10.1111/ijag.12125

Prak, M., 2011. Mega-structures of the Middle Ages: the construction of religious buildings in Europe and Asia, c.1000–1500. *J. Glob. Hist.* 6(2011), 381–406. doi:10.1017/S1740022811000386

Prak, M., 2008. Painters, Guilds, and the Art Market during the Dutch Golden Age, in: Epstein, S.R., Prak, M. (Eds.), *Guilds, Innovation and the European Economy, 1400 – 1800*. Cambridge University Press, Cambridge, 143–171. doi:10.1017/CBO9780511496738.006

Price, J., Freestone, I.C., Cartwright, C., 2005. 'All in a day 's work'? The colourless cylindrical glass cups found at Stonea revisited. *Image, Cr. Class. World. Essays honour Donald Bailey Catherine Johns (Monogr. Instrumentum 29)* 165–171.

Raguin, V.C., 1976. Windows of Saint-Germain-lès- Corbeil: A Traveling Glazing Atelier. *Gesta* 15(1), 265–272.

Raine, J., 1859. *The fabric rolls of York Minster*, The Publications of the Surtees Society. George Andrews, London.

Ramsay, N., 1987. Artists, Craftsmen and Design in England, 1200-1400, in: Alexander, J., Binski, P. (Eds.), *Age of Chivalry: Art in Plantagenet England 1200-1400*. Royal Academy of Arts, London.

Rauch, I., 2004. Konservierung und Restaurierung historische Glasmalereien. Eine Einführung in die Problematik [The Conservation and Restoration of Historical Stained and Painted Glass : An Introduction to the Problems]. *Die Denkmalpfl.* 2, 141–150, 154.

Rehren, T., 2000. Rationales in Old World base glass compositions. *J. Archaeol. Sci.* 27(12), 1225–1234. doi:10.1006/jasc.1999.0620

Rehren, T., Freestone, I.C., 2015. Ancient glass: from kaleidoscope to crystal ball. *J. Archaeol. Sci.* 56, 233–241. doi:10.1016/j.jas.2015.02.021

Reith, R., 2008. Circulation of Skilled Labour in Late Medieval and Early Modern Central Europe, in: Epstein, S.R., Prak, M. (Eds.), *Guilds, Innovation and the European Economy, 1400 – 1800*. Cambridge University Press, Cambridge, 114–142. doi:10.1017/CBO9780511496738.005

Reyerson, K.L., 1992. The Adolescent Apprentice/Worker in Medieval Montpellier. *J. Fam. Hist.* 17(4), 353–370.

Richardson, G., 2005. Craft Guilds and Christianity in Late-Medieval England: A Rational-Choice Analysis. *Ration. Soc.* 17(2), 139–189. doi:10.1177/1043463105051631

Richardson, G., 2001. A Tale of Two Theories: Monopolies and Craft Guilds in Medieval England and Modern Imagination. *J. Hist. Econ. Thought* 23(2), 217–242. doi:10.1080/10427710120049237

Rickers, J., 1994. Glazier and Illuminator: The Apocalypse Cycle in the East Window of York Minster and its Sources. *J. Stain. Glas.* XIX(3), 265–79.

Ringwood, A.E., 1955. The principles governing trace-element behaviour during magmatic crystallization: Part II. The role of complex formation. *Geochim. Cosmochim. Acta* 7(5–6), 242–254. doi:10.1016/0016-7037(55)90036-3

Rodrigues, A., Gutierrez-Patricio, S., Zélia Miller, A., Saiz-Jimenez, C., Wiley, R., Nunes, D., Vilarigues, M., Filomena Macedo, M., 2014. Fungal biodeterioration of stained-glass windows. *Int. Biodeterior. Biodegradation* 90, 152–160. doi:10.1016/j.ibiod.2014.03.007

Rouillon, M., Kristensen, L.J., Gore, D.B., 2015. Handheld x-ray fluorescence spectrometers: Radiation exposure risks of matrix-specific measurement scenarios. *Appl. Spectrosc.* 69(7), 815–822. doi:10.1366/14-07809

Roxburgh, M.A., Heeren, S., Huisman, D.J., Van Os, B.J.H., 2018. Non-Destructive Survey of Early Roman Copper-Alloy Brooches using Portable X-ray Fluorescence Spectrometry. *Archaeometry* (May 2017). doi:10.1111/arcm.12414

Royce-Roll, D., 1994. The colors of Romanesque stained glass. *J. Glass Stud.* 36, 71–80.

Salminen, R., Batista, M.J., Bidovec, M., Demetriades, A., 2005. *Geochemical Atlas of Europe. Part 1: Background Information, Methodology and Maps*.

Sanderson, D.C.W., Hunter, J.R., 1981. Composition variability in vegetable ash. *Sci. Archaeol.* 23, 27–30.

Santolaria Tura, A., 2014. *Vitralls sobre taules de vitraller: La taula de girona / Glazing on white-washed tables*. Institut Catal de Recerca en Patrimoni Cultural, Girona.

Sayre, E. V., 1963. The intentional use of antimony and manganese in ancient glasses. *Adv. Glas. Technol. Addit. Pap. from Sixth Int. Congr. Glas. held July 8-14, 1962, Was 2* 263–282.

Schalm, O., Anaf, W., 2016. Laminated altered layers in historical glass: Density variations of silica nanoparticle random packings as explanation for the observed lamellae. *J. Non. Cryst. Solids* 442, 1–16. doi:10.1016/j.jnoncrysol.2016.03.019

Schalm, O., Caluwé, D., Wouters, H., Janssens, K., Verhaeghe, F., Pieters, M., 2004. Chemical composition and deterioration of glass excavated in the 15th–16th century fishermen town of Raversijde (Belgium). *Spectrochim. Acta Part B At. Spectrosc.* 59(10–11), 1647–1656. doi:10.1016/j.sab.2004.07.012

Schalm, O., Janssens, K., Wouters, H., Caluwé, D., 2007. Composition of 12–18th century window glass in Belgium: Non-figurative windows in secular buildings and stained-glass windows in religious buildings. *Spectrochim. Acta - Part B At. Spectrosc.* 62(6–7), 663–668. doi:10.1016/j.sab.2007.03.006

Schibille, N., Freestone, I.C., 2013. Composition, production and procurement of glass at San Vincenzo Al Volturno: an early Medieval monastic complex in Southern Italy. *PLoS One* 8(10), e76479 1-13. doi:10.1371/journal.pone.0076479

Schreiner, M.R., 1984. Verwitterungserscheinungen an mittelalterlichen Glasgemälden österreichischer Provenienz, in: Vendl, A., Pichler, B., Weber, J. (Eds.), *Wiener Berichte Über Naturwissenschaft in Der Kunst*. Hochschule für Angewandte Kunst in Wien, Lehrkanzel für Technische Chemie, Wiener Arbeitskreis für Naturwissenschaft in der Kunst, Vienna, 96–117.

Schreiner, M.R., Woisetschläger, G., Schmitz, I., Wadsak, M., 1999. Characterisation of surface layers formed under natural environmental conditions on medieval stained glass and ancient copper alloys using SEM, SIMS and atomic force microscopy. *J. Anal. At. Spectrom.* 14, 395–403. doi:10.1039/a807305h

Scott, R.A., 2003. *The gothic enterprise: A guide to understanding the medieval cathedral*. University of California Press, London.

Scott, R.B., Braekmans, D., Brems, D., Degryse, P., 2012. Danger! High Voltage! The Application of Handheld X-ray Fluorescence (HH-XRF) to Experimental Glass: Pitfalls and Potentials. *Proc. 39th Int. Symp. Archaeom. Leuven* 268–273.

Sedláčková, H., Rohanová, D., Lesák, B., Šimončičová-Koóšová, P., 2014. Medieval glass from Bratislava (ca 1200–1450) in the context of contemporaneous glass production and trade contacts. *Památky Archeol. CV* 215–264.

Sellers, M., 1918. *The York Mercers and Merchant Adventurers, 1356-1917*, Surtees Society Publications. Andrews, Durham.

Sellers, M., 1912. *York Memorandum Book 1376-1419*. Surtees Society, York.

Sellet, F., 1993. Chaine Operatoire: The concept and its applications. *Lithic Technol.* 18(1/2), 106–112.

Sellner, C., Oel, H.J., Camara, B., 1979. Untersuchung alter Gläser (Waldglas) auf Zusammenhang von Zusammensetzung, Farbe und Schmelzatmosphäre mit der Elektronenspektroskopie und der Elektronenspinresonanz (ESR). *Glas. Berichte* 52(12), 255–264.

Shackley, M.S., 2010. Is There Reliability and Validity in Portable X-Ray Fluorescence Spectrometry (PXRF)? *SAA Archaeol. Rec.* 10(5), 17–20.

Shannon, R.D., 1976. Revised Effective Ionic Radii and Systematic Studies of Interatomic Distances in Halides and Chaleogenides. *Acta Crystallogr.* A 32, 751–767.

Sherman, J., 1955. The theoretical derivation of fluorescent X-ray intensities from mixtures. *Spectrochim. Acta* 7(x), 283–306. doi:10.1016/0371-1951(55)80041-0

Shortland, A., Schachner, L., Freestone, I., Tite, M., 2006. Natron as a flux in the early vitreous materials industry: Sources, beginnings and reasons for decline. *J. Archaeol. Sci.* 33(4), 521–530. doi:10.1016/j.jas.2005.09.011

Shugar, A.N., Mass, J.L., 2012. *Handheld XRF for Art and Archaeology*, Studies in Archaeological Science 3. Leuven University Press, Leuven.

Sillar, B., Tite, M.S., 2000. The challenge of "technological choices" for materials science approaches in archaeology. *Archaeometry* 42(1), 2–20.

Silvestri, A., Geoscienze, D., Giotto, V., Padova, I.-, 2008a. The coloured glass of Iulia Felix. *J. Archaeol. Sci.* 35, 1489–1501. doi:10.1016/j.jas.2007.10.014

Silvestri, A., Molin, G., Salviulo, G., 2008b. The colourless glass of Iulia Felix. *J. Archaeol. Sci.* 35, 331–341. doi:10.1016/j.jas.2007.03.010

Silvestri, A., Molin, G., Salviulo, G., Schievenin, R., 2006. Sand for Roman glass production: An experimental and philological study on source of supply. *Archaeometry* 48(3), 415–432. doi:10.1111/j.1475-4754.2006.00264.x

Simmons, C.T., Mysak, L. a., 2010. Transmissive properties of Medieval and Renaissance stained glass in European churches. *Archit. Sci. Rev.* 53(2), 251–274. doi:10.3763/asre.2009.0073

Sitko, R., 2009. Quantitative X-ray fluorescence analysis of samples of less than 'infinite thickness': Difficulties and possibilities. *Spectrochim. Acta Part B At. Spectrosc.* 64, 1161–1172. doi:10.1016/j.sab.2009.09.005

Smedley, J.W., Jackson, C.M., 2006. Medieval and post-medieval glass technology: Bracken as a sustainable resource for glassmaking. *Glas. Technol. Eur. J. Glas. Sci. Technol. Part A* 47(2), 39–47.

Smedley, J.W., Jackson, C.M., 2002a. Medieval and post-medieval glass technology: Batch measuring practices. *Glas. Technol.* 43(1), 22–27.

Smedley, J.W., Jackson, C.M., 2002b. Medieval and post-medieval glass technology: A review of bracken in glassmaking. *Glas. Technol.* 43(6), 221–224.

Smith, A., 1776. *An Inquiry into the Nature and Causes of the Wealth of Nations*. doi:http://dx.doi.org/10.1093/oseo/instance.00043218

Smith, C.S., Gnudi, M.T., 1943. *The Pirotechnia of Vannoccio Biringuccio*. The American Institute of Mining and Metallurgical Engineers, New Yrok.

Smrček, A., 1999. Batch and composition of typical Bohemian glasses from the 14th to 19th centuries, in: *Proceedings of the 5th ESG Conference*. 1–9.

Solé, V.A., Papillon, E., Cotte, M., Walter, P., Susini, J., 2007. A multiplatform code for the analysis of energy-dispersive X-ray fluorescence spectra. *Spectrochim. Acta - Part B At. Spectrosc.* 62(1), 63–68. doi:10.1016/j.sab.2006.12.002

Soulier, I., Gratuze, B., Barrandon, J.-N., 1996. The origin of cobalt blue pigments in French glass from the Bronze Age to the eighteenth century, in: Demirci, S., Özer, A.M., Summers, G.D. (Eds.), *Archaeometry 94: The Proceedings of the 29th International Symposium on Archaeometry, Ankara 9-14 May 1994*. Tübitak, Ankara, 133–140.

Speakman, R.J., Shackley, M.S., 2013. Silo science and portable XRF in archaeology: A response to Frahm. *J. Archaeol. Sci.* 40(2), 1435–1443. doi:10.1016/j.jas.2012.09.033

Spitzer-Aronson, M., 1975. Étude de vitraux rouge médiévaux á l'aide de microscope optique, microscope á balayage avec image par électrons rétrodiffusés et microsonde électronique á rayons X. *Verres et Réfractaires* 29, 145–153.

Stephan, H.-G., Wedepohl, K.H., Hartmann, G., 1997. Mittelalterliches Glas aus dem Reichskloster und der Stadtwüstung Corvey: Mit einem Nachtrag zu den Analyseergebnissen von Gläsern aus dem Kloster Brunshausen. *Germania* 75(2), 673–723.

Stern, W.B., Gerber, Y., 2004. Potassium - calcium glass: New data and experiments. *Archaeometry* 46(1), 137–156.

Sterpenich, J., Libourel, G., 2001. Using stained glass windows to understand the durability of toxic waste matrices. *Chem. Geol.* 174, 181–193.

Sterpenich, J., Libourel, G., 1997. Les vitraux médiévaux: caractérisation physico-chimique de l'altération. *Techne* 6, 70–78.

Sutton, A.F., 2009. The Merchant Adventurers of England: The Place of the Adventurers of York and the North in the Late Middle Ages. *North. Hist.* 46(2), 219–229. doi:10.1179/174587009X452314

Swanson, H., 1988. The Illusion of Economic Structure: Craft Guilds in Late Medieval English Towns. *Past Present* 121, 29–48.

Tehrani, J.J., Riede, F., 2008. Towards an archaeology of pedagogy: learning, teaching and the generation of material culture traditions. *World Archaeol.* 40(3), 316–331. doi:10.1080/00438240802261267

Thirlwall, M.F., 1991. Long-term reproducibility of multicollector Sr and Nd isotope ratio analysis. *Chem. Geol. (Isotope Geosci. Sect.* 94, 85–104. doi:10.1016/0168-9622(91)90002-E

Thirlwall, M.F., Anczkiewicz, R., 2004. Multidynamic isotope ratio analysis using MC-ICP-MS and the causes of secular drift in Hf, Nd and Pb isotope ratios. *Int. J. Mass Spectrom.* 235(1), 59–81. doi:10.1016/j.ijms.2004.04.002

Thomas, A., 1995. *The painter's practice in Renaissance Tuscany*. Cambridge University Press, Cambridge.

Thompson, D.V. (Jr. ., 1960. *Cennino D'Andrea Cennini: The Craftsman's Handbook*. Dover Publications, New York.

Thompson, N.M., 2014. Designers, Glaziers, and the Process of Making Stained Glass Windows in 14th- and 15th-Century Florence. *J. Glass Stud.* 56, 237–251.

Thorpe, W.A., 1949. *English Glass*. Adam and Charles Black, London.

Topić, N., Bogdanović Radović, I., Fazinić, S., Skoko, Ž., 2016. Analysis of medieval and post-medieval glass fragments from the Dubrovnik Region (Croatia). *Archaeometry* 58(4), 574–592. doi:10.1111/arcm.12191

Torre, J., 1691. *York Minster 1690-1691*. York Minster Library LI/2 and LI/7.

Turner, W.E.S., 1956a. Studies of Ancient Glass and Glass-making Processes. Part V. Raw Materials and Melting Processes. *J. Soc. Glas. Technol.* 40, 277–300.

Turner, W.E.S., 1956b. Studies of Ancient Glass and Glass-making Processes. Part III. The Chronology of the Glassmaking Constituents. *J. Soc. Glas. Technol.* 40, 39–52.

Tykot, R.H., 2017. A Decade of Portable (Hand-Held) X-Ray Fluorescence Spectrometer Analysis of Obsidian in the Mediterranean: Many Advantages and Few Limitations. *MRS Adv.* 1–8. doi:10.1557/adv.2017.148

Tykot, R.H., 2016. Using Nondestructive Portable X-ray Fluorescence Spectrometers on Stone, Ceramics, Metals, and Other Materials in Museums: Advantages and Limitations. *Appl. Spectrosc.* 70(1), 42–56. doi:10.1177/0003702815616745

UCL, n.d. Safe Use and Management of X-rays [WWW Document]. URL https://moodle.ucl.ac.uk/course/view.php?id=41165 (accessed 4.24.18).

Van der Snickt, G., Legrand, S., Caen, J., Vanmeert, F., Alfeld, M., Janssens, K., 2016. Chemical imaging of stained-glass windows by means of macro X-ray fluorescence (MA-XRF) scanning. *Microchem. J.* 124, 615–622. doi:10.1016/j.microc.2015.10.010

van Elteren, J.T., Tennent, N.H., Šelih, V.S., 2009. Multi-element quantification of ancient/historic glasses by laser ablation inductively coupled plasma mass spectrometry using sum normalization calibration. *Anal. Chim. Acta* 644(1–2), 1–9. doi:10.1016/j.aca.2009.04.025

Van Wersch, L., Loisel, C., Mathis, F., Strivay, D., Bully, S., 2016. Analyses of Early Medieval Stained Window Glass From the Monastery of Baume-Les-Messieurs (Jura, France). *Archaeometry* 58(6), 930–946. doi:10.1111/arcm.12207

Vance, D., Thirlwall, M.F., 2002. An assessment of mass discrimination in MC-ICPMS using Nd isotopes. *Chem. Geol.* 185(3–4), 227–240. doi:10.1016/S0009-2541(01)00402-8

Vassas, C.D., 1971. Etude chimique, thermographique et physique de verres de vitraux du Moyen-Age, in: *International Congress on Glass IX, Versailles, France, 1971*. 241–306.

Velde, B., 2013. Glass Compositions over Several Millennia in the Western World, in: Janssens, K. (Ed.), *Modern Methods for Analysing Archaeological and Historical Glass*. John Wiley & Sons, Chichester, UK, 67–78.

Velde, B., Barrera, J., 1986. Composition of medieval blown glass fragments found at Orleans.pdf. *Archéologie Médiévale* XVI, 93–103.

Verità, M., 2005. Comments on W. B. Stern and Y. Gerber,'Potassium–calcium glass: new data and experiments', Archaeometry, 46 (1)(2004), 137–56. *Archaeometry* 47(3), 667–669. doi:10.1111/j.1475-4754.2005.00225.x

Verità, M., 1996. Composition, structure et mécanisme de deterioration des grisailles, in: *Grisaille, Jaune d'argent, Sanguine, Émail et Peinture à Froid, Forum Pour La Conservation et Al Restauration Des Vitraux*. Commission Royale des Monuments Sites et Fouilles de la Règion Wallone, Liège, 61–67.

Verità, M., 1985. L'invenzione del cristallo muranese: una verifica analitica delle fonti storiche. *Riv. della Stn. Sper. del Vetro* 15, 17–29.

Vilarigues, M., da Silva, R.C., 2004. Ion beam and infrared analysis of medieval stained glass. *Appl. Phys. A Mater. Sci. Process.* 79, 373–378. doi:10.1007/s00339-004-2538-9

Vilarigues, M., Macedo, F., Rodrigues, A., Delgado, J., 2013. Medieval stained glass biocorrosion and cleaning.

Vilarigues, M., Redol, P., Machado, A., Rodrigues, P.A., Alves, L.C., da Silva, R.C., 2011. Corrosion of 15th and early 16th century stained glass from the monastery of Batalha studied with external ion beam. *Mater. Charact.* 62, 211–217. doi:10.1016/j.matchar.2010.12.001

von Simpson, O., 1962. *The Gothic Cathedral*. Harper and Row, New York.

Wallaert-Pêtre, H., 2001. Learning How to Make the Right Pots: Apprenticeship Strategies and Material Culture, a Case Study in Handmade Pottery from Cameroon. *J. Anthropol. Res.* 57(4), 471–493.

Ware, L., 2013. Revelations in the Study of Medieval Stained Glass Windows: The Scientific Analysis of Panel 3b of the Great East Window of York Minster Using EPMA and pXRF [Unpublished MSc Dissertation]. UCL.

Wedepohl, K.H., 2003. *Glas in Antike und Mittelalter: Geschichte eines Werkstoffs*. Schweizerbart'sche Verlagsbucchandlung, Stuttgart.

Wedepohl, K.H., 1998. Mittelalterliches Glas in Mitteleuropa: Zusammensetzung, Herstellung, Rohstoffe. *Nachrichten der Akad. der Wissenschaften Göttingen. 2, Math. Klasse, 1*.

Wedepohl, K.H., 1995. The composition of the continental crust. *Geochim. Cosmochim. Acta* 59(7), 1217–1232. doi:10.1016/0016-7037(95)00038-2

Wedepohl, K.H., Baumann, A., 2000. The Use of Marine Molluskan Shells for Roman Glass and Local Raw Glass Production in the Eifel Area (Western Germany). *Naturwissenschaften* 87, 129–132.

Wedepohl, K.H., Simon, K., 2010. The chemical composition of medieval wood ash glass from Central Europe. *Chemie der Erde - Geochemistry* 70(1), 89–97. doi:10.1016/j.chemer.2009.12.006

Welch, C.M., 2003. York Minster Glass from Staffordshire in the late 15th Century. *Glas. News* (January), 7–8.

Welch, C.M., 1997. Glass-making in Wolseley, Staffordshire. *Post-Medieval Archaeol.* 31(1), 1–60. doi:10.1179/pma.1997.001

Welch, C.M., Linford, P., 2005. Archaeomagnetic dating of medieval and Tudor glassmaking sites in Staffordshire, England, in: *Annales Du 16e Congrès de l'Association Internationale Pour l'Histoire Du Verre, Nottingham UK 2003*. AIHV, 210–213.

Wenger, E., 1998. *Communities of Practice: Learning, Meaning, and Identity*. Cambridge University Press, Cambridge, UK.

Westlake, N.J.H., 1886. *A History of Design in Painted Glass*. London.

Weyl, W.A., 1951. *Coloured Glasses*. The Society of Glass Technology, Sheffield, UK.

Whall, C.W., 1905. *Stained Glass Work: A Text-Book for Students and Workers in Glass. The Artistic Crafts Series of Technical Handbooks*. Sir Isaac Pitman & Sons, Ltd., London.

White, L., 1978. Cultural Climates and Technological Advance in the Middle Ages, in: *Medieval Religion and Technology*. University of California Press, Los Angeles, 217–254.

White, L., 1972. *Medieval technology and social change*. Oxford University Press, New York.

White, L., 1964. Theophilus Redivivus. *Johns Hopkins Univ. Press Soc. Hist. Technol.* 5(2), 224–233.

Wilk, D., Kamińska, M., Walczak, M., Bulska, E., 2017. Archaeometric investigations of medieval stained glass panels from Grodziec in Poland, in: Targowski (Ed.), *Lasers in the Conservation of Artworks XI, Proceedings of LACONA XI*. NCU Press, Torún, 263–278. doi:10.12775/3875-4.19

Wilke, D., Rauch, D., Rauch, P., 2016. Is Non-destructive Provenancing of Pottery Possible With Just a Few Discriminative Trace Elements? *STAR Sci. Technol. Archaeol. Res.* 0(0), 1–18. doi:10.1080/20548923.2016.1209030

Williams-Thorpe, O., Potts, P.J., Webb, P.C., 1999. Field-Portable Non-Destructive Analysis of Lithic Archaeological Samples by X-Ray Fluorescence Instrumentation using a Mercury Iodide Detector: Comparison with Wavelength-Dispersive XRF and a Case Study in British Stone Axe Provenancing. *J. Archaeol. Sci.* 26(2), 215–237. doi:10.1006/jasc.1998.0323

Willmott, H., 2005. *A History of English Glassmaking AD 43-1800*. Tempus, Stroud, Gloucestershire.

Wilson, C., 1990. *The Gothic Cathedral: The Architecture of the Great Church, 1130-1530*. Thames and Hudson, London.

Woisetschläger, G., Dutz, M., Paul, S., Schreiner, M.R., 2000. Weathering Phenomena on Naturally Weathered Potash-Lime-Silica-Glass with Medieval Composition Studied by Secondary Electron Microscopy and Energy Dispersive Microanalysis. *Mikrochim. Acta* 135, 121–130.

Wood, E.S., 1982. A 16th century glasshouse at Knightons, Alfold, Surrey. *Surrey Archaeol. Collect.* 73, 1–47.

Wypyski, M.T., Richter, R.W., 1997. Preliminary compositional study of 14th and 15th C. European enamels. *Technè la Sci. au Serv. l'histoire l'art des civilisations* (6), 48–57.

YGT (York Glaziers Trust), 2016e. Panel 15g (EMW arrangement) Art Historical Report [Unpublished].

YGT (York Glaziers Trust), 2016d. Panel 15f (EMW arrangement) Art Historical Report [Unpublished].

YGT (York Glaziers Trust), 2016c. Panel 15h (EMW arrangement) Art Historical Report [Unpublished].

YGT (York Glaziers Trust), 2016b. Panel 15b (EMW arrangement) Art Historical Report [Unpublished].

YGT (York Glaziers Trust), 2016a. Panel 15a (EMW arrangement) Art Historical Report [Unpublished].

YGT (York Glaziers Trust), 2015b. Panel 10j (EMW arrangement) Art Historical Report [Unpublished].

YGT (York Glaziers Trust), 2015c. Panel 10f (EMW arrangement) Art Historical Report [Unpublished].

YGT (York Glaziers Trust), 2015a. Panel 10d (EMW arrangement) Art Historical Report [Unpublished].

YGT (York Glaziers Trust), 2014a. Panel 1e (EMW arrangement) Art Historical Report [Unpublished].

YGT (York Glaziers Trust), 2014b. Panel 1g (EMW arrangement) Art Historical Report [Unpublished].

YGT (York Glaziers Trust), 2014c. Panel 1f (EMW arrangement) Art Historical Report [Unpublished].

YGT (York Glaziers Trust), 2013. Panel 3b (EMW arrangement) Art Historical Report [Unpublished].

Zhang, A.Y., Suetsugu, T., Kadono, K., 2007. Incorporation of silver into soda-lime silicate glass by a classical staining process. *J. Non. Cryst. Solids* 353, 44–50. doi:10.1016/j.jnoncrysol.2006.09.033

APPENDIX A

The Great East Window of York Minster: Supplementary materials and sampling

A.1 The contract for the glazing of the GEW

The contract for the glazing of the GEW was transcribed in the 17th century by James Torre (Latin and English) and Matthew Hutton (Latin), since which time the original has been lost; the English text by Torre and a translation of the Hutton text are given below (from Brown, 2018, 48–49).

A.1.1 James Torre, English version

> On 10 Aug[u]st Ad 1405 6H4
>
> An indenture was made between the Dean & Chapter on the one p[ar]t And John Thornton of Covintry glaziers on the other Whereby The s[ai]d John covenanted to make a Great Window at the E: end of the Quire, according to the best of his skill & Cunning And undertook to glaze the same w[i]th Glass, Lead, Sodder & other necessaries requisite, & to find all sufficient workmen to be disposed at the Costs of the s[ai]d Dean & Chapter. And to finish the same w[i]thin 3 years from the date hereof And obliging himself w[i]th his own hands to portrature the s[ai]d window w[i]th Historicall Images & other painted work, in the best Mannor & form that he possibly could And likewise paynt the same where need required according to the Ordination of the Dean & Chapter. For all w[hi]ch the Dean and Chapter should pay him 4s Sterling a week during the term afores[ai]d that he wrought in his Art. And besides that 100s sterling every one of those 3 years. And if he performed his work well & truly, & perfect it according to the tenor of these

Covenants, then he should receive more of the Dean & Chapter for his care therein, the sum of 10ll in silver

York Minster Library and Archive, MS LI/7, 7

A.1.2 Matthew Hutton (English translation)

Indenture between the Dean and Chapter of York and John Thornton of Coventry, glazier, for the glazing of the great window in the east gable of the Cathedral Church of York, which he shall complete within three years from the beginning of the said work. He shall portray the said window with his own hand, and the histories, images and other things to be painted on the same. He shall also paint the same as necessary, according to the ordination of the Dean and Chapter. And he shall also provide glass and lead and the workmen, at the expense of the Dean and Chapter, in the same manner as he would have done if the like had to be done at his own costs and chargers, whereunto he shall take his oath. And the said John shall receive of the Dean and Chapter for every week wherein he shall work at his art during the said three years four shillings, and each year of the same three years five pounds sterling, and after the work is completed ten pounds. Given at York etc., on the 10th day of December, 1405.

Translated by Harrison (1927, 129)

British Library Harleian MS 6971, fol. 141v

A.2 Timeline of the GEW

Table A.1 Timeline of the Great East Window since construction. Information compiled from French (2003).

1405-1408	Contract signed; Construction begins on the Great East Window Three years later, it is completed.
c. 1670	Henry Johnson describes heraldic emblems in the window
c. 1690	James Torre writes the first complete description of GEW. At least four panels out of place by this time, suggesting small repairs were made.
1730	Thomas Gent describes the window for a guidebook. At least 13 panels out of place, still not necessarily indicative of a general re-leading.
1736	Drake's Eboracum reproduces engravings of panels by Haynes/Toms.
1762	Thomas Gent writes rhyming couplets to describe each panel. Now 21 panels out of place, suggesting a large-scale re-leading had taken place.
1825	Entire window releaded, as evidenced by tracery graffiti.
1829	Fire devastates the quire; GEW is mostly undamaged.
1861	External glass plates added to GEW for protection.
1884	Camidge sketches main panels of the window.
1910	External plate glass replaced with colourless quarries.
1939-1940	Glass removed for safety during the Second World War.
1943-1953	Extensive project focused on the repair, releading and rearrangement of the glass under Eric Milner-White, Dean of York.
2006	York Minster Revealed, a massive project to restore the East End of York Minster, begins.

A.3 Images and sampling

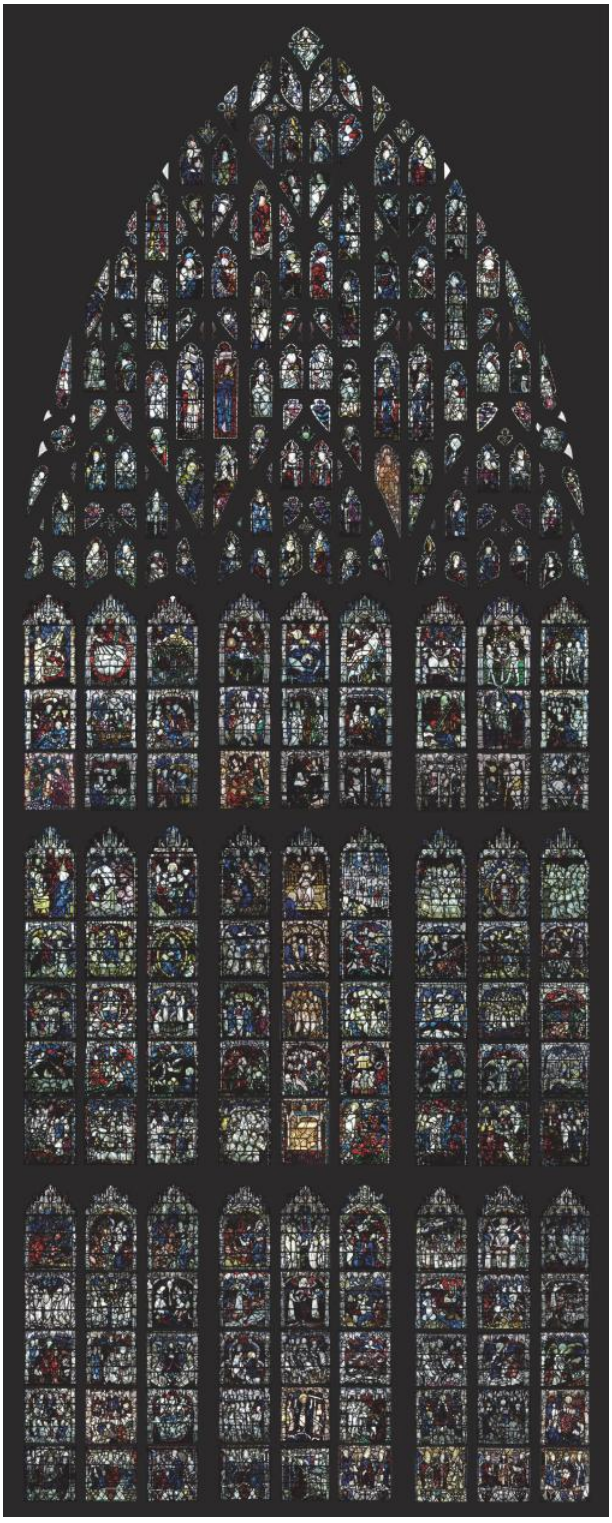

Figure A.1 Image of the GEW, compiled from individually photographed panels prior to their conservation (circa 2011). © *The York Glaziers Trust with the kind permission of Steve Farley.*

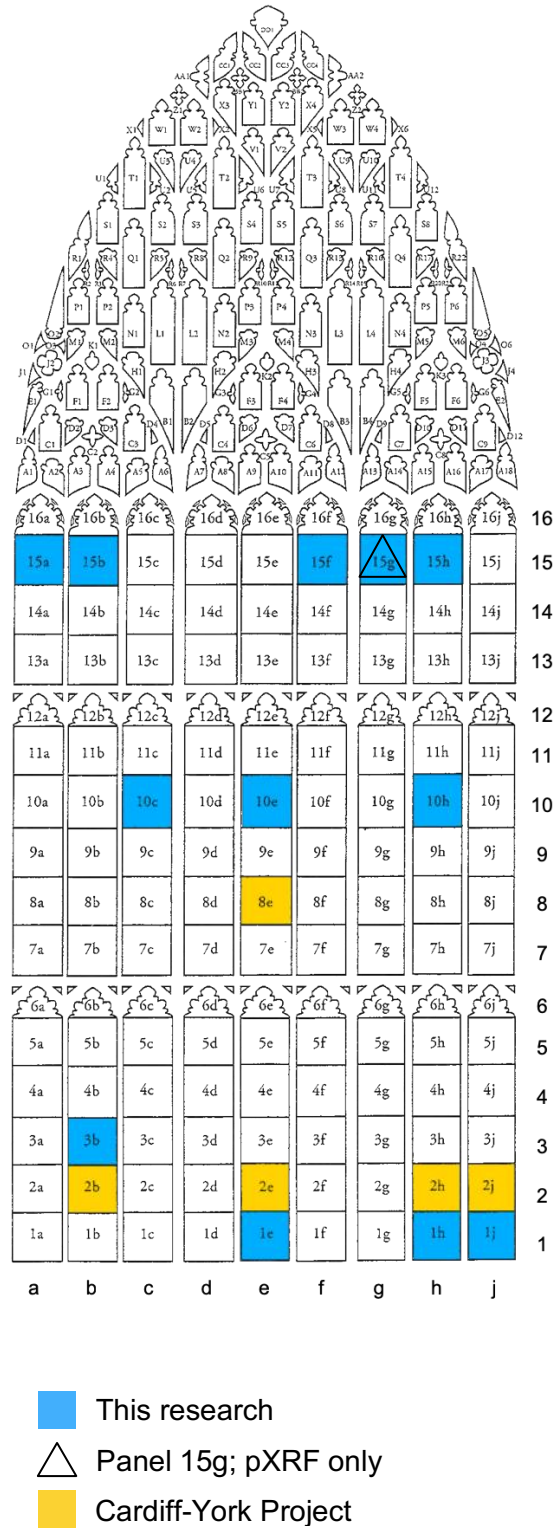

Figure A.2 Outline of the GEW with the panels studied in this research marked.

Table A.2 Numbers by panel and colour of samples analysed by pXRF and, in parentheses, subsamples taken for analysis by EPMA-WDS and other laboratory techniques. Below, the approximate percentage of the panel analysed by surface area, calculated using QGIS.

	15a	15b	15f	15g	15h	10c	10e	10h	3b	1e	1h	1j	Total
White	48 (11)	42 (10)	55 (0)	44 (11)	35 (12)	41 (13)	36 (8)	60 (19)	49 (13)	46 (12)	30 (5)	39 (8)	528 (122)
Blue	11 (4)		5 (1)	7 (4)	2 (1)	11 (6)	15 (5)	4 (1)	25 (9)	17 (6)	9 (2)	5 (2)	111 (40)
Red	21 (4)	22 (7)	8 (0)	11 (4)	8 (4)	1 (1)	17 (6)	22 (11)	14 (5)	10 (3)	5 (3)	7 (3)	147 (51)
Green	1 (1)		11 (4)	5 (2)	9 (5)		20 (5)	11 (5)	12 (3)			1 (0)	70 (26)
Yellow			10 (1)	3 (1)	6 (1)							1 (1)	20 (4)
Mn			2 (0)	8 (2)				16 (5)			8 (3)	1 (1)	9 (3)
Total	**81 (20)**	**64 (17)**	**91 (6)**	**78 (24)**	**60 (23)**	**53 (20)**	**88 (24)**	**112 (41)**	**100 (30)**	**73 (21)**	**52 (13)**	**54 (14)**	**911 (253)**
	47%	55%	52%	54%	52%	60%	44%	52%	49%	28%	27%	27%	

Figure A.3 Panel 1e. *Photo: The York Glaziers Trust: reproduced with the kind permission of the Chapter of York.*

Subject matter: Bishop Walter Skirlaw, donor of the window, kneeling before an altar with the words *[Hoc opus in]signe deus offero sume benigne,* "O God, I offer to thee this notable work. Receive it graciously", on a scroll behind him (Brown, 2018; French, 2003; Knowles, 1936, 220).

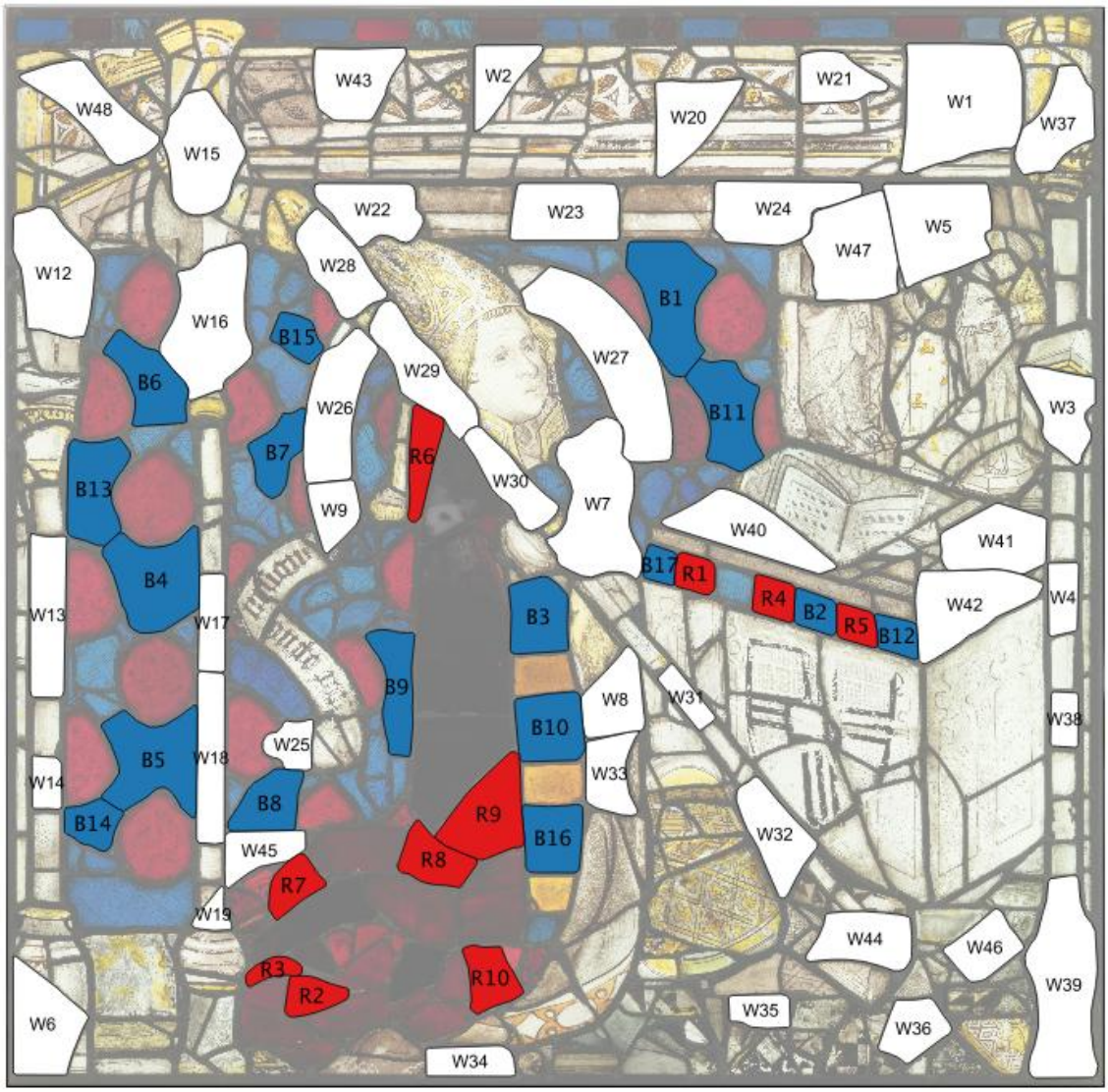

Figure A.4 Sample map of panel 1e.

Analysed by pXRF (73)
W1-W48 (excluding W10-W11)
B1-B17
R1-R10

Control group (21)
W1-W11, W48
B1-B6
R1-R3

LA-ICP-MS: W3, B4
TIMS: W48

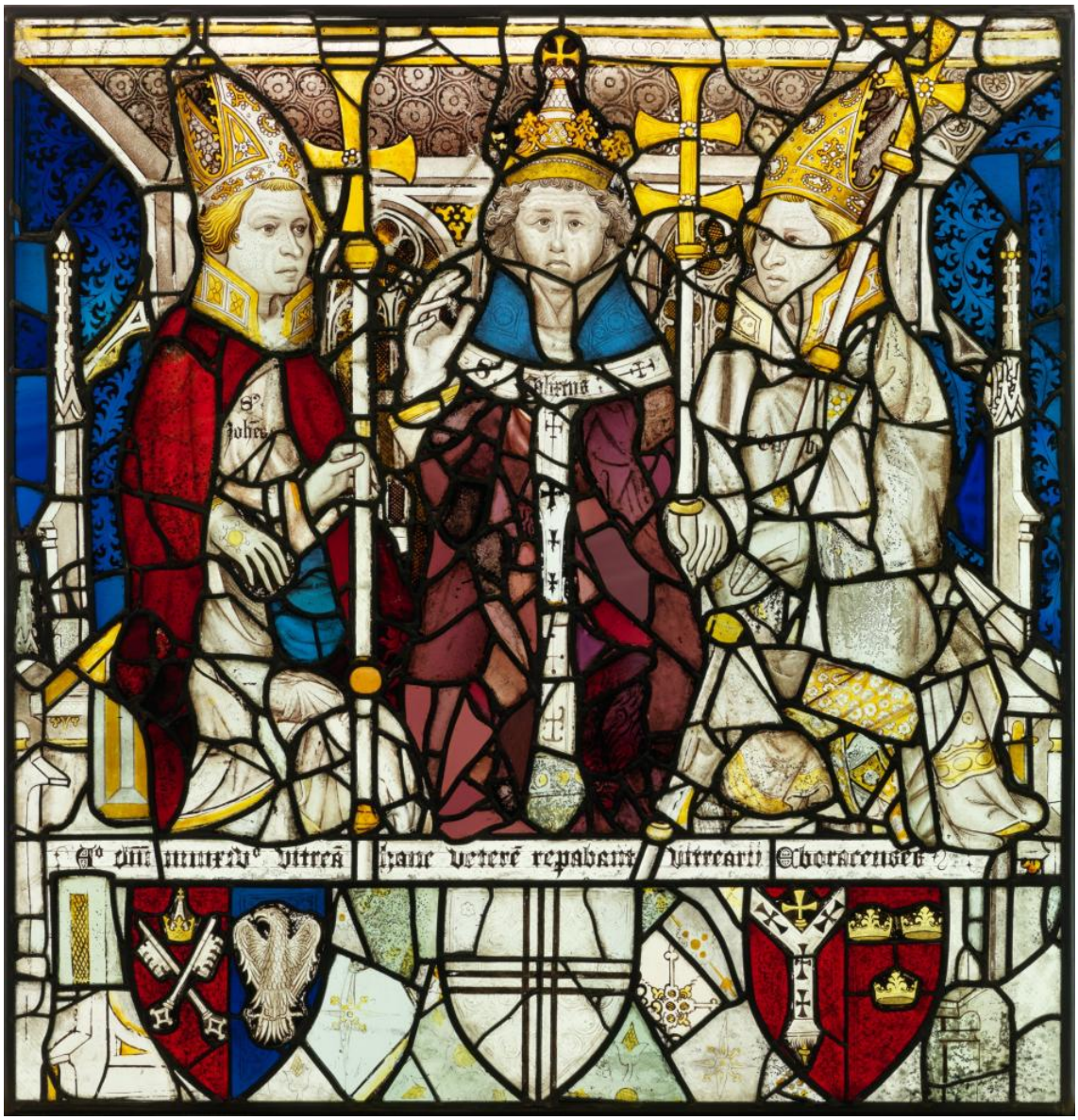

Figure A.5 Panel 1h, formerly in position 1g under the EMW arrangement. *Photo: The York Glaziers Trust: reproduced with the kind permission of the Chapter of York.*

Subject matter: St. John of Beverley, Pope Calixtus, and St. Egbert. St. John of Beverley and St. Egbert are two figures from the Anglo-Saxon period who were important to Christianity in northern England, while Pope Calixtus was an important 12th century figure (Brown, 2018; French, 2003).

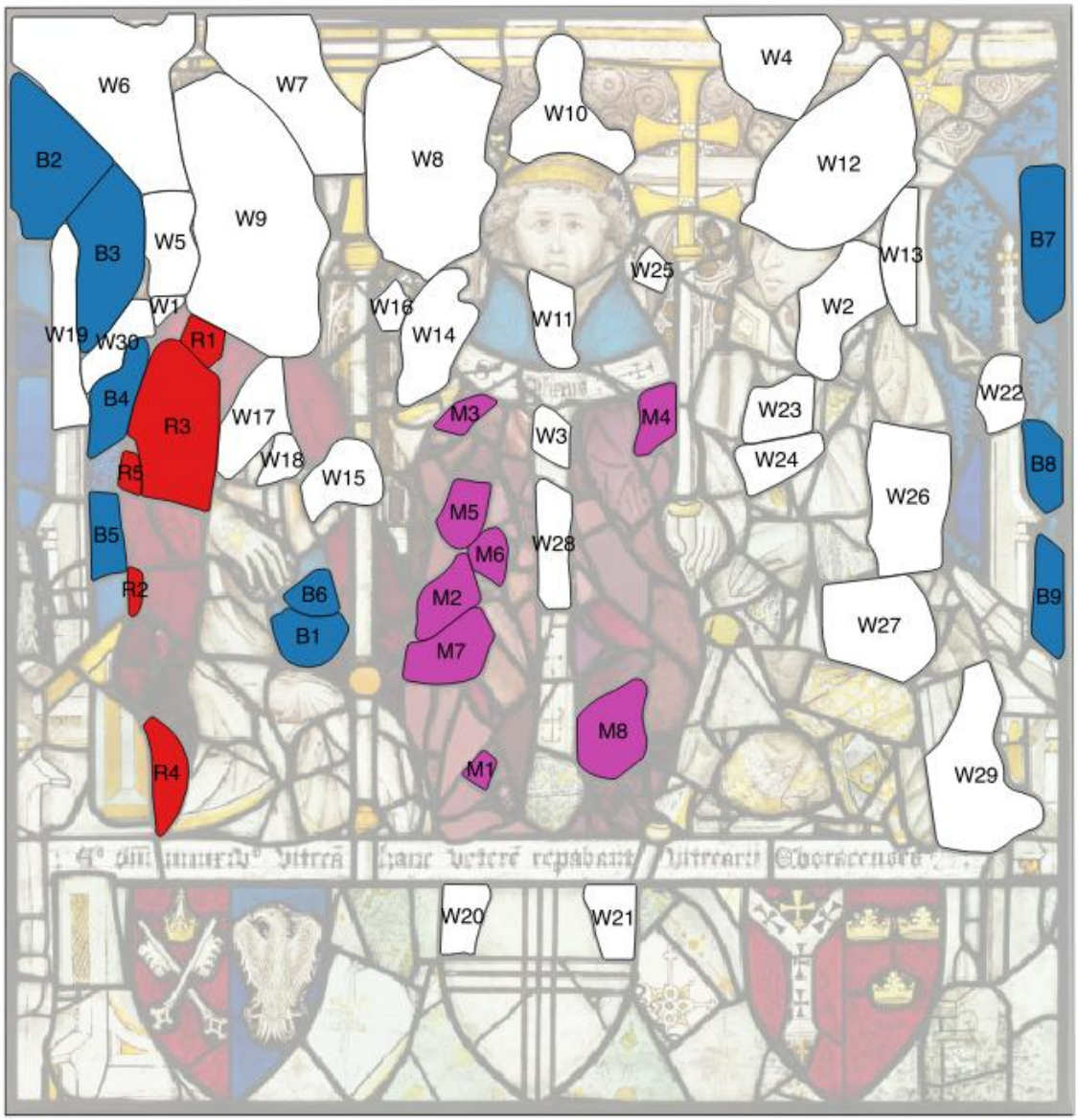

Figure A.6 Sample map of panel 1h.

Analysed by pXRF (52)
W1-W30
B1-B9
R1-R5
M1-M8

Control group (13)
W1-W4, W13
B1-B2
R1-R2, R5
M1-M3

LA-ICP-MS: M1, M3
TIMS: W13, B2, R5, M1

Figure A.7 Panel 1j, formerly in position 1f under the EMW arrangement. *Photo: The York Glaziers Trust: reproduced with the kind permission of the Chapter of York.*

Subject matter: An unidentified archbishop, Pope Celestine III, and St. William of York. St. William of York, a canonised archbishop, and Pope Celestine are two important figures from York's history in the 12th century (Brown, 2018; French, 2003).

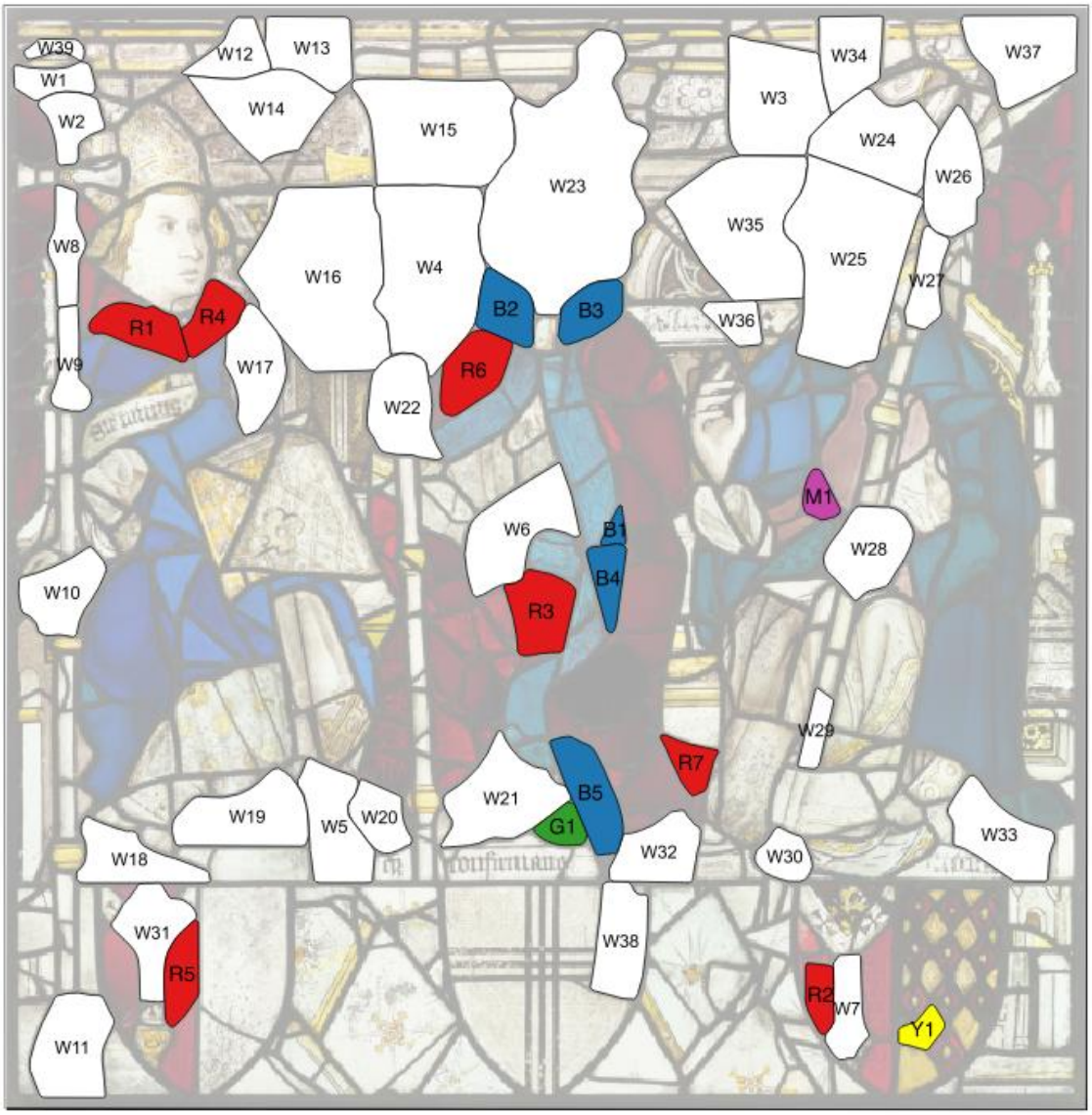

Figure A.8 Sample map of panel 1j.

Analysed by pXRF (54)
W1-W39
B1-B5
R1-R7
M1
Y1
G1

Control group (14)
W1-W7, W39
B1-B2
R1-R3
M1
Y1

LA-ICP-MS: W5
TIMS: W39

Figure A.9 Panel 3b. *Photo: The York Glaziers Trust: reproduced with the kind permission of the Chapter of York.*

Subject matter: The Merchants mourn the Fall of Babylon, *Revelation 18.* Three merchant look despondently down on the city of Babylon while an angle overhead announces the destruction of the city, subtly depicted by the crumbling walls near the bottom of the panel (Brown, 2018; French, 2003).

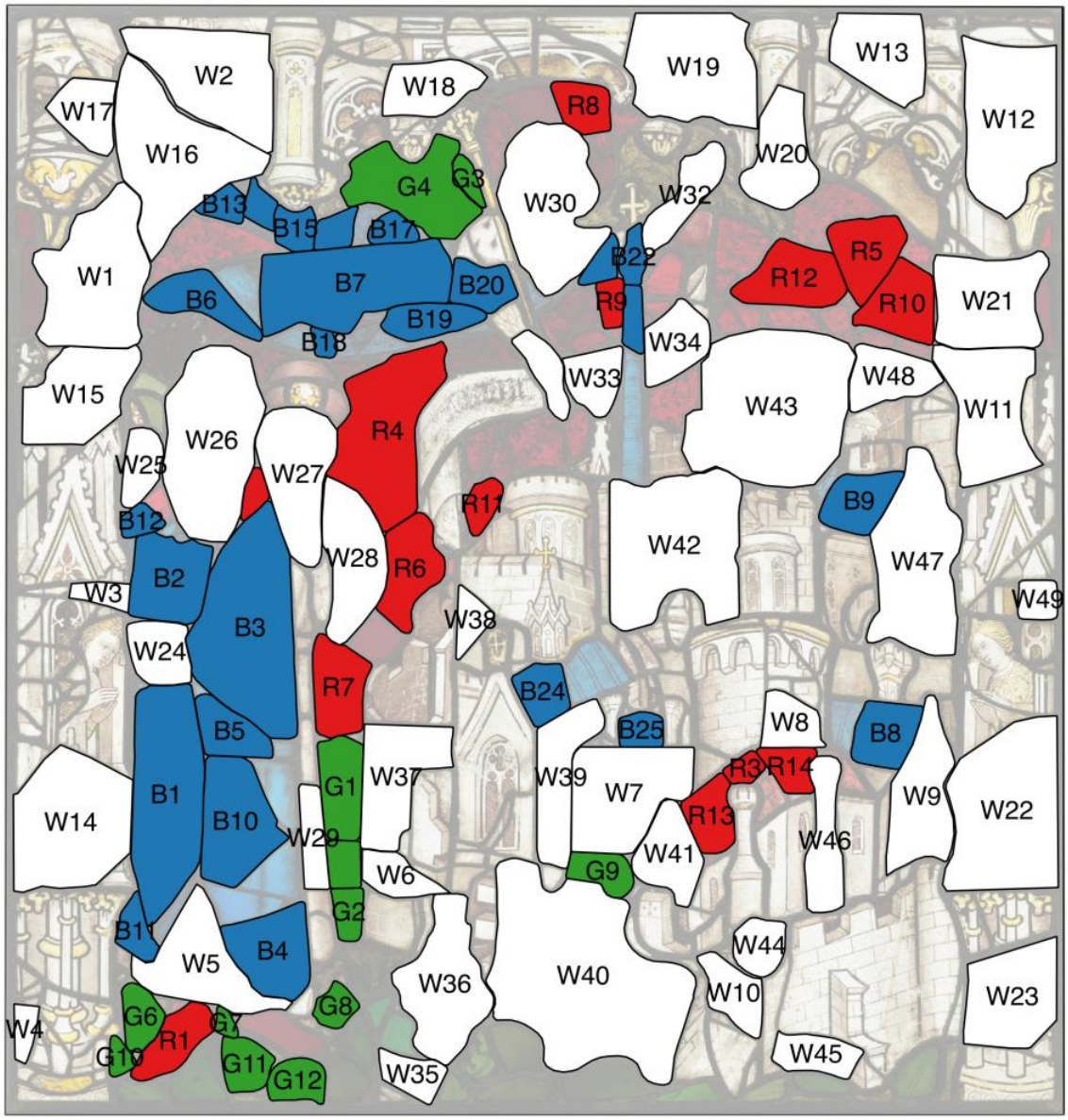

Figure A.10 Sample map of panel 3b.

Analysed by pXRF (100)
W1-W49
B1-B25
R1-R14
G1-G12

Control group (30)
W1-W13
B1-B9
R1-R5
G1-G3

LA-ICP-MS: W2, W7, B5, R1, G3

Figure A.11 Panel 10c, formerly in position 10d under the EMW arrangement. *Photo: The York Glaziers Trust: reproduced with the kind permission of the Chapter of York.*

Subject matter: The Elders worship the Lamb, *Revelation 5:8-10.* The Lamb, (representing Christ) opens the book that tells of events to come and other secrets known only to God, and the elders fall to their knees to worship him (Brown, 2018; French, 2003).

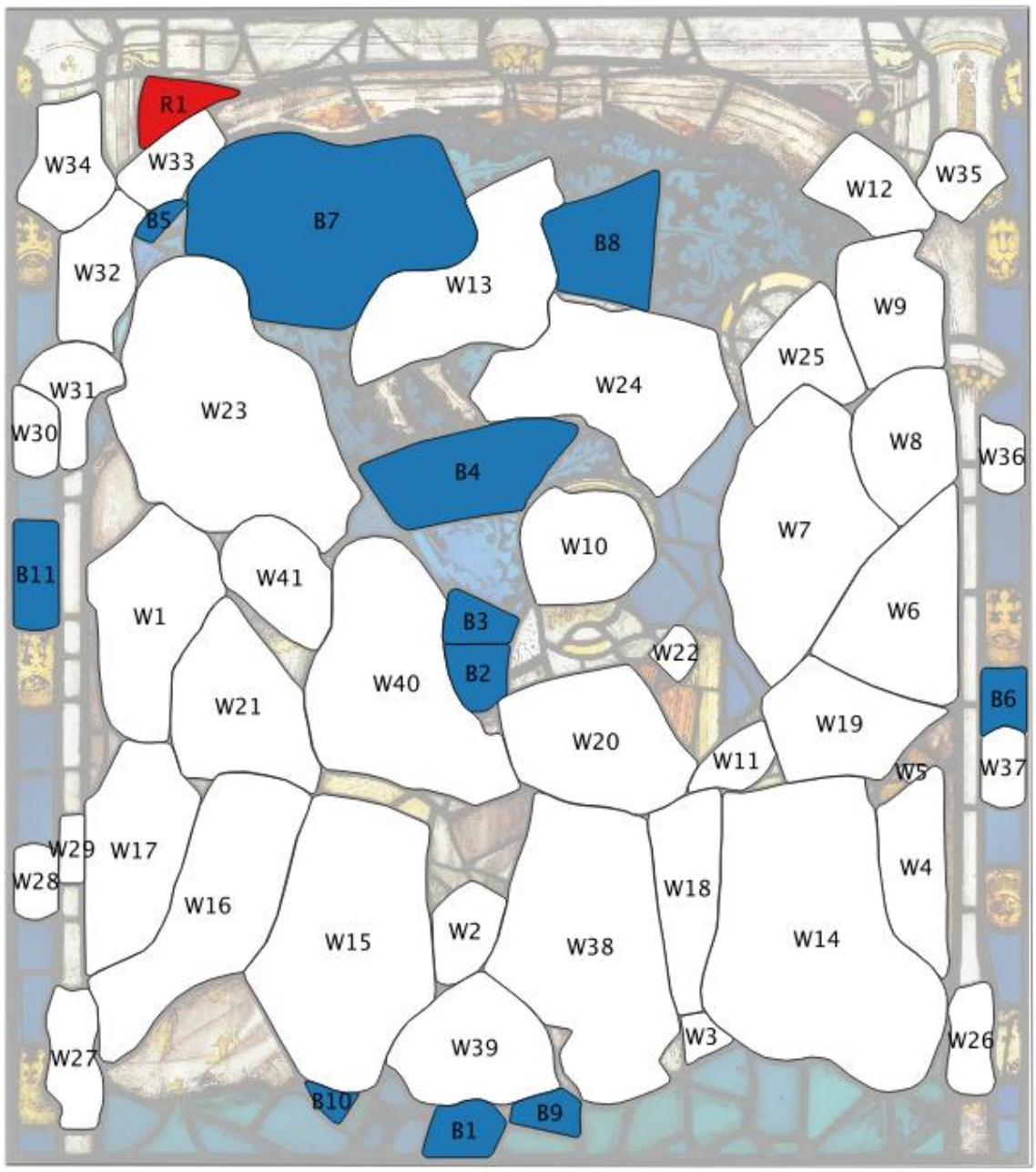

Figure A.12 Sample map of panel 10c.

Analysed by pXRF (53)
W1-W41
B1-B11
R1

Control group (20)
W1-W13
B1-B6
R1

LA-ICP-MS: W8, B1, B6

Figure A.13 Panel 10e, formerly in position 10f under the EMW arrangement. *Photo: The York Glaziers Trust: reproduced with the kind permission of the Chapter of York.*

Subject matter: The Opening of the First Seal, *Revelation 6:1-2.* St. John, left, observes as the Lamb opens the first of the seven seals which secure the Book of God, and the first Horseman of the Apocalypse rides forth on a white horse (Brown, 2018; French, 2003).

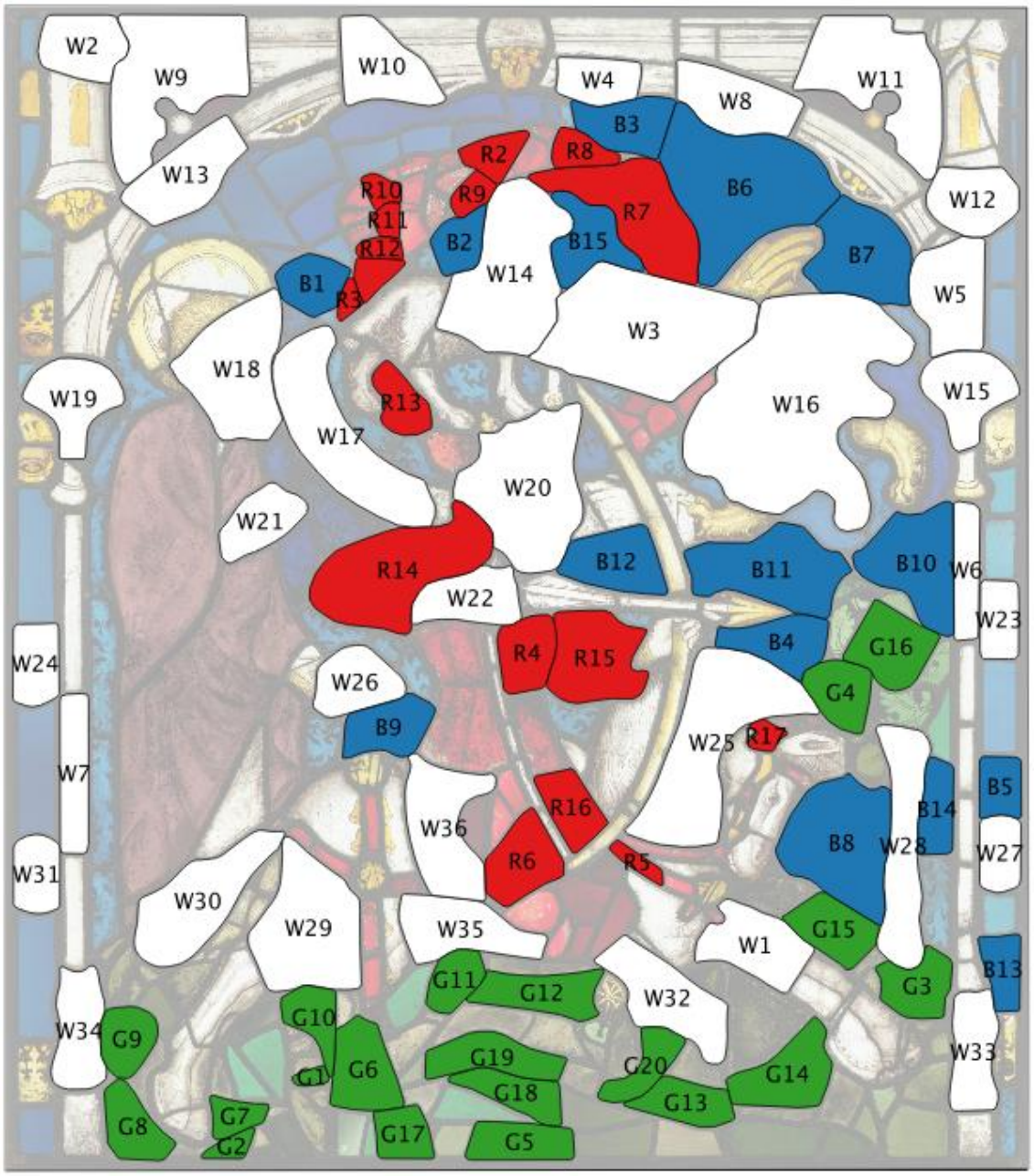

Figure A.14 Sample map of panel 10e.

Analysed by pXRF (88)	Control group (24)
W1-W36	W1-W8
B1-B15	B1-B5
R1-R17	R1-R6
G1-G20	G1-G5

Figure A.15 Panel 10h, formerly in position 10g under the EMW arrangement. *Photo: The York Glaziers Trust: reproduced with the kind permission of the Chapter of York.*

Subject matter: The Opening of the Fourth Seal, *Revelations 6:7-8.* The Lamb opens the fourth of the seven seals, unleashing the fourth Horseman of the Apocalypse (Death) followed by hell (Brown, 2018; French, 2003).

.

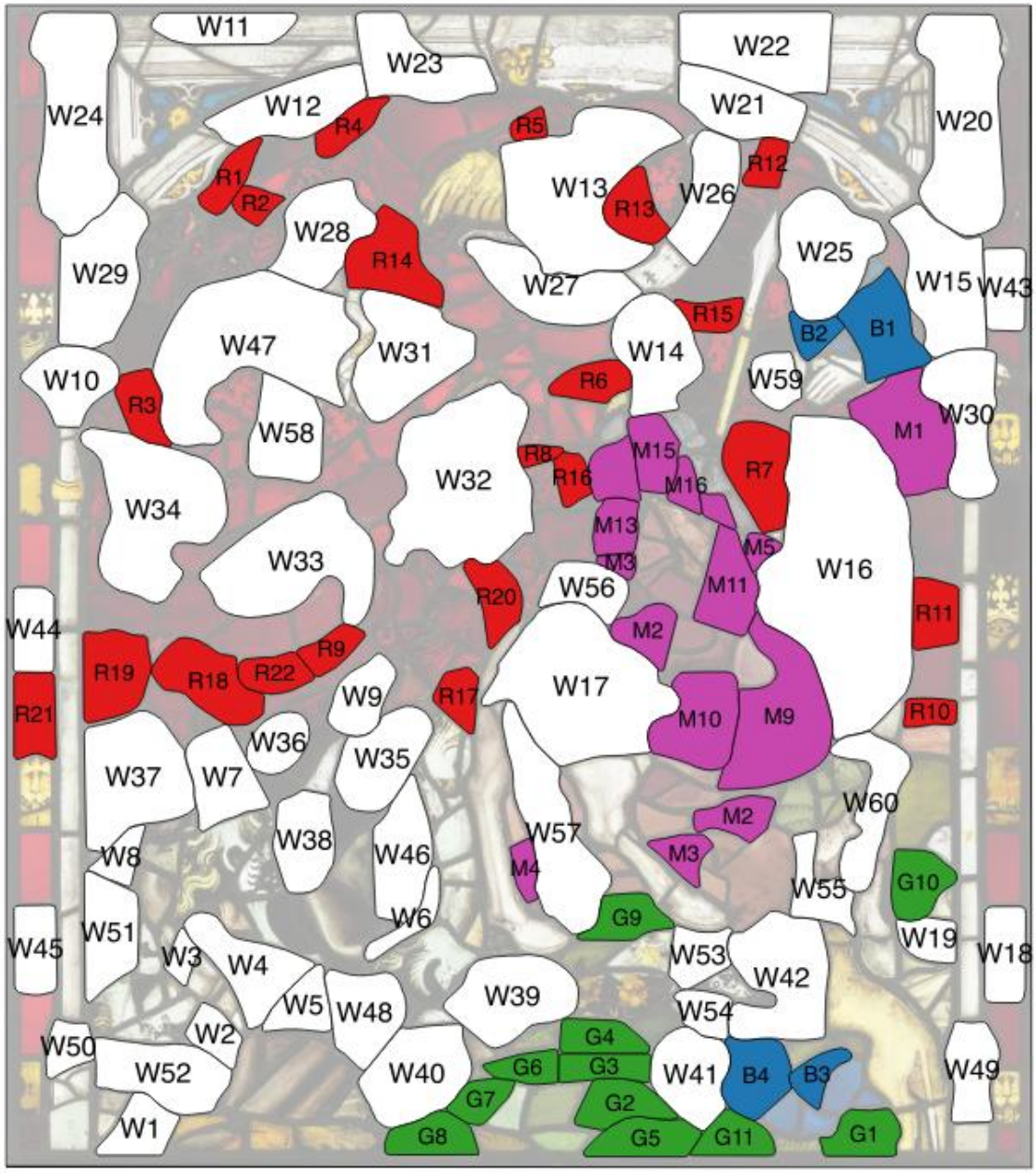

Figure A.16 Sample map of panel 10h.

Analysed by pXRF (112)	Control group (41)
W1-W60	W1-W19
B1-B4	B1
R1-R22	R1-R11
G1-G11	G1-G5
M1-M16	M1-M5
	LA-ICP-MS: M1, M2

Figure A.17 Panel 15a. *Photo: The York Glaziers Trust: reproduced with the kind permission of the Chapter of York.*

Subject matter: The First Day of Creation, *Genesis 1:1-5.* God creates heaven and earth, with angels above and two red rebel angels below (Brown, 2018; French, 2003).

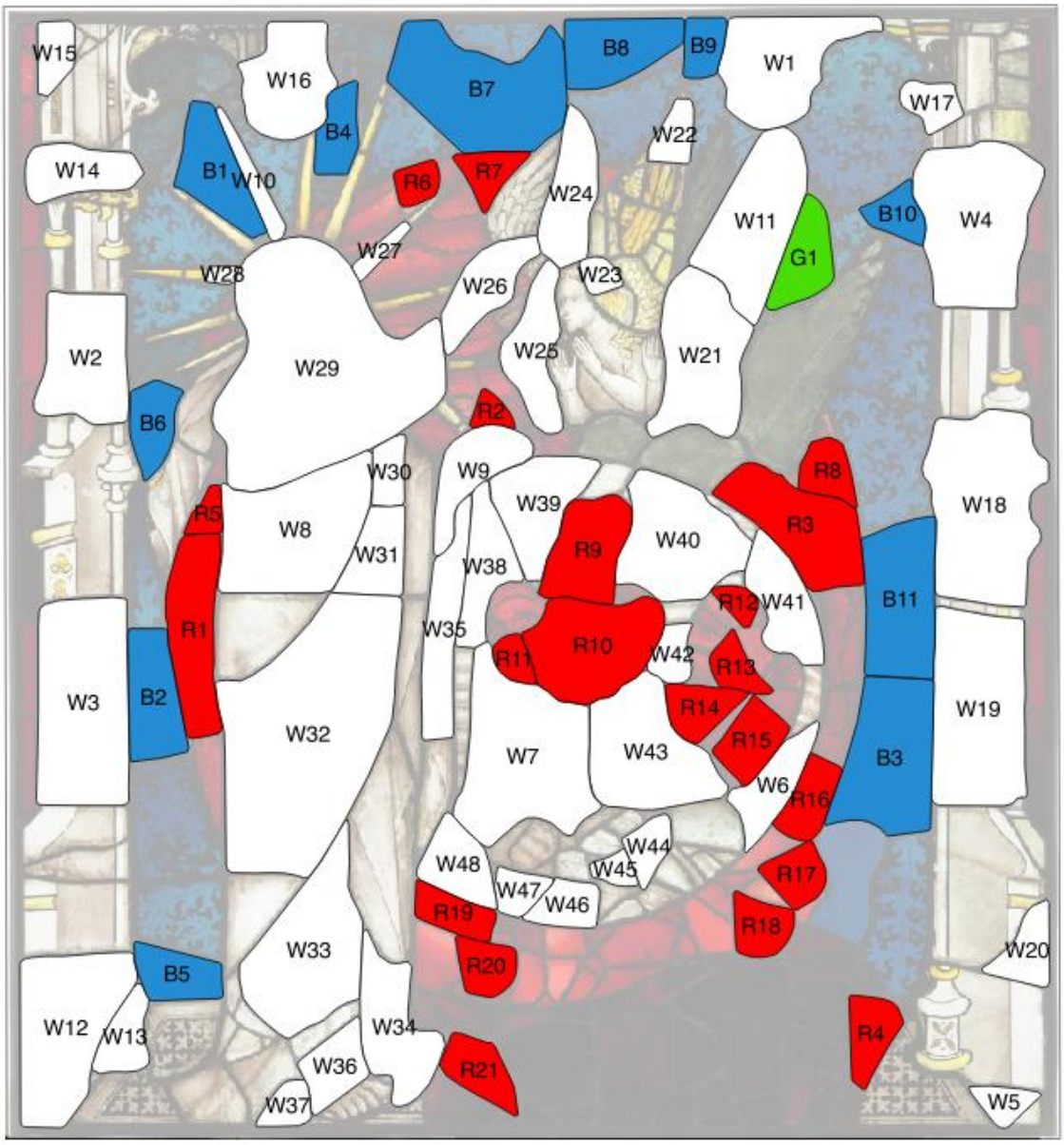

Figure A.18 Sample map of panel 15a.

Analysed by pXRF (81)
W1-W48
B1-B11
R1-R21
G1

Control group (20)
W1-W11
B1-B4
R1-R4
G1

LA-ICP-MS: R4

Figure A.19 Panel 15b. *Photo: The York Glaziers Trust: reproduced with the kind permission of the Chapter of York.*

Subject matter: The Second Day of Creation, *Genesis 1:6-8*. Rays emanate from the Hand of God onto the world below as he separates the heavens and the earth (Brown, 2018; French, 2003).

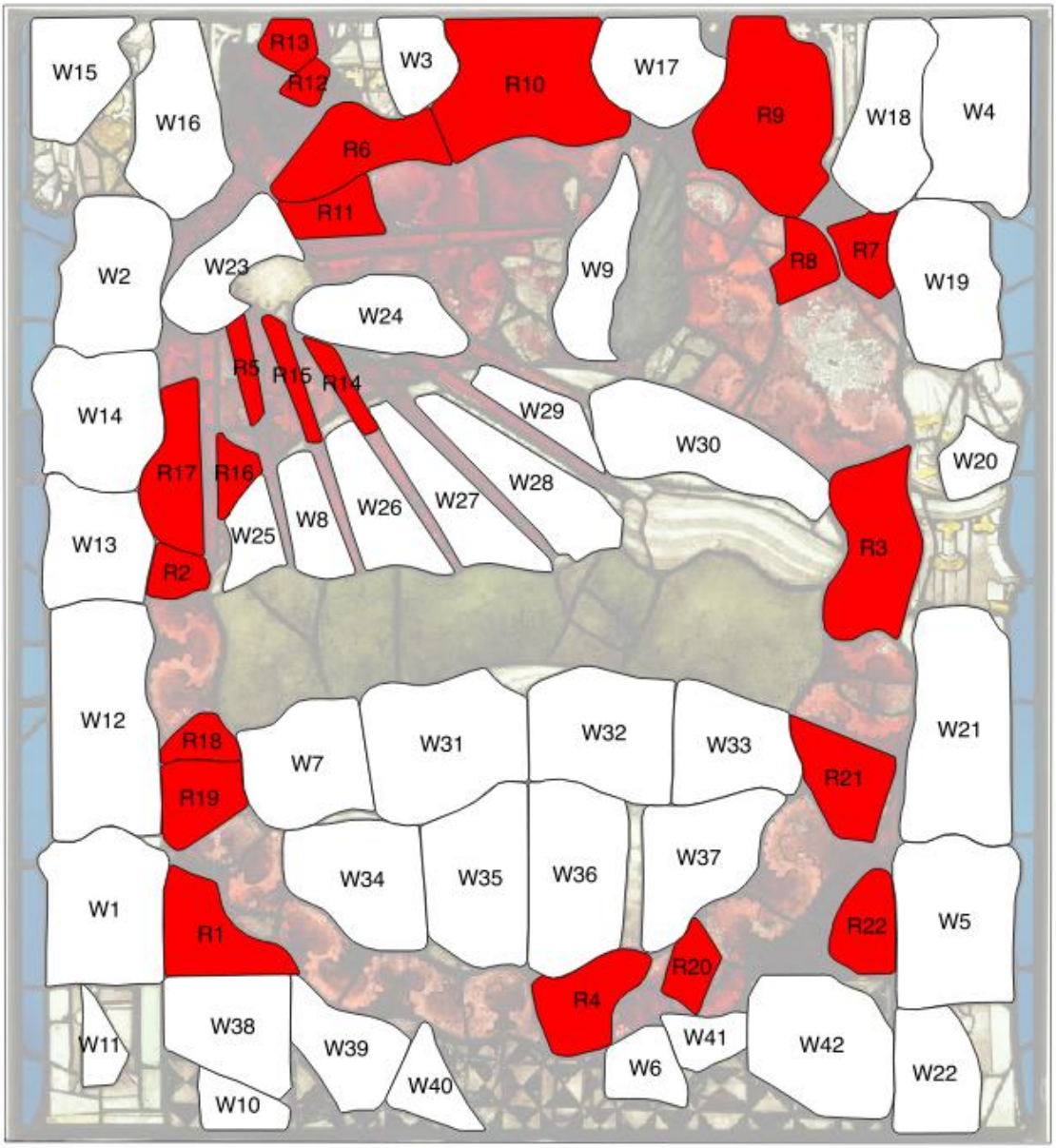

Figure A.20 Sample map of panel 15b.

Analysed by pXRF (64)
W1-W42
R1-R22

Control group (17)
W1-W10
R1-R7

LA-ICP-MS: W5

Figure A.21 Panel 15f. *Photo: The York Glaziers Trust: reproduced with the kind permission of the Chapter of York.*

Subject matter: The Sixth Day of Creation, *Genesis 1:24-31.* Rays emanate from the Hand of God, who blesses the newly created man, Adam (Brown, 2018; French, 2003).

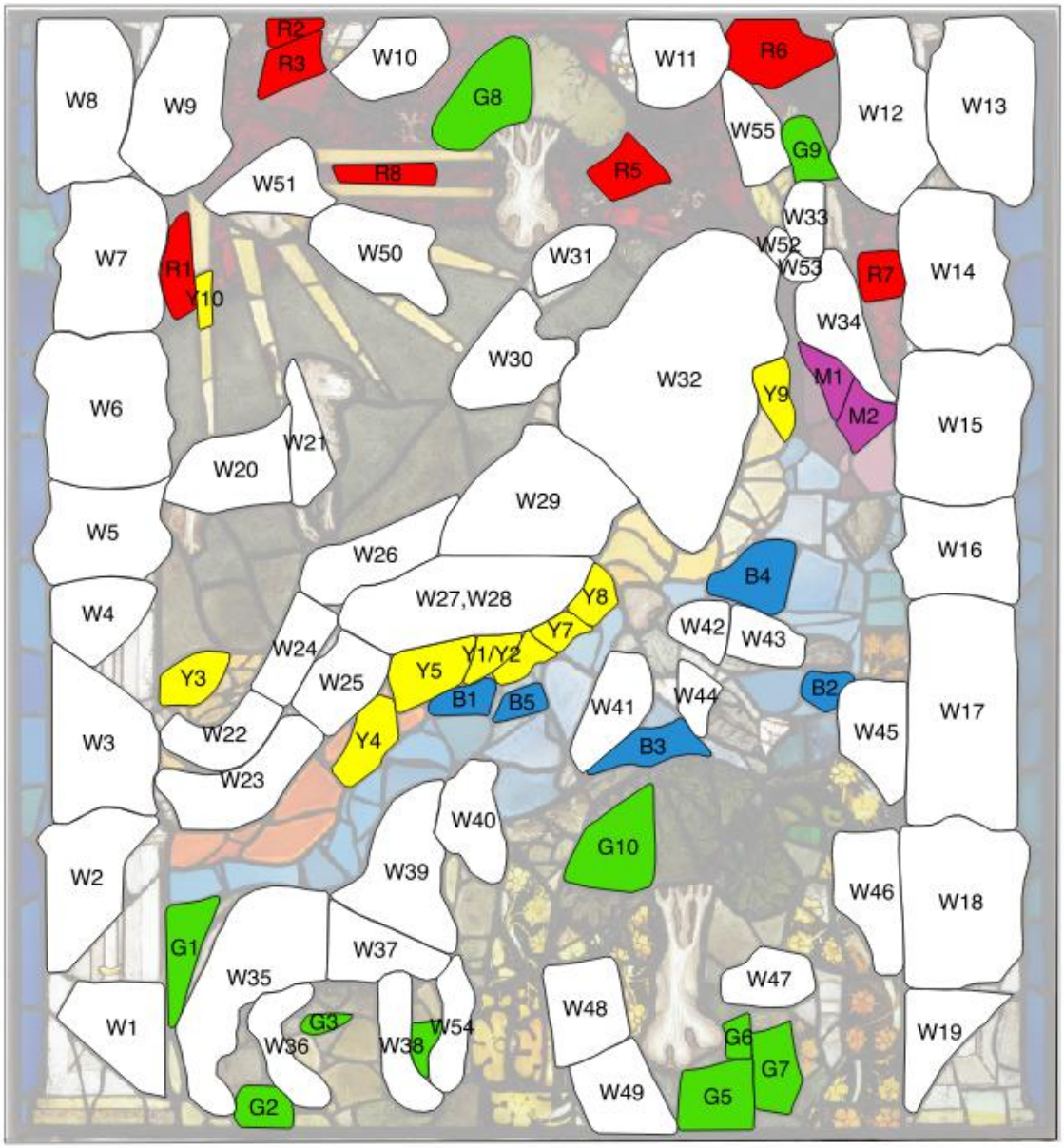

Figure A.22 Sample map of panel 15f.

Analysed by pXRF (90)
W1-W55
B1-B5
R1-R8
G1-G11
M1-M2
Y1-Y10

Control group (6)
B1
G1-G4
Y1

Not pictured: R4 and G11, non-original glass pieces no longer in the panel

Figure A.23 Panel 15g. *Photo: The York Glaziers Trust: reproduced with the kind permission of the Chapter of York.*

Subject matter: The Seventh Day of Creation, *Genesis 2:1-3.*God rests, surrounded by his Creation (Brown, 2018; French, 2003).

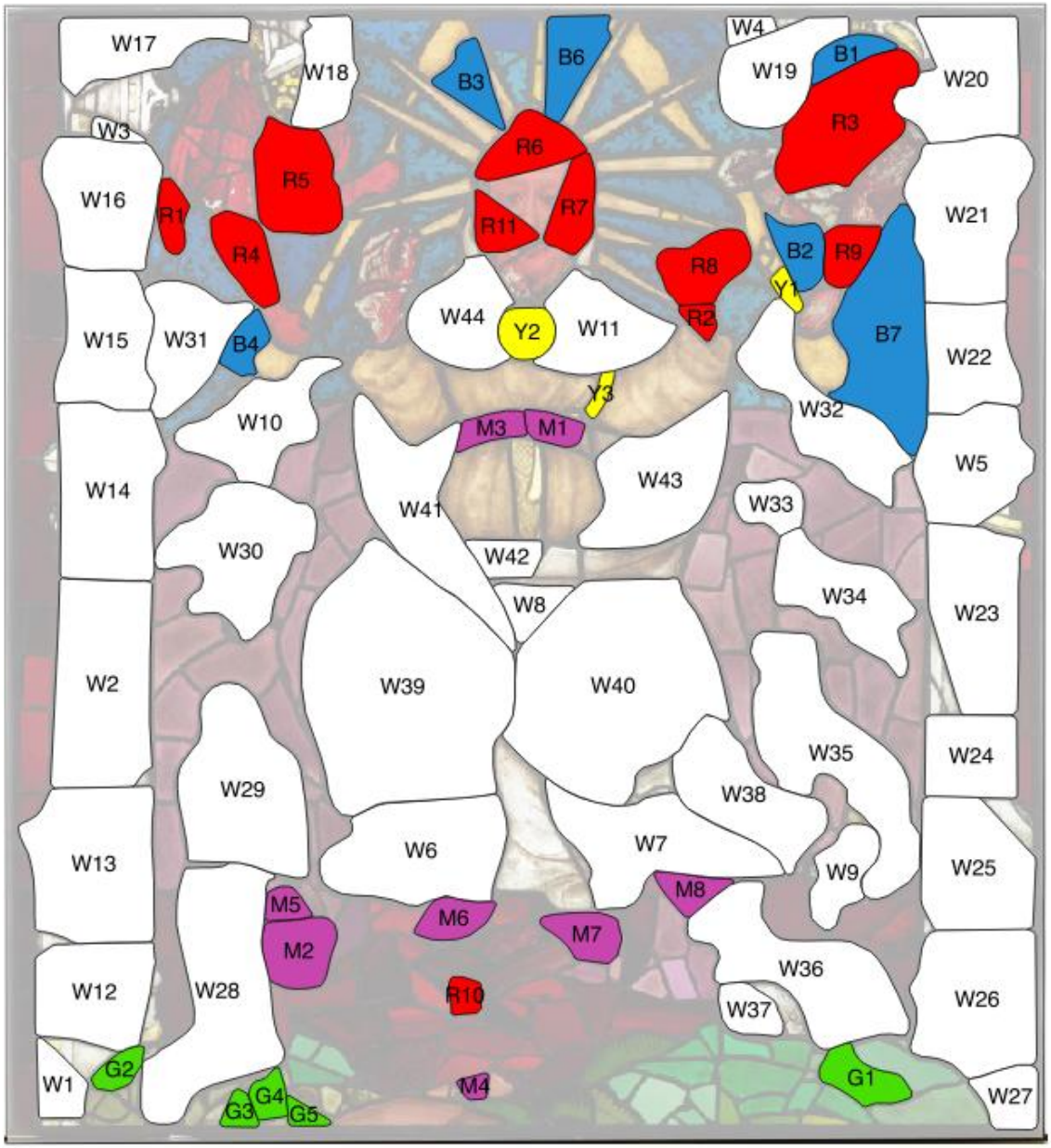

Figure A.24 Sample map of panel 15g.

Analysed by pXRF (78)
W1-W44
B1-B7
R1-R11
G1-G5
M1-M8
Y1-Y3

Not pictured: B5, non-original piece no longer in the panel

Control group (24)
W1-W11
B1-B4
R1-R4
G1-G2
M1-M2
Y1

LA-ICP-MS: G2, M1

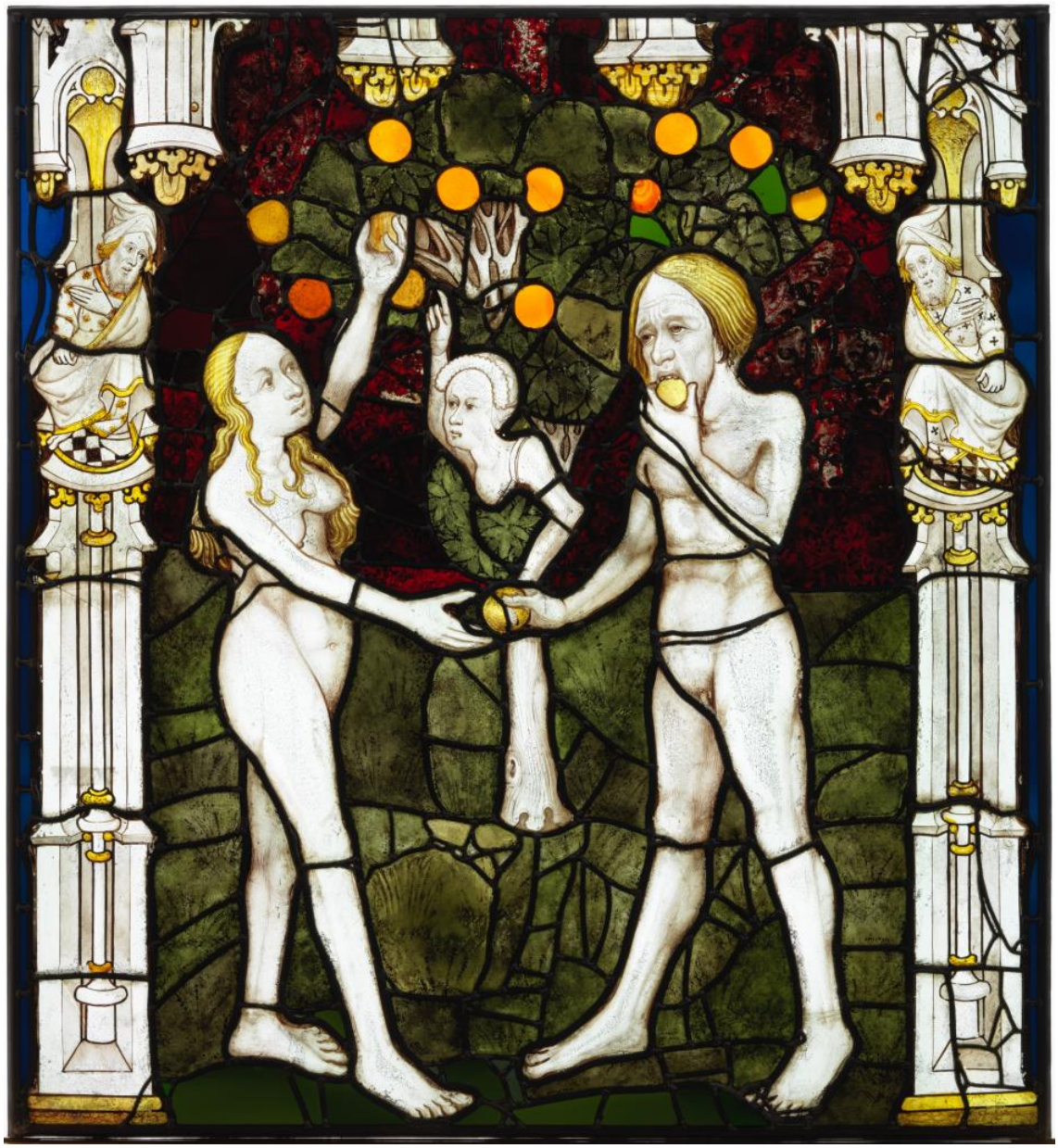

Figure A.25 Panel 15h. *Photo: The York Glaziers Trust: reproduced with the kind permission of the Chapter of York.*

Subject matter: The Temptation and Fall, *Genesis 3:1-6.* Satan points to the fruit on the forbidden Tree of Knowledge of Good and Evil, as Adam takes a bite of fruit and Eve reaches to pick another (Brown, 2018; French, 2003).

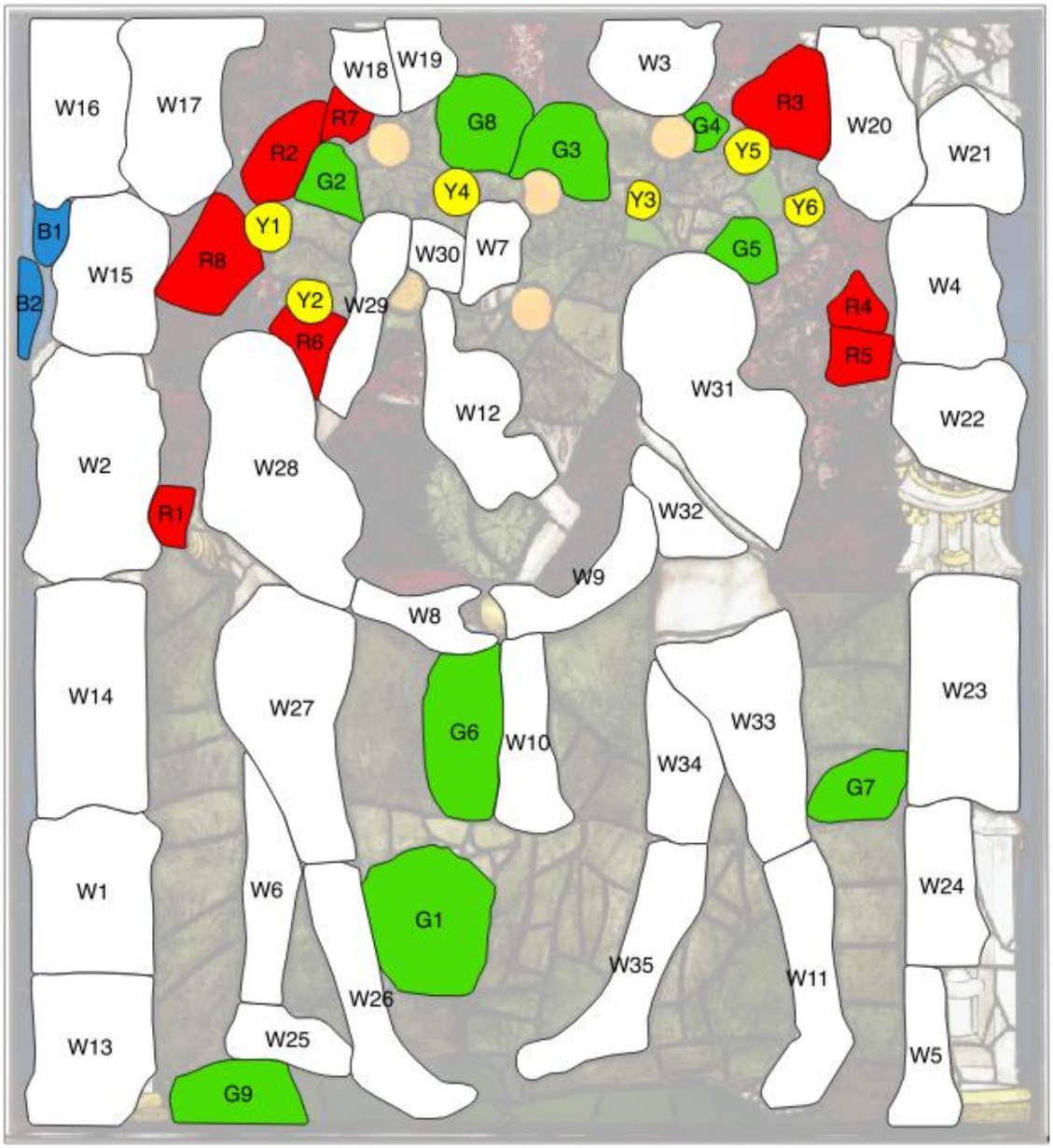

Figure A.26 Sample map of panel 15h.

Analysed by pXRF (60)	Control group (23)
W1-W35	W1-W12
B1-B2	B1
R1-R8	R1-R4
G1-G9	G1-G5
Y1-Y6	Y1

APPENDIX B

Analytical methods: Supplementary information

B.1 EPMA-WDS channels and crystals

The EPMA analyses were carried out over four periods, Summer 2013, Spring 2015, Autumn 2015 and Summer/Autumn 2016. The first analyses (June 2013) were carried out as part of MSc research, and were conducted by Dr. Kevin Reeves. Some details were not shared with me (such as which crystals were used for different elements and which X-ray lines were measured). Subsequent analyses were carried out by myself with help and advice from Dr. Tom Gregory, alongside whom I was trained. As we were both learning as we went along, the channels and crystals changed through the different periods as we learned what worked best through trial and error on standards.

The subsamples were analysed in the following periods:

June 2013: the control group of panel 3b

Spring 2015: selected samples from row 1 (1j-W2, W6, P1, Y1; 1e-W2-3, W5-W7, W10, B1-B4, R2)

Autumn 2015: row 10 samples

Summer/Autumn 2016: the remaining row 1 samples, row 15 samples, LBW samples

Table B.1 EPMA-WDS Spectrometers, Elements, Crystals, and Line

	Channel 1			Channel 2			Channel 3		
Summer 2013	Na Si Mg Al As			Cr Mn Zn Ba Ti V Co Pb Sb Sr			P K Cl S Ca Sn Cu Fe		
Spring 2015	Na	TAP	KA1,2	Ti	LIFH	KA1,2	K	PETJ	KA2
	Mg	TAP	KA1,2	Mn	LIFH	KA2	Ca	PETJ	KA2
	Al	TAP	KA1	Co	LIFH	KA2	Cl	PETJ	KA2
	Si	TAP	KA1	Ni	LIFH	KA2	S	PETJ	KA1
				Cu	LIFH	KA2	P	PETJ	KA1
				Zn	LIFH	KA2	Fe	PETJ	KA1,2
				Sr	PETH	LB1			
				Pb	PETH	MA1			
				Sn	PETH	LA1			
				Ba	PETH	LA1			
Autumn 2015	Na	TAP	KA1,2	Co	LIFH	KA2	Ca	PETJ	KA2
	Mg	TAP	KA1,2	Zn	LIFH	KA2	K	PETJ	KA2
	Al	TAP	KA2	Ba	PETH	LA2	Cl	PETJ	KA2
	Si	TAP	KA2	Fe	LIFH	KA2	S	PETJ	KA2
				Pb	LIFH	MA1	P	PETJ	KA1
				Mn	LIFH	KA2	Cu	LIF	KA1,2
				Sn	PETH	LA1	Ti	LIF	KA1
				Sb	PETH	LB1			
Summer/Autumn 2016	Na	TAP	KA1,2	Co	LIFH	KA2	Ca	PETJ	KA2
	Mg	TAP	KA1,2	Zn	LIFH	KA2	K	PETJ	KA2
	Al	TAP	KA2	Ba	PETH	LA2	Cl	PETJ	KA2
	Si	TAP	KA2	Fe	LIFH	KA2	S	PETJ	KA2
				Pb	PETH	MA1	P	PETJ	KA1
				Mn	LIFH	KA2	Cu	LIF	KA1,2
				Sn	PETH	LA1	Ti	LIF	KA1
				Sb	PETH	LB1			

B.2 Empirical calibrations for the pXRF analyses

Calibrations were made for the different analytical settings: for panel 3b, which was carried out using a DP4000 (a spectrometer that was on loan to the UCL Institute of Archaeology at the time); rows 1 and 15, which were carried out using a DP6000CC (which was subsequently purchased by the UCL Institute of Archaeology); and row 10, which was carried out on panels that had been reinstalled in their lead cames in *in situ* type circumstances. The calibrations for panel 3b and for rows 1 and 15 were based on the analysis of 22 matrix-matched standards, including one glass standard that was made for this research (AD1, see Appendix C), as well as the analysis of a small number of each set by LA-ICP-MS. The standards are listed in Table X.1. Corning D, which was used as a secondary standard to assess the accuracy and precision of the data, was only used for calibrations of the elements Co and Sr, and in these cases were not used as the standard with the highest concentrations as that data point has the most influence over the final calibration factor (Prichard and Barwick, 2003). For the row 10 analysis, since standards could not be analysed under the same conditions (i.e., with variable influence by lead cames), the control group of panel 3b was reanalysed at the same time under the same *in situ* conditions, and empirical calibrations were made based on this reanalysis. The exception is Ni, which is present in low concentrations in the control group of panel 3b and so a calibration curve based on standards (as in Table B.2) was used instead. No calibration was applied to Sn or Pb for panel 3b or rows 1 and 15, as measurements of Corning D were already sufficiently accurate. All calibrations were made using a best-fit linear trendline with the y-intercept set to 0, with the exception of Cu for panel 3b, Co and Zn for rows 1 and 15, and Sn for row 10; for these elements, the calibrations were bracketed as it was observed that a single calibration curve was not adequate for both higher and lower concentrations.

Table B.2 Standards used to make the empirical calibrations on the pXRF data. *AD1 was not available at the time of the panel 3b calibrations.

	K	Ca	Ti	Mn	Fe	Co	Ni	Cu	Zn	Rb	Sr	Zr
Corning A	X		X	X	X	X				X	X	X
Corning D						X					X	
Corning B	X		X	X	X	X	X			X	X	X
Newton 76-C-144				X	X							
Newton 76-C-145				X			X		X			
Newton 76-C-147		X	X					X	X		X	
Newton 76-C-148		X		X	X		X					
Newton 76-C-149	X	X	X	X				X				
Newton 76-C-150	X				X	X			X			
Newton 76-C-151	X	X	X	X								
Newton 76-C-158				X			X		X			
Newton 76-C-159		X		X	X			X				
Newton 77-C-33			X		X							
Sheffield 1	X	X			X							
NIST 612			X	X	X	X	X			X	X	
NIST 614							X				X	
SGT 4	X	X	X						X			
SGT 7	X	X	X									
SGT 11	X		X		X							X
Standardglas 1	X	X	X		X							
Standardglas 2			X		X							
AD1*	X	X			X	X		X	X	X	X	X
GEW samples	X	X	X	X	X	X	X	X	X	X	X	X

B.2.1 Empirical calibrations for the panel 3b analyses

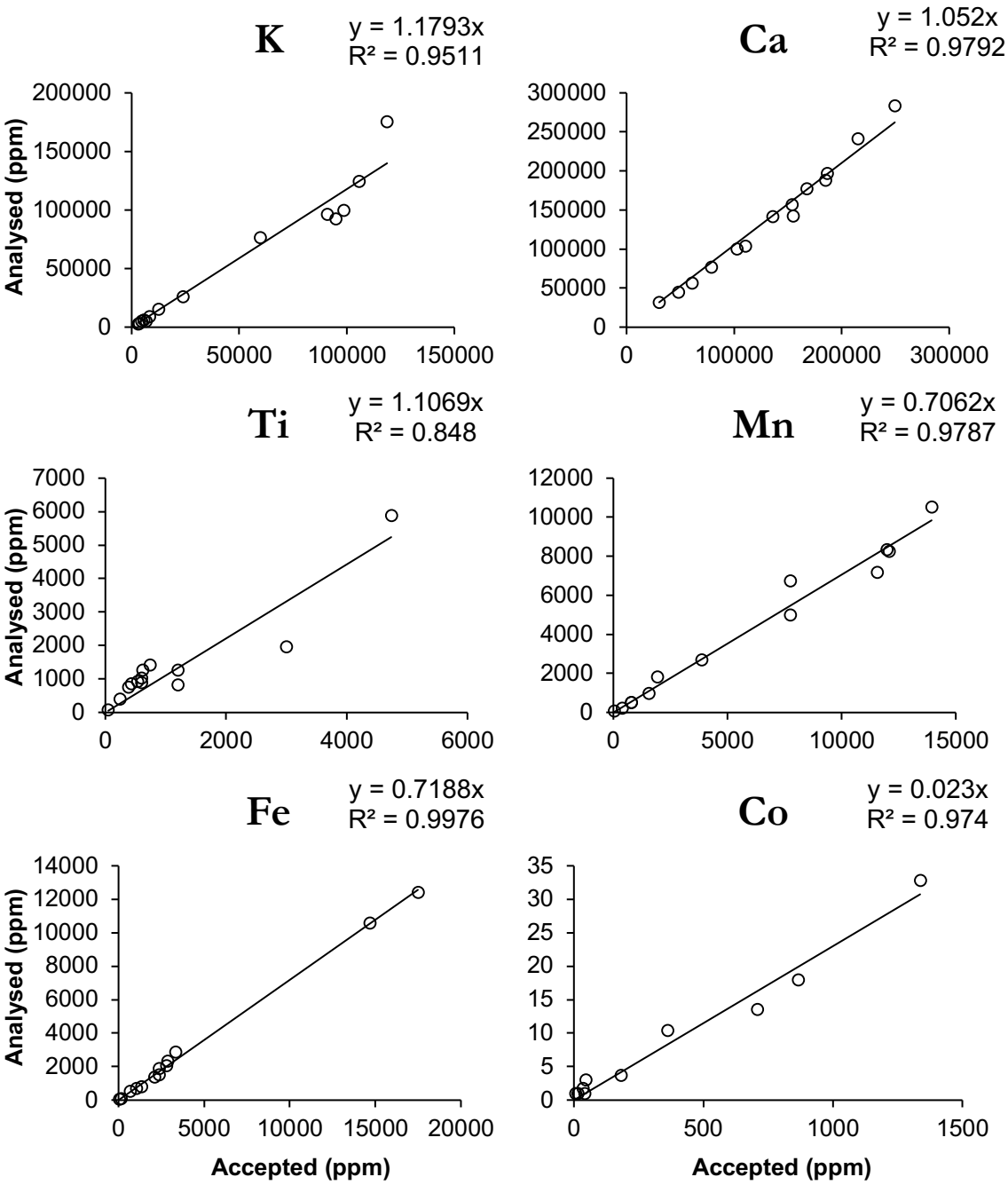

Figure B.1 Calibration curves for the pXRF analyses carried out on panel 3b. All graphs show Analysed values (ppm) against accepted values for standards (or, for GEW sampes, the result given by LA-ICP-MS). Continued next page.

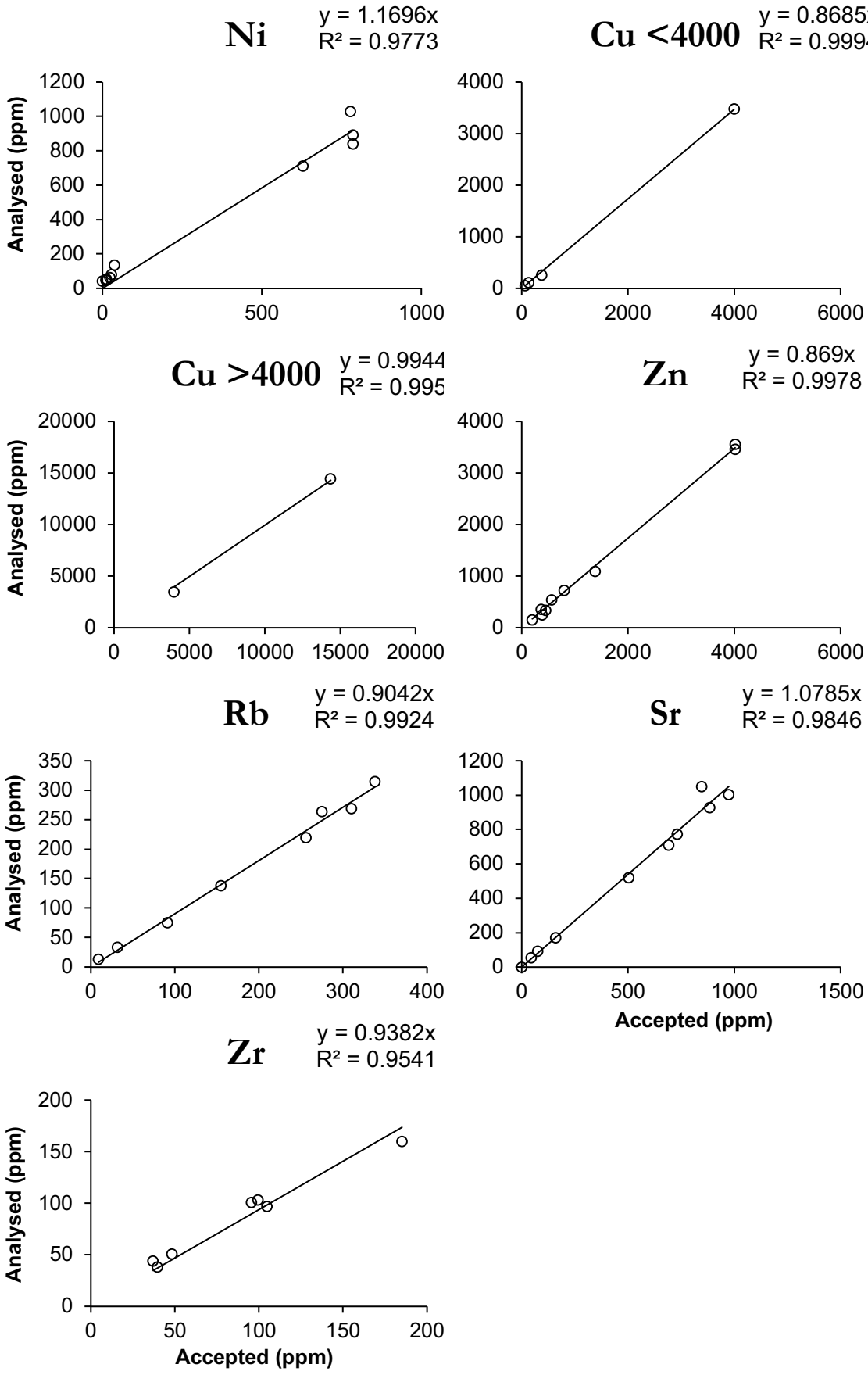
Ni
y = 1.1696x
R² = 0.9773
Analysed (ppm)
Cu <4000
y = 0.8685x
R² = 0.9994
Cu >4000
y = 0.9944
R² = 0.995
Zn
y = 0.869x
R² = 0.9978
Rb
y = 0.9042x
R² = 0.9924
Sr
y = 1.0785x
R² = 0.9846
Accepted (ppm)
Zr
y = 0.9382x
R² = 0.9541
Analysed (ppm)
Accepted (ppm)

B.2.2 Empirical calibrations for the rows 1 and 15 analyses

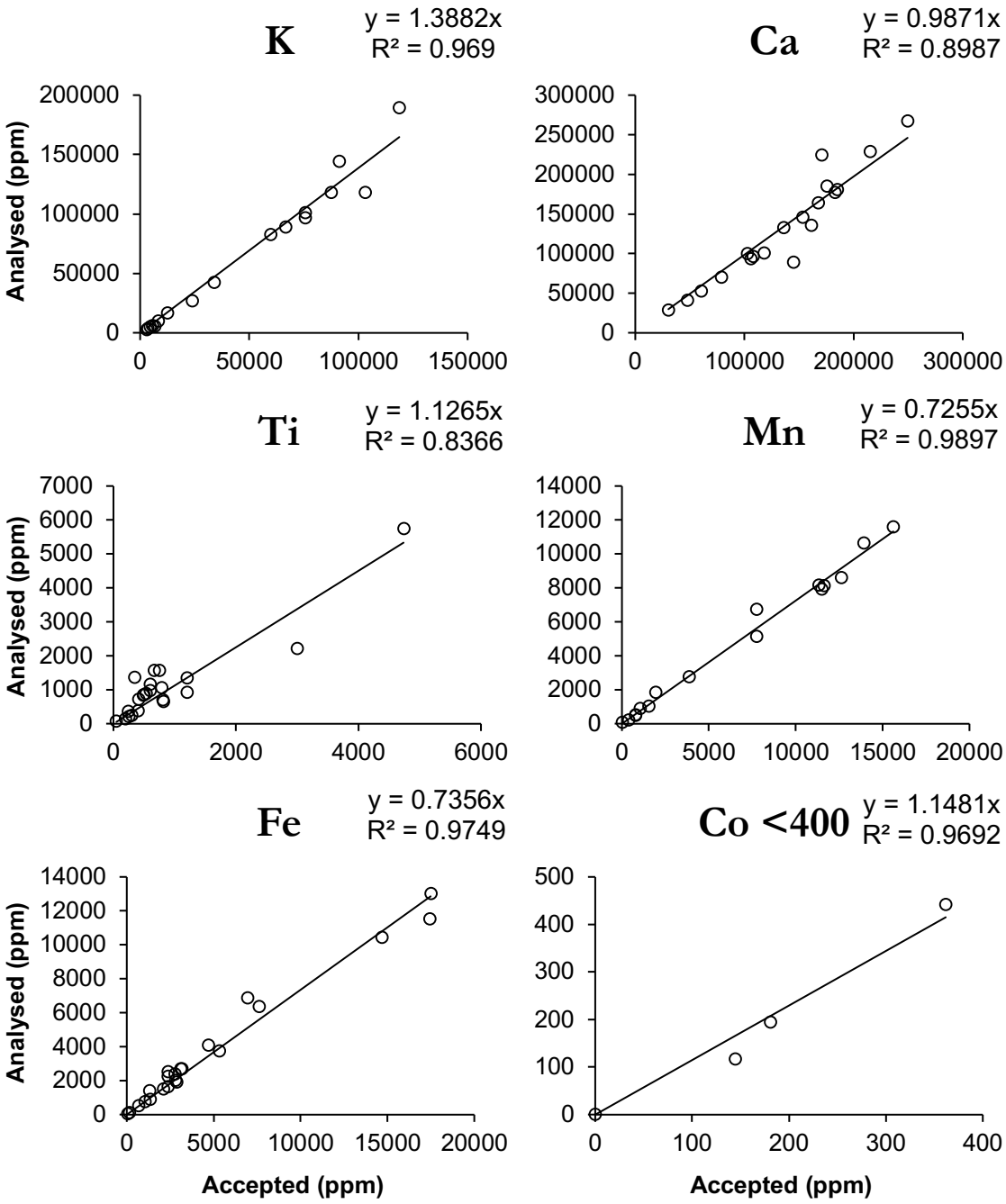

Figure B.2 Calibration curves for the pXRF analyses carried out on rows 1 and 15. All graphs show Analysed values (ppm) against accepted values for standards (or, for GEW sampes, the result given by LA-ICP-MS). Continued next page.

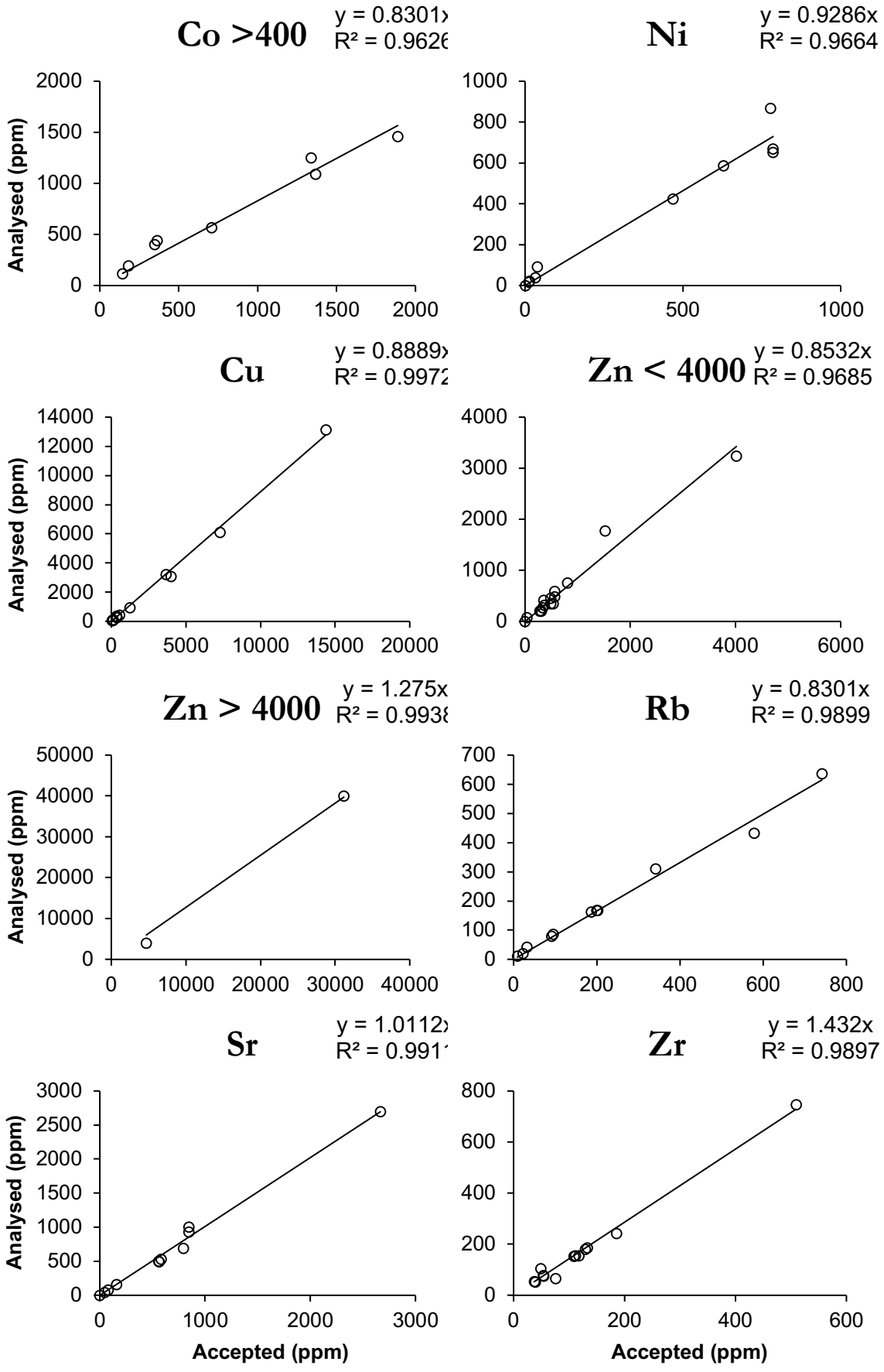
Co >400
y = 0.8301x
R² = 0.9626
Ni
y = 0.9286x
R² = 0.9664
Cu
y = 0.8889x
R² = 0.9972
Zn < 4000
y = 0.8532x
R² = 0.9685
Zn > 4000
y = 1.275x
R² = 0.9938
Rb
y = 0.8301x
R² = 0.9899
Sr
y = 1.0112x
R² = 0.9911
Zr
y = 1.432x
R² = 0.9897
Analysed (ppm)
Accepted (ppm)

B.2.3 Empirical calibrations for the row 10 analyses

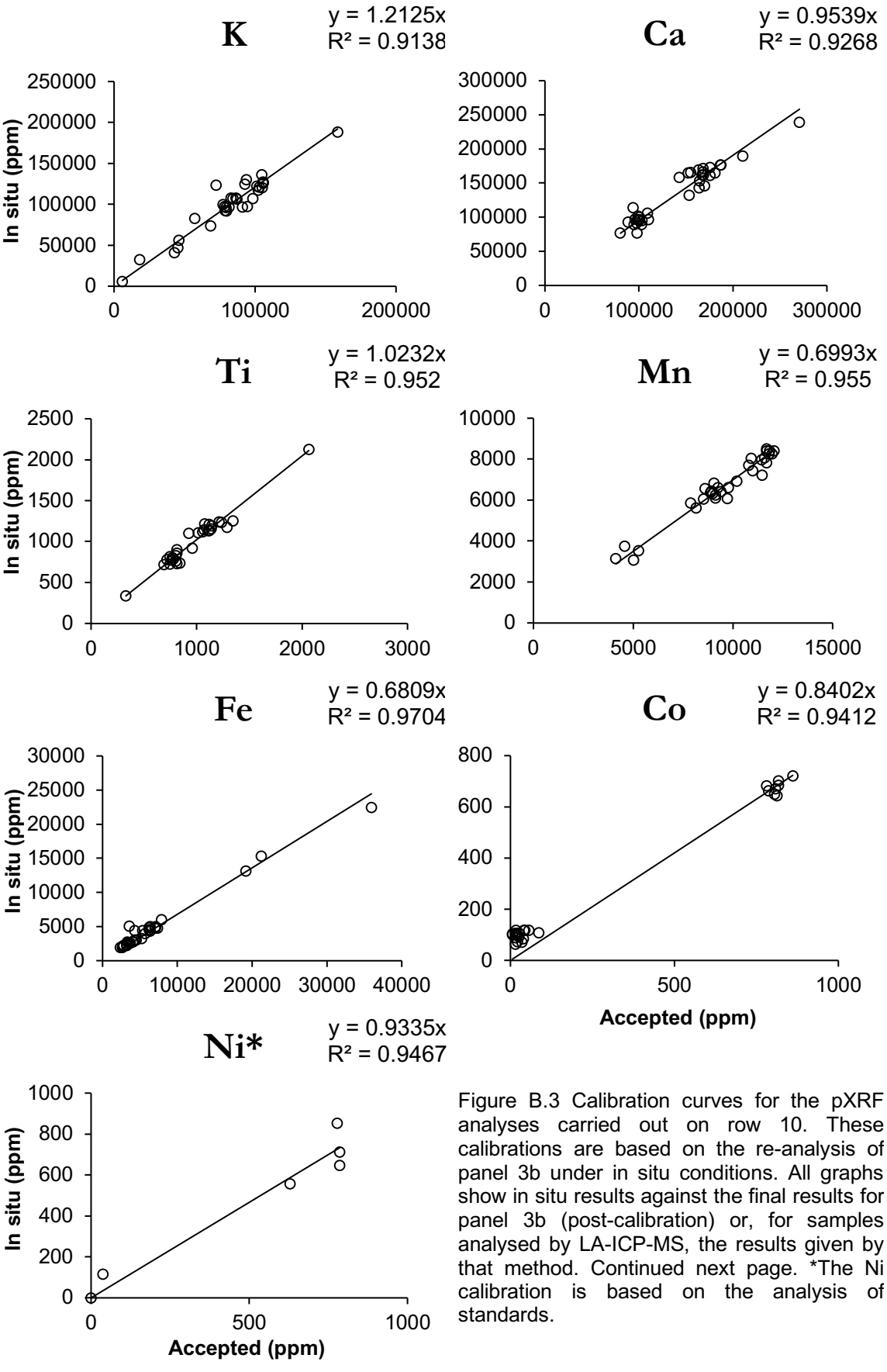

Figure B.3 Calibration curves for the pXRF analyses carried out on row 10. These calibrations are based on the re-analysis of panel 3b under in situ conditions. All graphs show in situ results against the final results for panel 3b (post-calibration) or, for samples analysed by LA-ICP-MS, the results given by that method. Continued next page. *The Ni calibration is based on the analysis of standards.

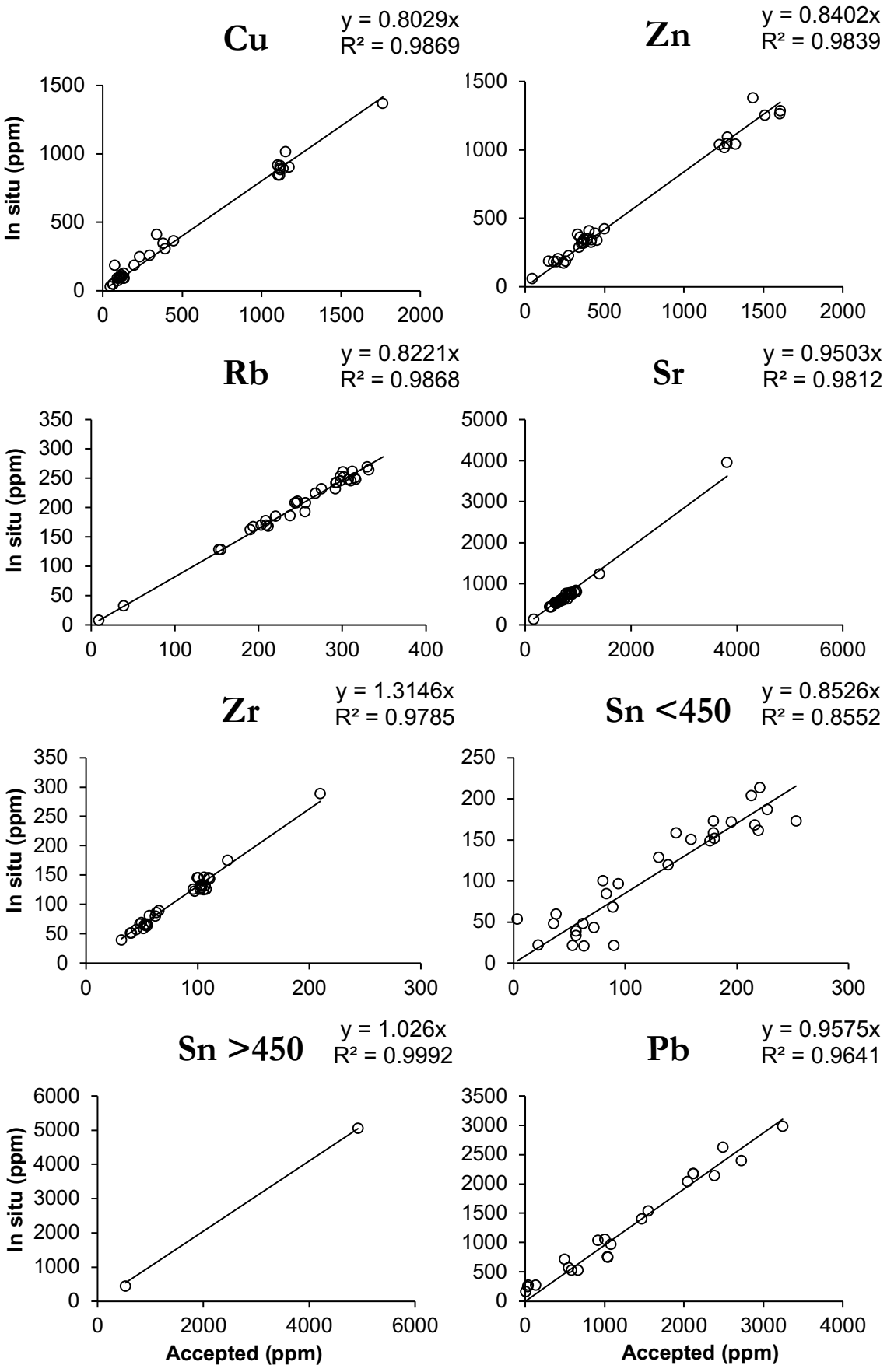
Cu
y = 0.8029x
R² = 0.9869
Zn
y = 0.8402x
R² = 0.9839
Rb
y = 0.8221x
R² = 0.9868
Sr
y = 0.9503x
R² = 0.9812
Zr
y = 1.3146x
R² = 0.9785
Sn <450
y = 0.8526x
R² = 0.8552
Sn >450
y = 1.026x
R² = 0.9992
Pb
y = 0.9575x
R² = 0.9641
In situ (ppm)
Accepted (ppm)

APPENDIX C

UCL Reference Glasses AD1, AD2 and AD3, based on medieval forest glass compositions

Three glass standards approximating medieval glass compositions were created as part of this PhD, although only the first (AD1) was made and characterised in time to include it in empirical calibrations on the pXRF data. Although other glass standards exist which resemble medieval compositions (including Corning D and the Newton Pilkington standards), none of these have an adequate range of trace elements.

A second aim of this project was to create the standards with relatively little expense; chemicals that were already owned by UCL (the Institute of Archaeology or the Department of Chemistry) were used, of variable purity, and the standards were melted in ceramic crucibles that likely added contamination to the batches. Contamination is regarded as unimportant, however, as long as the standard was homogeneous and ultimately well characterised.

C.1 Preparation of the standards

The raw materials were mixed together at the UCL Institute of Archaeology Wolfson Archaeological Laboratories and were calculated to yield approximately 200g of glass. The raw materials were weighed out in the proportions reported in **Error! Reference source not found.**, beginning with the smallest concentrations, and thoroughly stirred between each addition. Melting of AD3 resulted in visible heterogeneity on the surface (possible due to local reduction of copper, forming a streak of red glass), so that glass was pulverised with a ball mill and remelted.

Table C.1 Preparation of the AD standards: the below amounts of each raw material were weighed out and thoroughly mixed together before melting.

	AD1	**AD2**	**AD3**
Na_2CO_3	3.890	7.271	1.008
MgO	6.870	9.602	14.800
Al_2O_3	2.420	1.400	5.999
SiO_2	102.100	119.240	89.400
$Ca_3O_8P_2$	7.940	12.236	28.406
NaCl	1.980	3.298	1.154
K_2CO_3	38.240	24.356	59.863
$CaCO_3$	83.370	46.385	15.336
TiO_2	0.200	0.101	0.500
MnO_2	4.180	4.903	2.223
Fe_2O_3	1.430	0.342	2.399
CuO	1.010	0.201	2.002
CoO	0.500	0.200	0.101
$BaCO_3$	0.650	1.288	0.257
$SrCO_3$	0.337	0.134	0.674
Rb_2CO_3	0.274	0.095	0.034
ZrO_2	0.135	0.014	0.054
La_2O_3	0.047	0.005	0.024
ZnO	0.125	0.498	0.996
PbO	0.107	0.022	0.216
NiO		0.128	0.254
B_2O_3		0.064	0.129
SnO_2		0.055	0.634
Sb_2O_3		0.010	0.024
Y_2O_3		0.004	0.008
Nb_2O_5		0.002	0.005

The standards were melted by Mark Taylor of the Roman Glassmakers, using a ceramic crucible with a lid. The crucibles were made with 60% powdered (120 grit) molochite (calcined kaolin), 30% powdered kaolin, 10% powdered ball clay and a very small amount of deflocculent (c. 1 level teaspoon each of sodium carbonate and sodium silicate dissolved in a yoghurt-potful of boiling water). The slip is made with 10kg of mixed powder to 4.0-4.5 litres of cold water. The crucibles and lids are slipcast using small plaster moulds. They were allowed to dry, then fired to 1400°C.

The glasses were melted in a propane gas furnace at 1350°C for 4.5 hours, with a c. 15s stir using a stainless steel rod every 30 minutes, so seven stirs over the melting period; the rod was cleaned between stirs to remove the remains of glass from the previous stir. They were then annealed at 600°C.

C.2 Elemental analysis by EPMA-WDS and LA-ICP-MS

The standards were characterised by EPMA-WDS at the UCL Institute of Archaeology under the methods reported in this thesis. The AD standards are currently being analysed by several laboratories as part of an analytical round robin for LA-ICP-MS

Table C.2 Analysis of the standards by EPMA-WDS and LA-ICP-MS, showing the mean and standard deviation.

	EPMA						LA-ICP-MS					
(wt%)	AD1		AD2		AD3		AD1		AD2		AD3	
Na_2O	1.61	*0.03*	2.89	*0.11*	0.95	*0.04*	1.75	*0.06*	2.91	*0.08*	0.91	*0.03*
MgO	2.59	*0.02*	4.48	*0.15*	7.18	*0.10*	2.62	*0.05*	4.26	*0.18*	6.43	*0.05*
Al_2O_3	2.23	*0.10*	1.19	*0.01*	3.71	*0.01*	2.08	*0.11*	1.17	*0.09*	3.53	*0.25*
SiO_2	52.0	*0.43*	61.4	*0.31*	47.6	*0.10*	51.0	*1.19*	61.2	*1.14*	45.8	*0.56*
P_2O_5	1.67	*0.05*	2.17	*0.02*	5.00	*0.07*	1.56	*0.22*	2.47	*0.30*	5.62	*0.56*
Cl	0.13	*0.01*	0.33	*0.01*	0.04	*0.00*	0.15	*0.04*	0.34	*0.06*	0.07	*0.02*
K_2O	10.89	*0.21*	6.99	*0.05*	18.71	*0.32*	11.32	*0.32*	6.99	*0.26*	18.74	*0.82*
CaO	24.53	*0.37*	14.94	*0.26*	10.92	*0.01*	24.94	*0.76*	16.71	*0.76*	12.75	*0.51*
TiO_2	0.09	*0.02*	0.07	*0.01*	0.27	*0.00*	0.13	*0.04*	0.07	*0.01*	0.26	*0.02*
MnO	1.47	*0.03*	2.05	*0.01*	0.85	*0.00*	1.47	*0.06*	1.97	*0.15*	0.81	*0.04*
Fe_2O_3	0.69	*0.12*	0.25	*0.00*	1.66	*0.02*	0.82	*0.16*	0.31	*0.04*	1.67	*0.27*
CoO	0.24	*0.01*	0.10	*0.02*	0.04	*0.01*	0.24	*0.01*	0.10	*0.00*	0.05	*0.00*
CuO	0.45	*0.03*	0.06	*0.04*	0.91	*0.05*	0.48	*0.04*	0.10	*0.01*	0.92	*0.11*
ZnO	0.06	*0.02*	0.26	*0.01*	0.55	*0.04*	0.07	*0.00*	0.29	*0.02*	0.58	*0.07*
SnO_2	<		0.03	*0.00*	0.30	*0.03*						
BaO	0.27	*0.02*	0.48	*0.10*	0.14	*0.02*	0.25	*0.01*	0.48	*0.05*	0.11	*0.00*
PbO	0.07	*0.02*	<		0.14	*0.01*	0.05	*0.01*	0.01	*0.00*	0.10	*0.01*
					(ppm)	**B**	12	*2.9*	85	*19*	106	*17*
						Ni	22	*6.4*	572	*40*	1276	*89*
						Rb	762	*28*	250	*9.3*	137	*4.4*
						Sr	1028	*33*	456	*36*	1912	*206*
						Y	3.1	*0.6*	17	*0.8*	30	*2.1*
						Zr	556	*48*	69	*6.3*	231	*22*
						Nb	1.6	*0.3*	3.6	*0.6*	18	*1.1*
						La	211	*6.2*	16	*1.1*	89	*2.9*
						Sn	3.8	*1.0*	194	*18*	2215	*255*
						Sb	2.1	*0.8*	36	*2.9*	84	*8.1*

analysis of glass and ceramics under the leadership of Dr. Laure Dussubieux of the Field Museum. The below results (Table C.2) are preliminary, based on the results of five laboratories and the final recommended compositions will be updated upon completion of the round robin.

C.3 Recommended compositions based on elemental analysis

The following (Table C.3) are preliminary recommended compositions, determined based on the analysis by EPMA-WDS and LA-ICP-MS (Table C.2).

Table C.3 Preliminary recommended compositions of AD1, AD2 and AD3.

	AD1	AD2	AD3
Na_2O	1.61	2.89	0.95
MgO	2.59	4.48	7.18
Al_2O_3	2.23	1.19	3.71
SiO_2	52.02	61.38	47.63
P_2O_5	1.67	2.17	5.00
SO_3	0.04	0.05	0.04
Cl	0.13	0.33	0.04
K_2O	10.89	6.99	18.71
CaO	24.53	14.94	10.92
TiO_2	0.09	0.07	0.27
MnO	1.47	2.05	0.85
Fe_2O_3	0.69	0.25	1.66
CoO	0.24	0.10	0.05
CuO	0.45	0.10	0.91
ZnO	0.07	0.26	0.55
BaO	0.27	0.48	0.14
PbO	0.05	0.01	0.10
B	12.3	85	106
Ni	21.8	572	1276
Rb	762	250	137
Sr	1028	456	1912
Y	3.1	17	30
Zr	556	69	231
Nb	1.6	3.6	18
La	211	16	89
Sn	3.8	194	2215
Sb	2.1	36	84
Total	99.31	97.90	99.31

APPENDIX D

Results of the chemical analyses

Table D.1 EPMA-WDS results, in weight percent with oxides calculated by stoichiometry. ND = not detected. BD = below detection, or <0.03%. The identification of the sample as original or another type of glass is given in the right-most column.

Sample	Na_2O	MgO	Al_2O_3	SiO_2	P_2O_5	SO_3	Cl	K_2O	CaO	TiO_2	MnO	Fe_2O_3	CoO	CuO	ZnO	SnO_2	Sb_2O_5	BaO	PbO	Total	ID
1e-W1	2.42	7.56	1.44	58.7	3.22	0.17	0.25	9.20	15.35	0.07	1.43	0.48	BD	BD	0.04	BD	ND	0.16	0.07	100.49	Original
1e-W2	2.62	7.40	1.51	56.6	3.21	0.17	0.29	9.33	15.01	0.07	1.46	0.50	ND	BD	0.06	ND	ND	0.18	0.07	98.63	Original
1e-W3	2.47	7.45	1.46	56.6	3.11	0.19	0.30	9.53	15.43	0.07	1.48	0.48	ND	BD	0.06	BD	ND	0.19	0.06	99.07	Original
1e-W4	2.96	7.73	1.45	58.1	3.15	0.17	0.29	9.21	14.89	0.06	1.48	0.48	BD	BD	0.04	BD	BD	0.17	0.06	100.20	Original
1e-W5	2.28	7.46	1.44	57.3	3.20	0.18	0.25	9.13	15.07	0.07	1.40	0.43	ND	BD	0.04	ND	ND	0.16	0.04	98.60	Original
1e-W6	2.28	7.41	1.44	57.3	3.18	0.18	0.25	9.09	15.06	0.07	1.41	0.45	ND	BD	0.06	ND	ND	0.18	0.04	98.55	Original
1e-W7	2.57	7.26	1.50	56.3	3.32	0.17	0.32	9.46	15.30	0.07	1.44	0.48	ND	BD	0.04	ND	ND	0.18	0.08	98.68	Original
1e-W8	2.61	7.14	1.49	56.5	3.16	0.16	0.32	9.07	15.60	0.07	1.42	0.53	BD	0.03	0.04	BD	ND	0.16	0.10	98.30	Original
1e-W9	2.62	7.17	1.48	56.7	3.18	0.17	0.31	9.23	15.70	0.07	1.43	0.52	BD	BD	0.04	BD	BD	0.17	0.10	98.84	Original
1e-W10	2.49	7.32	1.42	57.5	3.17	0.18	0.30	9.18	14.68	0.07	1.43	0.44	ND	BD	0.04	ND	ND	0.18	0.12	98.66	Original
1e-W11	2.37	7.40	1.44	57.5	3.14	0.16	0.24	8.97	15.42	0.06	1.40	0.50	BD	BD	0.06	BD	BD	0.16	0.06	98.87	Original
1e-W48	2.68	7.29	1.48	58.0	3.24	0.13	0.28	9.39	14.68	0.07	1.47	0.54	BD	BD	0.05	BD	BD	0.17	0.09	99.57	Original
1e-B3	1.23	4.20	1.79	50.9	3.38	0.18	0.04	10.00	23.80	0.08	1.29	1.15	0.14	0.27	0.43	BD	ND	0.25	0.20	99.50	Original
1e-B6	1.38	4.29	1.82	50.2	3.71	0.16	0.05	9.86	24.17	0.08	1.19	1.04	0.13	0.24	0.28	BD	ND	0.24	0.22	99.02	Original
1e-R1	1.06	4.37	1.66	51.8	3.34	0.16	0.06	9.86	24.83	0.07	1.36	0.52	BD	0.07	BD	BD	ND	0.28	0.19	99.59	Original
1e-B1	1.47	3.51	2.82	52.7	4.09	0.04	0.30	7.43	22.79	0.07	2.06	0.69	0.13	0.16	BD	ND	ND	0.29	BD	98.87	Original? HLLA
1e-B2	1.47	3.56	2.84	53.1	4.08	0.05	0.30	7.48	23.02	0.07	2.07	0.69	0.14	0.16	0.03	ND	ND	0.31	BD	99.57	Original? HLLA
1e-B4	1.45	3.53	2.81	52.7	4.07	0.04	0.30	7.45	22.96	0.06	2.05	0.69	0.14	0.16	0.03	ND	ND	0.30	BD	99.01	Original? HLLA
1e-B5	1.48	3.54	2.79	53.0	4.02	0.06	0.28	7.25	23.00	0.05	2.05	0.74	0.17	0.17	0.03	BD	BD	0.30	BD	98.92	Original? HLLA
1e-R2	1.50	5.26	3.30	51.8	4.33	0.16	0.38	15.59	14.33	0.17	0.90	0.98	ND	0.10	0.06	ND	ND	0.21	BD	99.18	Medieval
1e-R3	2.16	4.79	2.20	55.7	3.47	0.07	0.45	12.38	15.79	0.10	0.96	0.59	BD	0.19	0.04	BD	ND	0.11	0.08	99.01	Medieval
1j-W1	2.61	7.26	1.42	56.5	3.20	0.21	0.34	9.90	16.20	0.06	1.46	0.50	BD	BD	0.06	BD	BD	0.18	0.11	99.91	Original
1j-W2	2.54	7.40	1.42	55.7	3.26	0.22	0.34	10.13	15.88	0.07	1.47	0.43	ND	BD	0.06	ND	ND	0.20	0.09	99.34	Original
1j-W3	2.55	7.42	1.44	57.1	2.97	0.18	0.30	9.03	15.41	0.07	1.44	0.48	BD	BD	0.05	BD	ND	0.17	0.08	98.58	Original
1j-W4	2.62	7.35	1.41	56.4	3.12	0.22	0.34	9.85	16.44	0.05	1.47	0.50	BD	BD	0.05	BD	ND	0.18	0.11	100.09	Original
1j-W5	2.62	7.45	1.46	57.8	3.03	0.18	0.31	9.42	15.83	0.06	1.49	0.42	BD	BD	0.04	BD	ND	0.18	0.07	100.41	Original
1j-W6	2.46	7.52	1.45	57.1	3.07	0.19	0.30	9.38	15.43	0.07	1.47	0.45	ND	BD	0.04	ND	ND	0.20	0.07	99.39	Original
1j-W7	2.41	7.46	1.44	58.4	3.05	0.21	0.26	8.97	15.40	0.07	1.42	0.48	BD	BD	0.04	BD	ND	0.17	0.06	99.80	Original
1j-W39	2.66	7.26	1.40	56.2	3.25	0.18	0.33	10.08	15.43	0.07	1.47	0.42	BD	0.04	0.05	BD	BD	0.19	0.12	99.08	Original
1j-B1	1.11	4.23	1.64	50.5	2.97	0.15	0.04	10.81	24.58	0.07	1.20	0.91	0.10	0.18	0.19	BD	ND	0.29	0.15	99.10	Original
1j-R1	1.02	4.38	1.64	50.1	3.34	0.16	0.04	10.25	25.46	0.08	1.39	0.48	BD	0.06	BD	BD	ND	0.26	0.17	98.80	Original
1j-R2	1.05	4.34	1.65	51.1	3.28	0.17	0.07	9.82	25.12	0.07	1.32	0.51	BD	0.08	BD	BD	ND	0.26	0.20	99.06	Original
1j-R3	1.18	4.43	1.59	49.7	3.46	0.20	0.05	10.48	26.67	0.06	1.43	0.49	BD	0.09	BD	BD	ND	0.28	0.50	100.60	Original

Sample	Na_2O	MgO	Al_2O_3	SiO_2	P_2O_5	SO_3	Cl	K_2O	CaO	TiO_2	MnO	Fe_2O_3	CoO	CuO	ZnO	SnO_2	Sb_2O_5	BaO	PbO	Total	ID
1j-M1	0.41	3.98	0.54	49.9	1.65	0.33	BD	18.77	20.92	BD	1.62	0.15	BD	0.04	BD	ND	ND	0.43	BD	98.96	Original (B)
1j-Y1	1.33	3.63	3.11	53.2	4.01	0.04	0.36	6.77	23.27	0.11	1.83	0.44	ND	BD	BD	ND	ND	0.31	BD	98.68	Original? HLLA
1h-W1	2.42	7.32	1.44	58.3	3.17	0.20	0.25	9.18	15.11	0.06	1.42	0.48	BD	BD	0.04	ND	BD	0.17	0.06	99.64	Original
1h-W2	2.40	7.26	1.45	58.1	3.18	0.20	0.25	9.22	14.96	0.08	1.40	0.48	BD	BD	0.06	BD	ND	0.16	0.07	99.28	Original
1h-W3	2.54	7.35	1.44	57.4	3.00	0.16	0.29	9.32	15.37	0.07	1.47	0.49	BD	BD	0.05	BD	ND	0.18	0.08	99.28	Original
1h-W4	2.42	7.37	1.44	58.2	3.21	0.19	0.25	9.21	14.98	0.08	1.42	0.48	BD	BD	0.05	BD	ND	0.15	0.07	99.56	Original
1h-W13	2.41	7.38	1.47	58.4	3.18	0.17	0.24	9.21	14.71	0.06	1.43	0.49	BD	0.03	0.04	BD	ND	0.16	0.05	99.37	Original
1h-B1	0.97	3.89	1.75	52.2	2.93	0.14	0.03	10.50	23.68	0.07	1.23	0.83	0.12	0.18	0.23	BD	ND	0.28	0.17	99.25	Original
1h-B2	0.95	3.92	1.76	52.4	2.88	0.14	0.04	10.50	23.94	0.08	1.22	1.01	0.13	0.19	0.22	BD	ND	0.27	0.18	99.88	Original
1h-R1	1.24	4.31	1.47	49.2	3.65	0.21	0.06	10.60	25.55	0.06	1.39	0.46	BD	0.09	BD	ND	ND	0.26	0.47	99.11	Original
1h-R2	1.03	4.30	1.62	50.0	3.37	0.15	0.05	10.54	25.55	0.08	1.43	0.49	BD	0.07	0.04	BD	ND	0.27	0.20	99.24	Original
1h-R5	1.02	4.37	1.63	50.3	3.17	0.18	0.06	10.23	26.65	0.06	1.39	0.48	BD	0.05	BD	ND	ND	0.27	0.17	100.02	Original
1h-M1	0.92	4.45	1.49	54.3	1.96	0.35	BD	11.01	22.45	0.04	1.58	0.36	BD	BD	BD	ND	ND	0.46	BD	99.43	Original (B/C)
1h-M2	0.88	3.37	1.08	53.6	1.91	0.24	0.13	14.55	20.23	0.03	1.72	0.14	BD	BD	BD	ND	ND	0.51	BD	98.41	Original (B/C)
1h-M3	0.43	3.90	0.51	50.8	1.63	0.27	BD	18.58	20.47	BD	1.60	0.16	BD	0.05	0.04	ND	BD	0.40	0.04	98.85	Original (B)
3b-W1	1.89	6.96	1.34	56.6	3.88	0.11	0.27	10.42	16.59	0.09	1.37	0.50	BD	BD	BD	ND	BD	0.22	0.09	100.46	Original
3b-W3	2.61	6.91	1.46	58.0	3.13	0.21	0.28	9.72	15.24	0.10	1.43	0.55	BD	0.03	0.04	BD	BD	0.21	0.09	100.21	Original
3b-W4	2.61	6.88	1.46	58.0	3.08	0.21	0.28	9.70	15.29	0.10	1.44	0.53	BD	BD	0.04	BD	ND	0.21	0.12	100.08	Original
3b-W5	2.26	6.77	1.22	58.6	3.33	0.18	0.49	10.02	14.80	0.08	1.41	0.45	ND	BD	0.04	ND	BD	0.22	0.05	100.09	Original
3b-W6	2.26	6.81	1.22	58.5	3.41	0.18	0.50	10.14	14.87	0.09	1.40	0.46	BD	0.04	0.04	ND	ND	0.23	0.05	100.27	Original
3b-W7	1.93	7.24	1.23	57.3	3.60	0.18	0.34	10.46	15.21	0.09	1.49	0.44	BD	BD	BD	ND	BD	0.24	0.06	99.98	Original
3b-W8	1.91	7.24	1.22	57.1	3.54	0.19	0.33	10.43	15.17	0.09	1.50	0.45	BD	BD	0.04	BD	BD	0.22	0.06	99.65	Original
3b-W9	1.95	7.24	1.21	56.9	3.62	0.17	0.34	10.37	15.01	0.09	1.49	0.45	BD	BD	0.05	ND	BD	0.22	0.06	99.29	Original
3b-W10	1.85	7.20	1.27	57.6	3.27	0.22	0.21	9.21	15.78	0.09	1.44	0.45	BD	BD	0.04	BD	ND	0.22	BD	99.00	Original
3b-W11	2.78	7.03	1.48	57.6	2.92	0.17	0.26	9.43	14.83	0.11	1.40	0.53	BD	BD	0.05	ND	BD	0.21	0.07	99.00	Original
3b-W12	2.62	6.86	1.47	57.7	3.04	0.19	0.29	9.48	14.71	0.10	1.42	0.53	BD	BD	0.03	BD	ND	0.21	0.10	98.91	Original
3b-B1	1.12	3.81	1.63	52.2	2.99	0.14	0.05	11.41	23.48	0.13	1.20	0.88	0.09	0.16	0.13	BD	BD	0.31	0.22	100.10	Original
3b-B2	1.09	3.84	1.64	51.9	2.95	0.14	0.05	11.36	23.68	0.13	1.19	0.85	0.09	0.16	0.13	BD	BD	0.33	0.21	99.86	Original
3b-B3	1.11	3.85	1.63	52.1	2.93	0.14	0.05	11.44	23.85	0.12	1.20	0.84	0.08	0.17	0.10	BD	BD	0.32	0.22	100.31	Original
3b-B4	1.09	3.83	1.63	52.0	3.01	0.13	0.05	11.37	23.63	0.12	1.20	0.84	0.08	0.16	0.13	BD	BD	0.34	0.23	99.93	Original
3b-B5	1.11	3.85	1.64	52.2	2.96	0.14	0.05	11.26	23.41	0.12	1.20	0.85	0.08	0.16	0.13	BD	BD	0.33	0.22	99.84	Original
3b-B6	1.12	4.13	1.60	50.2	2.92	0.16	0.04	11.72	24.48	0.11	1.21	0.93	0.07	0.14	0.16	BD	BD	0.36	0.16	99.70	Original
3b-B7	1.12	4.10	1.57	49.9	2.83	0.15	0.03	11.50	24.15	0.12	1.21	0.89	0.08	0.16	0.15	ND	BD	0.35	0.16	98.60	Original
3b-B8	1.13	4.02	1.62	50.5	2.82	0.15	0.03	11.33	23.86	0.11	1.19	0.95	0.09	0.16	0.16	BD	BD	0.34	0.15	98.80	Original
3b-B9	1.13	4.03	1.62	50.4	2.87	0.16	0.03	11.32	23.93	0.12	1.19	0.94	0.08	0.15	0.16	BD	BD	0.33	0.15	98.79	Original
3b-R1	1.16	4.19	1.67	50.9	3.28	0.14	0.04	10.25	25.74	0.12	1.19	0.51	BD	0.13	BD	ND	BD	0.31	0.22	100.05	Original
3b-R2	1.23	4.30	1.62	49.5	3.21	0.21	0.04	10.83	25.19	0.12	1.33	0.50	BD	0.08	0.04	ND	BD	0.32	0.29	99.01	Original
3b-R3	1.89	4.20	1.63	51.5	4.22	0.28	0.09	10.71	22.88	0.12	1.07	0.64	BD	0.03	0.04	BD	ND	0.28	0.09	99.84	Original
3b-R4	1.02	4.09	1.66	48.5	2.78	0.24	0.03	11.51	26.74	0.11	1.10	0.46	BD	0.07	BD	BD	0.04	0.32	0.20	98.98	Original
3b-G1	1.45	4.21	1.64	46.6	4.03	0.28	0.04	16.01	20.73	0.14	1.44	2.53	BD	0.07	BD	ND	ND	0.37	0.06	99.75	Original (A)
3b-G2	1.45	4.23	1.63	46.1	4.15	0.24	0.04	15.83	20.68	0.14	1.45	2.50	BD	0.07	0.05	BD	BD	0.38	0.08	99.17	Original (A)
3b-Y1	1.59	4.18	1.65	45.8	3.94	0.25	0.04	15.59	20.41	0.14	1.49	3.08	BD	0.04	0.04	BD	BD	0.38	0.04	98.76	Original (A); flashed
3b-W2	2.28	6.37	1.10	60.0	3.04	0.20	0.46	9.87	14.69	0.07	1.48	0.36	BD	BD	BD	ND	ND	0.19	BD	100.33	Medieval; Staffordshire?
3b-W13	1.93	6.76	1.50	55.2	3.92	0.10	0.23	12.40	14.60	0.11	1.30	0.52	BD	BD	BD	ND	BD	0.20	0.04	98.92	Medieval; Staffordshire?
3b-R5	0.40	4.75	1.86	51.5	3.81	0.18	0.35	18.99	14.78	0.13	1.11	0.37	BD	0.05	BD	BD	BD	0.38	BD	98.77	Medieval
10c-W1	2.05	7.19	1.36	55.6	3.95	0.14	0.33	10.27	16.07	0.10	1.40	0.51	BD	0.04	0.06	BD	ND	0.17	0.12	99.39	Original
10c-W2	2.05	7.20	1.36	55.6	4.00	0.14	0.34	10.50	16.27	0.08	1.37	0.51	BD	0.04	0.04	BD	BD	0.17	0.11	99.78	Original
10c-W3	2.02	7.22	1.34	55.8	3.96	0.13	0.33	10.36	16.33	0.07	1.39	0.53	BD	BD	0.05	BD	ND	0.17	0.13	99.83	Original
10c-W4	2.06	7.13	1.34	55.1	4.12	0.15	0.35	10.68	16.20	0.07	1.36	0.51	BD	0.05	0.06	BD	BD	0.17	0.13	99.50	Original
10c-B3	1.36	4.36	1.80	49.7	3.39	0.21	0.04	9.86	25.14	0.14	1.33	1.16	0.16	0.27	0.35	BD	ND	0.26	0.23	99.74	Original
10c-B5	2.07	4.61	1.77	49.4	4.32	0.23	0.10	10.46	23.22	0.09	1.32	1.25	0.10	0.18	0.17	BD	ND	0.25	0.17	99.74	Original (A); light blue
10c-B6	1.27	4.46	1.61	47.4	4.47	0.29	0.05	15.24	21.42	0.09	1.47	1.02	0.07	0.12	0.11	BD	ND	0.31	0.10	99.54	Medieval; Weald?
10c-W5	1.52	5.29	1.09	53.9	4.17	0.17	0.40	13.52	17.06	0.07	0.70	0.59	BD	BD	0.04	0.09	ND	0.09	0.44	99.19	HLLA
10c-W6	2.88	4.39	2.50	55.6	3.57	0.39	0.50	5.15	21.89	0.14	1.43	0.77	BD	BD	0.06	BD	BD	0.40	BD	99.74	Medieval; Staffordshire?
10c-W7	2.77	7.30	1.41	56.2	3.15	0.21	0.35	10.02	16.05	0.08	1.47	0.53	BD	0.04	0.05	BD	ND	0.19	0.12	100.00	HLLA
10c-W8	2.83	3.43	1.62	58.3	3.29	0.34	0.67	4.20	23.38	0.36	0.66	0.64	BD	BD	BD	ND	ND	0.19	BD	99.93	Medieval; Staffordshire?
10c-W9	1.78	7.09	1.38	56.5	3.35	0.21	0.24	9.48	17.57	0.09	1.62	0.48	BD	BD	0.05	BD	BD	0.18	0.05	100.09	Medieval; Staffordshire?

Sample	Na_2O	MgO	Al_2O_3	SiO_2	P_2O_5	SO_3	Cl	K_2O	CaO	TiO_2	MnO	Fe_2O_3	CoO	CuO	ZnO	SnO_2	Sb_2O_5	BaO	PbO	Total	ID
10c-W10	2.98	7.80	1.34	57.4	2.86	0.12	0.35	9.41	14.94	0.08	1.52	0.49	BD	BD	0.03	BD	ND	0.16	0.08	99.54	Medieval; Weald?
10c-W11	2.04	5.39	2.34	54.6	3.94	0.15	0.49	13.09	14.96	0.12	0.82	0.82	BD	0.17	0.06	0.03	ND	0.16	0.26	99.48	HLLA
10c-W12	2.92	4.39	2.54	55.8	3.52	0.38	0.48	5.18	21.66	0.17	1.45	0.79	BD	BD	BD	BD	ND	0.40	ND	99.74	HLLA
10c-W13	2.87	4.35	2.57	56.0	3.47	0.39	0.50	5.28	21.69	0.17	1.43	0.76	BD	BD	0.03	ND	BD	0.40	ND	99.98	Soda
10c-B1	12.23	0.05	1.00	70.7	BD	0.24	0.11	0.56	11.12	0.06	0.58	1.14	0.12	0.21	BD	0.60	ND	BD	BD	98.75	Medieval
10c-B2	0.46	2.98	1.81	55.7	4.02	0.09	0.39	11.58	20.40	0.14	0.45	1.15	0.11	0.08	0.07	BD	ND	0.08	BD	99.55	Not original; Comp. identical
10c-B4	1.21	3.56	3.53	54.8	1.88	0.15	0.21	11.51	19.04	0.12	1.44	1.10	0.13	0.20	BD	ND	ND	0.40	BD	99.33	Medieval; Ni-rich Co
10c-R1	2.36	3.25	3.71	56.5	2.83	0.03	0.64	6.32	22.35	0.16	0.84	0.78	BD	0.12	0.07	BD	ND	0.16	BD	100.12	HLLA
10e-W1	2.01	7.17	1.36	55.8	4.10	0.19	0.33	10.69	15.99	0.08	1.34	0.51	BD	0.05	0.04	BD	BD	0.18	0.09	99.96	Original
10e-W2	2.66	7.49	1.41	57.0	3.71	0.24	0.49	9.94	14.26	0.08	1.54	0.55	BD	0.03	0.05	BD	BD	0.18	0.09	99.70	Original
10e-W3	1.93	7.31	1.35	55.4	3.89	0.09	0.30	9.98	16.89	0.03	1.40	0.46	BD	BD	0.05	BD	ND	0.17	0.09	99.40	Original
10e-W5	2.29	7.46	1.34	59.5	3.26	0.14	0.28	7.96	14.67	0.07	1.59	0.49	BD	0.03	0.06	BD	ND	0.17	BD	99.37	Original
10e-W6	2.02	7.22	1.36	55.6	4.02	0.13	0.34	10.43	16.12	0.07	1.36	0.50	BD	0.04	0.04	BD	ND	0.18	0.12	99.53	Original
10e-W7	2.03	6.89	1.43	56.2	3.40	0.10	0.30	9.95	16.72	0.07	1.46	0.57	BD	BD	0.04	BD	ND	0.21	0.07	99.45	Original
10e-W8	2.66	7.47	1.45	56.9	3.63	0.22	0.47	9.96	14.08	0.09	1.53	0.54	BD	BD	0.03	BD	BD	0.18	0.09	99.35	Original
10e-B1	1.16	3.96	1.57	51.5	2.88	0.20	0.05	11.37	23.62	0.10	1.26	0.94	0.14	0.15	0.19	BD	ND	0.28	0.33	99.65	Original
10e-B2	1.82	4.42	1.93	49.7	4.11	0.13	0.08	10.57	23.24	0.09	1.13	1.31	0.14	0.22	0.21	BD	ND	0.25	0.13	99.47	Original
10e-B3	1.86	4.42	1.92	49.6	4.05	0.13	0.07	10.49	22.95	0.10	1.11	1.32	0.14	0.23	0.21	BD	ND	0.24	0.11	98.95	Original
10e-B4	2.07	4.60	1.74	49.6	4.21	0.19	0.10	10.43	22.58	0.10	1.30	1.22	0.11	0.17	0.16	BD	ND	0.25	0.16	98.95	Original
10e-B5	1.30	4.32	2.09	50.0	3.16	0.26	0.03	10.01	24.70	0.11	1.26	1.08	0.11	0.23	0.17	BD	ND	0.26	0.14	99.23	Original
10e-R1	1.12	4.40	1.75	49.7	3.06	0.13	0.04	10.55	25.62	0.12	1.43	0.52	BD	0.06	0.03	BD	ND	0.27	0.22	99.07	Original
10e-R4	1.12	4.43	1.73	49.6	3.09	0.13	0.05	10.44	25.97	0.11	1.42	0.53	BD	0.08	0.03	BD	ND	0.27	0.22	99.27	Original
10e-R5	1.14	4.44	1.73	49.6	3.11	0.13	0.05	10.47	25.68	0.12	1.44	0.53	BD	0.06	BD	BD	ND	0.27	0.21	98.99	Original (B)
10e-G1	0.59	4.77	1.18	46.0	3.46	0.21	BD	14.71	24.77	0.12	1.60	1.85	BD	0.11	0.06	ND	ND	0.44	BD	99.90	Original (B)
10e-G2	0.60	4.78	1.20	46.1	3.55	0.22	BD	14.56	24.53	0.10	1.59	1.89	BD	0.06	0.05	BD	ND	0.45	BD	99.69	Original (B)
10e-G3	0.55	4.70	1.22	46.0	3.53	0.19	BD	14.50	24.34	0.11	1.55	2.13	BD	0.07	0.04	BD	ND	0.45	BD	99.43	HLLA
10e-W4	3.91	5.19	1.82	51.6	4.52	0.32	0.30	4.36	25.81	0.15	0.95	0.57	BD	BD	0.05	BD	ND	0.18	BD	99.78	Not original; Comp. identical
10e-R2	2.19	4.91	2.24	55.5	3.43	0.10	0.45	12.31	15.90	0.11	0.99	0.64	BD	0.41	0.05	0.06	BD	0.11	0.14	99.50	Medieval
10e-R3	2.27	4.98	2.25	57.1	3.31	0.08	0.49	12.03	15.84	0.14	1.02	0.62	BD	BD	BD	BD	ND	0.12	0.07	100.25	Medieval
10e-R6	4.29	8.02	1.01	56.2	4.07	0.07	0.54	11.88	11.53	0.07	0.95	0.32	BD	0.12	0.04	BD	BD	0.11	BD	99.30	Medieval
10e-G4	1.71	5.52	1.97	50.2	5.04	0.14	0.40	14.46	14.69	0.08	0.83	0.70	BD	3.22	0.32	0.15	ND	0.17	0.06	99.66	Medieval
10e-G5	11.59	0.05	1.85	68.7	BD	0.40	0.09	0.40	11.00	0.12	3.14	0.93	BD	0.53	BD	BD	BD	0.04	ND	98.83	Soda
10h-W1	2.69	7.51	1.42	57.0	3.71	0.24	0.49	10.01	14.24	0.11	1.56	0.54	BD	BD	0.04	BD	ND	0.19	0.08	99.93	Original
10h-W3	1.95	7.31	1.22	57.0	3.37	0.17	0.31	10.69	15.69	0.08	1.43	0.45	BD	BD	0.06	BD	ND	0.17	0.05	99.99	Original
10h-W6	2.26	7.30	1.39	59.6	3.34	0.16	0.29	8.16	15.14	0.07	1.60	0.51	BD	BD	0.05	BD	ND	0.18	0.05	100.09	Original
10h-W9	2.03	7.33	1.35	55.8	3.91	0.10	0.30	9.80	16.99	0.09	1.38	0.45	BD	BD	0.07	BD	ND	0.17	0.12	99.89	Original
10h-W10	2.11	7.02	1.45	53.3	4.39	0.17	0.45	11.75	15.71	0.12	1.57	0.45	BD	BD	0.06	BD	ND	0.19	0.05	98.78	Original
10h-W12	2.14	7.00	1.44	53.5	4.41	0.19	0.47	11.84	15.92	0.06	1.55	0.45	BD	0.04	0.05	ND	ND	0.18	0.05	99.27	Original
10h-W13	1.90	7.27	1.33	55.5	3.90	0.12	0.30	9.85	17.12	0.06	1.38	0.46	BD	BD	0.06	BD	ND	0.18	0.10	99.55	Original
10h-W15	2.11	6.99	1.45	53.7	4.42	0.17	0.46	11.89	15.86	0.10	1.57	0.44	BD	BD	0.04	BD	ND	0.19	0.04	99.50	Original
10h-W16	2.15	6.97	1.42	53.7	4.42	0.18	0.47	11.87	15.84	0.07	1.56	0.43	BD	BD	0.08	BD	ND	0.17	0.05	99.34	Original
10h-W17	2.57	7.43	1.38	56.8	3.67	0.24	0.51	9.77	14.33	0.09	1.52	0.52	BD	0.05	0.05	BD	ND	0.18	0.09	99.20	Original
10h-B1	1.73	4.33	1.72	51.1	4.12	0.15	0.09	9.99	22.79	0.10	1.13	1.04	0.10	0.22	0.23	BD	ND	0.24	0.14	99.18	Original
10h-R7	1.59	4.44	1.73	50.1	3.93	0.16	0.06	10.38	23.97	0.11	1.25	0.67	BD	0.09	0.04	BD	ND	0.26	0.12	98.95	Original
10h-R8	1.78	4.47	1.64	51.3	4.45	0.15	0.09	10.20	22.47	0.08	1.21	0.71	BD	0.05	0.04	BD	BD	0.25	0.14	99.02	Original
10h-M1	0.94	4.85	1.53	52.8	1.92	0.29	BD	10.19	23.70	0.12	1.58	0.45	BD	0.03	0.04	BD	ND	0.54	BD	99.04	Original (B/C)
10h-M3 (pink)	0.48	4.26	0.79	46.0	2.19	0.22	BD	17.88	23.66	0.08	1.95	0.25	BD	0.03	0.05	ND	ND	0.44	BD	98.24	Original (B); blue/purple/blue
10h-M3 (blue)	0.52	4.51	1.27	46.2	3.09	0.21	BD	16.51	23.04	0.12	1.68	0.76	0.06	0.06	0.09	ND	ND	0.38	BD	98.58	Original (B); blue/purple/blue
10h-M5 (pink)	0.46	4.21	0.79	46.3	2.12	0.20	BD	18.04	23.54	0.08	1.97	0.25	ND	BD	0.04	BD	ND	0.46	BD	98.48	Original (B); blue/purple/blue
10h-M5 (blue)	0.52	4.49	1.26	46.4	3.09	0.20	BD	16.44	23.03	0.12	1.70	0.76	0.07	0.09	0.09	BD	ND	0.37	0.03	98.65	Original (B); blue/purple/blue
10h-M4	0.57	4.41	0.86	47.5	3.72	0.32	BD	17.83	21.57	0.10	1.29	0.28	BD	0.03	0.04	BD	ND	0.34	BD	98.89	Original (B)
10h-W2	1.71	5.82	2.02	51.1	5.27	0.15	0.44	14.94	16.46	0.13	0.89	0.69	BD	0.05	0.07	BD	BD	0.16	BD	99.87	Medieval; Weald?
10h-W4	3.02	5.44	2.84	56.1	3.35	0.13	0.46	11.06	15.45	0.13	0.78	0.98	BD	0.08	0.04	BD	ND	0.17	0.04	100.11	Medieval; Weald?
10h-W5	1.81	5.13	2.41	54.6	4.53	0.20	0.42	14.68	13.80	0.15	0.90	0.83	BD	0.08	0.08	BD	BD	0.11	0.10	99.87	Medieval; Weald?
10h-W7	2.92	5.36	2.84	55.6	3.33	0.13	0.44	10.93	15.19	0.16	0.77	0.97	BD	0.09	BD	BD	ND	0.16	BD	98.98	Medieval; Weald?
10h-W8	1.75	4.94	2.53	53.4	4.33	0.21	0.44	13.52	15.37	0.16	0.91	0.86	BD	0.06	0.06	BD	ND	0.14	0.18	98.86	Medieval; Weald?
10h-W11	1.87	6.78	1.57	55.4	3.39	0.20	0.24	9.48	17.47	0.07	1.32	0.57	BD	0.04	0.06	BD	BD	0.19	0.12	98.81	Medieval; Staffordshire?

Sample	Na_2O	MgO	Al_2O_3	SiO_2	P_2O_5	SO_3	Cl	K_2O	CaO	TiO_2	MnO	Fe_2O_3	CoO	CuO	ZnO	SnO_2	Sb_2O_5	BaO	PbO	Total	ID
10h-W14	2.10	5.72	2.23	54.9	4.12	0.11	0.47	14.06	13.95	0.12	0.80	0.70	BD	0.07	BD	BD	ND	0.17	0.04	99.56	Medieval; Weald?
10h-W18	2.67	6.57	1.48	55.7	3.28	0.12	0.35	9.81	16.74	0.07	1.38	0.51	BD	BD	0.07	BD	BD	0.19	0.14	99.09	Medieval; Staffordshire?
10h-W19	11.23	0.03	1.50	70.1	ND	0.36	0.07	0.29	11.54	0.09	2.27	0.68	BD	BD	BD	0.03	ND	BD	BD	98.32	Soda
10h-R1	4.48	7.66	0.96	53.0	4.11	0.13	0.56	11.37	15.39	0.05	1.71	0.34	BD	0.05	0.06	BD	BD	0.09	BD	99.95	Medieval
10h-R2	1.73	6.18	2.14	53.6	3.91	0.13	0.38	13.21	15.89	0.13	1.33	0.75	BD	0.08	0.04	BD	BD	0.18	BD	99.72	Medieval
10h-R3	13.72	0.62	0.70	71.9	ND	0.31	0.05	0.20	10.99	0.03	BD	0.21	BD	BD	BD	BD	ND	BD	0.03	98.82	Soda
10h-R4	2.06	4.64	2.71	53.5	4.27	0.11	0.43	13.32	16.52	0.13	0.74	1.01	BD	0.06	0.05	BD	ND	0.13	BD	99.59	Medieval
10h-R5	1.41	4.81	2.81	50.7	3.86	0.13	0.40	13.52	18.80	0.13	0.93	0.89	BD	0.08	0.06	BD	ND	0.20	BD	98.73	Medieval
10h-R6	1.68	5.46	2.00	51.5	5.09	0.14	0.44	14.81	15.87	0.08	0.82	0.67	BD	0.05	0.04	BD	BD	0.14	BD	98.79	Medieval
10h-R9	2.13	5.92	2.25	52.7	4.30	0.11	0.45	13.48	16.27	0.13	0.86	0.75	BD	0.09	0.06	BD	ND	0.17	0.07	99.73	Medieval
10h-R10	4.38	7.52	0.97	53.1	4.03	0.12	0.54	11.31	15.12	0.05	1.68	0.35	BD	0.04	0.06	BD	ND	0.08	BD	99.36	Medieval
10h-R11	1.62	5.48	2.02	51.6	5.08	0.13	0.45	14.79	16.10	0.10	0.82	0.66	BD	0.05	0.05	BD	BD	0.15	BD	99.19	Medieval
10h-G1	10.64	0.09	3.18	68.5	ND	0.34	0.13	0.57	10.93	0.23	3.03	1.59	BD	0.18	BD	BD	ND	BD	ND	99.42	Soda
10h-G2	11.78	0.06	1.86	69.1	BD	0.40	0.10	0.41	10.99	0.11	3.20	0.95	BD	0.51	BD	BD	BD	BD	BD	99.53	Soda
10h-G3	1.66	4.24	2.88	51.3	4.12	0.20	0.38	11.76	16.29	0.13	0.76	0.96	BD	3.26	0.15	0.24	ND	0.13	0.61	99.11	Medieval
10h-G4	1.65	4.80	2.36	50.0	5.07	0.08	0.43	12.12	17.88	0.14	0.74	0.77	BD	2.53	0.29	0.19	ND	0.19	0.17	99.36	Medieval
10h-G5	10.15	0.10	3.15	67.9	BD	0.35	0.13	0.56	10.92	0.19	2.96	1.54	BD	0.20	BD	BD	BD	BD	BD	98.18	Soda
10h-M2 (purple)	0.70	0.18	0.27	52.2	0.09	0.05	0.05	6.67	1.35	0.06	4.79	0.46	BD	BD	0.09	ND	0.06	0.05	36.13	103.18	High lead
10h-M2 (white)	7.53	5.26	1.24	68.4	1.47	0.11	0.71	3.53	10.61	0.13	BD	0.41	BD	BD	BD	BD	BD	ND	BD	99.52	Kelp ash
15a-W1	1.99	7.17	1.31	55.9	3.68	0.15	0.23	9.43	17.37	0.05	1.36	0.45	BD	BD	0.07	BD	ND	0.19	BD	99.34	Original
15a-W2	2.58	7.81	1.21	55.5	4.28	0.17	0.48	10.60	15.21	0.05	1.48	0.40	BD	BD	0.03	BD	ND	0.18	BD	99.95	Original
15a-W3	2.47	6.62	1.60	57.1	3.76	0.18	0.39	8.93	16.51	0.05	1.52	0.46	BD	BD	0.06	BD	BD	0.21	0.16	99.96	Original
15a-W4	2.88	7.86	1.14	55.1	4.45	0.24	0.45	10.78	14.06	0.04	1.52	0.39	BD	BD	0.03	BD	BD	0.18	BD	99.07	Original
15a-W5	2.86	7.81	1.16	55.5	4.35	0.28	0.47	10.82	14.13	0.05	1.53	0.39	BD	BD	0.04	BD	ND	0.18	0.03	99.51	Original
15a-W6	2.56	7.84	1.23	55.5	4.26	0.17	0.45	10.49	15.11	0.06	1.50	0.42	BD	BD	0.04	BD	BD	0.19	BD	99.76	Original
15a-W7	1.90	7.45	1.29	56.2	3.79	0.20	0.35	10.22	15.49	0.06	1.47	0.45	BD	BD	0.05	BD	ND	0.19	0.04	99.13	Original
15a-W8	2.32	7.82	1.05	55.8	3.61	0.16	0.34	10.54	16.04	BD	1.35	0.35	BD	BD	0.07	ND	ND	0.18	BD	99.58	Original
15a-W9	2.10	7.56	1.29	56.2	3.94	0.19	0.35	10.14	15.60	0.05	1.45	0.43	BD	BD	0.04	BD	BD	0.19	0.06	99.50	Original
15a-W10	2.59	7.81	1.23	55.6	4.29	0.18	0.48	10.53	14.94	0.05	1.50	0.40	BD	BD	0.05	BD	ND	0.19	BD	99.79	Original
15a-W11	2.36	7.47	1.36	59.2	3.51	0.08	0.28	7.93	14.87	0.05	1.52	0.43	BD	BD	0.05	ND	BD	0.18	BD	99.25	Original
15a-B1	1.46	4.58	1.83	46.8	3.66	0.20	BD	10.84	26.49	0.08	1.43	1.01	0.15	0.25	0.36	BD	ND	0.28	0.19	99.65	Original
15a-B2	1.47	4.38	1.84	49.3	3.67	0.19	0.03	10.09	25.23	0.08	1.31	1.11	0.15	0.26	0.37	BD	BD	0.25	0.25	100.02	Original
15a-B3	1.53	4.50	1.81	48.0	3.62	0.17	0.03	10.70	25.79	0.08	1.37	1.31	0.19	0.26	0.48	BD	ND	0.25	0.24	100.40	Original
15a-B4	1.47	4.59	1.83	47.3	3.63	0.22	BD	10.94	26.37	0.07	1.44	1.02	0.15	0.26	0.36	BD	ND	0.27	0.21	100.12	Original
15a-R1	1.34	4.40	1.55	50.5	3.62	0.16	0.07	9.94	25.21	0.07	1.33	0.49	BD	0.09	BD	BD	ND	0.26	1.04	100.14	Original
15a-R2	1.32	4.52	1.51	47.9	3.79	0.25	0.06	9.99	26.39	0.06	1.35	0.47	ND	0.08	0.05	BD	ND	0.28	0.94	98.95	Original
15a-R3	1.16	4.47	1.68	49.8	3.37	0.18	0.05	10.23	25.74	0.08	1.40	0.48	BD	0.09	BD	BD	ND	0.28	0.15	99.22	Original
15a-G1	0.51	4.33	2.24	46.8	2.15	0.20	BD	13.94	26.18	0.07	1.23	1.24	BD	0.10	BD	ND	ND	0.37	BD	99.40	Original (B)
15a-R4	5.90	4.65	2.16	62.7	1.62	0.13	0.40	4.11	13.73	0.13	0.13	0.94	BD	0.04	0.04	BD	BD	BD	2.43	99.09	Kelp ash
15b-W1	1.88	7.41	1.34	55.9	3.88	0.22	0.36	10.56	16.15	0.05	1.45	0.44	BD	BD	0.04	BD	ND	0.20	0.05	99.85	Original
15b-W2	1.90	7.40	1.34	56.1	3.96	0.23	0.37	10.77	16.10	0.06	1.47	0.44	BD	BD	0.04	BD	ND	0.19	0.06	100.41	Original
15b-W3	2.01	7.36	1.42	56.2	3.96	0.17	0.35	10.80	15.69	0.05	1.50	0.32	BD	BD	0.04	BD	ND	0.19	0.06	100.01	Original
15b-W4	2.29	7.18	1.43	59.1	3.62	0.15	0.28	8.79	14.83	0.07	1.59	0.52	BD	0.06	0.05	BD	BD	0.18	0.08	100.10	Original
15b-W5	2.20	7.47	1.04	56.3	3.69	0.11	0.36	10.90	15.90	0.05	1.44	0.39	BD	BD	0.05	BD	BD	0.19	BD	100.09	Original
15b-W6	2.17	7.73	1.06	56.4	3.68	0.12	0.36	10.39	15.72	0.03	1.42	0.31	BD	BD	0.04	ND	ND	0.17	BD	99.61	Original
15b-W7	2.21	7.39	1.41	60.1	3.47	0.14	0.26	8.14	14.82	0.06	1.59	0.48	BD	BD	0.05	BD	ND	0.18	0.05	100.30	Original
15b-W8	2.12	7.89	1.06	56.6	3.62	0.15	0.34	10.90	15.87	BD	1.42	0.38	BD	BD	0.07	ND	ND	0.19	BD	100.55	Original
15b-W9	1.96	7.35	1.37	55.8	4.48	0.13	0.30	10.91	16.04	0.08	1.31	0.50	BD	BD	0.05	BD	ND	0.16	0.19	100.64	Original
15b-W10	2.21	7.57	1.06	56.5	3.68	0.13	0.36	10.94	16.15	0.05	1.44	0.39	BD	BD	0.06	BD	ND	0.19	BD	100.69	Original
15b-R1	1.92	4.66	1.63	49.3	4.60	0.19	0.10	10.57	24.39	0.05	1.11	0.62	BD	BD	BD	BD	ND	0.24	0.07	99.52	Original
15b-R2	1.11	4.50	1.70	50.1	3.25	0.19	0.04	10.38	26.67	0.07	1.42	0.51	BD	0.07	BD	BD	ND	0.27	0.24	100.52	Original
15b-R4	1.11	4.46	1.72	50.5	3.25	0.19	0.04	10.37	26.61	0.06	1.41	0.36	BD	0.09	BD	BD	ND	0.29	0.23	100.67	Original
15b-R5	1.03	4.49	1.69	50.4	3.32	0.19	0.06	10.39	26.68	0.07	1.42	0.51	BD	0.05	BD	BD	ND	0.28	0.14	100.74	Original
15b-R6	1.13	4.50	1.72	50.3	3.33	0.17	0.04	10.48	26.45	0.09	1.44	0.51	BD	0.11	BD	BD	ND	0.29	0.23	100.75	Original
15b-R7	1.11	4.48	1.71	50.3	3.33	0.17	0.04	10.43	26.55	0.09	1.44	0.37	BD	0.10	BD	BD	ND	0.27	0.24	100.70	Original
15b-R3	1.86	4.00	1.39	53.7	3.19	0.12	0.20	10.38	23.77	0.07	1.04	0.48	BD	0.07	BD	BD	ND	0.25	0.26	100.78	Original?
15f-B1	0.64	4.30	1.44	45.2	3.79	0.29	0.05	17.98	21.89	0.09	1.28	0.90	0.09	0.12	0.10	ND	BD	0.35	0.03	98.56	Original (B); light blue

Sample	Na_2O	MgO	Al_2O_3	SiO_2	P_2O_5	SO_3	Cl	K_2O	CaO	TiO_2	MnO	Fe_2O_3	CoO	CuO	ZnO	SnO_2	Sb_2O_5	BaO	PbO	Total	ID
15f-G1	1.71	4.76	1.67	44.0	4.88	0.31	0.06	15.70	21.70	0.08	1.50	1.94	BD	0.04	0.04	BD	BD	0.34	0.08	98.82	Original (A)
15f-G2	0.51	4.64	1.12	46.3	2.80	0.17	BD	15.29	24.52	0.04	1.48	1.45	BD	0.08	0.03	ND	ND	0.43	BD	98.88	Original (B)
15f-G3	0.52	4.64	1.10	46.3	2.72	0.19	BD	15.48	24.11	0.06	1.50	1.35	BD	0.09	BD	ND	ND	0.44	BD	98.57	Original (B)
15f-G4	0.48	4.59	1.08	46.2	2.64	0.21	BD	15.16	24.78	0.04	1.53	1.38	BD	0.08	0.04	ND	ND	0.45	BD	98.68	Original (B)
15f-Y1	0.53	4.67	1.08	47.0	2.62	0.25	BD	15.49	24.56	0.06	1.50	0.26	BD	BD	BD	ND	ND	0.44	BD	98.50	Original
15g-W1	2.14	7.35	1.34	55.5	4.16	0.14	0.31	9.96	15.84	0.05	1.36	0.48	BD	0.03	0.05	BD	ND	0.18	0.13	99.01	Original
15g-W2	2.13	7.31	1.35	56.0	3.98	0.15	0.32	9.63	16.33	0.04	1.42	0.46	BD	BD	0.06	BD	BD	0.18	0.06	99.38	Original
15g-W3	2.17	7.49	1.32	56.1	4.08	0.14	0.31	9.58	16.04	0.04	1.42	0.43	BD	BD	0.06	BD	BD	0.18	0.07	99.40	Original
15g-W4	2.08	7.26	1.37	55.1	4.51	0.16	0.31	10.76	15.68	0.05	1.32	0.49	BD	0.03	0.07	BD	ND	0.18	0.16	99.42	Original
15g-W5	2.02	7.22	1.40	56.5	3.54	0.14	0.22	9.37	16.92	0.05	1.46	0.48	BD	BD	0.04	BD	ND	0.20	0.08	99.66	Original
15g-W6	2.08	7.32	1.39	56.2	3.99	0.15	0.31	9.61	16.80	0.05	1.38	0.44	BD	BD	0.05	BD	ND	0.19	0.13	100.06	Original
15g-W7	2.06	7.43	1.31	55.3	4.17	0.18	0.31	9.64	16.68	0.04	1.40	0.42	BD	BD	0.07	BD	BD	0.18	0.06	99.22	Original
15g-W8	2.10	7.38	1.30	55.4	4.19	0.17	0.31	9.58	16.56	0.04	1.40	0.42	BD	BD	0.05	BD	ND	0.18	0.08	99.13	Original
15g-W9	2.09	7.23	1.37	55.5	4.34	0.18	0.29	10.22	15.85	0.05	1.32	0.49	BD	0.04	0.07	BD	BD	0.17	0.12	99.25	Original
15g-W10	2.08	7.38	1.30	55.7	4.13	0.19	0.31	9.78	16.57	0.05	1.40	0.43	BD	BD	0.05	BD	BD	0.17	0.06	99.52	Original
15g-W11	2.09	7.26	1.36	55.9	4.26	0.19	0.31	10.52	16.04	0.05	1.32	0.49	BD	0.03	0.06	BD	ND	0.17	0.10	100.05	Original
15g-B1	1.41	4.53	1.81	47.0	3.64	0.24	0.03	10.19	26.39	0.07	1.38	1.00	0.14	0.22	0.33	BD	ND	0.28	0.21	98.92	Original
15g-B2	1.28	4.35	2.16	50.3	3.37	0.23	0.03	10.05	24.74	0.10	1.26	0.94	0.11	0.24	0.19	BD	ND	0.27	0.12	99.72	Original
15g-B3	1.27	4.34	2.15	50.3	3.39	0.24	0.03	10.02	24.66	0.09	1.26	1.13	0.12	0.21	0.18	BD	ND	0.27	0.13	99.81	Original
15g-B4	1.38	4.39	2.17	50.2	3.45	0.26	0.03	9.94	24.63	0.09	1.26	1.09	0.10	0.21	0.18	BD	0.08	0.26	0.15	99.93	Original
15g-R1	1.32	4.54	1.65	49.4	3.71	0.19	0.05	10.06	26.02	0.07	1.36	0.49	BD	0.09	0.03	BD	ND	0.27	0.75	99.98	Original
15g-R2	2.16	4.74	1.69	48.9	4.77	0.22	0.08	10.76	24.60	0.06	1.12	0.62	BD	0.05	0.05	BD	ND	0.25	0.09	100.13	Original
15g-R3	1.66	4.59	1.76	49.8	4.27	0.19	0.05	10.71	24.70	0.07	1.25	0.63	BD	0.06	0.04	BD	ND	0.27	0.19	100.28	Original
15g-G1	0.52	4.70	1.10	46.2	2.61	0.18	BD	14.75	25.37	0.04	1.50	1.49	BD	BD	BD	BD	ND	0.46	ND	99.02	Original?
15g-G2	0.68	4.33	1.31	46.3	2.57	0.24	BD	16.67	22.62	0.04	1.49	2.27	BD	BD	BD	BD	ND	0.54	0.05	99.19	Original (B)
15g-M1	1.07	4.91	1.52	50.1	2.16	0.20	BD	12.47	23.85	0.04	1.91	0.38	BD	BD	BD	BD	ND	0.48	BD	99.09	Original (B)
15g-M2	1.23	4.21	1.50	51.9	1.75	0.30	0.08	14.64	21.07	BD	1.69	0.31	BD	BD	0.05	ND	ND	0.35	BD	99.11	Original (B/C)
15g-Y1	0.54	4.69	1.09	47.0	2.69	0.26	BD	15.67	25.19	0.04	1.51	0.31	BD	BD	BD	BD	BD	0.48	BD	99.50	Not original
15g-R4	2.02	4.09	1.38	53.2	3.21	0.11	0.18	10.68	22.76	0.06	1.05	0.45	BD	0.21	0.05	BD	ND	0.25	0.24	99.90	Original
15h-W1	2.12	7.62	1.07	56.4	3.64	0.15	0.35	10.58	15.87	0.04	1.41	0.38	BD	BD	0.06	BD	BD	0.18	BD	99.96	Original
15h-W2	1.88	7.08	1.49	56.2	3.84	0.23	0.41	10.16	16.14	0.06	1.48	0.49	BD	BD	0.03	BD	ND	0.19	0.08	99.76	Original
15h-W3	1.96	7.26	1.36	56.7	4.00	0.14	0.31	9.81	16.41	0.06	1.43	0.47	BD	BD	0.04	BD	ND	0.18	0.06	100.20	Original
15h-W4	2.14	7.13	1.52	58.8	3.62	0.14	0.26	8.72	15.63	0.07	1.57	0.51	BD	BD	0.06	BD	BD	0.19	0.09	100.45	Original
15h-W5	1.95	7.30	1.36	56.7	4.00	0.14	0.30	9.93	16.21	0.07	1.45	0.47	BD	BD	0.05	BD	ND	0.18	0.05	100.21	Original
15h-W6	1.96	7.27	1.37	56.7	3.98	0.16	0.29	9.80	16.05	0.06	1.43	0.46	BD	BD	0.05	ND	ND	0.17	0.06	99.84	Original
15h-W7	1.96	7.25	1.35	56.4	3.94	0.14	0.27	9.64	15.87	0.06	1.43	0.47	BD	BD	0.05	BD	ND	0.17	0.06	99.13	Original
15h-W8	1.98	7.30	1.34	56.1	4.32	0.13	0.32	10.36	15.32	0.06	1.39	0.47	BD	BD	0.05	BD	ND	0.18	0.09	99.48	Original
15h-W9	1.91	7.21	1.37	56.0	4.36	0.14	0.29	10.81	15.21	0.06	1.33	0.51	BD	0.03	0.04	BD	BD	0.18	0.12	99.61	Original
15h-W10	1.96	7.29	1.36	56.7	3.96	0.14	0.29	9.82	16.26	0.06	1.45	0.47	BD	0.04	0.06	BD	ND	0.18	0.06	100.10	Original
15h-W11	1.96	7.24	1.35	56.7	3.97	0.13	0.30	9.85	16.10	0.06	1.43	0.48	BD	BD	0.05	BD	ND	0.18	0.06	99.85	Original
15h-W12	1.95	7.52	1.27	57.1	3.83	0.15	0.32	10.29	15.10	0.06	1.49	0.43	BD	0.03	0.05	BD	ND	0.18	BD	99.81	Original
15h-B1	1.23	4.23	1.78	51.3	3.39	0.25	0.04	10.20	24.30	0.08	1.28	0.60	0.12	0.24	0.27	BD	ND	0.26	0.17	99.70	Original
15h-R1	1.15	4.37	1.71	50.5	3.45	0.14	0.04	9.84	26.74	0.09	1.22	0.53	BD	0.13	BD	BD	BD	0.26	0.17	100.33	Original
15h-R2	1.93	4.65	1.68	49.5	4.74	0.17	0.08	10.79	24.37	0.06	1.10	0.62	BD	0.03	0.04	BD	ND	0.24	0.08	100.14	Original
15h-R3	1.94	4.63	1.65	49.1	4.73	0.17	0.09	10.83	24.30	0.08	1.12	0.62	BD	0.05	0.03	BD	ND	0.25	0.07	99.68	Original
15h-R4	1.38	4.41	1.66	49.6	3.70	0.18	0.05	9.72	27.34	0.07	1.12	0.41	BD	0.05	0.03	ND	ND	0.22	0.09	100.00	Original
15h-G1	0.44	4.23	1.20	46.3	2.74	0.20	BD	16.42	22.78	0.04	1.70	1.80	0.04	0.10	0.07	ND	ND	0.41	BD	98.49	Original (B)
15h-G2	0.64	4.39	1.21	46.4	4.33	0.28	0.10	17.90	20.12	0.07	1.14	2.03	BD	0.04	BD	ND	ND	0.32	BD	99.01	Original (B)
15h-G3	0.64	4.38	1.23	46.5	4.34	0.28	0.10	18.12	20.31	0.08	1.16	2.01	BD	BD	0.03	ND	ND	0.30	ND	99.43	Original (B)
15h-G4	0.64	4.40	1.20	46.5	4.36	0.29	0.10	18.25	20.68	0.08	1.14	2.03	BD	0.04	BD	BD	BD	0.31	BD	100.04	Original (B)
15h-G5	0.47	4.72	1.04	46.4	2.58	0.17	BD	16.15	24.96	0.03	1.57	1.24	BD	0.09	BD	BD	ND	0.46	BD	99.92	Original (B)
15h-Y1	1.51	3.64	2.41	55.4	3.74	0.08	0.37	5.24	25.12	0.05	1.88	0.48	BD	BD	0.03	BD	ND	0.29	BD	100.17	Original? HLLA

Table D.2 Results of the pXRF analyses. Not analysed: 1e-W10,W11; 1e-B6; 10e-R5,G2; 10h-M4. Analysis omitted: 10c-W3,B5; 10e-W7,G1,G7; 10h-W3,W6. Five elements were identified as measured well by pXRF and are presented as quantitative analyses. The rest are considered informational or semi-quantitative. *BD* = below detection. Identification of the glass is given in the right-most column.

	Quantitative. Element ppm					Semi-quantitative. Oxide weight per cent;								Element ppm					
Sample	**Cu**	**Zn**	**Rb**	**Sr**	**Zr**	**P_2O_5**	**SO_3**	**Cl**	**K_2O**	**CaO**	**TiO_2**	**MnO**	**Fe_2O_3**	**Co**	**Ni**	**Sn**	**Sb**	**Pb**	**ID**
1e-W1	123	392	200	510	59	2.2	0.3	0.2	8.1	13.2	0.13	1.44	0.54	78	BD	54	BD	651	Original
1e-W2	118	384	207	546	54	3.1	0.5	0.3	8.6	13.9	0.12	1.51	0.58	81	25	83	BD	905	Original
1e-W3	100	410	196	495	54	1.9	0.3	0.2	8.8	13.7	0.13	1.45	0.53	78	BD	80	BD	765	Original
1e-W4	92	397	208	528	57	2.7	0.5	0.2	8.5	13.4	0.13	1.51	0.53	94	BD	58	BD	521	Original
1e-W5	141	411	195	523	57	2.4	0.3	0.2	8.4	14.1	0.12	1.46	0.53	97	BD	58	BD	585	Original
1e-W6	130	414	199	531	56	3.1	1.5	0.3	8.2	13.5	0.13	1.44	0.54	94	19	80	BD	883	Original
1e-W7	138	369	202	519	52	3.4	0.3	0.2	8.5	13.6	0.13	1.44	0.55	92	BD	75	BD	807	Original
1e-W8	146	381	213	555	61	1.7	0.8	0.3	8.5	13.9	0.14	1.47	0.63	79	BD	94	BD	1020	Original
1e-W9	156	400	208	525	59	2.9	0.4	0.3	8.4	13.7	0.13	1.43	0.57	108	BD	83	BD	883	Original
1e-W12	126	359	206	517	58	2.4	0.5	0.2	8.4	13.7	0.13	1.49	0.54	93	BD	67	BD	944	Original
1e-W13	121	388	214	560	57	2.9	0.7	0.2	8.5	13.8	0.14	1.52	0.56	81	BD	103	BD	1446	Original
1e-W14	126	398	202	532	61	2.8	0.4	0.2	8.4	13.6	0.13	1.46	0.51	78	BD	70	BD	724	Original
1e-W15	117	370	205	516	54	2.3	0.7	0.2	8.0	12.8	0.13	1.40	0.58	81	BD	74	BD	1003	Original
1e-W16	129	376	200	531	57	1.9	0.5	0.3	8.3	13.1	0.13	1.45	0.56	85	BD	106	BD	959	Original
1e-W17	84	380	201	501	55	2.1	1.3	0.3	8.3	12.8	0.13	1.48	0.52	67	BD	38	BD	810	Original
1e-W18	85	393	201	529	57	2.4	0.8	0.3	8.3	12.9	0.13	1.49	0.54	89	19	62	BD	669	Original
1e-W19	108	407	210	530	54	2.2	1.5	0.3	8.4	13.0	0.13	1.44	0.56	72	25	135	BD	1598	Original
1e-W20	116	382	212	555	59	2.7	0.5	0.2	8.6	13.7	0.13	1.50	0.55	100	BD	72	BD	861	Original
1e-W21	115	401	198	519	61	3.8	0.4	0.2	8.3	13.5	0.13	1.45	0.53	98	BD	72	BD	670	Original
1e-W22	138	384	219	548	57	2.4	0.9	0.3	8.5	13.5	0.13	1.46	0.58	91	BD	95	BD	1042	Original
1e-W23	87	397	204	509	52	2.4	1.0	0.3	8.2	13.0	0.13	1.48	0.54	84	BD	56	BD	745	Original
1e-W24	83	372	201	499	59	3.0	0.6	0.2	8.4	13.2	0.12	1.49	0.51	76	BD	32	BD	550	Original
1e-W25	133	413	220	529	57	2.6	3.8	0.6	7.8	12.9	0.13	1.45	0.59	66	19	80	BD	1879	Original
1e-W26	134	395	213	544	60	2.8	1.8	0.4	8.3	13.3	0.12	1.44	0.58	111	25	79	BD	1371	Original
1e-W27	117	397	190	513	60	2.4	0.3	0.2	8.2	13.5	0.12	1.42	0.50	104	BD	52	BD	570	Original
1e-W28	142	382	212	539	58	3.1	0.8	0.3	8.3	13.3	0.12	1.43	0.57	98	23	131	BD	1011	Original
1e-W29	151	418	213	556	56	2.3	3.2	0.5	7.5	13.8	0.13	1.36	1.51	BD	BD	79	BD	2299	Original
1e-W30	125	377	218	556	64	2.6	0.8	0.2	8.5	13.5	0.13	1.48	0.56	104	BD	114	BD	1401	Original
1e-W31	119	388	213	546	60	2.7	4.3	0.6	7.6	13.0	0.14	1.41	0.61	85	BD	82	BD	2943	Original
1e-W32	83	366	200	508	51	3.1	3.4	0.6	7.5	12.5	0.14	1.42	0.53	70	BD	59	BD	2274	Original
1e-W33	128	393	219	569	64	3.2	2.2	0.4	8.1	13.1	0.14	1.43	0.63	101	BD	56	BD	1493	Original
1e-W36	287	508	211	575	53	3.1	5.6	0.7	10.1	14.9	0.13	1.04	2.08	BD	BD	298	BD	6926	Original
1e-W37	116	396	199	510	58	2.9	0.3	0.2	8.5	14.0	0.12	1.45	0.52	91	26	69	BD	568	Original
1e-W38	98	376	212	532	59	2.9	1.2	0.3	8.6	13.8	0.13	1.55	0.56	84	19	65	BD	853	Original
1e-W39	116	387	212	528	59	1.8	0.5	0.2	8.6	13.6	0.14	1.49	0.58	92	BD	65	BD	934	Original
1e-W40	147	416	216	564	56	3.5	4.1	0.6	7.3	12.4	0.18	1.38	1.45	BD	BD	75	BD	1940	Original
1e-W41	130	408	218	555	57	2.7	1.0	0.3	8.5	13.6	0.13	1.47	0.67	89	BD	75	BD	1060	Original
1e-W42	151	408	218	574	56	3.0	3.2	0.5	7.7	13.2	0.14	1.42	1.15	BD	BD	93	BD	1724	Original
1e-W44	93	391	204	535	50	3.6	2.0	0.4	8.0	12.9	0.13	1.49	0.74	72	BD	41	BD	1134	Original
1e-W45	116	413	213	544	55	4.4	7.7	1.0	6.5	10.7	0.12	1.34	0.60	74	BD	95	BD	3495	Original
1e-W47	142	402	196	516	57	2.6	0.2	0.2	8.4	13.9	0.12	1.45	0.54	93	BD	58	BD	568	Original
1e-W48	126	374	205	513	57	2.4	0.4	0.2	8.2	13.1	0.12	1.45	0.56	110	BD	67	BD	957	Original
1e-B1	1067	244	106	1107	112	3.6	0.6	0.2	8.0	23.9	0.18	2.09	0.82	1307	447	BD	BD	139	Original? HLLA
1e-B2	1106	237	110	1120	117	4.5	2.4	0.4	7.4	22.6	0.18	2.03	0.84	1260	481	BD	BD	675	Original? HLLA
1e-B3	1945	3458	276	828	92	3.8	3.6	0.4	9.6	21.9	0.18	1.25	1.29	1533	33	300	105	2629	Original
1e-B4	1074	240	103	1061	107	4.7	1.8	0.4	7.7	23.2	0.17	2.06	0.80	1316	457	BD	BD	477	Original? HLLA
1e-B5	1064	227	106	1075	110	3.6	0.8	0.2	7.7	23.0	0.17	2.03	0.78	1290	460	BD	BD	189	Original? HLLA
1e-B7	1078	261	108	1112	119	4.8	3.1	0.5	7.3	21.9	0.18	2.00	0.83	1286	470	BD	BD	926	Original? HLLA
1e-B8	1043	257	108	1080	110	5.3	3.3	0.6	7.2	21.9	0.19	2.02	0.83	1291	429	BD	BD	974	Original? HLLA
1e-B9	1014	259	110	1075	113	4.2	2.1	0.4	7.4	22.1	0.18	1.98	0.81	1274	437	BD	BD	658	Original? HLLA
1e-B10	1972	3445	289	837	96	3.3	3.2	0.4	9.7	22.4	0.18	1.27	1.27	1508	36	294	108	2571	Original
1e-B11	1038	245	103	1094	105	3.8	2.1	0.4	7.3	22.4	0.18	2.02	0.81	1262	417	BD	BD	588	Original? HLLA

	Quantitative. Element ppm					Semi-quantitative. Oxide weight per cent;								Element ppm					
Sample	Cu	Zn	Rb	Sr	Zr	P_2O_5	SO_3	Cl	K_2O	CaO	TiO_2	MnO	Fe_2O_3	Co	Ni	Sn	Sb	Pb	ID
1e-B12	1055	258	106	1129	115	5.2	3.3	0.6	7.4	22.6	0.19	2.05	0.82	1299	459	BD	BD	948	Original? HLLA
1e-B13	1080	237	107	1078	111	3.1	1.9	0.4	7.7	23.1	0.17	2.05	0.80	1291	464	BD	BD	520	Original? HLLA
1e-B14	1006	232	112	1084	113	5.2	3.2	0.5	7.2	22.0	0.18	1.99	0.81	1284	436	37	BD	915	Original? HLLA
1e-B15	1011	256	107	1135	107	5.9	3.7	0.6	7.2	22.1	0.18	2.02	0.84	1322	471	BD	BD	1082	Original? HLLA
1e-B16	1930	3435	272	834	96	3.8	2.1	0.3	10.1	23.0	0.18	1.30	1.27	1424	56	342	78	2204	Original
1e-B17	1272	2414	283	837	93	5.3	6.6	0.8	8.7	20.6	0.16	1.23	1.06	996	48	230	71	3361	Original
1e-B18	1050	260	109	1104	121	5.1	5.3	0.7	6.8	20.7	0.20	1.96	0.82	1338	439	BD	BD	1686	Original? HLLA
1e-R1	614	250	294	877	103	3.4	2.9	0.4	9.8	23.2	0.18	1.28	0.56	107	22	73	BD	2371	Original
1e-R4	552	260	293	886	107	4.1	2.3	0.3	10.0	23.5	0.17	1.29	0.53	136	23	87	BD	2161	Original
1e-R5	648	261	294	866	97	4.9	3.4	0.5	9.8	23.2	0.18	1.30	0.56	114	23	49	BD	2561	Original
1e-R6	522	252	308	857	101	3.7	2.1	0.3	10.0	23.5	0.17	1.28	0.55	130	BD	62	BD	2117	Original
1e-W34	647	450	181	423	56	1.8	1.0	0.3	8.2	13.9	0.12	1.37	0.98	BD	31	55	BD	979	Medieval - Staffordshire?
1e-W43	130	384	210	577	58	2.4	0.3	0.2	8.7	13.9	0.13	1.47	0.58	78	BD	87	BD	823	Medieval - Staffordshire?
1e-W46	465	376	231	433	78	2.9	5.4	0.6	10.6	12.8	0.12	0.77	1.84	BD	26	202	BD	2044	Medieval - Weald?
1e-W35	58	257	119	1214	136	3.5	2.6	0.5	6.0	22.2	0.22	2.02	0.56	74	27	BD	BD	1187	HLLA
1e-R2	675	457	190	443	87	3.5	0.5	0.3	14.3	12.1	0.20	0.88	1.05	61	20	154	BD	211	Medieval
1e-R3	451	394	208	548	66	3.1	3.5	0.6	10.5	13.1	0.11	0.93	0.64	62	BD	285	BD	1795	Medieval
1e-R7	399	479	371	607	72	3.9	19.2	0.2	8.9	11.1	0.15	0.89	0.79	77	20	72	BD	2191	Medieval
1e-R8	865	436	226	408	80	3.4	3.1	0.6	10.1	12.6	0.17	0.67	0.79	74	19	147	BD	1575	Medieval
1e-R9	2598	368	273	641	80	BD	16.4	0.5	4.5	19.9	0.19	0.94	0.83	51	33	BD	BD	1732	Medieval
1e-R10	609	394	242	531	74	5.8	1.0	0.3	14.0	12.5	0.15	0.81	0.85	91	19	276	BD	1472	Medieval
1h-W1	124	404	207	537	64	2.1	1.2	0.3	8.3	14.2	0.13	1.44	0.53	90	27	70	BD	967	Original
1h-W2	110	405	205	539	62	2.6	0.4	0.2	8.5	13.3	0.13	1.46	0.54	95	23	57	BD	683	Original
1h-W3	93	430	211	558	58	2.0	0.5	0.2	8.7	13.8	0.13	1.49	0.55	78	19	101	BD	847	Original
1h-W4	115	388	201	504	58	3.0	0.4	0.2	8.4	13.1	0.12	1.45	0.54	93	BD	65	BD	649	Original
1h-W5	116	411	208	510	60	2.2	0.6	0.2	8.1	13.4	0.12	1.41	0.51	95	BD	56	BD	714	Original
1h-W6	99	382	198	519	57	2.4	0.4	0.2	8.3	13.3	0.12	1.45	0.51	84	BD	74	BD	799	Original
1h-W7	106	398	205	518	62	2.3	0.2	0.2	8.5	13.3	0.13	1.44	0.54	98	BD	73	BD	657	Original
1h-W8	107	410	206	524	61	2.5	0.2	0.2	8.6	13.3	0.13	1.48	0.51	105	BD	72	BD	783	Original
1h-W9	108	416	210	536	60	2.5	1.3	0.3	8.1	14.0	0.13	1.45	0.69	66	18	133	BD	1208	Original
1h-W10	112	389	207	557	54	2.9	0.2	0.2	8.8	13.7	0.12	1.50	0.51	96	26	89	BD	785	Original
1h-W11	112	408	207	526	57	2.1	1.4	0.3	8.4	12.9	0.14	1.46	0.89	51	BD	106	BD	1209	Original
1h-W12	116	391	204	530	59	2.7	0.4	0.2	8.3	13.1	0.13	1.42	0.55	67	BD	84	BD	678	Original
1h-W13	119	390	201	533	64	1.9	0.5	0.2	8.2	13.2	0.12	1.42	0.51	106	BD	78	BD	722	Original
1h-W14	94	396	195	497	52	3.1	0.3	0.2	8.3	13.0	0.12	1.45	0.51	98	BD	81	BD	763	Original
1h-W15	121	387	211	530	52	2.1	4.7	0.7	7.5	12.2	0.13	1.41	0.74	68	24	72	BD	2147	Original
1h-W16	87	406	208	527	62	1.8	0.6	0.2	8.7	13.5	0.14	1.46	0.53	95	31	89	BD	840	Original
1h-W17	111	427	211	601	59	2.3	0.5	0.2	8.4	14.2	0.13	1.58	0.52	84	BD	109	BD	895	Original
1h-W18	108	420	210	622	54	3.6	2.7	0.5	7.7	13.5	0.13	1.54	0.55	78	BD	104	BD	1568	Original
1h-W19	124	410	202	526	61	2.4	1.5	0.3	8.1	13.3	0.13	1.42	0.53	99	24	68	BD	1034	Original
1h-W20	129	383	216	563	64	3.4	2.6	0.5	8.2	12.7	0.13	1.44	0.58	84	BD	81	BD	1787	Original
1h-W21	120	383	216	548	59	4.2	2.5	0.5	8.1	13.0	0.12	1.46	0.56	108	25	72	BD	1790	Original
1h-W23	100	420	210	532	50	3.6	3.7	0.6	7.9	12.3	0.13	1.44	0.81	60	BD	106	BD	1853	Original
1h-W24	92	418	214	534	54	2.3	0.8	0.3	8.7	13.5	0.13	1.49	0.55	65	25	103	BD	954	Original
1h-W25	117	415	210	546	59	2.6	0.5	0.2	8.7	13.6	0.13	1.47	0.55	86	BD	60	BD	705	Original
1h-W26	271	462	249	539	48	3.6	6.4	0.8	7.9	11.6	0.12	1.22	1.28	BD	BD	159	BD	2991	Original
1h-W30	145	422	205	509	58	2.6	1.4	0.3	8.4	13.8	0.12	1.50	0.53	109	BD	104	BD	1152	Original
1h-B1	1209	1732	293	784	108	2.7	0.8	0.1	10.8	23.9	0.18	1.21	1.06	937	30	170	BD	1705	Original
1h-B2	1270	1729	290	766	101	3.0	0.4	0.1	10.8	23.7	0.18	1.20	1.05	974	37	206	68	1566	Original
1h-B3	1198	1690	287	750	103	2.5	0.4	0.1	10.4	23.1	0.19	1.18	1.02	929	40	178	BD	1549	Original
1h-B4	1216	1762	292	754	105	2.9	0.6	0.1	10.8	23.9	0.18	1.22	1.04	980	55	198	40	1608	Original
1h-B5	1338	1746	298	759	103	3.7	0.7	0.1	10.8	23.9	0.17	1.22	1.05	978	44	204	52	1631	Original
1h-B7	1209	1699	288	750	103	4.3	0.5	0.1	10.8	24.1	0.18	1.22	1.05	956	39	181	61	1622	Original
1h-B8	1250	1779	294	755	106	2.6	0.5	0.1	11.0	24.5	0.18	1.25	1.06	969	33	189	74	1559	Original
1h-B9	1264	1721	288	767	103	2.3	0.4	0.1	10.7	24.1	0.18	1.21	1.05	940	38	170	45	1569	Original

	Quantitative. Element ppm					Semi-quantitative. Oxide weight per cent;								Element ppm					
Sample	Cu	Zn	Rb	Sr	Zr	P_2O_5	SO_3	Cl	K_2O	CaO	TiO_2	MnO	Fe_2O_3	Co	Ni	Sn	Sb	Pb	ID
1h-R1	404	231	267	840	76	BD	8.6	0.7	3.1	33.6	0.11	0.76	0.50	84	BD	81	BD	9567	Original
1h-R2	516	220	267	842	92	3.2	8.5	0.7	6.8	24.1	0.15	1.03	1.35	BD	BD	132	BD	7447	Original
1h-R3	667	217	295	870	103	4.3	3.3	0.4	9.9	24.6	0.16	1.29	0.53	109	BD	76	BD	2580	Original
1h-R5	569	237	308	907	101	3.9	10.2	1.1	6.9	21.2	0.18	1.11	1.62	BD	31	116	BD	5631	Original
1h-M1	88	247	373	1242	130	3.6	4.5	0.5	10.2	19.2	0.23	1.53	0.50	74	24	BD	BD	1518	Original (B/C)
1h-M4	106	340	332	630	107	2.5	2.5	0.2	6.4	11.7	0.28	1.42	0.51	85	BD	BD	BD	368	Original (B)
1h-M2	135	274	445	984	78	1.9	0.7	0.2	14.5	17.9	0.25	1.62	0.27	78	39	BD	BD	174	Original (B/C)
1h-M3	320	315	520	684	73	1.8	3.1	0.4	7.3	12.6	0.20	1.47	0.27	106	40	68	BD	1804	Original (B)
1h-M5	252	346	355	571	68	BD	9.3	0.8	4.5	34.0	0.14	0.72	0.42	75	BD	277	BD	14522	Medieval
1h-M6	130	305	218	799	56	1.5	3.7	0.5	8.7	14.6	0.35	0.75	0.39	71	47	BD	BD	2385	Original (B)
1h-M7	136	273	445	991	82	BD	1.9	0.3	14.0	17.9	0.24	1.58	0.34	57	33	BD	BD	482	Original (B/C)
1h-W22	47	437	159	456	36	3.3	4.3	0.6	7.6	12.2	0.11	1.44	0.39	108	BD	BD	BD	1500	Medieval - Staffordshire?
1h-W29	70	431	120	413	41	2.5	0.3	0.3	9.4	14.6	0.11	1.45	0.38	75	BD	BD	BD	227	Medieval - Staffordshire?
1h-W27	121	408	255	625	99	2.5	0.9	0.3	10.2	12.7	0.19	1.09	0.79	91	BD	87	BD	804	Medieval - Weald?
1h-W28	130	241	187	313	119	2.9	0.3	0.4	8.2	12.9	0.16	0.65	0.62	100	27	52	BD	375	Medieval - Weald?
1h-B6	903	293	47	756	105	1.9	1.8	0.6	4.6	23.1	0.28	1.18	0.79	1077	914	BD	BD	603	HLLA; Ni-rich Co
1h-R4	564	483	371	407	65	4.1	1.6	0.4	13.1	13.8	0.14	0.84	0.76	70	22	72	BD	1168	Medieval
1h-M8	330	270	60	708	94	2.7	0.6	0.4	5.0	23.2	0.23	0.94	0.48	78	31	BD	BD	115	Medieval?
1j-W1	141	431	206	545	57	2.5	1.3	0.4	8.9	13.9	0.13	1.43	0.59	86	BD	146	BD	1495	Original
1j-W2	130	429	214	559	54	4.1	1.6	0.4	9.0	13.9	0.13	1.46	0.53	105	24	135	BD	1470	Original
1j-W3	99	413	204	519	57	2.5	1.9	0.4	8.3	13.2	0.12	1.48	0.52	105	BD	86	BD	1160	Original
1j-W4	124	413	211	542	51	3.2	0.9	0.3	9.1	14.1	0.12	1.46	0.53	100	18	111	BD	1214	Original
1j-W5	91	404	201	528	53	2.4	0.5	0.3	8.4	13.2	0.12	1.45	0.53	64	BD	91	BD	802	Original
1j-W6	91	398	198	506	53	2.3	1.1	0.3	8.2	12.7	0.12	1.43	0.51	87	BD	104	BD	995	Original
1j-W7	128	414	204	528	60	2.0	3.0	0.5	7.5	13.0	0.13	1.40	0.63	70	22	84	BD	1443	Original
1j-W8	127	436	211	529	55	2.9	1.5	0.3	9.0	13.7	0.12	1.44	0.55	93	23	130	BD	1497	Original
1j-W9	128	414	217	553	60	3.0	1.7	0.4	8.9	14.0	0.13	1.43	0.56	94	19	148	BD	1666	Original
1j-W10	106	410	205	525	53	2.2	0.6	0.2	8.5	13.6	0.12	1.49	0.52	91	BD	86	BD	861	Original
1j-W11	110	417	214	550	59	2.5	1.4	0.3	8.4	14.4	0.15	1.49	0.53	84	26	93	BD	908	Original
1j-W12	153	436	216	551	56	2.6	1.3	0.3	9.0	14.5	0.13	1.43	0.55	90	24	114	BD	1345	Original
1j-W13	144	431	212	532	58	2.2	1.5	0.4	9.0	14.7	0.13	1.45	0.53	104	BD	124	BD	1320	Original
1j-W14	128	408	205	514	49	2.1	0.8	0.3	8.7	14.2	0.12	1.41	0.50	113	BD	111	BD	1150	Original
1j-W15	134	421	214	543	59	3.6	0.5	0.3	9.5	14.2	0.14	1.46	0.55	98	22	107	BD	1101	Original
1j-W16	127	424	213	549	56	2.4	0.4	0.2	9.4	14.4	0.14	1.48	0.54	88	BD	140	BD	1177	Original
1j-W17	114	428	213	544	58	1.9	3.0	0.4	7.9	13.5	0.14	1.42	1.03	62	20	96	BD	1512	Original
1j-W18	83	418	207	530	52	2.5	1.7	0.4	8.4	13.2	0.12	1.48	0.53	80	BD	98	BD	1201	Original
1j-W19	82	417	204	525	58	2.2	4.0	0.5	7.9	13.0	0.13	1.42	0.53	92	BD	97	BD	2081	Original
1j-W20	108	410	205	528	58	2.5	2.5	0.4	7.9	12.9	0.13	1.44	0.75	67	BD	108	BD	1579	Original
1j-W21	126	414	214	548	54	3.9	1.3	0.4	9.0	13.7	0.13	1.46	0.54	81	BD	135	BD	1356	Original
1j-W22	98	403	204	528	52	1.6	1.4	0.3	8.2	12.9	0.13	1.45	0.78	70	30	105	BD	1440	Original
1j-W23	102	395	199	510	52	2.1	0.9	0.3	8.3	13.1	0.13	1.45	0.55	84	BD	104	BD	915	Original
1j-W24	142	437	212	534	59	2.4	0.6	0.3	9.5	14.2	0.13	1.49	0.55	92	BD	123	BD	1145	Original
1j-W25	146	420	213	537	58	2.7	1.6	0.4	8.8	13.5	0.14	1.43	0.72	60	BD	92	BD	1477	Original
1j-W26	151	434	220	546	54	1.3	0.5	0.3	9.4	14.2	0.13	1.46	0.55	109	BD	123	BD	1172	Original
1j-W27	153	443	216	543	54	3.3	1.2	0.4	9.3	14.4	0.12	1.49	0.56	96	25	127	BD	1374	Original
1j-W29	153	402	226	569	54	1.8	2.6	0.4	7.1	12.2	0.13	1.49	0.89	47	BD	92	BD	1584	Original
1j-W30	108	435	216	617	54	3.2	2.2	0.4	7.9	14.0	0.13	1.58	0.55	85	BD	137	BD	1411	Original
1j-W31	91	447	207	602	59	4.1	4.3	0.7	7.4	13.2	0.13	1.56	0.55	78	BD	108	BD	1976	Original
1j-W32	91	408	211	548	54	2.3	3.1	0.8	7.7	12.5	0.13	1.41	0.56	77	25	92	BD	1726	Original
1j-W33	112	424	208	541	53	2.3	2.2	0.4	8.9	13.6	0.13	1.48	0.55	96	BD	115	BD	1542	Original
1j-W34	98	424	210	527	55	2.5	0.8	0.3	8.5	13.6	0.14	1.49	0.56	76	BD	74	BD	918	Original
1j-W35	109	400	198	523	54	2.5	1.6	0.4	8.2	13.2	0.12	1.48	0.53	78	BD	105	BD	1139	Original
1j-W36	119	449	216	543	59	2.5	0.4	0.3	10.3	14.4	0.14	1.38	0.58	98	BD	120	BD	1364	Original
1j-W37	117	401	196	523	50	2.2	0.9	0.3	9.1	13.3	0.13	1.43	0.51	106	BD	113	BD	1193	Original
1j-W38	100	451	210	639	59	3.6	1.7	0.4	8.3	14.0	0.14	1.58	0.56	91	28	111	BD	1206	Original

	Quantitative. Element ppm					Semi-quantitative. Oxide weight per cent;								Element ppm					
Sample	Cu	Zn	Rb	Sr	Zr	P_2O_5	SO_3	Cl	K_2O	CaO	TiO_2	MnO	Fe_2O_3	Co	Ni	Sn	Sb	Pb	ID
1j-W39	142	447	224	578	58	3.0	2.2	0.5	9.1	14.1	0.13	1.49	0.58	112	BD	125	BD	1742	Original
1j-B1	1157	1709	330	804	99	5.1	4.6	0.6	11.0	23.0	0.18	1.20	1.03	861	45	182	54	2661	Original
1j-B2	1077	1633	317	760	97	2.9	1.9	0.2	10.7	22.9	0.18	1.16	1.01	817	28	182	64	1895	Original
1j-B3	1055	1485	313	788	100	2.0	4.2	0.6	9.1	22.7	0.18	1.09	1.57	674	42	196	48	3212	Original
1j-B4	1105	1656	318	803	95	3.6	2.8	0.4	11.1	23.4	0.18	1.19	1.01	921	31	180	40	2237	Original
1j-B5	1167	1609	293	833	91	2.4	8.3	0.9	6.1	17.6	0.17	0.96	3.00	226	82	243	66	5242	Original
1j-R1	334	207	263	859	90	2.4	7.6	0.4	6.7	28.2	0.15	0.94	0.55	101	BD	106	BD	4089	Original
1j-R2	469	270	298	869	105	4.0	2.3	0.3	10.0	23.7	0.17	1.29	0.58	117	24	84	BD	2320	Original
1j-R3	476	220	275	843	88	BD	8.0	0.5	3.6	22.9	0.15	0.89	0.57	106	BD	61	BD	5765	Original
1j-R4	530	256	286	830	86	2.4	13.4	0.5	3.5	18.8	0.15	0.90	0.63	98	BD	61	BD	5958	Original
1j-R5	486	248	299	889	101	2.3	1.6	0.2	10.2	24.2	0.16	1.31	0.56	125	BD	105	BD	2008	Original
1j-R6	431	226	295	897	103	3.0	7.9	0.8	7.7	20.4	0.19	1.19	1.58	BD	32	87	BD	4001	Original
1j-R7	1987	281	302	844	96	2.1	11.2	1.2	4.9	14.1	0.14	0.99	4.37	BD	BD	69	BD	8792	Original
1j-G1	253	380	327	637	97	3.4	13.2	0.4	5.0	18.0	0.20	1.11	1.79	71	24	184	BD	2391	Original
1j-M1	310	303	500	657	68	1.5	7.6	0.3	4.5	8.8	0.24	1.41	0.30	104	26	56	BD	1127	Original (B)
1j-Y1	55	294	126	1177	131	4.4	3.2	0.5	6.6	22.4	0.22	1.77	0.66	62	27	BD	BD	1002	Original? HLLA
1j-W28	126	479	213	524	52	3.3	2.7	0.5	8.1	13.3	0.14	1.24	0.61	88	28	87	BD	1607	Medieval - Staffordshire?
3b-W1	123	440	208	568	49	3.8	0.9	0.3	10.4	15.2	0.13	1.39	0.53	17	52	139	4	1006	Original
3b-W3	134	372	211	606	64	2.2	1.3	0.4	9.6	13.9	0.14	1.51	0.62	26	52	94	10	1360	Original
3b-W4	154	369	201	600	60	3.2	0.9	0.2	9.7	14.8	0.14	1.50	0.58	39	55	94	6	1208	Original
3b-W5	100	390	220	589	51	3.0	2.0	0.5	9.3	14.5	0.12	1.41	0.50	17	53	63	11	1036	Original
3b-W6	108	419	238	592	45	3.9	1.0	0.5	9.8	13.7	0.12	1.48	0.51	39	53	56	11	708	Original
3b-W7	130	414	243	658	54	3.2	1.0	0.3	10.2	13.8	0.13	1.51	0.46	26	45	90	8	664	Original
3b-W8	121	367	247	671	53	4.2	0.5	0.2	10.5	14.1	0.13	1.53	0.47	39	46	72	19	546	Original
3b-W9	93	354	246	645	54	3.2	2.0	0.4	10.0	13.4	0.13	1.51	0.46	26	52	89	6	1043	Original
3b-W10	232	501	209	610	52	2.6	2.2	0.3	8.3	14.1	0.14	1.42	0.62	26	44	56	BD	1074	Original
3b-W11	113	360	194	581	56	1.4	1.3	0.3	9.6	13.6	0.14	1.49	0.59	22	56	83	11	1078	Original
3b-W12	116	370	203	570	63	3.0	1.4	0.3	9.5	14.0	0.13	1.48	0.89	15	50	80	BD	1554	Original
3b-W14	133	362	199	569	62	2.4	1.1	0.4	9.3	13.6	0.14	1.48	0.64	13	55	70	BD	1248	Original
3b-W15	115	357	202	562	60	1.3	2.6	0.4	7.8	12.8	0.14	1.28	0.84	65	38	93	20	1806	Original
3b-W16	115	380	191	557	55	3.4	1.1	0.3	9.3	13.6	0.13	1.46	1.20	22	56	67	BD	1526	Original
3b-W17	213	425	252	579	49	2.3	1.6	0.4	9.6	15.3	0.13	1.32	0.64	48	43	121	3	1729	Original
3b-W18	246	466	252	612	51	4.5	1.7	0.4	10.6	14.8	0.13	1.37	1.40	BD	54	182	BD	2929	Original
3b-W19	122	364	197	568	61	2.2	2.3	0.5	8.9	13.4	0.14	1.45	0.70	35	50	76	BD	1355	Original
3b-W20	124	380	192	568	58	1.9	3.6	0.7	8.2	14.8	0.14	1.39	0.79	52	50	82	BD	1812	Original
3b-W21	133	373	203	579	66	0.8	1.5	0.4	9.1	14.5	0.14	1.43	0.62	78	42	85	BD	1833	Original
3b-W22	130	394	199	577	59	2.5	0.8	0.3	9.6	13.9	0.15	1.51	0.71	39	42	93	2	1043	Original
3b-W23	143	368	201	576	60	2.8	2.5	0.4	8.3	14.1	0.13	1.38	1.30	BD	59	106	BD	2191	Original
3b-W24	122	381	233	605	55	3.0	2.1	0.5	9.4	15.0	0.14	1.41	0.56	39	51	83	8	1501	Original
3b-W25	90	371	241	650	50	3.2	0.7	0.3	11.0	14.5	0.13	1.54	0.49	13	57	85	BD	611	Original
3b-W26	207	383	243	551	50	3.2	0.4	0.3	11.1	14.5	0.13	1.43	0.49	39	50	145	BD	839	Original
3b-W27	112	396	226	596	42	3.8	2.0	0.5	9.2	13.1	0.11	1.42	0.47	52	51	45	BD	930	Original
3b-W28	96	396	230	609	48	1.8	0.7	0.4	9.9	13.7	0.12	1.44	0.47	48	53	37	BD	577	Original
3b-W29	322	427	254	593	51	2.9	7.6	1.2	6.9	10.6	0.14	1.21	1.26	BD	47	157	BD	4407	Original
3b-W30	196	419	251	562	58	3.9	0.8	0.3	11.2	14.5	0.12	1.45	0.56	9	56	168	18	955	Original
3b-W31	126	412	242	650	51	3.2	3.7	0.5	8.1	14.7	0.13	1.27	0.67	43	40	111	BD	2467	Original
3b-W32	151	395	228	640	59	2.9	2.5	0.5	9.2	15.3	0.14	1.39	0.70	4	50	110	15	1831	Original
3b-W33	226	419	249	558	54	3.1	2.3	0.5	9.2	12.9	0.13	1.33	0.80	13	54	154	BD	1945	Original
3b-W34	243	441	251	580	55	3.3	2.6	0.5	9.9	15.5	0.13	1.34	0.63	52	52	227	12	2159	Original
3b-W35	164	406	217	625	59	2.8	1.0	0.3	9.0	13.7	0.14	1.59	0.54	BD	53	133	BD	980	Original
3b-W36	107	422	227	591	48	2.8	2.1	0.5	9.3	14.1	0.13	1.43	0.61	17	53	69	BD	812	Original
3b-W37	107	386	218	579	49	3.4	2.1	0.6	9.0	14.2	0.12	1.38	0.54	17	46	67	5	1011	Original
3b-W38	145	417	225	597	46	2.2	3.9	0.7	8.6	13.3	0.12	1.38	0.78	30	44	74	BD	1375	Original
3b-W39	123	367	250	657	52	2.8	3.2	0.7	7.9	16.2	0.12	1.29	0.57	52	50	124	23	2156	Original
3b-W40	108	350	239	631	47	2.6	2.1	0.4	8.9	14.2	0.12	1.38	0.53	BD	47	105	13	1448	Original

	Quantitative. Element ppm					Semi-quantitative. Oxide weight per cent;								Element ppm					
Sample	Cu	Zn	Rb	Sr	Zr	P_2O_5	SO_3	Cl	K_2O	CaO	TiO_2	MnO	Fe_2O_3	Co	Ni	Sn	Sb	Pb	ID
3b-W41	120	399	234	587	45	3.0	1.3	0.4	9.8	13.9	0.12	1.44	0.99	13	58	48	10	1505	Original
3b-W42	136	371	244	680	50	3.3	1.8	0.4	9.1	13.8	0.13	1.40	0.55	22	44	91	BD	1310	Original
3b-W43	133	379	244	639	51	2.7	1.0	0.3	10.1	14.3	0.13	1.51	0.47	35	51	61	BD	717	Original
3b-W44	307	470	228	591	59	2.8	3.6	0.6	8.2	13.2	0.14	1.21	0.99	13	41	208	16	2624	Original
3b-W45	139	411	217	607	46	2.7	1.2	0.3	9.6	15.2	0.12	1.42	0.49	17	54	72	BD	924	Original
3b-W46	115	435	206	618	53	1.5	1.4	0.3	8.1	13.4	0.18	1.40	0.57	17	44	57	BD	932	Original
3b-W47	110	362	241	656	49	3.7	1.5	0.4	10.1	16.0	0.13	1.47	0.50	17	58	71	6	1010	Original
3b-W48	196	425	231	585	58	3.1	2.2	0.5	9.4	16.0	0.13	1.29	0.60	43	50	160	BD	2160	Original
3b-B1	1119	1323	307	835	110	3.5	2.1	0.4	11.2	21.3	0.19	1.15	1.05	781	64	195	26	2724	Original
3b-B2	1118	1223	293	788	106	2.2	0.8	0.1	11.3	21.7	0.18	1.11	0.91	809	56	180	26	2386	Original
3b-B3	1117	1273	302	815	103	3.0	0.5	0.1	12.6	23.5	0.18	1.17	0.89	817	70	176	12	2047	Original
3b-B4	1101	1272	298	772	100	3.2	0.9	0.2	12.2	22.8	0.19	1.15	0.91	813	72	179	38	2177	Original
3b-B5	1137	1255	298	859	110	4.1	0.7	0.2	12.7	23.6	0.19	1.19	0.91	787	68	179	36	2118	Original
3b-B6	1114	1605	316	839	107	4.6	2.0	0.4	12.6	24.5	0.18	1.18	1.01	804	75	227	57	2011	Original
3b-B7	1104	1602	315	860	103	3.4	1.8	0.3	12.4	25.3	0.19	1.18	1.02	870	51	219	58	2493	Original
3b-B8	1153	1434	301	835	102	3.5	4.9	0.6	8.7	20.0	0.21	0.96	1.45	817	43	253	45	4762	Original
3b-B9	1175	1507	312	855	103	2.2	0.8	0.2	12.7	24.5	0.19	1.21	1.01	861	62	216	70	1470	Original
3b-B10	1089	1291	307	853	110	2.4	1.7	0.3	11.8	23.0	0.19	1.16	0.93	796	69	191	31	2310	Original
3b-B11	1847	2657	288	860	100	5.2	2.4	0.3	12.1	25.0	0.18	1.20	1.22	1130	74	289	90	2106	Original
3b-B13	1485	1678	281	837	93	3.8	2.6	0.3	10.0	21.6	0.17	1.02	1.34	1030	64	282	51	1884	Original
3b-B18	1139	1586	310	845	99	3.9	4.2	0.6	11.0	24.2	0.20	1.10	1.35	787	71	228	58	3578	Original
3b-B20	1116	1640	326	854	99	3.1	2.1	0.4	12.4	23.8	0.19	1.16	0.99	874	76	206	18	2190	Original
3b-B21	1010	1466	291	825	97	1.1	6.5	0.6	5.2	33.1	0.15	0.69	1.13	696	60	256	31	5717	Original
3b-B22	1171	1372	309	848	119	5.2	4.9	0.7	11.4	22.0	0.18	1.15	0.91	796	48	207	43	3585	Original
3b-B23	1138	1547	300	848	106	3.7	6.5	0.8	10.4	22.2	0.20	1.12	1.18	791	68	196	4	6092	Original
3b-B24	1229	1764	315	877	110	2.5	2.4	0.3	12.8	25.0	0.19	1.23	1.04	935	52	205	60	1984	Original
3b-B25	1236	1680	332	874	111	5.1	4.6	0.6	11.4	23.0	0.18	1.16	1.07	922	65	213	30	2930	Original
3b-R1	847	180	292	931	108	4.2	5.8	0.6	9.5	26.2	0.15	1.10	0.58	43	41	62	10	3310	Original
3b-R2	392	148	280	961	103	BD	8.0	0.4	2.2	37.9	0.14	0.53	0.74	17	45	159	3	6280	Original
3b-R3	198	255	255	752	92	2.3	7.1	0.5	5.2	23.0	0.16	0.65	0.81	87	48	167	13	3877	Original
3b-R4	430	170	307	872	95	1.6	8.7	0.4	5.9	21.8	0.16	0.86	0.54	61	44	126	BD	2643	Original
3b-R6	444	173	309	868	101	1.7	5.8	0.4	5.9	23.0	0.17	0.87	0.54	57	50	119	14	2945	Original
3b-R7	510	184	302	811	85	5.4	5.9	0.8	10.0	21.9	0.16	1.12	0.70	87	45	137	BD	3144	Original
3b-R13	262	403	276	796	95	3.8	2.1	0.3	10.8	23.0	0.16	1.02	0.66	67	50	101	BD	1519	Original
3b-R14	209	188	258	798	91	4.4	3.5	0.5	9.0	27.1	0.15	0.93	0.65	65	52	125	3	2973	Original
3b-G1	339	330	332	686	102	1.5	5.9	0.7	5.6	29.4	0.17	1.16	2.74	174	37	213	BD	3242	Original (A)
3b-G2	381	344	349	727	105	3.3	3.8	0.5	12.5	22.9	0.21	1.26	3.03	188	49	220	4	2677	Original (A)
3b-G5	370	365	349	709	104	3.3	5.4	0.7	10.2	18.2	0.22	1.16	3.98	96	68	226	6	4218	Original
3b-G6	335	388	336	701	95	2.4	5.4	0.7	3.6	25.3	0.17	1.00	1.02	39	53	153	6	3586	Original
3b-G7	210	287	349	744	103	3.3	10.1	0.3	5.3	16.8	0.26	1.57	2.48	143	51	152	10	1154	Original
3b-G8	308	369	314	684	100	BD	7.1	1.0	4.0	34.7	0.14	0.93	1.11	65	66	193	6	5793	Original
3b-G9	390	423	327	702	98	2.7	5.5	0.7	4.3	26.3	0.19	1.07	0.95	74	59	178	11	4835	Original
3b-G3	297	289	348	716	103	2.8	5.5	0.5	12.3	18.9	0.21	1.31	3.82	133	53	126	1	3031	Original (A)
3b-G4	295	339	330	696	97	3.2	6.9	1.0	6.9	21.4	0.22	1.02	5.14	57	41	130	4	5875	Original
3b-W2	63	389	153	481	41	2.5	0.6	0.3	9.8	13.3	0.12	1.52	0.38	22	42	3	BD	131	Medieval - Staffordshire?
3b-W13	77	402	190	464	62	2.9	0.8	0.3	12.3	13.1	0.13	1.32	0.52	35	49	38	2	499	Medieval - Staffordshire?
3b-W49	92	470	233	832	113	4.5	5.9	0.9	9.7	13.1	0.17	1.13	1.24	57	55	78	BD	2868	Medieval - Weald?
3b-B19	659	372	264	652	77	3.0	5.0	0.7	10.5	17.2	0.17	1.13	1.96	765	65	52	BD	1842	Medieval
3b-B12	999	245	65	643	119	2.5	4.2	0.7	4.2	30.4	0.21	0.86	1.12	1739	984	20	BD	1357	HLLA; Ni-rich Co
3b-B14	1065	250	69	673	126	2.8	1.4	0.4	4.9	27.8	0.24	0.97	0.99	1909	1053	BD	BD	512	HLLA; Ni-rich Co
3b-B15	1184	272	51	780	113	1.2	4.6	0.8	4.7	26.3	0.31	1.09	1.03	1500	955	34	14	1250	HLLA; Ni-rich Co
3b-B16	1024	246	67	669	124	3.1	1.3	0.4	5.3	26.3	0.23	0.98	0.73	1900	1047	BD	BD	319	HLLA; Ni-rich Co
3b-B17	1024	243	67	673	120	2.7	2.5	0.5	4.3	30.8	0.22	0.90	0.77	1826	1017	8	2	817	HLLA; Ni-rich Co
3b-R5	445	207	268	626	65	3.9	2.3	0.5	19.1	12.4	0.20	1.05	0.40	57	66	22	BD	918	Medieval
3b-R8	1663	681	445	682	72	3.1	3.1	0.6	16.4	20.6	0.18	1.02	0.52	4	63	34	BD	1431	Medieval

	Quantitative. Element ppm					Semi-quantitative. Oxide weight per cent;								Element ppm					
Sample	Cu	Zn	Rb	Sr	Zr	P_2O_5	SO_3	Cl	K_2O	CaO	TiO_2	MnO	Fe_2O_3	Co	Ni	Sn	Sb	Pb	ID
3b-R9	305	218	142	572	80	2.0	4.2	0.8	7.6	14.3	0.15	0.70	1.07	63	58	91	11	1305	Medieval
3b-R10	764	410	205	697	94	1.7	8.8	0.5	4.5	30.6	0.18	0.50	0.85	61	68	862	5	5173	Medieval
3b-R11	189	345	226	622	80	BD	6.7	0.6	4.9	25.6	0.17	0.72	0.63	61	61	250	17	4140	Medieval
3b-R12	462	177	248	612	63	3.7	3.2	0.4	16.4	17.9	0.19	0.95	0.40	35	70	45	BD	2251	Medieval
3b-G8	20947	5334	280	415	78	4.4	1.4	0.5	13.8	13.8	0.18	0.89	1.15	70	52	4275	51	3160	Medieval
3b-G9	22699	157	ND	ND	ND	0.3	13.8	1.6	4.8	4.4	0.08	1.48	17.26	957	BD	1073	BD	208675	Soda or Lead
3b-G10	4869	78	14	163	52	BD	4.5	0.5	0.7	11.5	0.16	4.15	2.23	574	84	187	1	2035	Soda
10c-W1	330	474	250	578	56	9.2	2.7	0.6	9.9	13.8	0.14	1.38	1.32	BD	BD	142	BD	1977	Original
10c-W2	339	458	259	571	52	BD	4.9	0.8	8.8	11.6	0.14	1.28	2.11	BD	BD	162	BD	3200	Original
10c-W4	295	453	256	577	56	BD	0.4	0.4	11.3	14.1	0.13	1.39	0.55	121	BD	211	BD	1209	Original
10c-W14	300	467	269	613	53	10.5	1.0	0.4	11.3	14.6	0.14	1.41	0.61	161	BD	159	BD	1436	Original
10c-W15	227	451	248	592	57	7.4	0.7	0.3	11.1	14.6	0.14	1.44	0.65	126	BD	135	BD	1215	Original
10c-W16	226	445	245	554	51	9.2	1.3	0.4	10.2	13.9	0.13	1.37	0.66	120	BD	190	BD	1523	Original
10c-W18	221	445	253	579	57	7.2	0.6	0.3	11.2	14.7	0.13	1.43	0.57	99	BD	201	BD	1202	Original
10c-W21	251	453	247	567	59	10.1	1.5	0.4	10.8	14.5	0.14	1.44	0.75	124	BD	128	BD	1450	Original
10c-W22	137	427	214	613	54	10.2	2.4	0.5	9.7	15.7	0.15	1.44	0.75	BD	BD	71	BD	1262	Original
10c-W23	155	436	213	625	58	8.3	0.9	0.3	10.0	15.0	0.14	1.48	0.60	118	BD	75	BD	957	Original
10c-W24	333	471	261	569	57	8.2	1.0	0.3	11.5	14.3	0.13	1.38	0.55	144	BD	188	BD	1372	Original
10c-W26	113	459	210	543	53	7.4	1.6	0.4	10.1	14.3	0.12	1.36	0.52	142	BD	152	BD	1375	Original
10c-W27	91	457	225	556	54	8.5	3.4	0.6	9.9	14.4	0.14	1.36	0.52	113	BD	148	BD	1991	Original
10c-W28	237	379	242	583	60	7.9	1.2	0.5	9.9	11.8	0.12	1.54	0.57	148	BD	211	BD	1222	Original
10c-W30	126	446	206	572	49	8.1	1.7	0.4	8.6	15.3	0.14	1.41	0.49	149	BD	128	BD	860	Original
10c-W31	142	383	213	581	54	9.0	2.6	0.5	7.5	12.1	0.13	1.54	0.54	113	BD	96	BD	1151	Original
10c-W32	76	395	219	599	57	8.2	1.6	0.5	8.4	13.1	0.13	1.66	0.53	112	BD	BD	BD	722	Original
10c-W33	81	392	214	581	57	BD	1.4	0.4	8.4	13.0	0.12	1.62	0.50	115	BD	BD	BD	583	Original
10c-W34	83	400	216	585	58	BD	0.9	0.3	8.5	13.0	0.14	1.64	0.56	108	BD	BD	BD	395	Original
10c-W35	103	413	266	603	45	9.2	1.7	0.6	11.3	12.3	0.11	1.64	0.50	127	BD	189	BD	1686	Original
10c-W36	161	436	209	564	55	9.1	3.1	0.7	9.1	13.3	0.14	1.41	0.63	119	BD	136	BD	1498	Original
10c-W37	173	433	250	523	54	10.1	1.7	0.5	9.9	14.4	0.13	1.35	0.54	BD	BD	235	BD	1475	Original
10c-W38	222	442	238	580	51	9.0	1.4	0.4	10.3	15.1	0.15	1.37	0.85	103	BD	158	BD	1836	Original
10c-W39	244	451	230	554	47	BD	5.4	0.8	7.3	11.9	0.13	1.17	1.74	BD	BD	176	BD	3833	Original
10c-W40	231	455	247	589	57	8.3	2.1	0.4	9.6	16.1	0.13	1.31	0.88	BD	BD	186	BD	2099	Original
10c-W41	249	423	236	536	47	BD	6.0	0.8	8.0	11.5	0.13	1.25	2.00	BD	BD	173	BD	3748	Original
10c-B3	1791	2683	273	879	93	11.1	1.8	0.3	11.2	24.9	0.19	1.30	1.28	1170	BD	317	96	2736	Not original; Composition identical
10c-B6	928	820	344	665	102	BD	7.7	0.5	6.3	15.8	0.22	1.28	1.19	494	BD	232	BD	3638	Original - light blue
10c-W7	141	422	213	566	57	7.9	1.1	0.4	10.8	14.4	0.14	1.53	0.60	125	BD	140	BD	1443	Medieval - Staffordshire?
10c-W9	133	394	191	583	56	8.6	0.7	0.3	10.3	16.3	0.16	1.63	0.55	124	BD	BD	BD	650	Medieval - Staffordshire?
10c-W10	77	369	208	554	54	8.2	3.0	0.6	8.8	12.7	0.14	1.47	0.90	BD	BD	75	BD	1778	Medieval - Staffordshire?
10c-W25	125	415	187	548	64	8.3	1.7	0.4	9.7	15.7	0.16	1.62	0.64	145	BD	BD	BD	1005	Medieval - Staffordshire?
10c-W11	1510	544	231	434	84	8.7	0.5	0.4	14.1	13.9	0.18	0.88	0.92	BD	BD	424	BD	2335	Medieval - Weald?
10c-W6	135	298	65	756	133	9.1	0.5	0.4	6.2	21.8	0.28	1.42	0.90	BD	BD	BD	BD	156	HLLA
10c-W8	39	269	40	835	220	10.3	0.7	0.5	4.7	24.0	0.35	0.66	0.65	124	BD	BD	BD	174	HLLA
10c-W12	119	285	60	739	123	BD	1.0	0.4	5.8	22.4	0.30	1.45	0.81	BD	BD	BD	BD	256	HLLA
10c-W13	62	287	64	755	138	9.6	1.2	0.5	6.2	21.5	0.29	1.39	0.85	BD	BD	BD	BD	366	HLLA
10c-W19	133	310	63	775	139	9.4	1.3	0.5	5.8	21.5	0.28	1.39	0.94	BD	BD	BD	BD	415	HLLA
10c-W20	157	305	60	750	129	11.1	0.6	0.4	6.3	22.7	0.30	1.46	0.87	BD	BD	BD	BD	118	HLLA
10c-W17	ND	36	14	77	51	BD	0.1	BD	0.2	7.4	0.03	0.02	0.08	115	BD	70	BD	92	Soda
10c-B2	630	569	93	517	79	9.3	0.3	0.3	14.0	19.3	0.15	0.46	1.18	878	BD	77	BD	221	Medieval
10c-B4	1261	369	133	545	93	BD	1.4	0.3	12.7	18.4	0.26	1.46	1.20	995	569	BD	BD	503	Medieval; Ni-rich Co
10c-B7	1163	375	134	576	90	BD	1.1	0.3	12.5	19.1	0.26	1.45	1.19	1037	580	BD	BD	395	Medieval; Ni-rich Co
10c-B8	1218	405	141	551	90	BD	1.1	0.3	12.5	18.9	0.27	1.45	1.20	1037	580	BD	BD	425	Medieval; Ni-rich Co
10c-B1	1707	71	10	151	30	BD	0.7	0.1	0.6	11.2	0.06	0.69	1.27	907	BD	4919	BD	267	Soda
10c-B9	6374	190	ND	ND	ND	BD	16.4	1.8	5.8	2.5	0.03	0.55	5.23	735	BD	561	BD	198055	Soda
10c-B10	5471	208	ND	ND	ND	BD	17.6	2.1	5.2	3.4	0.03	0.59	5.63	982	BD	608	BD	196426	Soda
10c-B11	8646	189	ND	151	31	BD	0.7	0.5	0.3	13.4	0.03	0.99	1.62	696	503	BD	BD	11686	Soda

	Quantitative. Element ppm					Semi-quantitative. Oxide weight per cent;								Element ppm					
Sample	Cu	Zn	Rb	Sr	Zr	P_2O_5	SO_3	Cl	K_2O	CaO	TiO_2	MnO	Fe_2O_3	Co	Ni	Sn	Sb	Pb	ID
10c-R1	683	523	73	548	92	10.5	0.5	0.5	7.3	21.4	0.19	0.83	0.81	182	63	BD	BD	385	HLLA
10e-W1	288	469	253	553	55	9.8	6.4	1.0	8.5	13.1	0.14	1.24	1.86	114	46	144	BD	3501	Original
10e-W2	206	387	245	603	61	6.2	1.2	0.4	10.0	12.0	0.14	1.57	0.64	148	BD	131	BD	1314	Original
10e-W3	105	442	207	535	51	9.8	0.7	0.3	10.3	14.3	0.13	1.36	0.51	125	BD	127	BD	1108	Original
10e-W5	68	422	224	617	60	6.7	2.7	0.5	8.5	12.9	0.14	1.67	0.56	114	BD	BD	BD	1059	Original
10e-W8	194	398	244	585	60	6.9	2.1	0.6	9.4	11.3	0.14	1.52	0.59	127	BD	148	BD	1584	Original
10e-W9	204	406	248	614	62	BD	1.3	0.4	10.5	12.4	0.13	1.62	0.58	140	BD	91	BD	1103	Original
10e-W10	217	430	250	606	62	8.9	1.8	0.5	10.4	12.6	0.17	1.58	0.62	87	BD	89	BD	1357	Original
10e-W11	182	392	246	592	61	8.7	1.3	0.5	10.6	12.1	0.14	1.61	0.60	117	BD	105	BD	1177	Original
10e-W12	224	389	247	616	62	9.6	1.4	0.5	10.3	12.2	0.14	1.61	0.63	130	BD	146	BD	1336	Original
10e-W13	187	381	247	576	63	7.4	0.9	0.4	10.1	12.3	0.14	1.58	0.59	170	BD	122	BD	1049	Original
10e-W14	115	457	208	558	50	10.8	1.5	0.5	10.5	15.1	0.14	1.45	0.50	122	BD	117	BD	1147	Original
10e-W15	82	400	215	596	58	7.1	2.2	0.4	8.1	12.7	0.13	1.62	0.62	98	BD	77	BD	1372	Original
10e-W16	111	436	212	541	51	10.5	1.9	0.5	10.3	15.0	0.13	1.41	0.51	120	BD	164	BD	1429	Original
10e-W17	143	423	210	605	58	9.7	1.3	0.3	10.0	14.9	0.13	1.49	0.56	150	BD	98	BD	1127	Original
10e-W18	124	464	212	556	50	9.9	3.2	0.6	10.1	14.8	0.14	1.41	0.80	102	BD	153	BD	1912	Original
10e-W19	207	392	249	598	60	9.2	3.8	0.8	8.9	10.8	0.13	1.46	0.66	131	BD	153	BD	2494	Original
10e-W20	318	473	265	566	55	9.1	1.5	0.4	11.2	14.2	0.15	1.37	0.65	141	BD	179	BD	1644	Original
10e-W21	258	446	242	566	51	8.5	4.7	0.9	9.6	13.1	0.14	1.27	0.74	113	BD	175	BD	3374	Original
10e-W22	100	457	218	556	55	11.1	3.4	0.7	9.6	14.4	0.14	1.38	0.52	133	BD	133	BD	2082	Original
10e-W23	202	380	239	594	55	BD	1.8	0.6	9.8	12.0	0.12	1.54	0.50	118	BD	108	BD	1257	Original
10e-W24	133	375	229	633	60	14.2	3.2	0.8	9.5	12.1	0.13	1.45	0.60	108	BD	115	BD	1891	Original
10e-W25	129	434	212	566	55	8.0	1.1	0.3	10.6	15.1	0.14	1.45	0.54	113	BD	137	BD	1055	Original
10e-W26	116	467	208	544	49	9.5	2.1	0.5	10.0	14.3	0.13	1.40	0.54	115	BD	145	BD	1561	Original
10e-W27	203	399	247	591	50	7.6	1.1	0.5	10.3	12.4	0.14	1.57	0.50	113	BD	144	BD	1053	Original
10e-W28	124	433	206	528	49	9.0	3.4	0.7	9.2	13.8	0.13	1.39	0.51	127	BD	143	BD	2058	Original
10e-W29	140	440	214	568	54	12.5	4.2	0.8	9.3	13.5	0.13	1.34	0.54	132	BD	127	BD	2296	Original
10e-W30	292	471	250	547	51	10.6	4.7	0.9	9.6	12.6	0.13	1.30	0.91	130	BD	161	BD	2546	Original
10e-W31	106	406	261	606	46	12.0	1.9	0.7	11.1	11.8	0.11	1.62	0.50	97	BD	189	BD	1689	Original
10e-W32	111	425	207	530	51	10.9	3.5	0.7	9.3	13.4	0.12	1.35	0.48	139	BD	113	BD	1898	Original
10e-W33	116	457	214	546	52	9.4	1.3	0.4	10.3	14.9	0.13	1.40	0.53	120	47	130	BD	1273	Original
10e-W34	128	429	214	532	51	7.3	0.7	0.3	10.5	14.9	0.13	1.39	0.53	107	BD	151	BD	1059	Original
10e-W35	142	428	210	541	47	9.3	5.7	0.9	8.2	12.8	0.13	1.29	1.18	126	BD	129	BD	2951	Original
10e-W36	102	439	214	544	48	9.8	2.2	0.5	10.1	15.6	0.13	1.37	0.50	150	BD	162	BD	1708	Original
10e-B1	1009	1439	300	774	104	BD	1.1	0.3	12.6	22.0	0.18	1.21	0.96	978	BD	226	BD	2910	Not original; Composition identical
10e-B2	1297	1575	278	768	91	11.5	5.3	0.8	9.5	24.0	0.17	0.98	1.33	1000	BD	247	BD	4992	Original
10e-B3	1337	1534	277	767	86	10.2	4.8	0.7	10.6	20.8	0.17	1.06	1.31	1013	BD	255	82	2727	Original
10e-B4	1256	1296	239	782	90	14.7	3.6	0.6	11.2	22.3	0.17	1.26	1.27	742	BD	182	BD	3275	Original
10e-B5	1650	1311	289	840	98	9.3	2.8	0.5	10.8	22.5	0.19	1.24	1.15	824	BD	185	74	2201	Original
10e-B6	1444	1597	283	770	93	13.3	2.4	0.4	11.9	23.0	0.17	1.13	1.42	994	63	249	BD	2057	Original
10e-B7	1450	1539	277	738	90	14.0	2.5	0.4	11.9	22.6	0.18	1.11	1.35	1036	BD	228	72	1915	Original
10e-B8	1361	1306	249	806	86	11.0	4.0	0.7	10.8	22.2	0.16	1.24	1.28	802	BD	219	BD	3662	Original
10e-B9	1521	1235	289	801	94	9.8	3.1	0.5	11.8	22.9	0.18	1.13	1.54	1077	BD	221	BD	2025	Original
10e-B10	1294	1197	277	790	85	11.7	4.9	0.8	10.5	21.4	0.17	1.07	1.57	1085	BD	233	69	3136	Original
10e-B11	1262	1271	239	798	86	9.5	2.5	0.4	11.3	21.5	0.18	1.25	1.28	800	BD	207	BD	2560	Original
10e-B12	1374	1575	281	768	85	11.9	2.5	0.4	11.5	21.7	0.17	1.09	1.37	1028	59	267	72	1829	Original
10e-B14	1152	1303	238	756	90	11.4	3.8	0.6	9.7	21.7	0.15	1.16	1.34	749	BD	186	67	3939	Original
10e-B15	1411	1545	275	749	88	11.1	3.5	0.5	11.3	21.9	0.18	1.09	1.37	1012	BD	232	BD	2458	Original
10e-R1	395	216	273	885	92	12.0	5.4	0.7	9.3	30.6	0.16	1.13	0.55	132	BD	170	BD	9535	Original
10e-R4	445	196	296	884	104	9.4	3.6	0.5	10.4	25.1	0.17	1.26	1.05	124	BD	126	BD	3802	Original
10e-R7	401	194	286	900	101	BD	3.9	0.5	9.5	27.6	0.17	1.18	0.64	121	BD	110	BD	6072	Original
10e-R8	489	202	305	892	105	10.5	6.2	0.9	9.9	23.3	0.17	1.25	0.60	129	BD	113	BD	5134	Original
10e-R10	427	204	284	908	97	BD	5.4	0.8	9.0	26.0	0.15	1.17	0.58	154	BD	348	BD	8823	Original
10e-R11	405	221	293	896	94	12.6	10.2	1.2	8.1	22.5	0.16	1.11	0.61	117	BD	302	BD	10327	Original
10e-R12	285	240	273	709	108	8.7	4.6	0.8	9.8	18.9	0.15	0.94	0.53	137	BD	167	BD	4934	Original

	Quantitative. Element ppm					Semi-quantitative. Oxide weight per cent;								Element ppm					
Sample	Cu	Zn	Rb	Sr	Zr	P_2O_5	SO_3	Cl	K_2O	CaO	TiO_2	MnO	Fe_2O_3	Co	Ni	Sn	Sb	Pb	ID
10e-R13	481	244	284	898	98	10.8	3.8	0.6	10.4	26.3	0.18	1.27	0.58	144	BD	108	BD	4629	Original
10e-R14	508	210	283	887	96	8.7	4.7	0.7	9.8	24.3	0.18	1.19	0.68	141	BD	94	BD	4854	Original
10e-R15	512	200	299	920	104	9.3	6.4	0.8	9.2	24.3	0.18	1.22	2.05	BD	BD	120	BD	4264	Original
10e-R16	366	188	259	842	85	BD	7.3	0.7	6.4	28.6	0.17	0.93	0.91	BD	BD	175	BD	8470	Original
10e-R17	355	202	286	897	98	BD	6.8	0.9	7.7	29.2	0.16	0.98	1.11	BD	BD	216	BD	10658	Original
10e-G3	413	374	284	737	89	BD	6.5	0.7	3.2	26.4	0.21	1.19	2.40	BD	BD	88	BD	4700	Original (B)
10e-G6	491	447	296	771	97	BD	9.7	0.7	2.5	24.0	0.22	1.44	2.04	BD	BD	87	BD	4353	Original
10e-G8	242	324	311	597	114	BD	6.3	0.7	4.9	20.0	0.22	1.11	2.76	BD	BD	94	BD	3244	Original
10e-G9	512	432	285	727	91	BD	8.4	0.5	2.7	19.8	0.25	1.45	2.41	BD	BD	106	BD	3556	Original
10e-G10	444	403	284	715	91	BD	9.6	0.6	3.0	28.2	0.20	1.35	2.23	BD	BD	133	BD	5992	Original
10e-G11	608	555	342	665	59	BD	7.6	0.4	5.8	20.3	0.21	1.86	2.06	330	BD	88	BD	2320	Original?
10e-G14	496	420	298	778	98	BD	9.4	0.5	4.7	17.5	0.27	1.71	2.36	BD	BD	BD	BD	2063	Original
10e-G15	246	386	290	573	104	BD	8.4	1.0	3.3	39.0	0.12	0.68	3.10	BD	BD	108	BD	8492	Original
10e-W4	86	356	45	1255	144	11.3	1.0	0.4	5.1	26.7	0.16	0.93	0.60	145	BD	BD	BD	591	HLLA
10e-B13	581	310	94	763	207	BD	5.9	1.0	7.2	19.3	0.32	1.15	0.58	669	369	BD	BD	2789	HLLA; Ni-rich Co
10e-R2	498	371	199	552	70	BD	0.7	0.4	12.6	13.8	0.15	0.98	0.73	99	BD	374	BD	1176	Medieval
10e-R3	268	328	160	491	28	BD	10.7	1.2	10.8	12.3	0.12	0.85	0.63	BD	BD	2923	164	34982	Medieval
10e-R6	925	358	410	657	47	8.8	4.2	0.9	10.2	8.9	0.09	0.94	0.40	96	BD	261	BD	1762	Medieval
10e-R9	200	319	192	536	71	6.9	0.4	0.3	12.3	13.2	0.14	0.99	0.68	105	BD	119	BD	747	Medieval
10e-G4	23129	2646	328	355	45	BD	5.6	1.0	10.7	11.4	0.12	0.71	5.99	BD	BD	1486	82	8429	Medieval
10e-G16	20800	2440	214	328	65	BD	4.0	0.6	11.7	12.5	0.14	0.77	2.54	BD	BD	1301	87	2976	Medieval
10e-G17	3105	7884	21	2808	46	BD	0.9	0.4	3.8	12.3	0.09	0.10	1.55	BD	BD	252	358	12081	Kelp ash
10e-G5	4091	107	10	144	36	BD	1.9	0.3	0.9	11.7	0.10	3.83	1.17	264	BD	159	BD	1094	Soda
10e-G12	47	942	22	146	55	BD	8.7	1.1	0.1	7.9	0.19	1.65	3.93	BD	BD	BD	BD	6910	Soda
10e-G13	33	1262	18	152	52	BD	8.7	1.0	0.1	7.1	0.18	1.66	4.15	BD	BD	BD	BD	6400	Soda
10e-G18	30262	677	16	101	33	BD	2.9	0.4	0.3	16.1	0.09	0.26	2.90	BD	BD	BD	168	17569	Soda
10e-G19	3954	103	9	148	40	BD	1.6	0.2	0.7	12.5	0.10	3.68	1.11	232	BD	156	BD	562	Soda
10e-G20	800	113	ND	165	50	BD	3.7	0.4	0.6	14.7	0.20	4.95	2.36	294	54	647	BD	5642	Soda
10h-W1	171	392	251	588	59	7.0	2.5	0.7	9.5	11.5	0.14	1.54	0.58	109	BD	122	BD	1724	Original
10h-W9	106	437	212	569	47	9.9	3.1	0.6	9.7	14.2	0.13	1.39	0.50	126	BD	154	BD	1966	Original
10h-W10	99	379	242	669	64	10.7	2.4	0.7	12.0	13.1	0.14	1.58	0.48	119	BD	81	BD	1289	Original
10h-W12	81	397	244	651	57	9.9	1.3	0.5	13.0	13.6	0.13	1.62	0.52	98	BD	81	BD	837	Original
10h-W13	101	807	213	563	52	9.5	2.0	0.5	9.8	15.7	0.14	1.38	1.00	BD	BD	153	BD	1799	Original
10h-W15	87	419	260	701	70	9.4	2.3	0.7	12.4	13.2	0.14	1.58	0.52	137	BD	99	BD	1153	Original
10h-W16	91	384	254	675	66	9.0	6.1	0.9	9.7	15.4	0.14	1.39	1.49	BD	BD	90	BD	3585	Original
10h-W17	217	440	266	625	58	7.6	0.4	0.4	11.1	13.4	0.14	1.68	0.60	107	BD	103	BD	897	Original
10h-W20	95	397	241	647	58	11.7	0.6	0.5	12.4	13.4	0.14	1.57	0.47	127	BD	131	BD	589	Original
10h-W21	66	404	238	649	58	12.2	2.5	0.6	11.8	12.7	0.13	1.55	0.50	129	BD	66	BD	2126	Original
10h-W22	83	398	249	646	57	8.4	1.2	0.4	12.5	13.5	0.13	1.57	0.48	104	BD	63	BD	812	Original
10h-W23	69	390	237	659	58	8.0	2.2	0.6	11.7	12.7	0.13	1.52	0.51	146	BD	68	BD	1435	Original
10h-W24	105	392	253	676	62	8.8	1.1	0.5	12.6	13.7	0.14	1.61	0.49	148	BD	127	BD	768	Original
10h-W25	111	465	220	563	48	9.8	1.3	0.4	10.6	15.6	0.13	1.45	0.61	87	BD	147	BD	1255	Original
10h-W26	114	456	212	521	54	9.8	2.1	0.5	10.3	15.1	0.14	1.42	0.51	123	BD	117	BD	1570	Original
10h-W27	126	442	207	512	46	BD	4.8	0.7	7.6	12.9	0.14	1.16	2.29	BD	BD	177	BD	6149	Original
10h-W28	92	393	270	693	61	8.6	1.4	0.5	12.4	13.9	0.15	1.58	0.62	BD	BD	81	BD	1219	Original
10h-W29	82	402	246	660	59	8.1	2.1	0.6	12.0	13.1	0.14	1.55	0.53	113	BD	66	BD	1401	Original
10h-W30	102	392	249	643	59	11.4	1.1	0.4	12.5	13.4	0.14	1.59	0.54	141	BD	121	BD	847	Original
10h-W31	122	448	199	544	50	10.3	0.8	0.3	10.3	15.0	0.12	1.42	0.48	142	BD	140	BD	936	Original
10h-W32	119	467	218	572	50	8.3	3.1	0.6	9.3	15.1	0.13	1.34	2.14	BD	48	169	BD	2158	Original
10h-W33	110	454	215	568	52	10.7	3.0	0.6	9.7	14.6	0.15	1.37	0.70	123	43	161	BD	1830	Original
10h-W34	136	478	210	553	48	7.7	6.9	1.1	6.7	15.5	0.10	1.15	2.91	BD	BD	152	BD	4499	Original
10h-W35	135	378	239	619	54	9.7	7.0	1.1	7.1	12.2	0.14	1.52	1.48	118	BD	147	BD	3662	Original
10h-W36	233	443	250	565	51	9.7	3.6	0.7	9.7	14.0	0.13	1.39	0.91	BD	BD	147	BD	2331	Original
10h-W38	113	446	223	568	54	8.6	1.8	0.5	9.8	14.6	0.13	1.39	0.66	143	BD	114	BD	1115	Original
10h-W41	94	450	215	564	46	8.3	1.1	0.3	10.3	15.4	0.13	1.44	0.55	87	BD	75	BD	834	Original

	Quantitative. Element ppm					Semi-quantitative. Oxide weight per cent;								Element ppm					
Sample	Cu	Zn	Rb	Sr	Zr	P_2O_5	SO_3	Cl	K_2O	CaO	TiO_2	MnO	Fe_2O_3	Co	Ni	Sn	Sb	Pb	ID
10h-W42	95	413	252	680	61	10.5	0.7	0.4	12.6	13.7	0.13	1.56	0.51	104	BD	109	BD	636	Original
10h-W43	97	417	265	583	42	9.5	3.2	0.8	10.6	12.2	0.13	1.60	0.47	142	BD	170	BD	2716	Original
10h-W44	310	447	268	530	53	10.8	2.8	0.6	10.6	13.0	0.12	1.32	0.62	145	BD	267	BD	2609	Original
10h-W45	160	372	260	589	54	8.7	1.6	0.4	9.8	11.6	0.13	1.55	0.60	119	BD	145	BD	1332	Original
10h-W47	129	435	236	654	59	14.4	7.6	1.1	6.8	13.8	0.12	1.16	4.43	BD	BD	115	BD	8041	Original
10h-W49	76	384	241	651	58	8.2	1.3	0.5	11.8	13.0	0.14	1.51	0.49	142	BD	58	BD	1023	Original
10h-W50	107	450	206	531	50	8.1	2.7	0.6	9.5	14.4	0.12	1.37	0.50	129	BD	122	BD	2379	Original
10h-W56	217	447	235	561	56	9.2	1.0	0.4	10.7	14.3	0.13	1.41	0.54	110	BD	152	BD	1390	Original
10h-W57	176	407	262	608	62	7.5	0.4	0.4	11.0	12.8	0.14	1.63	0.59	128	BD	118	BD	810	Original
10h-W58	103	444	212	558	51	8.6	1.5	0.4	10.3	15.2	0.13	1.41	0.50	125	BD	138	BD	1301	Original
10h-W59	97	390	240	608	52	10.4	1.8	0.6	10.5	13.3	0.13	1.64	0.56	125	BD	167	BD	1678	Original
10h-W60	196	391	245	592	61	6.3	2.7	0.6	9.8	11.9	0.14	1.56	0.59	120	BD	138	BD	1878	Original
10h-B1	1581	1936	281	745	95	11.8	1.9	0.3	11.6	22.9	0.18	1.16	1.31	798	BD	217	73	1812	Original
10h-B2	1360	1282	280	737	83	13.3	4.9	0.8	11.0	21.7	0.18	1.09	1.46	1095	BD	235	BD	4963	Original
10h-B3	1165	1702	324	764	91	14.4	9.8	1.4	9.8	18.0	0.18	1.12	1.03	1080	BD	235	87	8463	Original
10h-B4	1472	1308	288	773	83	9.5	2.9	0.5	11.5	21.6	0.18	1.09	1.45	1095	BD	224	BD	1911	Original
10h-R7	626	235	298	870	92	13.9	4.6	0.7	10.5	20.8	0.16	1.20	0.71	136	BD	153	BD	2681	Original
10h-R8	252	252	285	784	82	10.8	5.5	0.8	10.1	19.4	0.15	1.13	0.76	147	BD	201	BD	8014	Original
10h-R14	494	217	275	789	86	12.5	5.1	0.7	9.6	24.2	0.16	1.09	0.69	126	BD	177	BD	5884	Original
10h-R16	242	252	281	782	85	9.6	3.9	0.6	10.4	19.8	0.16	1.16	0.74	137	BD	207	BD	2672	Original
10h-R18	583	237	287	814	93	11.1	3.3	0.5	10.7	22.7	0.16	1.14	0.70	142	BD	158	BD	3372	Original
10h-R19	602	232	294	847	101	11.2	3.2	0.5	11.1	22.0	0.16	1.20	0.72	152	BD	155	BD	2439	Original
10h-M1	93	205	294	1306	133	9.2	6.9	0.9	9.0	21.0	0.25	1.33	1.72	BD	BD	63	BD	2655	Original (B/C)
10h-M3	254	361	355	767	72	BD	6.2	0.4	5.9	13.3	0.26	1.75	0.54	205	51	185	BD	4793	Original (B); blue/purple/blue flashed glass
10h-M5	390	484	330	757	83	BD	7.1	0.5	6.0	12.3	0.26	1.67	0.71	280	BD	187	BD	7574	Original (B); blue/purple/blue flashed glass
10h-M12	279	257	387	616	62	BD	9.1	0.7	8.7	29.2	0.16	1.00	0.44	118	BD	140	BD	19964	Medieval
10h-M13	352	476	367	802	86	BD	8.5	0.5	4.6	14.0	0.28	1.73	0.71	273	BD	93	BD	1652	Original (B)
10h-M14	1092	406	273	700	93	BD	8.7	0.6	6.0	14.4	0.25	1.29	0.98	485	BD	113	BD	2597	Original (B)
10h-M15	175	501	367	776	40	12.7	1.8	0.4	16.3	11.6	0.12	1.76	0.52	124	BD	80	BD	1506	Original (B)
10h-W11	165	442	168	555	55	8.6	7.9	1.1	6.4	19.1	0.18	1.05	0.70	127	BD	178	BD	6416	Medieval - Staffordshire?
10h-W18	119	378	178	553	54	7.8	0.5	0.3	11.4	14.9	0.14	1.44	0.60	142	BD	161	BD	1273	Medieval - Staffordshire?
10h-W2	347	440	330	423	55	11.1	4.3	0.7	11.7	14.2	0.14	0.76	0.77	108	BD	105	BD	7472	Medieval - Weald?
10h-W4	689	259	226	583	92	10.6	2.5	0.5	10.8	13.4	0.18	0.78	1.08	165	BD	139	BD	1231	Medieval - Weald?
10h-W5	565	564	204	464	75	BD	10.4	1.3	7.0	12.2	0.14	0.68	4.03	BD	BD	154	BD	6597	Medieval - Weald?
10h-W7	638	267	244	595	88	8.0	2.1	0.5	11.1	12.9	0.17	0.78	1.07	124	BD	95	BD	1156	Medieval - Weald?
10h-W8	417	571	214	504	92	10.2	3.8	0.7	12.2	11.9	0.16	0.88	1.37	BD	BD	281	BD	3294	Medieval - Weald?
10h-W14	538	383	235	333	74	9.7	0.2	0.3	15.3	12.1	0.16	0.84	0.69	121	BD	110	BD	392	Medieval - Weald?
10h-W37	7845	342	98	437	105	BD	19.7	2.4	2.9	9.6	0.04	0.15	6.71	2122	1051	104	BD	28844	Medieval - Weald?
10h-W39	701	255	227	551	84	BD	6.4	0.9	9.0	13.3	0.15	0.73	2.14	BD	BD	131	BD	3213	Medieval - Weald?
10h-W40	568	249	243	583	91	BD	1.4	0.5	11.7	14.3	0.18	0.81	1.03	138	BD	82	BD	854	Medieval - Weald?
10h-W46	519	397	235	335	72	8.4	0.4	0.3	15.2	12.1	0.18	0.84	0.74	111	BD	116	BD	472	Medieval - Weald?
10h-W48	262	384	312	430	46	11.6	14.4	1.6	5.9	20.8	0.12	0.52	2.34	BD	BD	127	BD	12484	Medieval - Weald?
10h-W51	544	246	236	586	93	6.5	3.4	0.7	10.4	13.1	0.18	0.75	1.03	153	BD	106	BD	1572	Medieval - Weald?
10h-W52	549	257	236	585	86	6.8	1.1	0.4	11.8	15.2	0.18	0.80	1.03	130	BD	91	BD	1209	Medieval - Weald?
10h-W53	874	410	246	408	62	BD	4.9	0.8	9.5	12.0	0.16	0.84	3.33	BD	BD	345	BD	4355	Medieval - Weald?
10h-W54	1341	495	221	401	75	9.2	6.7	1.2	10.6	10.8	0.16	0.79	0.85	119	BD	328	BD	4235	Medieval - Weald?
10h-W19	300	114	ND	163	38	BD	4.5	0.5	0.4	9.4	0.09	2.64	1.24	445	BD	276	BD	2641	Soda
10h-W55	26	594	14	27	27	BD	8.1	0.9	0.2	5.0	0.06	0.12	0.75	BD	45	92	BD	7301	Soda
10h-R1	4638	705	170	440	81	10.5	0.4	0.3	15.2	15.0	0.16	0.77	1.09	133	BD	423	BD	847	Medieval
10h-R2	571	409	420	725	87	8.8	1.4	0.3	14.7	14.0	0.18	1.35	0.81	156	BD	163	BD	3459	Medieval
10h-R4	268	334	159	495	24	9.9	10.1	1.2	3.2	28.6	0.06	0.78	0.42	111	BD	243	BD	16187	Medieval
10h-R5	390	351	182	544	77	10.9	4.0	0.7	13.7	16.1	0.20	0.93	0.91	133	BD	153	BD	4828	Medieval
10h-R6	347	430	332	407	55	11.5	4.7	0.8	12.1	19.3	0.14	0.71	0.69	112	BD	163	BD	7477	Medieval
10h-R9	409	403	247	384	75	8.3	1.0	0.3	13.1	13.7	0.17	0.84	0.77	175	BD	186	BD	962	Medieval
10h-R10	325	396	171	519	31	9.4	5.0	0.7	5.0	14.7	0.08	1.13	0.53	129	BD	151	BD	9259	Medieval

	Quantitative. Element ppm					Semi-quantitative. Oxide weight per cent;								Element ppm					
Sample	Cu	Zn	Rb	Sr	Zr	P_2O_5	SO_3	Cl	K_2O	CaO	TiO_2	MnO	Fe_2O_3	Co	Ni	Sn	Sb	Pb	ID
10h-R11	321	473	346	404	63	12.1	4.0	0.8	12.8	12.2	0.15	0.81	0.73	98	BD	88	BD	2000	Medieval
10h-R12	407	393	246	390	72	9.9	0.9	0.4	15.0	14.8	0.16	0.91	0.80	BD	BD	165	BD	2562	Medieval
10h-R13	374	436	325	401	58	8.7	7.0	1.0	9.5	15.9	0.12	0.66	0.71	129	BD	172	BD	5775	Medieval
10h-R15	419	384	255	394	73	10.6	2.9	0.7	12.3	13.3	0.17	0.84	0.80	131	BD	142	BD	1812	Medieval
10h-R17	384	335	176	549	84	10.3	0.7	0.3	14.0	16.1	0.20	0.92	0.92	BD	BD	120	BD	498	Medieval
10h-R20	324	447	374	406	64	10.4	1.2	0.5	14.4	13.5	0.16	0.82	0.76	144	BD	93	BD	598	Medieval
10h-R21	379	336	176	478	82	10.7	2.1	0.5	14.1	13.7	0.20	0.82	0.88	167	BD	138	BD	1036	Medieval
10h-R3	6246	118	ND	56	28	BD	0.2	0.1	0.5	5.8	0.04	0.06	0.77	118	BD	1661	BD	1354	Soda
10h-R22	6296	137	ND	59	26	BD	0.8	0.2	0.5	5.6	0.04	0.06	0.79	129	BD	1701	BD	4329	Soda
10h-G3	29328	1498	193	599	78	10.7	2.1	0.6	12.9	17.5	0.19	0.91	1.28	BD	BD	2277	151	6897	Medieval
10h-G4	19592	2751	185	456	77	13.4	5.8	1.0	12.2	16.6	0.20	0.78	0.90	BD	BD	1868	81	3757	Medieval
10h-G9	27099	3033	212	358	78	9.8	3.5	0.7	12.9	13.4	0.21	0.83	1.27	BD	BD	1921	149	2780	Medieval
10h-G1	1632	100	10	145	123	BD	3.6	0.5	0.6	10.4	0.20	3.56	1.99	184	BD	92	BD	1572	Soda
10h-G2	4278	115	12	159	40	BD	2.9	0.4	0.4	11.0	0.11	3.89	1.22	306	60	147	BD	1170	Soda
10h-G5	1565	83	8	139	126	BD	1.1	0.2	0.5	11.6	0.21	3.69	1.91	154	BD	77	BD	469	Soda
10h-G6	5160	119	12	153	66	BD	1.5	0.2	0.5	12.0	0.19	4.42	2.17	564	58	178	BD	669	Soda
10h-G8	2733	136	9	155	59	BD	3.0	0.4	0.4	11.0	0.21	4.94	2.24	201	44	95	BD	1268	Soda
10h-G10	4466	107	9	158	42	BD	1.1	0.2	0.4	11.7	0.11	3.95	1.19	196	BD	169	BD	444	Soda
10h-G7	31403	14602	ND	92	ND	BD	19.3	2.4	5.0	1.5	0.04	0.23	1.83	524	BD	256	399	222263	Soda or Lead
10h-G11	15578	182	57	ND	ND	BD	9.2	1.1	5.3	5.9	0.06	1.17	10.74	BD	BD	609	BD	121248	Soda or Lead
10h-M8	482	553	ND	2578	30	6.3	5.9	0.8	3.6	12.4	0.11	0.14	1.41	BD	BD	270	85	40700	Kelp ash
10h-M2	ND	33	15	4166	43	BD	0.2	0.4	2.9	9.2	0.08	0.03	0.46	108	BD	BD	64	760	High lead glass on white kelp ash base
10h-M9	ND	36	12	4297	57	BD	0.2	0.4	3.1	9.5	0.08	0.03	0.47	101	BD	BD	BD	270	High lead glass on white kelp ash base
10h-M10	ND	32	16	4354	50	BD	BD	0.4	3.0	9.3	0.07	0.03	0.47	121	BD	BD	58	554	High lead glass on white kelp ash base
10h-M6	521	90	8	161	55	BD	1.9	0.2	0.5	10.8	0.13	5.57	1.29	230	BD	BD	BD	692	Soda
10h-M7	522	154	10	156	32	BD	4.6	0.6	0.3	9.6	0.08	5.18	1.06	323	58	59	BD	2314	Soda
10h-M11	47	1241	ND	211	34	BD	4.4	1.0	0.5	11.2	0.08	1.02	1.38	BD	57	70	177	21282	Soda
10h-M16	ND	36	12	76	45	BD	0.9	0.1	0.2	7.9	0.03	0.02	0.09	115	BD	424	BD	4479	Soda
15a-W1	128	443	222	588	48	3.7	0.8	0.2	9.3	15.9	0.14	1.42	0.51	93	BD	62	BD	585	Original
15a-W2	69	409	224	551	52	5.1	0.6	0.4	10.2	13.5	0.13	1.58	0.47	71	BD	67	BD	243	Original
15a-W3	85	425	212	631	62	4.7	2.1	0.4	8.5	14.5	0.14	1.57	0.54	87	BD	139	BD	1770	Original
15a-W4	64	376	260	563	48	3.8	0.9	0.4	10.0	12.1	0.12	1.60	0.46	68	19	34	BD	371	Original
15a-W5	83	389	263	591	53	3.9	1.0	0.4	9.8	11.8	0.12	1.57	0.47	75	19	47	BD	410	Original
15a-W6	67	411	229	555	47	4.5	2.5	0.6	9.6	13.1	0.13	1.52	0.47	80	20	36	BD	694	Original
15a-W7	99	395	242	599	54	3.7	0.5	0.3	9.9	13.5	0.12	1.50	0.55	90	BD	99	BD	544	Original
15a-W8	80	481	210	512	34	3.6	4.7	0.6	9.1	14.0	0.12	1.35	0.64	60	BD	BD	BD	971	Original
15a-W9	103	403	259	621	52	3.4	0.3	0.2	9.8	14.3	0.12	1.52	0.49	88	19	92	BD	535	Original
15a-W10	114	388	228	526	47	6.3	4.5	0.8	8.7	12.0	0.12	1.46	0.48	76	BD	103	BD	1206	Original
15a-W11	88	416	218	576	55	2.8	4.1	0.5	6.5	13.8	0.12	1.45	0.73	48	BD	45	BD	1583	Original
15a-W12	84	403	228	570	50	4.0	0.9	0.3	10.1	13.1	0.13	1.56	0.48	66	BD	49	BD	288	Original
15a-W13	88	408	228	555	47	4.2	1.3	0.4	9.7	13.0	0.13	1.53	0.47	75	23	41	BD	405	Original
15a-W14	75	413	243	549	53	4.6	4.8	0.8	8.9	12.3	0.11	1.53	0.47	85	BD	36	BD	1646	Original
15a-W15	82	421	220	622	59	4.1	2.1	0.4	8.3	14.4	0.14	1.52	0.54	78	BD	138	BD	1703	Original
15a-W16	110	445	212	561	46	3.7	1.1	0.3	9.2	15.9	0.13	1.35	0.51	78	19	104	BD	451	Original
15a-W17	80	400	270	644	57	4.9	0.9	0.4	11.6	13.5	0.13	1.63	0.50	76	BD	71	BD	649	Original
15a-W18	96	424	222	626	59	3.5	0.3	0.3	8.8	15.5	0.13	1.61	0.55	84	27	160	BD	1258	Original
15a-W19	91	421	222	636	58	3.2	0.7	0.3	8.7	14.8	0.14	1.57	0.53	98	19	160	BD	1338	Original
15a-W20	81	382	259	570	46	3.8	0.5	0.4	10.0	12.0	0.12	1.58	0.45	77	BD	BD	BD	276	Original
15a-W21	70	403	219	571	60	2.8	2.0	0.4	7.5	13.0	0.14	1.61	0.51	87	BD	BD	BD	526	Original
15a-W24	93	407	240	633	54	4.3	1.3	0.4	9.9	13.6	0.14	1.53	0.55	102	BD	100	BD	731	Original
15a-W25	127	406	201	570	58	3.4	3.6	0.4	9.8	15.1	0.14	1.43	0.78	52	20	113	BD	1505	Original
15a-W26	97	394	260	616	55	4.9	0.4	0.2	10.0	14.2	0.12	1.52	0.47	92	BD	68	BD	525	Original
15a-W27	90	482	207	502	31	5.0	8.0	1.1	8.2	12.6	0.10	1.30	0.48	73	BD	BD	BD	3536	Original
15a-W28	151	421	205	582	52	7.1	12.3	1.5	7.2	11.2	0.12	1.24	0.68	81	25	148	BD	5783	Original
15a-W29	75	494	203	509	37	3.7	0.9	0.3	10.3	14.4	0.11	1.41	0.40	81	27	BD	BD	243	Original

	Quantitative. Element ppm					Semi-quantitative. Oxide weight per cent;								Element ppm					
Sample	Cu	Zn	Rb	Sr	Zr	P_2O_5	SO_3	Cl	K_2O	CaO	TiO_2	MnO	Fe_2O_3	Co	Ni	Sn	Sb	Pb	ID
15a-W30	109	394	254	561	41	2.9	9.7	1.1	7.1	10.0	0.10	1.38	1.52	BD	BD	BD	BD	3423	Original
15a-W31	74	498	208	503	28	3.6	4.9	0.7	9.0	13.2	0.11	1.34	0.56	61	BD	BD	BD	1160	Original
15a-W32	80	495	213	515	34	3.8	4.0	0.6	9.5	13.6	0.11	1.37	0.44	71	26	BD	BD	1009	Original
15a-W33	80	499	211	517	36	3.4	0.6	0.2	10.9	15.1	0.12	1.48	0.40	68	BD	BD	BD	144	Original
15a-W34	89	500	206	515	34	5.2	7.0	0.9	8.6	12.4	0.10	1.32	0.71	44	27	39	BD	2015	Original
15a-W35	92	482	212	512	35	4.5	12.4	1.3	6.9	10.9	0.10	1.23	1.85	BD	BD	BD	BD	3927	Original
15a-W38	126	422	219	547	53	3.6	0.8	0.2	9.5	16.3	0.13	1.38	0.46	90	BD	36	BD	535	Original
15a-W39	83	400	233	547	52	4.2	0.3	0.4	10.4	13.6	0.13	1.61	0.47	68	32	49	BD	156	Original
15a-W40	128	463	218	542	67	3.9	0.4	0.2	10.9	15.2	0.14	1.41	0.59	84	22	127	BD	936	Original
15a-W41	114	391	242	590	53	4.4	3.6	0.6	9.5	13.5	0.13	1.51	0.55	79	BD	117	BD	1357	Original
15a-W42	100	395	236	585	55	4.0	0.6	0.3	10.0	13.8	0.13	1.51	0.53	97	19	87	BD	609	Original
15a-W43	108	415	249	605	47	4.9	1.1	0.3	10.0	13.9	0.13	1.55	0.55	97	22	104	BD	686	Original
15a-W44	101	388	216	580	63	3.8	1.7	0.5	9.8	14.2	0.13	1.45	0.52	80	BD	89	BD	1086	Original
15a-W48	109	463	217	555	52	3.8	0.6	0.2	9.6	16.0	0.12	1.37	0.48	91	18	56	BD	350	Original
15a-W22	64	422	159	447	38	2.4	0.2	0.3	8.8	13.5	0.11	1.52	0.38	91	BD	37	BD	99	Medieval - Staffordshire?
15a-W36	307	465	239	457	50	4.2	3.2	0.5	8.6	16.3	0.12	1.28	0.62	53	26	59	BD	503	Medieval - Staffordshire?
15a-W45	87	408	140	490	43	4.6	6.0	0.8	7.8	12.8	0.13	1.23	0.47	106	50	79	BD	2162	Medieval - Staffordshire?
15a-W23	703	287	243	584	68	3.3	1.2	0.3	9.7	16.2	0.16	0.76	0.78	57	BD	85	BD	1007	Medieval - Weald?
15a-W37	325	516	172	552	79	4.8	4.2	0.6	12.6	14.7	0.15	0.95	1.02	53	24	47	BD	2256	Medieval - Weald?
15a-W47	578	286	320	555	73	3.8	1.4	0.4	11.9	12.6	0.12	0.57	0.79	51	19	44	BD	469	Medieval - Weald?
15a-W46	279	63	16	3871	26	BD	5.5	0.8	3.1	9.4	0.06	0.02	0.39	91	BD	BD	BD	3396	Kelp ash
15a-B8	606	836	49	884	180	4.9	2.7	0.7	6.0	23.6	0.29	0.96	1.19	721	50	112	BD	849	HLLA; Ni-rich Co
15a-B9	703	270	81	696	244	4.0	0.3	0.3	5.8	22.9	0.38	1.24	0.79	763	626	BD	BD	35	HLLA; Ni-rich Co
15a-R11	267	318	140	384	97	5.4	2.0	0.3	13.1	14.7	0.20	0.72	0.79	69	37	37	BD	550	Medieval
15a-R12	394	347	189	530	80	4.3	0.7	0.4	13.0	16.6	0.20	0.93	0.93	83	18	67	BD	217	Medieval
15a-R14	2637	688	349	414	62	5.2	0.6	0.4	14.6	14.8	0.14	0.88	0.72	85	25	183	BD	307	Medieval
15a-R15	535	481	353	409	62	5.1	0.8	0.3	13.9	14.1	0.14	0.85	0.73	79	27	97	BD	444	Medieval
15a-R13	40	252	47	603	126	3.6	0.4	0.5	4.8	22.2	0.13	0.54	0.53	84	34	BD	BD	70	HLLA
15a-R4	400	560	24	2668	45	1.4	1.8	0.4	3.7	14.2	0.10	0.16	1.35	90	BD	229	70	23002	Kelp ash
15a-R17	39	101	6	158	27	BD	1.0	0.2	0.2	11.0	0.04	0.25	0.32	72	20	101	BD	308	Soda
15a-R18	26	124	5	152	29	BD	0.9	0.1	0.2	10.5	0.04	0.24	0.32	79	17	111	BD	240	Soda
15a-R20	28	96	3	180	29	BD	0.4	0.0	0.2	11.7	0.04	0.37	0.32	78	BD	123	BD	105	Soda
15a-R21	ND	98	ND	ND	ND	BD	28.7	2.5	6.0	0.1	0.02	0.06	0.06	BD	BD	319	65	257359	Soda
15a-B1	1356	2370	281	885	82	BD	9.4	1.3	2.6	41.5	0.10	0.79	1.19	731	44	290	91	8947	Original
15a-B2	1753	2577	287	838	94	2.5	9.0	1.0	6.8	22.3	0.14	1.04	5.14	555	83	353	96	6727	Original
15a-B3	1565	3277	284	884	85	4.0	6.0	0.6	8.3	33.7	0.14	1.05	1.36	1290	44	353	94	7526	Original
15a-B4	1473	2471	288	863	82	BD	10.7	1.8	3.5	34.8	0.11	0.85	1.12	777	59	293	99	8027	Original
15a-B5	1654	2784	289	862	94	5.8	5.5	0.6	9.5	23.7	0.17	1.27	1.24	1242	46	303	76	3678	Original
15a-B6	1271	2471	276	833	79	BD	10.1	1.0	2.3	38.7	0.10	0.69	1.51	627	43	301	100	10925	Original
15a-B7	1960	2880	296	887	101	4.0	1.1	0.2	11.6	25.8	0.18	1.36	1.27	1306	32	289	64	2011	Original
15a-B10	1739	2818	292	869	92	4.1	1.1	0.2	11.0	25.7	0.17	1.34	1.25	1243	60	276	70	1996	Original
15a-B11	1932	3013	294	869	100	5.6	2.0	0.2	10.9	25.2	0.19	1.35	1.30	1399	50	333	96	2299	Original
15a-R1	549	294	275	840	96	3.3	6.4	0.5	6.7	22.2	0.16	0.97	0.76	63	BD	116	BD	10557	Original
15a-R2	3500	293	284	845	91	2.8	10.7	0.8	5.1	19.2	0.19	0.90	0.74	78	BD	115	BD	8693	Original
15a-R3	445	227	287	882	101	3.7	6.2	0.5	7.0	26.7	0.17	1.06	0.61	105	BD	114	BD	4171	Original
15a-R5	618	271	284	805	92	3.4	4.3	0.5	9.3	24.9	0.15	1.19	0.58	115	BD	53	BD	9850	Original
15a-R6	987	240	273	730	95	3.3	2.8	0.5	10.3	21.5	0.15	1.01	0.50	87	BD	78	BD	2552	Original
15a-R7	594	230	306	904	96	4.9	3.7	0.5	9.9	24.7	0.17	1.32	0.58	105	23	77	BD	3173	Original
15a-R8	385	218	290	876	93	2.4	5.3	0.5	6.8	31.5	0.14	1.03	0.56	90	BD	84	BD	5025	Original
15a-R9	4339	305	298	861	94	2.1	6.0	0.9	3.6	13.9	0.23	0.87	1.01	BD	36	72	BD	5392	Original
15a-R10	3733	248	305	881	98	2.7	4.2	0.5	8.3	22.6	0.17	1.17	0.95	78	BD	93	BD	3362	Original
15a-R16	3294	253	313	893	94	4.0	1.5	0.2	10.1	25.0	0.18	1.31	0.55	128	36	59	BD	1911	Original
15a-R19	451	234	286	900	92	3.2	6.6	0.3	8.5	27.4	0.15	1.10	0.56	108	BD	109	BD	4437	Original
15a-G1	595	265	261	675	83	BD	7.6	0.5	5.6	26.7	0.18	0.97	1.36	148	46	49	BD	3755	Original (B)
15b-W1	101	375	219	571	49	3.1	0.4	0.3	10.3	14.5	0.12	1.47	0.48	83	BD	74	BD	562	Original

	Quantitative. Element ppm					Semi-quantitative. Oxide weight per cent;								Element ppm					
Sample	Cu	Zn	Rb	Sr	Zr	P_2O_5	SO_3	Cl	K_2O	CaO	TiO_2	MnO	Fe_2O_3	Co	Ni	Sn	Sb	Pb	ID
15b-W2	111	408	224	605	57	4.1	2.3	0.5	9.8	13.7	0.12	1.46	0.51	64	BD	85	BD	1057	Original
15b-W3	105	398	255	586	52	3.6	1.2	0.3	9.7	14.0	0.13	1.51	0.48	106	BD	64	BD	715	Original
15b-W4	121	408	223	575	54	3.0	0.5	0.2	7.3	13.5	0.13	1.64	0.52	82	BD	56	BD	389	Original
15b-W5	70	474	201	489	37	2.8	0.8	0.4	10.2	14.2	0.11	1.41	0.38	86	18	BD	BD	238	Original
15b-W6	75	476	214	512	34	3.4	1.2	0.4	9.7	14.1	0.11	1.41	0.44	78	28	BD	BD	405	Original
15b-W7	134	375	228	577	57	4.4	1.8	0.3	7.8	13.0	0.14	1.57	0.55	88	BD	81	BD	1032	Original
15b-W8	60	492	202	498	35	3.5	0.9	0.4	10.1	14.1	0.11	1.39	0.39	76	18	BD	BD	204	Original
15b-W9	153	456	251	560	54	4.0	3.3	0.5	8.9	13.1	0.14	1.22	0.82	47	BD	358	BD	2730	Original
15b-W10	73	461	212	523	34	4.4	1.3	0.4	10.0	14.1	0.11	1.43	0.43	71	22	BD	BD	410	Original
15b-W11	199	447	248	569	52	3.7	1.0	0.3	9.8	15.5	0.13	1.40	0.54	96	22	140	BD	1416	Original
15b-W12	108	395	229	593	55	3.5	0.4	0.3	10.4	14.8	0.12	1.50	0.51	94	BD	97	BD	571	Original
15b-W13	83	373	252	574	48	3.0	0.8	0.3	9.6	13.7	0.12	1.49	0.46	91	BD	71	BD	626	Original
15b-W14	107	396	254	617	51	3.1	1.2	0.3	9.8	14.0	0.13	1.52	0.48	80	BD	89	BD	756	Original
15b-W15	115	394	231	601	53	3.7	0.6	0.3	10.4	14.6	0.12	1.49	0.50	83	BD	63	BD	661	Original
15b-W16	94	387	255	609	50	3.9	0.6	0.3	10.0	14.0	0.13	1.52	0.48	103	BD	85	BD	580	Original
15b-W17	91	402	229	596	55	3.3	0.8	0.2	7.8	13.5	0.13	1.64	0.53	71	BD	42	BD	358	Original
15b-W18	98	398	254	594	49	3.8	0.8	0.3	9.8	14.0	0.13	1.53	0.49	78	36	88	BD	631	Original
15b-W19	189	420	220	589	50	2.9	0.6	0.3	8.5	13.7	0.13	1.60	0.51	87	BD	120	BD	994	Original
15b-W20	64	482	206	512	37	3.5	0.7	0.3	10.1	14.2	0.11	1.40	0.41	74	22	BD	BD	201	Original
15b-W21	200	389	228	613	56	3.5	0.4	0.2	9.6	14.2	0.13	1.62	0.54	112	BD	172	BD	1123	Original
15b-W22	69	507	208	504	37	3.7	1.0	0.3	10.0	14.0	0.15	1.40	0.40	84	23	45	BD	258	Original
15b-W23	80	505	204	520	36	3.9	2.9	0.6	9.4	13.3	0.10	1.37	0.41	93	BD	BD	BD	769	Original
15b-W24	80	498	201	478	32	3.4	1.3	0.4	9.6	13.7	0.11	1.38	0.38	82	BD	BD	BD	336	Original
15b-W25	116	459	258	540	61	3.9	3.3	0.5	9.3	13.4	0.12	1.26	0.71	60	BD	359	BD	2751	Original
15b-W26	75	490	201	500	35	3.4	1.3	0.4	9.7	13.5	0.12	1.37	0.40	79	BD	BD	BD	319	Original
15b-W27	69	468	198	488	35	3.6	0.9	0.4	9.9	13.9	0.11	1.38	0.39	72	BD	BD	BD	230	Original
15b-W28	72	452	198	486	36	3.7	0.7	0.3	9.9	13.8	0.11	1.37	0.38	84	BD	37	BD	167	Original
15b-W29	67	479	206	491	35	3.4	2.1	0.5	9.4	13.3	0.10	1.35	0.37	109	BD	BD	BD	578	Original
15b-W30	132	391	205	577	52	3.8	1.2	0.3	8.0	13.7	0.14	1.56	0.54	73	BD	90	BD	1052	Original
15b-W31	143	389	219	557	52	3.2	1.0	0.3	7.7	13.3	0.13	1.56	0.55	84	BD	91	BD	825	Original
15b-W32	139	434	222	611	57	3.3	2.3	0.4	8.1	13.9	0.14	1.55	0.52	100	BD	141	BD	1480	Original
15b-W33	124	409	213	621	64	4.3	1.2	0.3	8.4	14.4	0.14	1.59	0.51	87	BD	102	BD	1123	Original
15b-W34	182	404	220	626	61	3.3	1.9	0.4	9.3	14.1	0.14	1.59	0.60	93	BD	153	BD	1470	Original
15b-W35	195	407	229	650	56	3.5	1.0	0.3	9.8	14.3	0.13	1.61	0.58	112	BD	185	BD	1318	Original
15b-W36	142	377	216	555	57	3.6	0.3	0.2	7.9	13.5	0.13	1.59	0.54	84	BD	81	BD	636	Original
15b-W37	159	417	229	600	58	3.3	2.1	0.4	7.7	13.6	0.13	1.58	0.66	57	19	113	BD	1184	Original
15b-W38	84	499	220	500	35	3.5	1.2	0.3	10.0	14.1	0.11	1.42	0.45	57	19	BD	BD	482	Original
15b-W39	72	465	207	503	33	3.1	1.3	0.3	9.7	13.7	0.11	1.37	0.42	71	BD	BD	BD	444	Original
15b-W40	154	398	236	593	58	3.3	0.8	0.2	8.1	13.8	0.14	1.61	0.58	70	BD	82	BD	766	Original
15b-W41	75	478	218	509	33	3.7	4.4	0.7	9.1	13.0	0.11	1.36	0.42	70	BD	BD	BD	1365	Original
15b-W42	75	482	217	518	39	3.3	1.2	0.3	9.9	14.2	0.11	1.42	0.43	89	BD	BD	BD	389	Original
15b-R1	3640	302	284	771	82	1.9	8.0	1.2	4.4	23.4	0.18	0.82	0.85	66	BD	103	BD	3435	Original
15b-R2	3153	282	307	898	105	3.4	3.6	0.5	8.1	18.7	0.20	1.13	1.62	BD	BD	64	BD	3885	Original
15b-R4	488	263	290	853	98	1.9	5.9	0.4	5.1	25.7	0.18	0.96	0.64	88	BD	78	BD	3813	Original
15b-R5	3781	306	289	825	105	2.4	6.9	0.7	3.2	20.0	0.18	0.90	0.79	67	23	86	BD	4453	Original
15b-R6	498	226	292	898	94	2.5	2.0	0.2	10.2	24.9	0.17	1.28	0.55	126	BD	59	BD	2756	Original
15b-R7	475	223	301	927	94	3.9	4.4	0.5	9.7	23.5	0.16	1.29	0.56	109	28	98	BD	3294	Original
15b-R8	484	222	266	707	106	4.2	3.2	0.5	9.9	20.6	0.15	0.97	0.53	94	BD	102	BD	2979	Original
15b-R9	513	226	271	813	89	2.0	2.6	0.3	7.7	23.8	0.16	1.08	0.55	102	BD	74	BD	2304	Original
15b-R10	484	234	300	916	96	3.4	1.7	0.3	10.4	24.6	0.18	1.31	0.54	130	27	66	BD	2219	Original
15b-R11	442	231	270	689	92	3.9	1.7	0.4	10.0	20.7	0.15	0.97	0.52	96	BD	55	BD	2577	Original
15b-R14	346	234	301	883	94	4.6	8.3	0.8	7.7	26.5	0.16	1.13	0.59	111	BD	83	BD	5658	Original
15b-R15	346	277	298	885	107	3.5	10.1	0.6	5.5	22.9	0.16	0.97	0.72	90	BD	82	BD	6297	Original
15b-R16	2545	213	298	874	95	5.1	4.6	0.4	8.8	26.6	0.16	1.20	0.56	82	BD	84	BD	2703	Original
15b-R17	470	225	276	705	98	3.9	1.8	0.4	10.3	21.8	0.16	1.02	0.50	105	BD	75	BD	2668	Original

	Quantitative. Element ppm					Semi-quantitative. Oxide weight per cent;								Element ppm					
Sample	Cu	Zn	Rb	Sr	Zr	P_2O_5	SO_3	Cl	K_2O	CaO	TiO_2	MnO	Fe_2O_3	Co	Ni	Sn	Sb	Pb	ID
15b-R18	444	258	294	880	93	6.2	8.6	0.9	7.0	25.4	0.16	1.11	0.63	95	BD	80	BD	4883	Original
15b-R19	447	237	292	847	94	3.6	3.5	0.4	9.0	24.1	0.18	1.21	0.60	98	BD	80	BD	2996	Original
15b-R20	462	241	284	881	96	4.0	3.8	0.3	7.7	33.2	0.15	1.08	0.56	118	BD	106	BD	3622	Original
15b-R21	418	257	283	854	93	2.4	4.8	0.4	7.1	31.0	0.16	1.05	0.57	111	BD	94	BD	6329	Original
15b-R22	1547	325	281	757	80	3.8	8.0	1.0	5.6	24.1	0.13	0.77	2.19	BD	BD	163	BD	6614	Original
15b-R3	506	218	273	684	97	3.6	1.3	0.3	10.5	21.7	0.15	0.99	0.51	87	BD	73	BD	2452	Original?
15b-R12	309	438	341	382	60	4.5	4.5	0.5	8.9	16.4	0.14	0.65	0.72	78	BD	91	BD	2779	Medieval
15b-R13	294	425	342	401	61	4.2	3.3	0.5	11.2	20.2	0.12	0.70	0.66	82	BD	82	BD	3418	Medieval
15f-W1	234	459	260	557	50	5.3	8.5	1.1	8.1	11.6	0.11	1.26	0.52	97	BD	125	BD	3318	Original
15f-W2	244	464	263	551	50	4.3	5.2	0.7	8.8	12.6	0.13	1.29	0.52	80	BD	127	BD	2488	Original
15f-W3	94	435	204	509	41	5.4	6.0	0.9	8.0	12.7	0.12	1.31	0.45	84	BD	86	BD	2402	Original
15f-W4	92	428	210	523	50	5.1	7.2	0.9	8.0	13.0	0.12	1.32	0.46	70	22	98	BD	2715	Original
15f-W5	83	421	230	534	48	4.3	4.6	0.7	8.4	13.0	0.12	1.33	0.45	83	BD	96	BD	1732	Original
15f-W6	100	451	229	539	47	5.2	5.2	0.8	8.1	12.9	0.12	1.34	0.47	89	BD	103	BD	1992	Original
15f-W7	94	448	202	566	45	3.8	4.2	0.6	7.9	13.6	0.13	1.40	0.48	92	BD	43	BD	1354	Original
15f-W8	220	457	259	557	51	4.3	5.7	0.8	8.8	12.0	0.13	1.26	0.53	73	BD	121	BD	2592	Original
15f-W9	240	469	263	543	52	4.0	3.0	0.5	9.5	13.2	0.13	1.31	0.54	76	BD	147	BD	1778	Original
15f-W10	192	442	253	563	48	4.5	5.7	0.8	8.2	12.2	0.12	1.29	0.54	72	25	133	BD	2769	Original
15f-W11	87	438	231	532	42	4.3	4.8	0.7	8.3	12.8	0.12	1.32	0.47	89	BD	64	BD	1921	Original
15f-W12	89	416	225	504	50	4.0	6.0	0.8	7.8	11.8	0.11	1.29	0.45	85	BD	71	BD	2452	Original
15f-W13	180	479	253	514	54	4.5	2.6	0.5	9.6	12.6	0.13	1.27	0.52	98	22	129	BD	1607	Original
15f-W14	231	475	278	551	52	4.5	6.5	0.8	8.6	11.2	0.13	1.23	0.60	64	BD	144	BD	3509	Original
15f-W15	100	420	204	481	41	5.9	7.3	1.0	7.2	12.0	0.10	1.26	0.46	80	BD	77	BD	2760	Original
15f-W16	102	444	216	499	43	4.9	7.3	1.0	7.7	12.5	0.11	1.30	0.47	78	BD	93	BD	2701	Original
15f-W17	97	430	201	561	45	4.5	3.4	0.5	7.8	13.1	0.12	1.36	0.49	64	23	BD	BD	1433	Original
15f-W18	216	468	263	537	47	5.8	7.4	0.9	8.4	12.0	0.11	1.28	0.52	97	20	123	BD	3071	Original
15f-W19	223	442	259	548	53	6.1	8.8	1.1	7.6	10.6	0.13	1.21	0.54	89	BD	154	BD	3671	Original
15f-W20	120	427	223	551	52	4.5	2.0	0.4	9.2	14.0	0.14	1.41	0.50	86	BD	74	BD	1046	Original
15f-W21	120	443	230	564	49	4.6	1.3	0.3	9.5	14.0	0.13	1.40	0.50	98	BD	107	BD	935	Original
15f-W22	198	457	258	535	52	6.6	11.1	1.4	7.4	10.9	0.12	1.24	0.68	75	BD	140	BD	4356	Original
15f-W23	180	434	248	538	56	5.0	4.9	0.7	9.1	12.7	0.12	1.33	0.54	96	BD	131	BD	2448	Original
15f-W24	213	437	251	552	50	4.7	2.0	0.4	9.8	13.8	0.13	1.34	0.58	85	BD	141	BD	1593	Original
15f-W25	186	447	248	536	50	3.6	1.7	0.3	9.7	14.1	0.13	1.37	0.55	74	BD	116	BD	1302	Original
15f-W26	240	466	263	535	47	6.5	11.6	1.4	7.5	11.0	0.12	1.22	0.74	51	20	142	BD	4468	Original
15f-W27	208	452	251	561	53	3.8	1.2	0.4	10.1	14.5	0.13	1.41	0.55	78	18	126	BD	1237	Original
15f-W28	193	435	247	528	52	4.3	2.0	0.4	9.6	14.2	0.13	1.38	0.54	95	BD	121	BD	1435	Original
15f-W29	211	438	245	541	50	4.5	1.8	0.4	9.7	14.4	0.13	1.39	0.58	84	BD	123	BD	1386	Original
15f-W30	137	427	222	545	52	4.9	2.1	0.4	9.0	14.1	0.12	1.41	0.50	81	BD	106	BD	1133	Original
15f-W31	125	438	226	554	52	3.2	1.2	0.3	9.3	14.6	0.13	1.43	0.51	90	BD	101	BD	882	Original
15f-W32	112	468	220	551	54	3.4	0.7	0.3	9.7	15.8	0.13	1.41	0.48	82	BD	128	BD	804	Original
15f-W35	208	458	251	539	52	3.6	0.4	0.3	10.0	14.6	0.12	1.39	0.53	89	BD	117	BD	1026	Original
15f-W36	186	441	248	558	50	5.6	8.0	1.1	8.1	12.0	0.12	1.30	0.52	91	BD	140	BD	3076	Original
15f-W37	214	441	248	540	52	4.0	0.8	0.2	10.1	14.8	0.12	1.41	0.54	90	23	136	BD	1127	Original
15f-W38	184	427	246	537	50	3.6	1.5	0.4	9.8	13.8	0.13	1.38	0.52	98	BD	127	BD	1307	Original
15f-W39	183	440	247	560	52	4.5	0.7	0.3	10.1	14.8	0.12	1.42	0.53	87	BD	140	BD	1100	Original
15f-W40	116	442	222	565	54	4.6	1.6	0.3	9.2	15.8	0.13	1.41	0.50	122	25	BD	BD	769	Original
15f-W50	118	451	231	550	50	5.4	6.9	0.9	7.9	12.3	0.12	1.35	0.50	86	BD	92	BD	2700	Original
15f-W51	118	431	223	528	53	4.1	6.8	0.9	7.7	11.9	0.12	1.31	0.49	92	BD	114	BD	2559	Original
15f-W54	180	438	248	543	53	4.3	5.0	0.7	8.8	13.1	0.13	1.35	0.53	92	BD	128	BD	2239	Original
15f-W55	189	398	205	550	60	3.3	0.3	0.2	8.5	14.9	0.13	1.44	0.60	97	19	187	BD	1353	Original
15f-B1	420	496	298	622	108	3.9	4.1	0.4	6.4	11.2	0.26	1.36	1.07	319	40	47	BD	1477	Original? - light blue
15f-B2	952	933	352	639	117	4.6	6.7	0.4	7.0	11.2	0.26	1.52	1.16	538	28	84	BD	2016	Original? - light blue
15f-R1	305	227	282	859	94	2.5	6.2	0.5	4.4	24.7	0.16	0.94	0.60	81	22	117	BD	3739	Original
15f-R5	1518	261	301	823	82	3.4	4.7	0.6	7.8	24.1	0.15	0.98	0.96	53	29	50	BD	2494	Original
15f-R6	345	220	295	883	105	BD	8.6	0.6	5.0	18.0	0.16	1.02	0.64	78	BD	117	BD	3215	Original

	Quantitative. Element ppm					Semi-quantitative. Oxide weight per cent;								Element ppm					
Sample	Cu	Zn	Rb	Sr	Zr	P_2O_5	SO_3	Cl	K_2O	CaO	TiO_2	MnO	Fe_2O_3	Co	Ni	Sn	Sb	Pb	ID
15f-R8	319	202	264	842	82	3.3	13.6	1.2	3.5	40.0	0.12	0.66	0.52	86	BD	149	BD	12501	Original
15f-G1	499	319	320	761	92	3.1	7.0	0.2	8.2	13.3	0.27	1.64	1.79	113	BD	BD	BD	438	Original (A)
15f-G2	205	361	326	642	79	3.0	14.0	0.4	3.7	23.9	0.18	1.08	2.16	BD	BD	121	BD	3144	Original (B)
15f-G3	503	372	341	749	98	2.7	4.7	0.3	6.0	10.4	0.31	1.51	1.87	106	33	BD	BD	1342	Original (B)
15f-G4	516	445	346	799	102	BD	10.3	0.6	4.9	26.9	0.20	1.26	1.75	172	39	BD	BD	4364	Original (B)
15f-G5	819	326	270	652	75	3.3	7.5	0.5	7.3	15.8	0.23	1.26	1.94	187	32	50	BD	1659	Original
15f-G7	495	349	306	721	92	BD	9.2	0.6	5.4	28.7	0.18	1.30	2.24	138	28	60	BD	3087	Original
15f-G8	493	323	334	741	101	3.8	7.0	0.1	8.6	15.6	0.26	1.55	1.71	115	30	BD	BD	534	Original
15f-G10	249	258	348	629	118	4.3	5.4	0.4	8.5	16.8	0.24	1.15	2.90	BD	34	45	BD	1466	Original
15f-Y1	186	287	320	759	108	BD	9.8	0.5	4.7	22.0	0.19	1.28	0.41	62	BD	BD	BD	2603	Original
15f-Y2	234	325	358	807	99	2.2	11.1	0.3	6.2	15.7	0.24	1.41	0.47	65	BD	BD	BD	1089	Original
15f-W41	130	454	182	511	53	2.6	7.9	0.7	6.0	26.2	0.11	0.97	0.76	71	BD	150	BD	4648	Medieval - Staffordshire?
15f-W42	136	479	195	523	50	BD	10.5	0.9	4.1	27.1	0.08	0.85	1.50	BD	BD	191	BD	6752	Medieval - Staffordshire?
15f-W43	118	434	194	511	55	3.8	5.7	0.9	8.6	22.9	0.11	1.04	0.69	73	BD	138	BD	4288	Medieval - Staffordshire?
15f-W44	162	436	190	534	38	BD	15.6	1.1	4.1	26.1	0.07	0.77	2.73	BD	BD	218	BD	9964	Medieval - Staffordshire?
15f-W47	135	452	170	544	52	3.2	1.6	0.3	9.1	15.3	0.14	1.52	0.92	52	38	133	BD	1249	Medieval - Staffordshire?
15f-W52	98	406	151	464	54	3.6	2.3	0.5	9.1	14.5	0.13	1.25	0.50	125	32	325	BD	1969	Medieval - Staffordshire?
15f-W53	1209	509	161	475	54	2.3	8.1	0.9	7.5	14.7	0.11	1.29	2.18	BD	29	95	BD	4728	Medieval - Staffordshire?
15f-W45	403	377	229	313	66	2.5	7.7	0.9	8.4	8.6	0.14	0.68	0.80	60	BD	125	39	3976	Medieval - Weald?
15f-W46	513	400	246	329	62	4.3	2.5	0.6	10.1	12.7	0.15	0.80	0.63	57	BD	158	BD	1030	Medieval - Weald?
15f-W48	649	384	234	313	75	4.5	1.6	0.5	11.8	12.0	0.16	0.79	0.68	84	22	129	BD	845	Medieval - Weald?
15f-W49	1470	534	220	380	70	3.9	0.9	0.5	11.0	13.9	0.16	0.84	0.82	64	BD	400	BD	2273	Medieval - Weald?
15f-W33	29	265	39	975	125	2.7	1.6	0.5	3.7	24.1	0.22	1.08	0.66	57	BD	BD	BD	249	HLLA
15f-W34	65	299	114	1143	141	4.0	2.2	0.5	6.0	26.7	0.19	1.22	0.73	86	23	BD	BD	1565	HLLA
15f-B3	1633	790	65	2091	ND	BD	19.2	1.8	3.8	0.2	0.04	0.03	0.70	5588	5286	BD	BD	62630	HLLA
15f-B4	2353	1227	51	1251	ND	BD	21.7	2.1	4.6	0.2	0.05	0.04	0.86	7471	7564	67	BD	110273	HLLA
15f-B5	496	332	47	612	109	2.9	0.7	0.3	4.3	23.8	0.22	1.04	1.07	1142	588	BD	BD	118	HLLA; Ni-rich Co
15f-R2	28	93	6	162	25	BD	3.3	0.3	0.3	10.6	0.03	0.41	0.41	132	22	149	BD	1020	Soda
15f-R3	5285	118	6	61	26	BD	0.3	0.1	0.5	5.7	0.04	0.08	0.77	64	BD	1413	41	1393	Soda
15f-R4	22	120	5	183	29	BD	1.6	0.2	0.2	11.0	0.04	0.41	0.36	89	BD	193	BD	468	Soda
15f-R7	38	90	4	171	27	BD	0.5	0.1	0.2	11.4	0.04	0.37	0.33	82	BD	201	BD	128	Soda
15f-G9	1137	474	237	530	91	5.9	1.9	0.4	11.6	17.2	0.21	0.98	0.93	73	BD	152	BD	754	Medieval
15f-G6	49291	16089	ND	ND	ND	BD	31.9	2.8	4.2	0.3	0.04	0.19	0.96	BD	BD	418	280	247914	Soda or Lead
15f-G11	26717	8661	ND	ND	ND	BD	30.3	2.7	5.4	0.4	0.03	0.11	2.99	BD	BD	346	732	238884	Soda or Lead
15f-M1	61	97	6	134	40	BD	1.0	0.2	0.1	11.7	0.05	5.64	0.46	327	BD	BD	BD	9687	Soda
15f-M2	92	69	28	70	20	BD	1.0	0.2	0.9	8.8	0.08	3.22	0.25	106	BD	37	BD	10785	Soda
15f-Y6	35	267	38	690	159	4.2	0.2	0.6	4.4	23.5	0.23	1.04	0.63	93	BD	BD	BD	58	Medieval?
15f-Y4	27	52	20	4043	34	1.4	0.2	0.4	3.5	9.9	0.06	0.03	0.54	95	BD	105	BD	40	Kelp ash
15f-Y3	269	88	8	143	85	BD	0.2	0.2	0.1	12.4	0.10	11.42	3.11	546	BD	BD	BD	112	Soda
15f-Y7	261	552	8	120	22	BD	0.8	0.1	0.1	8.2	0.44	3.73	4.02	BD	BD	155	261	8702	Soda
15f-Y8	269	89	7	144	83	BD	3.2	0.4	0.2	12.3	0.10	11.16	3.02	507	32	44	BD	821	Soda
15f-Y9	800	307	10	69	ND	BD	2.4	0.3	0.4	7.3	0.08	3.99	4.48	134	335	95	298	35391	Soda
15f-Y5	ND	ND	ND	ND	ND	BD	27.8	2.5	7.1	0.7	0.02	0.07	11.45	BD	BD	207	BD	220460	Soda or Lead
15f-Y10	ND	122	ND	ND	ND	BD	30.4	2.6	6.5	0.6	0.06	0.09	10.05	BD	BD	256	BD	233876	Soda or Lead
15g-W1	196	443	246	556	50	5.0	4.4	0.6	8.8	13.4	0.12	1.35	0.52	98	BD	146	BD	2063	Original
15g-W2	111	418	224	541	45	3.6	1.5	0.3	8.8	14.2	0.12	1.43	0.50	84	BD	93	BD	897	Original
15g-W3	119	462	239	590	52	3.8	1.0	0.3	9.5	14.9	0.12	1.50	0.50	78	BD	73	BD	733	Original
15g-W4	272	498	284	560	53	4.4	3.1	0.6	9.8	13.5	0.12	1.31	0.58	84	BD	133	BD	2272	Original
15g-W5	144	423	213	605	57	3.6	1.3	0.3	8.9	15.2	0.13	1.46	0.54	85	BD	77	BD	907	Original
15g-W6	84	414	201	526	45	3.6	1.1	0.3	9.2	15.0	0.12	1.40	0.46	91	BD	65	BD	720	Original
15g-W7	107	434	234	557	46	5.9	7.4	1.0	8.0	12.9	0.12	1.36	0.47	91	BD	94	BD	2589	Original
15g-W8	157	418	228	526	43	4.6	17.9	1.8	4.1	10.0	0.15	1.04	3.01	BD	BD	121	BD	6774	Original
15g-W9	228	484	257	520	42	5.0	3.0	0.6	9.5	13.4	0.13	1.31	0.56	90	BD	136	BD	1604	Original
15g-W10	78	422	219	520	43	4.4	2.2	0.4	9.0	13.9	0.12	1.38	0.46	75	BD	77	BD	1003	Original
15g-W11	238	466	259	527	52	3.8	2.3	0.4	9.5	13.6	0.12	1.29	0.55	83	BD	120	BD	1442	Original

	Quantitative. Element ppm					Semi-quantitative. Oxide weight per cent;								Element ppm					
Sample	Cu	Zn	Rb	Sr	Zr	P_2O_5	SO_3	Cl	K_2O	CaO	TiO_2	MnO	Fe_2O_3	Co	Ni	Sn	Sb	Pb	ID
15g-W12	207	438	243	561	49	4.6	1.0	0.3	9.9	14.6	0.12	1.41	0.52	100	BD	123	BD	1245	Original
15g-W13	213	432	242	530	50	3.8	0.6	0.3	9.7	14.4	0.12	1.36	0.53	87	24	124	BD	1077	Original
15g-W14	211	452	260	549	52	6.0	6.6	1.0	8.4	12.0	0.11	1.24	0.57	81	19	145	BD	2918	Original
15g-W15	201	447	241	533	50	4.2	1.2	0.3	9.3	14.0	0.12	1.36	0.52	78	BD	112	BD	1300	Original
15g-W16	186	442	246	554	52	4.0	1.3	0.4	9.5	14.2	0.12	1.37	0.52	103	23	139	BD	1240	Original
15g-W17	107	428	230	548	50	4.4	0.4	0.3	9.5	14.9	0.12	1.49	0.47	76	BD	72	BD	466	Original
15g-W18	306	458	275	514	52	4.0	1.0	0.4	9.9	13.4	0.12	1.29	0.60	74	BD	218	BD	1603	Original
15g-W19	251	458	276	553	50	3.6	0.9	0.3	10.5	14.1	0.13	1.35	0.56	88	BD	141	BD	1571	Original
15g-W20	120	489	202	516	43	4.5	1.3	0.3	9.4	15.0	0.12	1.35	0.50	90	BD	136	BD	1287	Original
15g-W21	200	452	245	548	54	4.1	0.5	0.3	9.7	14.6	0.12	1.39	0.53	92	BD	121	BD	1005	Original
15g-W22	200	444	242	548	52	4.1	0.9	0.3	9.4	14.0	0.12	1.35	0.53	86	BD	106	BD	1161	Original
15g-W23	135	417	213	576	52	3.4	1.7	0.3	8.6	14.8	0.13	1.42	0.54	84	BD	69	BD	1013	Original
15g-W24	191	457	254	552	53	5.0	5.5	0.8	8.5	12.9	0.13	1.34	0.58	78	BD	121	BD	2570	Original
15g-W25	188	428	237	512	45	4.2	3.3	0.6	8.6	12.9	0.12	1.32	0.51	98	BD	132	BD	1796	Original
15g-W26	208	427	246	553	53	3.8	0.6	0.3	9.8	14.6	0.13	1.40	0.52	78	19	124	BD	1075	Original
15g-W27	197	431	242	531	50	4.3	2.4	0.5	9.2	13.7	0.12	1.34	0.53	111	BD	123	BD	1507	Original
15g-W28	199	450	247	541	51	4.3	0.7	0.3	9.8	14.7	0.13	1.38	0.52	86	BD	139	BD	1116	Original
15g-W29	226	458	247	542	53	4.3	0.9	0.3	9.9	14.8	0.13	1.40	0.53	89	BD	138	BD	1171	Original
15g-W30	89	428	216	529	49	4.1	1.3	0.4	9.0	14.9	0.12	1.40	0.49	77	BD	68	BD	856	Original
15g-W31	91	436	229	542	49	4.0	3.0	0.5	8.7	13.7	0.12	1.37	0.49	98	BD	82	BD	1302	Original
15g-W32	88	413	219	505	43	5.2	6.3	0.9	7.8	12.7	0.10	1.32	0.52	83	BD	126	BD	2256	Original
15g-W33	229	379	260	586	55	3.1	9.7	1.2	6.7	9.7	0.12	1.41	1.54	BD	BD	104	BD	3645	Original
15g-W34	211	390	253	560	60	4.4	4.2	0.6	8.0	11.9	0.15	1.50	0.82	40	BD	85	BD	1855	Original
15g-W35	253	454	272	509	48	5.1	4.7	0.7	9.2	12.4	0.13	1.27	0.54	95	BD	176	BD	2587	Original
15g-W36	103	424	195	516	46	3.8	1.4	0.2	8.4	14.6	0.12	1.43	0.48	87	BD	68	BD	641	Original
15g-W37	114	438	234	532	47	5.7	6.1	0.8	7.8	12.7	0.12	1.38	0.48	69	19	101	BD	2070	Original
15g-W38	91	415	228	525	47	5.3	6.6	0.9	7.6	12.6	0.12	1.32	0.49	82	BD	61	BD	2368	Original
15g-W39	101	441	221	553	52	4.2	1.7	0.4	9.2	15.5	0.13	1.43	0.57	85	24	106	BD	920	Original
15g-W40	109	458	239	551	49	5.4	2.5	0.4	9.1	14.5	0.12	1.42	0.51	80	27	98	BD	1135	Original
15g-W41	103	427	214	541	45	4.1	4.3	0.7	8.1	13.1	0.13	1.32	0.66	56	BD	89	BD	1663	Original
15g-W42	116	437	231	532	44	4.0	7.8	0.9	7.5	12.6	0.14	1.30	1.10	BD	BD	95	BD	2636	Original
15g-W43	80	417	210	534	48	2.5	0.8	0.3	9.3	14.8	0.12	1.40	0.46	74	BD	92	BD	665	Original
15g-W44	98	437	214	552	42	4.1	1.8	0.4	9.2	15.2	0.13	1.44	0.51	77	BD	82	BD	946	Original
15g-B1	1479	2343	298	933	95	3.6	6.5	0.4	5.5	17.4	0.19	1.15	1.35	876	BD	340	BD	3241	Original
15g-B2	1491	1519	296	878	98	4.6	3.7	0.5	10.3	24.1	0.18	1.23	1.19	900	46	162	85	2210	Original
15g-B3	1467	1455	293	873	96	3.8	0.9	0.2	10.7	24.9	0.19	1.23	1.19	875	29	175	64	1383	Original
15g-B4	1401	1497	290	902	101	6.6	2.2	0.3	10.9	25.0	0.21	1.26	1.21	934	44	205	66	1764	Original
15g-B6	1507	1499	288	869	97	4.2	1.1	0.1	10.8	25.3	0.18	1.26	1.17	897	50	175	57	1363	Original
15g-B7	1540	1469	294	816	95	4.6	1.2	0.2	10.2	24.2	0.19	1.21	1.17	865	34	155	92	1449	Original
15g-R1	650	233	293	883	84	3.4	4.8	0.4	7.3	26.4	0.16	1.08	0.61	98	BD	72	BD	8058	Original
15g-R2	313	274	284	777	90	3.4	3.1	0.2	7.0	17.1	0.18	1.00	0.78	91	BD	81	BD	1303	Original
15g-R3	315	202	273	807	87	3.0	7.4	0.3	8.0	28.4	0.13	0.89	0.60	103	BD	160	BD	3479	Original
15g-R4	477	212	269	724	95	4.8	2.6	0.4	10.2	21.3	0.15	0.99	0.51	83	BD	70	BD	2798	Original?
15g-R5	516	223	264	729	100	3.7	1.8	0.4	10.6	21.6	0.15	1.00	0.51	89	BD	68	BD	2558	Original
15g-R6	507	214	276	701	94	4.6	6.8	0.9	9.2	19.4	0.15	0.97	0.51	80	BD	57	BD	4052	Original
15g-R7	512	223	271	669	94	5.1	7.5	0.8	7.9	17.0	0.19	0.90	1.02	BD	BD	90	BD	4598	Original
15g-R8	296	288	290	751	89	2.9	2.3	0.2	5.4	12.2	0.20	0.96	0.85	74	BD	87	BD	1269	Original
15g-R9	339	270	300	778	79	BD	6.1	0.8	4.0	28.1	0.12	0.88	0.70	78	BD	146	BD	4017	Original
15g-R11	502	220	273	698	92	5.6	5.1	0.6	9.3	19.8	0.15	0.97	0.60	84	BD	88	BD	3539	Original
15g-G1	218	474	281	721	94	BD	12.0	0.9	2.7	24.1	0.19	1.41	1.87	BD	27	120	BD	5442	Original (B)
15g-G2	295	377	405	675	109	BD	12.5	1.4	4.9	31.8	0.16	0.84	2.27	102	BD	143	BD	7182	Original (B)
15g-G4	484	476	313	725	88	3.5	12.1	1.1	5.5	20.2	0.19	1.30	2.94	112	34	99	BD	4865	Original
15g-M1	105	239	388	1337	126	BD	4.2	0.5	8.0	25.0	0.23	1.42	0.47	72	BD	BD	BD	3169	Original (B/C)
15g-M3	93	257	401	1416	124	BD	5.4	0.6	8.3	25.8	0.20	1.45	0.47	72	BD	50	BD	3124	Original (B/C)
15g-M4	94	342	376	957	83	4.2	6.6	0.4	5.5	16.3	0.30	3.03	0.38	86	36	BD	BD	1259	Original (B)

	Quantitative. Element ppm					Semi-quantitative. Oxide weight per cent;								Element ppm					
Sample	Cu	Zn	Rb	Sr	Zr	P_2O_5	SO_3	Cl	K_2O	CaO	TiO_2	MnO	Fe_2O_3	Co	Ni	Sn	Sb	Pb	ID
15g-M2	115	277	228	728	54	BD	9.9	0.8	7.5	25.5	0.13	1.01	0.39	73	31	125	BD	6323	Medieval
15g-Y1	249	329	342	804	102	2.6	6.7	0.6	7.0	14.3	0.27	1.46	1.17	53	39	38	BD	5295	Original
15g-Y2	463	316	332	746	94	2.6	10.2	1.1	4.4	19.4	0.19	1.08	2.60	BD	BD	43	BD	9225	Original
15g-Y3	216	353	355	852	102	2.7	6.5	0.6	6.0	15.9	0.28	1.45	0.87	44	28	42	BD	3598	Original
15g-B5	241	261	39	655	255	3.0	1.4	0.4	4.1	22.9	0.35	0.71	0.76	886	179	BD	BD	276	HLLA; Ni-rich Co
15g-R10	507	311	400	559	75	4.6	3.2	0.5	14.5	12.2	0.12	0.79	0.69	83	19	74	BD	1217	Medieval
15g-G3	22269	3275	187	430	67	5.1	4.9	0.7	12.2	14.2	0.17	0.81	1.25	BD	39	1457	92	2274	Medieval
15g-G5	15191	1453	245	590	78	2.6	12.6	1.1	3.1	22.4	0.14	0.81	1.61	BD	BD	1360	52	9586	Medieval
15g-M5	62	93	4	134	34	BD	1.0	0.2	0.1	11.6	0.04	5.55	0.47	331	BD	BD	BD	9888	Soda
15g-M6	58	90	6	141	40	BD	0.9	0.2	0.1	11.5	0.04	5.55	0.44	332	BD	32	BD	9714	Soda
15g-M8	62	84	ND	137	42	BD	1.0	0.2	0.1	11.7	0.05	5.52	0.44	328	BD	BD	BD	9468	Soda
15g-M7	ND	36	11	3892	59	1.2	0.1	0.4	2.7	9.4	0.07	0.03	0.43	58	BD	BD	37	282	High lead glass flashed on white kelp ash base
15h-W1	70	472	211	508	35	4.8	6.3	0.9	8.3	11.7	0.09	1.30	0.41	70	BD	50	BD	1992	Original
15h-W2	87	352	201	540	54	3.2	1.6	0.4	9.6	13.3	0.13	1.43	0.49	85	BD	86	BD	1008	Original
15h-W3	114	427	225	565	53	3.0	1.2	0.3	9.5	14.4	0.13	1.41	0.50	93	BD	117	BD	882	Original
15h-W4	117	401	213	607	61	3.0	1.1	0.3	8.3	13.7	0.14	1.56	0.61	64	BD	80	BD	1122	Original
15h-W5	135	436	222	520	45	4.1	2.9	0.5	8.6	13.9	0.13	1.40	0.50	78	BD	89	BD	1416	Original
15h-W6	139	443	228	558	52	4.3	2.8	0.5	9.0	14.4	0.13	1.43	0.56	87	23	132	BD	1416	Original
15h-W7	126	434	229	573	57	3.4	4.5	0.7	8.6	13.6	0.13	1.39	0.67	72	BD	121	BD	1996	Original
15h-W8	193	428	261	546	51	6.6	13.7	1.7	6.7	10.0	0.11	1.24	0.51	88	BD	144	BD	5101	Original
15h-W9	232	438	263	534	50	4.7	5.9	0.9	8.9	12.5	0.12	1.29	0.57	90	BD	146	BD	2945	Original
15h-W10	109	430	219	526	50	3.2	2.2	0.4	9.0	14.2	0.11	1.36	0.48	83	BD	112	BD	1091	Original
15h-W11	139	434	225	537	49	3.4	1.1	0.3	9.3	14.7	0.12	1.41	0.50	86	BD	105	BD	887	Original
15h-W12	85	377	231	564	50	3.4	2.1	0.5	9.6	12.9	0.13	1.48	0.52	105	BD	65	BD	1042	Original
15h-W13	67	450	210	493	38	3.2	2.5	0.5	9.3	12.8	0.10	1.35	0.40	88	BD	34	BD	809	Original
15h-W14	84	490	214	519	39	3.8	1.3	0.3	10.0	14.4	0.11	1.43	0.43	91	BD	BD	BD	385	Original
15h-W15	123	396	202	557	58	3.6	1.8	0.4	9.2	13.9	0.14	1.44	0.57	91	BD	100	BD	1246	Original
15h-W16	69	479	204	496	34	3.6	1.1	0.4	9.8	13.7	0.10	1.37	0.49	70	BD	BD	BD	304	Original
15h-W17	70	459	200	473	38	3.3	1.5	0.4	9.5	13.3	0.10	1.33	0.37	84	BD	BD	BD	487	Original
15h-W18	123	437	230	540	50	3.9	4.4	0.7	8.4	13.1	0.13	1.37	0.50	98	BD	97	BD	1873	Original
15h-W19	119	421	225	538	48	3.3	7.9	1.0	7.6	11.8	0.13	1.32	0.51	88	BD	112	BD	3174	Original
15h-W20	128	427	218	519	47	3.9	0.9	0.3	9.2	14.2	0.12	1.40	0.49	92	BD	74	BD	839	Original
15h-W21	126	411	217	537	47	3.4	0.5	0.2	9.4	14.6	0.12	1.42	0.48	88	BD	78	BD	693	Original
15h-W22	130	442	223	521	44	3.5	0.9	0.3	9.3	14.5	0.12	1.42	0.50	84	BD	108	BD	785	Original
15h-W23	128	435	220	527	50	3.0	1.8	0.4	8.8	14.1	0.12	1.36	0.59	94	BD	98	BD	1386	Original
15h-W24	134	409	217	532	48	4.3	1.0	0.3	9.2	14.6	0.13	1.40	0.50	90	BD	98	BD	810	Original
15h-W25	119	452	228	548	50	6.7	9.3	1.1	7.4	12.1	0.12	1.33	0.50	109	22	112	BD	3175	Original
15h-W26	147	437	228	546	51	3.5	1.6	0.4	8.9	14.8	0.13	1.42	0.57	85	BD	101	BD	928	Original
15h-W27	147	443	229	539	52	3.2	0.6	0.3	9.4	14.9	0.12	1.42	0.50	96	BD	86	BD	712	Original
15h-W28	152	440	222	563	57	3.5	3.0	0.5	8.5	14.2	0.13	1.38	0.89	53	BD	101	BD	1385	Original
15h-W29	119	443	230	545	52	3.3	1.1	0.3	9.3	14.5	0.12	1.42	0.50	99	BD	107	BD	988	Original
15h-W30	145	423	229	556	50	3.7	4.0	0.6	8.4	13.1	0.13	1.32	0.88	49	20	110	BD	1967	Original
15h-W31	152	440	237	564	59	4.6	0.6	0.3	9.6	15.6	0.13	1.48	0.51	105	19	113	BD	718	Original
15h-W32	111	381	239	570	50	4.0	1.5	0.4	9.9	13.9	0.13	1.51	0.62	71	BD	79	BD	884	Original
15h-W33	102	379	228	555	53	3.1	0.6	0.3	10.2	13.8	0.13	1.49	0.52	79	19	86	BD	633	Original
15h-W34	70	388	260	582	53	3.1	2.3	0.5	9.5	11.6	0.12	1.53	0.47	92	BD	BD	BD	701	Original
15h-W35	123	414	213	525	48	4.2	2.9	0.5	8.3	13.7	0.12	1.36	0.46	86	BD	80	BD	1343	Original
15h-B1	1666	2661	289	837	101	4.7	1.1	0.2	11.3	24.4	0.16	1.31	1.14	1187	51	214	62	1827	Original
15h-B2	1716	2686	293	856	93	4.1	1.0	0.2	11.4	24.6	0.18	1.31	1.14	1242	45	213	82	1901	Original
15h-R1	691	206	276	848	96	3.4	3.0	0.5	8.4	23.2	0.15	1.12	1.36	BD	BD	57	BD	2478	Original
15h-R2	162	195	228	693	61	BD	6.3	0.6	3.7	55.8	0.08	0.46	0.44	105	BD	145	BD	12374	Original
15h-R3	256	265	277	738	77	2.5	5.5	0.5	4.6	19.5	0.15	0.80	0.77	57	BD	72	BD	3378	Original
15h-R4	1541	268	300	846	98	4.1	5.9	0.8	7.6	25.1	0.15	0.98	0.81	73	33	59	BD	3243	Original
15h-R6	602	195	284	844	98	3.8	2.6	0.3	9.3	27.3	0.16	1.10	0.63	85	BD	68	41	2846	Original
15h-R7	529	220	305	917	96	2.3	3.8	0.4	8.9	21.4	0.18	1.23	0.58	99	BD	74	BD	3038	Original

	Quantitative. Element ppm					Semi-quantitative. Oxide weight per cent;								Element ppm					
Sample	Cu	Zn	Rb	Sr	Zr	P_2O_5	SO_3	Cl	K_2O	CaO	TiO_2	MnO	Fe_2O_3	Co	Ni	Sn	Sb	Pb	ID
15h-G1	618	635	379	747	70	2.9	7.5	0.6	7.0	21.0	0.21	1.89	2.07	233	56	53	BD	1407	Original (B)
15h-G2	180	401	318	578	112	3.7	10.1	1.2	4.6	20.6	0.16	1.13	2.35	BD	BD	45	BD	3986	Original (B)
15h-G3	183	408	322	565	112	3.3	8.9	1.4	3.9	20.5	0.18	1.01	2.42	BD	27	66	BD	3881	Original (B)
15h-G4	189	394	334	592	113	3.2	7.5	1.2	4.5	25.1	0.17	1.06	2.34	77	BD	48	BD	3620	Original (B)
15h-G5	586	388	345	727	98	2.6	7.4	0.2	5.0	11.9	0.28	1.73	1.67	154	24	BD	BD	1519	Original (B)
15h-G6	204	474	322	551	111	2.3	7.7	0.6	5.0	20.4	0.19	1.10	2.44	BD	BD	37	BD	2108	Original
15h-G7	191	372	337	575	109	3.4	7.7	1.0	5.7	19.0	0.19	1.21	2.38	66	24	56	BD	3096	Original
15h-G8	174	366	306	548	101	BD	7.2	1.2	2.8	27.8	0.15	1.09	2.18	82	BD	70	BD	3989	Original
15h-Y1	65	289	90	1286	76	4.3	2.7	0.5	5.5	22.0	0.21	1.65	0.74	85	25	BD	BD	1197	Original? HLLA
15h-R5	183	193	241	669	68	BD	7.7	0.7	2.3	48.6	0.07	0.42	0.50	106	BD	116	BD	10442	Medieval
15h-R8	8455	4135	ND	ND	ND	BD	28.7	2.5	6.3	0.1	0.02	0.08	6.44	BD	BD	313	79	237593	Soda
15h-G9	7015	226	17	116	25	BD	1.2	0.5	0.5	11.1	0.12	2.59	4.84	199	1157	BD	309	14546	Soda
15h-Y6	119	211	80	495	112	2.8	0.5	0.1	6.1	23.3	0.11	0.13	1.25	71	24	BD	BD	214	Medieval?
15h-Y2	112	53	5	206	27	BD	2.9	0.5	0.5	14.0	0.04	0.43	0.51	81	BD	28	BD	881	Soda
15h-Y3	291	33	15	4090	59	1.0	0.3	0.4	3.1	9.6	0.09	0.03	0.41	101	BD	67	BD	90	Kelp ash
15h-Y4	12	56	15	3897	43	1.3	0.1	0.4	3.4	10.0	0.06	0.03	0.45	71	BD	101	BD	26	Kelp ash
15h-Y5	13	47	15	4258	34	1.6	0.2	0.4	3.4	10.8	0.07	0.04	0.49	78	BD	41	BD	40	Kelp ash
15j-W1	250	468	267	538	54	4.2	1.4	0.3	10.3	14.3	0.14	1.37	0.56	74	18	125	BD	1324	Original
15j-W3	216	455	242	542	52	4.4	0.8	0.3	9.8	14.6	0.13	1.39	0.60	91	BD	122	BD	1206	Original
15j-W2	102	397	173	571	51	2.1	1.5	0.3	8.0	13.9	0.17	1.46	0.56	87	BD	66	BD	811	Medieval - Staffordshire?
15j-R1	22771	2323	260	602	64	6.8	3.6	0.7	13.3	14.3	0.15	1.20	1.17	78	29	2483	103	5054	Medieval
15j-G1	102	343	143	428	57	3.3	1.8	0.5	10.7	13.6	0.16	0.74	0.67	79	28	BD	BD	453	Medieval

Table D.3 Results of the LA-ICP-MS analyses.

	1e-W3	1j-W5	3b-W7	15b-W5	3b-B5	3b-R1	3b-G3	10c-B6	15g-G2	1h-M1	10h-M1	15g-M1	1e-B4	3b-W2	10c-W8	15a-R4	10h-M2	10c-B1
Na_2O	2.70	2.81	2.03	2.03	1.15	1.22	1.63	0.58	0.52	0.92	0.89	0.82	1.54	2.28	2.76	5.01	7.35	12.17
MgO	8.17	8.21	8.46	7.81	4.61	5.02	4.81	4.55	4.31	4.72	5.38	4.71	3.84	7.34	3.85	4.74	5.48	0.11
Al2O3	1.33	1.30	1.11	1.01	1.44	1.48	1.66	1.21	1.19	1.36	1.40	1.35	2.66	1.00	1.53	1.99	1.14	1.01
SiO2	56.98	57.04	54.72	54.95	50.18	48.61	44.59	44.04	44.70	52.34	50.21	48.54	51.74	58.39	56.70	62.54	67.54	71.27
P_2O_5	3.94	4.07	3.69	4.58	3.03	3.29	4.95	3.17	3.32	2.73	2.38	2.90	4.89	3.22	3.94	2.21	1.81	0.08
K_2O	9.12	9.11	11.87	10.55	12.73	11.42	16.36	18.33	16.83	12.41	12.91	12.72	8.04	10.96	5.44	4.08	4.53	0.71
CaO	15.14	14.80	15.42	16.55	23.41	26.12	21.66	23.56	23.94	22.55	23.75	25.61	23.44	14.34	23.52	14.38	10.75	11.24
TiO_2	0.08	0.08	0.07	0.07	0.10	0.10	0.12	0.12	0.13	0.11	0.10	0.13	0.10	0.06	0.34	0.13	0.09	0.06
MnO	1.46	1.50	1.56	1.49	1.26	1.31	1.49	1.45	1.58	1.63	1.50	1.95	2.02	1.55	0.68	0.14	0.04	0.59
Fe_2O_3	0.45	0.45	0.41	0.41	0.76	0.48	1.98	2.02	2.49	0.34	0.43	0.40	0.67	0.34	0.64	1.00	0.39	1.13
Li	20	19	13	8.6	14	10	14	7.8	8.7	4.9	6.1	6.3	96	7.4	19	14	9.9	7.6
B	287	285	301	325	173	175	127	124	145	194	179	183	176	326	187	384	409	12
V	7.5	7.5	6.6	6.1	7.5	8.1	9.3	6.9	7.6	6.3	6.6	7.3	5.7	5.6	11	20	12	17
Cr	8.5	8.6	7.7	7.6	7.1	7.2	8.8	7.2	8.4	7.0	6.7	6.6	6.8	7.5	13	16	11	3054
Co	25	23	15	9.0	865	42	47	131	144	8.2	6.6	6.2	1367	5.7	7.1	24	4.7	964
Ni	14	15	13	12	29	14	24	29	32	14	15	15	468	12	25	31	15	35
Cu	131	129	136	92	1333	1044	379	374	386	104	96	109	1259	66	49	362	4.8	1764
Zn	484	531	369	676	1381	199	381	331	365	286	243	312	280	453	273	563	14	44
Ge	0.7	0.61	0.49	0.57	3.4	0.64	1.0	0.78	0.92	0.68	0.71	0.75	2.3	0.72	0.86	1.7	1.7	2.0
As	2.8	3.0	1.7	2.6	9.9	4.8	12	11	11	2.4	2.0	2.1	48	1.8	2.3	3963	45	826
Rb	187	202	256	200	310	275	338	414	449	341	292	391	95	155	39	22	9.4	9.2
Sr	556	583	691	562	883	975	731	797	836	1317	1405	1531	1180	504	881	2666	3816	161
Y	3.0	3.1	2.6	2.5	3.2	3.1	4.0	3.5	3.5	3.0	3.0	3.1	5.1	2.7	5.8	5.6	3.7	4.3
Zr	53	54	48	39	100	96	105	120	118	133	127	129	109	40	210	76	55	32
Nb	1.6	1.7	1.4	1.2	2.2	2.2	2.6	2.6	2.6	2.2	2.1	2.3	2.3	1.2	7.7	2.7	2.1	1.6
Ag	0.37	0.44	0.43	0.28	0.85	0.7	0.24	0.23	0.29	0.28	0.17	0.26	0.52	0.2	0.44	1.1	0.15	0.22
Sb	2.3	2.0	1.4	1.1	37	8.3	2.8	3.8	4.1	0.94	0.7	0.92	1.2	0.67	0.61	69	4.8	1.8
Cs	1.8	2.0	2.2	1.7	1.6	1.5	0.68	0.84	0.88	1.0	0.92	1.1	1.8	1.3	0.43	0.29	0.08	0.22
Ba	1773	1747	2053	1606	2920	2598	3072	4787	4604	4268	5311	3908	2729	1656	2431	248	107	195
La	13	12	10	13	4.8	4.7	4.6	4.1	3.9	3.7	4.3	3.5	7.4	20	8.8	6.6	4.4	5.9
Ce	18	17	15	16	9.8	9.4	8.5	7.4	7.1	6.6	7.7	6.3	13	28	16	13	8.7	8.6
Pr	1.9	1.8	1.7	1.7	1.0	1.0	0.99	0.85	0.8	0.72	0.87	0.69	1.6	3.0	1.7	1.5	0.97	1.1
Nd	6.3	5.7	5.3	5.7	3.6	3.5	3.7	3.0	2.8	2.6	3.0	2.6	5.8	9.8	6.0	5.5	3.7	4.2
Sm	0.88	0.8	0.75	0.7	0.64	0.63	0.7	0.61	0.59	0.5	0.59	0.48	1.2	1.1	1.1	1.1	0.69	0.83
Eu	0.18	0.18	0.17	0.16	0.18	0.17	0.2	0.23	0.21	0.18	0.22	0.15	0.34	0.21	0.27	0.24	0.14	0.17
Gd	0.66	0.62	0.52	0.49	0.55	0.53	0.62	0.53	0.56	0.44	0.53	0.4	0.95	0.71	1.0	0.98	0.67	0.78
Tb	0.09	0.08	0.07	0.06	0.09	0.08	0.09	0.09	0.08	0.07	0.08	0.07	0.13	0.08	0.16	0.14	0.1	0.11
Dy	0.47	0.44	0.43	0.33	0.54	0.5	0.62	0.51	0.49	0.47	0.54	0.43	0.81	0.47	0.97	0.78	0.63	0.7
Ho	0.1	0.09	0.09	0.07	0.11	0.11	0.14	0.11	0.11	0.09	0.11	0.09	0.16	0.08	0.21	0.18	0.12	0.14
Er	0.3	0.29	0.26	0.21	0.32	0.34	0.42	0.35	0.35	0.3	0.37	0.31	0.48	0.24	0.67	0.47	0.39	0.43
Tm	0.04	0.04	0.04	0.03	0.05	0.05	0.06	0.05	0.05	0.05	0.06	0.05	0.07	0.03	0.1	0.07	0.06	0.06
Yb	0.29	0.28	0.26	0.19	0.37	0.38	0.43	0.37	0.39	0.37	0.43	0.36	0.5	0.25	0.83	0.49	0.41	0.4
Lu	0.05	0.04	0.04	0.03	0.06	0.06	0.07	0.06	0.06	0.06	0.07	0.06	0.08	0.04	0.13	0.09	0.06	0.06
Pb	762	693	583	114	2112	1901	385	470	559	160	75	209	6.4	40	4.8	23606	1816	35
Bi	0.07	0.1	0.08	0.02	0.12	0.07	0.06	0.08	0.08	0.02	0.03	0.02	0.01	0.02	0.02	11	2.0	2.1
Th	1.1	1.1	0.99	0.81	1.3	1.4	1.3	1.0	1.1	1.1	1.3	1.1	2.1	0.87	2.5	1.6	0.99	0.91
U	0.35	0.32	0.34	0.23	0.46	0.46	0.38	0.35	0.41	0.35	0.42	0.37	0.71	0.28	1.2	3.1	4.9	0.49
	Original	Original	Original	Original	Original	Original	Original	Original	Original	Original	Original	Original	Original?	Medieval	HLLA	Kelp ash	Lead on	Soda

Table D.4 Results of the TIMS analyses. Samples marked by an asterisk (*) were analysed by the Static IsoProbe instead of the Multidynamic IsoProbe.

	$^{87}Sr/^{86}Sr$	$^{143}Nd/^{144}Nd$	
GEW-1e-W48	0.715968	0.512119	*
GEW-1j-W39	0.716109	0.512122	*
GEW-1h-W13	0.716034	0.512104	
GEW-1h-B2	0.714135	0.511918	*
GEW-1h-R5	0.713500	0.511909	*
GEW-1h-M1	0.716196		
SWW-21b-M44	0.715109	0.511869	
SWW-25c-W37	0.715861	0.512098	
SWW-20b-W52	0.708154	0.512149	*
SWW-24e-B26	0.713823		
LBW 22	0.715393	0.512059	
LBW 23	0.716082	0.512070	
LBW 24	0.716873	0.512039	
LBW 1.1	0.716613	0.512109	
LBW 36	0.716354	0.512129	
LBW 45	0.716000	0.512108	

APPENDIX E

Identification of batches

Two approaches for the identification of batches in the original white glass of the GEW were tried for this research, as described in Chapter 6 and Chapter 9. The first of these, the panel-by-panel (PBP) approach, is described in this appendix in more detail. The other, the cross-window (XW) approach, was selected as the final method because of its agreement with the PBP approach and because it would allow comparisons to be made between panels across the window.

The following sections will report the PBP results for each panel in the same way, following the sequence of the methodology (see Chapter 6 for details). First, glass pieces that were identical within experimental error were identified in the control group; this is reported using a "sigma matrix" (Figure E.1). In this graphical tool, if the square at the intersection of two samples is shaded green, they are identical within experimental error.

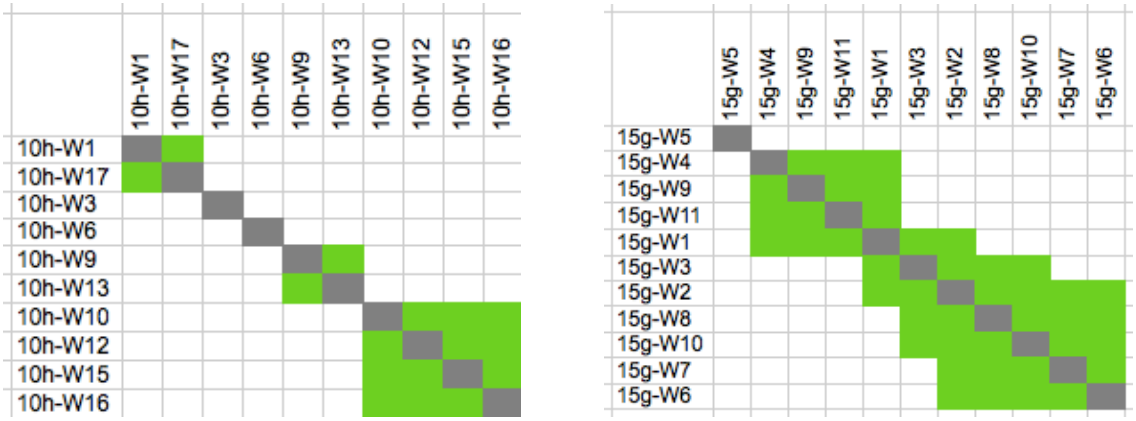

Figure E.1 Two examples of a "sigma matrix". If the square at the intersection of two samples is shaded green, they are within two standard deviations for all elements analysed by EPMA-WDS. On the left, an example of a panel where all identified batches were distinct. On the right, an example of a panel where identified batches had shared members and could not be defined without hierarchical clustering.

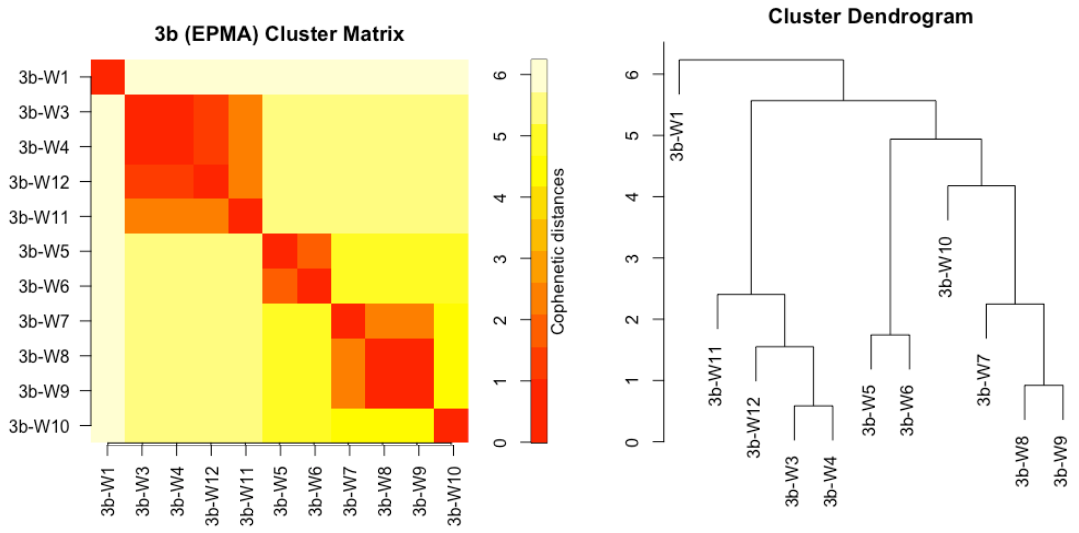

Figure E.2 An example of a "cluster matrix" (left) and a corresponding dendrogram. The colour scale with cophenetic numbers corresponds to the "tree height" of the dendrogram: closer to dark red means the two samples are more closely related, while pale yellow and white means the two samples are less closely related. This example reports EPMA data for the control group of a panel; the cluster matrix is easier to interpret especially for the larger sample population analysed by pXRF.

In some cases, the identification of identical groups was straightforward (Figure E.1, left), while in others, there were several groups with shared members (Figure E.1, right). This latter obstacle was overcome through hierarchical clustering. The results of the cluster analysis are presented using a “cluster matrix”, as an alternative to the standard dendrogram (Figure E.2), which can become cumbersome for larger datasets (such as the pXRF data). The cophenetic distances on the colour scale relate to the "tree” height of the dendrogram; the lower the number (the closer the colour is to deep red) the more closely related the two samples are. The cluster boundaries (i.e., the cophenetic distance at which to define the clusters) were determined by the previously determined identical groups.

With batches in the control group identified, the focus turned to the full sample set from each panel, the glass pieces analysed by pXRF. The five quantifiable elements (Cu, Zn, Rb, Sr, and Zr) of the original white glass of each panel were analysed by hierarchical clustering, again reported using a cluster matrix. The control group batches are marked on each pXRF cluster matrix, and used to guide the cluster boundary decisions. Scatterplots with error bars equal to ±1 standard deviation were also examined for the five elements to ensure sensible groupings.

E.1 Panel 1e

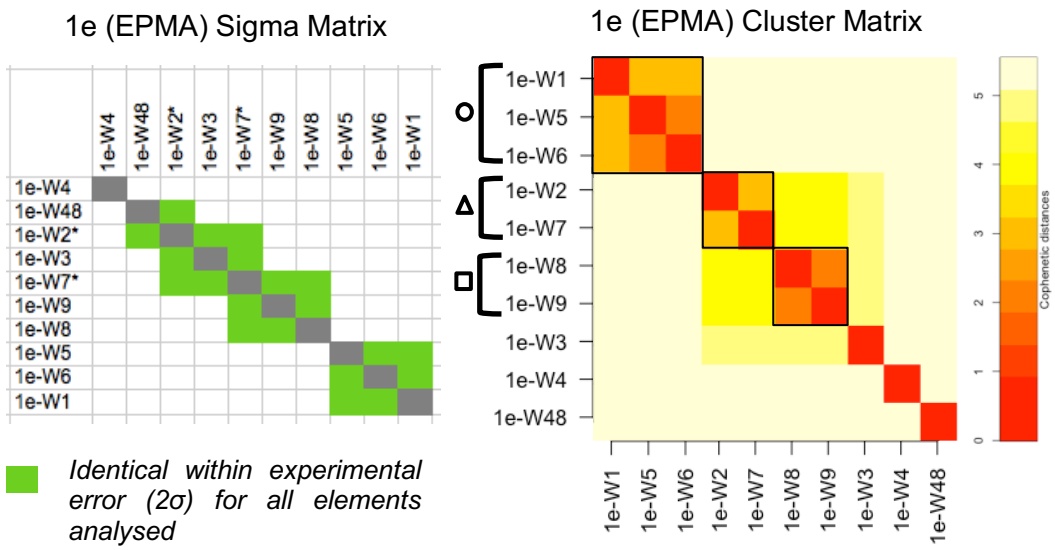

Figure E.3 The sigma matrix (left) and cluster matrix (right) for the control group of panel 1e white glass.

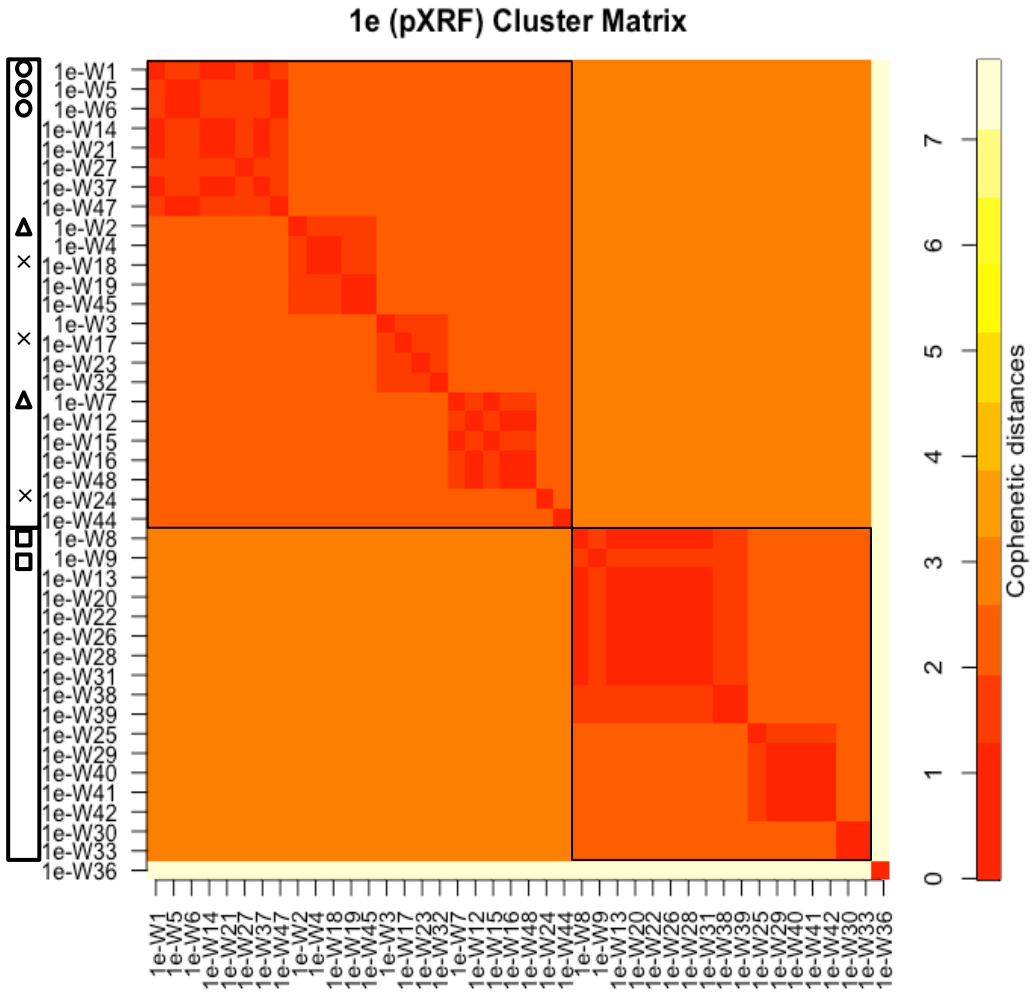

Figure E.4 Cluster matrix showing the results of the hierarchical clustering of the panel 1e white glass (pXRF data).

E.2 Panel 1h

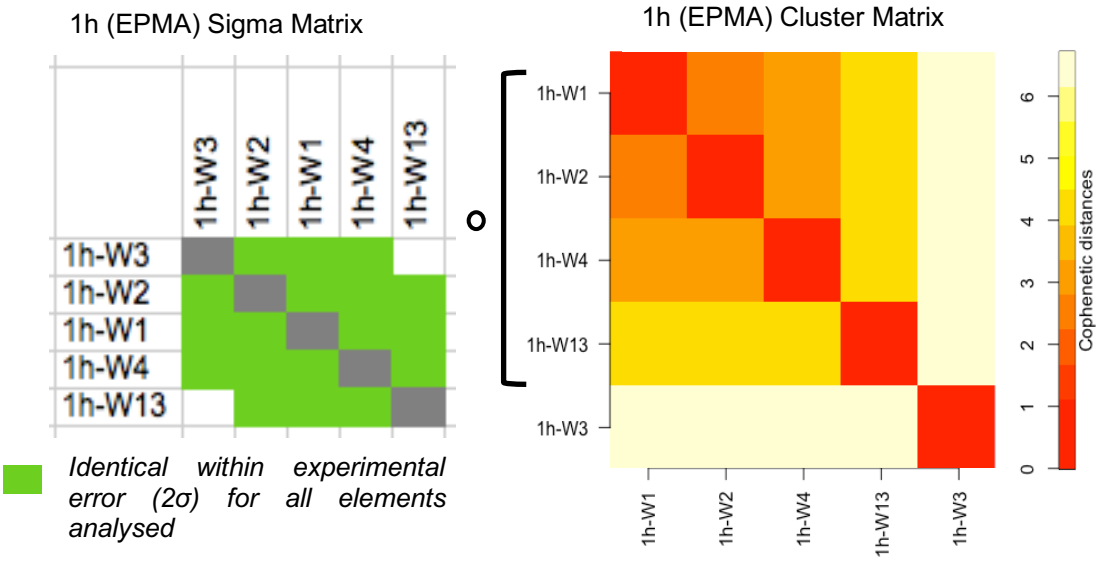

Figure E.5 The sigma matrix (top) and cluster matrix (bottom) for the control group of panel 1h white glass.

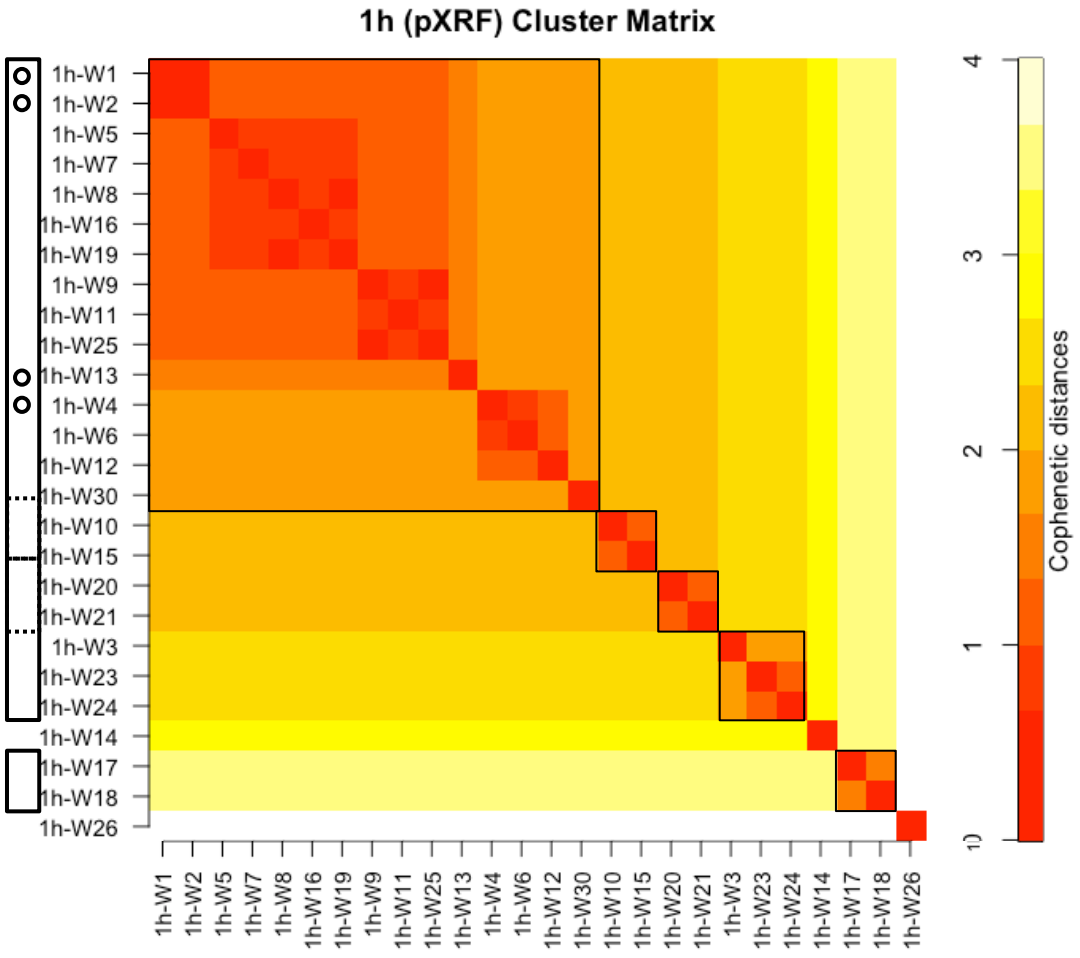

Figure E.6 Cluster matrix showing the results of the hierarchical clustering of the panel 1h white glass (pXRF data).

E.3 Panel 1j

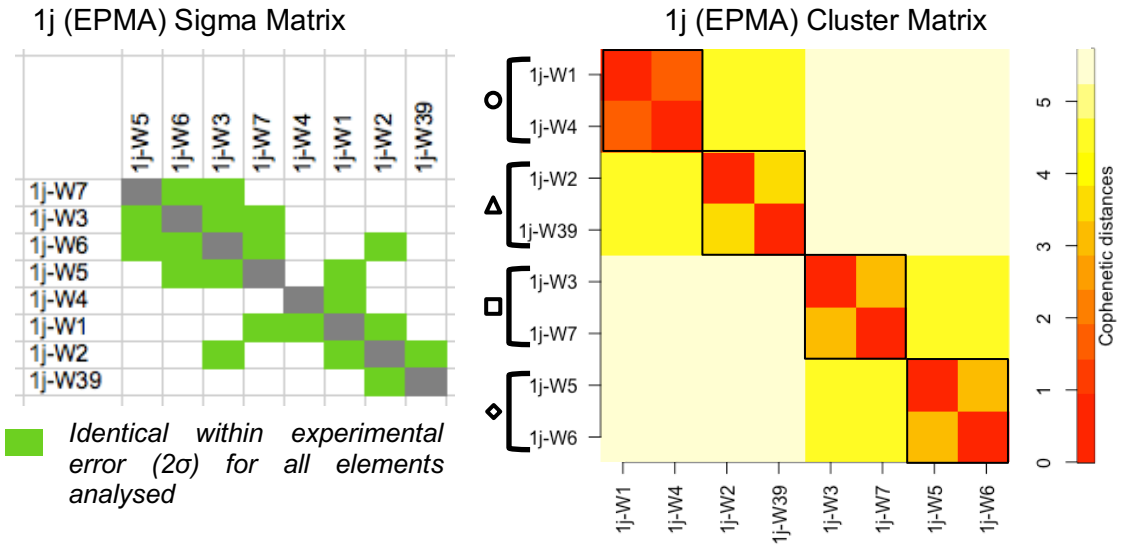

Figure E.8 The sigma matrix (top) and cluster matrix (bottom) for the control group of panel 1j white glass.

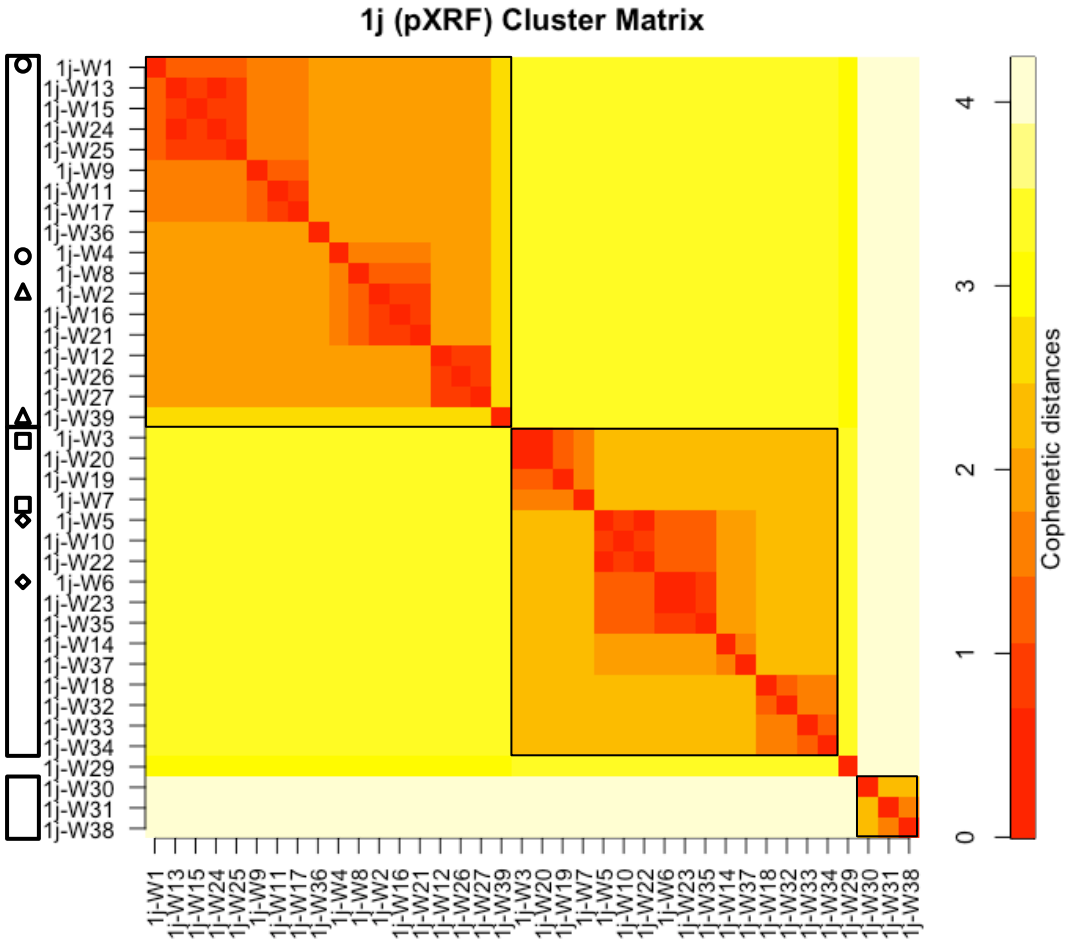

Figure E.7 Cluster matrix showing the results of the hierarchical clustering of the panel 1j white glass (pXRF data).

E.4 Panel 3b

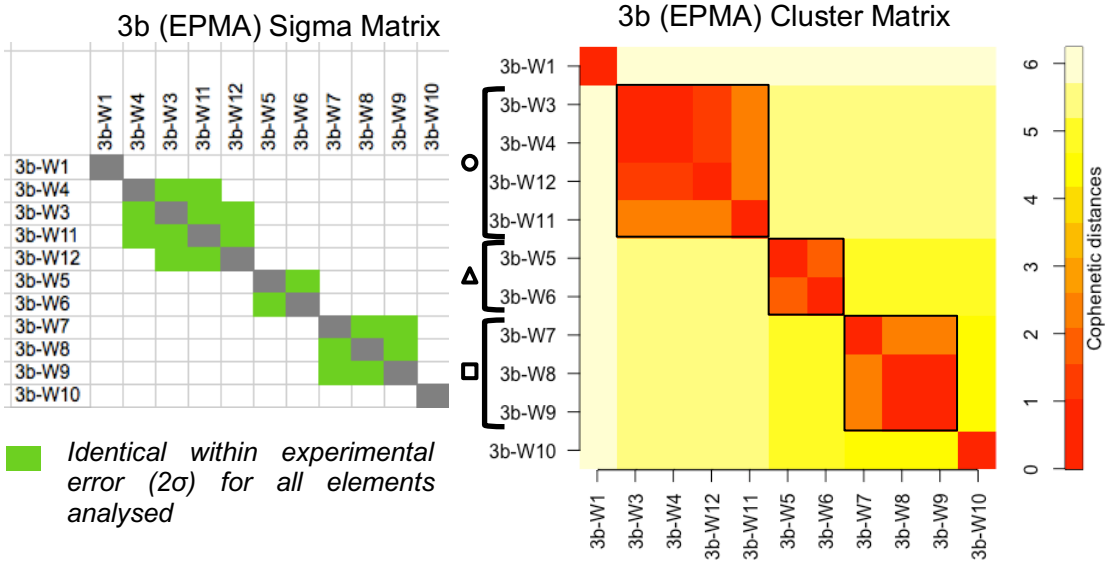

Figure E.9 The sigma matrix (top) and cluster matrix (bottom) for the control group of panel 3b white glass.

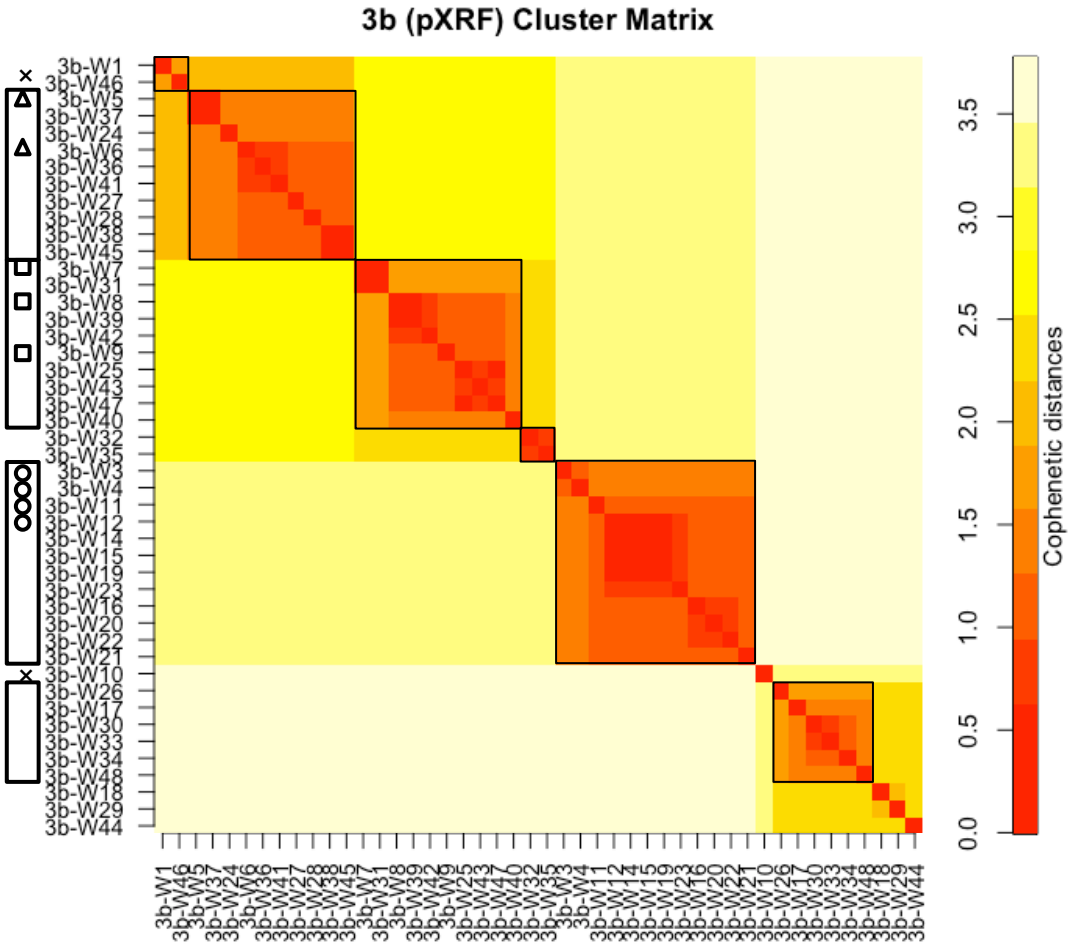

Figure E.10 Cluster matrix showing the results of the hierarchical clustering of the panel 3b white glass (pXRF data).

E.5 Panel 10c

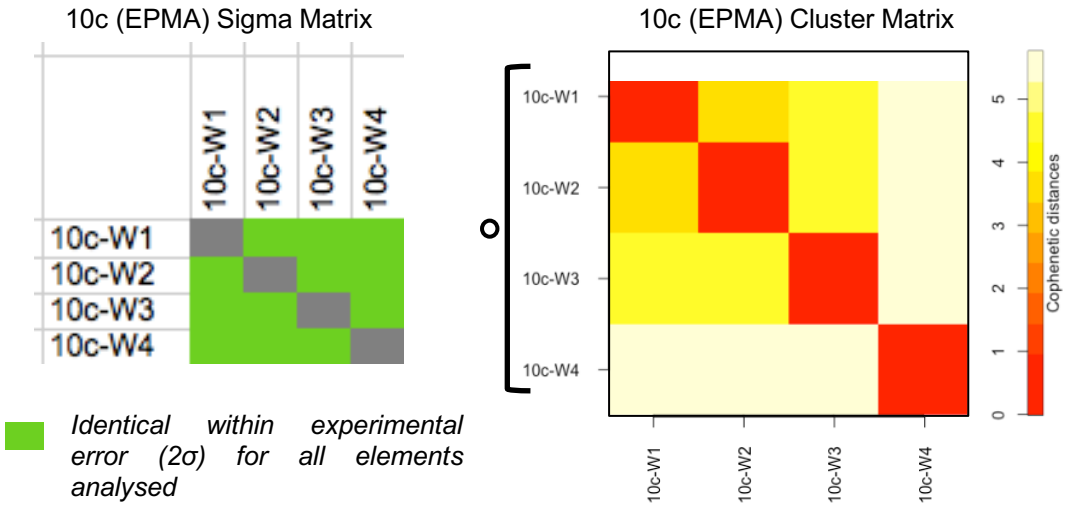

Figure E.11 The sigma matrix (top) and cluster matrix (bottom) for the control group of panel 10c white glass.

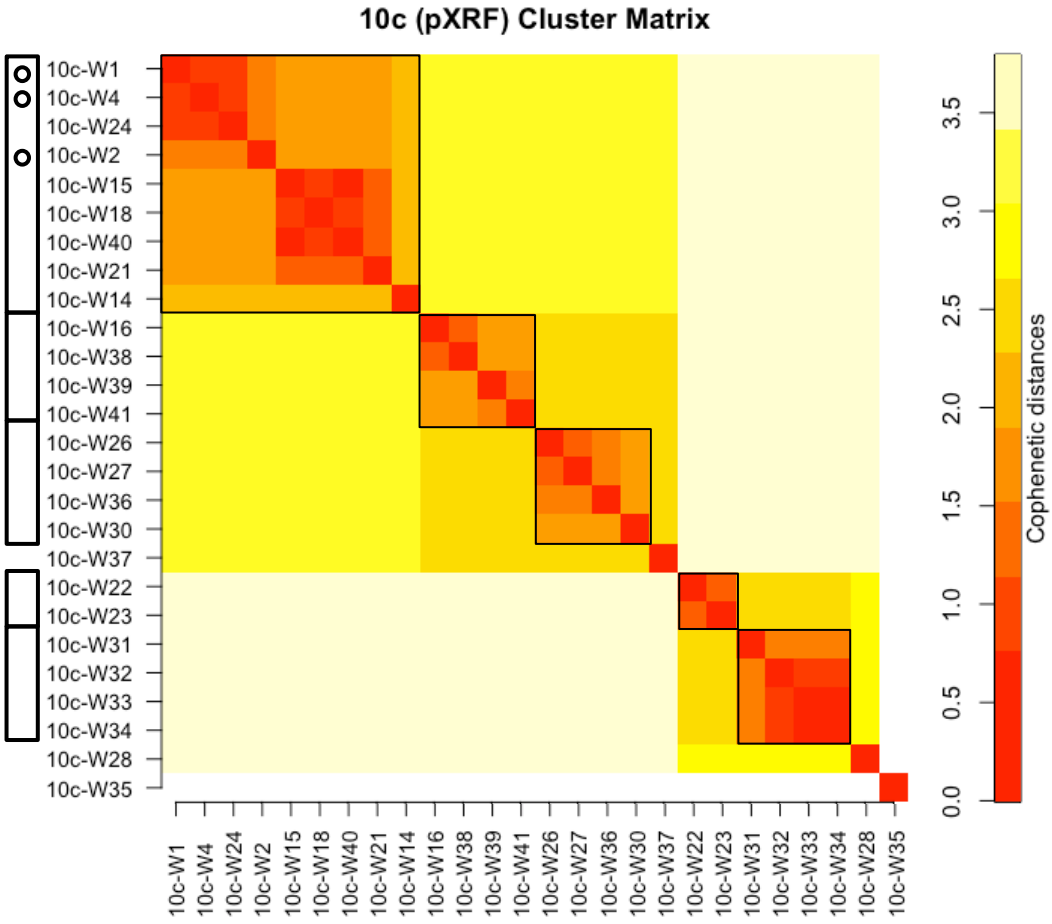

Figure E.12 Cluster matrix showing the results of the hierarchical clustering of the panel 10c white glass (pXRF data).

E.6 Panel 10e

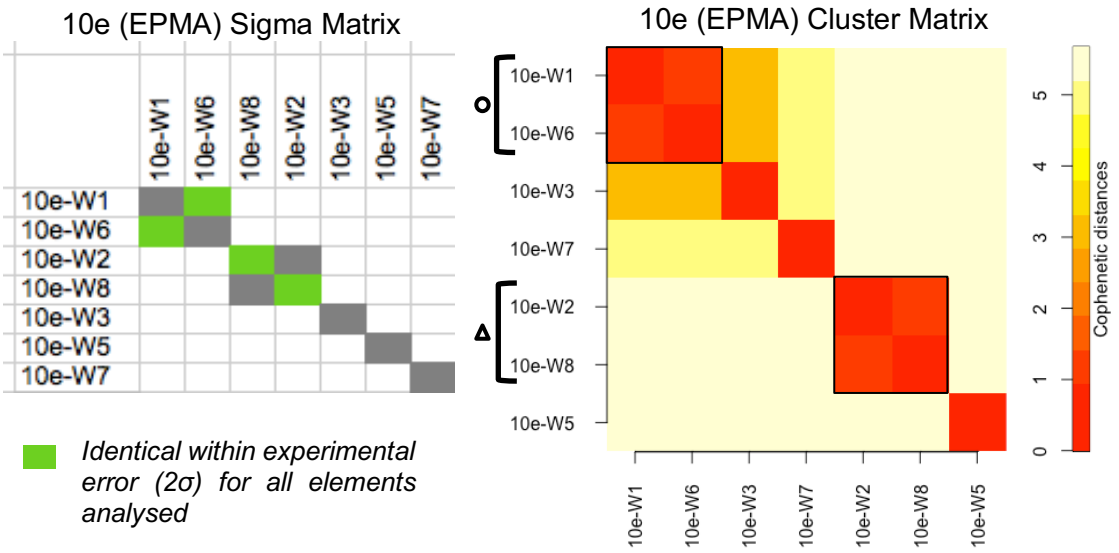

Figure E.13 The sigma matrix (top) and cluster matrix (bottom) for the control group of panel 10e white glass.

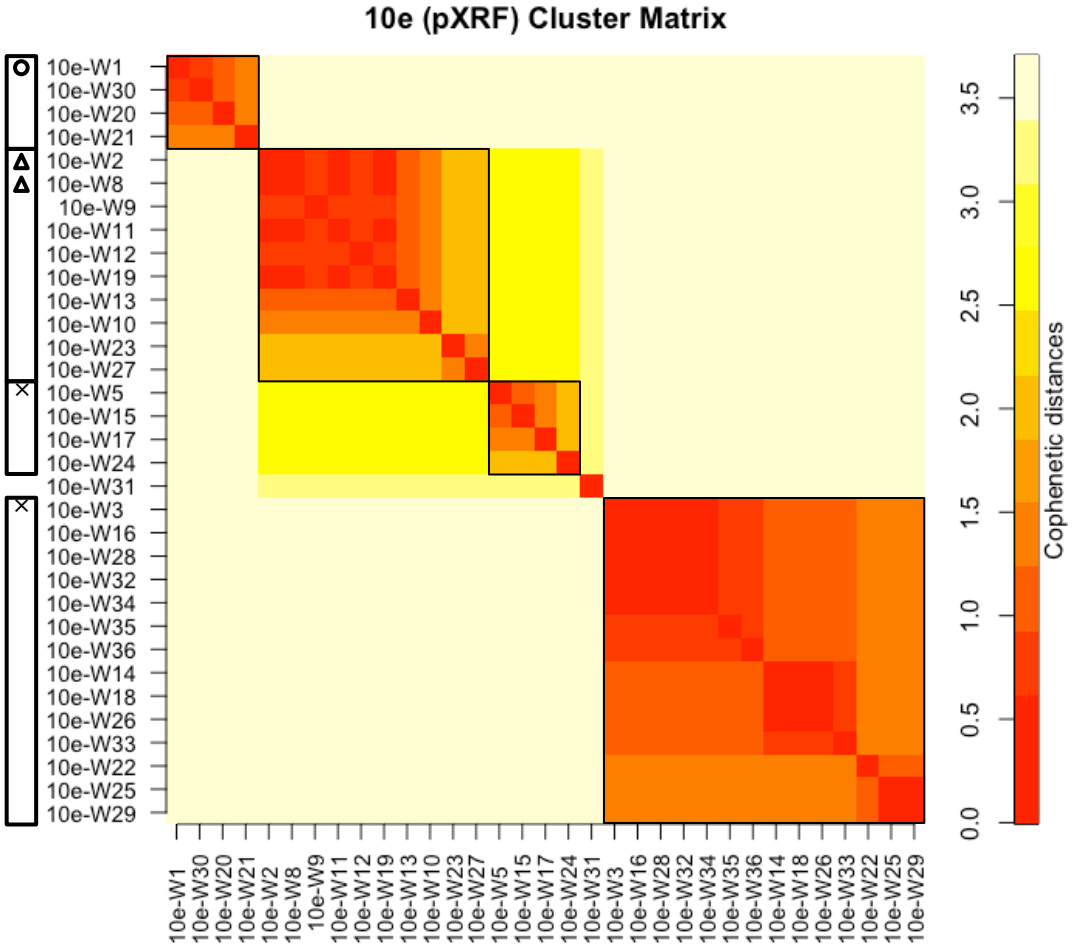

Figure E.14 Cluster matrix showing the results of the hierarchical clustering of the panel 10e white glass (pXRF data).

E.7 Panel 10h

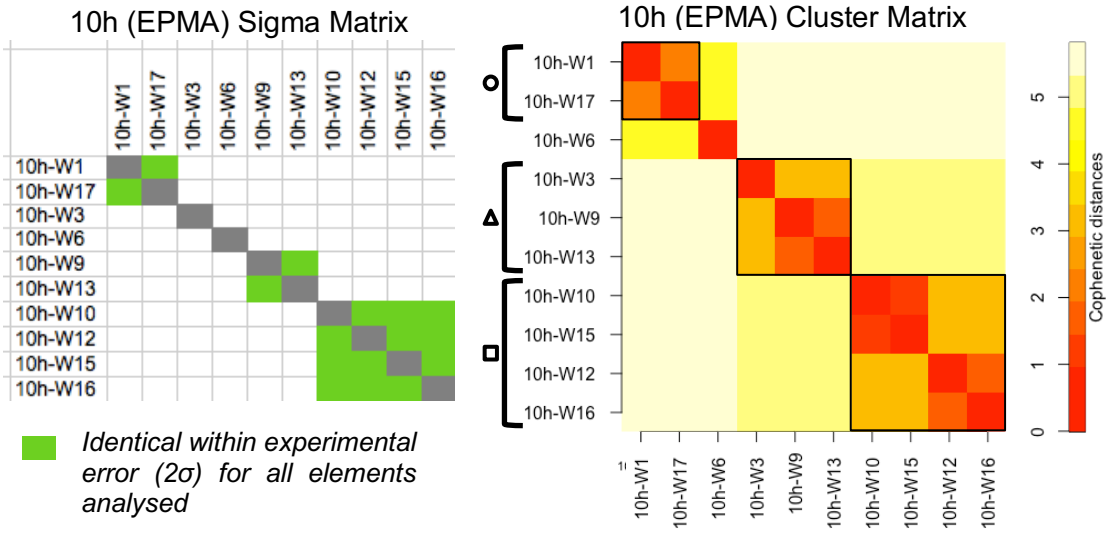

Figure E.15 The sigma matrix (top) and cluster matrix (bottom) for the control group of panel 10h white glass.

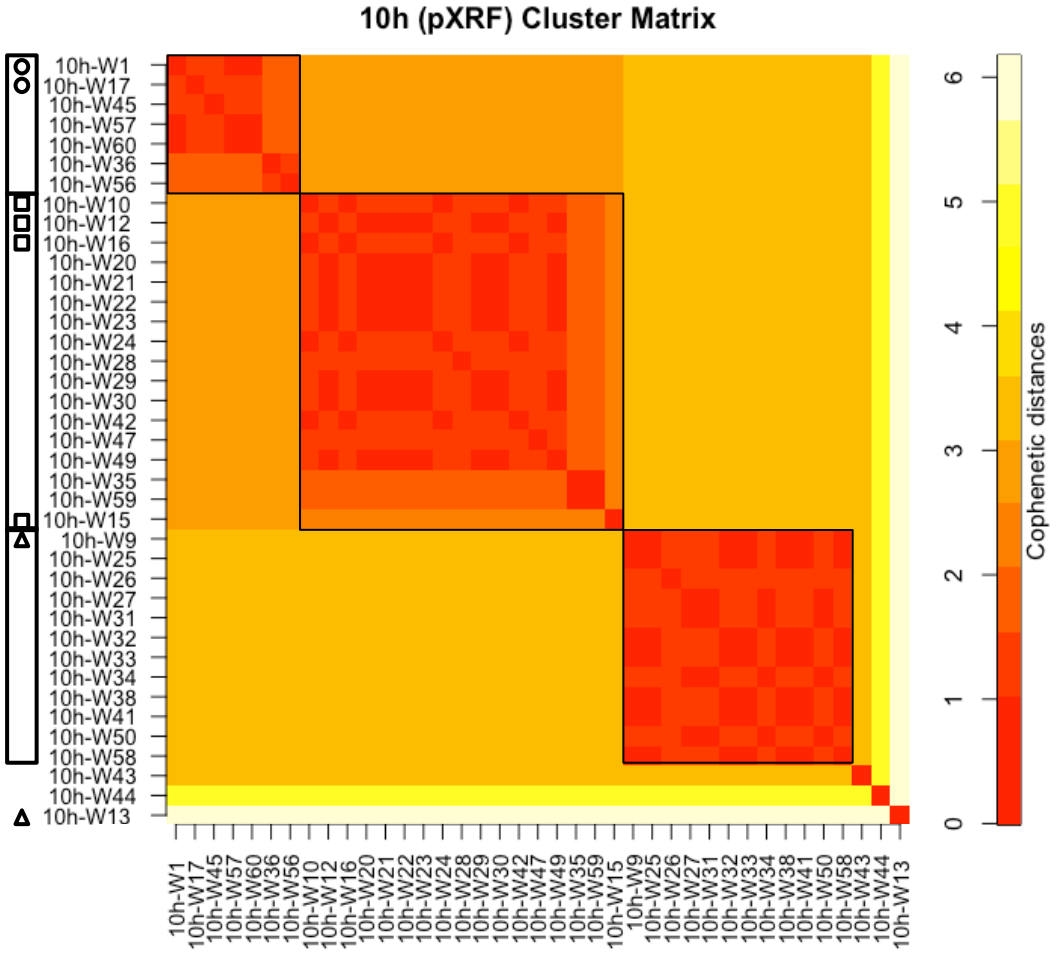

Figure E.16 Cluster matrix showing the results of the hierarchical clustering of the panel 10h white glass (pXRF data). 10h-W13 was measured with about twice the amount of copper as the other pieces due to it being completely covered with yellow stain.

E.8 Panel 15a

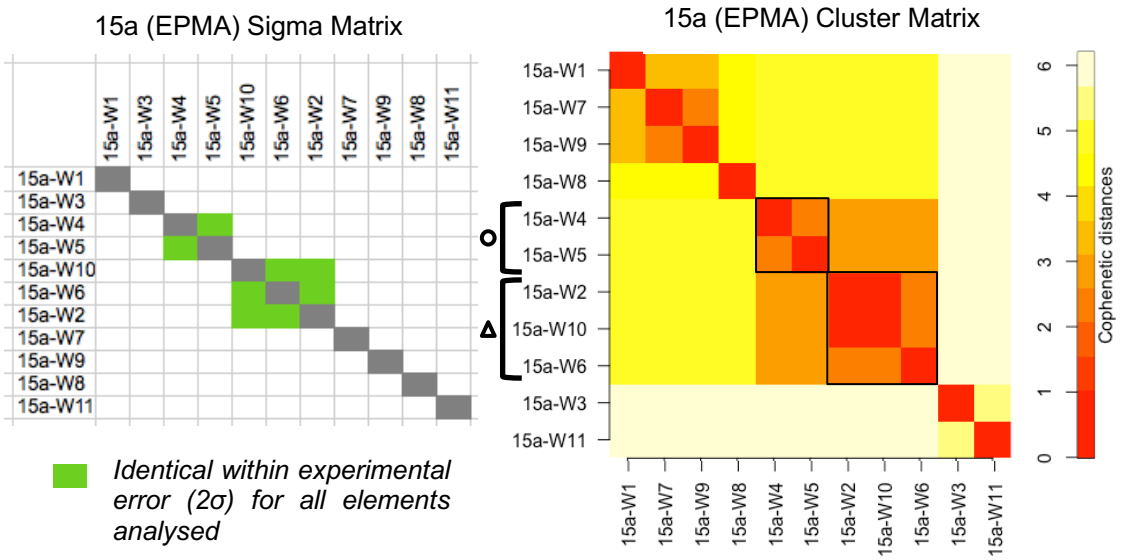

Figure E.17 The sigma matrix (top) and cluster matrix (bottom) for the control group of panel 15a white glass.

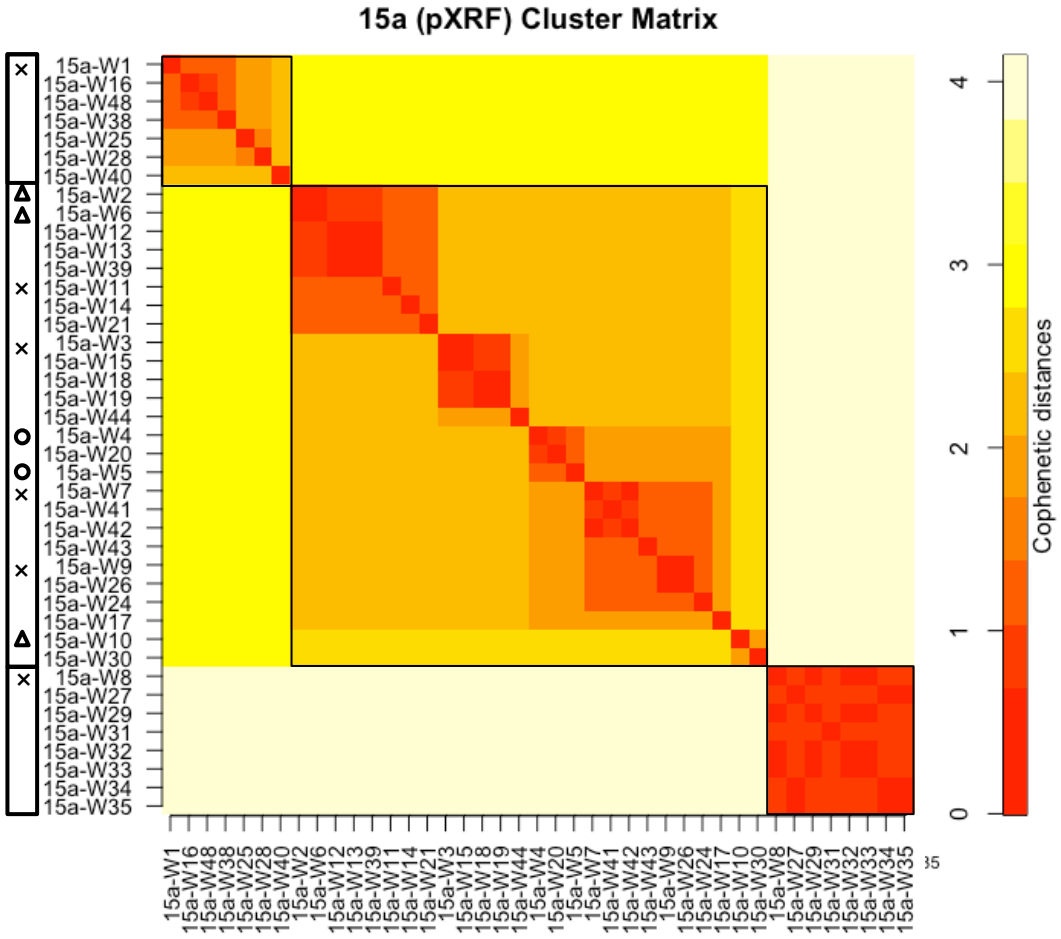

Figure E.18 Cluster matrix showing the results of the hierarchical clustering of the panel 15a white glass (pXRF data).

E.9 Panel 15b

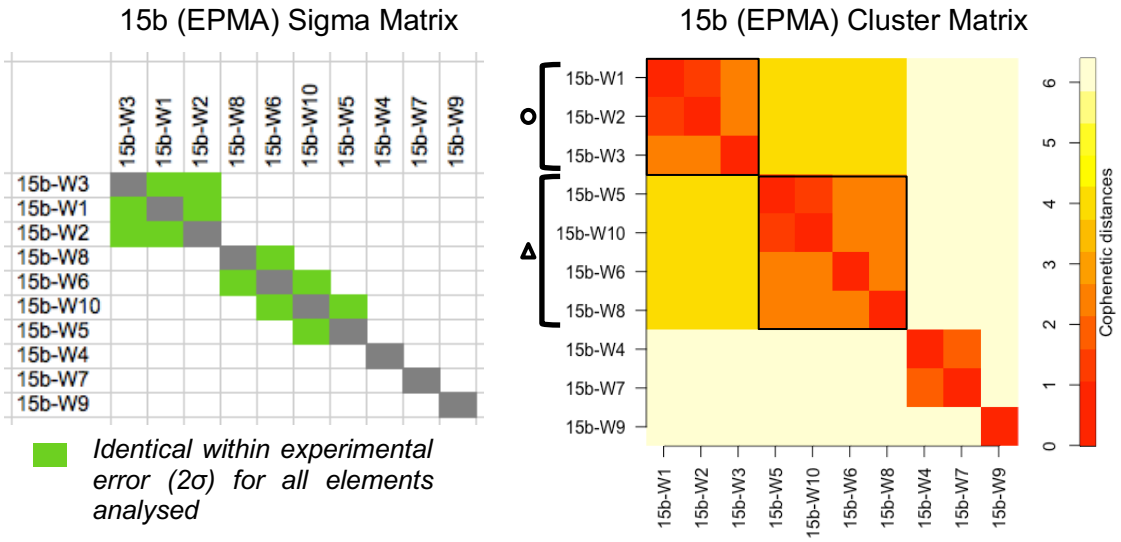

Figure E.19 The sigma matrix (top) and cluster matrix (bottom) for the control group of panel 15b white glass.

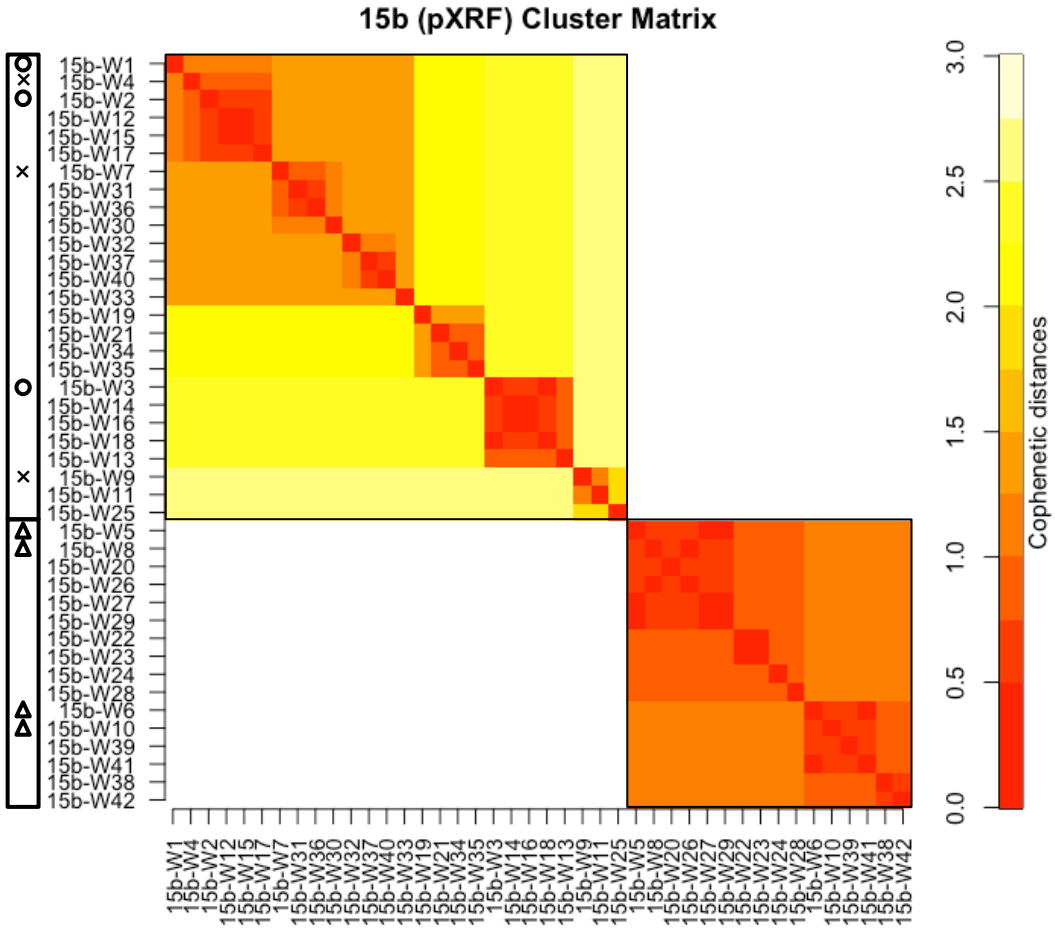

Figure E.20 Cluster matrix showing the results of the hierarchical clustering of the panel 15b white glass (pXRF data).

E.10 Panel 15f

No subsamples were taken from panel 15f for EPMA analysis; this panel was analysed by pXRF alone. The cluster boundaries had to be determined without the guidance of control group batches in the PBP approach.

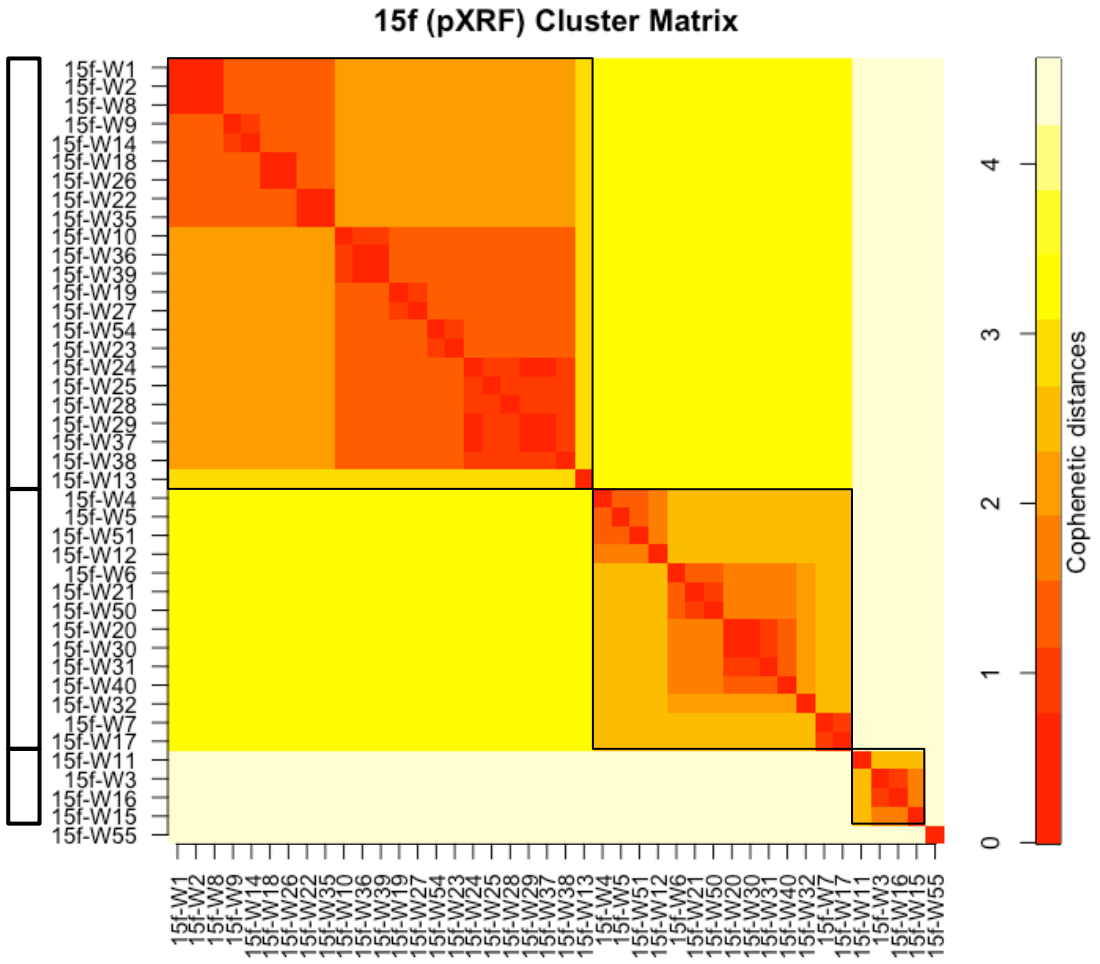

Figure E.21 Cluster matrix showing the results of the hierarchical clustering of the panel 15f white glass (pXRF data).

E.11 Panel 15g

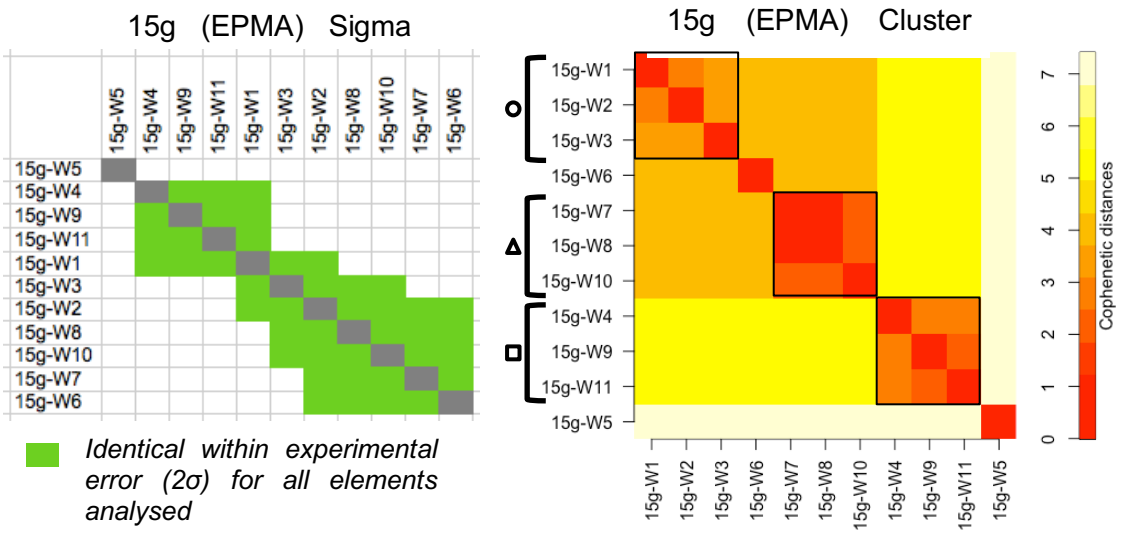

Figure E.22 The sigma matrix (top) and cluster matrix (bottom) for the control group of panel 15g white glass.

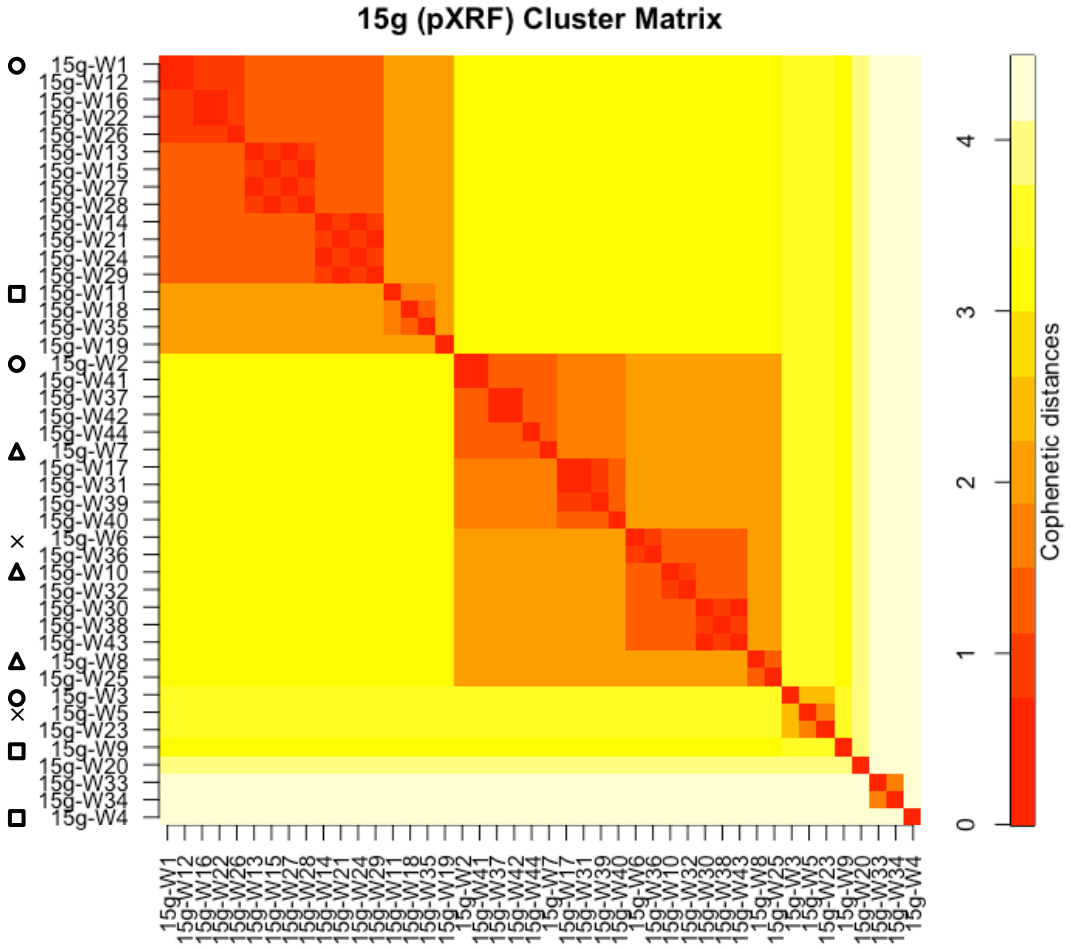

Figure E.23 Cluster matrix showing the results of the hierarchical clustering of the panel 15g white glass (pXRF data). In this panel, the control group batches did not correspond to the cluster results and so no groupings were made by the PBP approach.

E.12 Panel 15h

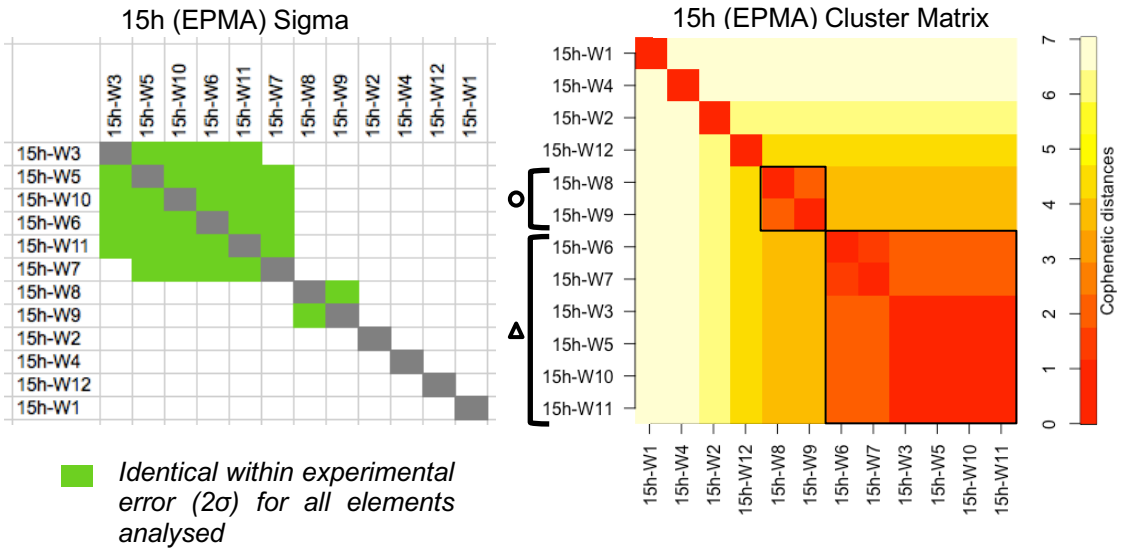

Figure E.24 The sigma matrix (top) and cluster matrix (bottom) for the control group of panel 15h white glass.

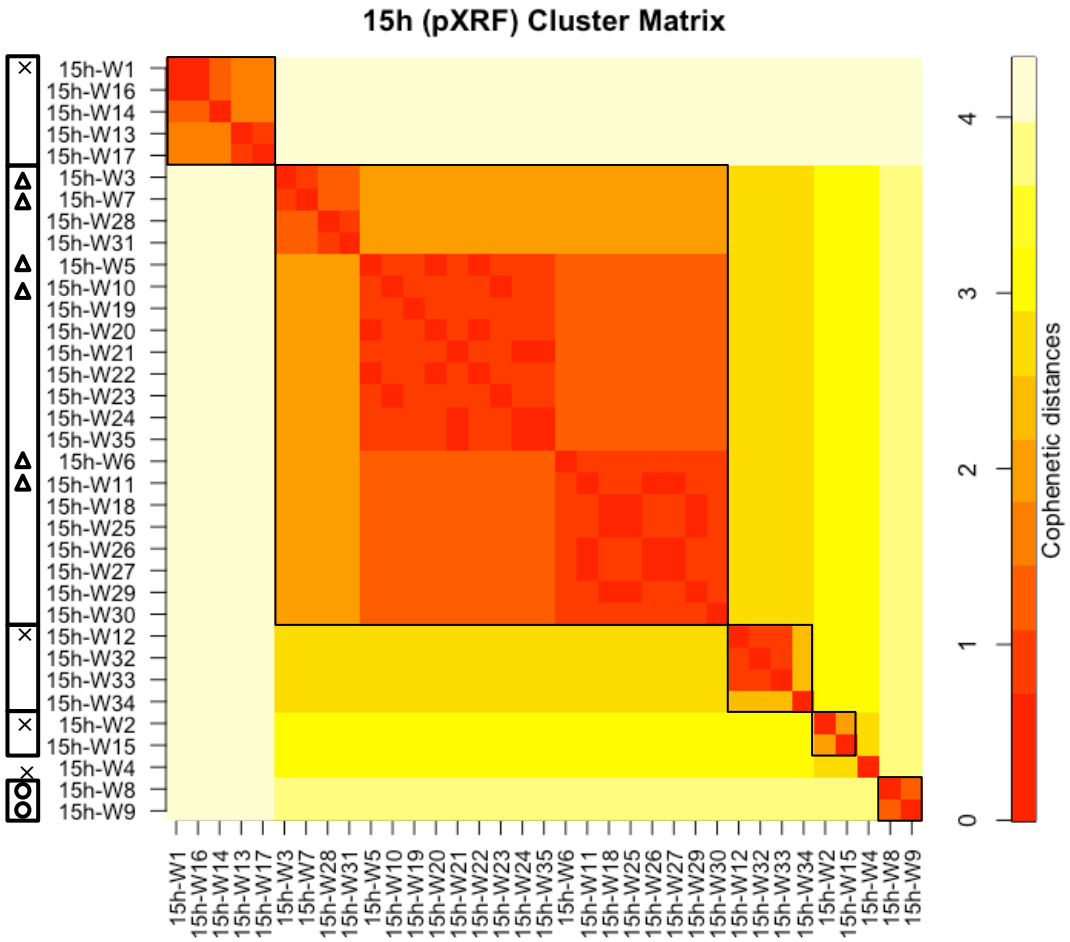

Figure E.25 Cluster matrix showing the results of the hierarchical clustering of the panel 15h white glass (pXRF data).